

CHEMISTRY

A European Journal

Supporting Information

Functionalization of Piperidine Derivatives for the Site-Selective and Stereoselective Synthesis of Positional Analogues of Methylphenidate

Wenbin Liu,^[a] Tobias Babl,^[a, b] Alexander Röther,^[b] Oliver Reiser,^{*[b]} and Huw M. L. Davies^{*[a]}

chem_201905773_sm_miscellaneous_information.pdf

Content

1. General Considerations.....	2
2. Full Conditions Optimization Tables.....	3
2.1. C2 Functionalization.....	4
2.2. C3 Functionalization.....	6
2.3. C4 Functionalization.....	8
3. Acquisition and Preparation of Compounds.....	11
4. C–H Insertion Reactions	17
4.1 General Procedures	17
5. Cyclopropanation and Ring-Opening Reactions for C3-Analogs	42
5.1 General Procedures	42
5.2. Diastereomer and Enantiomer Ratios Determination	42
5.3. Characterization Data for Cyclopropanation and Ring-Opening Products.....	43
6. Reference	59
7. Crude NMR for Diastereo- (and/or Regio-) Selectivity Determination:	60
8. Characterization NMR Spectra	109
9. HPLC Spectra for Enantioselectivity Determination	173
10.1. C2 Functionalization Products	173
10.2. Cyclopropanation and C3 Functionalization Products	226
10.3. C4 Functionalization Products	263
10. X-Ray Crystallographic Data of the Products for Absolute Stereochemistry.....	290
10.1. X-Ray Crystallographic Data for 6a	290
10.2. X-Ray Crystallographic Data for 8b	300
10.3. X-Ray Crystallographic Data for N-COCF₃-9a	305
10.4. X-Ray Crystallographic Data for 13b	315

1. General Considerations

All solvents for reactions were purified and dried by a *Glass Contour Solvent System* unless otherwise stated. The dichloromethane used in reactions was dried and degassed at reflux over activated 4 Å molecular sieves for 1 hours under argon, then stored with activated 4 Å molecular sieves under argon atmosphere and was used directly.

Thin layer chromatographic (TLC) analysis was performed on Kieselgel 60 F254 aluminum-backed silica plates, visualizing with UV light and/or staining with aqueous KMnO₄ stain.

Flash chromatography was used for product purification and performed on a Biotage® Isolera™ device. Depending on the scale of the reactions, different sizes of columns were employed. The normal phase silica columns were purchased from RediSep® and Biotage ZIP®. Ethylacetate (EtOAc) in combination with hexanes or Methanol (MeOH) in combination with dichloromethane (DCM) was used in a certain gradient as the mobile phase.

¹H and ¹³C NMR spectra were recorded at 600 MHz (¹³C at 150 MHz) on Bruker-600 spectrometer or IVONA-600 spectrometer, or 500 MHz (¹³C at 126 MHz) on INOVA-500 spectrometer. ¹⁹F NMR spectra were recorded at 565 MHz on Bruker-600 spectrometer or 283 MHz on Mercury 300. Unless otherwise stated, NMR spectra were run in solutions of deuterated chloroform (CDCl₃) with tetramethylsilane (TMS) as an internal standard (0 ppm for ¹H, and 0 ppm for ¹³C), and were reported in parts per million (ppm). Abbreviations for signal multiplicity are as follow: s = singlet, d = doublet, t = triplet, q = quartet, m = multiplet, dd = doublet of doublet, etc. Coupling constants (*J* values) were calculated directly from the spectra.

IR spectra were collected on a Nicolet iS10 FT-IR spectrometer and reported in unit of cm⁻¹.

Mass spectra were taken on a Thermo Finnigan LTQ-FTMS spectrometer with APCI, ESI or NSI.

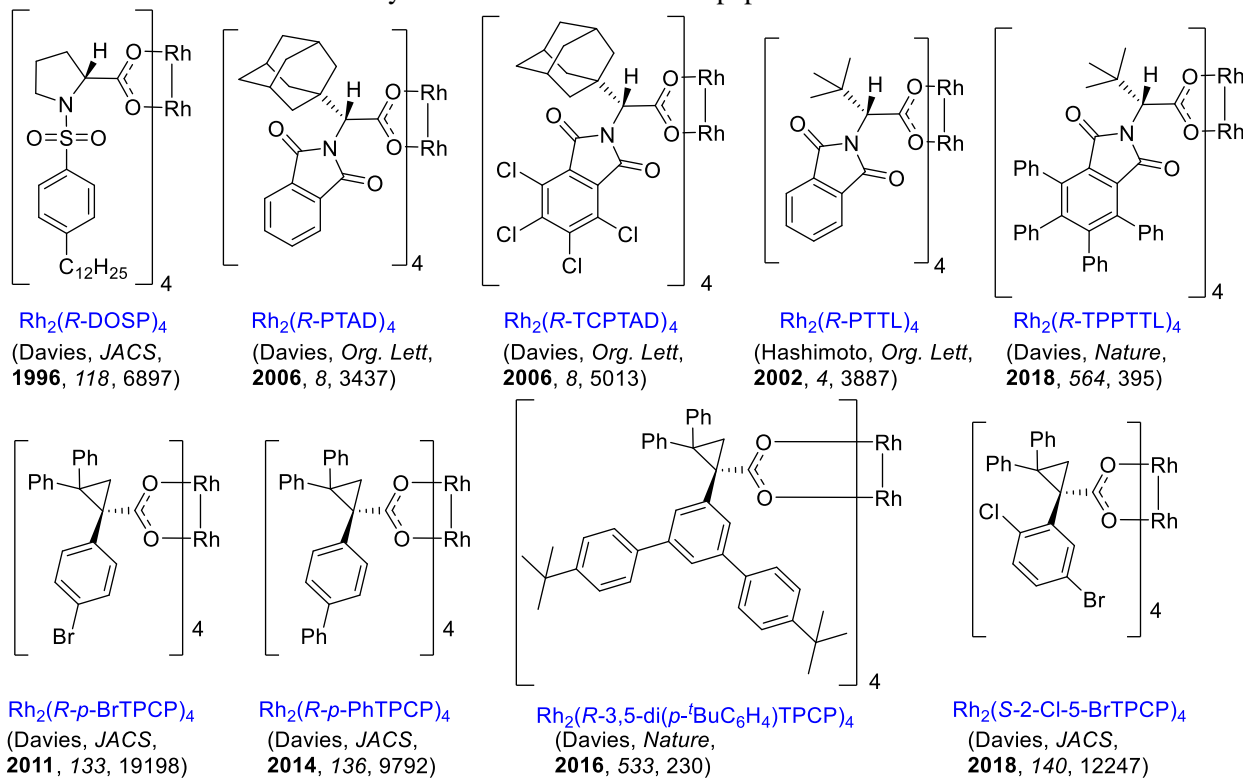
Melting points (mp) were measured in open capillary tubes with a Mel-Temp Electrothermal melting points apparatus and are uncorrected.

Optical rotations were measured on Jasco P-2000 polarimeters.

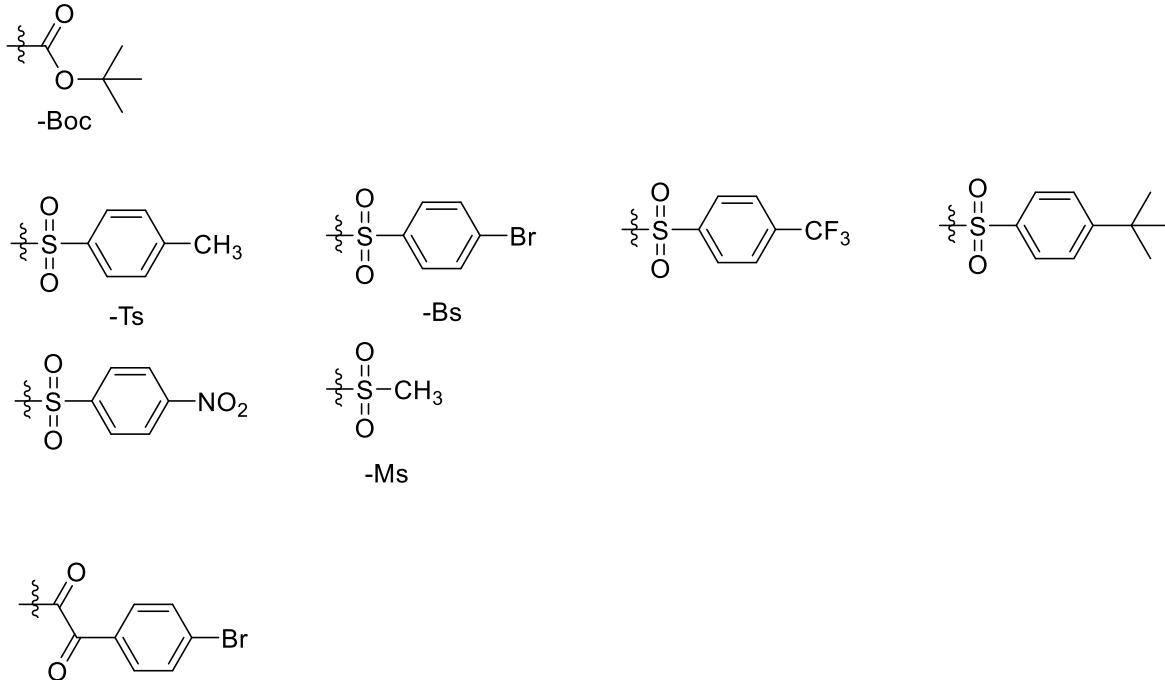
Analytical enantioselective chromatographs were measured on either Varian Prostar instrument or Agilent-1100 series instrument, and used isopropanol/hexane as gradient. Chiral HPLC conditions were determined by obtaining separation of the racemic products using Rh₂(OAc)₄, Rh₂(R/S-DOSP)₄ or Rh₂(R/S-2-Cl-5-BrTPCP)₄.

2. Full Conditions Optimization Tables

Structures of the dirhodium catalysts that are relevant to this paper:



Structure of protecting groups:



2.1. C2 Functionalization

Table S1. Catalyst and Condition Optimization for C2 Functionalization (Boc-protected)^a

entry	PG	L	R	solvent	temp. (°C)	yield (%) ^b	d.r. ^c	ee (%) ^d (major d)	ee (%) ^d (minor d)
1	Boc	S-DOSP	CH ₃	pentane	23	69	1.5:1	-69%	-44%
2		S-DOSP	CH ₃	CH ₂ Cl ₂	23	53	1.1:1	-41%	-29%
3		R-PTAD	CH ₃	CH ₂ Cl ₂	23	62	2.2:1	-70%	-14%
4		R-TCPTAD	CH ₃	CH ₂ Cl ₂	23	69	1.4:1	66%	72%
5		R-p-BrTPCP	CH ₃	CH ₂ Cl ₂	23	41	1.2:1	27%	-30%
6		R-p-PhTPCP	CH ₃	CH ₂ Cl ₂	23	40	1.5:1	33%	-45%
7		R-3,5-di(<i>p</i> - <i>t</i> BuC ₆ H ₄)TPCP	CH ₃	CH ₂ Cl ₂	23	55	2.0:1	44%	20%
8		S-2-Cl-5-BrTPCP	CH ₃	CH ₂ Cl ₂	23	83	5.3:1	83%	85%
9		R-TPPTTL	CH ₃	CH ₂ Cl ₂	23	69	1.5:1	54%	-32%
10		R-PTTL	CH ₃	CH ₂ Cl ₂	23	69	2.3:1	-69%	-10%
11	Boc	R-DOSP	CH ₂ CCl ₃	CH ₂ Cl ₂	23	52	3.4:1	14%	
12		R-PTAD	CH ₂ CCl ₃	CH ₂ Cl ₂	23	58	16.4:1	-80%	
13		R-TCPTAD	CH ₂ CCl ₃	CH ₂ Cl ₂	23	83	10.5:1	93%	
14		S-2-Cl-5-BrTPCP	CH ₂ CCl ₃	CH ₂ Cl ₂	23	73	3.6:1	65%	
15		R-TPPTTL	CH ₂ CCl ₃	CH ₂ Cl ₂	23	80	27.0:1	69%	
16		R-PTTL	CH ₂ CCl ₃	CH ₂ Cl ₂	23	78	23.7:1	-84%	

^aReaction condition are using general procedures with variants as indicated in the table. Results were determined on free secondary amines obtained after N-Boc deprotection by treatment of TFA. ^bIsolated yield of the C2-H insertion product. ^cDetermined from crude ¹H-NMR. ^dDetermined by chiral HPLC analysis of isolated product.

Variation of catalysts and conditions were examined for C–H functionalization at C2 position of N-Boc-piperidine. Using methyl diazoacetates (entry 1-10), most the dirhodium tetracarboxylate catalysts gave 1:2:1 diastereomeric ratio (d.r.), while the sterically demanding catalyst, Rh₂(S-2-Cl-5-BrTPCP)₄, gave highest d.r. (5.3:1, entry 8). Due to the recent advance in improving selectivity by using trichloroethyl (TCE) diazoacetates¹, some of the typical catalysts were examined. The d.r. for Rh₂(S-2-Cl-5-BrTPCP)₄-catalyzed reaction was decreased significantly, while the phthalimido-base dirhodium catalysts gave better d.r.. The highest enantioselectivity was obtained by using Rh₂(R-TCPTAD)₄ with good d.r. (10.5:1 d.r., 93% ee in entry 13).

Noticeably, the Rh₂(R-TPPTTL)₄-catalyzed reaction gave nearly single diastereomer (27:1 d.r. in entry 15), but its enantioselectivity was only moderate. Therefore, further exploration by changing the protecting group on the piperidine substrate was conducted (Table S2).

Table S2. Catalyst and Condition Optimization for C2 Functionalization (Sulfonyl-protected)^a

entry	PG	L	R	solvent	tempt. (°C)	yield (%) ^b	d.r. ^c	ee (%) ^d
1	Ts	<i>R</i> -DOSP	CH ₂ CCl ₃	CH ₂ Cl ₂	23	38	8.2:1	57%
2		<i>S</i> -2-Cl-5-BrTPCP	CH ₂ CCl ₃	CH ₂ Cl ₂	23	13*	7.3:1	84%
						(other C-H insertion products: @ C4 and CH ₃)		
3		<i>R</i> -TPPTTL	CH ₂ CCl ₃	CH ₂ Cl ₂	23	65	10.2:1	76%
4	Bs	<i>R</i> -DOSP	CH ₂ CCl ₃	CH ₂ Cl ₂	23	61	17.7:1	67%
5		<i>R</i> -DOSP	CH ₂ CCl ₃	pentane/TFT	23	13	>30:1	76%
6		<i>R</i> -DOSP	CH ₂ CCl ₃	TFT	23		no C-H insertion product	
7		<i>R</i> -PTAD	CH ₂ CCl ₃	CH ₂ Cl ₂	23	67	13.5:1	-72%
8		<i>R</i> -TCPTAD	CH ₂ CCl ₃	CH ₂ Cl ₂	23	75	3.2:1	97%
9		<i>R</i> - <i>p</i> -BrTPCP	CH ₂ CCl ₃	CH ₂ Cl ₂	23		trace C-H insertion product in crude ¹ H-NMR	
10		<i>R</i> - <i>p</i> -PhTPCP	CH ₂ CCl ₃	CH ₂ Cl ₂	23		trace C-H insertion product in crude ¹ H-NMR	
11		<i>R</i> -3,5-di(<i>p</i> - ^t Bu C ₆ H ₄)TPCP	CH ₂ CCl ₃	CH ₂ Cl ₂	23		trace C-H insertion product in crude ¹ H-NMR	
12		<i>S</i> -2-Cl-5-BrTPCP	CH ₂ CCl ₃	CH ₂ Cl ₂	23	16*	>30:1	66%
						(other C-H insertion products: @ C4)		
13		<i>R</i> -TPPTTL	CH ₂ CCl ₃	CH ₂ Cl ₂	23	76	>30:1	77%
14		<i>R</i> -PTTL	CH ₂ CCl ₃	CH ₂ Cl ₂	23	65	7.1:1	-74%
15		<i>R</i> -TPPTTL	CH ₂ CCl ₃	CH ₂ Cl ₂	39	87	21.5:1	76%
16		<i>R</i> -TPPTTL	CH ₂ CCl ₃	CH ₂ Cl ₂	0	42	26.4:1	72%

^aReaction condition are using general procedures with variants as indicated in the table. ^bIsolated yield of the C2-H insertion product. ^cDetermined from crude ¹H-NMR. ^dDetermined by chiral HPLC analysis of isolated product.

When the piperidine was protected by tosyl group, the standard catalyst, Rh₂(*R*-DOSP)₄, resulted in improved d.r. comparing to its selectivity on Boc-protected piperidine, but its yield and enantioselectivity were declined largely (entry 1). In addition, other C–H insertion products were observed in the reaction using Rh₂(*S*-2-Cl-5-BrTPCP)₄, in which the dirhodium carbene intermediate was reacted with the primary benzylic C–H bonds, so *p*-bromobenzenesulfonyl group was applied for further examination.

When the piperidine was protected by *p*-bromobenzenesulfonyl group, Rh₂(*R*-TPPTTL)₄ gave highest diastereoselectivity (entry 13, >30:1 d.r.). The yield for Rh₂(*R*-TPPTTL)₄-catalyzed reaction could be improved using higher temperature with small decrease in diastereoselectivity (entry 15), while the lower temperature (0 °C) resulted in significant loss in yield and decreased enantioselectivity.

Noticeably, most of the triarylcylopropanated (TPCP)-based dirhodium gave only trace amount of C–H functionalization product, while Rh₂(*S*-2-Cl-5-BrTPCP)₄-catalyzed reaction produced C–H functionalization product at C4 position of the piperidine in addition to the C2-products. It led to the further studies on C4 functionalization using Rh₂(*S*-2-Cl-5-BrTPCP)₄ (Section 2.4.)

2.2. C3 Functionalization

Table S3. Catalyst and Condition Optimization for Cyclopropanation at C2/C3 site^a

entry	L	R ¹ / R ²	solvent	tempt. (°C)	yield (%) ^b	ee (%) ^c
1	S-DOSP	H / CH ₃	pentane	23	83	92
2	S-DOSP	H / CH ₃	pentane	0	87	95
3	S-DOSP	H / CH ₃	pentane	-40	85	95
4	R-DOSP	H / CH ₃	trifluorotoluene	23	87	-79
5	R-DOSP	H / CH ₃	dichloromethane	23	52	-71
6	R-DOSP	H / CH ₃	toluene	23	76	-87
7	R-DOSP	Br / CH ₂ CCl ₃	pentane	23	70	-80
8	R-DOSP	Br / CH ₃	pentane	23	76	-89
9	S-TCPTAD	Br / CH ₃	pentane	23	75	3
10	R-p-BrTPCP	Br / CH ₃	pentane	23	85	-46
11	S-o-CITPCP	Br / CH ₃	pentane	23	92	-33
12	R-PTAD	Br / CH ₃	pentane	23	70	58
13	S-PTTL	Br / CH ₃	pentane	23	86	-43
14	S-TPPTTL	Br / CH ₃	pentane	23	79	5
15	S-p-BrTPCP	Br / CH ₃	dichloromethane	23	73	8
16	R-p-PhTPCP	Br / CH ₃	dichloromethane	23	85	-30
17	S-2-Cl-5-BrTPCP	Br / CH ₃	dichloromethane	23	77	-69

^aReaction condition are using general procedures with variants as indicated in the table.

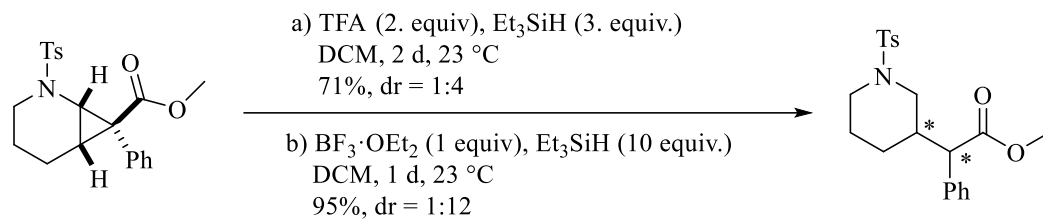
^bIsolated yield of the cyclopropanation product. ^cDetermined by chiral HPLC analysis of isolated product.

Rh₂(DOSP)₄ gives good yields using non-polar solvents (pentane, trifluorotoluene and toluene in entry 1, 4 and 6). Remarkable decrease of the yield as well as the ee is observed with DCM as solvent (entry 5). This behavior was already observed in other reactions using Rh₂(DOSP)₄²⁻³. The performance of trichloroethyl (TCE) diazoacetates¹ was also examined here in comparison to its methyl analog (entry 8), and decreased enantioselectivity was observed with TCE diazoacetates (80% ee in entry 7). Further examination of different dirhodium catalysts was conducted using methyl 2-(4-bromophenyl)-2-diazoacetate, and Rh₂(R-DOSP)₄ was found unmatched for this type of cyclopropanation (76% yield and 89% ee in entry 8), while all other dirhodium catalysts tested gave 3-69% ee (entry 9-17) in either pentane or dichloromethane as solvents.

In an attempt of further enhancing the ee, the reaction was carried out at lower temperatures. Using Rh₂(DOSP)₄ as catalyst, in combination with methyl 2-diazo-2-phenylacetate in pentane, 0 °C as well as -40 °C

gave a very good ee of 95% while the yields stayed the same. As 0 °C is easier to handle as it only takes a bath of ice in water, further reactions were carried out at 0 °C.

In order to synthesize the 3-substituted piperidines that are aim of this part of the work, the cyclopropanes had to be opened in an acid catalyzed way. According to the strategies of Pilsl *et al.*,⁴ the same reaction with the cyclopropanated piperidines as substrate. In contrast to Pilsl's substrate the ring-opened product would contain two chiral centers and one of them would be affected by the enol-form during the transition state. The desired product was able to be obtained *via* Brønsted and Lewis acid catalyzed ring-openings in good to excellent yields. The Lewis acid, $\text{BF}_3\cdot\text{OEt}_2$, gave yields of 95% with a good d.r. of 1:12. The ring-opening of Boc-protected substrate was then conducted using the $\text{BF}_3\cdot\text{OEt}_2$ condition, and the deprotection of Boc group was observed, so the reaction was extended to 2 days to ensure the full conversion.



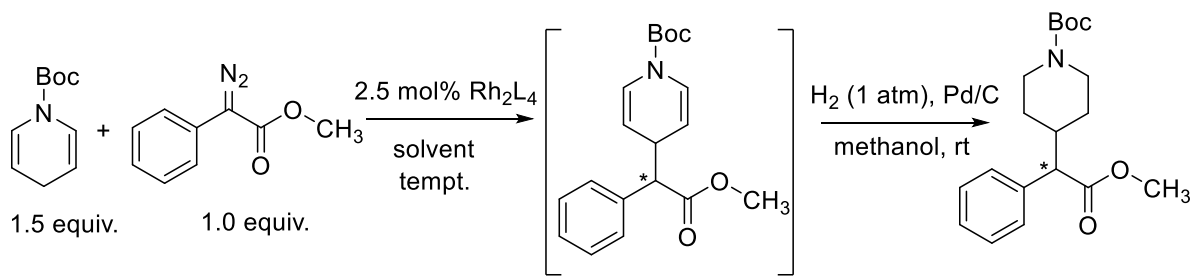
Scheme S1. Ring-opening of Ts-protected 2-azabicyclo[4.1.0]heptanes.

2.3. C4 Functionalization

N-Boc-1,4-dihydropyridine was chosen as substrate for the synthesis of 4-substituted piperidines. The double vinyl position and the +M effect of the nitrogen in addition should give this substrate an enormous reactivity and chemoselectivity towards C–H insertion making the possible cyclopropanation less favored.⁵

In the initial attempt for 4-substituted piperidine, a combination of methyl 2-diazo-2-phenylacetate and 0.5 mol% Rh₂(DOSP)₄ was applied. However, decomposition of the starting-material to pyridine and the poisoning of the catalyst was thought to be the major problem, as pyridine was found in the crude NMR-analysis of the reaction. A higher catalyst loading should ensure the presence of active catalyst (2.5 mol%). In addition, the freshly made N-Boc-1,4-dihydropyridine was used for the dirhodium carbene reaction, followed by immediately hydrogenation of the C–H insertion product after isolation to prevent loss due to decomposition.

Table S4. Catalyst and Condition Optimization for C–H Insertion at C4-position using 1,4-Dihydropyridine^a



entry	L	solvent	tempt. (°C)	yield (%) ^b	ee (%) ^c
1	Rh ₂ (S-DOSP) ₄	pentane	23	no activity	
2	Rh ₂ (S-DOSP) ₄	dichloromethane	23	no activity	
3	Rh ₂ (S-DOSP) ₄	trifluorotoluene	23	no activity	
4	Rh ₂ (S-DOSP) ₄	ethyl acetate	23	no activity	
5	Rh ₂ (S-DOSP) ₄	-- (neat)	23	52	-55
6	Rh ₂ (R-DOSP) ₄	-- (neat)	0	54	61
7	Rh ₂ (R-PTAD) ₄	-- (neat)	23	62	-37
8	Rh ₂ (R-TCPTAD) ₄	-- (neat)	23	35	6
9	Rh ₂ (R-TPPTTL) ₄	-- (neat)	23	19	32
10	Rh ₂ (S-PTTL) ₄	-- (neat)	23	45	30
11	Rh ₂ (R-p-BrTPCP) ₄	-- (neat)	23	58	-13
12	Rh ₂ (R-3,5-di(^t BuC ₆ H ₄)TPCP) ₄	-- (neat)	23	no activity	
13	Rh ₂ (S-2-Cl-5-Br-TPCP) ₄	-- (neat)	23	68	6

^aReaction condition are using general procedures with variants as indicated in the table. ^bIsolated yield of the product after hydrogenation. ^cDetermined by chiral HPLC analysis of isolated product.

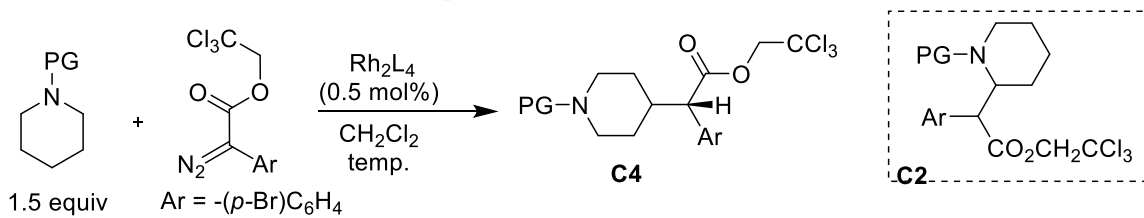
No reaction activity was observed using various solvent. However, decomposition of diazoacetate (bubble formation and heat generated) was observed when solvent was removed under reduced pressure. The analysis of the crude ¹H-NMR clearly showed the formation of the desired product. Then, the reactions were carried out under neat conditions without any solvent. To obtain more reproducible results, the setup of the reaction was changed. Instead of adding the diazo compound slowly to a solution of substrate and catalyst, the catalyst and the substrate were dissolved in small amounts of DCM (pentane for Rh₂(DOSP)₄). Stirring the mixture 1 min

before adding the diazo compound in one portion, makes sure that all catalyst is inactive. Afterwards, the solvent was removed under reduced pressure. Residues of solvent were removed under vacuum. The reaction started after a few minutes under HV conditions. In the course of the reaction, the viscosity of the mixture increased, inhibiting proper stirring. Therefore, the viscous mixture was dissolved again, stirred and then dried again twice. The catalysts were consecutively screened under the new conditions.

Screening the catalyst gave moderate yields of 50-60% in many cases. The highest yield of 68% was obtained using $\text{Rh}_2(2\text{-Cl-5-Br-TPCP})_4$. However, this catalyst gives almost no chirality induction and only an ee of 5%. $\text{Rh}_2(\text{DOSP})_4$ gives reasonable yields of up to 52% with the best value in enantiomeric excess of 55%. A lower temperature of 0 °C while using $\text{Rh}_2(\text{DOSP})_4$ gives a small rise in yield (54%) as well as in enantiomeric access (61%).

As yields and enantioselectivity was not very good even after catalyst screening and experiments with lower temperatures, investigations using N-Boc-1,4-dihydropyridine were stopped. A more innovative approach was explored with direct C–H functionalization at C4 position on piperidines controlled by catalyst with appropriate combination of protection group.

Table S5. Catalyst and Condition Optimization for C4 Functionalization^a



entry	PG	L	temp. (°C)	r.r. (C4:C2) ^b	yield (%) ^c	ee (%) ^d
1		R-DOSP	23	<1:30	--	--
2		R-TCPTAD	23	<1:30	--	--
3		R-TPPTTL	23	<1:30	--	--
4		R- <i>p</i> -BrTPCP	23	trace C-H insertion product in crude ¹ H-NMR		
5		S-2-Cl-5-BrTPCP	23	4.2:1	67	90
6		S-2-Cl-5-BrTPCP	23	4.0:1	30	96
7		S-2-Cl-5-BrTPCP	23	3.9:1	--	--
8		S-2-Cl-5-BrTPCP	23	4.7:1	65	96
9		S-2-Cl-5-BrTPCP	23	no C-H insertion product in crude ¹ H-NMR		
10	1e	S-2-Cl-5-BrTPCP	23	5.6:1	78	97
11	1f	S-2-Cl-5-BrTPCP	23	>30:1	50	97
12	1f	S-2-Cl-5-BrTPCP	39	>30:1	57	97
13 ^e	1f	S-2-Cl-5-BrTPCP	39	>30:1	61	97

^aReaction condition are using general procedures with variants as indicated in the table. ^bDetermined from crude ¹H-NMR. ^cIsolated yield of the C4-H insertion product. ^dDetermined by chiral HPLC analysis of isolated product. ^eProtected piperidine was used as limiting reagent, with 1.5 equivalent of diazoacetates.

Variation of catalysts and conditions were examined for C–H functionalization at C4 position of N-protected piperidines. The sterically demanding catalyst, Rh₂(S-2-Cl-5-BrTPCP)₄, was found to be the only catalyst gave C4-functionalization product (entry 5 vs entry 1-4). Variation of the substituent on the *para*-position of the benzenesulfonyl groups showed small change of the regioselectivity with electron-withdrawing CF₃ substituent giving highest selectivity for C4 product (4.7:1 r.r. in entry 8). When it was a simple methyl group next to the sulfonyl group (entry 10), which is expected to give lower selectivity due to diminished steric hindrance, the selectivity for C4 product is unexpectedly higher than arylsulfonyl-protected ones (5.6:1 r.r.). Significant improvement was achieved using strong electron-withdrawing oxalyl group, in which C4 product was observed as single regio-isomer with 97% ee.

3. Acquisition and Preparation of Compounds

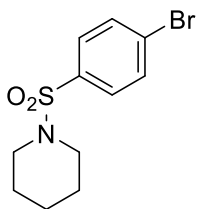
The substrates and reagents were purchased from commercial sources (Sigma-Aldrich, Alfa-Aesar, Acros Organic, TCI America, Oakwood Chemical, Fisher Scientific and Strem Chemicals) and used directly without further purification. The chiral dirhodium catalysts are available in our lab and they were made according to literature procedures.

The following substrates were prepared by procedures adapted from literatures:

2,2,2-Trichloroethyl 2-(4-bromophenyl)-2-diazoacetate;¹ 2,2,2-trichloroethyl 2-diazo-2-phenylacetate;² 2,2,2-Trifluoroethyl 2-diazo-2-(4-(trifluoromethyl)phenyl)acetate;⁶ 2,2,2-Trichloroethyl 2-(4-acetoxyphenyl)-2-diazoacetate;⁶ 2,2,2-Trifluoroethyl 2-diazoacetate;⁶ Methyl 2-(4-bromophenyl)-2-diazoacetate;⁶ Methyl 2-diazo-2-phenylacetate;⁷ Methyl 2-diazo-2-(4-(trifluoromethyl)phenyl)acetate;⁷ Methyl 2-([1,1'-biphenyl]-4-yl)-2-diazoacetate;⁸ *tert*-Butyl piperidine-1-carboxylate;⁹ 1-Tosylpiperidine;⁹ 1-(4-Bromophenyl)-2-(piperidin-1-yl)ethane-1,2-dione;¹⁰ *o*-NBSA (*o*-nitrobenzenesulfonyl azide);¹¹ 2-(3,4-Dibromophenyl)acetic acid;¹² *tert*-Butyl pyridine-1(4H)-carboxylate.¹³

Other sulfonyl protected piperidines were prepared using adapted procedure similar to the one for 1-tosylpiperidine:⁹

To a solution of corresponding sulfonyl chloride (50 mmol, 1.0 equiv.) in 150 mL of CH₂Cl₂, piperidine (5.9 mL, 60 mmol, 1.2 equiv.) was added drop-wise with the generation of white fume, followed by the slow addition of triethylamine (10.5 mL, 75 mmol, 1.5 equiv.). The mixture was allowed to stir at room temperature (23 °C) for 15 hours. The consumption of piperidine was monitored by TLC (30% ethyl acetate in hexane). The solvent was removed under reduced pressure and the residue was purified by flash silica gel column chromatography using gradient as indicated.

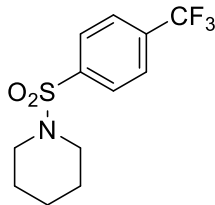


1-((4-Bromophenyl)sulfonyl)piperidine (1b)

Purification was carried out with 8-12% ethyl acetate in hexane to give **1b** as white solid in 78% yield (39 mmol, 11.9 g). The NMR data are consistent with literature values.¹⁴

¹H NMR (600 MHz, CDCl₃) δ 7.67 (d, *J* = 8.6 Hz, 2H), 7.62 (d, *J* = 8.6 Hz, 2H), 2.99 (t, *J* = 5.5 Hz, 4H), 1.69 – 1.61 (m, 4H), 1.48 – 1.39 (m, 2H).

¹³C NMR (151 MHz, CDCl₃) δ 135.5, 132.2, 129.1, 127.6, 46.9, 25.1, 23.5.



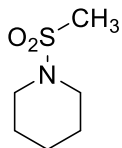
1-((4-(Trifluoromethyl)phenyl)sulfonyl)piperidine (1d)

It was done in 30 mmol scale of 4-(trifluoromethyl)benzenesulfonyl chloride. Purification was carried out with 8-15% ethyl acetate in hexane to give **1d** as white solid in 93% yield (28 mmol, 8.2 g). The NMR data are consistent with literature values.¹⁴

¹H NMR (500 MHz, CDCl₃) δ 7.90 (dt, *J* = 8.1, 0.7 Hz, 2H), 7.81 (dt, *J* = 8.3, 0.6 Hz, 2H), 3.03 (t, *J* = 5.5 Hz, 4H), 1.74 – 1.59 (m, 4H), 1.53 – 1.38 (m, 2H).

¹³C NMR (126 MHz, CDCl₃) δ 140.2, 134.3 (q, *J* = 32.9 Hz), 128.2, 128.0, 126.2 (q, *J* = 3.6 Hz), 123.4 (d, *J* = 272.6 Hz), 47.0, 25.2, 23.5.

¹⁹F NMR (282 MHz, CDCl₃) δ -63.12.

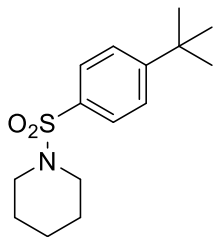


1-(Methylsulfonyl)piperidine (1e)

It was done in 30 mmol scale of methanesulfonyl chloride. Purification was carried out with 8-15% ethyl acetate in hexane to give **1e** as white solid in 82% yield (24.5 mmol, 4.0 g). The NMR data are consistent with literature values.¹⁵

¹H NMR (500 MHz, CDCl₃) δ 3.18 (t, *J* = 5.6 Hz, 4H), 2.77 (s, 3H), 1.72 – 1.64 (m, 4H), 1.61 – 1.53 (m, 2H).

¹³C NMR (126 MHz, CDCl₃) δ 46.6, 34.1, 25.2, 23.5.

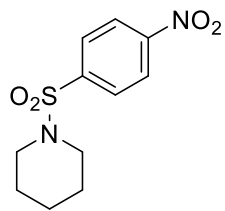


1-((4-(tert-Butyl)phenyl)sulfonyl)piperidine (1g)

Purification was carried out with 10-12% ethyl acetate in hexane to give **1g** as white solid in 98% yield (49 mmol, 13.8 g). The NMR data are consistent with literature values.¹⁴

¹H NMR (600 MHz, CDCl₃) δ 7.67 (d, *J* = 8.2 Hz, 2H), 7.52 (d, *J* = 8.5 Hz, 2H), 2.99 (t, *J* = 5.5 Hz, 4H), 1.68 – 1.61 (m, 4H), 1.47 – 1.39 (m, 2H), 1.35 (s, 9H).

¹³C NMR (151 MHz, CDCl₃) δ 156.2, 133.3, 127.6, 125.9, 46.9, 35.1, 31.1, 25.2, 23.5.



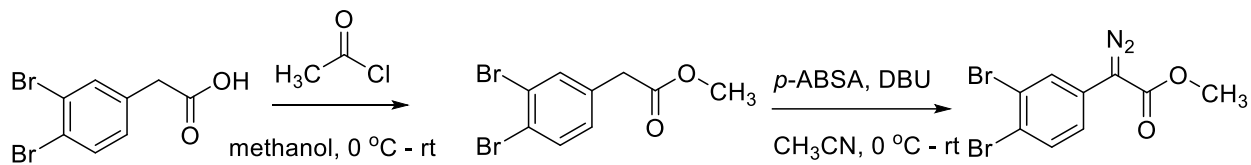
1-((4-Nitrophenyl)sulfonyl)piperidine (1h)

It was done in 30 mmol scale of 4-nitrobenzenesulfonyl chloride. Purification was carried out with 8-15% ethyl acetate in hexane to give **1h** as white solid in 83% yield (25 mmol, 6.7 g). The NMR data are consistent with literature values.¹⁶

¹H NMR (500 MHz, CDCl₃) δ 8.39 (d, *J* = 8.9 Hz, 2H), 7.96 (d, *J* = 8.9 Hz, 2H), 3.06 (t, *J* = 5.5 Hz, 4H), 1.67 (p, *J* = 5.9 Hz, 4H), 1.47 (tt, *J* = 8.3, 4.6 Hz, 2H).

¹³C NMR (126 MHz, CDCl₃) δ 150.1, 142.6, 128.8, 124.3, 47.0, 25.2, 23.4.

Other diazoacetate compounds were prepared using procedures in literatures from corresponding starting materials.^{1,6-7}



Methyl 2-diazo-2-(3,4-dibromophenyl)acetate (2e)

The synthesis is adapted from literatures:³ In a 250 mL round-bottom flask with argon atmosphere inside, 2-(3,4-dibromophenyl)acetic acid (4.6 g, 15.6 mmol, 1.0 equiv) was dissolved in 100 mL of methanol and cooled to 0 °C via ice bath. Acetyl chloride (2 mL, 18.8 mmol, 1.2 equiv) was added via a syringe. The reaction mixture was stirred for 15 hours, at which point it was warmed up to room temperature (23 °C). The reacted mixture was diluted with 100 mL of ethyl acetate and washed with NaHCO_3 . The organic layer was concentrated under reduced pressure and purified by flash column chromatography (10% ethyl acetate in hexane) to afford the orange solid in 93% yield (4.5 g). It was used immediately in the next step.

Methyl 2-(3,4-dibromophenyl)acetate (3.0 g, 9.7 mmol) was added in a flame-dried round-bottom flask, together with *p*-ABSA (*p*-acetamidobenzenesulfonyl azide) (3.03 g, 12.6 mmol, 1.3 equiv.). After the flask was flushed with argon gas (3 times), 50 mL of dry acetonitrile was added to the mixture for dissolving. Then, the reaction mixture was cooled to 0 °C via ice bath. DBU (1,8-diazabicyclo[5.4.0]undec-7-ene) (2.0 mL, 12.6 mmol, 1.3 equiv.) was added drop-wise at 0 °C. The mixture was allowed to stir at 0 °C for an additional 15 min, followed by 24 hours at room temperature (23 °C) after removing the ice bath. The resulting orange solution was quenched with 60 mL of saturated aqueous NH_4Cl . The aqueous layer was extracted with diethyl ether (50 mL X 3) and the combined organic layer was washed with brine. Then, it was concentrated under reduced pressure and purified by flash column chromatography (5-8% diethyl ether in hexane) to provide orange solid in 95% yield (3.1 g).

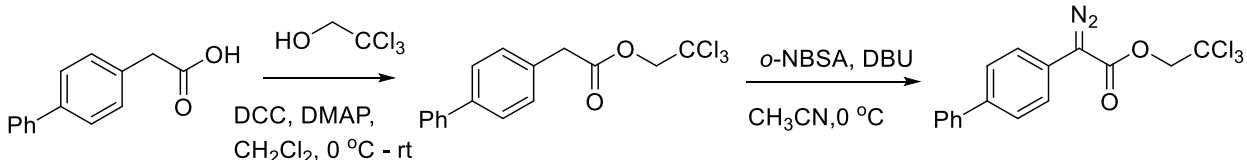
Rf = 0.20 (5% diethyl ether in hexane);

¹H NMR (500 MHz, CDCl_3) δ 7.77 (d, J = 2.3 Hz, 1H), 7.57 (d, J = 8.5 Hz, 1H), 7.25 (dd, J = 8.6, 2.3 Hz, 1H), 3.87 (s, 3H);

¹³C NMR (126 MHz, CDCl_3) δ 164.8, 133.9, 128.3, 126.9, 125.6, 123.5, 121.4, 52.4 (The resonance resulting from the diazo carbon was not observed);

IR (neat) 3091, 3005, 2952, 2092, 1702, 1470, 1358, 1238, 1196, 1160, 1049, 806, 737 cm^{-1} ;

HRMS (+p ESI) calcd for $\text{C}_9\text{H}_7\text{Br}_2\text{N}_2\text{O}_2$ ($\text{M}+\text{H}$)⁺ 332.8869 found 332.88715.



2,2,2-Trichloroethyl 2-([1,1'-biphenyl]-4-yl)-2-diazoacetate (3c)

The synthesis is adapted from literatures:¹ A dry 100 mL round-bottom flask was charged with 2-([1,1'-biphenyl]-4-yl)acetic acid (2.12g, 10 mmol, 1.0 equiv), DMAP (4-dimethylaminopyridine) (122.2 mg, 1 mmol, 0.1 equiv.) and 2,2,2-trichloroethanol (1.2 mL, 12 mmol, 1.2 equiv.). After the flask was flushed with argon gas (3 times), 20 mL of dry dichloromethane was added to the mixture. Then, the reaction mixture was cooled to 0 °C via ice bath. The solution of DCC (N,N'-dicyclohexylcarbodiimide) (2.27 g, 11 mmol, 1.1 equiv) in 20 mL of dry dichloromethane was then added slowly at 0 °C. The reaction mixture was stirred for 15 hours, at which point it was warmed up to room temperature (23 °C). The reacted mixture was filtered through Celite under reduced pressure and washed with dichloromethane. The filtrate was collected and concentrated under reduced pressure. The crude compound was purified by silica plug (3.8 cm diameter, 6 cm height, 5% ethyl acetate in hexane) to afford the white solid in 99% yield (9.9 mmol, 3.4 g). The product was used immediately in the next step.

The 2,2,2-trichloroethyl 2-([1,1'-biphenyl]-4-yl)acetate (3.4 g, 9.9 mmol, 1.0 equiv.) was added in a flame-dried round-bottom flask, together with *o*-NBSA (*o*-nitrobenzenesulfonyl azide) (3.39 g, 14.85 mmol, 1.5 equiv.). After the flask was flushed with argon gas (3 times), 30 mL of dry acetonitrile was added to the mixture for dissolving. Then, the reaction mixture was cooled to 0 °C via ice bath. DBU (1,8-diazabicyclo[5.4.0]undec-7-ene) (3.3 mL, 21.78 mmol, 2.2 equiv.) was added drop-wise at 0 °C. The mixture was allowed to stir for 1 hour at 0 °C, followed by pouring into a separation funnel with 40 mL of saturated aqueous NH₄Cl for quenching. The aqueous layer was extracted with diethyl ether (30 mL X 2) and the combined organic layer was washed with brine. Then, it was concentrated under reduced pressure and purified by flash column chromatography (5-8% dichloromethane in hexane) to provide orange solid in 82% yield.

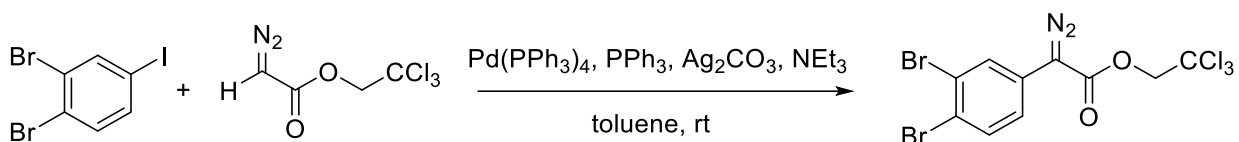
Rf = 0.50 (20% dichloromethane in hexane);

¹H NMR (500 MHz, CDCl₃) δ 7.62 (d, *J* = 8.5 Hz, 2H), 7.57 (d, *J* = 7.9 Hz, 2H), 7.54 (d, *J* = 8.5 Hz, 2H), 7.42 (t, *J* = 7.7 Hz, 2H), 7.33 (t, *J* = 7.4 Hz, 1H), 4.90 (s, 2H);

¹³C NMR (126 MHz, CDCl₃) δ 163.4, 140.2, 139.1, 129.0, 127.8, 127.6, 127.0, 124.4, 123.5, 95.1, 73.9 (The resonance resulting from the diazo carbon was not observed);

IR (neat) 3054, 3037, 2954, 2086, 1699, 1489, 1376, 1342, 1230, 1151, 1054, 760, 718, 582 cm⁻¹;

HRMS (+p APCI) calcd for C₁₆H₁₂Cl₃O₂ (M+H-N₂)⁺ 340.9897 found 340.99004.



2,2,2-Trichloroethyl 2-diazo-2-(3,4-dibromophenyl)acetate (3e)

The synthesis is adapted from literatures.² A 100-mL round-bottom flask was charged with 1,2-dibromo-4-iodobenzene (3.62 g, 10 mmol, 1.0 equiv.), Pd(PPh₃)₄ (577.8 mg, 0.5 mmol, 5 mol%), PPh₃ (262.3 mg, 1 mmol, 10 mol%) and Ag₂CO₃ (1.38 g, 5 mmol, 0.5 equiv.). After the flask was flushed with argon, 40 mL of dry toluene was added, followed by the addition of NEt₃ (1.8 mL, 13 mmol, 1.3 equiv.) and 2,2,2-trifluoroethyl 2-diazoacetate (2.18 g, 13 mmol, 1.3 equiv.). The resulted mixture was stirred at room temperature for 4 h and then, filtered through a short silica plug (3.5 cm *diameter*, 5 cm *height*), eluting with ethyl acetate (20 mL). The crude product was concentrated and purified by column chromatography (6% diethyl ether in pentane) to afford 2,2,2-trichloroethyl 2-diazo-2-(3,4-dibromophenyl)acetate as yellow solid in % yield (or 2,2,2-trifluoroethyl 2-diazo-2-(4-nitrophenyl)acetate as yellow solid in 66% yield (6.6 mmol, 3.0 g).

Rf = 0.69 (10% diethyl ether in pentane);

¹H NMR (500 MHz, CDCl₃) δ 7.80 (d, *J* = 2.3 Hz, 1H), 7.60 (d, *J* = 8.5 Hz, 1H), 7.29 – 7.21 (m, 1H), 4.91 (s, 2H);

¹³C NMR (126 MHz, CDCl₃) δ 162.6, 134.1, 128.5, 126.0, 125.8, 123.6, 122.1, 94.9, 74.1 (The resonance resulting from the diazo carbon was not observed);

IR (neat) 3098, 2954, 2094, 1711, 1469, 1372, 1340, 1273, 1234, 1139, 1046, 790, 712, 579 cm⁻¹;

HRMS (+p ESI) calcd for C₁₀H₆Br₂Cl₃N₂O₂ (M+H)⁺ 448.7856 found 448.78616.

4. C–H Insertion Reactions

4.1 General Procedures

GP-I: A 16-mL reaction vial (21x70mm) with screw cap (open top with PTFE faced silicone septum) was charged with Rh₂L₄ (0.0025 mmol, 0.5 mol%) and corresponding substrate (0.75 mmol, 1.5 equiv.). The reaction vessel was then evacuated and back filled with argon (3 times), followed by the addition of dry degassed CH₂Cl₂ (2 mL). Corresponding donor/acceptor diazo compounds (0.5 mmol, 1.0 equiv.) was weighed in a 20-mL scintillation vial and dissolved in 4 mL of dry degassed CH₂Cl₂ under argon atmosphere. Then, under room temperature (23 °C) and argon atmosphere, the diazo solution was added to the reaction vessel dropwise via syringe pump over 2 h. The reaction mixture was stirred at room temperature (23 °C) for another 4 h, and crude ¹H NMR was obtained after the resulted mixture was concentrated under vacuum. Finally, the desired product was obtained after purification using flash column chromatography with indicated eluting gradient.

GP-II: Similar to GP-II, but an additional step was added after the completion of the reaction, before the concentration for crude ¹H NMR: After the reaction mixture was stirred at room temperature (23 °C) for another 4 h, 1 mL of TFA (trichluoroacetic acid) was added to the reaction mixture slowly and stirred at room temperature (23 °C) for 15 h. The resulted mixture was concentrated under reduce pressure and dissolved in 4 mL of dichloromethane, followed by addition of aqueous saturated NaHCO₃ drop-wise until no more bubble generated (~4 mL). The aqueous layer was extracted by 10 mL dichloromethane (3 times). The combined organic layer was concentrated for crude ¹H NMR and purified using flash column chromatography with indicated eluting gradient.

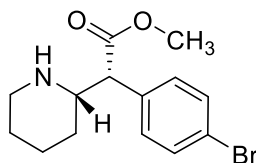
GP-III: In a round bottom flask, *tert*-butyl pyridine-1(4H)-carboxylate (91 mg, 0.5 mmol, 1.5 equiv.) and 2.5 mol% rhodium catalyst were dissolved in 5 mL dry solvent. Methyl 2-diazo-2-phenylacetate (59 mg, 0.333 mmol, 1 equiv.) was dissolved in 4 mL of the corresponding dry solvent and added within 2 h using a syringe pump. After addition, the reaction mixture was stirred for 30 min and the solvent was evaporated under reduced pressure.

GP-IV: In a round bottom flask, *tert*-butyl pyridine-1(4H)-carboxylate (91 mg, 0.5 mmol, 1.5 equiv.) and 2.5 mol% rhodium catalyst were dissolved in 5 mL dry pentane and stirred for 1 min. Methyl 2-diazo-2-phenylacetate (59 mg, 0.333 mmol, 1 equiv.) dissolved in 5 mL dry pentane was added to the mixture. The solvent was removed under reduced pressure and high vacuum was applied under stirring. After complete removal of the solvent the reaction starts under high vacuum conditions. With progressive conversion, the viscosity of the mixture increased. For better homogeneity solvent was added, the mixture was stirred for 1 min and the solvent was removed again before applying high vacuum. This was repeated for 2 times. The reaction is completed when gas formation stops. The crude product was purified by FC (EA/HEX: 2-10% EA gradient). As the product is decomposing under normal conditions complete analysis of the compound was not carried out. Enantiomeric excess was measured after hydrogenation of the 1,4-dihydropyridine.

4.2. Regioisomer and Diastereomer Ratios Determination

The crude ¹H NMR spectra in general procedures were utilized for regioisomer and diastereomer ratios determination, and it was obtained using Bruker-600 MHz spectrometer with a Prodigy probe, and the acquisition was done with 16 times of scans and 1 seconds of relaxation time.

4.3. Characterization Data of C–H Functionalization Products



Methyl (R)-2-(4-bromophenyl)-2-((S)-piperidin-2-yl)acetate (4a-*erythro*)

Following *GP-II* (*tert*-butyl piperidine-1-carboxylate as substrate, reacting with methyl 2-(4-bromophenyl)-2-diazoacetate), the desired C2-product (mixture of both diastereomers) was obtained using 0–4% methanol in dichloromethane as eluting gradient in flash column chromatography.

Characterization data for the *erythro*-diastereomer was conducted on sample obtained in Rh₂(S-2-Cl-5-BrTPCP)₄-catalyzed reaction (83% ee).

Yellow oil

Rf = 0.36 (5% methanol in dichloromethane);

[α]²⁰_D: +22.2° (c = 0.45, CHCl₃, 83% ee);

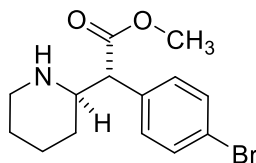
¹H NMR (500 MHz, CDCl₃) δ 7.47 (d, *J* = 8.4 Hz, 2H), 7.29 (d, *J* = 8.4 Hz, 2H), 3.66 (s, 3H), 3.43 (d, *J* = 10.0 Hz, 1H), 3.06 (td, *J* = 10.2, 2.3 Hz, 1H), 2.93 (d, *J* = 11.7 Hz, 1H), 2.50 (td, *J* = 11.5, 2.9 Hz, 1H), 1.88 – 1.70 (m, 2H), 1.61 – 1.54 (m, 1H), 1.46 – 1.33 (m, 2H), 1.30 – 1.17 (m, 1H);

¹³C NMR (126 MHz, CDCl₃) δ 172.8, 135.2, 132.1, 130.5, 122.1, 59.1, 57.9, 52.2, 47.2, 31.2, 25.9, 24.6;

IR (neat) 2934, 2854, 1734, 1488, 1435, 1331, 1161, 1119, 1011, 763 cm⁻¹;

HRMS (+p APCI) calcd for C₁₄H₁₉BrNO₂ (M+H)⁺ 312.0594 found 312.05941;

HPLC (ODH column, 1% *i*-propanol in hexane, 0.5 mL min⁻¹, 1 mg mL⁻¹, 30 min, UV 230 nm) retention times of 11.17 min (major) and 12.59 min (minor) 83% ee with Rh₂(S-2-Cl-5-BrTPCP)₄.



Methyl 2-(4-bromophenyl)-2-(piperidin-2-yl)acetate (4a-*threo*)

Characterization data for the *threo*-diastereomer was conducted on sample obtained in Rh₂(*R*-DOSP)₄-catalyzed reaction (ee not determined).

Yellow oil

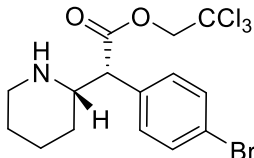
Rf = 0.32 (5% methanol in dichloromethane);

¹H NMR (500 MHz, CDCl₃) δ 7.44 (d, *J* = 8.4 Hz, 2H), 7.17 (d, *J* = 8.4 Hz, 2H), 3.65 (s, 3H), 3.41 (d, *J* = 10.0 Hz, 1H), 3.08 (td, *J* = 10.4, 2.6 Hz, 2H), 2.68 (td, *J* = 11.9, 2.7 Hz, 1H), 2.01 (s, broad, 1H), 1.75 – 1.65 (m, 1H), 1.64 – 1.52 (m, 1H), 1.37 (qt, *J* = 12.4, 3.9 Hz, 1H), 1.29 – 1.19 (m, 2H), 1.01 – 1.87 (m, 1H);

¹³C NMR (126 MHz, CDCl₃) δ 173.4, 135.4, 131.8, 130.2, 121.6, 58.8, 58.1, 52.1, 46.9, 30.0, 26.1, 24.3;

IR (neat) 2931, 2853, 1731, 1489, 1434, 1196, 1163, 1012, 824, 765 cm⁻¹;

HRMS (+p APCI) calcd for C₁₄H₁₉BrNO₂ (M+H)⁺ 312.0594 found 312.05945;



2,2,2-Trichloroethyl (*R*)-2-(4-bromophenyl)-2-((*S*)-piperidin-2-yl)acetate (5a-*erythro***)**

Following *GP-II* (*tert*-butyl piperidine-1-carboxylate as substrate, reacting 2,2,2-trichloroethyl 2-(4-bromophenyl)-2-diazoacetate), the desired C2-product (mixture of both diastereomers) was obtained using 0–4% methanol in dichloromethane as eluting gradient in flash column chromatography.

Characterization data for the *erythro*-diastereomer was conducted on sample obtained in Rh₂(*R*-TCPTAD)₄-catalyzed reaction (93% ee).

Yellow oil

Rf = 0.36 (5% methanol in dichloromethane);

[α]²⁰_D: -2.8° (c = 1.00, CHCl₃, 93% ee);

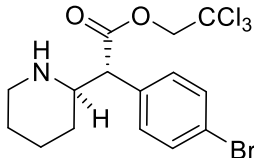
¹H NMR (500 MHz, CDCl₃) δ 7.49 (d, *J* = 8.4 Hz, 2H), 7.32 (d, *J* = 8.4 Hz, 2H), 4.76 (d, *J* = 12.0 Hz, 1H), 4.66 (d, *J* = 12.0 Hz, 1H), 3.58 (d, *J* = 10.0 Hz, 1H), 3.15 (td, *J* = 10.1, 2.2 Hz, 1H), 2.96 (d, *J* = 11.5 Hz, 1H), 2.53 (td, *J* = 11.4, 2.7 Hz, 1H), 1.90 – 1.74 (m, 2H), 1.63 – 1.54 (m, 1H), 1.47 – 1.34 (m, 2H), 1.33 – 1.25 (m, 1H);

¹³C NMR (126 MHz, CDCl₃) δ 170.5, 134.3, 132.2, 130.7, 122.5, 94.8, 74.2, 58.7, 57.9, 47.1, 31.1, 25.9, 24.5;

IR (neat) 2935, 2855, 1749, 1488, 1452, 1139, 1116, 1073, 1012, 761, 722 cm⁻¹;

HRMS (+p APCI) calcd for C₁₅H₁₈BrCl₃NO₂ (M+H)⁺ 427.9581 found 427.95886;

HPLC (ODH column, 0.5% *i*-propanol in hexane, 0.35 mL min⁻¹, 1 mg mL⁻¹, 60 min, UV 230 nm) retention times of 26.84 min (major) and 28.93 min (minor) 93% ee with Rh₂(*R*-TCPTAD)₄.



2,2,2-Trichloroethyl 2-(4-bromophenyl)-2-(piperidin-2-yl)acetate (5a-*threo***)**

Characterization data for the *threo*-diastereomer was conducted on sample obtained in Rh₂(*R*-DOSP)₄-catalyzed reaction (ee not determined).

Yellow oil

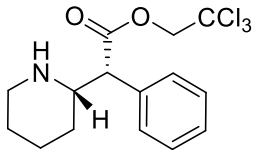
Rf = 0.29 (5% methanol in dichloromethane);

¹H NMR (500 MHz, CDCl₃) δ 7.46 (d, *J* = 8.6 Hz, 2H), 7.22 (d, *J* = 8.1 Hz, 2H), 4.72 (s, 2H), 3.56 (d, *J* = 10.1 Hz, 1H), 3.18 (td, *J* = 10.5, 2.6 Hz, 1H), 3.08 (d, *J* = 12.3 Hz, 1H), 2.69 (td, *J* = 11.9, 2.8 Hz, 1H), 1.80 – 1.66 (m, 1H), 1.59 (d, *J* = 12.9 Hz, 1H), 1.44 – 1.18 (m, 3H), 0.96 (qd, *J* = 12.2, 3.6 Hz, 1H);

¹³C NMR (126 MHz, CDCl₃) δ 171.4, 134.7, 132.0, 130.6, 122.0, 94.8, 74.3, 58.9, 58.2, 46.9, 30.2, 26.4, 24.4;

IR (neat) 2936, 2922, 2857, 1652, 1568, 1380, 1013, 763, 724, 529 cm⁻¹;

HRMS (+p APCI) calcd for C₁₅H₁₈BrCl₃NO₂ (M+H)⁺ 427.9581 found 427.95871;



2,2,2-Trichloroethyl (*R*)-2-phenyl-2-((*S*)-piperidin-2-yl)acetate (5b-*erythro***)**

Following *GP-II* (*tert*-butyl piperidine-1-carboxylate as substrate, reacting 2,2,2-trichloroethyl 2-diazo-2-phenylacetate), the desired C2-product (mixture of both diastereomers) was obtained using 0-4% methanol in dichloromethane as eluting gradient in flash column chromatography.

Characterization data for the *erythro*-diastereomer was conducted on sample obtained in Rh₂(*R*-TCPTAD)₄-catalyzed reaction (73% ee).

Yellow oil

Rf = 0.30 (5% methanol in dichloromethane);

[\alpha]²⁰_D: +6.4° (c = 1.00, CHCl₃, 73% ee);

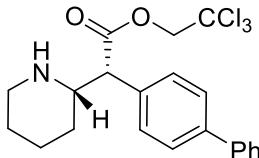
¹H NMR (500 MHz, CDCl₃) δ 7.49 – 7.41 (m, 2H), 7.39 – 7.28 (m, 3H), 4.76 (d, *J* = 12.0 Hz, 1H), 4.65 (d, *J* = 12.0 Hz, 1H), 3.61 (d, *J* = 10.2 Hz, 1H), 3.19 (td, *J* = 10.2, 2.4 Hz, 1H), 2.94 (d, *J* = 11.5 Hz, 1H), 2.53 (td, *J* = 11.5, 2.8 Hz, 1H), 1.88 (d, *J* = 14.2 Hz, 1H), 1.82 (d, *J* = 13.7 Hz, 1H), 1.62 – 1.56 (m, 1H), 1.50 – 1.36 (m, 2H), 1.36 – 1.26 (m, 1H);

¹³C NMR (126 MHz, CDCl₃) δ 170.9, 135.3, 129.1, 129.0, 128.3, 94.9, 74.2, 58.7, 58.5, 47.1, 31.2, 25.9, 24.5;

IR (neat) 2934, 2854, 1748, 1454, 1332, 1289, 1138, 1115, 774, 718, 699 cm⁻¹;

HRMS (+p APCI) calcd for C₁₅H₁₉Cl₃NO₂ (M+H)⁺ 350.0476. found 350.04780;

HPLC (ODH column, 1% *i*-propanol in hexane, 1 mL min⁻¹, 1 mg mL⁻¹, 30 min, UV 230 nm) retention times of 5.41 min (minor) and 5.94 min (major) 73% ee with Rh₂(*R*-TCPTAD)₄.



2,2,2-Trichloroethyl (*R*)-2-([1,1'-biphenyl]-4-yl)-2-((*S*)-piperidin-2-yl)acetate (5c-erythro**)**

Following *GP-II* (*tert*-butyl piperidine-1-carboxylate as substrate, reacting 2,2,2-trichloroethyl 2-([1,1'-biphenyl]-4-yl)-2-diazoacetate), the desired C2-product (mixture of both diastereomers) was obtained using 0-4% methanol in dichloromethane as eluting gradient in flash column chromatography.

Characterization data for the *erythro*-diastereomer was conducted on sample obtained in Rh₂(*R*-TCPTAD)₄-catalyzed reaction (61% ee).

Yellow oil

Rf = 0.36 (5% methanol in dichloromethane);

[α]²⁰_D: -4.3° (c = 0.91, CHCl₃, 61% ee);

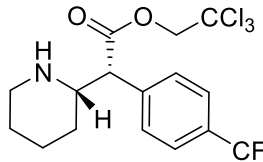
¹H NMR (500 MHz, CDCl₃) δ 7.62 – 7.56 (m, 4H), 7.51 (d, *J* = 8.3 Hz, 2H), 7.44 (t, *J* = 7.6 Hz, 2H), 7.39 – 7.32 (m, 1H), 4.80 (d, *J* = 12.0 Hz, 1H), 4.66 (d, *J* = 12.0 Hz, 1H), 3.65 (d, *J* = 10.1 Hz, 1H), 3.23 (td, *J* = 10.1, 2.4 Hz, 1H), 2.97 (d, *J* = 11.6 Hz, 1H), 2.56 (td, *J* = 11.5, 2.8 Hz, 1H), 1.97 – 1.86 (m, 1H), 1.86 – 1.81 (m, 1H), 1.65 – 1.56 (m, 1H), 1.53 – 1.39 (m, 2H), 1.39 – 1.28 (m, 1H);

¹³C NMR (126 MHz, CDCl₃) δ 170.9, 141.2, 140.6, 134.3, 129.4, 129.0, 127.8, 127.6, 127.2, 94.9, 74.3, 58.8, 58.2, 47.2, 31.3, 26.0, 24.6;

IR (neat) 3030, 2935, 2854, 1749, 1487, 1451, 1331, 1139, 1117, 776, 741, 725, 698 cm⁻¹;

HRMS (+p APCI) calcd for C₂₁H₂₂Cl₃NO₂ (M+H)⁺ 426.0789 found 426.07943;

HPLC (obtained on its 2,2,2-trifluoroacetamide derivative) (ADH column, 3% *i*-propanol in hexane, 1 mL min⁻¹, 1 mg mL⁻¹, 40 min, UV 230 nm) retention times of 23.99 min (major) and 27.95 min (minor) 61% ee with Rh₂(*R*-TCPTAD)₄.



2,2,2-Trichloroethyl (*R*)-2-((*S*)-piperidin-2-yl)-2-(4-(trifluoromethyl)phenyl)acetate (5d-*erythro***)**

Following *GP-II* (*tert*-butyl piperidine-1-carboxylate as substrate, reacting 2,2,2-trichloroethyl 2-diazo-2-(4-(trifluoromethyl)phenyl)acetate), the desired C2-product (mixture of both diastereomers) was obtained using 0-4% methanol in dichloromethane as eluting gradient in flash column chromatography.

Characterization data for the *erythro*-diastereomer was conducted on sample obtained in Rh₂(*R*-TCPTAD)₄-catalyzed reaction (37% ee).

White solid:

Rf = 0.40 (5% methanol in dichloromethane);

[α]²⁰_D: +1.7° (c = 0.91, CHCl₃, 37% ee);

¹H NMR (500 MHz, CDCl₃) δ 7.63 (d, *J* = 8.7 Hz, 2H), 7.58 (d, *J* = 8.2 Hz, 2H), 4.77 (d, *J* = 12.0 Hz, 1H), 4.66 (d, *J* = 11.9 Hz, 1H), 3.69 (d, *J* = 9.9 Hz, 1H), 3.22 (td, *J* = 10.0, 2.4 Hz, 1H), 2.96 (d, *J* = 12.8 Hz, 1H), 2.54 (td, *J* = 11.5, 2.9 Hz, 1H), 1.92 – 1.77 (m, 2H), 1.65 – 1.54 (m, 1H), 1.48 – 1.36 (m, 2H), 1.35 – 1.26 (m, 1H);

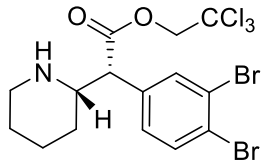
¹³C NMR (126 MHz, CDCl₃) δ 170.3, 139.4, 130.6 (q, *J* = 32.6 Hz), 129.5, 126.0 (q, *J* = 3.8 Hz), 124.1 (q, *J* = 272.2 Hz), 94.7, 74.3, 58.8, 58.3, 47.1, 31.1, 25.9, 24.5;

¹⁹F NMR (282 MHz, CDCl₃) δ -62.67;

IR (neat) 2938, 2957, 1750, 1324, 1164, 1117, 1068, 1019, 846, 758, 718, 601, 571 cm⁻¹;

HRMS (+p APCI) calcd for C₁₆H₁₈Cl₃F₃NO₂ (M+H)⁺ 418.0350 found 418.03508;

HPLC (ODH column, 0.5% *i*-propanol in hexane, 1.5 mL min⁻¹, 1 mg mL⁻¹, 30 min, UV 230 nm) retention times of 3.84 min (major) and 4.58 min (minor) 37% ee with Rh₂(*R*-TCPTAD)₄.



2,2,2-Trichloroethyl (*R*)-2-(3,4-dibromophenyl)-2-((*S*)-piperidin-2-yl)acetate (5e-erythro**)**

Following *GP-II* (*tert*-butyl piperidine-1-carboxylate as substrate, reacting 2,2,2-trichloroethyl 2-diazo-2-(3,4-dibromophenyl)acetate), the desired C2-product (mixture of both diastereomers) was obtained using 0-4% methanol in dichloromethane as eluting gradient in flash column chromatography.

Characterization data for the *erythro*-diastereomer was conducted on sample obtained in Rh₂(*R*-TCPTAD)₄-catalyzed reaction (37% ee).

Yellow oil

Rf = 0.43 (5% methanol in dichloromethane);

[α]²⁰_D: -4.3° (c = 1.00, CHCl₃, 29% ee);

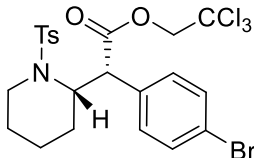
¹H NMR (500 MHz, CDCl₃) δ 7.73 (d, *J* = 2.1 Hz, 1H), 7.60 (d, *J* = 8.2 Hz, 1H), 7.26 (dd, *J* = 8.4, 2.3 Hz, 1H), 4.79 (d, *J* = 12.0 Hz, 1H), 4.65 (d, *J* = 11.9 Hz, 1H), 3.55 (d, *J* = 9.8 Hz, 1H), 3.13 (td, *J* = 10.1, 2.3 Hz, 1H), 2.97 (d, *J* = 11.8 Hz, 1H), 2.55 (td, *J* = 11.6, 2.9 Hz, 1H), 1.87 – 1.78 (m, 2H), 1.65 – 1.58 (m, 1H), 1.46 – 1.32 (m, 2H), 1.32 – 1.23 (m, 1H);

¹³C NMR (126 MHz, CDCl₃) δ 170.0, 136.3, 134.1, 134.1, 129.2, 125.5, 124.8, 94.7, 74.3, 58.7, 57.6, 47.0, 31.1, 25.8, 24.4;

IR (neat) 2936, 2855, 1747, 1461, 1139, 1113, 1014, 907, 727, 571 cm⁻¹;

HRMS (+p APCI) calcd for C₁₅H₁₇Br₂Cl₃NO₂ (M+H)⁺ 505.8686 found 505.86927;

HPLC (ODH column, 0.5% *i*-propanol in hexane, 1 mL min⁻¹, 1 mg mL⁻¹, 30 min, UV 230 nm) retention times of 7.69 min (major) and 8.32 min (minor) 29% ee with Rh₂(*R*-TCPTAD)₄.



2,2,2-Trichloroethyl (*R*)-2-(4-bromophenyl)-2-((*S*)-1-tosylpiperidin-2-yl)acetate

Following *GP-I* (1-tosylpiperidine as substrate, reacting 2,2,2-trichloroethyl 2-(4-bromophenyl)-2-diazoacetate), the desired C2-product was obtained using 0-12% ethyl acetate in hexane as eluting gradient in flash column chromatography (a 2nd column with 35-100% dichloromethane in hexane was conducted if the product is not pure enough).

Characterization data for the *erythro*-diastereomer was conducted on sample obtained in Rh₂(*R*-TPPTTL)₄-catalyzed reaction (76% ee).

White solid: **m.p.** 131-133 °C

Rf = 0.45 (20% ethyl acetate in hexane);

[α]²⁰_D: +24.9° (c = 1.00, CHCl₃, 76% ee);

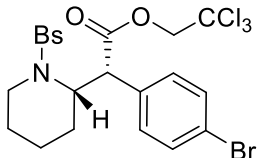
¹H NMR (600 MHz, CDCl₃) δ 7.35 (d, *J* = 8.5 Hz, 2H), 7.23 (d, *J* = 8.5 Hz, 2H), 7.17 (d, *J* = 8.3 Hz, 2H), 7.11 (d, *J* = 8.0 Hz, 2H), 4.88 (dd, *J* = 11.6, 4.5 Hz, 1H), 4.84 (d, *J* = 12.0 Hz, 1H), 4.58 (d, *J* = 12.0 Hz, 1H), 4.22 (d, *J* = 11.7 Hz, 1H), 3.55 (d, *J* = 15.1 Hz, 1H), 2.92 – 2.82 (m, 1H), 2.40 (s, 3H), 1.88 – 1.80 (m, 1H), 1.80 – 1.66 (m, 3H), 1.54 – 1.46 (m, 2H).;

¹³C NMR (151 MHz, CDCl₃) δ 170.2, 143.2, 137.6, 134.0, 131.9, 130.5, 129.5, 127.2, 122.5, 94.6, 74.4, 54.5, 50.8, 41.3, 27.3, 24.2, 21.7, 18.9;

IR (neat) 2945, 2869, 1750, 1489, 1338, 1325, 1294, 1155, 1092, 932, 908, 816, 767, 718, 657, 552 cm⁻¹;

HRMS (+p APCI) calcd for C₂₂H₂₄BrCl₃SNO₄ (M+H)⁺ 581.9670 found 581.96713;

HPLC (ADH column, 5% *i*-propanol in hexane, 0.5 mL min⁻¹, 1 mg mL⁻¹, 80 min, UV 230 nm) retention times of 40.94 min (major) and 55.33 min (minor) 76% ee with Rh₂(*R*-TPPTTL)₄.



2,2,2-Trichloroethyl (R)-2-(4-bromophenyl)-2-((S)-1-((4-bromophenyl)sulfonyl)piperidin-2-yl)acetate (6a)

Following *GP-I* (1-((4-bromophenyl)sulfonyl)piperidine as substrate, reacting 2,2,2-trichloroethyl 2-(4-bromophenyl)-2-diazoacetate), the desired C2-product was obtained using 0-12% ethyl acetate in hexane as eluting gradient in flash column chromatography (a 2nd column with 35-100% dichloromethane in hexane was conducted if the product is not pure enough).

Characterization data for the *erythro*-diastereomer was conducted on sample obtained in Rh₂(*R*-TCPTAD)₄-catalyzed reaction (97% ee).

White solid: **m.p.** 159-161 °C

Rf = 0.44 (20% ethyl acetate in hexane);

[α]²⁰_D: +29.4° (c = 1.00, CHCl₃, 97% ee);

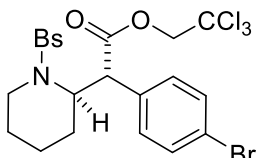
¹H NMR (600 MHz, CDCl₃) δ 7.45 (d, *J* = 8.6 Hz, 2H), 7.38 (d, *J* = 8.5 Hz, 2H), 7.23 (d, *J* = 8.5 Hz, 2H), 7.11 (d, *J* = 8.6 Hz, 2H), 4.90 – 4.80 (m, 2H), 4.59 (d, *J* = 12.0 Hz, 1H), 4.21 (d, *J* = 11.8 Hz, 1H), 3.58 – 3.47 (m, 1H), 2.90 (ddd, *J* = 14.8, 12.5, 3.6 Hz, 1H), 1.89 – 1.80 (m, 1H), 1.81 – 1.67 (m, 3H), 1.60 – 1.50 (m, 2H);

¹³C NMR (151 MHz, CDCl₃) δ 169.9, 139.3, 133.8, 132.1, 131.9, 130.3, 128.6, 127.3, 122.5, 94.4, 74.3, 54.7, 50.5, 41.3, 27.3, 24.1, 18.7;

IR (**neat**) 2946, 2869, 1751, 1489, 1327, 1158, 1011, 933, 822, 768, 755, 609 cm⁻¹;

HRMS (+p APCI) calcd for C₂₁H₂₁Br₂Cl₃SNO₄ (M+H)⁺ 645.8618 found 645.86216;

HPLC (ADH column, 5% *i*-propanol in hexane, 0.5 mL min⁻¹, 1 mg mL⁻¹, 80 min, UV 230 nm) retention times of 44.54 min (major) and 66.29 min (minor) 97% ee with Rh₂(*R*-TCPTAD)₄.



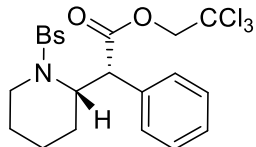
2,2,2-Trichloroethyl 2-(4-bromophenyl)-2-(1-((4-bromophenyl)sulfonyl)piperidin-2-yl)acetate

Characterization data for the *threo*-diastereomer was conducted on sample obtained in Rh₂(*R*-TCPTAD)₄-catalyzed reaction (ee not determined).

White solid, **Rf** = 0.45 (20% ethyl acetate in hexane);

¹H NMR (600 MHz, CDCl₃) δ 7.73 (d, *J* = 8.8 Hz, 2H), 7.65 (d, *J* = 8.6 Hz, 2H), 7.50 (d, *J* = 8.6 Hz, 2H), 7.37 (d, *J* = 8.5 Hz, 2H), 4.79 (dd, *J* = 11.6, 4.7 Hz, 1H), 4.58 (d, *J* = 11.9 Hz, 1H), 4.45 (d, *J* = 11.9 Hz, 1H), 4.25 (d, *J* = 11.7 Hz, 1H), 3.80 (dd, *J* = 15.0, 4.7 Hz, 1H), 3.36 – 3.23 (m, 1H), 1.60 – 1.41 (m, 3H), 1.38 – 1.27 (m, 2H), 1.24 – 1.18 (m, 1H);

¹³C NMR (151 MHz, CDCl₃) δ 169.7, 140.4, 133.4, 132.3, 132.2, 130.5, 128.8, 127.5, 122.6, 94.4, 74.5, 56.0, 50.8, 41.4, 24.5, 23.7, 18.0.



2,2,2-Trichloroethyl (R)-2-((S)-1-((4-bromophenyl)sulfonyl)piperidin-2-yl)-2-phenylacetate (6b)

Following *GP-I* (1-((4-bromophenyl)sulfonyl)piperidine as substrate, reacting 2,2,2-trichloroethyl 2-diazo-2-phenylacetate) with reaction under reflux dichloromethane (39 °C), the desired C2-product was obtained using 0-12% ethyl acetate in hexane as eluting gradient in flash column chromatography (a 2nd column with 35-100% dichloromethane in hexane was conducted if the product is not pure enough).

Characterization data for the *erythro*-diastereomer was conducted on sample obtained in Rh₂(*R*-TPPTTL)₄-catalyzed reaction (52% ee).

White solid: **m.p.** 146-148 °C

Rf = 0.48 (20% ethyl acetate in hexane);

[α]²⁰_D: +9.9° (c = 1.00, CHCl₃, 52% ee);

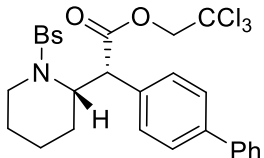
¹H NMR (600 MHz, CDCl₃) δ 7.38 (d, *J* = 7.4 Hz, 2H), 7.33 (dd, *J* = 11.9, 7.8 Hz, 3H), 7.29 (d, *J* = 7.7 Hz, 2H), 7.00 (d, *J* = 8.4 Hz, 2H), 4.97 (dd, *J* = 11.9, 4.7 Hz, 1H), 4.86 (d, *J* = 11.9 Hz, 1H), 4.58 (d, *J* = 12.0 Hz, 1H), 4.26 (d, *J* = 11.7 Hz, 1H), 3.40 (d, *J* = 14.5, 1H), 2.96 – 2.87 (m, 1H), 1.92 – 1.70 (m, 4H), 1.61 – 1.53 (m, 2H);

¹³C NMR (151 MHz, CDCl₃) δ 170.4, 139.4, 135.0, 132.1, 129.0, 128.9, 128.3, 127.1, 94.7, 74.3, 54.6, 51.2, 41.3, 27.6, 24.2, 18.8;

IR (neat) 2947, 2868, 1749, 1575, 1470, 1455, 1319, 1287, 1156, 1089, 1067, 1010, 934, 907, 761 cm⁻¹;

HRMS (+p APCI) calcd for C₂₁H₂₂BrCl₃SNO₄ (M+H)⁺ 567.9513 found 567.95184;

HPLC (ODH column, 2% *i*-propanol in hexane, 0.6 mL min⁻¹, 1 mg mL⁻¹, 60 min, UV 230 nm) retention times of 39.84 min (minor) and 44.79 min (major) 52% ee with Rh₂(*R*-TPPTTL)₄.



2,2,2-Trichloroethyl (R)-2-((1,1'-biphenyl)-4-yl)-2-((S)-1-((4-bromophenyl)sulfonyl)piperidin-2-yl)acetate (6c)

Following *GP-I* (1-((4-bromophenyl)sulfonyl)piperidine as substrate, reacting 2,2,2-trichloroethyl 2-((1,1'-biphenyl)-4-yl)-2-diazoacetate) with reaction under reflux dichloromethane (39 °C), the desired C2-product was obtained using 0-12% ethyl acetate in hexane as eluting gradient in flash column chromatography (a 2nd column with 35-100% dichloromethane in hexane was conducted if the product is not pure enough).

Characterization data for the *erythro*-diastereomer was conducted on sample obtained in $\text{Rh}_2(\text{R-TPPTTL})_4$ -catalyzed reaction (62% ee).

White solid: **m.p.** 52–54 °C

Rf = 0.46 (20% ethyl acetate in hexane);

$[\alpha]^{20}_{\text{D}}$: +31.3° (c = 1.00, CHCl_3 , 62% ee);

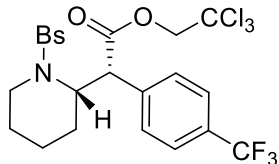
$^1\text{H NMR}$ (600 MHz, CDCl_3) δ 7.60 (dd, J = 8.3, 1.2 Hz, 2H), 7.51 (d, J = 8.4 Hz, 2H), 7.47 (t, J = 7.7 Hz, 2H), 7.43 (d, J = 8.3 Hz, 2H), 7.38 (tt, J = 6.9, 1.2 Hz, 1H), 7.27 (d, J = 8.7 Hz, 2H), 7.04 (d, J = 8.7 Hz, 2H), 4.99 (dd, J = 11.8, 4.8 Hz, 1H), 4.89 (d, J = 12.0 Hz, 1H), 4.59 (d, J = 12.0 Hz, 1H), 4.31 (d, J = 11.8 Hz, 1H), 3.50 – 3.43 (m, 1H), 2.95 (ddd, J = 14.7, 12.2, 3.8 Hz, 1H), 1.97 – 1.88 (m, 1H), 1.87 – 1.74 (m, 3H), 1.68 – 1.57 (m, 2H);

$^{13}\text{C NMR}$ (151 MHz, CDCl_3) δ 170.4, 141.3, 140.2, 139.4, 134.0, 132.0, 129.3, 129.1, 128.9, 127.8, 127.5, 127.1, 127.1, 94.7, 74.4, 54.6, 50.9, 41.4, 27.7, 24.4, 18.9;

IR (neat) 3031, 2947, 2868, 1749, 1575, 1487, 1326, 1156, 1089, 1068, 1009, 933, 908, 760, 729 cm^{-1} ;

HRMS (+p APCI) calcd for $\text{C}_{27}\text{H}_{26}\text{BrCl}_3\text{SNO}_4$ ($\text{M}+\text{H}$)⁺ 643.9826 found 643.98294;

HPLC (R,R-Whelk column, 10% *i*-propanol in hexane, 1 mL min^{-1} , 1 mg mL^{-1} , 60 min, UV 230 nm) retention times of 41.77 min (minor) and 45.52 min (major) 62% ee with $\text{Rh}_2(\text{R-TPPTTL})_4$.



**2,2,2-Trichloroethyl
(trifluoromethyl)phenyl)acetate (6d)**

(R)-2-((S)-1-((4-bromophenyl)sulfonyl)piperidin-2-yl)-2-(4-

Following *GP-I* (1-((4-bromophenyl)sulfonyl)piperidine as substrate, reacting 2,2,2-trichloroethyl 2-diazo-2-(4-(trifluoromethyl)phenyl)acetate), the desired C2-product was obtained using 0-12% ethyl acetate in hexane as eluting gradient in flash column chromatography (a 2nd column with 35-100% dichloromethane in hexane was conducted if the product is not pure enough).

Characterization data for the *erythro*-diastereomer was conducted on sample obtained in Rh₂(*R*-TPPTTL)₄-catalyzed reaction (74% ee).

White solid: **m.p.** 119-121 °C

Rf = 0.43 (20% ethyl acetate in hexane);

[α]²⁰_D: +11.8° (c = 1.00, CHCl₃, 74% ee);

¹H NMR (600 MHz, CDCl₃) δ 7.55 (d, *J* = 8.3 Hz, 2H), 7.51 (d, *J* = 8.3 Hz, 2H), 7.41 (d, *J* = 8.7 Hz, 2H), 7.11 (d, *J* = 8.6 Hz, 2H), 4.95 (dd, *J* = 11.8, 4.7 Hz, 1H), 4.85 (d, *J* = 12.0 Hz, 1H), 4.60 (d, *J* = 12.0 Hz, 1H), 4.33 (d, *J* = 11.7 Hz, 1H), 3.54 – 3.46 (m, 1H), 2.90 (ddd, *J* = 14.9, 12.8, 3.4 Hz, 1H), 1.89 – 1.81 (m 1H), 1.80 – 1.71 (m, 3H), 1.59 – 1.49 (m, 2H);

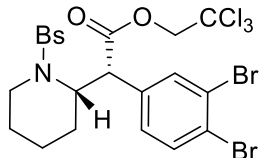
¹³C NMR (151 MHz, CDCl₃) δ 169.6, 139.2, 138.7, 132.1, 130.6 (q, *J* = 32.6 Hz), 129.2, 128.6, 127.4, 125.7 (q, *J* = 3.8 Hz), 123.9 (q, *J* = 272.2 Hz), 94.4, 74.3, 54.5, 51.0, 41.3, 27.1, 23.9, 18.6;

¹⁹F NMR (282 MHz, CDCl₃) δ -62.45;

IR (neat) 2948, 2870, 1750, 1575, 1322, 1291, 1156, 1122, 1068, 907, 829, 766, 752, 730, 609, 535 cm⁻¹;

HRMS (+p APCI) calcd for C₂₂H₂₁BrCl₃F₃SNO₄ (M+H)⁺ 635.9387 found 635.93908;

HPLC (ADH column, 5% *i*-propanol in hexane, 1 mL min⁻¹, 1 mg mL⁻¹, 40 min, UV 230 nm) retention times of 26.67 min (major) and 29.89 min (minor) 74% ee with Rh₂(*R*-TPPTTL)₄.



**2,2,2-Trichloroethyl
dibromophenyl)acetate (6e)**

(*R*)-2-((*S*)-1-((4-bromophenyl)sulfonyl)piperidin-2-yl)-2-(3,4-

Following *GP-I* (1-((4-bromophenyl)sulfonyl)piperidine as substrate, reacting 2,2,2-trichloroethyl 2-diazo-2-(3,4-dibromophenyl)acetate), the desired C2-product was obtained using 0-12% ethyl acetate in hexane as eluting gradient in flash column chromatography (a 2nd column with 35-100% dichloromethane in hexane was conducted if the product is not pure enough).

Characterization data for the *erythro*-diastereomer was conducted on sample obtained in Rh₂(*R*-TPPTTL)₄-catalyzed reaction (67% ee).

White solid: **m.p.** 134-136 °C

Rf = 0.40 (20% ethyl acetate in hexane);

[α]²⁰_D: +11.4° (c = 1.00, CHCl₃, 67% ee);

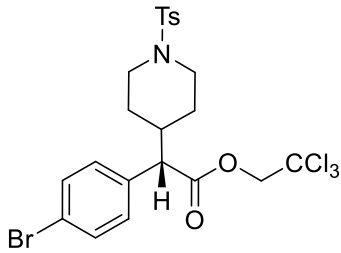
¹H NMR (600 MHz, CDCl₃) δ 7.59 (d, *J* = 2.2 Hz, 1H), 7.50 – 7.42 (m, 3H), 7.22 – 7.17 (m, 3H), 4.88 (d, *J* = 11.9 Hz, 1H), 4.81 (dd, *J* = 11.7, 4.7 Hz, 1H), 4.58 (d, *J* = 12.0 Hz, 1H), 4.18 (d, *J* = 11.7 Hz, 1H), 3.68 – 3.61 (m, 1H), 2.92 (ddd, *J* = 14.7, 13.0, 3.0 Hz, 1H), 1.87 – 1.79 (m, 1H), 1.77 – 1.70 (m, 3H), 1.63 – 1.56 (m, 1H), 1.54 – 1.46 (m, 1H);

¹³C NMR (151 MHz, CDCl₃) δ 169.4, 139.5, 135.5, 133.8, 133.8, 132.1, 128.6, 128.2, 127.4, 125.1, 124.9, 94.3, 74.3, 55.0, 50.2, 41.4, 27.3, 24.2, 18.6;

IR (neat) 2945, 2869, 1749, 1575, 1464, 1326, 1155, 1089, 1068, 1010, 908, 821, 764, 729, 609 cm⁻¹;

HRMS (+p APCI) calcd for C₂₁H₂₀Br₃Cl₃SNO₄ (M+H)⁺ 723.7723 found 723.77275;

HPLC (ADH column, 5% *i*-propanol in hexane, 1 mL min⁻¹, 1 mg mL⁻¹, 60 min, UV 230 nm) retention times of 28.28 min (major) and 37.17 min (minor) 67% ee with Rh₂(*R*-TPPTTL)₄.



2,2,2-Trichloroethyl (S)-2-(4-bromophenyl)-2-(1-tosylpiperidin-4-yl)acetate (13b)

Following GP-I (1-tosylpiperidine as substrate, reacting 2,2,2-trichloroethyl 2-(4-bromophenyl)-2-diazoacetate, Rh₂(S-2-Cl-5-BrTPCP)₄ as catalyst), the desired C4-product was obtained using 0-10% ethyl acetate in hexane as eluting gradient in flash column chromatography.

Characterization data was conducted on sample obtained in Rh₂(S-2-Cl-5-BrTPCP)₄-catalyzed reaction (96% ee).

White solid: **m.p.** 61-63 °C

Rf = 0.38 (20% ethyl acetate in hexane);

[α]²⁰_D: -40.5° (c = 1.00, CHCl₃, 96% ee);

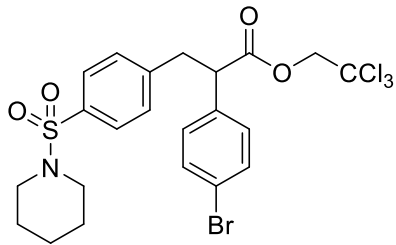
¹H NMR (600 MHz, CDCl₃) δ 7.61 (d, *J* = 8.2 Hz, 2H), 7.44 (d, *J* = 8.5 Hz, 2H), 7.31 (d, *J* = 7.8 Hz, 2H), 7.16 (d, *J* = 8.5 Hz, 2H), 4.74 (d, *J* = 12.0 Hz, 1H), 4.61 (d, *J* = 12.0 Hz, 1H), 3.85 – 3.78 (m, 1H), 3.75 – 3.67 (m, 1H), 3.34 (d, *J* = 10.6 Hz, 1H), 2.43 (s, 3H), 2.27 (td, *J* = 12.0, 2.7 Hz, 1H), 2.13 (td, *J* = 12.0, 2.7 Hz, 1H), 2.00 – 1.87 (m, 2H), 1.48 (qd, *J* = 12.2, 4.2 Hz, 1H), 1.34 (dp, *J* = 13.3, 2.8 Hz, 1H), 1.18 (qd, *J* = 12.1, 4.3 Hz, 1H);

¹³C NMR (151 MHz, CDCl₃) δ 171.0, 143.7, 134.9, 133.0, 132.1, 130.3, 129.8, 127.9, 122.2, 94.7, 74.3, 56.9, 46.2, 38.5, 30.4, 29.0, 21.7;

IR (neat) 2948, 2924, 2848, 1749, 1489, 1355, 1338, 1165, 932, 817, 726, 549 cm⁻¹;

HRMS (+p APCI) calcd for C₂₂H₂₄BrCl₃SNO₄ (M+H)⁺ 581.9670 found 581.96752;

HPLC (OD column, 10% *i*-propanol in hexane, 1 mL min⁻¹, 1 mg mL⁻¹, 60 min, UV 230 nm) retention times of 21.61 min (major) and 37.29 min (minor) 96% ee with Rh₂(S-2-Cl-5-BrTPCP)₄.



2,2,2-Trichloroethyl 2-(4-bromophenyl)-3-(4-(piperidin-1-ylsulfonyl)phenyl)propanoate

Following *GP-I* (1-tosylpiperidine as substrate, reacting 2,2,2-trichloroethyl 2-(4-bromophenyl)-2-diazoacetate, Rh₂(S-2-Cl-5-BrTPCP)₄ as catalyst), the primary benzylic insertion byproduct was obtained using 0-10% ethyl acetate in hexane as eluting gradient in flash column chromatography.

Characterization data was conducted on sample obtained in Rh₂(S-2-Cl-5-BrTPCP)₄-catalyzed reaction (ee not determined).

White solid: **m.p.** 42-44 °C

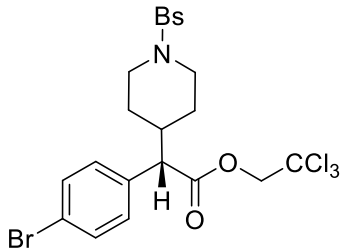
Rf = 0.33 (20% ethyl acetate in hexane);

¹H NMR (600 MHz, CDCl₃) δ 7.63 (d, *J* = 8.4 Hz, 2H), 7.45 (d, *J* = 8.4 Hz, 2H), 7.28 (d, *J* = 8.3 Hz, 2H), 7.20 (d, *J* = 8.5 Hz, 2H), 4.72 (d, *J* = 12.0 Hz, 1H), 4.64 (d, *J* = 12.0 Hz, 1H), 3.98 (dd, *J* = 8.6, 7.1 Hz, 1H), 3.52 (dd, *J* = 13.9, 8.6 Hz, 1H), 3.14 (dd, *J* = 13.9, 7.1 Hz, 1H), 2.94 (t, *J* = 5.5 Hz, 4H), 1.63 (p, *J* = 5.9 Hz, 4H), 1.46 – 1.39 (m, 2H);

¹³C NMR (151 MHz, CDCl₃) δ 171.0, 143.2, 136.0, 135.0, 132.1, 129.9, 129.7, 128.0, 122.2, 94.7, 74.3, 52.5, 47.1, 39.1, 25.3, 23.7;

IR (neat) 2941, 2854, 1751, 1489, 1340, 1166, 1149, 930, 720, 588, 564 cm⁻¹;

HRMS (+p APCI) calcd for C₂₂H₂₄BrCl₃SNO₄ (M+H)⁺ 581.9670 found 581.96710;



2,2,2-Trichloroethyl (S)-2-(4-bromophenyl)-2-(1-((4-bromophenyl)sulfonyl)piperidin-4-yl)acetate (13a)

Following GP-I (1-((4-bromophenyl)sulfonyl)piperidine as substrate, reacting 2,2,2-trichloroethyl 2-(4-bromophenyl)-2-diazoacetate, Rh₂(S-2-Cl-5-BrTPCP)₄ as catalyst), the desired C4-product was obtained using 0-10% ethyl acetate in hexane as eluting gradient in flash column chromatography.

Characterization data was conducted on sample obtained in Rh₂(S-2-Cl-5-BrTPCP)₄-catalyzed reaction (90% ee).

White solid: **m.p.** 154-156 °C

Rf = 0.46 (20% ethyl acetate in hexane);

[α]²⁰_D: -29.1° (c = 1.00, CHCl₃, 90% ee);

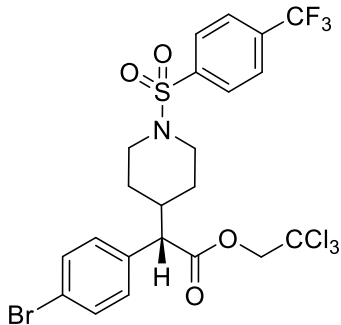
¹H NMR (600 MHz, CDCl₃) δ 7.67 (d, *J* = 8.6 Hz, 2H), 7.59 (d, *J* = 8.6 Hz, 2H), 7.44 (d, *J* = 8.5 Hz, 2H), 7.16 (d, *J* = 8.4 Hz, 2H), 4.75 (d, *J* = 12.0 Hz, 1H), 4.62 (d, *J* = 12.0 Hz, 1H), 3.83 (ddt, *J* = 11.7, 4.6, 2.6 Hz, 1H), 3.71 (ddt, *J* = 11.7, 4.5, 2.5 Hz, 1H), 3.35 (d, *J* = 10.6 Hz, 1H), 2.30 (td, *J* = 12.0, 2.7 Hz, 1H), 2.17 (td, *J* = 12.0, 2.7 Hz, 1H), 2.03 – 1.87 (m, 2H), 1.48 (qd, *J* = 12.3, 4.3 Hz, 1H), 1.36 (dt, *J* = 13.4, 2.7 Hz, 1H), 1.19 (qd, *J* = 12.2, 4.3 Hz, 1H);

¹³C NMR (151 MHz, CDCl₃) δ 170.8, 135.1, 134.6, 132.3, 132.0, 130.1, 129.1, 127.9, 122.1, 94.5, 74.1, 56.7, 46.1, 46.0, 38.3, 30.2, 28.8;

IR (neat) 2949, 2849, 1749, 1575, 1489, 1358, 1341, 1166, 1011, 934, 825, 750, 595 cm⁻¹;

HRMS (+p APCI) calcd for C₂₁H₂₁Br₂Cl₃SNO₄ (M+H)⁺ 645.8618 found 645.86207;

HPLC (OD column, 15% *i*-propanol in hexane, 1 mL min⁻¹, 1 mg mL⁻¹, 60 min, UV 230 nm) retention times of 21.66 min (major) and 34.30 min (minor) 90% ee with Rh₂(S-2-Cl-5-BrTPCP)₄.



2,2,2-Trichloroethyl (S)-2-(4-bromophenyl)-2-(1-((4-(trifluoromethyl)phenyl)sulfonyl)piperidin-4-yl)acetate (13c)

Following *GP-I* (1-((4-(trifluoromethyl)phenyl)sulfonyl)piperidine as substrate, reacting 2,2,2-trichloroethyl 2-(4-bromophenyl)-2-diazoacetate, $\text{Rh}_2(\text{S}-2-\text{Cl}-5-\text{BrTPCP})_4$ as catalyst), the desired C4-product was obtained using 0-10% ethyl acetate in hexane as eluting gradient in flash column chromatography.

Characterization data was conducted on sample obtained in $\text{Rh}_2(\text{S}-2-\text{Cl}-5-\text{BrTPCP})_4$ -catalyzed reaction (96% ee).

White solid: **m.p.** 158-160 °C

R_f = 0.49 (20% ethyl acetate in hexane);

$[\alpha]^{20}_{\text{D}}$: -29.1° (c = 1.00, CHCl_3 , 96% ee);

¹H NMR (600 MHz, CDCl_3) δ 7.86 (d, J = 8.2 Hz, 2H), 7.80 (d, J = 8.2 Hz, 2H), 7.45 (d, J = 8.5 Hz, 2H), 7.16 (d, J = 8.4 Hz, 2H), 4.75 (d, J = 12.0 Hz, 1H), 4.62 (d, J = 12.0 Hz, 1H), 3.88 (ddt, J = 11.7, 4.4, 2.4 Hz, 1H), 3.76 (ddq, J = 11.7, 4.5, 2.5 Hz, 1H), 3.35 (d, J = 10.6 Hz, 1H), 2.34 (td, J = 12.0, 2.7 Hz, 1H), 2.20 (td, J = 12.0, 2.7 Hz, 1H), 2.07 – 1.88 (m, 2H), 1.50 (qd, J = 12.3, 4.3 Hz, 1H), 1.38 (dt, J = 13.4, 3.0 Hz, 1H), 1.20 (qd, J = 12.2, 4.3 Hz, 1H);

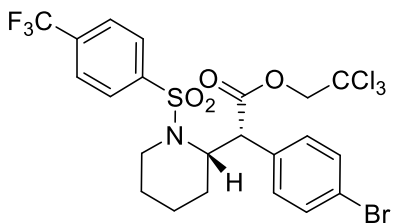
¹³C NMR (151 MHz, CDCl_3) δ 170.8, 139.8, 134.6, 134.5 (q, J = 33.0 Hz), 132.1, 130.1, 128.1, 126.2 (q, J = 3.6 Hz), 123.2 (d, J = 272.9 Hz), 122.2, 94.5, 74.1, 56.7, 46.1, 46.0, 38.2, 30.2, 28.8;

¹⁹F NMR (282 MHz, CDCl_3) δ -63.12;

IR (neat) 2951, 1750, 1489, 1404, 1323, 1170, 1134, 1062, 726, 596 cm^{-1} ;

HRMS (+p APCI) calcd for $\text{C}_{22}\text{H}_{21}\text{BrCl}_3\text{F}_3\text{SNO}_4$ ($\text{M}+\text{H}$)⁺ 635.9387 found 635.93897;

HPLC (R,R-Whelk column, 20% *i*-propanol in hexane, 1 mL min^{-1} , 1 mg mL^{-1} , 60 min, UV 230 nm) retention times of 31.20 min (major) and 50.10 min (minor) 96% ee with $\text{Rh}_2(\text{S}-2-\text{Cl}-5-\text{BrTPCP})_4$.



2,2,2-Trichloroethyl (R)-2-(4-bromophenyl)-2-((S)-1-((4-(trifluoromethyl)phenyl)sulfonyl)piperidin-2-yl)acetate

Following GP-I (1-((4-(trifluoromethyl)phenyl)sulfonyl)piperidine as substrate, reacting 2,2,2-trichloroethyl 2-(4-bromophenyl)-2-diazoacetate, $\text{Rh}_2(\text{S}-2\text{-Cl-5-BrTPCP})_4$ as catalyst), the desired C2-product was obtained using 0-10% ethyl acetate in hexane as eluting gradient in flash column chromatography.

Characterization data was conducted on sample obtained in $\text{Rh}_2(\text{S}-2\text{-Cl-5-BrTPCP})_4$ -catalyzed reaction (81% ee).

White solid: **m.p.** 136-138 °C

R_f = 0.45 (20% ethyl acetate in hexane);

[\alpha]²⁰_D: +22.5° (c = 0.66, CHCl₃, 81% ee);

¹H NMR (600 MHz, CDCl₃) δ 7.58 (d, *J* = 8.2 Hz, 2H), 7.37 (dd, *J* = 10.4, 8.4 Hz, 4H), 7.23 (d, *J* = 8.5 Hz, 2H), 4.89 (dd, *J* = 11.6, 4.8 Hz, 1H), 4.85 (d, *J* = 12.0 Hz, 1H), 4.59 (d, *J* = 12.0 Hz, 1H), 4.22 (d, *J* = 11.7 Hz, 1H), 3.56 (dd, *J* = 14.9, 4.4 Hz, 1H), 2.93 (ddd, *J* = 14.7, 12.9, 3.1 Hz, 1H), 1.92 – 1.70 (m, 4H), 1.60 (d, *J* = 13.7 Hz, 1H), 1.58 – 1.48 (m, 2H);

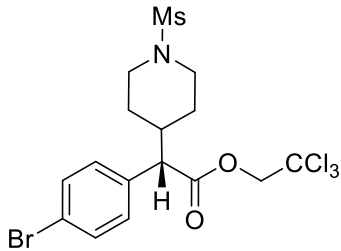
¹³C NMR (151 MHz, CDCl₃) δ 169.8, 143.9, 134.0 (d, *J* = 33.1 Hz), 133.7, 131.9, 130.3, 127.5, 125.9 (q, *J* = 3.8 Hz), 123.2 (q, *J* = 273.0 Hz), 122.5, 94.4, 74.3, 54.9, 50.5, 41.4, 27.4, 24.2, 18.6;

¹⁹F NMR (282 MHz, CDCl₃) δ -62.99;

IR (neat) 2947, 1752, 1489, 1323, 1161, 1136, 1063, 934, 720 cm⁻¹;

HRMS (+p APCI) calcd for C₂₂H₂₁BrCl₃F₃SNO₄ (M+H)⁺ 635.9387 found 635.93888;

HPLC (ADH column, 5% *i*-propanol in hexane, 1 mL min⁻¹, 1 mg mL⁻¹, 60 min, UV 230 nm) retention times of 16.01 min (major) and 31.83 min (minor) 81% ee with $\text{Rh}_2(\text{S}-2\text{-Cl-5-BrTPCP})_4$.



2,2,2-Trichloroethyl (S)-2-(4-bromophenyl)-2-(1-(methylsulfonyl)piperidin-4-yl)acetate (13d)

Following GP-I (1-(methylsulfonyl)piperidine as substrate, reacting 2,2,2-trichloroethyl 2-(4-bromophenyl)-2-diazoacetate, Rh₂(S-2-Cl-5-BrTPCP)₄ as catalyst), the desired C4-product was obtained using 0-10% ethyl acetate in hexane as eluting gradient in flash column chromatography.

Characterization data was conducted on sample obtained in Rh₂(S-2-Cl-5-BrTPCP)₄-catalyzed reaction (97% ee).

White solid: **m.p.** 170-172 °C

Rf = 0.08 (20% ethyl acetate in hexane);

[α]²⁰_D: +18.6° (c = 1.00, CHCl₃, 97% ee);

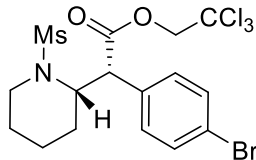
¹H NMR (600 MHz, CDCl₃) δ 7.48 (d, *J* = 8.4 Hz, 2H), 7.22 (d, *J* = 8.5 Hz, 2H), 4.78 (d, *J* = 12.0 Hz, 1H), 4.65 (d, *J* = 11.9 Hz, 1H), 3.88 – 3.80 (m, 1H), 3.77 – 3.70 (m, 1H), 3.40 (d, *J* = 10.7 Hz, 1H), 2.76 (s, 3H), 2.70 (td, *J* = 12.1, 2.7 Hz, 1H), 2.57 (td, *J* = 12.1, 2.7 Hz, 1H), 2.20 – 2.12 (m, 2H), 1.98 (dt, *J* = 13.1, 3.0 Hz, 1H), 1.49 (qd, *J* = 12.1, 4.3 Hz, 1H), 1.42 (dt, *J* = 13.3, 2.2 Hz, 1H), 1.20 (qd, *J* = 12.1, 4.3 Hz, 1H);

¹³C NMR (151 MHz, CDCl₃) δ 170.9, 134.7, 132.1, 130.2, 122.2, 94.6, 74.2, 56.8, 45.9, 45.8, 38.5, 34.8, 30.5, 29.0;

IR (**neat**) 3023, 2948, 2851, 1748, 1489, 1332, 1255, 1216, 1155, 957, 934, 827, 759, 723, 517, 505 cm⁻¹;

HRMS (+p APCI) calcd for C₁₆H₂₀BrCl₃SNO₄ (M+H)⁺ 505.9357 found 505.93616;

HPLC (R,R-Whelk column, 20% *i*-propanol in hexane, 1 mL min⁻¹, 1 mg mL⁻¹, 80 min, UV 230 nm) retention times of 41.56 min (major) and 53.30 min (minor) 97% ee with Rh₂(S-2-Cl-5-BrTPCP)₄.



2,2,2-Trichloroethyl (*R*)-2-(4-bromophenyl)-2-((*S*)-1-(methylsulfonyl)piperidin-2-yl)acetate

Following *GP-I* (1-(methylsulfonyl)piperidine as substrate, reacting 2,2,2-trichloroethyl 2-(4-bromophenyl)-2-diazoacetate, $\text{Rh}_2(\text{S}-2\text{-Cl-5-BrTPCP})_4$ as catalyst), the desired C2-product was obtained using 0-10% ethyl acetate in hexane as eluting gradient in flash column chromatography.

Characterization data was conducted on sample obtained in $\text{Rh}_2(\text{S}-2\text{-Cl-5-BrTPCP})_4$ -catalyzed reaction (80% ee).

White solid: **m.p.** 84-86 °C

Rf = 0.18 (20% ethyl acetate in hexane);

$[\alpha]^{20}_{\text{D}}$: +11.8° (c = 1.00, CHCl_3 , 80% ee);

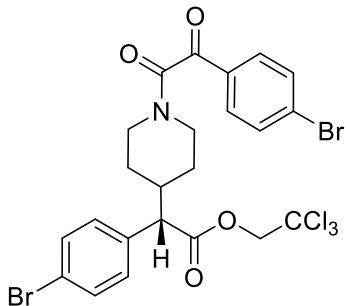
$^1\text{H NMR}$ (600 MHz, CDCl_3) δ 7.51 (d, J = 8.5 Hz, 2H), 7.38 (d, J = 8.5 Hz, 2H), 4.91 – 4.82 (m, 2H), 4.61 (d, J = 12.0 Hz, 1H), 4.24 (d, J = 11.8 Hz, 1H), 3.56 (dd, J = 14.7, 4.4 Hz, 1H), 2.95 – 2.86 (m, 1H), 2.06 (s, 3H), 1.92 – 1.84 (m, 1H), 1.84 – 1.76 (m, 3H), 1.72 – 1.59 (m, 2H);

$^{13}\text{C NMR}$ (151 MHz, CDCl_3) δ 170.0, 134.6, 132.2, 130.8, 122.7, 94.6, 74.4, 55.1, 50.7, 41.0, 39.9, 28.2, 25.2, 18.9;

IR (neat) 2938, 2856, 1749, 1489, 1320, 1146, 1053, 959, 940, 777, 715, 519 cm^{-1} ;

HRMS (+p APCI) calcd for $\text{C}_{16}\text{H}_{20}\text{BrCl}_3\text{SNO}_4$ ($\text{M}+\text{H}$)⁺ 505.9357 found 505.93578;

HPLC (ADH column, 5% *i*-propanol in hexane, 1 mL min^{-1} , 1 mg mL^{-1} , 45 min, UV 230 nm) retention times of 28.79 min (major) and 33.36 min (minor) 80% ee with $\text{Rh}_2(\text{S}-2\text{-Cl-5-BrTPCP})_4$.



2,2,2-Trichloroethyl (S)-2-(4-bromophenyl)-2-(1-(2-(4-bromophenyl)-2-oxoacetyl)piperidin-4-yl)acetate (13e)

Following *GP-I* (1-(4-bromophenyl)-2-(piperidin-1-yl)ethane-1,2-dione as substrate, reacting 2,2,2-trichloroethyl 2-(4-bromophenyl)-2-diazoacetate, Rh₂(S-2-Cl-5-BrTPCP)₄ as catalyst) with reaction under reflux dichloromethane (39 °C) and 1.5: 1 (diazoacetate: protected-piperidine), the desired C4-product was obtained using 0-10% ethyl acetate in hexane as eluting gradient in flash column chromatography.

Characterization data was conducted on sample obtained in Rh₂(S-2-Cl-5-BrTPCP)₄-catalyzed reaction (97% ee) as mixture with 1:1 ratio of rotamers.

White solid: **m.p.** 58-60 °C

Rf = 0.31 (20% ethyl acetate in hexane);

[α]²⁰_D: +46.1° (c = 1.00, CHCl₃, 97% ee);

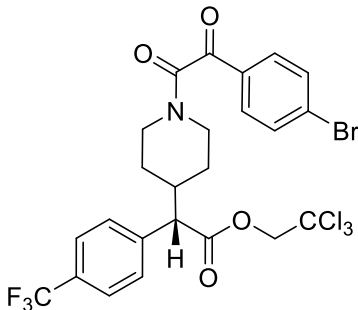
¹H NMR (600 MHz, CDCl₃) (*mixture of both rotamers with 1:1 ratio*) δ 7.79 (dd, *J* = 13.0, 8.5 Hz, 2H), 7.65 (dd, *J* = 9.9, 8.5 Hz, 2H), 7.47 (dd, *J* = 23.4, 8.5 Hz, 2H), 7.22 (dd, *J* = 13.7, 8.4 Hz, 2H), 4.81 (d, *J* = 12.0 Hz, 0.5H), 4.75 (d, *J* = 12.0 Hz, 0.5H), 4.73 – 4.67 (m, 0.5H), 4.64 (t, *J* = 11.9 Hz, 1H), 4.61 – 4.54 (m, 0.5H), 3.60 (dt, *J* = 13.7, 2.2 Hz, 0.5H), 3.48 (dt, *J* = 13.7, 2.1 Hz, 0.5H), 3.41 (dd, *J* = 10.6, 3.1 Hz, 1H), 3.17 – 3.07 (m, 0.5H), 3.03 – 2.93 (m, 0.5H), 2.84 (td, *J* = 13.1, 2.9 Hz, 0.5H), 2.70 (td, *J* = 13.0, 2.9 Hz, 0.5H), 2.35 (qt, *J* = 11.5, 3.7 Hz, 1H), 2.04 (dt, *J* = 13.4, 2.8 Hz, 0.5H), 1.89 (dt, *J* = 13.1, 2.9 Hz, 0.5H), 1.52 – 1.28 (m, 2H), 1.14 (qd, *J* = 12.5, 4.4 Hz, 0.5H), 1.06 (qd, *J* = 12.5, 4.3 Hz, 0.5H);

¹³C NMR (151 MHz, CDCl₃) (*mixture of both rotamers with 1:1 ratio*) δ 190.3, (190.3), 170.8, (170.8), 164.7, (164.7), 134.5, (134.5), 132.4, (132.4), 132.1, (132.1), 131.9, (131.9), 131.0, (130.9), 130.3, (130.3), 130.1, (130.1), 122.2, (122.2), 94.6, (94.5), 74.2, (74.1), 56.8, (56.8), 45.9, (45.8), 41.3, (41.2), 39.1, (39.0), 31.1, (30.5), 29.8, (29.0);

IR (neat) 2949, 2867, 1749, 1681, 1643, 1585, 1488, 1449, 1399, 1267, 1228, 1140, 1071, 762 cm⁻¹;

HRMS (+p APCI) calcd for C₂₂H₂₁Br₂Cl₃NO₄ (M)+ 637.8897 found 637.88974;

HPLC (ADH column, 5% *i*-propanol in hexane, 1 mL min⁻¹, 1 mg mL⁻¹, 80 min, UV 230 nm) retention times of 49.67 min (major) and 60.07 min (minor) 97% ee with Rh₂(S-2-Cl-5-BrTPCP)₄.



2,2,2-Trichloroethyl (S)-2-(1-(2-(4-bromophenyl)-2-oxoacetyl)piperidin-4-yl)-2-(4-trifluoromethylphenyl)acetate (13f)

Following *GP-I* (1-(4-bromophenyl)-2-(piperidin-1-yl)ethane-1,2-dione as substrate, reacting 2,2,2-trichloroethyl 2-diazo-2-(4-(trifluoromethyl)phenyl)acetate, Rh₂(S-2-Cl-5-BrTPCP)₄ as catalyst) with reaction under reflux dichloromethane (39 °C) and 1.5: 1 (diazoacetate: protected-piperidine), the desired C4-product was obtained using 0-10% ethyl acetate in hexane as eluting gradient in flash column chromatography.

Characterization data was conducted on sample obtained in Rh₂(S-2-Cl-5-BrTPCP)₄-catalyzed reaction (96% ee) as mixture with 1:1 ratio of rotamers.

White solid: **m.p.** 50–52 °C

R_f = 0.37 (20% ethyl acetate in hexane);

[\alpha]²⁰_D: +42.3° (c = 1.00, CHCl₃, 96% ee);

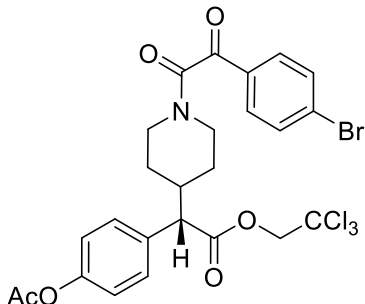
¹H NMR (600 MHz, CDCl₃) (*mixture of both rotamers with 1:1 ratio*) δ 7.79 (dd, *J* = 15.6, 8.6 Hz, 2H), 7.68 – 7.62 (m, 3H), 7.62 – 7.58 (m, 1H), 7.48 (dd, *J* = 12.7, 8.1 Hz, 2H), 4.83 (d, *J* = 12.0 Hz, 0.5H), 4.77 (d, *J* = 12.0 Hz, 0.5H), 4.72 (ddt, *J* = 13.4, 4.6, 2.4 Hz, 0.5H), 4.68 – 4.58 (m, 1.5H), 3.62 (ddt, *J* = 13.8, 4.4, 2.3 Hz, 0.5H), 3.53 (dd, *J* = 10.6, 3.4 Hz, 1H), 3.49 (ddt, *J* = 13.9, 4.6, 2.4 Hz, 0.5H), 3.13 (ddd, *J* = 13.7, 12.4, 2.9 Hz, 0.5H), 2.99 (ddd, *J* = 13.8, 12.3, 2.8 Hz, 0.5H), 2.89 – 2.81 (m, 0.5H), 2.71 (ddd, *J* = 13.4, 12.5, 3.0 Hz, 0.5H), 2.46 – 2.36 (m, 1H), 2.07 (dt, *J* = 13.5, 2.8 Hz, 0.5H), 1.92 (dt, *J* = 13.1, 3.0 Hz, 0.5H), 1.51 – 1.35 (m, 1.5H), 1.29 (dt, *J* = 13.3, 3.0 Hz, 0.5H), 1.17 (dtd, *J* = 13.6, 12.3, 4.5 Hz, 0.5H), 1.09 (dtd, *J* = 13.3, 12.2, 4.4 Hz, 0.5H);

¹³C NMR (151 MHz, CDCl₃) (*mixture of both rotamers with 1:1 ratio*) δ 190.5, (190.5), 170.7, (170.7), 164.9, (164.9), 139.7, (139.7), 132.6, (132.6), 132.1, (132.0), 131.1, (131.1), 130.7 (d, *J* = 32.7 Hz), (130.6 (d, *J* = 32.7 Hz)), 130.5, (130.5), 129.1, 126.1 (q, *J* = 3.7 Hz), (126.0 (q, *J* = 3.9 Hz)), 124.0 (d, *J* = 272.2 Hz), (124.0 (d, *J* = 272.2 Hz)), 94.6, (94.6), 74.4, (74.3), 57.4, (57.4), 46.0, (46.0), 41.4, (41.3), 39.4, (39.3), 31.3, (30.6), 30.0, (29.2);

IR (neat) 2950, 2869, 1751, 1682, 1643, 1586, 1325, 1127, 1068, 760 cm⁻¹;

HRMS (+p APCI) calcd for C₂₄H₂₁BrCl₃F₃NO₄ (M+H)⁺ 627.9666 found 627.96735;

HPLC (ODH column, 10% *i*-propanol in hexane, 1 mL min⁻¹, 1 mg mL⁻¹, 45 min, UV 230 nm) retention times of 18.09 min (minor) and 28.06 min (major) 96% ee with Rh₂(S-2-Cl-5-BrTPCP)₄.



2,2,2-Trichloroethyl

(S)-2-(4-acetoxyphenyl)-2-(1-(2-(4-bromophenyl)-2-oxoacetyl)piperidin-4-yl)acetate (13g)

Following *GP-I* (1-(4-bromophenyl)-2-(piperidin-1-yl)ethane-1,2-dione as substrate, reacting 2,2,2-trichloroethyl 2-(4-acetoxyphenyl)-2-diazoacetate, Rh₂(S-2-Cl-5-BrTPCP)₄ as catalyst) with reaction under reflux dichloromethane (39 °C) and 1.5: 1 (diazoacetate: protected-piperidine), the desired C4-product was obtained using 0-10% ethyl acetate in hexane as eluting gradient in flash column chromatography.

Characterization data was conducted on sample obtained in Rh₂(S-2-Cl-5-BrTPCP)₄-catalyzed reaction (75% ee) as mixture with 1:1 ratio of rotamers.

White solid: **m.p.** 55-58 °C

Rf = 0.18 (20% ethyl acetate in hexane);

[α]²⁰_D: +29.8° (c = 0.45, CHCl₃, 75% ee);

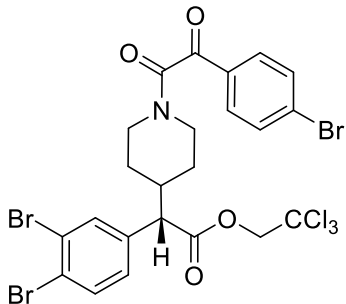
¹H NMR (600 MHz, CDCl₃) (*mixture of both rotamers with 1:1 ratio*) δ 7.79 (dd, *J* = 13.8, 8.6 Hz, 2H), 7.66 (dd, *J* = 10.2, 8.6 Hz, 2H), 7.35 (dd, *J* = 14.0, 8.6 Hz, 2H), 7.07 (dd, *J* = 25.2, 8.6 Hz, 2H), 4.85 (d, *J* = 12.0 Hz, 0.5H), 4.79 (d, *J* = 12.0 Hz, 0.5H), 4.71 (ddt, *J* = 13.4, 4.5, 2.2 Hz, 0.5H), 4.64 – 4.57 (m, 1.5H), 3.60 (ddt, *J* = 13.7, 4.4, 2.3 Hz, 0.5H), 3.51 – 3.41 (m, 1.5H), 3.13 (ddd, *J* = 13.8, 12.4, 2.9 Hz, 0.5H), 2.98 (ddd, *J* = 13.8, 12.3, 2.8 Hz, 0.5H), 2.84 (td, *J* = 13.1, 3.0 Hz, 0.5H), 2.71 (td, *J* = 13.1, 3.0 Hz, 0.5H), 2.40 – 2.32 (m, 1H), 2.31 (s, 1.5H), 2.29 (s, 1.5H), 2.05 (dt, *J* = 13.4, 3.1 Hz, 0.5H), 1.90 (dt, *J* = 13.0, 2.9 Hz, 0.5H), 1.51 (dt, *J* = 13.0, 2.7 Hz, 0.5H), 1.48 – 1.31 (m, 1.5H), 1.15 (dtd, *J* = 13.7, 12.3, 4.4 Hz, 0.5H), 1.06 (qd, *J* = 12.5, 4.3 Hz, 0.5H);

¹³C NMR (151 MHz, CDCl₃) (*mixture of both rotamers with 1:1 ratio*) δ 190.4, (190.4), 171.1, (171.0), 169.3, (169.3), 164.8, (164.7), 150.5, (150.4), 133.0, (133.0), 132.5, (132.4), 131.9, (131.9), 131.0, (131.0), 130.3, (130.3), 129.5, (129.5), 122.1, (122.0), 94.6, (94.6), 74.2, (74.1), 56.8, 46.0, (45.9), 41.3, (41.2), 39.3, (39.2), 31.1, (30.5), 29.9, (29.1), 21.2, (21.1);

IR (neat) 2950, 1750, 1682, 1641, 1586, 1506, 1370, 1201, 1170, 1139, 911, 728 cm⁻¹;

HRMS (+p APCI) calcd for C₂₅H₂₄BrCl₃NO₆ (M+H)⁺ 617.9847 found 617.98471;

HPLC (ODH column, 15% *i*-propanol in hexane, 1 mL min⁻¹, 1 mg mL⁻¹, 80 min, UV 230 nm) retention times of 23.99 min (minor) and 45.95 min (major) 75% ee with Rh₂(S-2-Cl-5-BrTPCP)₄.



**2,2,2-trichloroethyl
dibromophenylacetate (13h)**

(S)-2-(1-(2-(4-bromophenyl)-2-oxoacetyl)piperidin-4-yl)-2-(3,4-

Following *GP-I* (1-(4-bromophenyl)-2-(piperidin-1-yl)ethane-1,2-dione as substrate, reacting 2,2,2-trichloroethyl 2-diazo-2-(3,4-dibromophenyl)acetate, Rh₂(S-2-Cl-5-BrTPCP)₄ as catalyst) with reaction under reflux dichloromethane (39 °C) and 1.5: 1 (diazoacetate: protected-piperidine), the desired C4-product was obtained using 0-10% ethyl acetate in hexane as eluting gradient in flash column chromatography.

Characterization data was conducted on sample obtained in Rh₂(S-2-Cl-5-BrTPCP)₄-catalyzed reaction (98% ee) as mixture with 1:1 ratio of rotamers.

White solid: **m.p.** 62-64 °C

Rf = 0.31 (20% ethyl acetate in hexane);

[α]²⁰_D: +42.6° (c = 1.00, CHCl₃, 98% ee);

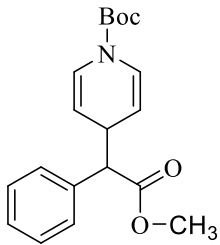
¹H NMR (500 MHz, CDCl₃) (*mixture of both rotamers with 1:1 ratio*) δ 7.79 (dd, *J* = 10.9, 8.6 Hz, 2H), 7.68 – 7.55 (m, 4H), 7.15 (ddd, *J* = 9.3, 8.2, 2.1 Hz, 1H), 4.84 (d, *J* = 11.9 Hz, 0.5H), 4.78 (d, *J* = 12.0 Hz, 0.5H), 4.74 – 4.68 (m, 0.5H), 4.68 – 4.58 (m, 1.5H), 3.65 – 3.57 (m, 0.5H), 3.55 – 3.46 (m, 0.5H), 3.39 (dd, *J* = 10.6, 1.9 Hz, 1H), 3.12 (ddd, *J* = 13.8, 12.3, 2.9 Hz, 0.5H), 3.00 (ddd, *J* = 13.8, 12.3, 2.8 Hz, 0.5H), 2.87 – 2.78 (m, 0.5H), 2.77 – 2.67 (m, 0.5H), 2.39 – 2.27 (m, 1H), 2.07 – 1.98 (m, 0.5H), 1.91 – 1.84 (m, 0.5H), 1.53 – 1.47 (m, 0.5H), 1.47 – 1.30 (m, 1.5H), 1.13 (dq, *J* = 42.3, 12.5, 4.4 Hz, 1H);

¹³C NMR (126 MHz, CDCl₃) (*mixture of both rotamers with 1:1 ratio*) δ 190.3, (190.3), 170.3, (170.3), 164.7, (164.7), 136.4, (136.4), 134.1, (134.0), 133.5, (133.5), 132.5, 131.9, (131.9), 131.0, (131.0), 130.4, 128.7, (128.7), 125.5, (125.4), 124.7, (124.6), 94.5, (94.4), 74.3, (74.2), 56.5, 45.9, (45.8), 41.2, (41.1), 39.2, (39.1), 31.1, (30.4), 29.9, (29.0);

IR (neat) 3010, 2949, 2867, 1750, 1682, 1643, 1585, 1486, 1141, 761 cm⁻¹;

HRMS (+p APCI) calcd for C₂₃H₂₀B_r₃Cl₃NO₄ (M+H)⁺ 715.8003 found 715.80147;

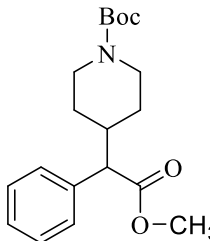
HPLC (R,R-Whelk column, 20% *i*-propanol in hexane, 1 mL min⁻¹, 1 mg mL⁻¹, 100 min, UV 230 nm) retention times of 66.36 min (major) and 84.85 min (minor) 98% ee with Rh₂(S-2-Cl-5-BrTPCP)₄.



tert-Butyl 4-(2-methoxy-2-oxo-1-phenylethyl)pyridine-1(4H)-carboxylate (11)

Following GP-IV, the desired insertion product was obtained in $\text{Rh}_2(\text{S}-\text{DOSP})_4$ -catalyzed reaction once for ^1H NMR characterization. However, the product decomposed too fast for a ideal ^{13}C NMR and other characterizations.

$^1\text{H NMR}$ (500 MHz, CDCl_3) δ 7.31 – 7.11 (m, 5H), 6.63 (dd, $J = 103.6, 34.2$ Hz, 2H), 4.85 (d, $J = 42.6$ Hz, 1H), 4.32 (d, $J = 49.2$ Hz, 1H), 3.59 (s, 4H), 3.45 (d, $J = 10.3$ Hz, 1H), 1.42 (s, 9H).



tert-Butyl 4-(2-methoxy-2-oxo-1-phenylethyl)piperidine-1-carboxylate (12)

Following GP-IV at 0 °C, the desired insertion product was obtained in $\text{Rh}_2(\text{S}-\text{DOSP})_4$ -catalyzed and followed by hydrogenation to get the sample for characterization data: *tert*-butyl 4-(2-methoxy-2-oxo-1-phenylethyl)pyridine-1(4H)-carboxylate (84 mg, 0.255 mmol, 1 equiv.) was dissolved in dry methanol (5 mL) and Pd/C (27 mg, 10 mol%, 10 wt%) was added. The flask was evacuated and flushed with hydrogen several times. Two hydrogen filled balloons were connected to the flask and the mixture was stirred under hydrogen atmosphere overnight. The palladium was filtered off by a short celite plug which was washed thoroughly with diethyl ether. The solvent was removed under reduced pressure to give a colorless solid in quantitative yields.

White solid: **m.p.:** 69–72 °C

Rf = 0.47 (10% ethyl acetate in hexane);

[α] $^{20}_{\text{D}}$: +31.8° (c = 1.00, CHCl_3 , 61% ee).

$^1\text{H NMR}$ (600 MHz, CDCl_3) δ 7.35 – 7.22 (m, 5H), 4.04 (s, 2H), 3.64 (s, 3H), 3.23 (d, $J = 10.6$ Hz, 1H), 2.65 (d, $J = 99.6$ Hz, 2H), 2.14 (qt, $J = 11.4, 3.5$ Hz, 1H), 1.76 (d, $J = 13.5$ Hz, 1H), 1.42 (s, 9H), 1.21 (tt, $J = 12.9, 6.2$ Hz, 2H), 0.94 (q, $J = 13.2$ Hz, 1H);

$^{13}\text{C NMR}$ (75 MHz, CDCl_3) δ 173.8, 154.7, 137.0, 128.7, 128.4, 127.5, 79.3, 57.8, 51.9, 39.4, 31.0, 29.5, 28.4;

IR (neat) 2972, 2931, 2853, 1733, 1692, 1447, 1413, 1391, 1365, 1285, 1247, 1156, 1128, 1086, 1019, 991, 965, 949, 902, 870, 771, 741, 703, 531 cm^{-1} ;

FTMS (+p NSI) calcf for $\text{C}_{19}\text{H}_{28}\text{NO}_4$ ($\text{M}+\text{H}$)⁺ 334.2013 found 334.20168;

HPLC (R,R-Whelk column, 5% *i*-propanol in hexane, 1 mL min⁻¹, 1 mg mL⁻¹, 45 min, UV 230 nm) retention times of 24.65 min (minor) and 27.08 min (major) 61% ee with $\text{Rh}_2(\text{S}-\text{DOSP})_4$.

5. Cyclopropanation and Ring-Opening Reactions for C3-Analogs

5.1 General Procedures

General Procedure for Cyclopropanation Reactions:

In a 25 mL round bottom flask under argon atmosphere, Boc-1,2,3,4-tetrahydropyridine (137 mg, 0.75 mmol, 1.5 equiv.) and 0.5 mol% Rh₂L₄ were dissolved in 2 mL dry solvent under indicated temperature. Corresponding donor/acceptor diazo compounds (0.5 mmol, 1.0 equiv.) was dissolved in 12 mL dry solvent under argon atmosphere and added over 2 h via a syringe pump under indicated temperature. After addition, the reaction mixture was stirred for another 30 min, and crude ¹H NMR was obtained after the resulted mixture was concentrated under vacuum. Finally, the desired product was obtained after purification using flash column chromatography with 1-15% ethyl acetate in hexane as eluting gradient.

General Procedure for Ring-opening Reactions:

In a flame-dried 10-mL round bottom flask, corresponding cyclopropanation product from last step (1 equiv.) was dissolved in dry dichloromethane (5 mL). BF₃-OEt₂ (2 equiv.) and triethylsilane (10 equiv.) were added. The mixture was stirred for 3 days at 23 °C. The crude product was purified by flash column chromatography (20% ethyl acetate in hexane to remove byproducts, then the product was eluted with 2% triethylamine in ethyl acetate). Further purification was done by a 2nd flash column chromatography (10% methanol in dichloromethane).

5.2. Diastereomer and Enantiomer Ratios Determination

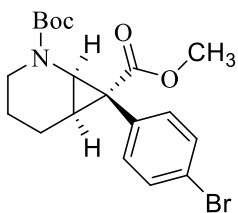
Diastereomer ratio was determined from crude ¹H NMR spectra.

Enantiomer ratio were determined by chiral HPLC on purified samples without derivation (cyclopropanation products), or after derivatizing the secondary amine to 2,2,2-trifluoroacetamide (ring-opening products).

General Procedure for Derivatizing the Secondary Amine to 2,2,2-Trifluoroacetamide:

Triethylamine (1 equiv.) and corresponding amine from ring-opening reactions (1 equiv.) were dissolved in 2 mL dichloromethane and cooled to 0 °C. Trifluoroacetic acid anhydride (1.2 equiv.) was added dropwise. The mixture was stirred at 0 °C for 1 h and was allowed to warm up to 23 °C. At 23 °C, the mixture was stirred overnight. The solvent was evaporated under reduced pressure and the crude product was purified by flash column chromatography (5-10% ethyl acetate in hexane as eluting gradient).

5.3. Characterization Data for Cyclopropanation and Ring-Opening Products



2-(*tert*-Butyl) 7-methyl (1*R*,6*R*,7*S*)-7-(4-bromophenyl)-2-azabicyclo[4.1.0]heptane-2,7-dicarboxylate (8a)

Following *General Procedure for Cyclopropanation Reactions* (methyl 2-(4-bromophenyl)-2-diazoacetate (128 mg), Rh₂(S-DOSP)₄ as catalyst, pentane as solvent, at 0 °C), the desired cyclopropanation product was obtained for characterization (92% ee).

White solid: **m.p.** 113–118 °C

Rf = 0.11 (5% ethyl acetate in hexane);

[α]²⁰_D: +135.2° (c = 1.00, CHCl₃, 92% ee);

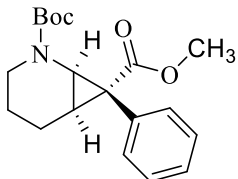
¹H NMR (600 MHz, CDCl₃) *Rotamer1* : (*Rotamer2*) (1.04:1) δ 7.39 (d, *J* = 8.4 Hz, 2H), (7.36 (d, *J* = 8.5 Hz, 2H)), 7.10 (d, *J* = 8.4 Hz, 2H), (7.08 (d, *J* = 8.4 Hz, 2H)), 3.65 (d, *J* = 9.2 Hz, 1H), (3.60 (d, *J* = 9.3 Hz, 1H)), (3.50 (s, 3H)), 3.48 (s, 3H), 3.18 (dt, *J* = 12.5, 4.4 Hz, 1H), (3.08 (dt, *J* = 12.4, 4.4 Hz, 1H)), 2.72 – 2.52 (m, 2H) (both rotamers), 2.34 – 2.29 (m, 1H), (2.29 – 2.25 (m, 1H)), 1.92 – 1.80 (m, 2H) (both rotamers), 1.75 – 1.62 (m, 1H) (both rotamers), (1.49 (s, 9H)), 1.43 (s, 9H), 1.20 – 1.10 (m, 2H) (both rotamers), 0.47 – 0.20 (m, 2H) (both rotamers);

¹³C NMR (126 MHz, CDCl₃) δ 173.1, (173.0), 156.3, (155.7), 133.6, (133.2), 132.7, (132.4), 131.7, (131.5), 121.6, (121.6), 80.5, (80.3), 52.5, (52.4), 43.3, (42.3), 41.5, (40.1), 34.4, (34.1), 28.4, (28.3), 25.0, (24.6), 21.2, (21.0), 18.5, (18.5);

IR (neat) 2974, 2951, 2867, 2252, 1779, 1691, 1593, 1489, 1476, 1435, 1409, 1391, 1365, 1301, 1246, 1216, 1202, 1157, 1143, 1102, 1084, 1074, 1012, 970, 937, 907, 888, 842, 827, 809, 771, 729, 724 cm⁻¹;

HRMS (+p NSI) calcd for C₁₉H₂₅BrNO₄ (M+H)⁺ 410.0962 found 410.09648;

HPLC (ADH column, 1% *i*-propanol in hexane, 1 mL min⁻¹, 1 mg mL⁻¹, 60 min, UV 230 nm) retention times of 11.83 min (major) and 13.33 min (minor) 92% ee with Rh₂(S-DOSP)₄.



2-(tert-Butyl) 7-methyl (1*R*,6*R*,7*S*)-7-phenyl-2-azabicyclo[4.1.0]heptane-2,7-dicarboxylate (8b)

Following *General Procedure for Cyclopropanation Reactions* (methyl 2-diazo-2-phenylacetate (88 mg), Rh₂(S-DOSP)₄ as catalyst, pentane as solvent, at 0 °C), the desired cyclopropanation product was obtained for characterization (95% ee).

White solid: **m.p.** 68–72 °C

R_f = 0.19 (5% ethyl acetate in hexane);

[α]²⁰_D: +149.6° (c = 1.00, CHCl₃, 95% ee);

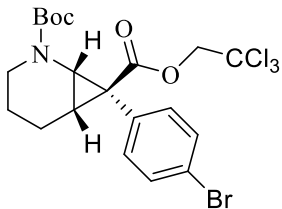
¹H NMR (500 MHz, CDCl₃) *Rotamer1* : (*Rotamer2*) (1.22:1) δ 7.27 (m, 10H) (both rotamers), (3.73 (d, *J* = 9.3 Hz, 1H)), 3.67 (d, *J* = 9.4 Hz, 1H), 3.55 (s, 3H), (3.53 (s, 3H)), 3.19 (dt, *J* = 12.4, 4.3 Hz, 1H), (3.08 (dt, *J* = 12.4, 4.4 Hz, 1H)), 2.77 – 2.58 (m, 2H) (both rotamers), (2.40 – 2.34 (m, 1H)), 2.34 – 2.28 (m, 1H), 1.89 (m, 2H) (both rotamers), 1.78 (t, *J* = 13.4 Hz, 2H) (both rotamers), 1.56 (s, 9H), (1.49 (s, 9H)), 1.16 (m, 2H) (both rotamers), 0.35 (m, 2H) (both rotamers).;

¹³C NMR (126 MHz, CDCl₃) δ 173.7, (173.5), 156.3, (155.8), 133.5, (133.3), 131.8, (131.5), 128.4, (128.2), 127.3, (127.2), 80.3, (80.0), 52.4, (52.4), 43.2, (42.2), 41.5, (40.13), 34.80, (34.56), 28.38, (28.36), 24.90, (24.51), 21.15, (20.92), 18.62, (18.57);

IR (neat) 2973, 2951, 2867, 1693, 1604, 1498, 1476, 1446, 1435, 1408, 1390, 1366, 1302, 1245, 1216, 1203, 1158, 1142, 1102, 1085, 1076, 1031, 1014, 982, 968, 939, 901, 888, 854, 842, 809, 773, 759, 746, 706, 677 cm⁻¹;

HRMS (+p NSI) calcd for C₁₉H₂₆NO₂ (M+H)⁺ 332.1856 found 332.18697;

HPLC (ADH column, 0.3% *i*-propanol in hexane, 1 mL min⁻¹, 1 mg mL⁻¹, 45 min, UV 230 nm) retention times of 22.90 min (major) and 28.27 min (minor) 95% ee with Rh₂(S-DOSP)₄.



2-(*tert*-Butyl) 7-(2,2,2-trichloroethyl) (1*R*,6*R*,7*S*)-7-phenyl-2-azabicyclo[4.1.0]heptane-2,7-dicarboxylate

Following *General Procedure for Cyclopropanation Reactions* (2,2,2-trichloroethyl 2-(4-bromophenyl)-2-diazoacetate (186.8 mg), Rh₂(*R*-DOSP)₄ as catalyst, pentane as solvent, at 23 °C), the desired cyclopropanation product was obtained for characterization (80% ee).

White solid: **m.p.** 43–45 °C

R_f = 0.30 (5% ethyl acetate in hexane);

[α]²⁰_D: -90.4° (c = 1.00, CHCl₃, xx% ee);

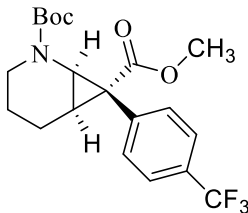
¹H NMR (600 MHz, CDCl₃) *Rotamer1* : (*Rotamer2*) (1.13:1) δ 7.48 (d, *J* = 8.4 Hz, 1H), (7.45 (d, *J* = 8.5 Hz, 1H)), (7.20 (d, *J* = 8.5 Hz, 1H)), 7.18 (d, *J* = 8.4 Hz, 1H), (4.71 (d, *J* = 11.9 Hz, 1H)), 4.66 (d, *J* = 11.9 Hz, 1H), 4.60 (d, *J* = 11.9 Hz, 1H), (4.53 (d, *J* = 11.9 Hz, 1H)), (3.88 (d, *J* = 9.6 Hz, 1H)), 3.86 (d, *J* = 9.6 Hz, 1H), 3.26 (dt, *J* = 12.7, 4.6 Hz, 1H), (3.17 (dt, *J* = 12.2, 4.4 Hz, 1H)), 2.81 – 2.65 (m, 2H) (both rotamers), (2.48 (t, *J* = 8.2 Hz, 1H)), 2.43 (t, *J* = 8.2 Hz, 1H), 2.03 – 1.91 (m, 2H) (both rotamers), 1.83 (t, *J* = 4.6 Hz, 1H), (1.81 (t, *J* = 4.4 Hz, 1H)), 1.55 (s, 9H), (1.51 (s, 9H)), 1.30 – 1.20 (m, 2H) (both rotamers), 0.49 (m, 2H) (both rotamers);

¹³C NMR (126 MHz, CDCl₃) δ 171.0, (170.9), 156.2, (155.6), 133.6, (133.2), 131.7, (131.7), 131.5, (131.5), 121.9, (121.8), 94.9, (94.8), 80.8, (80.4), 74.4, (74.3), 43.5, (42.8), 41.5, (40.3), 34.4, (34.1), 28.5, (28.4), 25.8, (25.6), 21.2, (21.0), 18.6, (18.5);

IR (neat) 2973, 2867, 1731, 1692, 1477, 1444, 1379, 1301, 1229, 1212, 1194, 1154, 1143, 1102, 910, 888, 832, 808, 769, 719, 608, 573, 530 cm⁻¹;

HRMS (+p NSI) calcd for C₂₀H₂₄BrCl₃NO₄ (M+H)⁺ 525.9949 found 525.9953;

HPLC (ADH column, 1% *i*-propanol in hexane, 1 mL min⁻¹, 1 mg mL⁻¹, 45 min, UV 230 nm) retention times of 9.47 min (major) and 11.27 min (minor) 80% ee with Rh₂(*R*-DOSP)₄.



2-(*tert*-Butyl) 7-(2,2,2-trichloroethyl)azabicyclo[4.1.0]heptane-2,7-dicarboxylate (8c)

Following *General Procedure for Cyclopropanation Reactions* (methyl 2-diazo-2-(4-(trifluoromethyl)phenyl)acetate (122 mg), Rh₂(S-DOSP)₄ as catalyst, pentane as solvent, at 0 °C), the desired cyclopropanation product was obtained for characterization (90% ee).

Colorless oil

Rf = 0.10 (5% ethyl acetate in hexane);

[α]²⁰_D: +129.7° (c = 1.00, CHCl₃, 90% ee);

¹H NMR (600 MHz, CDCl₃) *Rotamer1 : Rotamer2 (1:1)* δ 7.52 (d, *J* = 8.1 Hz, 2H), 7.49 (d, *J* = 8.2 Hz, 2H), 7.35 (d, *J* = 8.4 Hz, 2H), 7.33 (d, *J* = 8.2 Hz, 2H), 3.70 (d, *J* = 9.2 Hz, 1H), 3.65 (d, *J* = 9.3 Hz, 1H), 3.51 (s, 3H), 3.49 (s, 3H), 3.18 (dt, *J* = 12.5, 4.3 Hz, 1H), 3.09 (dt, *J* = 12.5, 4.4 Hz, 1H), 2.67 – 2.62 (m, 1H), 2.60 (td, *J* = 13.0, 3.1 Hz, 1H), 2.38 – 2.30 (m, 2H) (both rotamers), 1.94 – 1.84 (m, 2H) (both rotamers), 1.75 – 1.67 (m, 12.5 Hz, 2H) (both rotamers), 1.51 (s, 9H), 1.44 (s, 9H), 1.19 – 1.10 (m, 2H) (both rotamers), 0.34 – 0.14 (m, 2H) (both rotamers);

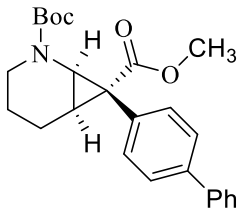
¹³C NMR (126 MHz, CDCl₃) δ 172.9, (172.7), 156.3, (155.7), 137.8, (137.7), 132.2, (131.9), 129.5 (q, *J* = 32.2 Hz), (129.4 (q, *J* = 32.2 Hz)), 125.3 (q, *J* = 3.6 Hz), (125.2 (q, *J* = 3.6 Hz)), 124.2 (q, *J* = 204.1 Hz), (124.2 (q, *J* = 204.1 Hz)), 80.6, (80.4), 52.5, (52.5) 43.3, (42.3), 41.4, (40.1), 34.7, 34.4, 28.4, (28.3), 25.0, (24.7), 21.2, (21.0), 18.5, (18.4);

¹⁹F NMR (282 MHz, CDCl₃) (Rotamers) δ -62.41, (-62.57).

IR (neat) 2974, 2954, 2870, 1692, 1618, 1477, 1445, 1436, 1409, 1391, 1366, 1323, 1246, 1216, 1159, 1143, 1122, 1108, 1085, 1075, 1066, 1020, 971, 938, 906, 889, 844, 809, 771, 760, 735, 691 cm⁻¹;

HRMS (+p NSI) calcd for C₂₀H₂₄F₃NO₄Na (M+Na)+ 422.1550 found 422.15535;

HPLC (ADH column, 0.65% *i*-propanol in hexane, 0.65 mL min⁻¹, 1 mg mL⁻¹, 45 min, UV 230 nm) retention times of 15.73 min (major) and 17.49 min (minor) 90% ee with Rh₂(S-DOSP)₄.



2-(*tert*-Butyl) 7-(2,2,2-trichloroethyl) (1*R*,6*R*,7*S*)-7-([1,1'-biphenyl]-4-yl)-2-azabicyclo[4.1.0]heptane-2,7-dicarboxylate (8d)

Following *General Procedure for Cyclopropanation Reactions* (methyl 2-([1,1'-biphenyl]-4-yl)-2-diazoacetate (126 mg), Rh₂(S-DOSP)₄ as catalyst, pentane as solvent, at 0 °C), the desired cyclopropanation product was obtained for characterization (86% ee).

Colorless oil

Rf = 0.10 (5% ethyl acetate in hexane);

[\alpha]²⁰_D: +149.5° (c = 1.00, CHCl₃, 86% ee);

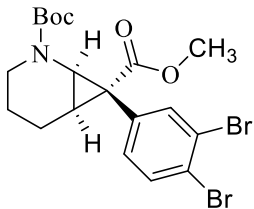
¹H NMR (600 MHz, CDCl₃) *Rotamer1* : (*Rotamer2*) (1.20:1) δ 7.52 (t, *J* = 7.8 Hz, 4H) (both rotamers), 7.48 (d, *J* = 8.2 Hz, 2H), (7.46 (d, *J* = 8.4 Hz, 2H)), (7.33 (t, *J* = 7.8, 2H)), 7.33 (t, *J* = 7.8, 2H), 7.25 (m, 6H) (both rotamers), (3.69 (d, *J* = 9.2 Hz, 1H)), 3.63 (d, *J* = 9.3 Hz, 1H), 3.51 (s, 3H), (3.49 (s, 3H)), 3.17 (dt, *J* = 12.4, 4.3 Hz, 1H), (3.04 (dt, *J* = 12.3, 4.4 Hz, 1H)), 2.70 – 2.56 (m, 2H) (both rotamers), (2.32 (t, *J* = 7.5 Hz, 1H)), 2.28 (t, *J* = 7.7 Hz, 1H), 1.92 – 1.79 (m, 2H) (both rotamers), 1.74 (t, *J* = 15.7 Hz, 2H) (both rotamers), 1.51 (s, 9H), (1.44 (s, 9H)), 1.16 – 1.05 (m, 2H) (both rotamers), 0.47 – 0.26 (m, 2H) (both rotamers);

¹³C NMR (126 MHz, CDCl₃) δ 173.7, (173.5), 156.4, (155.9), 140.7, (140.6), 140.0, (139.8), 132.6, (132.4), 132.2, (131.8), 128.7, 127.3, (127.3), 127.1, (127.0), (126.9), 80.4, (80.1), 52.5, (52.5), 43.3, (42.3), 41.5, (40.2), 34.6, (34.3), 28.5, (28.4), 25.0, (24.7), 21.3, (21.1), 18.7, (18.6);

IR (neat) 3029, 2973, 2951, 2866, 2251, 1691, 1600, 1581, 1522, 1488, 1476, 1448, 1435, 1406, 1390, 1365, 1303, 1245, 1216, 1203, 1158, 1142, 1103, 1085, 1075, 1060, 1009, 969, 938, 907, 889, 843, 809, 764, 746, 728, 697 cm⁻¹;

HRMS (+p NSI) calcd for C₂₅H₃₀NO₄ (M+H)⁺ 408.2169 found 408.21752;

HPLC (S4900 column, 1% *i*-propanol in hexane, 1 mL min⁻¹, 1 mg mL⁻¹, 30 min, UV 230 nm) retention times of 11.41 min (major) and 13.64 min (minor) 86% ee with Rh₂(S-DOSP)₄.



2-(*tert*-Butyl) 7-(2,2,2-trichloroethyl) (1*R*,6*R*,7*S*)-7-(3,4-dibromophenyl)-2-azabicyclo[4.1.0]heptane-2,7-dicarboxylate (8e)

Following *General Procedure for Cyclopropanation Reactions* (methyl 2-diazo-2-(3,4-dibromophenyl)acetate (167 mg), Rh₂(S-DOSP)₄ as catalyst, pentane as solvent, at 0 °C), the desired cyclopropanation product was obtained for characterization (81% ee).

White solid: **m.p.** 133–134 °C

Rf = 0.09 (5% ethyl acetate in hexane);

[α]²⁰_D: +96.8° (c = 1.00, CHCl₃, 81% ee);

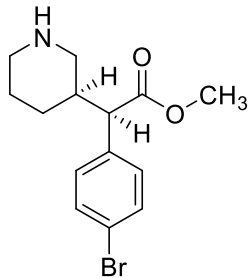
¹H NMR (500 MHz, CDCl₃) *Rotamer1* : (*Rotamer2*) (1.27:1) δ 7.62 – 7.45 (m, 4H) (both rotamers), 7.13 – 6.99 (m, 2H) (both rotamers), 3.70 (d, *J* = 9.2 Hz, 1H), (3.64 (d, *J* = 9.3 Hz, 1H)), (3.57 (s, 3H)), 3.55 (s, 3H), (3.29 (dt, *J* = 12.3, 4.0 Hz, 1H)), 3.20 (dt, *J* = 12.2, 4.1 Hz, 1H), 2.75 – 2.58 (m, 2H) (both rotamers), 2.38 – 2.30 (m, 2H) (both rotamers), 1.98 – 1.86 (m, 2H) (both rotamers), 1.75 (d, *J* = 14.7 Hz, 2H) (both rotamers), (1.55 (s, 9H)), 1.50 (s, 9H), 1.31 – 1.16 (m, 2H) (both rotamers), 0.52 – 0.29 (m, 2H) (both rotamers);

¹³C NMR (126 MHz, CDCl₃) δ 172.6, (172.5), 156.2, (155.5), 136.9, (136.5), 134.7, (134.5), 133.6, (133.4), 132.1, (131.7), 124.8, (124.6), 124.0, (123.9), 80.7, (80.5), 52.6, (52.6), 43.4, (42.4), 41.4, (40.1), 34.2, (33.9), 28.4, (28.4), 25.1, (24.7), 21.3, (21.1), 18.5, (18.4);

IR (neat) 2973, 2951, 2867, 2254, 1690, 1585, 1548, 1464, 1443, 1435, 1411, 1390, 1365, 1246, 1202, 1160, 1143, 1104, 1085, 1076, 1059, 1013, 975, 939, 908, 868, 842, 810, 788, 774, 760, 729, 703, 661 cm⁻¹;

HRMS (+p NSI) calcd for C₁₉H₂₄Br₂NO₄ (M+H)⁺ 488.0067 found 488.00748;

HPLC (ADH column, 1% *i*-propanol in hexane, 1 mL min⁻¹, 1 mg mL⁻¹, 60 min, UV 230 nm) retention times of 11.82 min (major) and 16.48 min (minor) 81% ee with Rh₂(S-DOSP)₄.



Methyl (R)-2-(4-bromophenyl)-2-((R)-piperidin-3-yl)acetate (9a)

Following *General Procedure for Ring-opening Reactions* (2-(*tert*-butyl) 7-methyl (1*R*,6*R*,7*S*)-7-(4-bromophenyl)-2-azabicyclo[4.1.0]heptane-2,7-dicarboxylate with 92% ee as starting material), the desired ring-opened product was obtained for characterization (93% ee).

White solid: **m.p.** 115–117 °C

Rf = 0.03 (100% ethyl acetate);

Rf = 0.19 (10% methanol in dichloromethane);

$[\alpha]^{20}_{\text{D}}$: -40.4° (c = 1.00, MeOH, 93% ee);

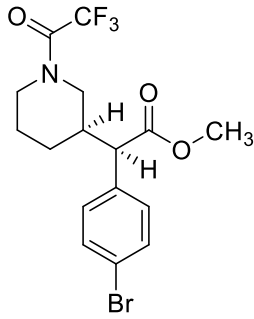
1H NMR (300 MHz, CD₃OD) δ 7.43 (d, *J* = 8.5 Hz, 2H), 7.19 (d, *J* = 8.3 Hz, 2H), 3.57 (d, *J* = 0.7 Hz, 3H), 3.40 (d, *J* = 10.1 Hz, 1H), 3.18 (d, *J* = 14.6 Hz, 1H), 2.83 – 2.59 (m, 2H), 2.44 (t, *J* = 11.7 Hz, 1H), 2.34 (qt, *J* = 11.7, 3.1 Hz, 1H), 2.00 – 1.76 (m, 2H), 1.63 (qt, *J* = 13.5, 3.9 Hz, 1H), 1.27 (qd, *J* = 11.9, 3.9, 1H);

13C NMR (75 MHz, CD₃OD) δ 174.8, 137.4, 134.1, 132.3, 124.0, 56.7, 53.7, 49.0, 46.4, 39.2, 29.7, 24.6;

IR (neat) 3367, 2927, 2852, 2419, 1732, 1610, 1553, 1488, 1434, 1407, 1337, 1244, 1293, 1219, 1197, 1161, 1101, 1073, 1011, 961, 914, 868, 824, 763, 720, 652, 618 cm⁻¹;

HRMS (+p APCI) calcd for C₁₄H₁₉BrNO₂ (M+H)⁺ 312.0594 found 312.06974;

HPLC (obtained on its 2,2,2-trifluoroacetamide derivative) (ASH column, 3% *i*-propanol in hexane, 1 mL min⁻¹, 1 mg mL⁻¹, 30 min, UV 230 nm) retention times of 13.22 min (minor) and 19.33 min (major) 93% ee.



Methyl (R)-2-(4-dibromophenyl)-2-((R)-1-(2,2,2-trifluoroacetyl)piperidin-3-yl)acetate

Following *General Procedure for Derivatizing the Secondary Amine to 2,2,2-Trifluoroacetamide* (methyl (R)-2-(4-bromophenyl)-2-((R)-piperidin-3-yl)acetate as starting material), the desired derivatized product was obtained for characterization and enantiomeric ratio determination.

Colorless oil

Rf = 0.32 (20% ethyl acetate in hexane);

1H NMR (600 MHz, CDCl₃) δ *Rotamer1* : (*Rotamer2*) (1.10:1) δ 7.44 – 7.39 (m, 4H) (both rotamers), 7.15 – 7.12 (m, 4H) (both rotamers), (4.45 (dd, *J* = 13.2, 3.8 Hz, 1H)), 3.96 – 3.91 (m, 1H), 3.83 (s, 1H), (3.60 (s, 3H)), 3.59 (s, 3H), (3.52 – 3.48 (m, 1H)), 3.25 (d, *J* = 10.5 Hz, 1H), (3.19 (d, *J* = 10.5 Hz, 1H)), 3.04 (ddd, *J* = 14.3, 11.7, 3.0 Hz, 1H), 2.59 – 2.49 (m, 2H) (both rotamers), 2.40 – 2.33 (m, 1H), 2.21 (pt, *J* = 11.5, 3.6 Hz, 2H) (both rotamers), 1.94 (t, *J* = 15.7 Hz, 2H) (both rotamers), 1.80 – 1.73 (m, 2H) (both rotamers), 1.59 – 1.50 (m, 2H) (both rotamers), (1.37 – 1.29 (m, 1H)), 1.29 – 1.21 (m, 1H);

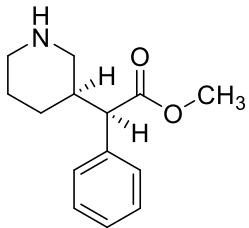
13C NMR (151 MHz, CDCl₃) δ 172.5, (172.3), 155.5 (q, *J* = 35.7 Hz), (155.3 (d, *J* = 35.6 Hz)), 134.7, (134.3), 132.2, (132.1), 130.0, (129.9), 122.3, (122.2), 116.5 (q, *J* = 288.0 Hz), (116.3 (q, *J* = 288.1 Hz)), 55.1, (54.9), 52.3, (52.3), 49.3 (q, *J* = 3.6 Hz), 47.0, (46.4 (q, *J* = 3.5 Hz)), (44.2), 39.8, (38.7), 29.8, (29.3), 25.3, (24.6).;

19F NMR (565 MHz, CDCl₃) δ -69.02, (-69.10).;

IR (neat) 2926, 2856, 1736, 1691, 1489, 1466, 1447, 1409, 1345, 1290, 1271, 1235, 1190, 1141, 1073, 1011, 835, 755 cm⁻¹;

HRMS (+p NSI) calcd for C₁₆H₁₈BrF₃NO₃ (M+H)⁺ 408.0417 found 408.04204;

HPLC (ASH column, 3% *i*-propanol in hexane, 1 mL min⁻¹, 1 mg mL⁻¹, 30 min, UV 230 nm) retention times of 13.22 min (minor) and 19.33 min (major) 93% ee.



Methyl (R)-2-phenyl-2-((R)-piperidin-3-yl)acetate (9b)

Following *General Procedure for Ring-opening Reactions* (2-(*tert*-butyl) 7-methyl (1*R*,6*R*,7*S*)-7-phenyl-2-azabicyclo[4.1.0]heptane-2,7-dicarboxylate with 95% ee as starting material), the desired ring-opened product was obtained for characterization (91% ee).

White solid: **m.p.** 173–175 °C

Rf = 0.02 (100% ethyl acetate);

Rf = 0.37 (10% methanol in dichloromethane);

[α]²⁰_D: -43.1° (c = 1.00, MeOH, 91% ee);

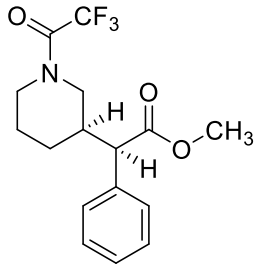
¹H NMR (600 MHz, CDCl₃) δ 7.29 – 7.16 (m, 5H), 3.58 (s, 3H), 3.23 (d, *J* = 10.8 Hz, 1H), 2.91 (d, *J* = 12.1 Hz, 1H), 2.56 (d, *J* = 12.0 Hz, 1H), 2.46 (td, *J* = 11.9, 2.9 Hz, 1H), 2.27 (bs, 1H), 2.15 (qt *J* = 10.5, 3.3 Hz, 3H), 2.06 (q, *J* = 10.4 Hz, 1H), 1.84 (d, *J* = 11.4 Hz, 1H), 1.63 (dq, *J* = 13.4, 3.1 Hz, 1H), 1.45 (qt, *J* = 13.0, 3.9 Hz, 1H), 1.13 (qd, *J* = 10.6, 3.9 Hz, 1H);

¹³C NMR (101 MHz, CDCl₃) δ 173.7, 137.0, 128.6, 128.4, 127.4, 56.3, 51.8, 50.2, 46.6, 40.1, 30.2, 26.0;

IR (neat) 3320, 3062, 3028, 2929, 2850, 2735, 1731, 1558, 1439, 1454, 1424, 1338, 1272, 1242, 1217, 1197, 1135, 1018, 959, 892, 864, 779, 733, 700, 625, 614, 577 cm⁻¹;

HRMS (+p APCI) calcd for C₁₄H₂₀NO₂ (M+H)⁺ 234.1489 found 234.14904;

HPLC (obtained on its 2,2,2-trifluoroacetamide derivative) (ASH column, 3% *i*-propanol in hexane, 1 mL min⁻¹, 1 mg mL⁻¹, 30 min, UV 230 nm) retention times of 10.89 min (minor) and 15.22 min (major) 91% ee.



Methyl (R)-2-phenyl-2-((R)-1-(2,2,2-trifluoroacetyl)piperidin-3-yl)acetate

Following *General Procedure for Derivatizing the Secondary Amine to 2,2,2-Trifluoroacetamide* (methyl (R)-2-phenyl-2-((R)-piperidin-3-yl)acetate as starting material), the desired derivatized product was obtained for characterization and enantiomeric ratio determination.

Colorless oil

Rf = 0.39 (20% ethyl acetate in hexane);

¹H NMR (600 MHz, CDCl₃) δ *Rotamer1* : (*Rotamer2*) (1.11:1) δ 7.31 – 7.20 (m, 10H) (both rotamers), 4.45 (ddq, *J* = 13.1, 4.1, 2.0 Hz, 1H), (3.97 (ddt, *J* = 12.8, 3.7, 1.8 Hz, 1H)), (3.83 (d, *J* = 13.4 Hz, 1H)), 3.60 (s, 3H), (3.59 (s, 3H)), 3.53 – 3.41 (m, 1H), (3.28 (d, *J* = 10.3 Hz, 1H)), 3.21 (d, *J* = 10.6 Hz, 1H), (3.01 (ddd, *J* = 14.2, 11.9, 3.0 Hz, 1H)), 2.58 – 2.48 (m, 2H) (both rotamers), (2.38 – 2.30 (m, 1H)), 2.30 – 2.19 (m, 2H) (both rotamers), 2.03 – 1.91 (m, 2H) (both rotamers), 1.81 – 1.72 (m, 2H) (both rotamers), 1.61 – 1.46 (m, 2H) (both rotamers), (1.36 – 1.27 (m, 1H)), 1.27 – 1.21 (m, 1H).;

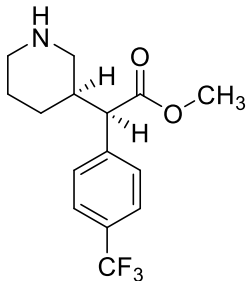
¹³C NMR (151 MHz, CDCl₃) δ 172.9 , (172.7) , 155.4 (q, *J* = 35.6 Hz), (155.3 (q, *J* = 35.6 Hz)), 135.7, (135.4) , 129.0 , (128.9) , 128.2, (128.2), 128.2, (128.1), 116.5 (q, *J* = 288.0 Hz), (116.3 (q, *J* = 288.0 Hz)), 55.8 , (55.6) , 52.2 , (52.1), 49.4 (q, *J* = 3.6 Hz), 47.2, (46.4 (q, *J* = 3.5 Hz)), (44.3), 40.0 , (38.7) , 29.9 , (29.4) , 25.5 , (24.7).;

¹⁹F NMR (282 MHz, CDCl₃) δ -69.01, (-69.20).;

IR (neat) 3031, 2951, 2860, 1733, 1685, 1497, 1466, 1456, 1436, 1345, 1291, 1274, 1236, 1183, 1134, 1044, 1005, 973, 956, 920, 882, 855, 827, 779, 754, 733, 699, 662, 622, 558, 531 cm⁻¹;

HRMS (+p NSI) calcd for C₁₆H₁₉F₃NO₃ (M+H)⁺ 330.1312 found 330.13131;

HPLC (ASH column, 3% *i*-propanol in hexane, 1 mL min⁻¹, 1 mg mL⁻¹, 30 min, UV 230 nm) retention times of 10.89 min (minor) and 15.22 min (major) 91% ee.



Methyl (*R*)-2-((*R*)-piperidin-3-yl)-2-(4-(trifluoromethyl)phenyl)acetate (9c)

Following *General Procedure for Ring-opening Reactions* (2-(*tert*-butyl) 7-(2,2,2-trichloroethyl) (1*R*,6*R*,7*S*)-7-(4-(trifluoromethyl)phenyl)-2-azabicyclo[4.1.0]heptane-2,7-dicarboxylate with 90% ee as starting material), the desired ring-opened product was obtained for characterization (90% ee).

White solid: **m.p.** 79–82 °C

Rf = 0.18 (100% ethyl acetate);

Rf = 0.34 (10% methanol in dichloromethane);

$[\alpha]^{20}_{\text{D}}$: -31.8° (c = 1.00, MeOH, 90% ee);

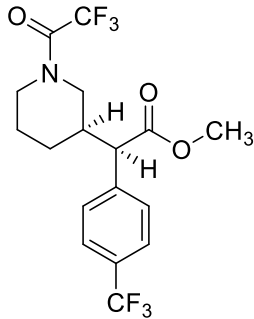
$^1\text{H NMR}$ (600 MHz, CD_3OD) δ 7.56 (d, J = 8.3 Hz, 2H), 7.46 (d, J = 8.2 Hz, 2H), 3.57 (s, 3H), 3.45 (d, J = 10.1 Hz, 1H), 2.99 (d, J = 12.5 Hz, 1H), 2.59 – 2.48 (m, 2H), 2.26 (qt, J = 11.1, 3.3 Hz, 1H), 2.23 (t, J = 11.3 Hz, 1H), 1.86 (d, J = 12.9 Hz, 1H), 1.72 (dp, J = 14.0, 3.2 Hz, 1H), 1.53 (qt, J = 13.9, 4.0 Hz, 1H), 1.22 (qd, J = 10.7, 3.4 Hz, 1H);

$^{13}\text{C NMR}$ (126 MHz, CD_3OD) δ 172.6, 140.9, 129.6 (q, J = 32.8 Hz), 128.8, 125.3 (q, J = 3.8 Hz), 124.1 (q, J = 271.1 Hz), 55.2, 51.3, 44.9, 38.3, 28.5, 23.8 (1 carbon not visible);

IR (neat) 2947, 2798, 2735, 1727, 1617, 1423, 1435, 1423, 1324, 1279, 1241, 1202, 1189, 1156, 1119, 1067, 1019, 961, 934, 901, 865, 852, 838, 816, 782, 756, 722, 647, 599, 582 cm^{-1} ;

HRMS (+p APCI) calcd for $\text{C}_{15}\text{H}_{19}\text{F}_3\text{NO}_2$ ($\text{M}+\text{H}$)⁺ 302.1362 found 302.13656;

HPLC (obtained on its 2,2,2-trifluoroacetamide derivative) (ASH column, 3% *i*-propanol in hexane, 1 mL min⁻¹, 1 mg mL⁻¹, 30 min, UV 230 nm) retention times of 9.09 min (minor) and 13.86 min (major) 90% ee.



Methyl (R)-2-((R)-1-(2,2,2-trifluoroacetyl)piperidin-3-yl)-2-(4-(trifluoromethyl)phenyl)acetate

Following *General Procedure for Derivatizing the Secondary Amine to 2,2,2-Trifluoroacetamide* (methyl (R)-2-((R)-piperidin-3-yl)-2-(4-(trifluoromethyl)phenyl)acetate as starting material), the desired derivatized product was obtained for characterization and enantiomeric ratio determination.

Colorless oil

R_f = 0.55 (20% ethyl acetate in hexane);

¹H NMR (600 MHz, CDCl₃) δ *Rotamer1* : (*Rotamer2*) (1.20:1) δ 7.56 (d, *J* = 8.1 Hz, 2H), (7.53 (d, *J* = 8.0 Hz 2H)), 7.39 (d, *J* = 8.1 Hz, 2H), (7.37 (d, *J* = 8.0 Hz, 2H)), (4.44 (ddd, *J* = 13.0, 4.1, 2.1 Hz, 1H)), 3.91 (ddt, *J* = 13.0, 3.7, 1.7 Hz, 1H), 3.81 (d, *J* = 14.0 Hz, 1H), (3.61 (s, 3H)), 3.60 (s, 3H), (3.45 (ddd, *J* = 13.7, 3.7, 1.8 Hz, 1H)), 3.37 (d, *J* = 10.5 Hz, 1H), (3.31 (d, *J* = 10.5 Hz, 1H)), 3.06 (ddd, *J* = 14.2, 11.6, 3.0 Hz, 1H), 2.59 – 2.52 (m, 2H) (both rotamers), 2.40 (dd, *J* = 13.0, 10.6 Hz, 1H), 2.33 – 2.20 (m, 2H) (both rotamers), 2.04 – 1.89 (m, 2H) (both rotamers), 1.81 – 1.74 (m, 2H) (both rotamers), 1.60 – 1.47 (m, 2H) (both rotamers), 1.40 – 1.32 (m, 1H), (1.31 – 1.23 (m, 1H));

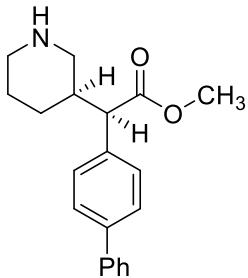
¹³C NMR (151 MHz, CDCl₃) δ 172.2, (172.0), 155.5 (q, *J* = 35.8 Hz), (155.2 (d, *J* = 35.5 Hz)), 139.8, (139.4), 130.5 (q, *J* = 32.6 Hz), (130.3 (q, *J* = 32.5 Hz)), 128.8, (128.7), 125.9 (q, *J* = 3.5 Hz), (125.8 (q, *J* = 3.4 Hz)), 124.0 (q, *J* = 272.1 Hz), (123.9 (q, *J* = 272.1 Hz)), 116.5 (q, *J* = 287.9 Hz), 116.2 (q, *J* = 288.1 Hz), 55.4, (55.2), 52.4, (52.3), 49.2 (q, *J* = 3.5 Hz), 46.9, (46.4 (q, *J* = 3.4 Hz)), (44.2), 40.0, (38.8), 29.7, (29.2), 25.3, (24.6);

¹⁹F NMR (565 MHz, CDCl₃) δ 62.69, (-62.77), -69.09, (-69.24);

IR (neat) 2954, 1735, 1686, 1619, 1466, 1438, 1422, 1324, 1280, 1186, 1159, 1116, 1067, 1019, 975, 954, 936, 905, 883, 844, 784, 755, 723, 694, 660, 602, 530 cm⁻¹;

HRMS (+p NSI) calcd for C₁₇H₁₈F₆NO₃ (M+H)⁺ 398.1185 found 398.11859;

HPLC (ASH column, 3% *i*-propanol in hexane, 1 mL min⁻¹, 1 mg mL⁻¹, 30 min, UV 230 nm) retention times of 9.09 min (minor) and 13.86 min (major) 90% ee.



Methyl (R)-2-([1,1'-biphenyl]-4-yl)-2-((R)-piperidin-3-yl)acetate (9d)

Following *General Procedure for Ring-opening Reactions* (2-(*tert*-butyl) 7-(2,2,2-trichloroethyl) (1*R*,6*R*,7*S*)-7-([1,1'-biphenyl]-4-yl)-2-azabicyclo[4.1.0]heptane-2,7-dicarboxylate with 86% ee as starting material), the desired ring-opened product was obtained for characterization (87% ee).

White solid: **m.p.** 184–185 °C

Rf = 0.09 (100% ethyl acetate);

Rf = 0.44 (10% methanol in dichloromethane);

[α]²⁰_D: -54.6° (c = 1.00, MeOH, 87% ee);

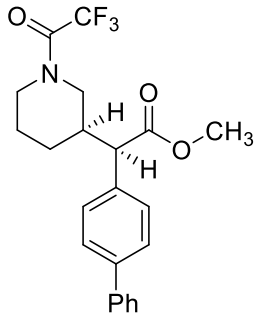
¹H NMR (600 MHz, CD₃OD) δ 7.57 – 7.45 (m, 4H), 7.32 (dt, *J* = 7.8, 3.5 Hz, 4H), 7.23 (t, *J* = 7.4 Hz, 1H), 3.56 (s, 3H), 3.43 (d, *J* = 10.1 Hz, 1H), 3.17 (d, *J* = 12.3 Hz, 1H), 2.72 (qd, *J* = 13.0, 3.2 Hz, 2H), 2.46 (t, *J* = 11.9 Hz, 1H), 2.41 (qt, 11.8, 2.8 Hz, 1H), 1.90 (d, *J* = 12.9 Hz, 1H), 1.83 (dp, *J* = 14.5, 3.0 Hz, 1H), 1.65 (qt, *J* = 14.3, 4.0 Hz, 1H), 1.28 (qd, *J* = 12.9, 3.7 Hz, 1H);

¹³C NMR (126 MHz, CD₃OD) δ 175.2, 143.2, 142.6, 137.1, 130.9, 130.9, 129.5, 128.9, 57.1, 53.6, 49.2, 46.5, 39.3, 29.9, 24.8;

IR (neat) 3325, 3029, 2927, 2851, 2733, 1730, 1675, 1653, 1600, 1582, 1558, 1521, 1486, 1448, 1434, 1412, 1387, 1337, 1262, 1240, 1216, 1191, 1157, 1132, 1075, 1008, 959, 898, 863, 840, 759, 739, 697, 642, 620, 582, 558 cm⁻¹;

HRMS (+p APCI) calcd for C₂₀H₂₃NO₂ (M+H)⁺ 310.1802 found 310.18048;

HPLC (obtained on its 2,2,2-trifluoroacetamide derivative) (ASH column, 3% *i*-propanol in hexane, 1 mL min⁻¹, 1 mg mL⁻¹, 30 min, UV 230 nm) retention times of 14.78 min (minor) and 17.97 min (major) 87% ee.



Methyl (R)-2-([1,1'-biphenyl]-4-yl)-2-((R)-1-(2,2,2-trifluoroacetyl)piperidin-3-yl)acetate

Following *General Procedure for Derivatizing the Secondary Amine to 2,2,2-Trifluoroacetamide* (methyl (R)-2-([1,1'-biphenyl]-4-yl)-2-((R)-piperidin-3-yl)acetate as starting material), the desired derivatized product was obtained for characterization and enantiomeric ratio determination.

Colorless oil

Rf = 0.33 (20% ethyl acetate in hexane);

1H NMR (600 MHz, CDCl₃) δ *Rotamer1 : Rotamer2 (1:1)* δ 7.53-7.48 (m, 8H) (both rotamers), 7.40 – 7.33 (m, 4H) (both rotamers), 7.33 – 7.24 (m, 6H) (both rotamers), 4.45 (ddt, *J* = 15.0, 4.0, 1.9 Hz, 1H), 4.05 (ddt, *J* = 12.9, 3.7, 1.8 Hz, 1H), 3.84 (d, *J* = 13.9 Hz, 1H), 3.62 (s, 3H), 3.61 (s, 3H), 3.58 – 3.54 (m, 1H), 3.33 (d, *J* = 10.3 Hz, 1H), 3.27 (d, *J* = 10.5 Hz, 1H), 3.03 (ddd, *J* = 14.2, 11.9, 2.9 Hz, 1H), 2.59 – 2.51 (m, 1H), 2.55 (dd, *J* = 13.9, 11.6 Hz, 1H), 2.38 (dd, *J* = 12.9, 10.9 Hz, 1H), 2.35 – 2.20 (m, 2H), 2.04 – 1.90 (m, 2H), 1.81 – 1.74 (m, 1H) (both rotamers), 1.60 – 1.49 (m, 2H), 1.38 – 1.23 (m, 2H);

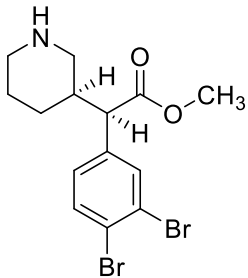
13C NMR (151 MHz, CDCl₃) δ 172.9 , (172.7) , 155.4 (q, *J* = 35.5 Hz), (155.3 (q, *J* = 35.6 Hz)), 141.1, (141.0), 140.5, (140.4), 134.7, (134.3), 128.8, (128.8) , 128.7, (128.6), 127.7, (127.6), 127.5, (127.4), 127.1, (127.1), 116.5 (q, *J* = 288.0 Hz), (116.3 (q, *J* = 288.1 Hz)), 55.4, (55.3) , 52.3, (52.2) , 49.4 (q, *J* = 3.4 Hz), 47.2, (46.5 (q, *J* = 3.5 Hz)), (44.3), 39.9, (38.7), 29.9, (29.4), 25.4, (24.7);

19F NMR (282 MHz, CDCl₃) δ -68.98, (-69.11);

IR (neat) 3031, 2950, 2857, 1735, 1691, 1487, 1466, 1448, 1413, 1345, 1279, 1267, 1235, 1188, 1158, 1142, 1009, 974, 845, 760, 740, 699 cm⁻¹;

HRMS (+p NSI) calcd for C₂₂H₂₃F₃NO₃ (M+H)⁺ 406.1625 found 406.16250;

HPLC (ASH column, 3% *i*-propanol in hexane, 1 mL min⁻¹, 1 mg mL⁻¹, 30 min, UV 230 nm) retention times of 14.78 min (minor) and 17.97 min (major) 87% ee.



Methyl (R)-2-(3,4-dibromophenyl)-2-((R)-piperidin-3-yl)acetate (9e)

Following *General Procedure for Ring-opening Reactions* (2-(*tert*-butyl) 7-(2,2,2-trichloroethyl) (1*R*,6*R*,7*S*)-7-(3,4-dibromophenyl)-2-azabicyclo[4.1.0]heptane-2,7-dicarboxylate with 81% ee as starting material), the desired ring-opened product was obtained for characterization (80% ee).

Colorless oil

Rf = 0.15 (100% ethyl acetate);

Rf = 0.50 (10% methanol in dichloromethane);

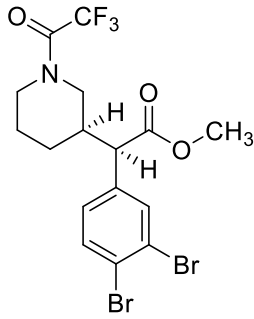
[α]²⁰_D: -27.5° (c = 1.00, MeOH, 80% ee);

¹H NMR (600 MHz, CD₃OD) δ 7.60 (d, *J* = 2.1 Hz, 1H), 7.54 (d, *J* = 8.3 Hz, 1H), 7.15 (dd, *J* = 8.3, 2.1 Hz, 1H), 3.56 (s, 3H), 3.29 (d, *J* = 10.2 Hz, 1H), 2.88 (d, *J* = 12.3 Hz, 1H), 2.41 – 2.50 (m, 2H), 2.16 – 2.05 (m, 2H), 1.84 – 1.72 (m, 1H), 1.64 (dp, *J* = 13.4, 3.3 Hz, 1H), 1.45 (qt, *J* = 12.3, 4.0 Hz, 1H), 1.20 – 1.08 (m, 1H); **¹³C NMR** (75 MHz, CD₃OD) δ 172.7, 138.2, 133.7, 133.3, 128.7, 124.4, 123.3, 54.6, 51.3, 48.5, 45.2, 39.0, 29.0, 24.6.;

IR (neat) 3325, 2928, 2851, 2806, 2733, 1730, 1653, 1582, 1553, 1459, 1434, 1395, 1337, 1298, 1260, 1238, 1193, 1158, 1131, 1111, 1076, 1013, 959, 940, 905, 865, 826, 777, 729, 698, 670, 595, 559 cm⁻¹;

HRMS (+p APCI) calcd for C₁₄H₁₈Br₂NO₂ (M+H)⁺ 389.9699 found 389.97030;

HPLC (obtained on its 2,2,2-trifluoroacetamide derivative) (ASH column, 3% *i*-propanol in hexane, 1 mL min⁻¹, 1 mg mL⁻¹, 30 min, UV 230 nm) retention times of 15.21 min (minor) and 24.16 min (major) 80% ee.



Methyl (R)-2-(3,4-dibromophenyl)-2-((R)-1-(2,2,2-trifluoroacetyl)piperidin-3-yl)acetate

Following *General Procedure for Derivatizing the Secondary Amine to 2,2,2-Trifluoroacetamide* (methyl (R)-2-(3,4-dibromophenyl)-2-((R)-piperidin-3-yl)acetate as starting material), the desired derivatized product was obtained for characterization and enantiomeric ratio determination.

Colorless oil

Rf = 0.39 (20% ethyl acetate in hexane);

1H NMR (600 MHz, CDCl₃) δ *Rotamer1* : (*Rotamer2*) (1.18:1) δ 7.57 – 7.48 (m, 4H) (both rotamer), 7.09 (dd, *J* = 8.3, 2.2 Hz, 1H), (7.06 (dd, *J* = 8.3, 2.2 Hz, 1H)), (4.45 (ddd, *J* = 13.1, 4.2, 2.1 Hz, 1H)), 3.94 (ddt, *J* = 13.1, 3.7, 1.7 Hz, 1H), 3.82 (d, *J* = 14.1 Hz, 1H), (3.61 (s, 3H)), 3.61 (s, 3H), (3.52 (ddd, *J* = 13.7, 3.8, 1.9 Hz, 1H)), 3.23 (d, *J* = 10.5 Hz, 1H), (3.17 (d, *J* = 10.5 Hz, 1H)), 3.05 (ddd, *J* = 14.2, 11.6, 3.0 Hz, 1H), 2.65 – 2.48 (m, 2H) (both rotamers), 2.47 – 2.33 (m, 1H), 2.27 – 2.13 (m, 2H) (both rotamers), 1.98 – 1.87 (m, 2H) (both rotamers), 1.80 – 1.74 (m, 2H) (both rotamers), 1.61 – 1.46 (m, 2H) (both rotamers), 1.38 – 1.29 (m, 1H), (1.25 (m, 1H));

13C NMR (151 MHz, CDCl₃) δ 172.0, (171.8), 155.5 (q, *J* = 35.7 Hz), (155.2 (q, *J* = 35.7 Hz)), 136.7, (136.3), 134.2, (134.0), 133.6, (133.5), 128.3, (128.2), 125.4, (125.3), 124.6, (124.6), 116.5 (d, *J* = 288.0 Hz), (116.3 (d, *J* = 288.2 Hz)), 54.7, (54.4), 52.5, (52.4), 49.2 (q, *J* = 3.4 Hz), 46.9, (46.4 (q, *J* = 3.4 Hz)), (44.2), 39.8, (38.7), 29.7, (29.2), 25.2, (24.6);

19F NMR (282 MHz, CDCl₃) δ -69.01, (-69.06);

IR (neat) 2950, 2858, 1734, 1685, 1463, 1397, 1343, 1267, 1291, 1235, 1187, 1138, 1113, 1044, 1014, 975, 956, 909, 854, 832, 778, 754, 733, 699, 661 cm⁻¹;

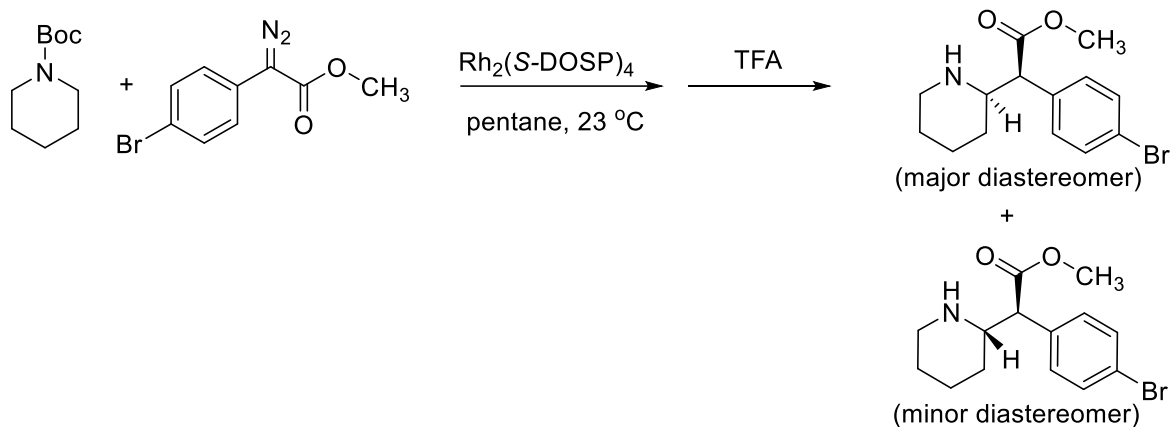
HRMS (+p NSI) calcd for C₁₆H₁₇Br₂F₃NO₃ (M+H)⁺ 485.9522 found 485.95260;

HPLC (ASH column, 3% *i*-propanol in hexane, 1 mL min⁻¹, 1 mg mL⁻¹, 30 min, UV 230 nm) retention times of 15.21 min (minor) and 24.16 min (major) 80% ee.

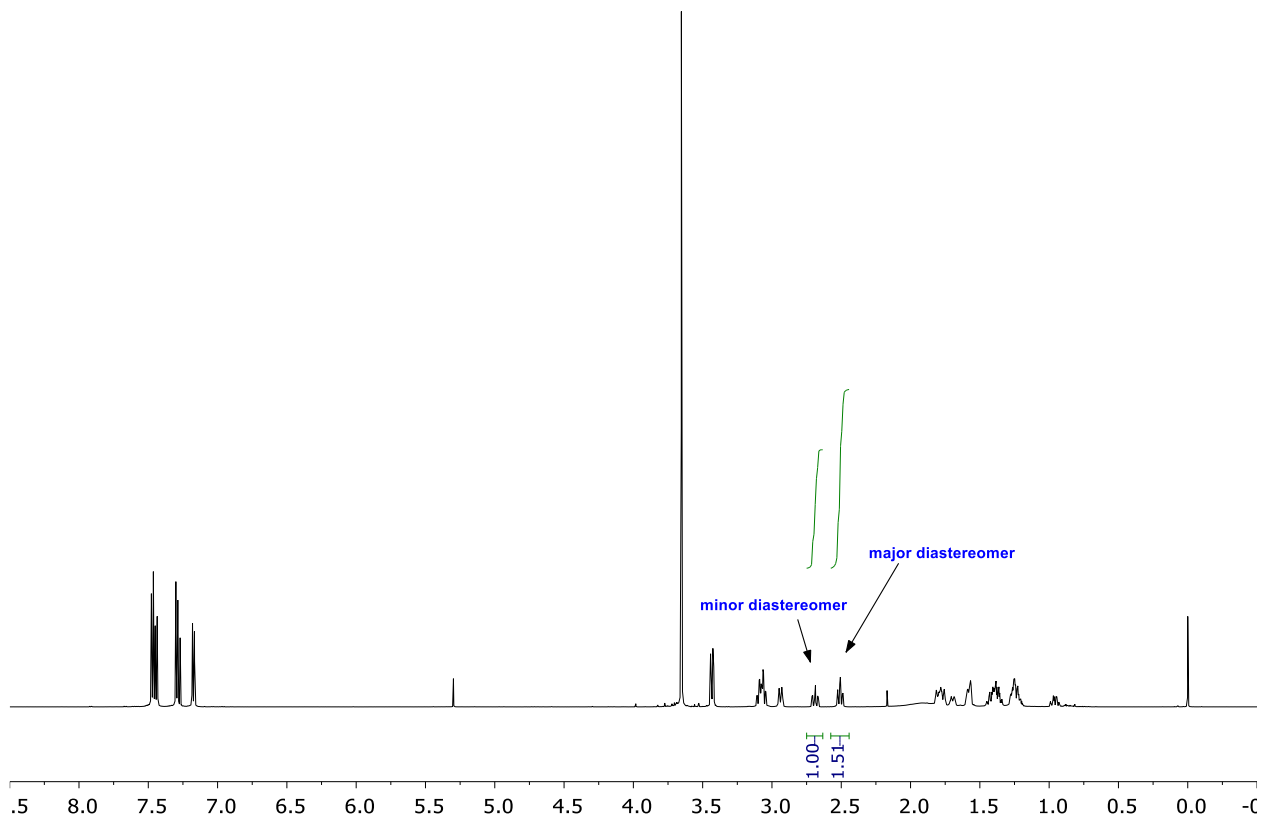
6. Reference

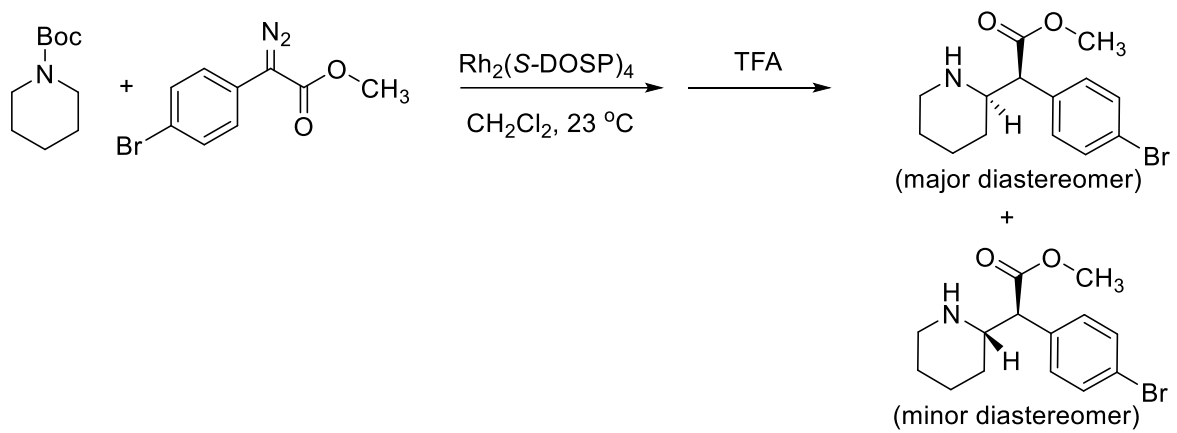
1. Guptill, D. M.; Davies, H. M. L. *J. Am. Chem. Soc.* **2014**, *136*, 17718.
2. Briones, J. F.; Hansen, J.; Hardcastle, K. I.; Autschbach, J.; Davies, H. M. L. *J. Am. Chem. Soc.* **2010**, *132*, 17211.
3. Chepiga, K. M.; Qin, C.; Alford, J. S.; Chennamadhavuni, S.; Gregg, T. M.; Olson, J. P.; Davies, H. M. L.; *Tetrahedron* **2013**, *69*, 5765.
4. Pilsl, L. K. A.; Ertl, T.; Reiser, O. *Org. Lett.* **2017**, *19*, 2754.
5. Davies, H. M. L; Morton, D. *Chem. Soc. Rev.* **2011**, *40*, 1857.
6. Fu, L.; Hoang, K.; Tortoreto, C.; Liu, W.; Davies, H. M. L. *Org. Lett.* **2018**, *20*, 2399.
7. Davies, H. M. L.; Hansen, T.; Churchill, M. R. *J. Am. Chem. Soc.* **2000**, *122*, 3063.
8. Qu, Z.; Shi, W.; Wang, J. *J. Org. Chem.* **2001**, *66*, 8139.
9. Takasu, N.; Oisaki, K.; Kanai, M. *Org. Lett.* **2013**, *15*, 1918.
10. Du, F.-T.; Ji, J.-X. *Chem. Sci.* **2012**, *3*, 460.
11. Brodsky, B. H.; Du Bois, J. *Org. Lett.* **2004**, *15*, 2619.
12. Pour, M.; Špulák, M.; Balšánek, V.; Kuneš, J.; Kubanová, P.; Buchta, V. *Bioorg. Med. Chem.* **2003**, *11*, 2843.
13. Sundberg, R. J; Bloom, J. D. *J. Org. Chem.* **1981**, *46*, 4836.
14. Zhang,W.; Luo, M. *Chem. Commun.* **2016**, *52*, 2980.
15. Zhou, G.; Ting, P.; Aslanian, R.; Piwinski, J. J. *Org. Lett.* **2008**, *10*, 2517.
16. Kweon, D.-H.; Kim, H.-K.; Kim, J.-J.; Chung, H. A; Lee, W. S.; Kim, S.-K.; Yoon, Y.-J. *J. Heterocycl. Chem.* **2002**, *39*, 203.

7. Crude NMR for Diastereo- (and/or Regio-) Selectivity Determination:

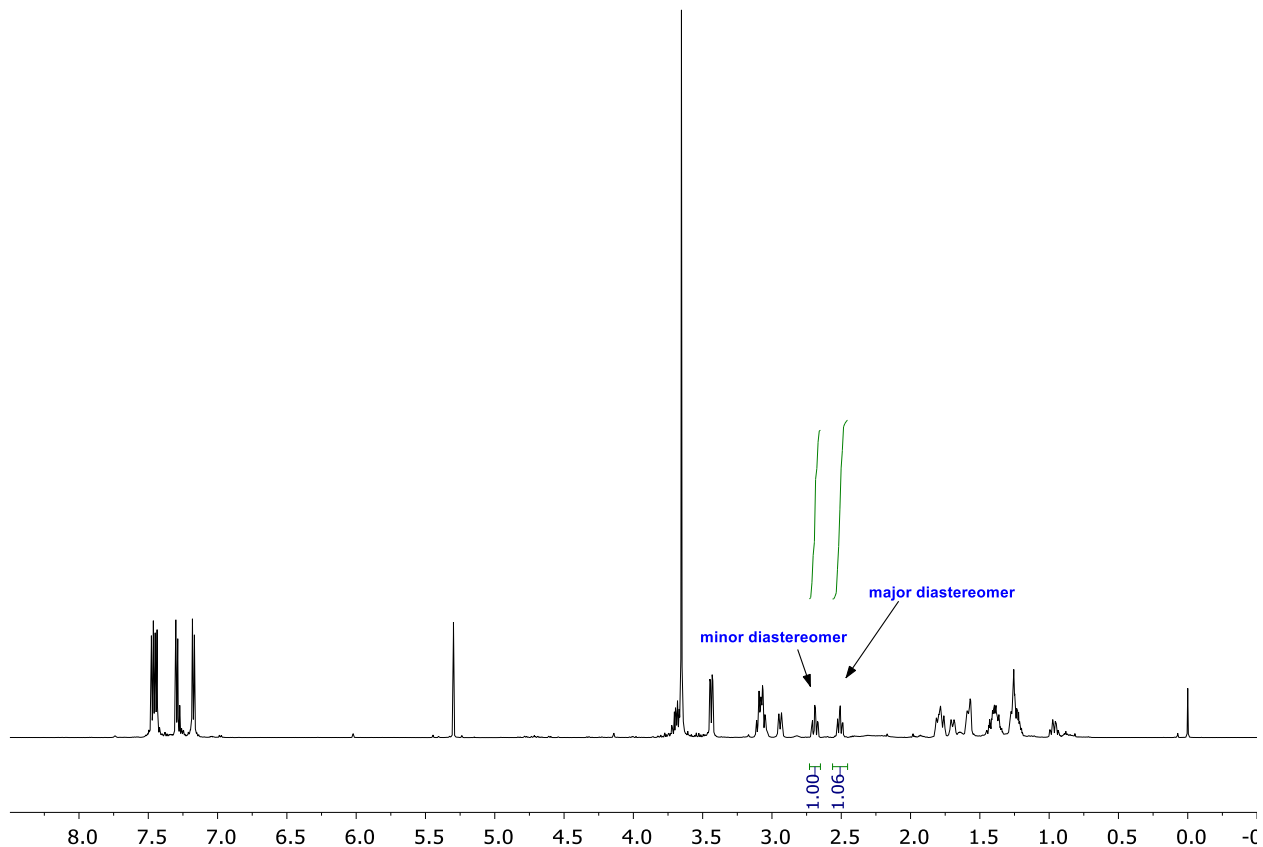


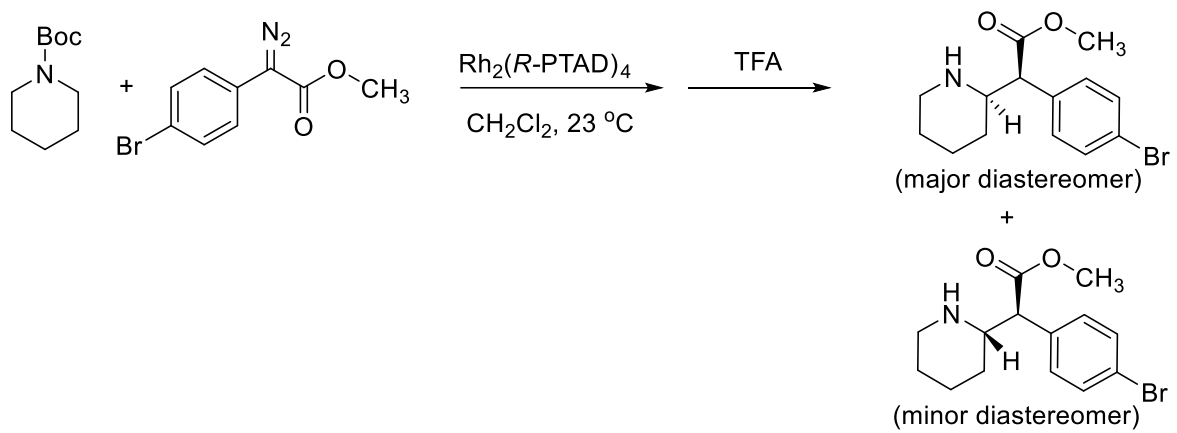
(Table S1, entry 1)



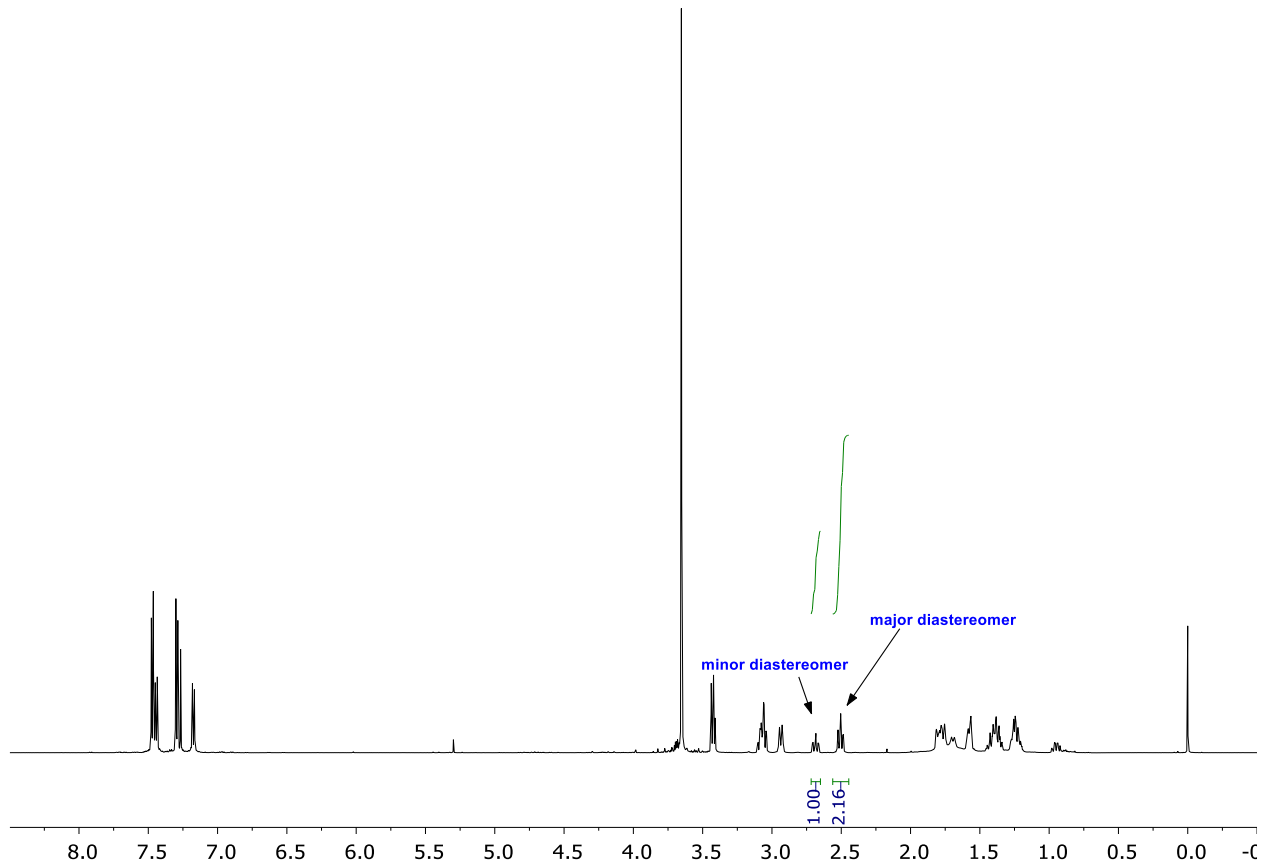


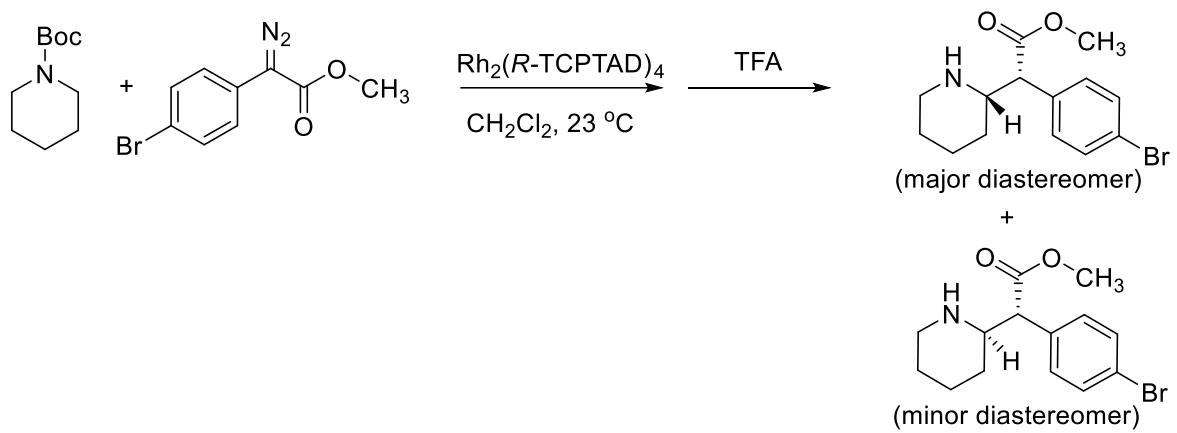
(Table 1, entry 1) (Table S1, entry 2)



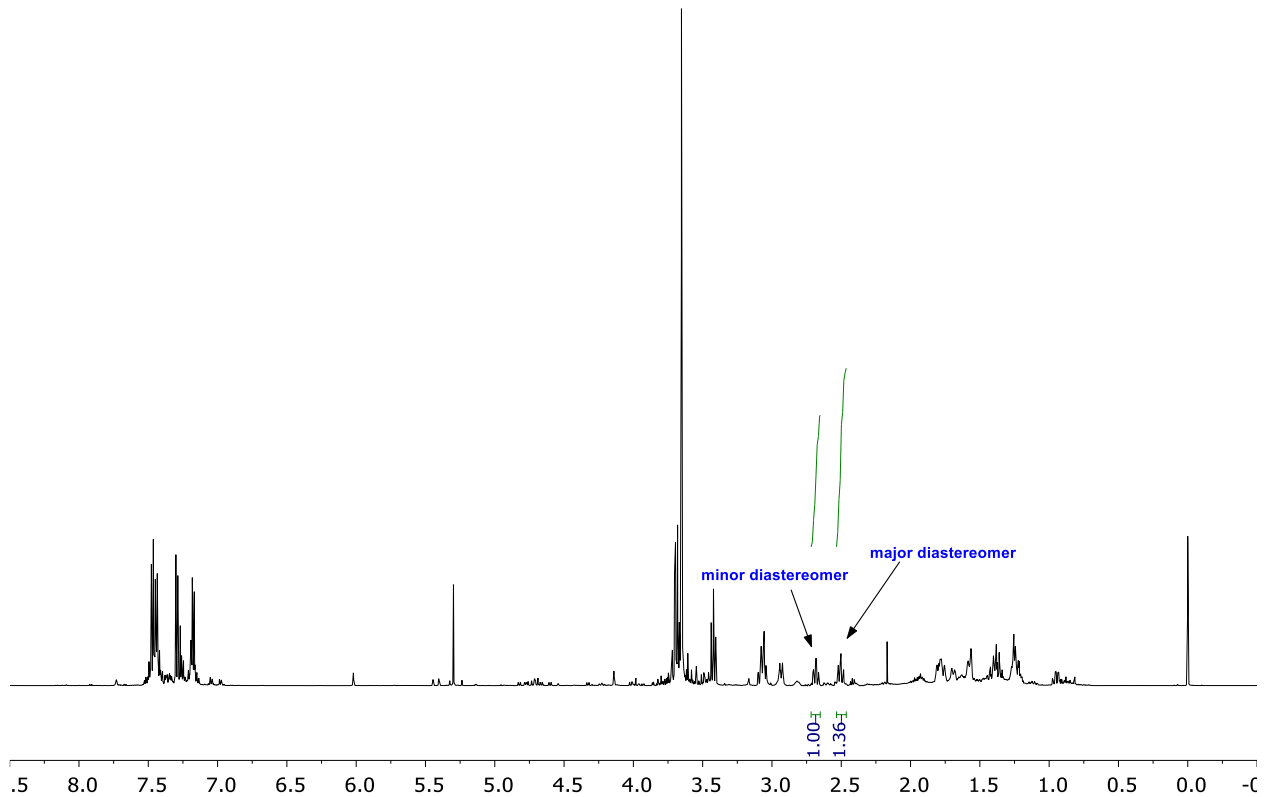


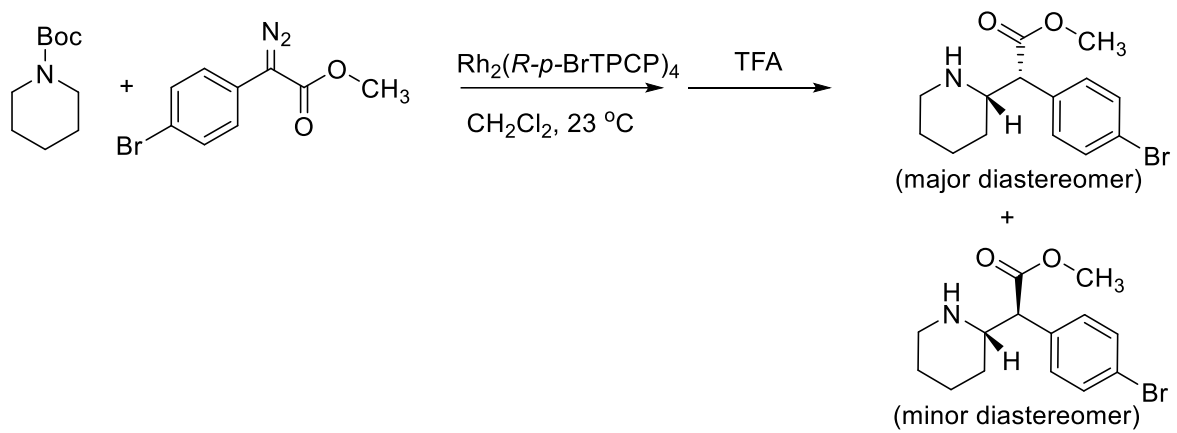
(Table S1, entry 3)



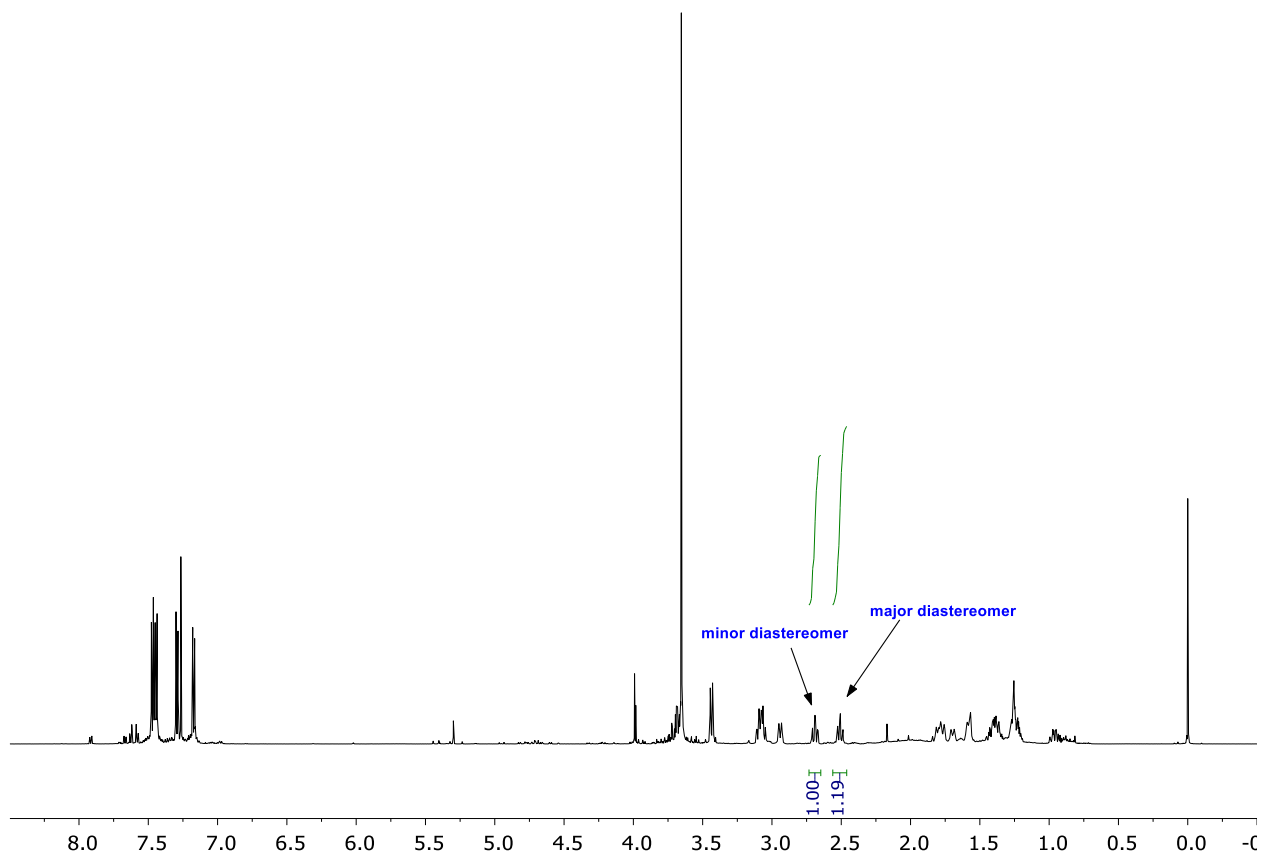


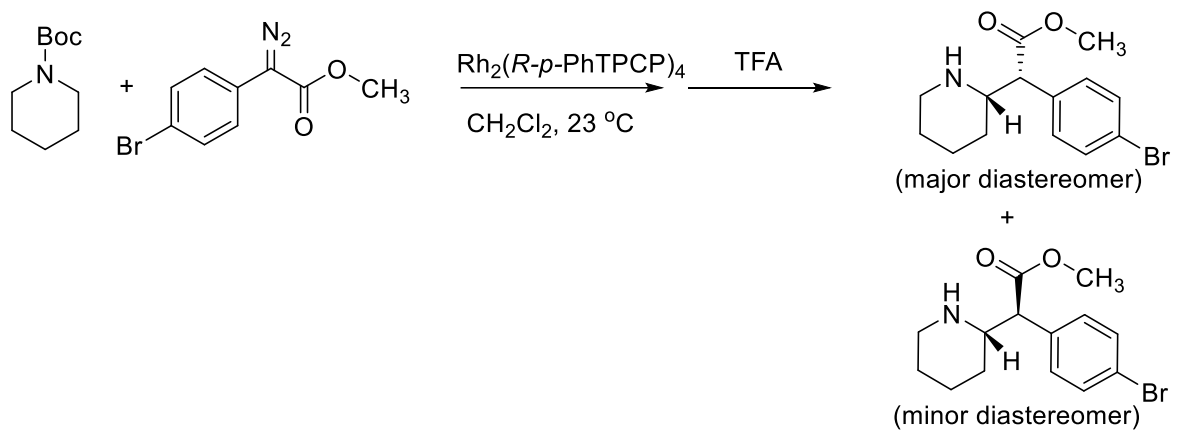
(Table 1, entry 2) (Table S1, entry 4)



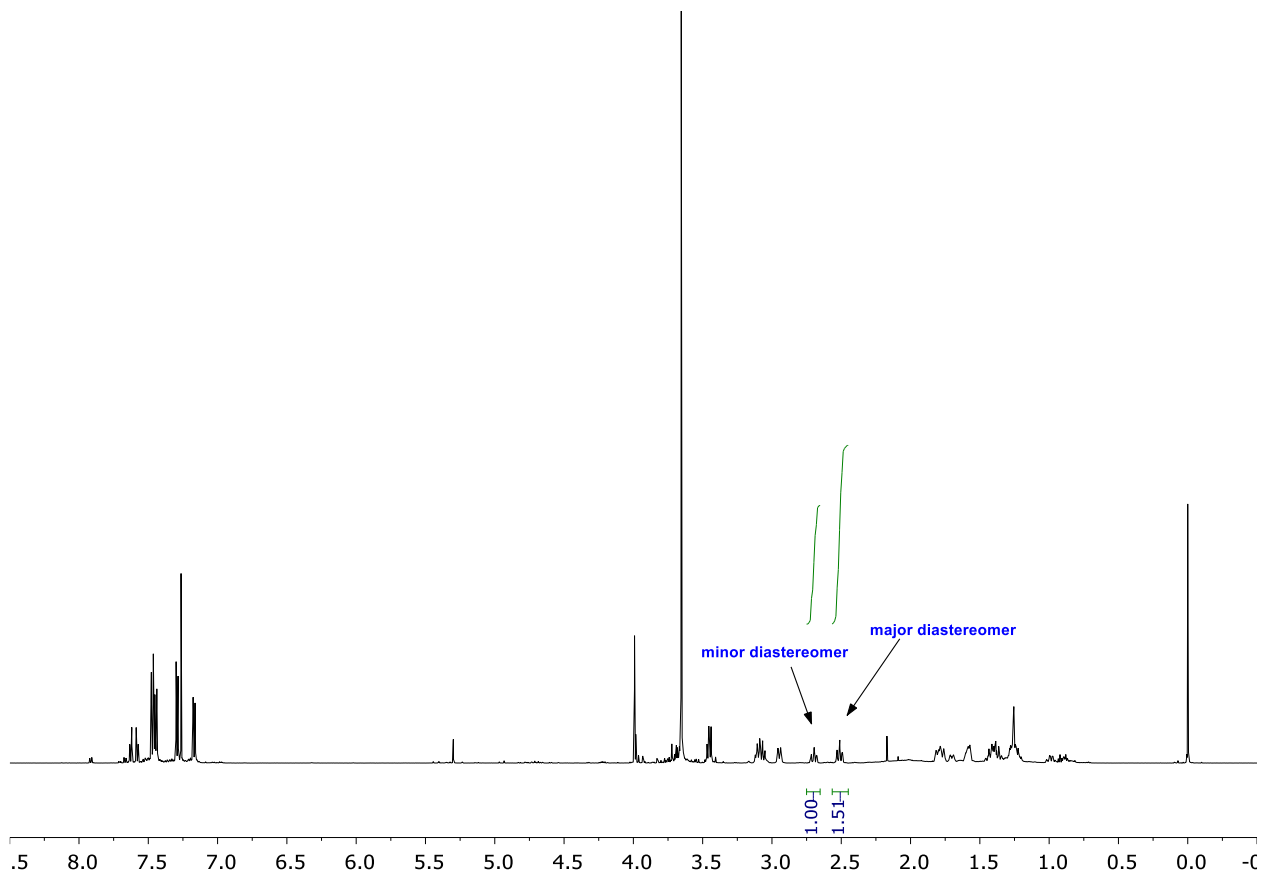


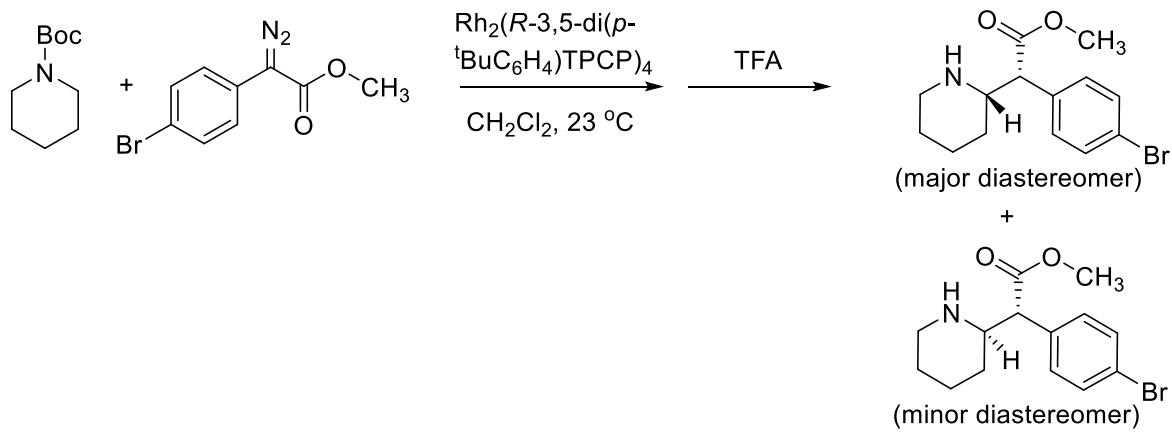
(Table 1, entry 3) (Table S1, entry 5)



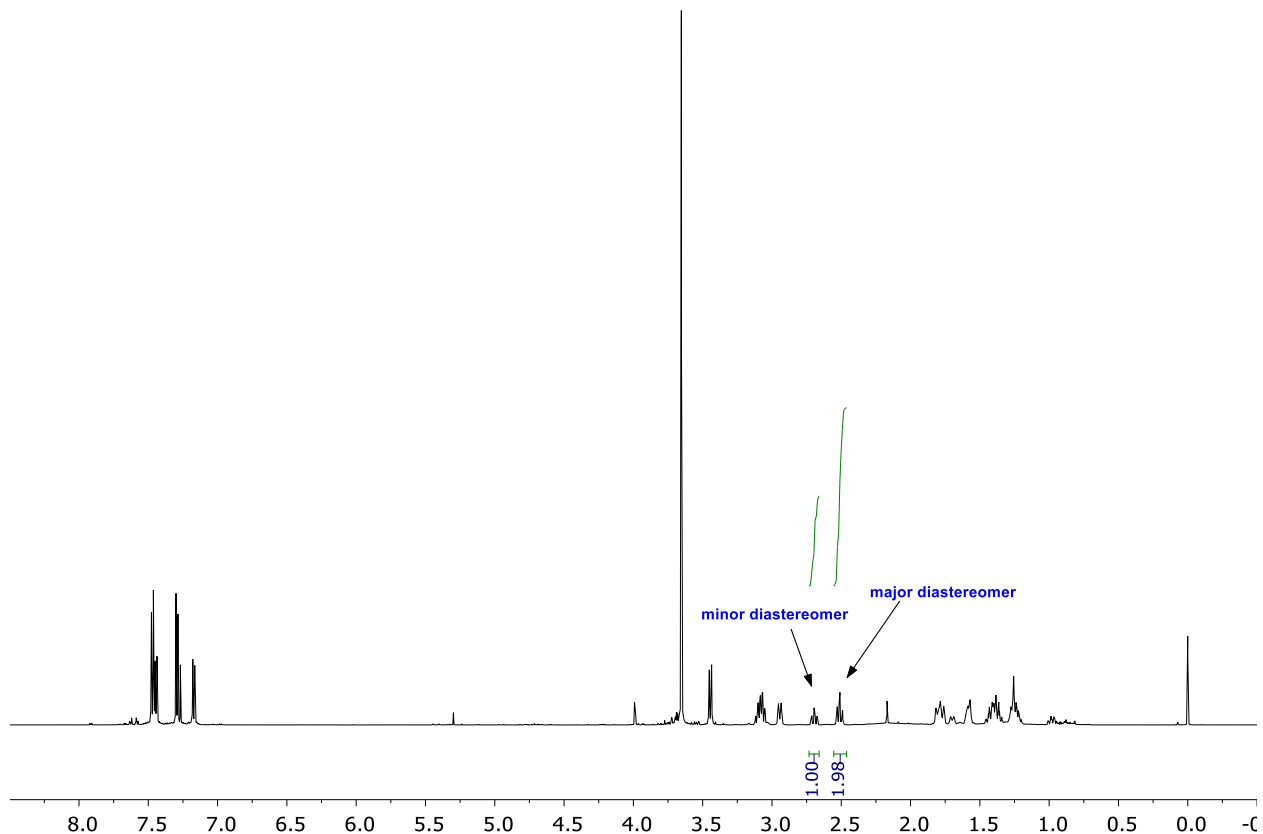


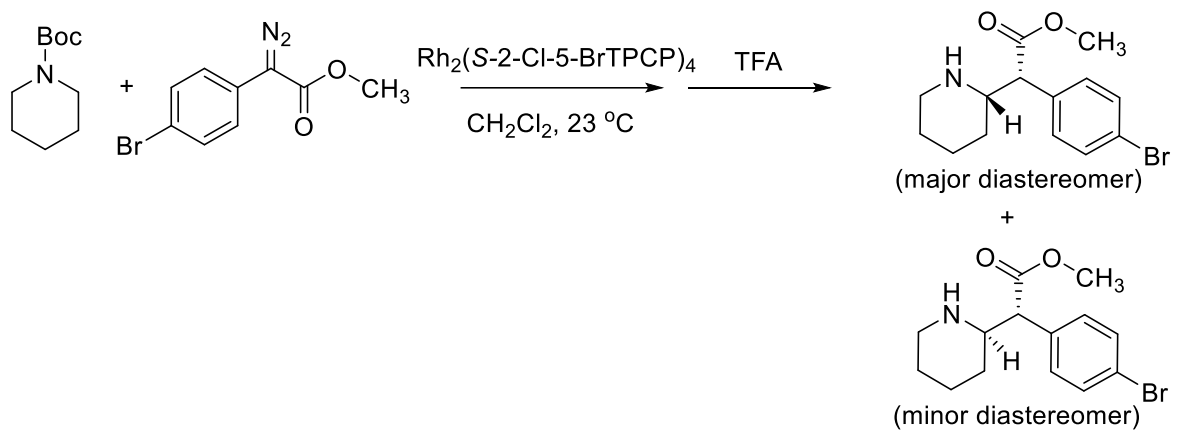
(Table S1, entry 6)



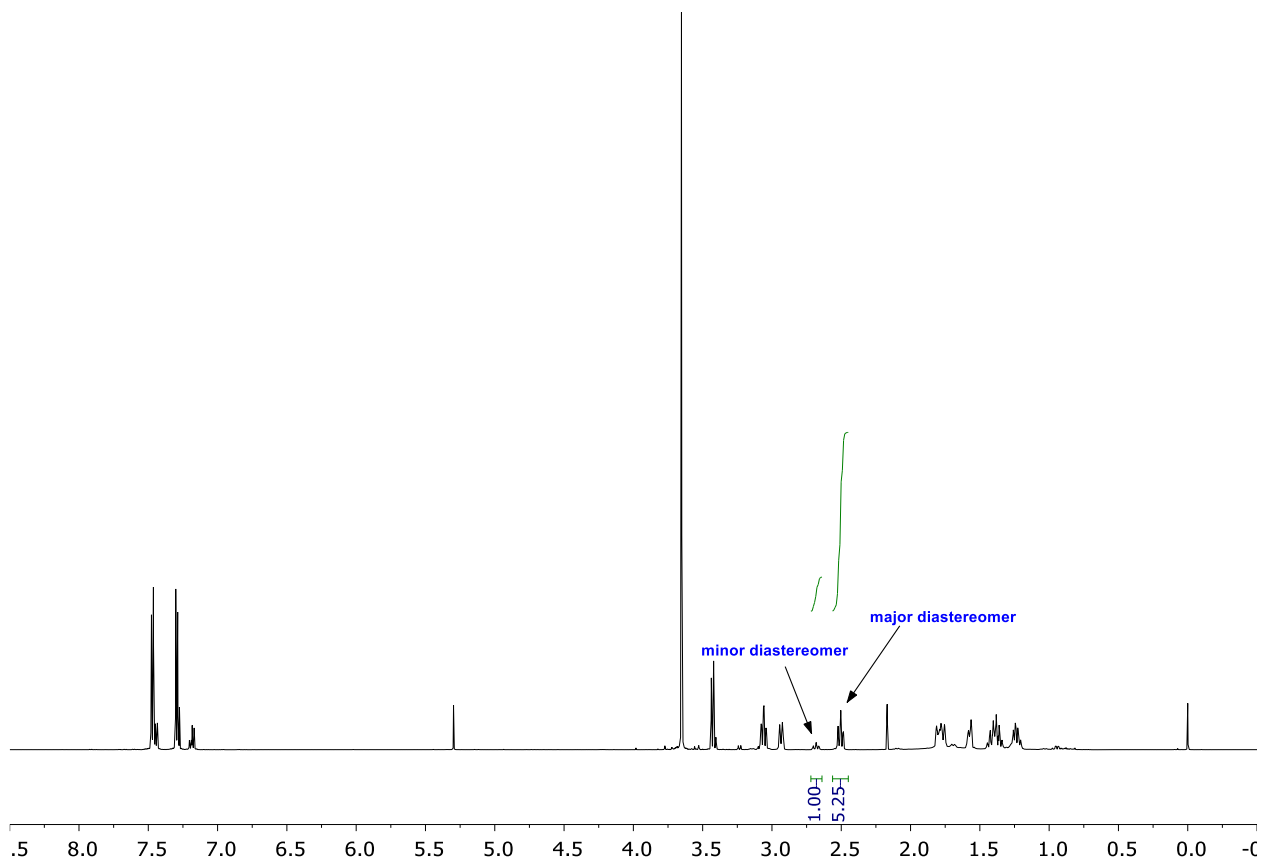


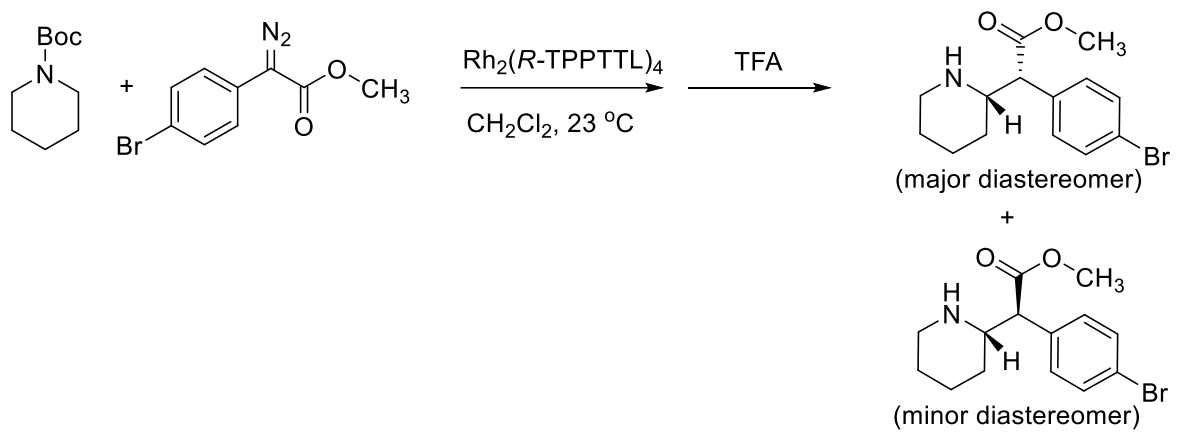
(Table S1, entry 7)



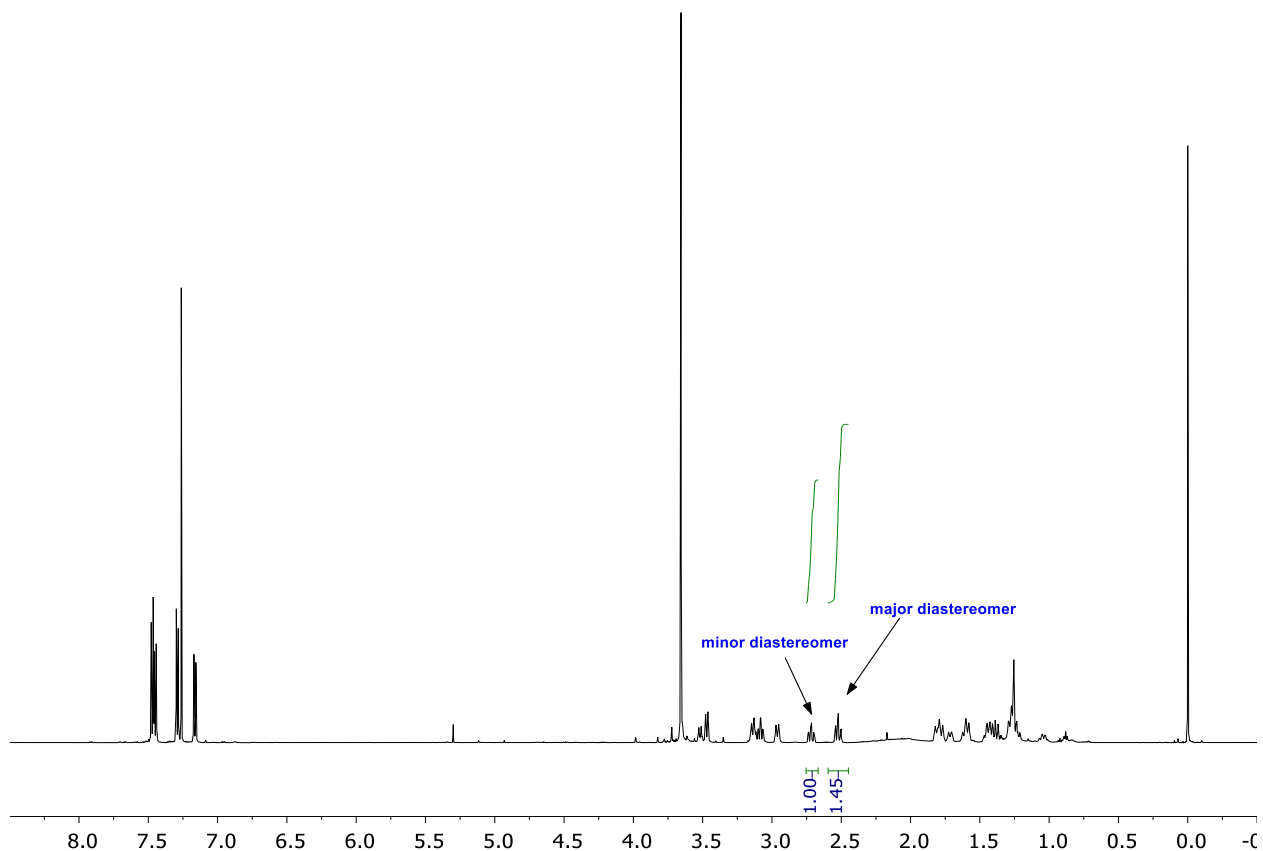


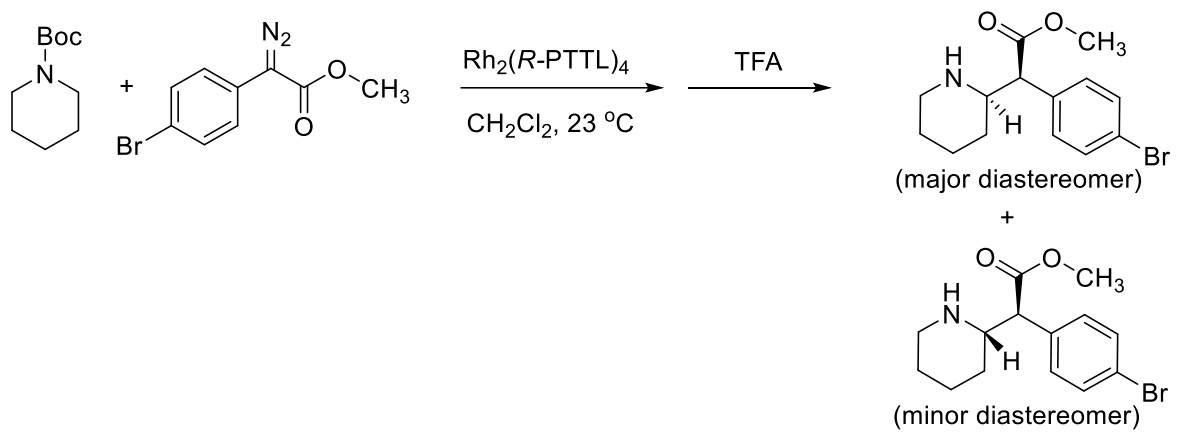
(Table 1, entry 5) (Table S1, entry 8)



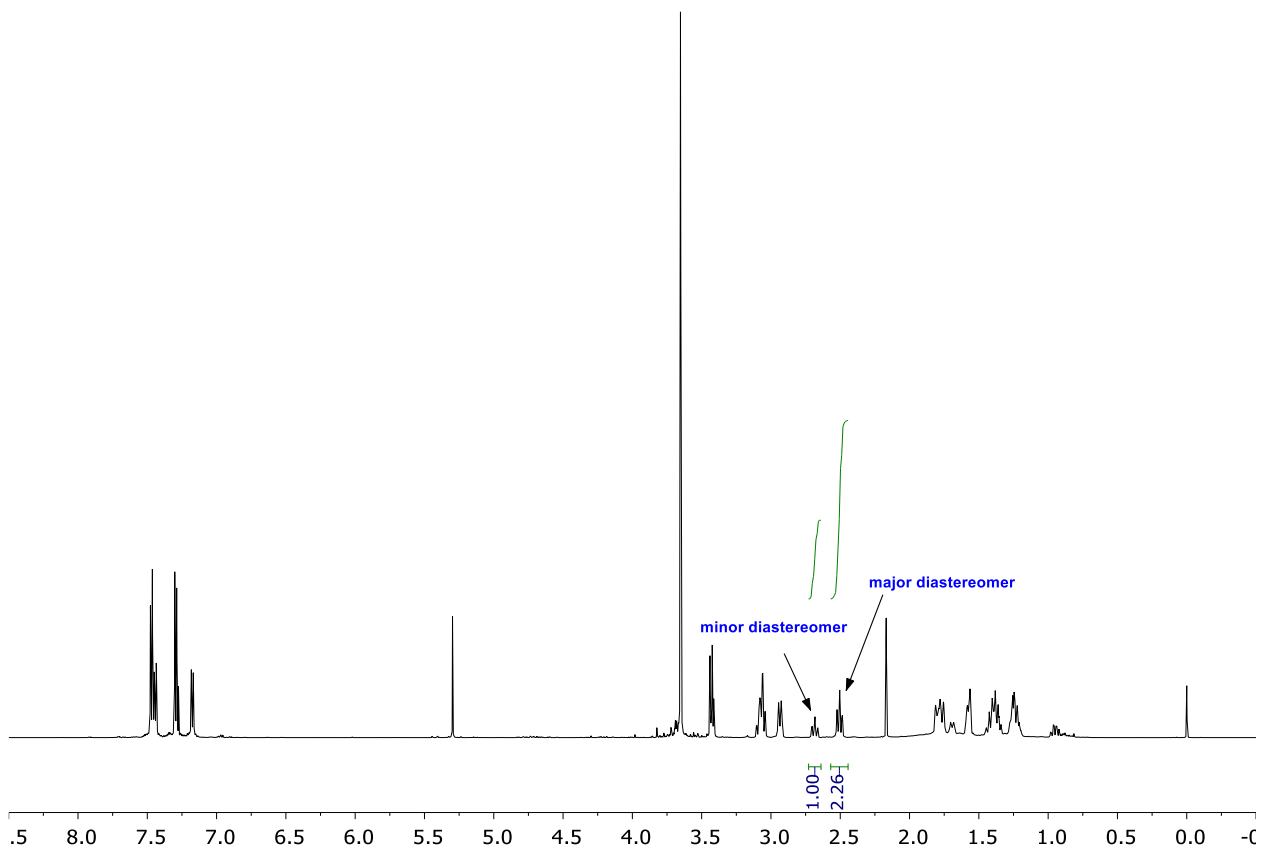


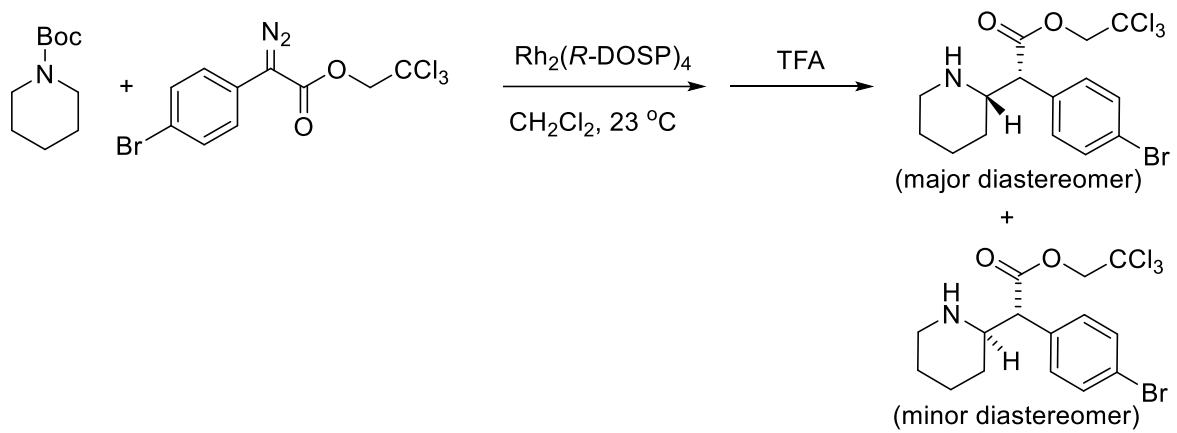
(Table S1, entry 9)



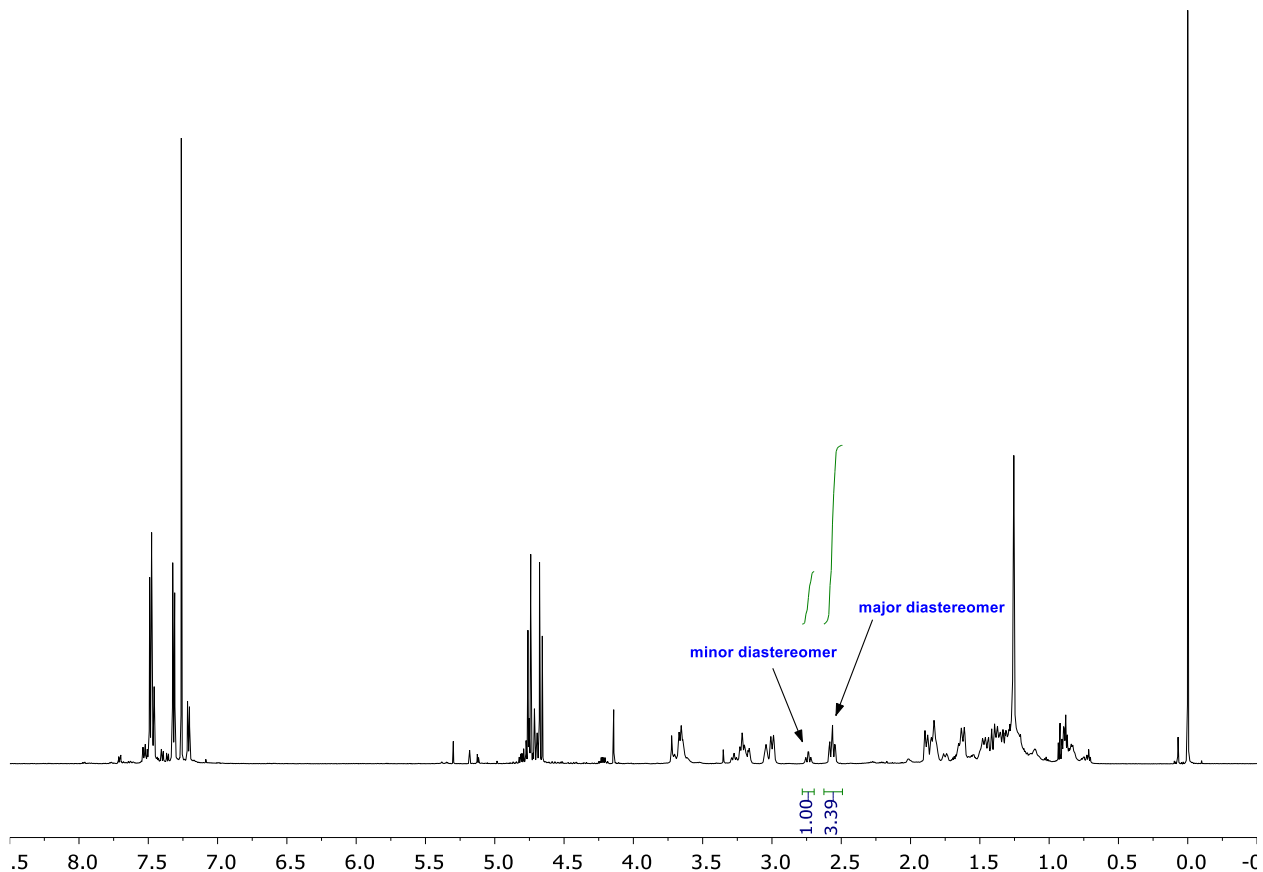


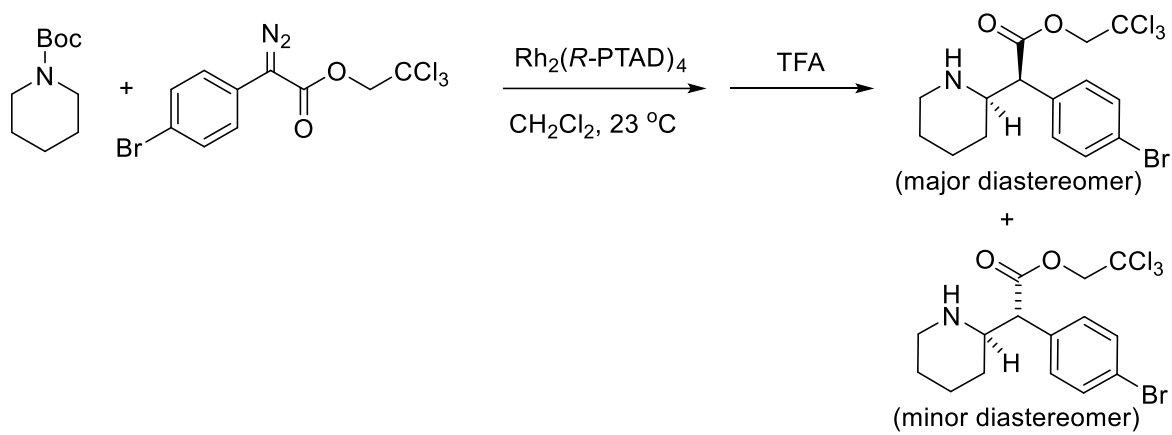
(Table S1, entry 10)



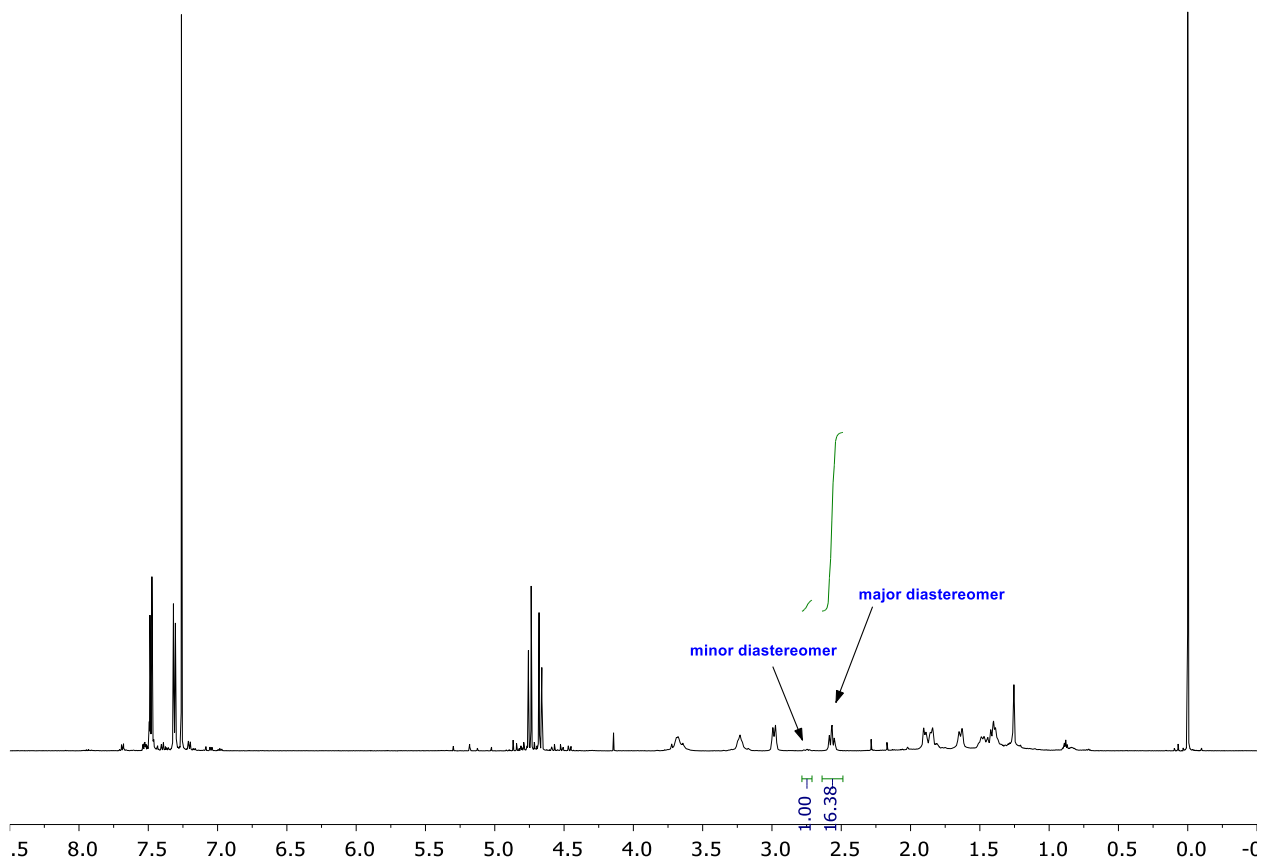


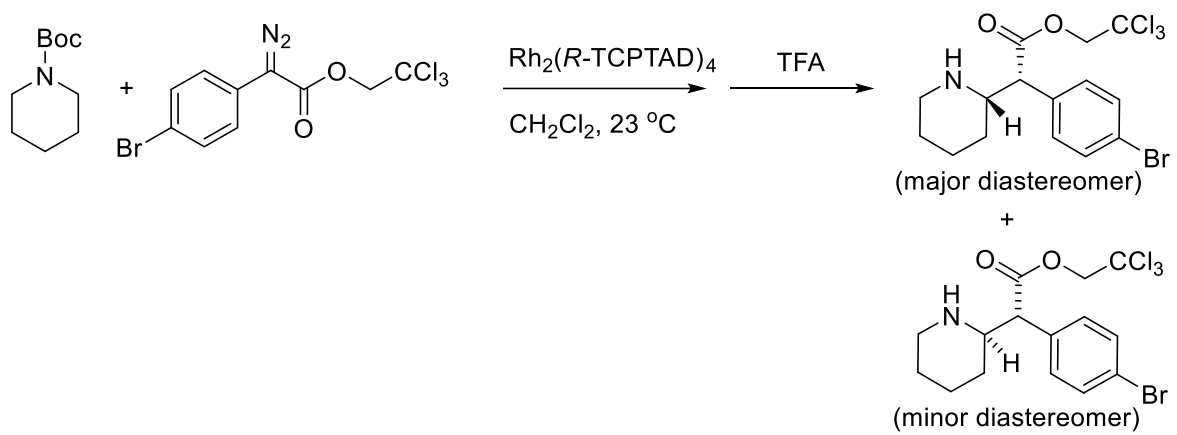
(Table S1, entry 11)



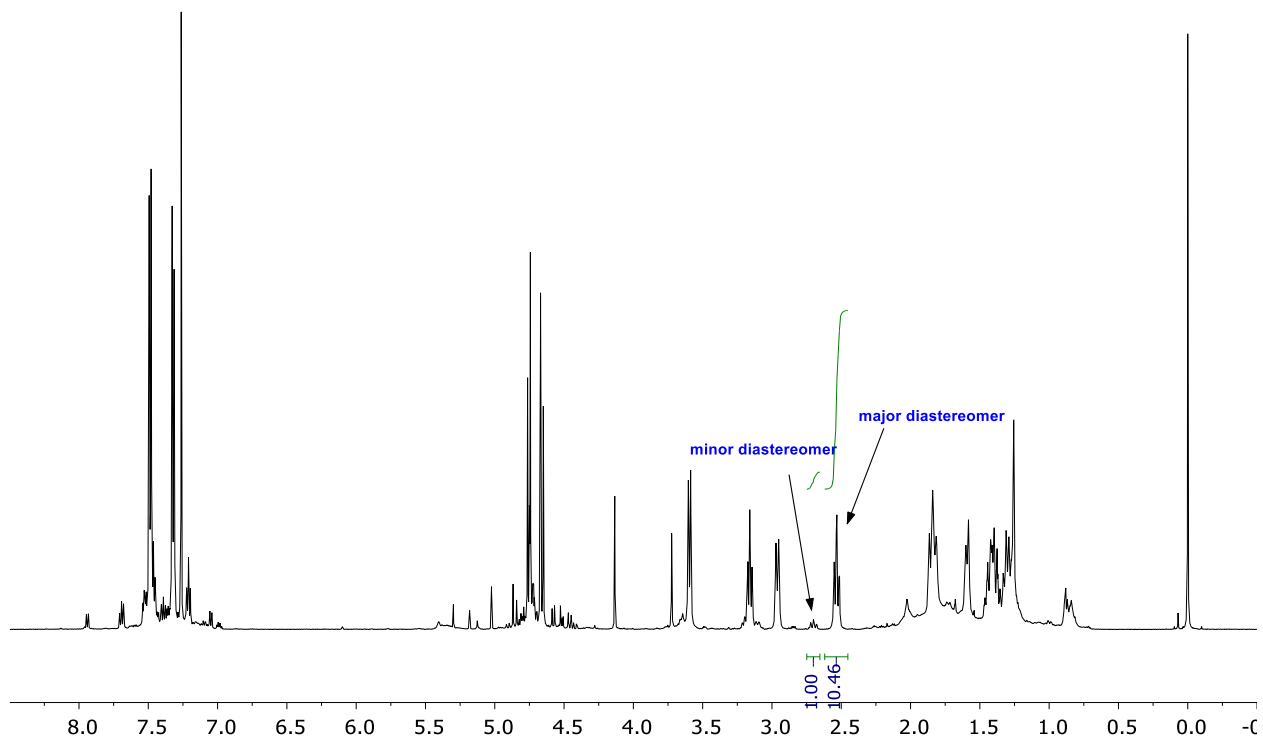


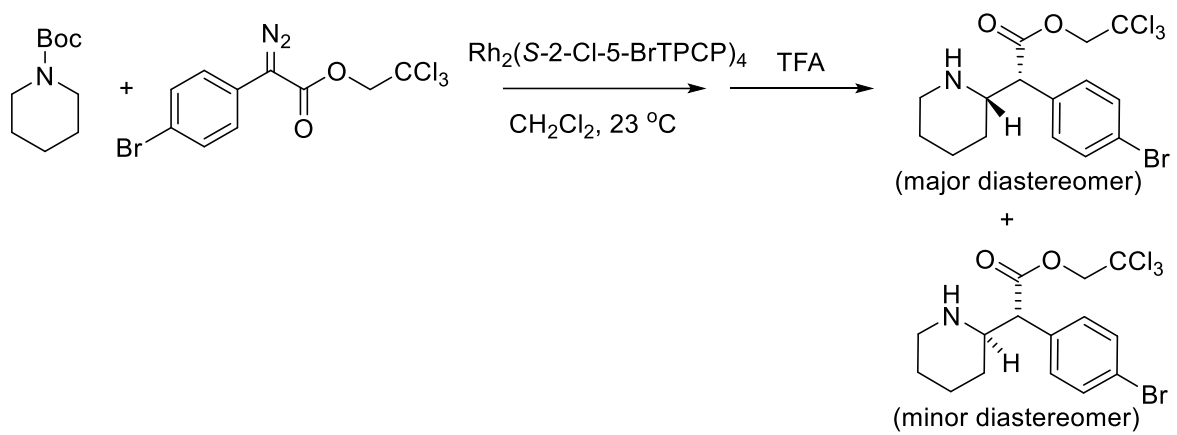
(Table S1, entry 12)



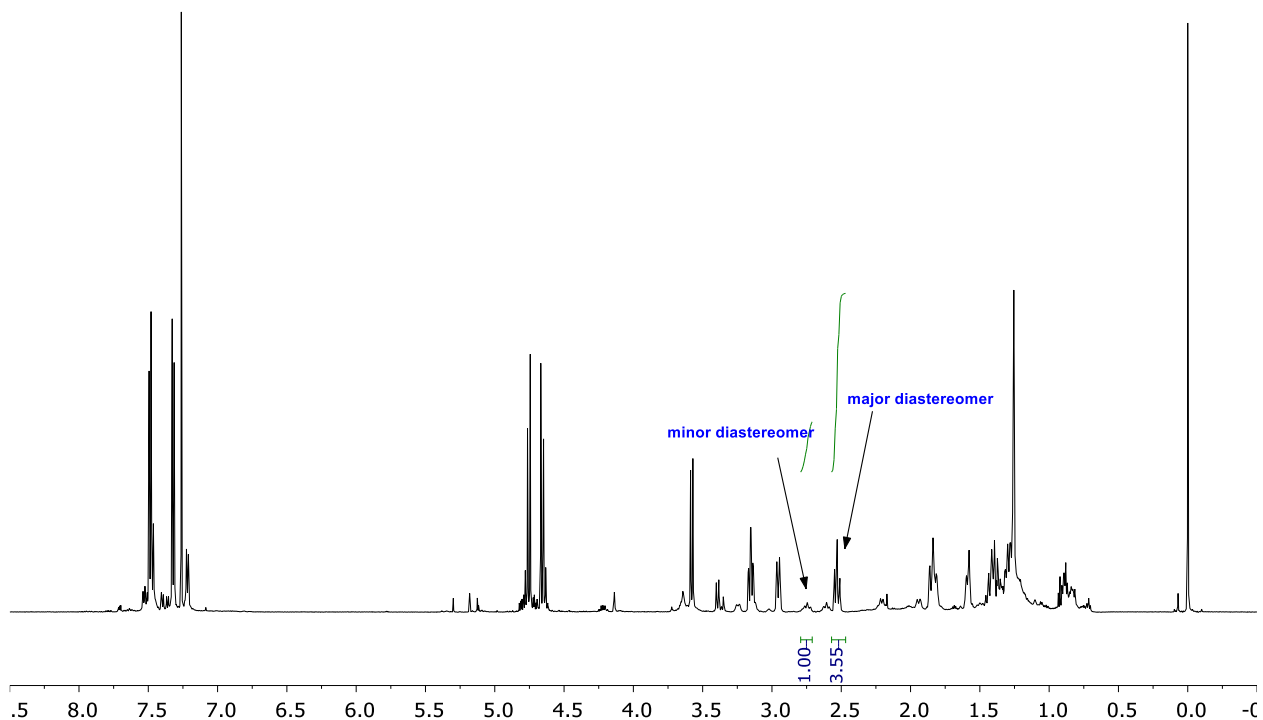


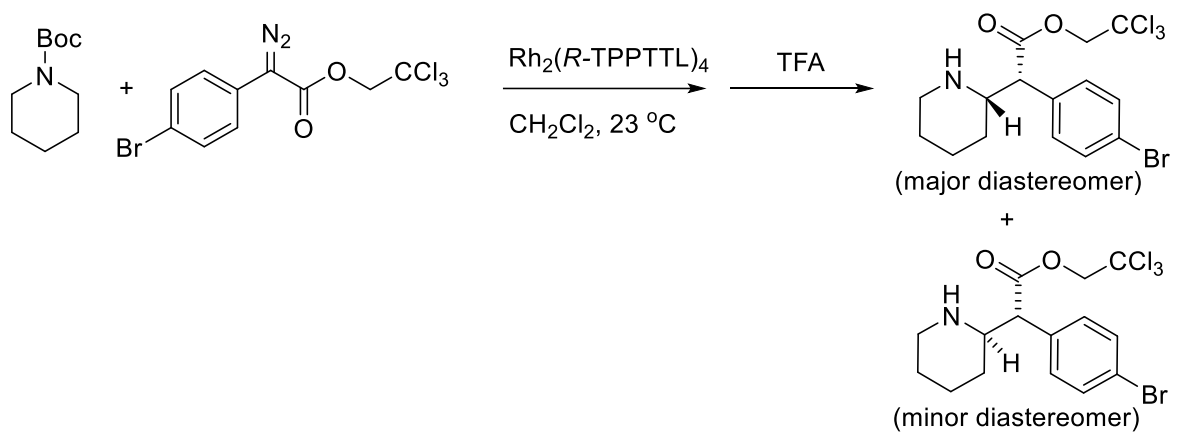
(Table 1, entry 7) (Table S1, entry 13)



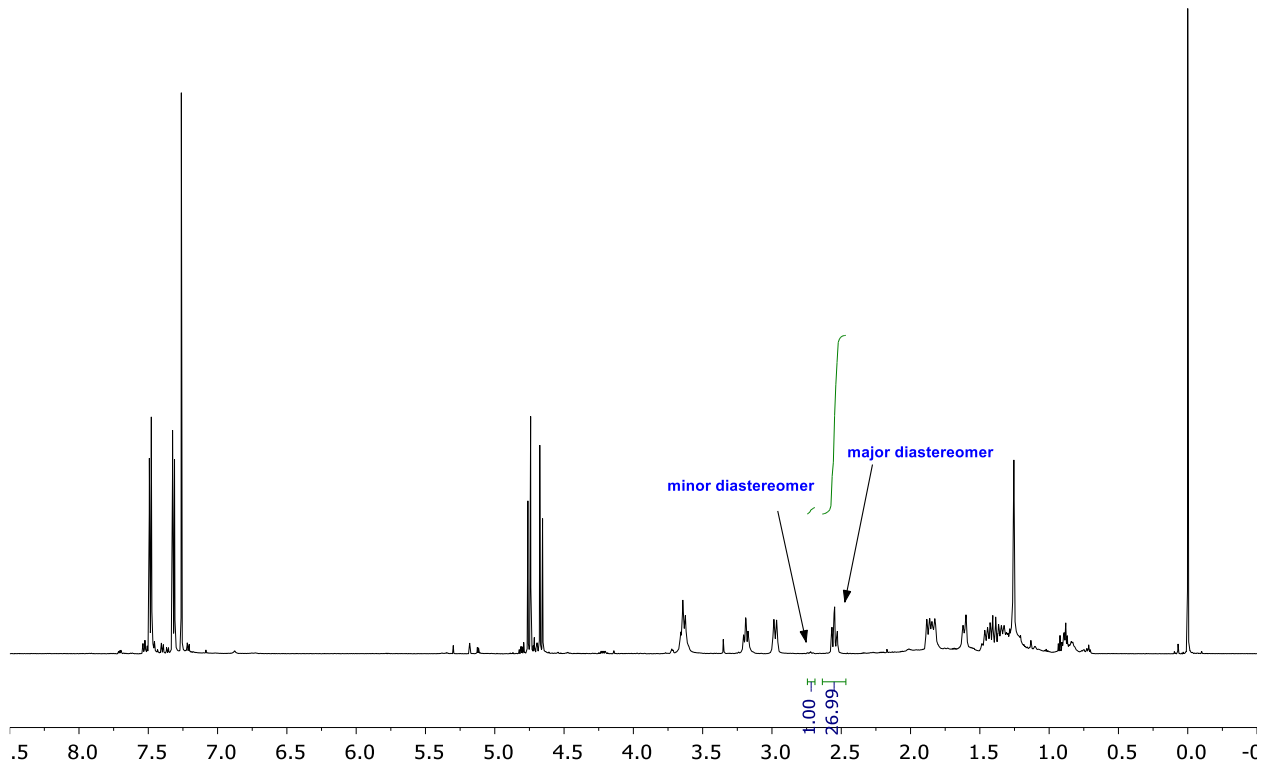


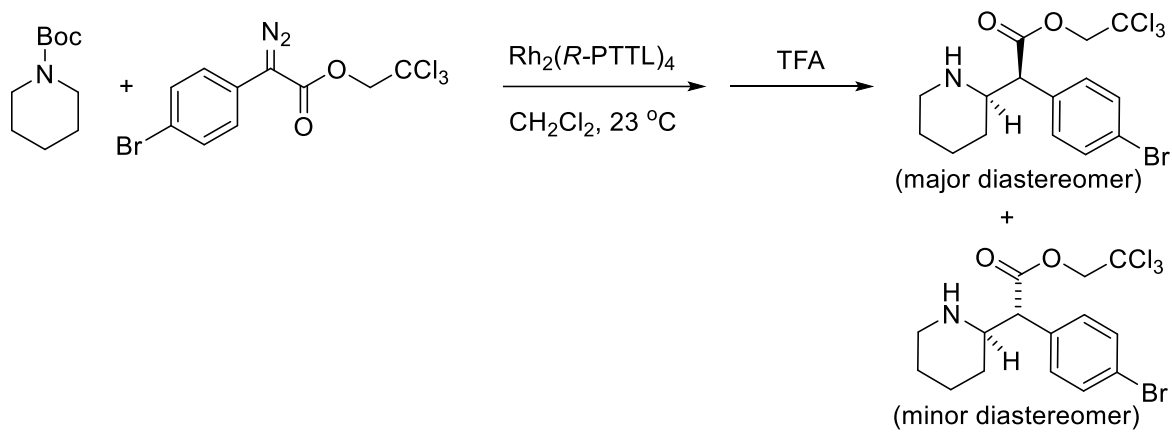
(Table 1, entry 6) (Table S1, entry 14)



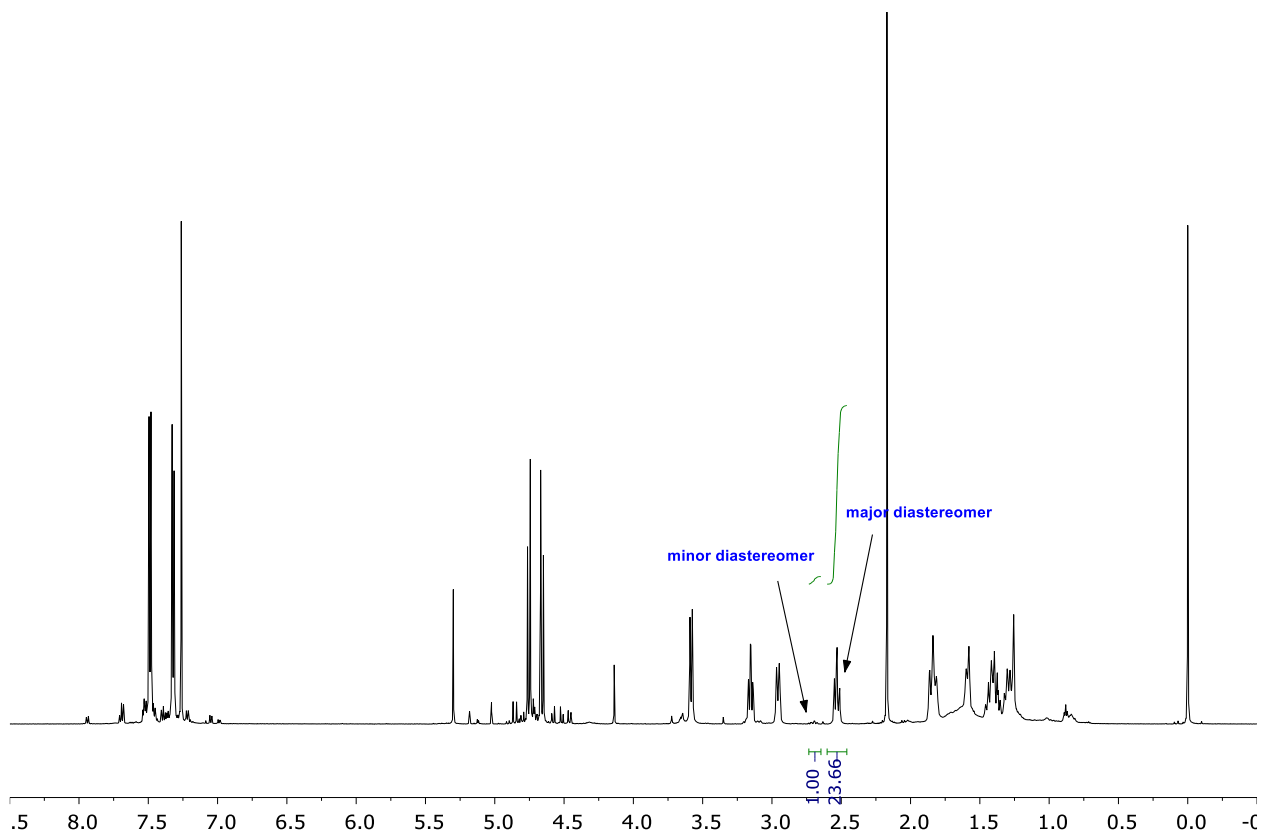


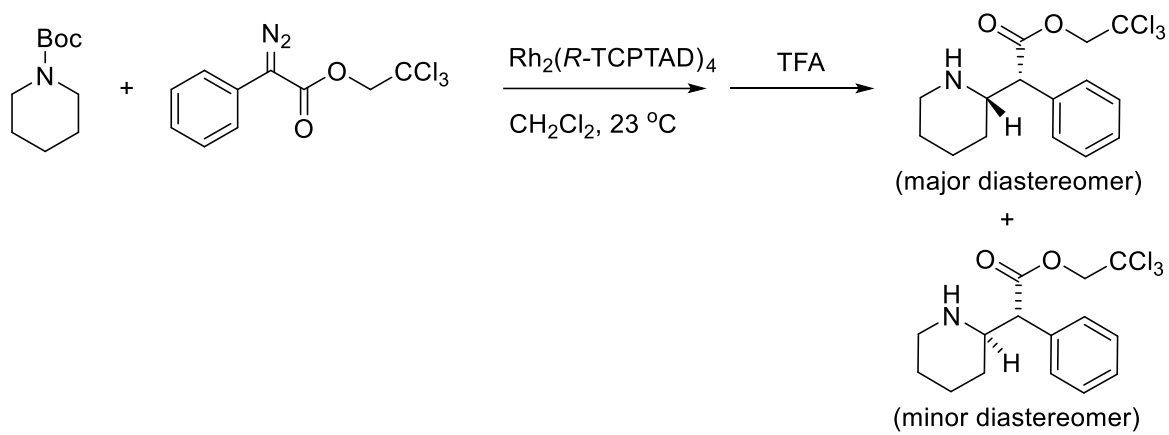
(Table 1, entry 8) (Table S1, entry 15)



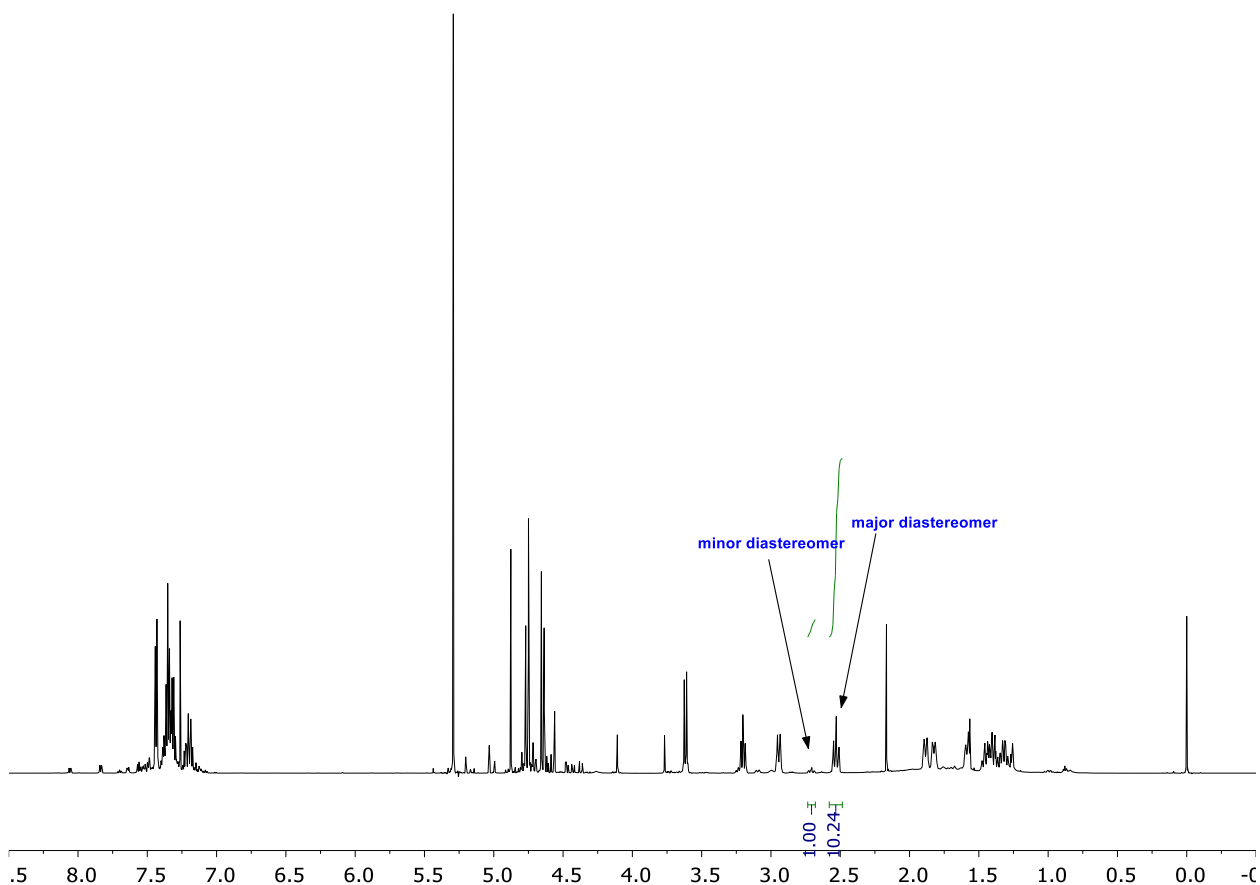


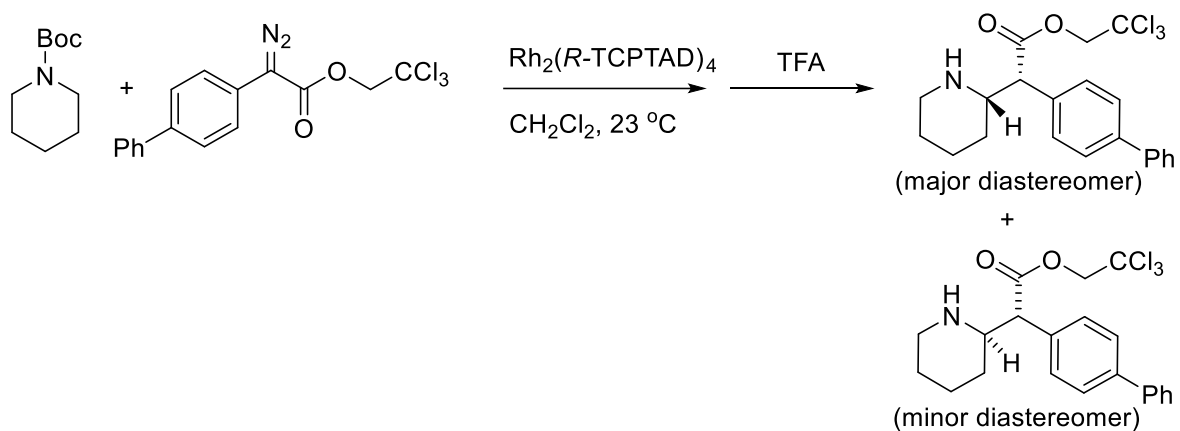
(Table S1, entry 16)



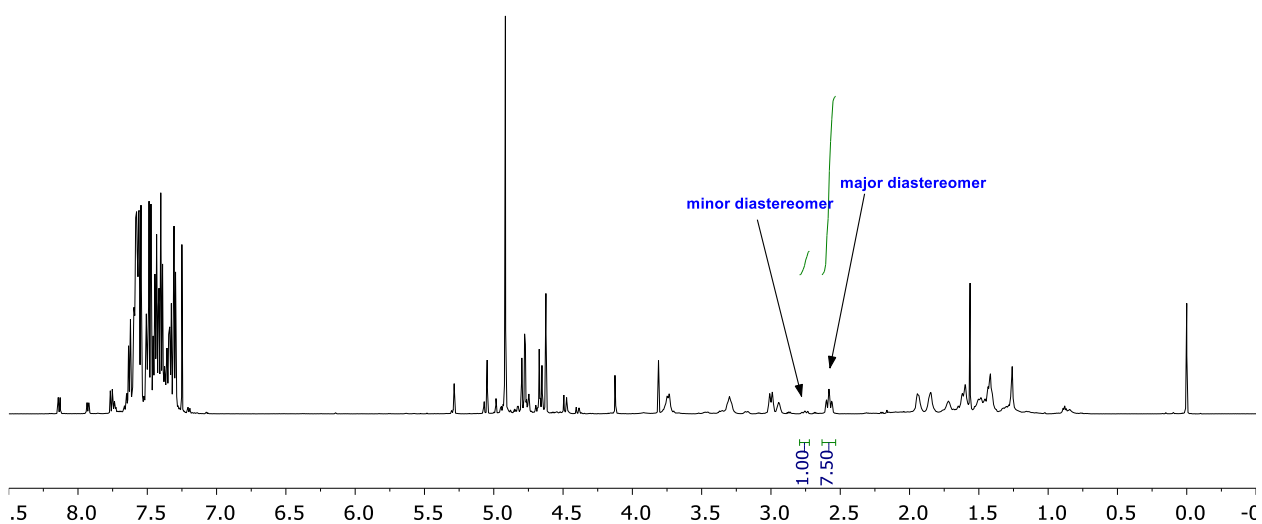


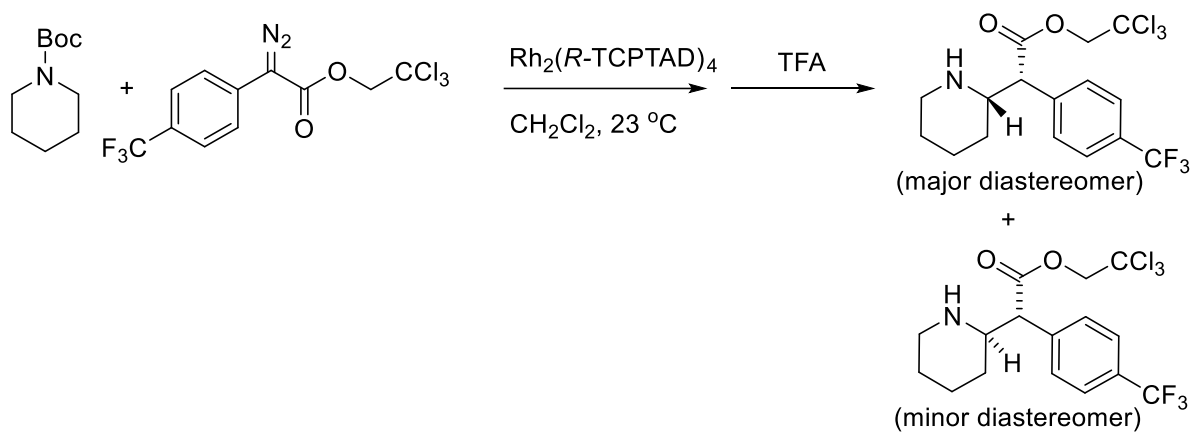
(Scheme 2, 5b)



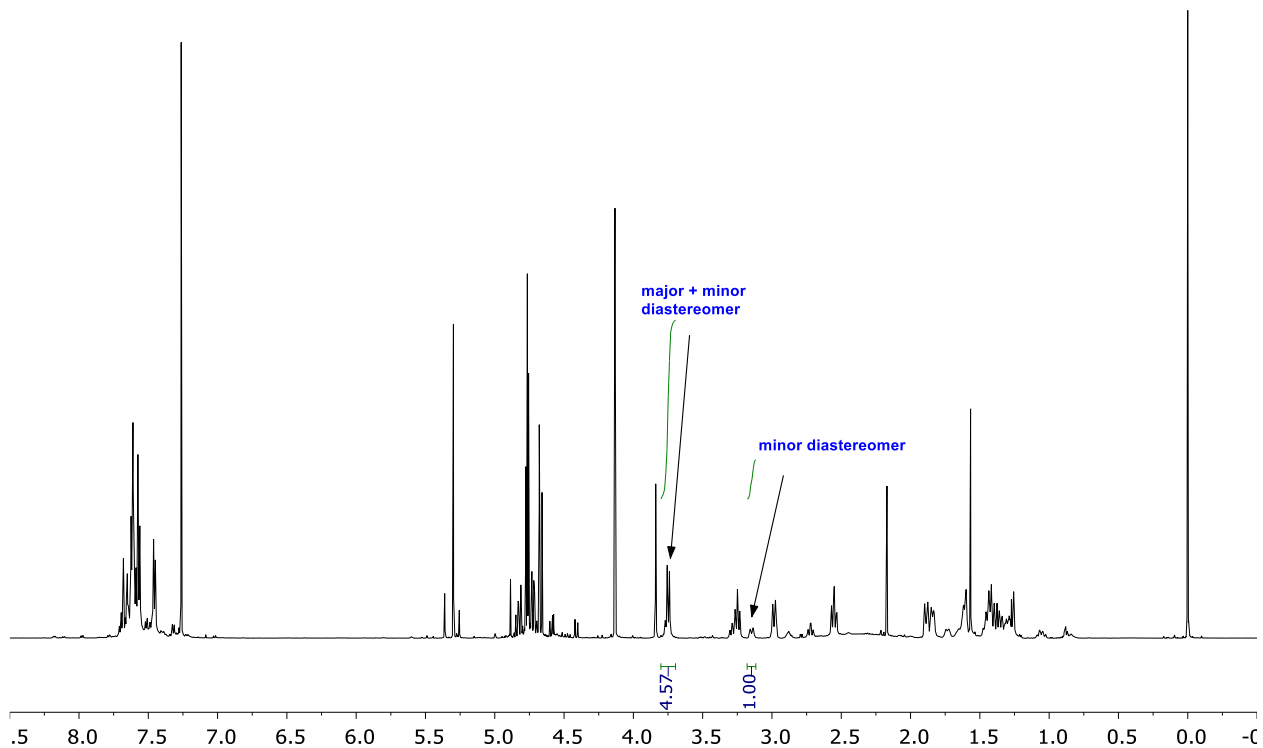


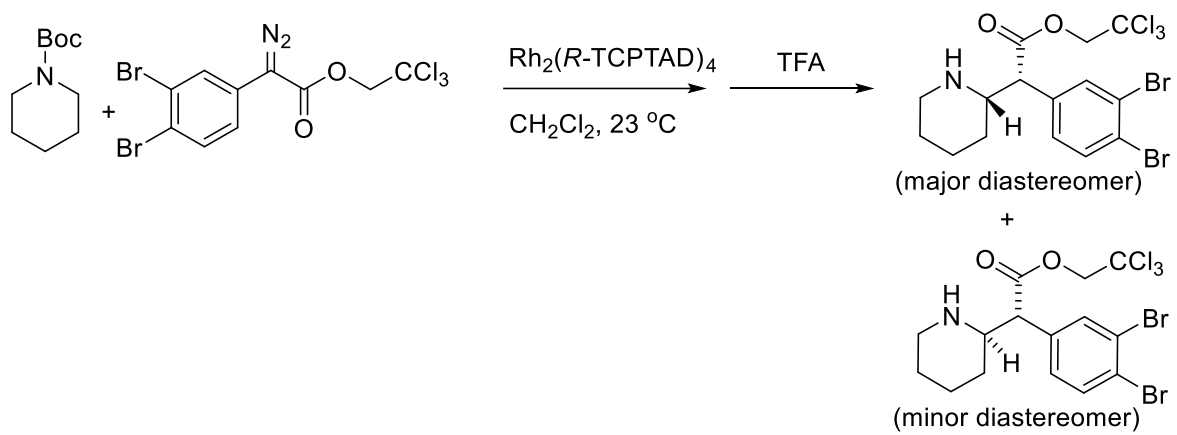
(Scheme 2, 5c)



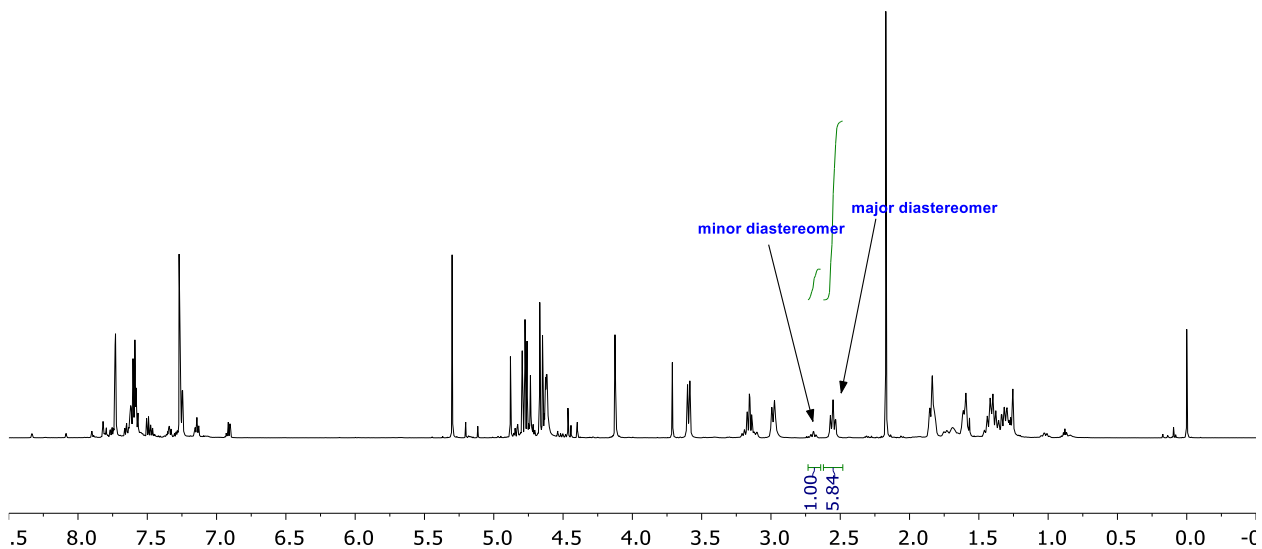


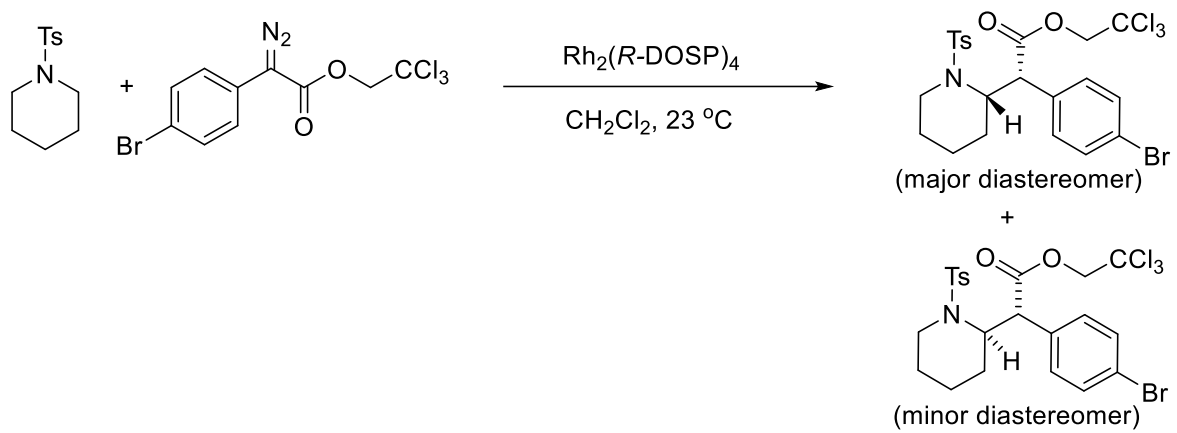
(Scheme 2, 5d)



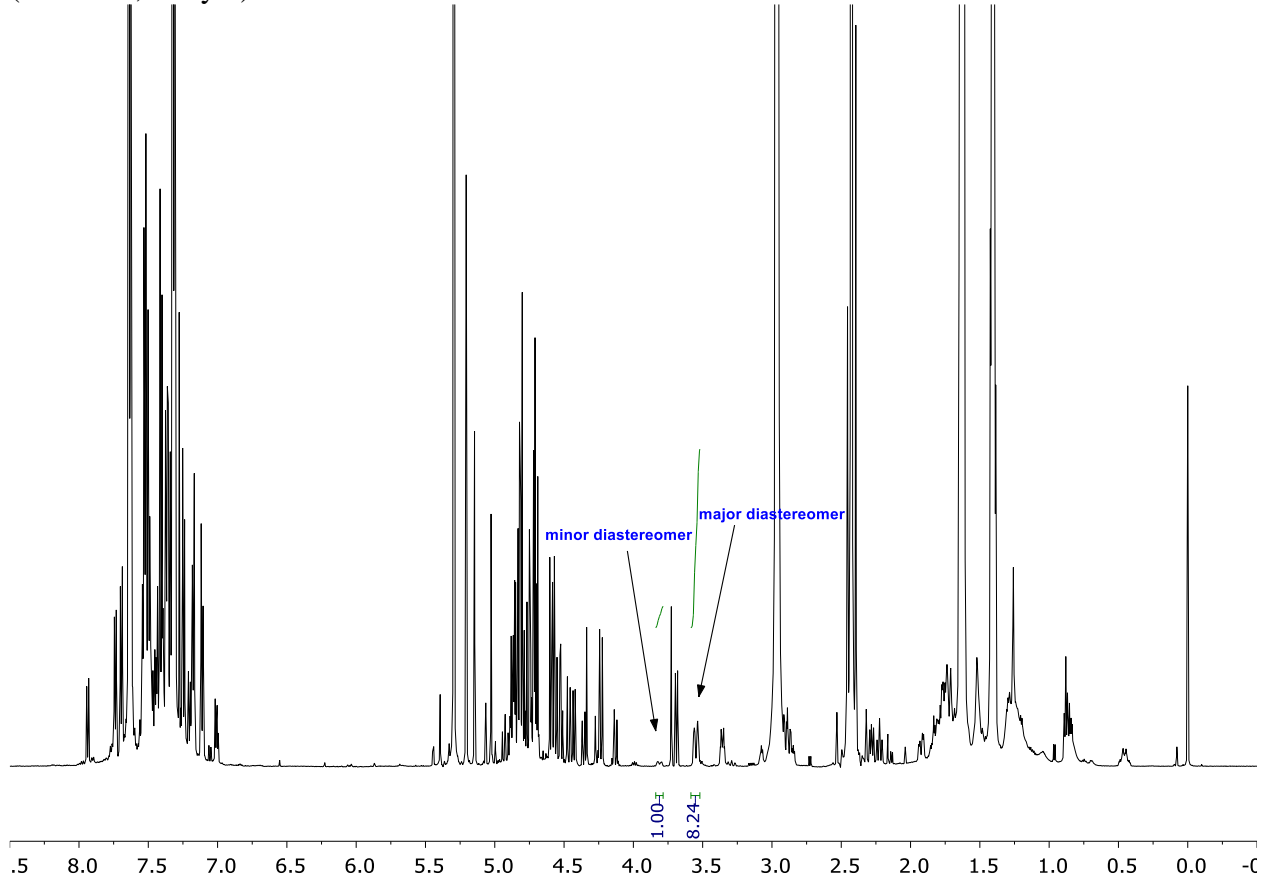


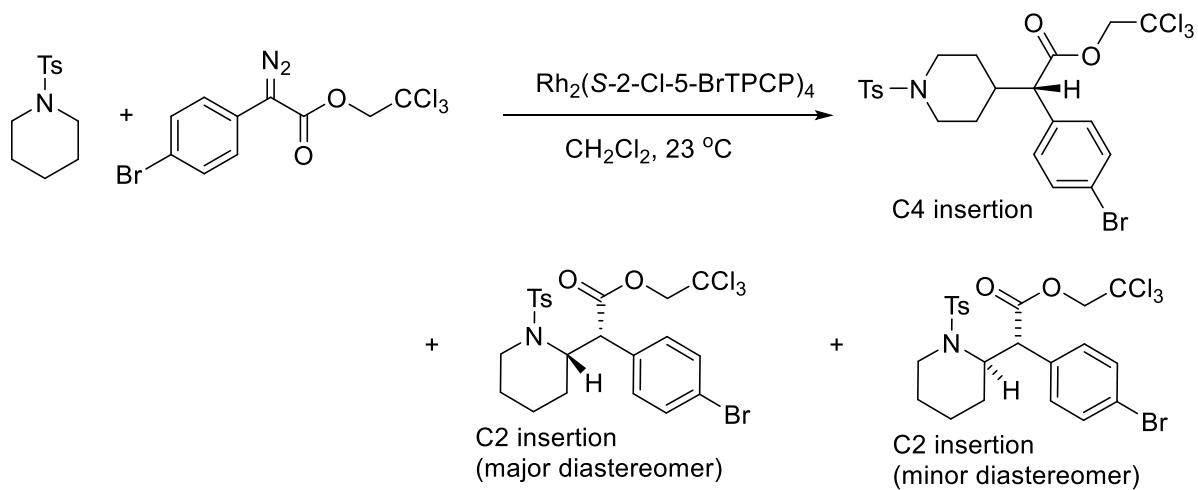
(Scheme 2, 5e)



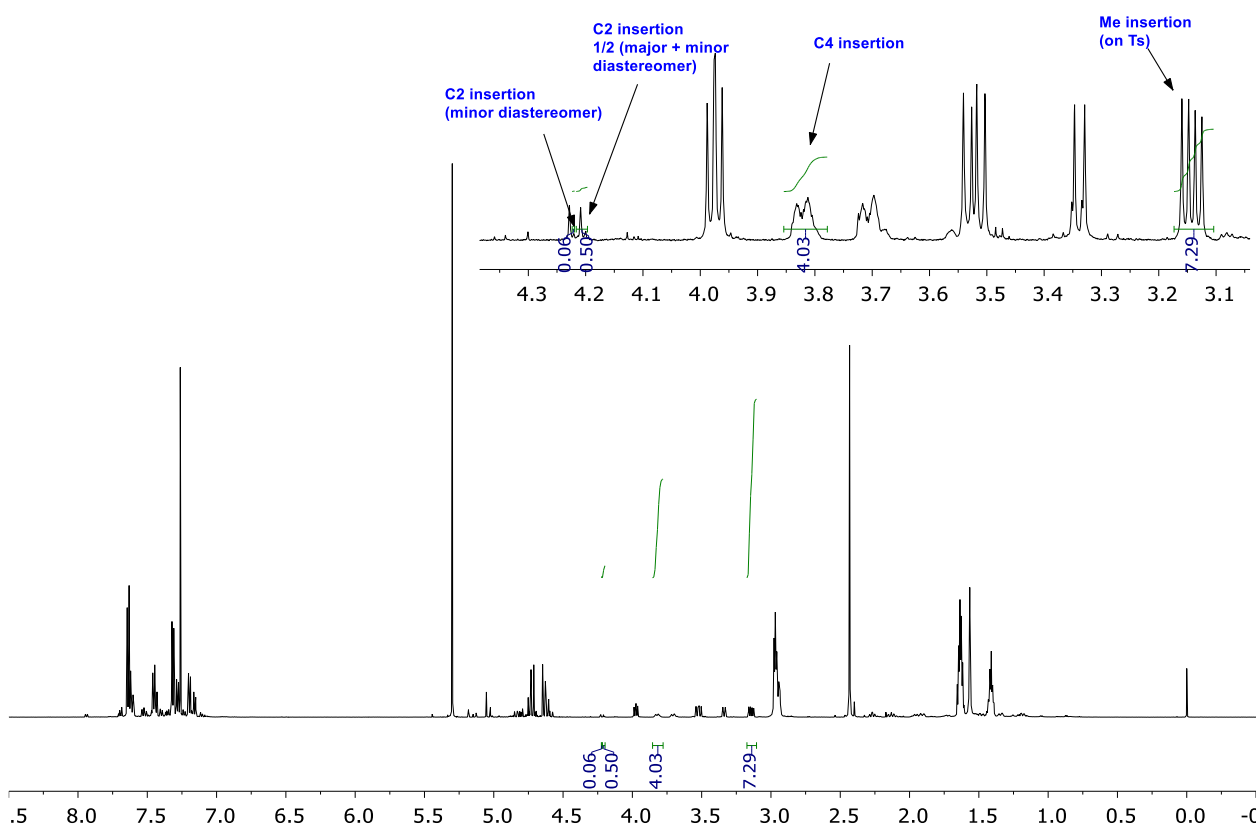


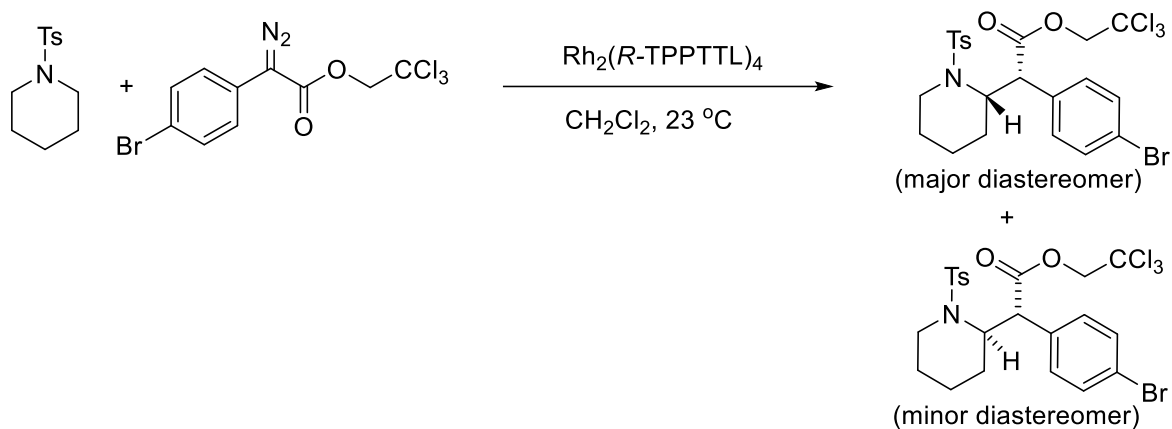
(Table S2, entry 1)



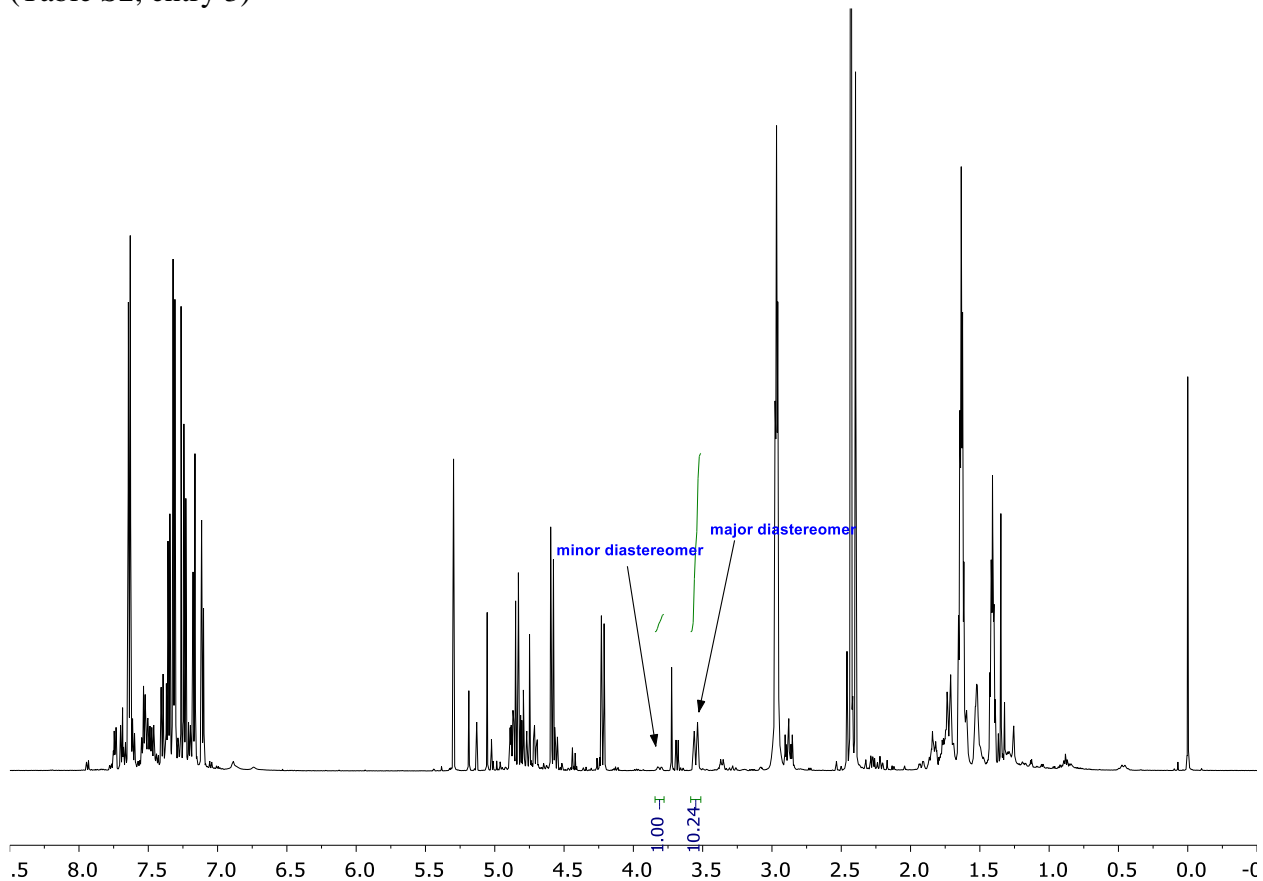


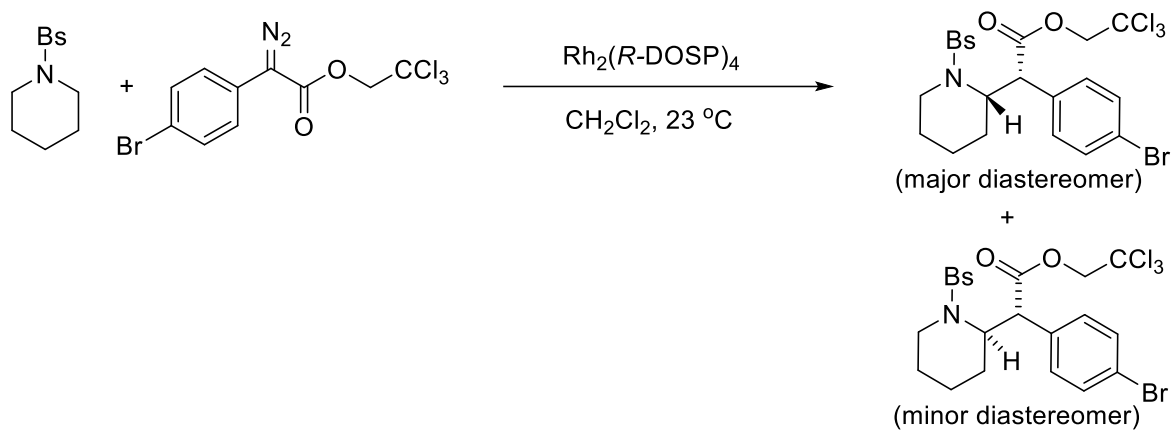
(Table S2, entry 2)



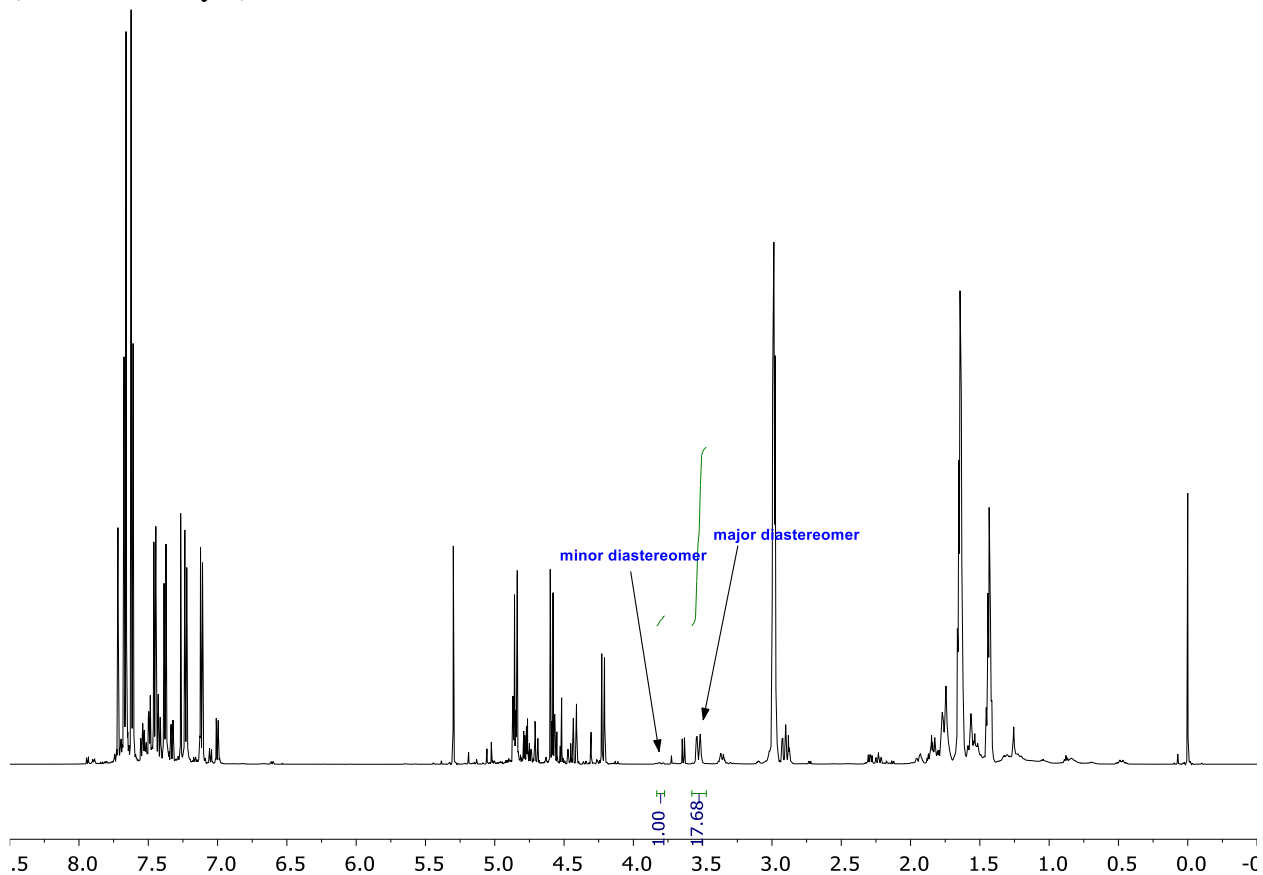


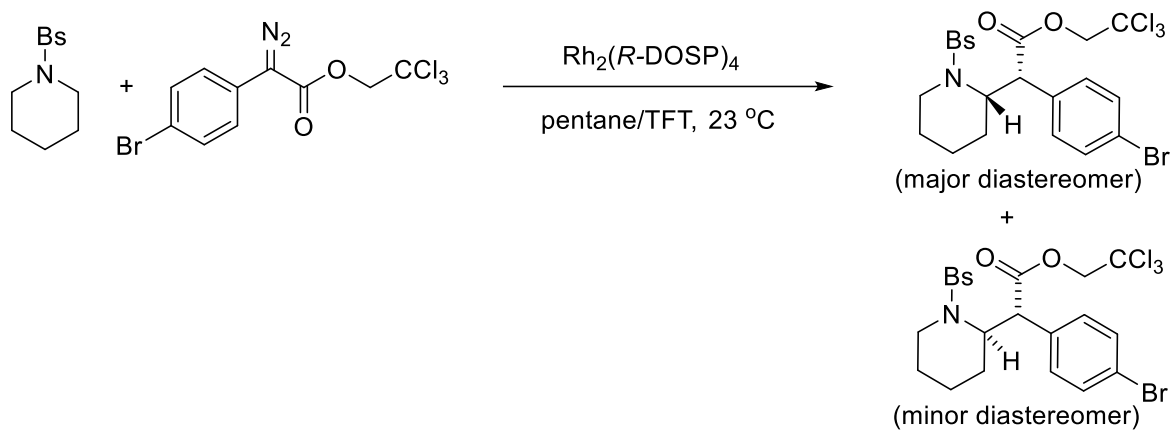
(Table S2, entry 3)



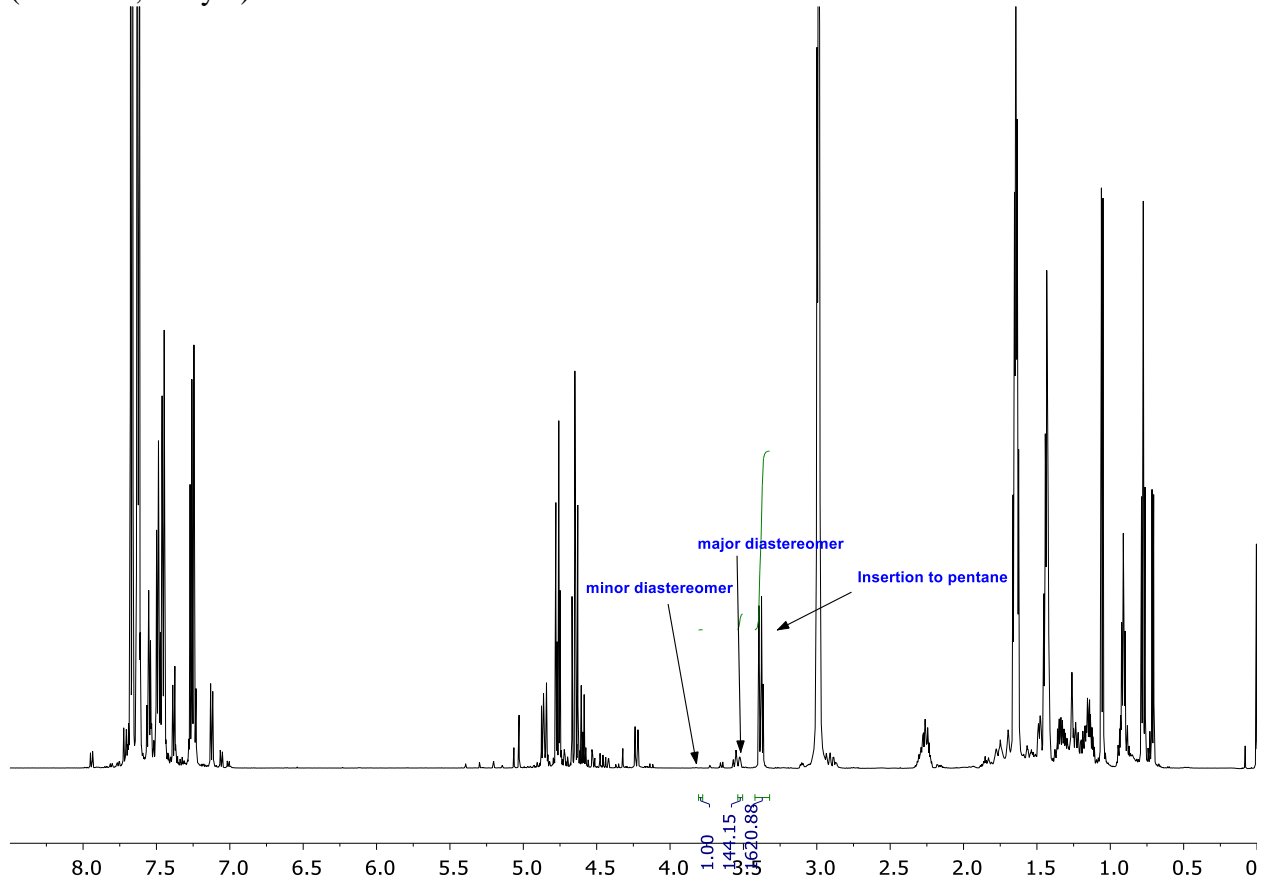


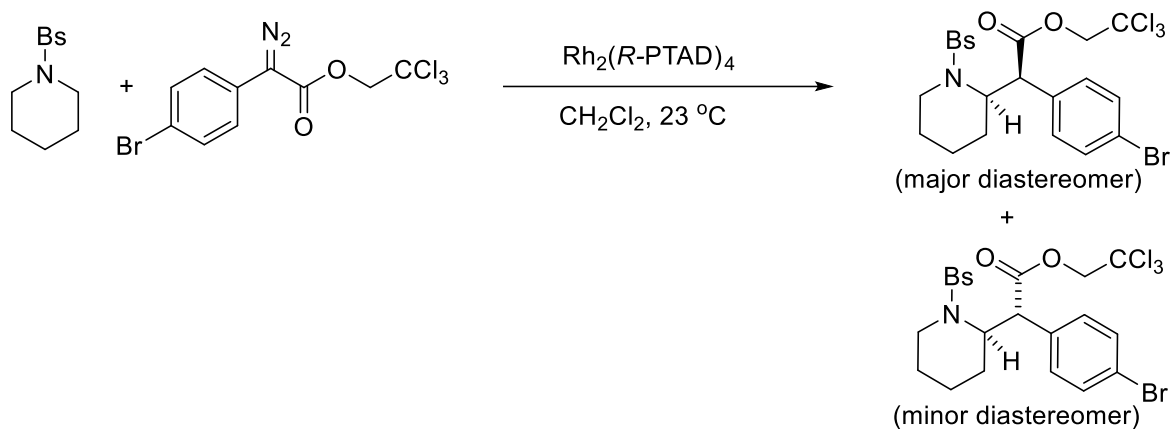
(Table S2, entry 4)



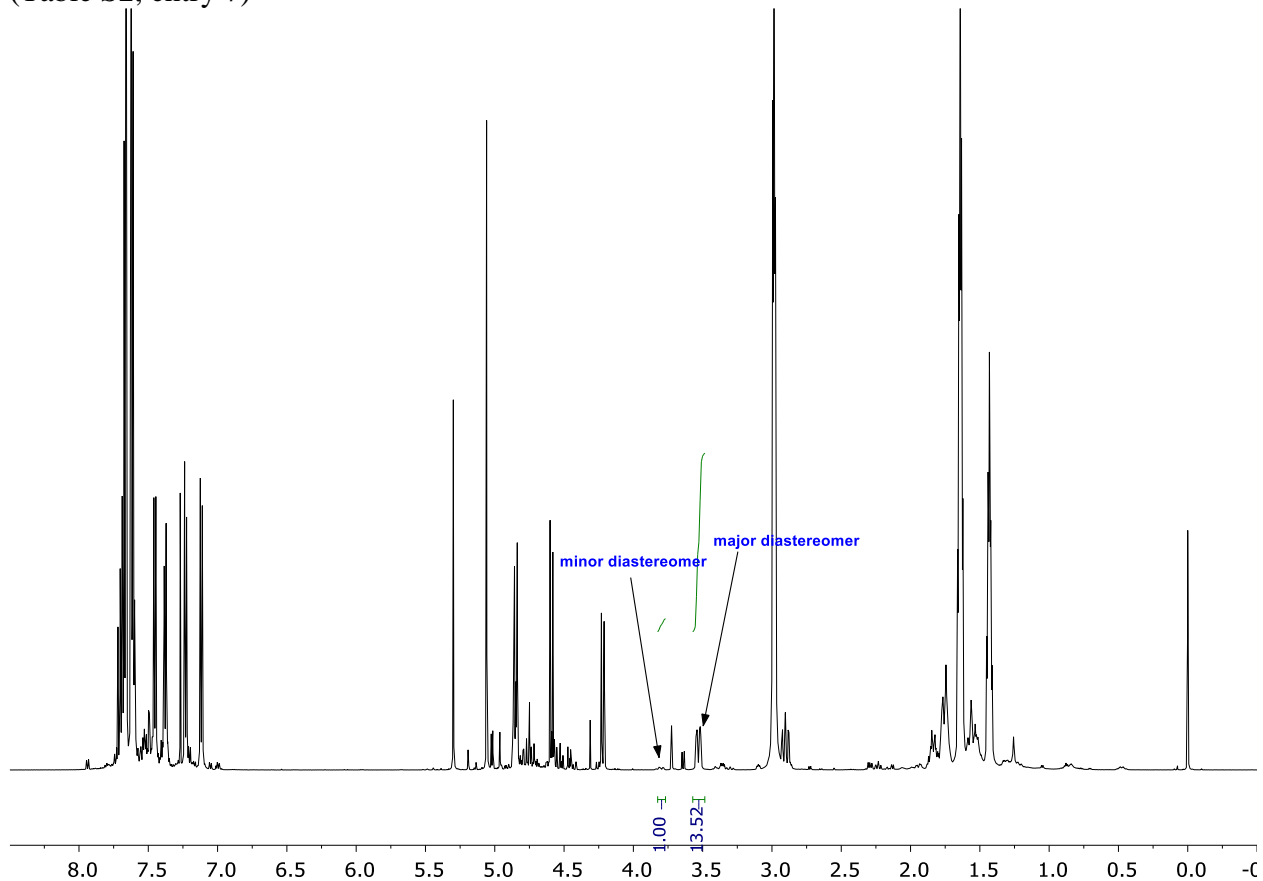


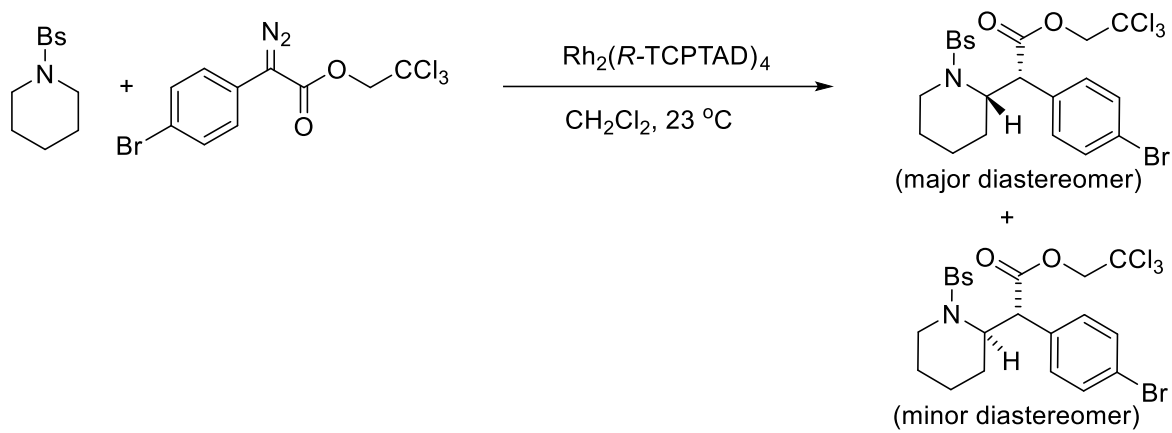
(Table S2, entry 5)



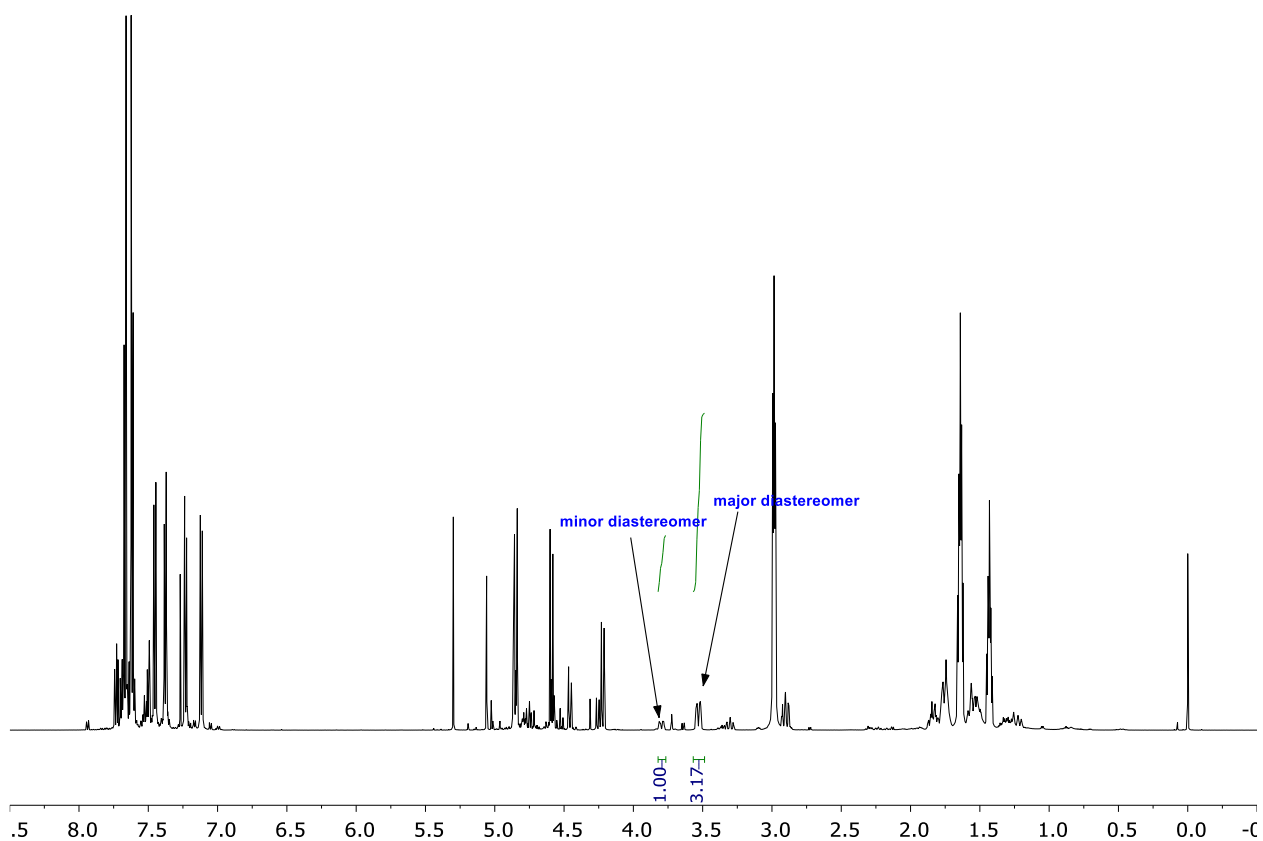


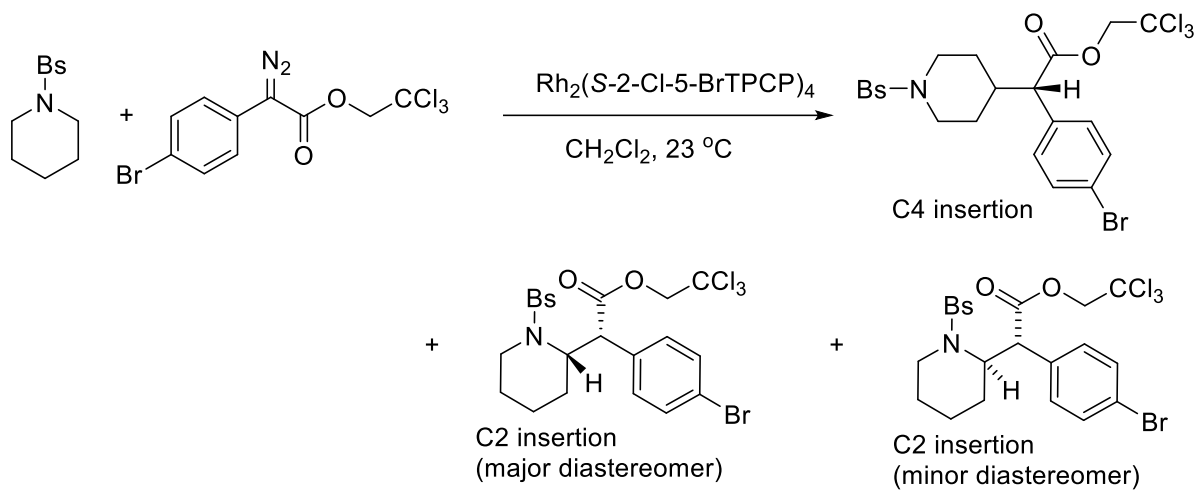
(Table S2, entry 7)



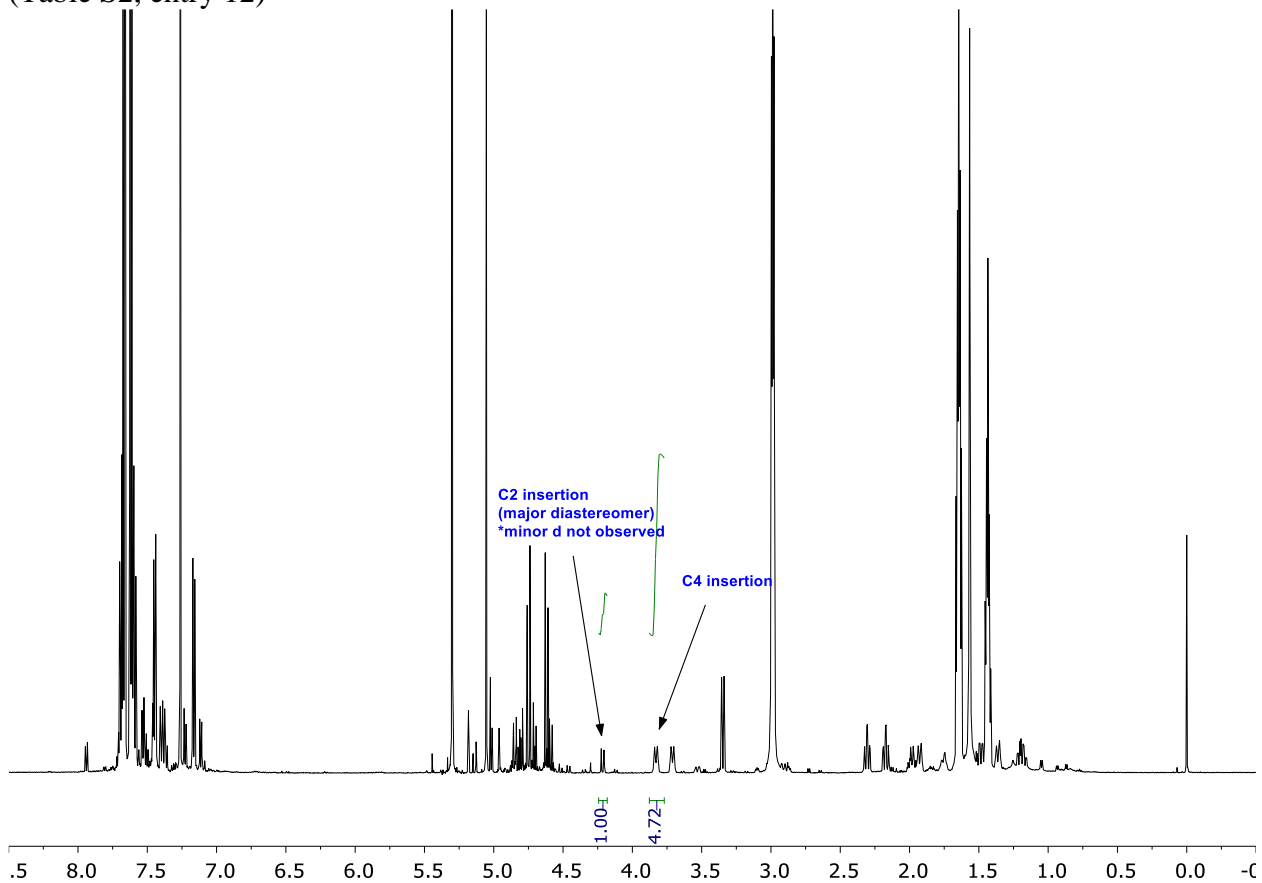


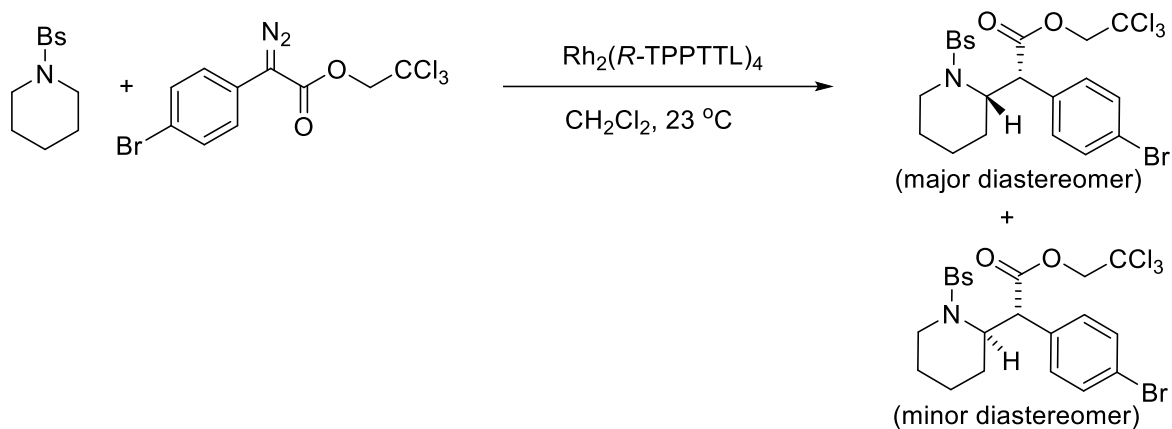
(Table S2, entry 8)



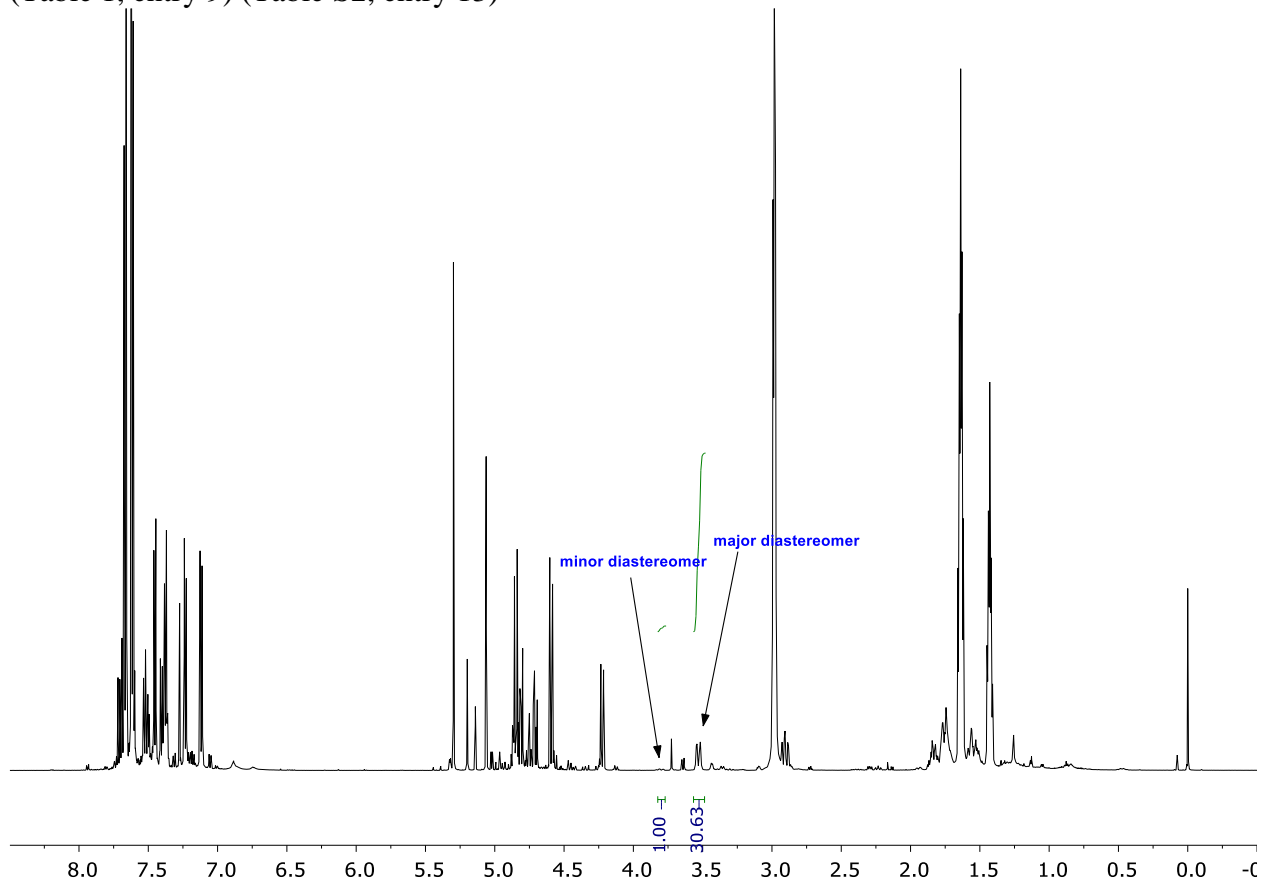


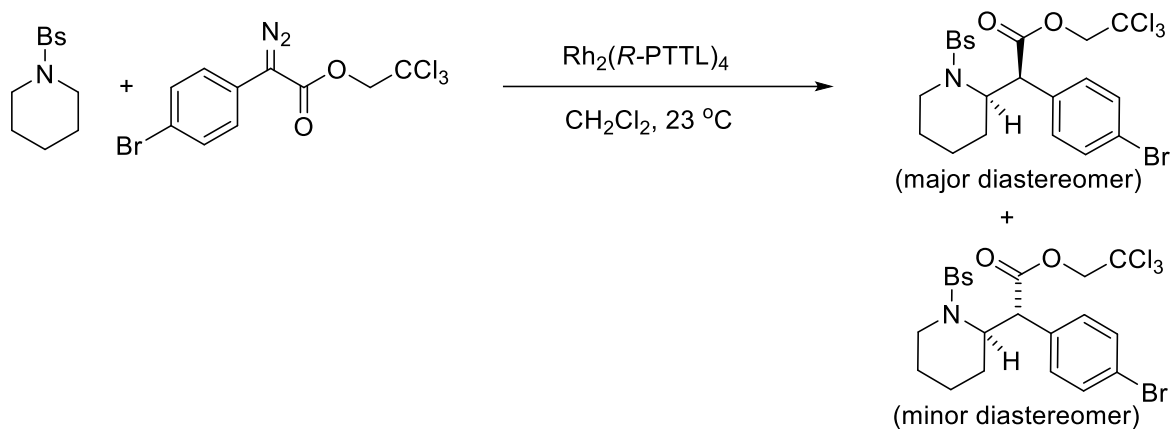
(Table S2, entry 12)



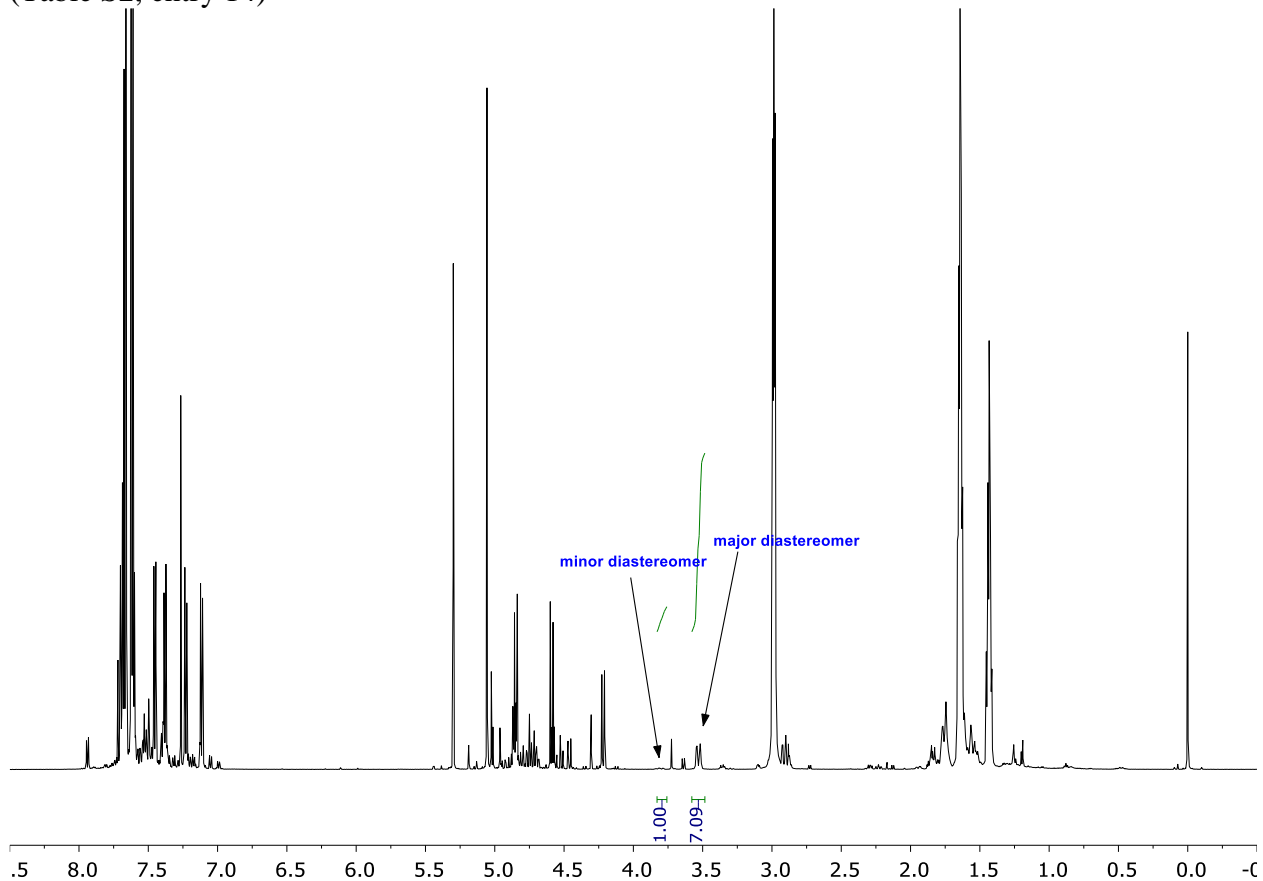


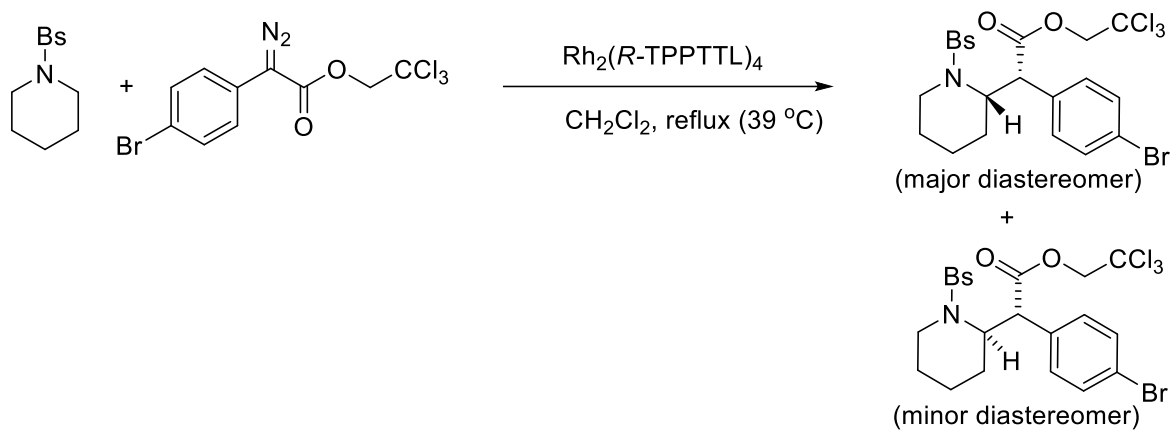
(Table 1, entry 9) (Table S2, entry 13)



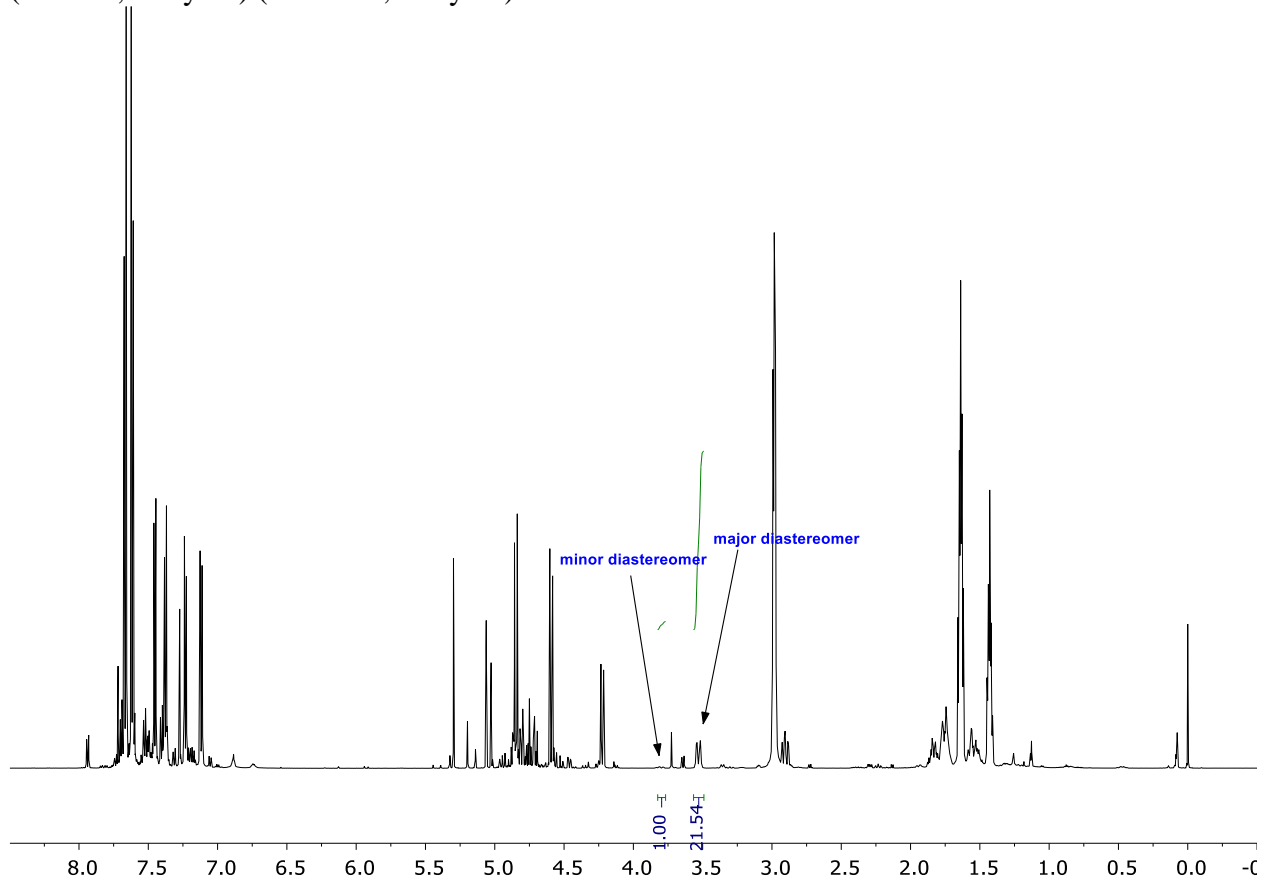


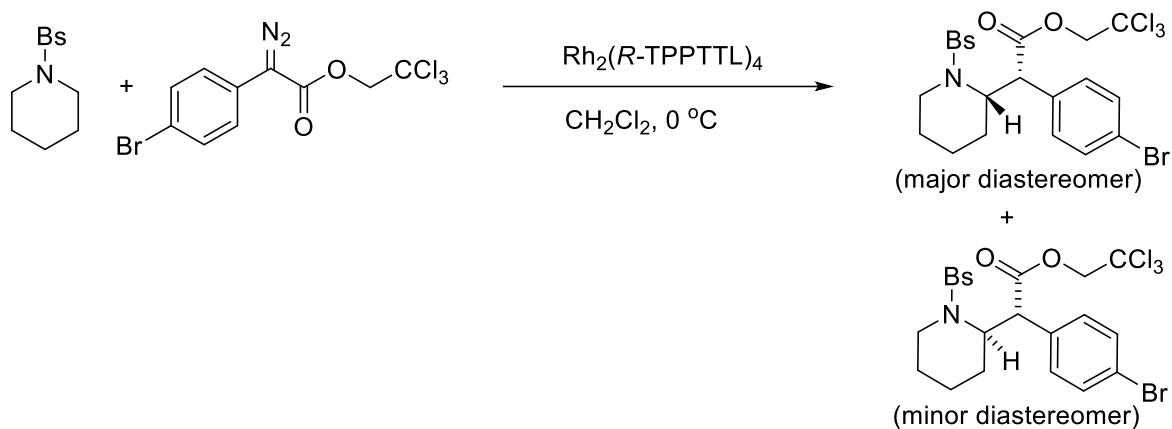
(Table S2, entry 14)



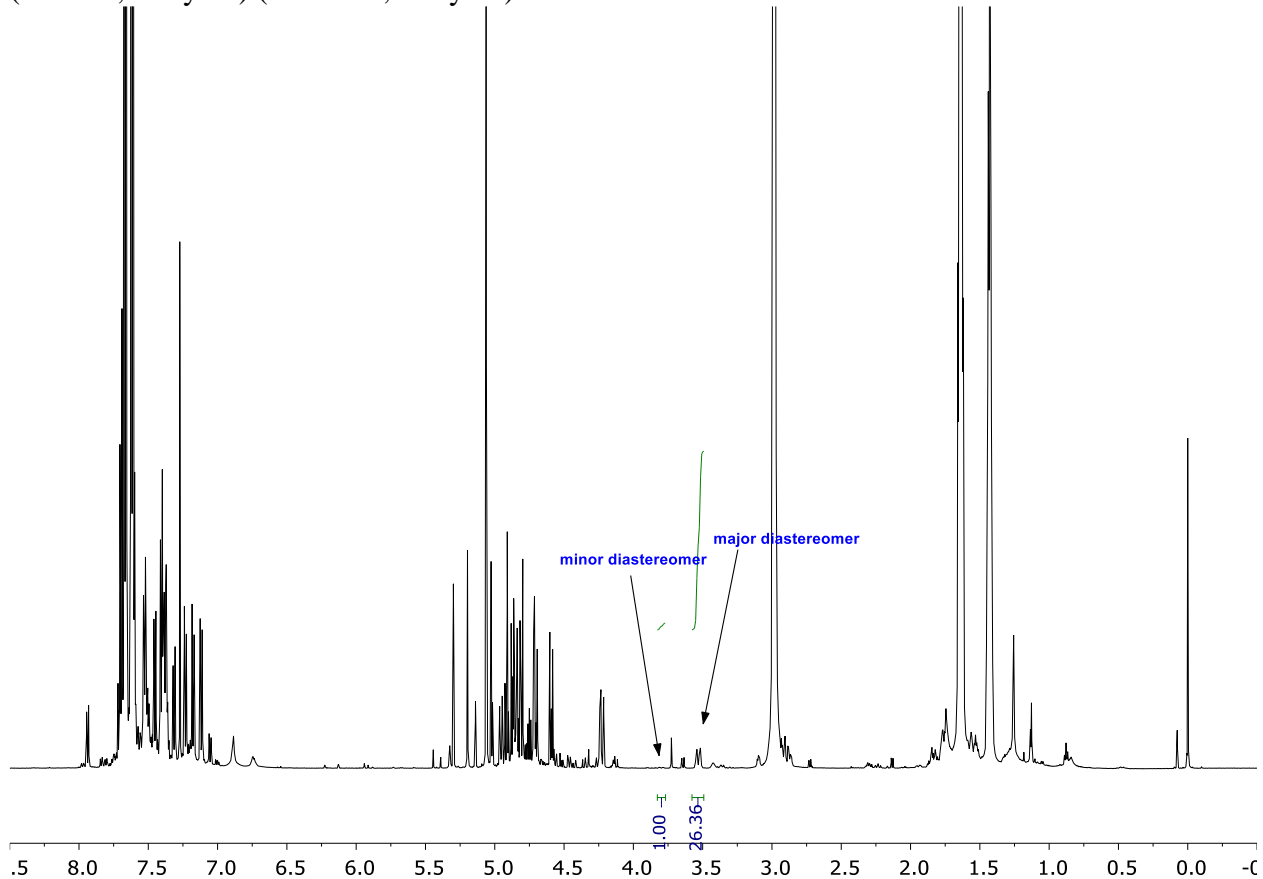


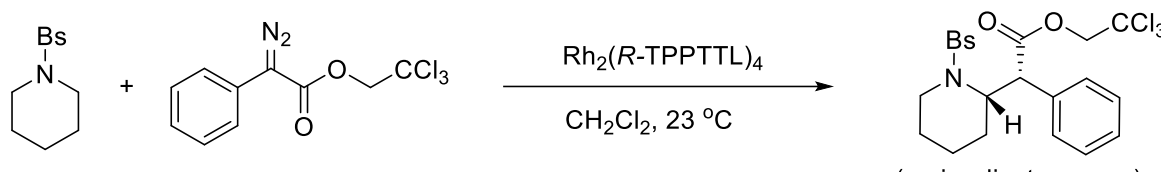
(Table 1, entry 10) (Table S2, entry 15)





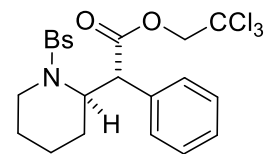
(Table 1, entry 11) (Table S2, entry 16)



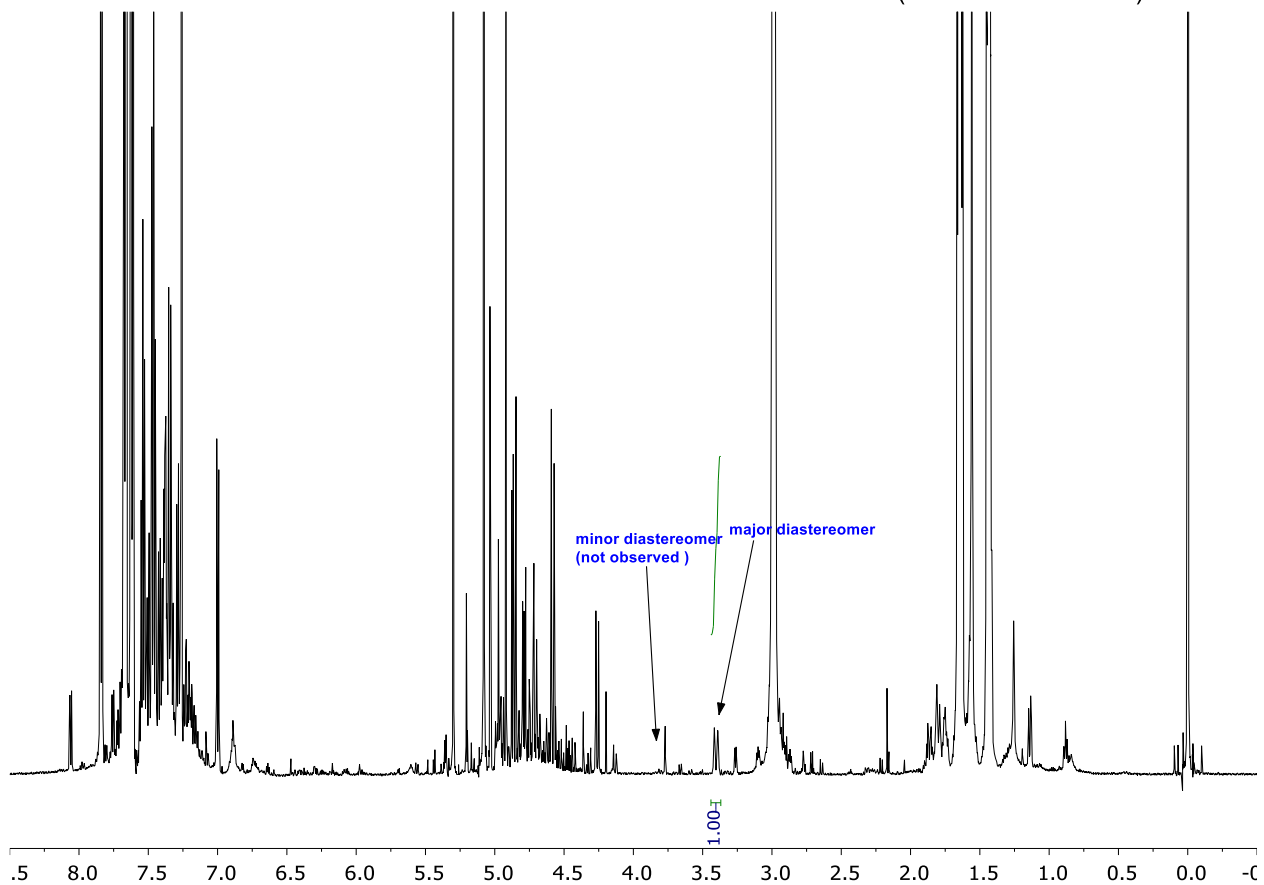


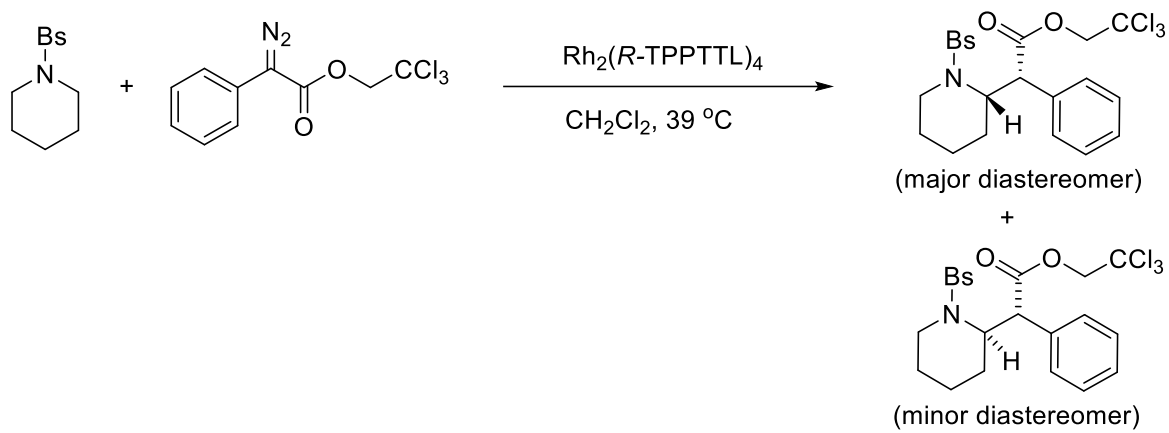
(major diastereomer)

+

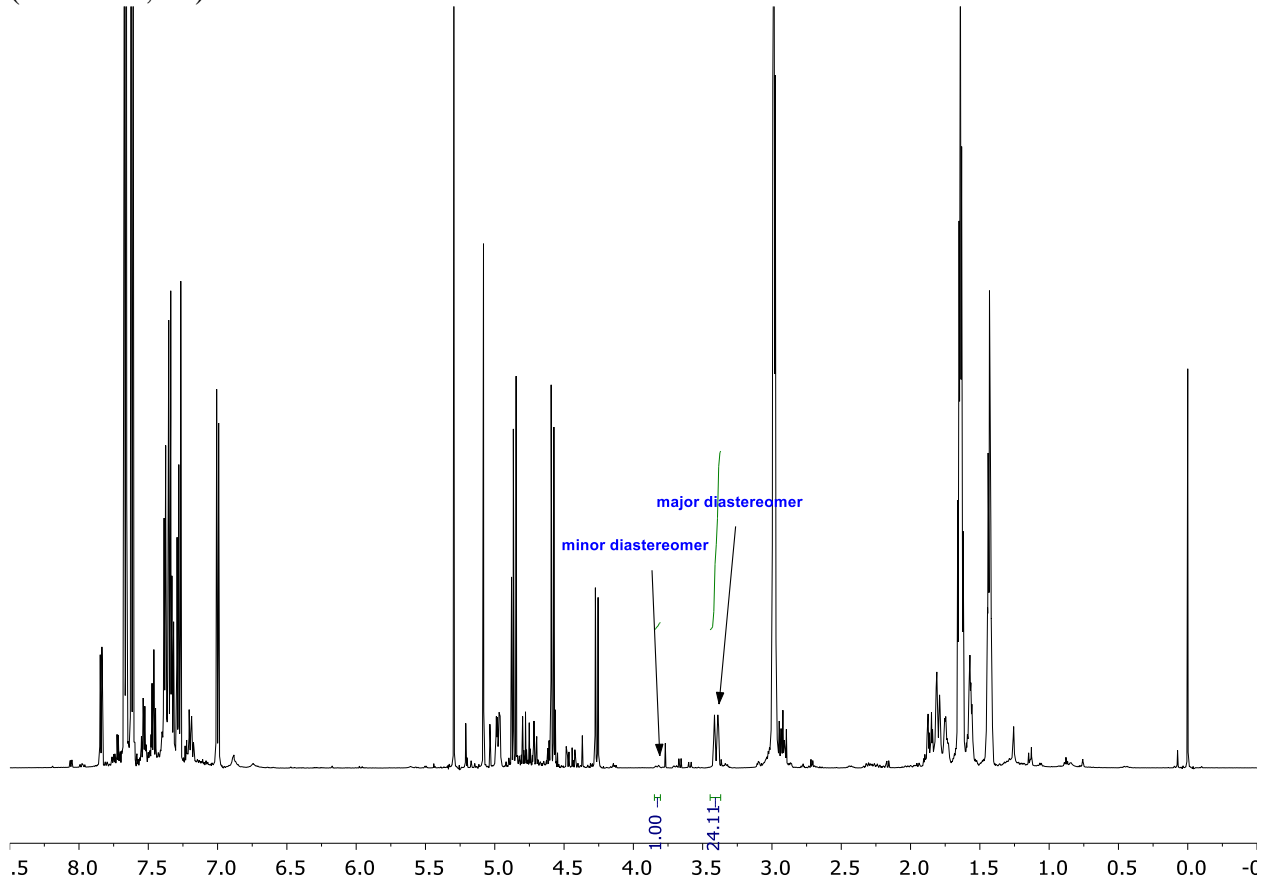


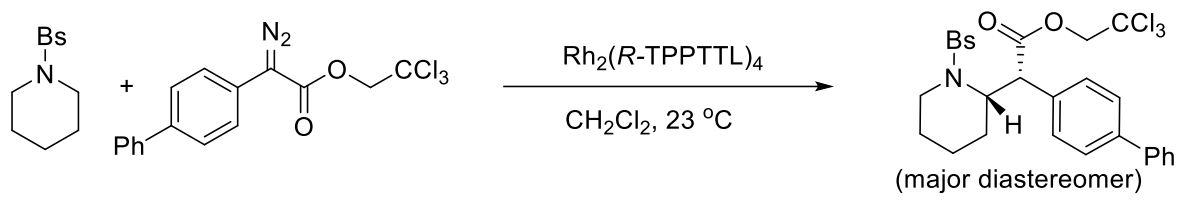
(minor diastereomer)





(Scheme 2, **6b**)

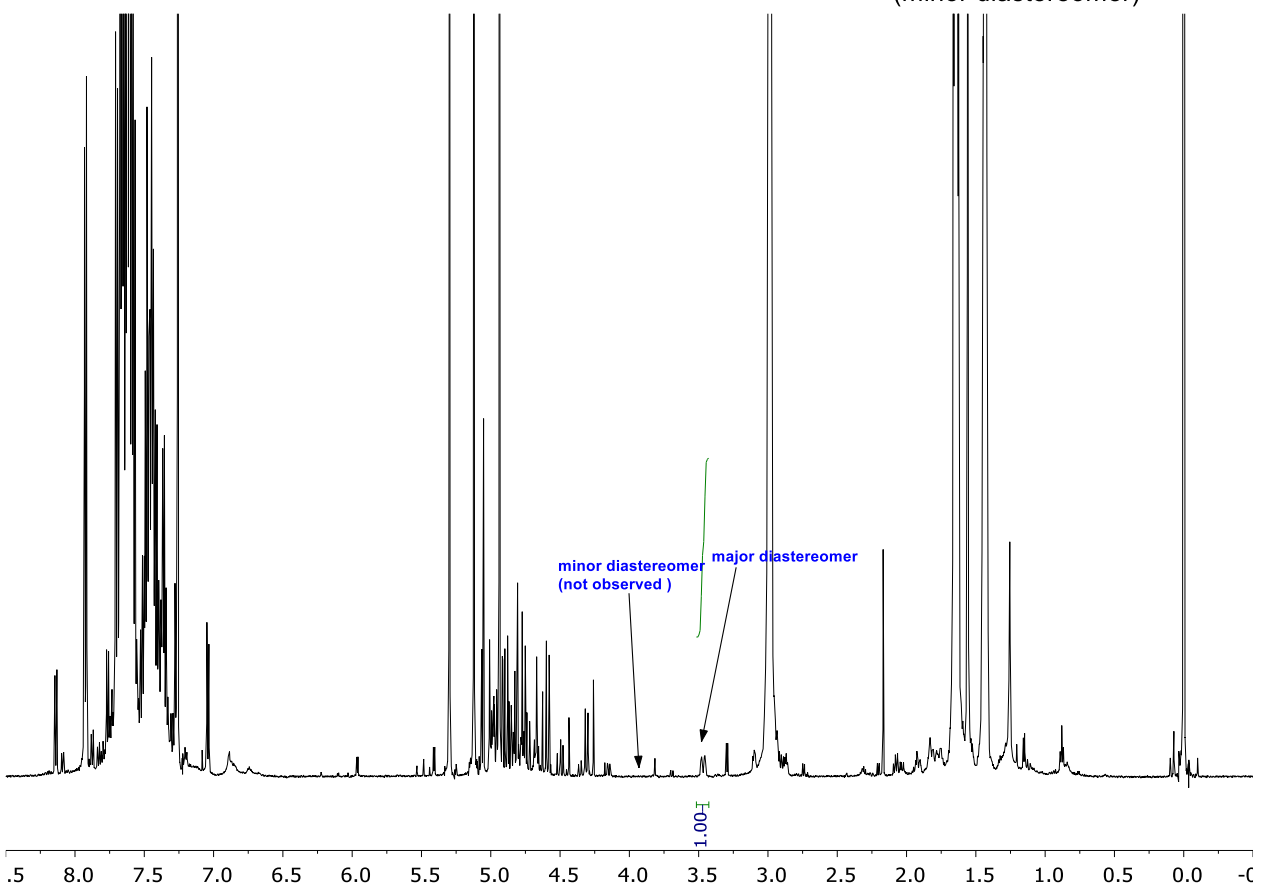


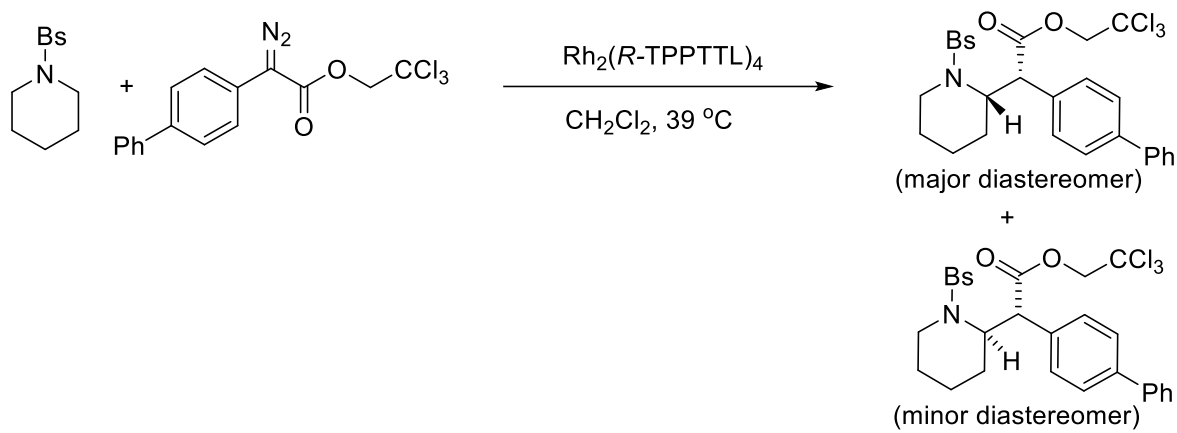


(major diastereomer)

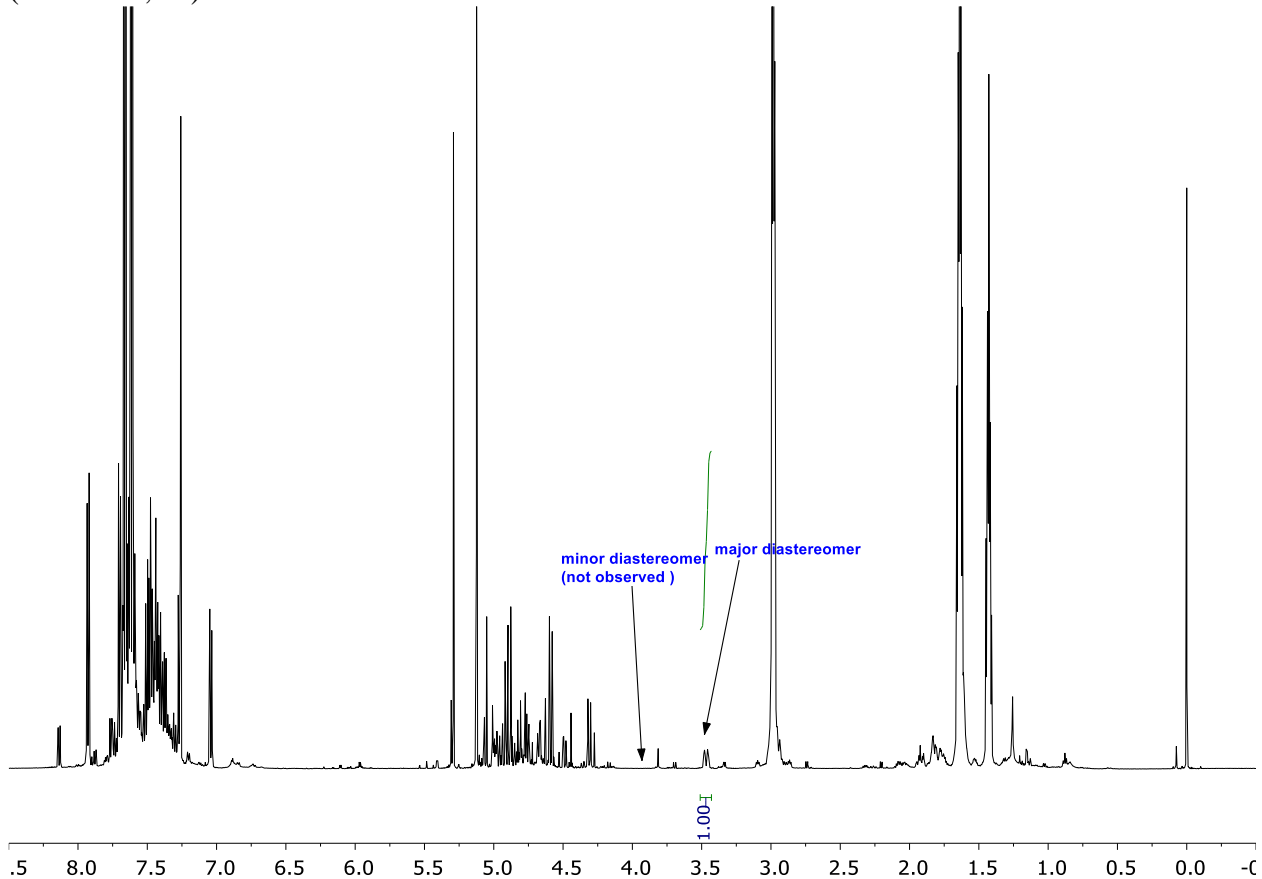
+

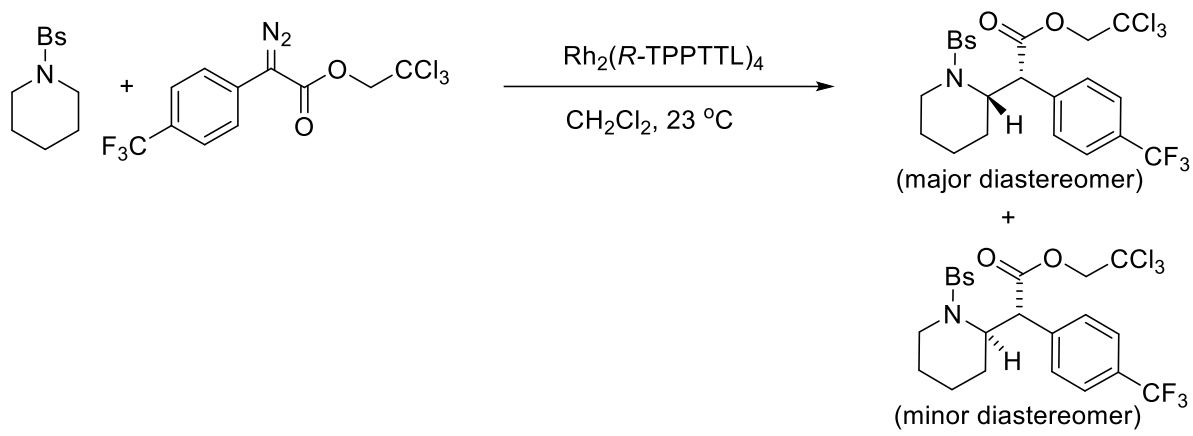
(minor diastereomer)



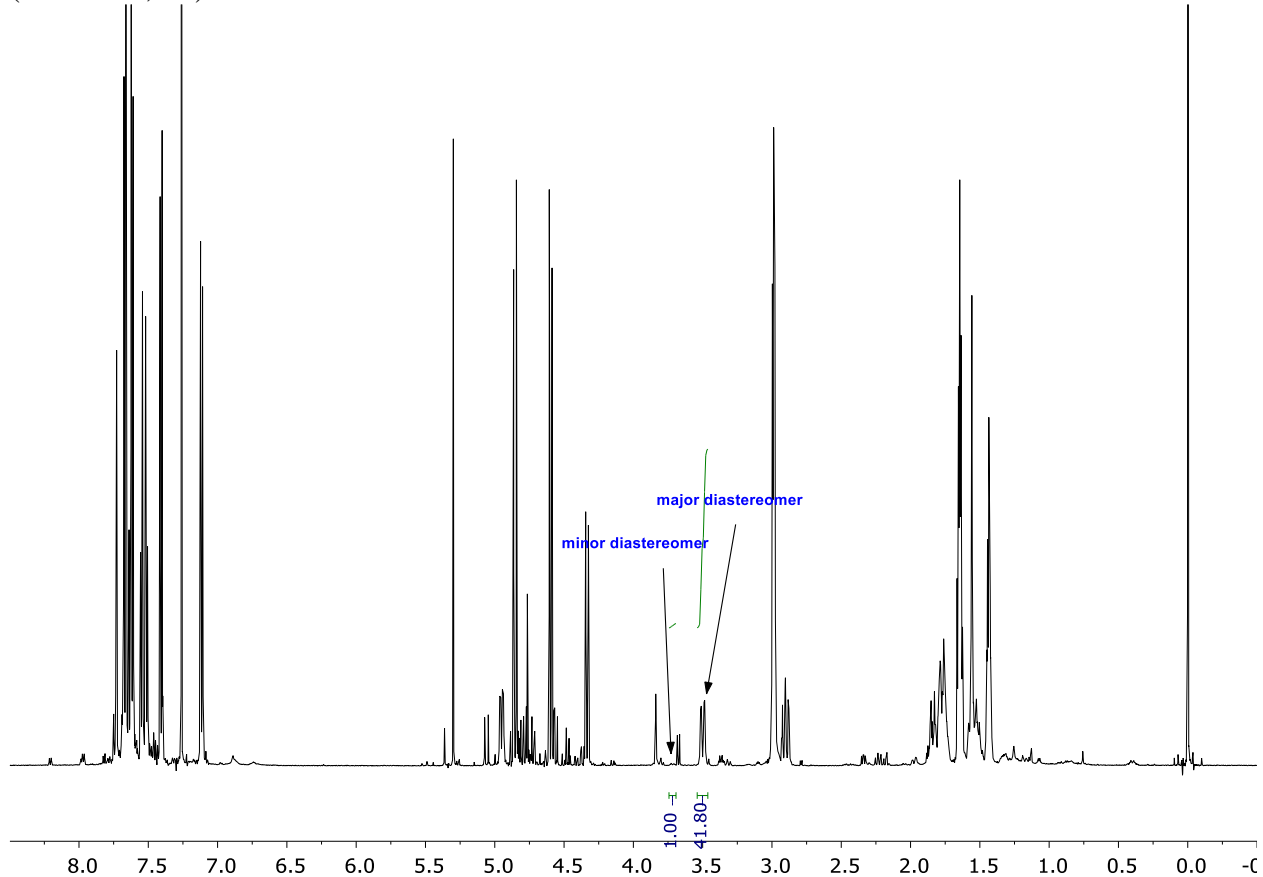


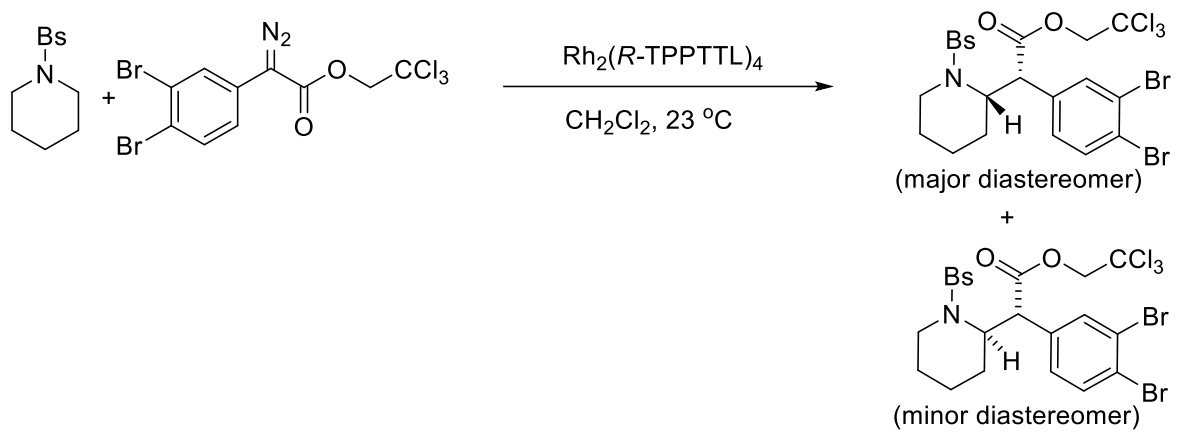
(Scheme 2, **6c**)



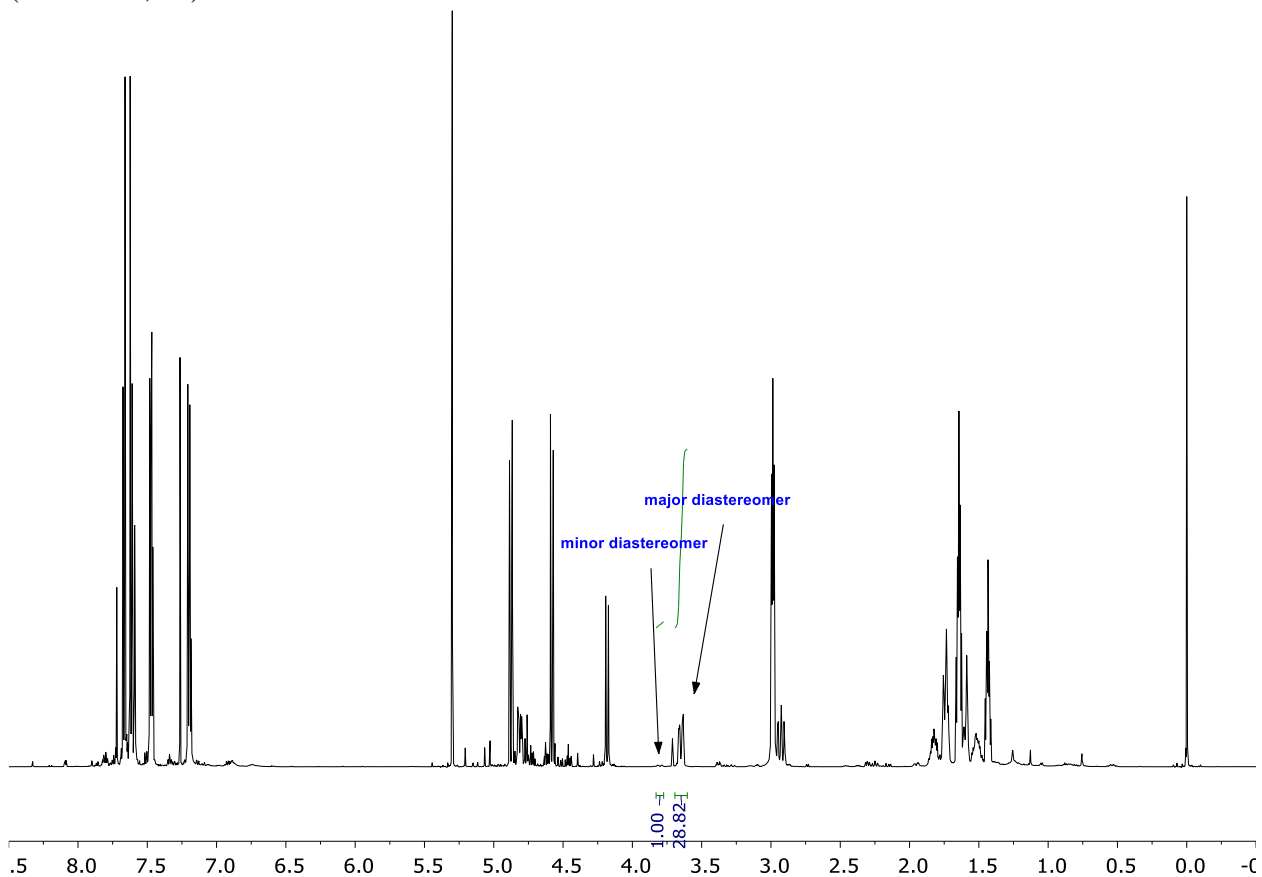


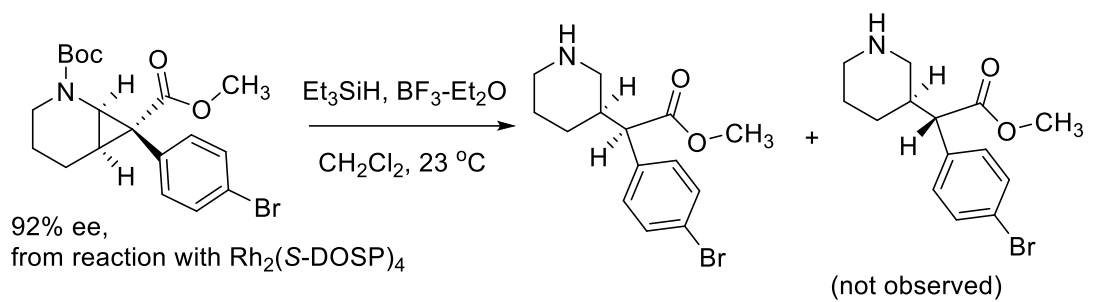
(Scheme 2, **6d**)



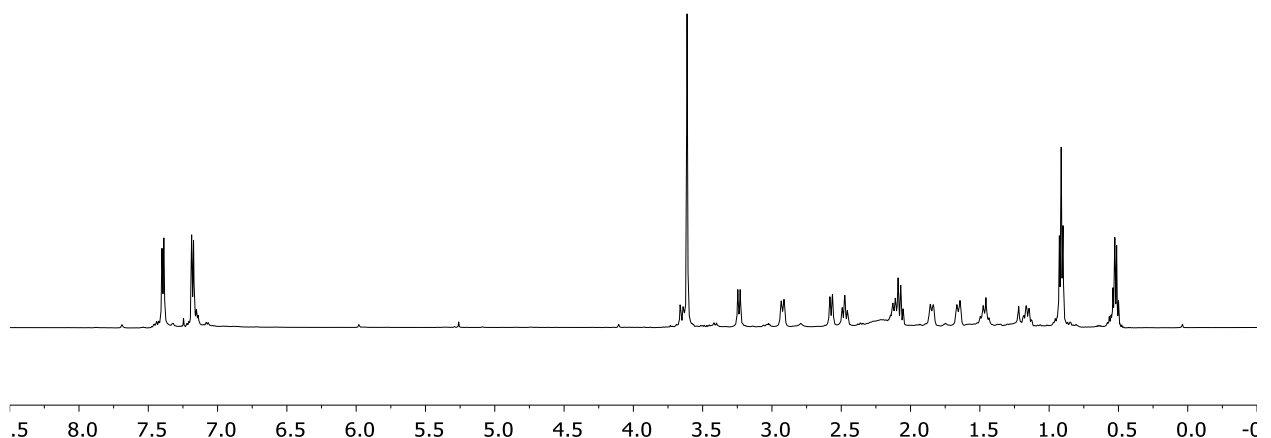


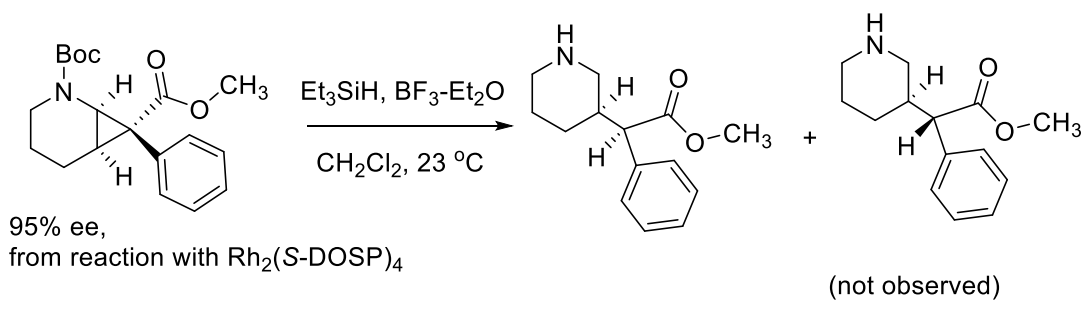
(Scheme 2, **6e**)



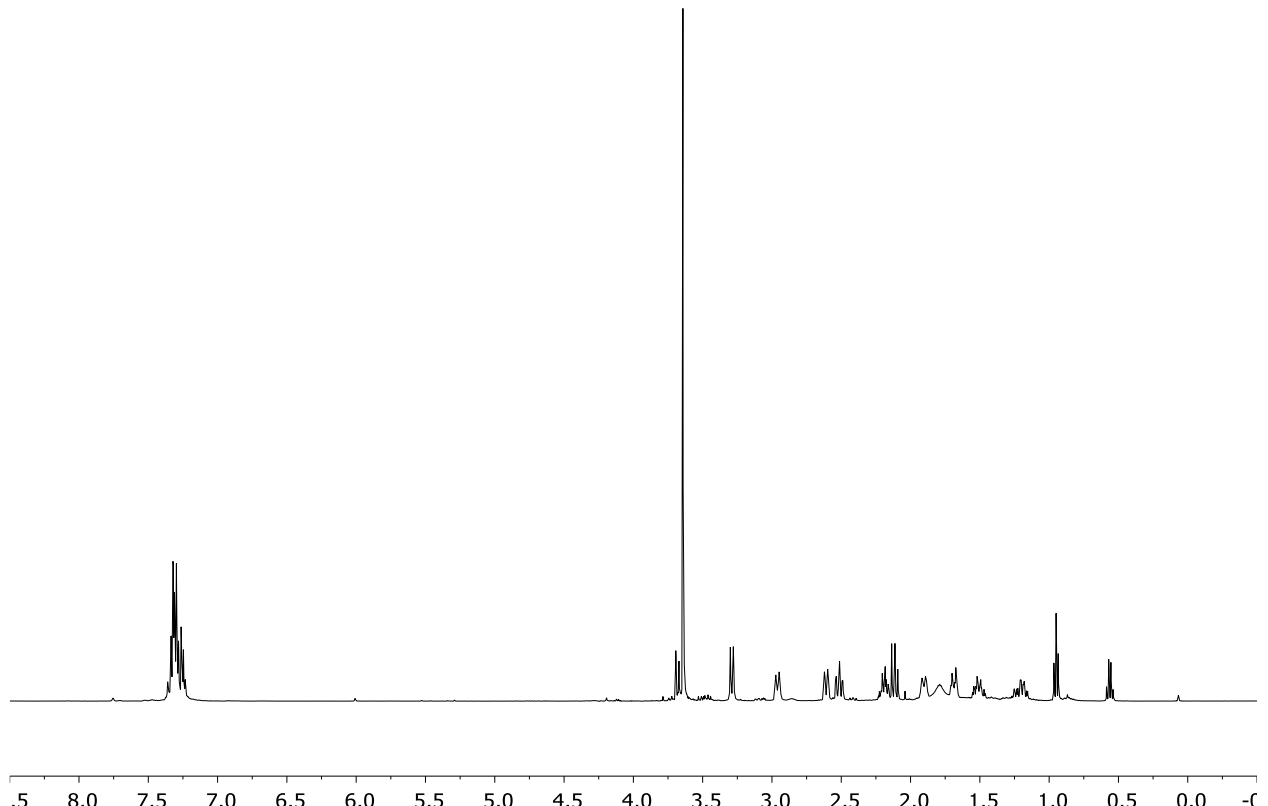


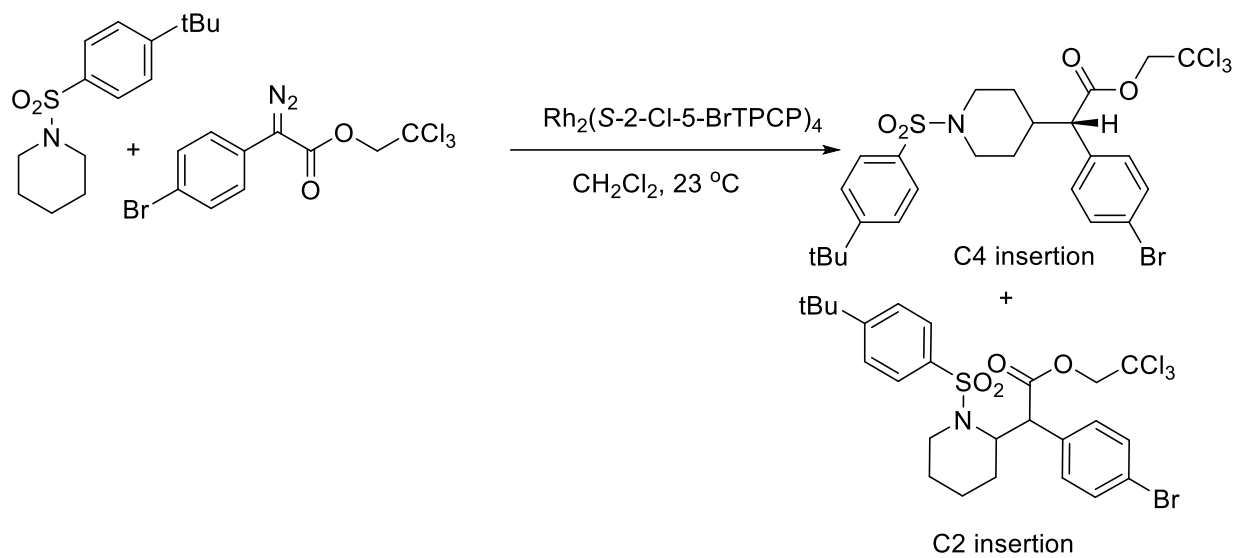
(Table 3, **9a**)



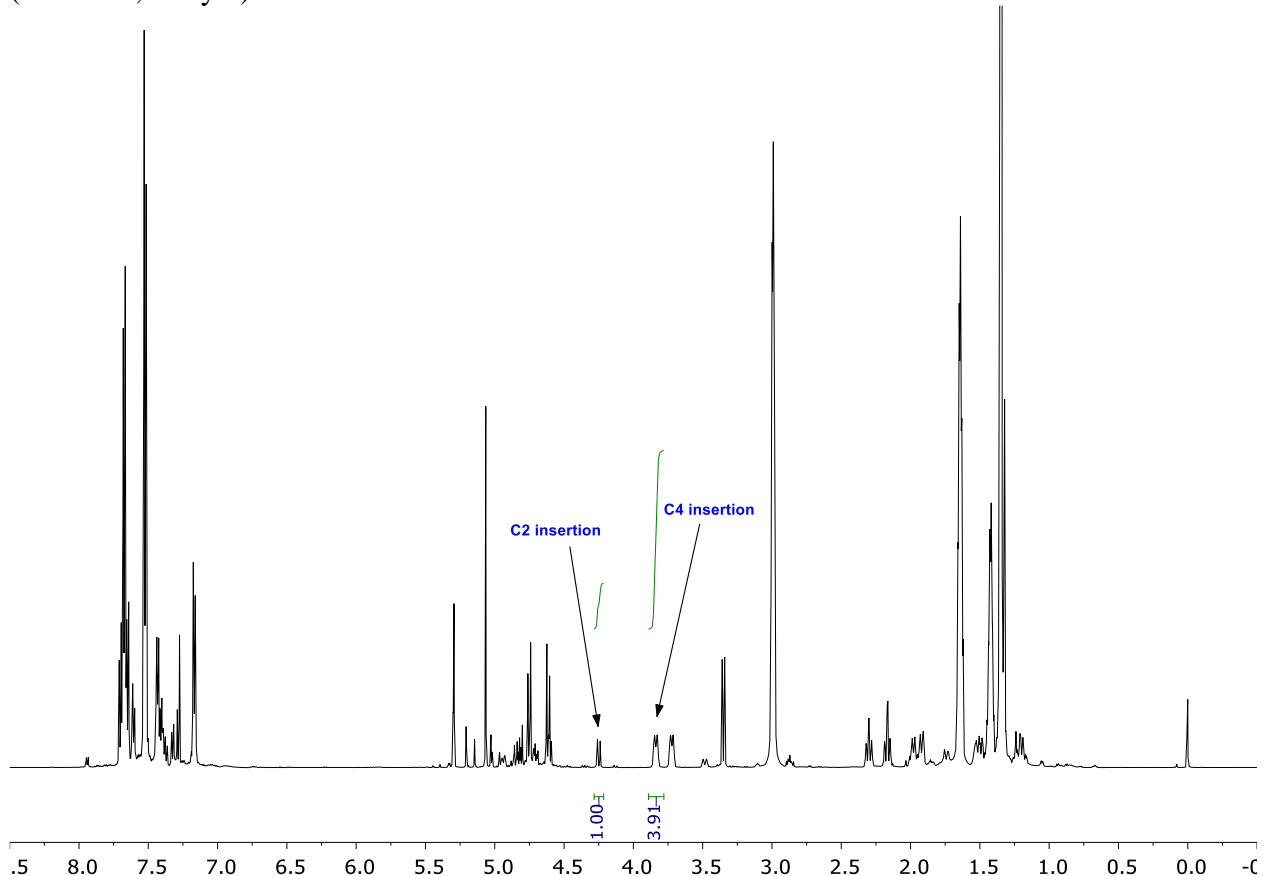


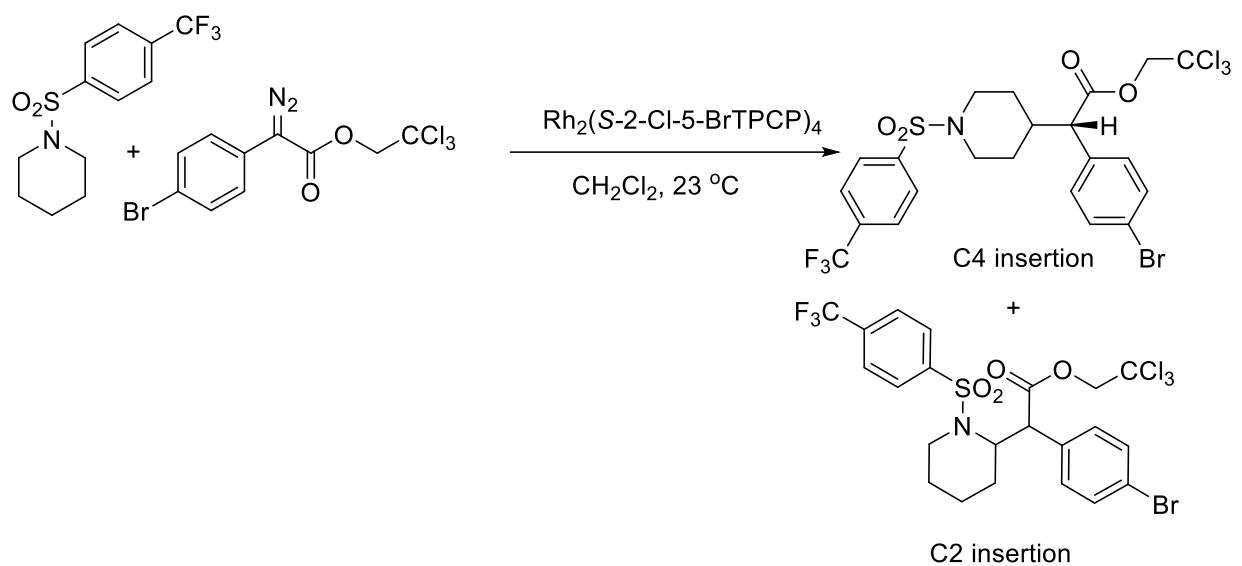
(Table 3, **9b**)



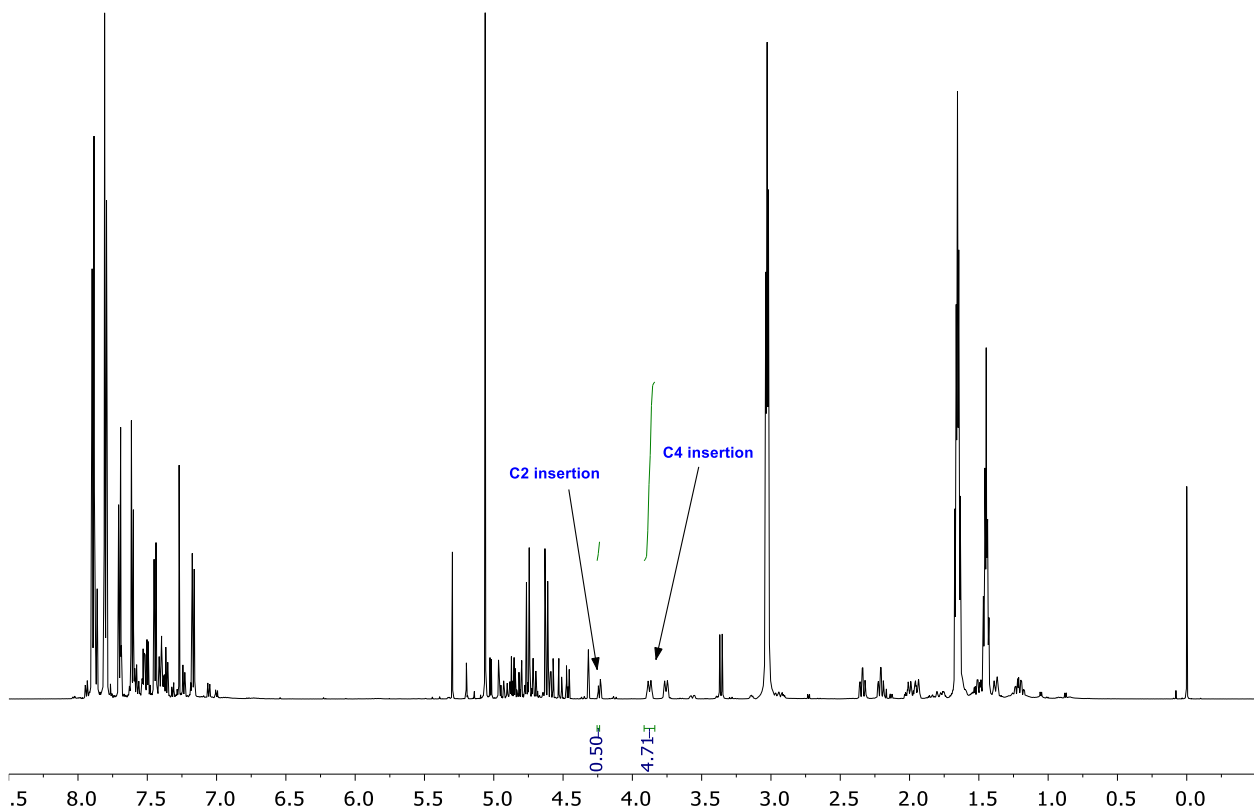


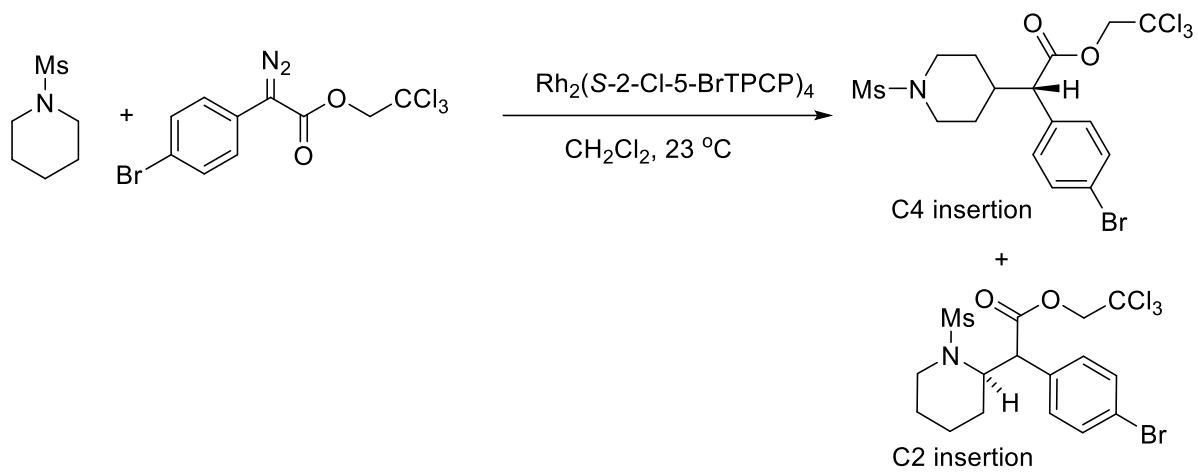
(Table S5, entry 7)



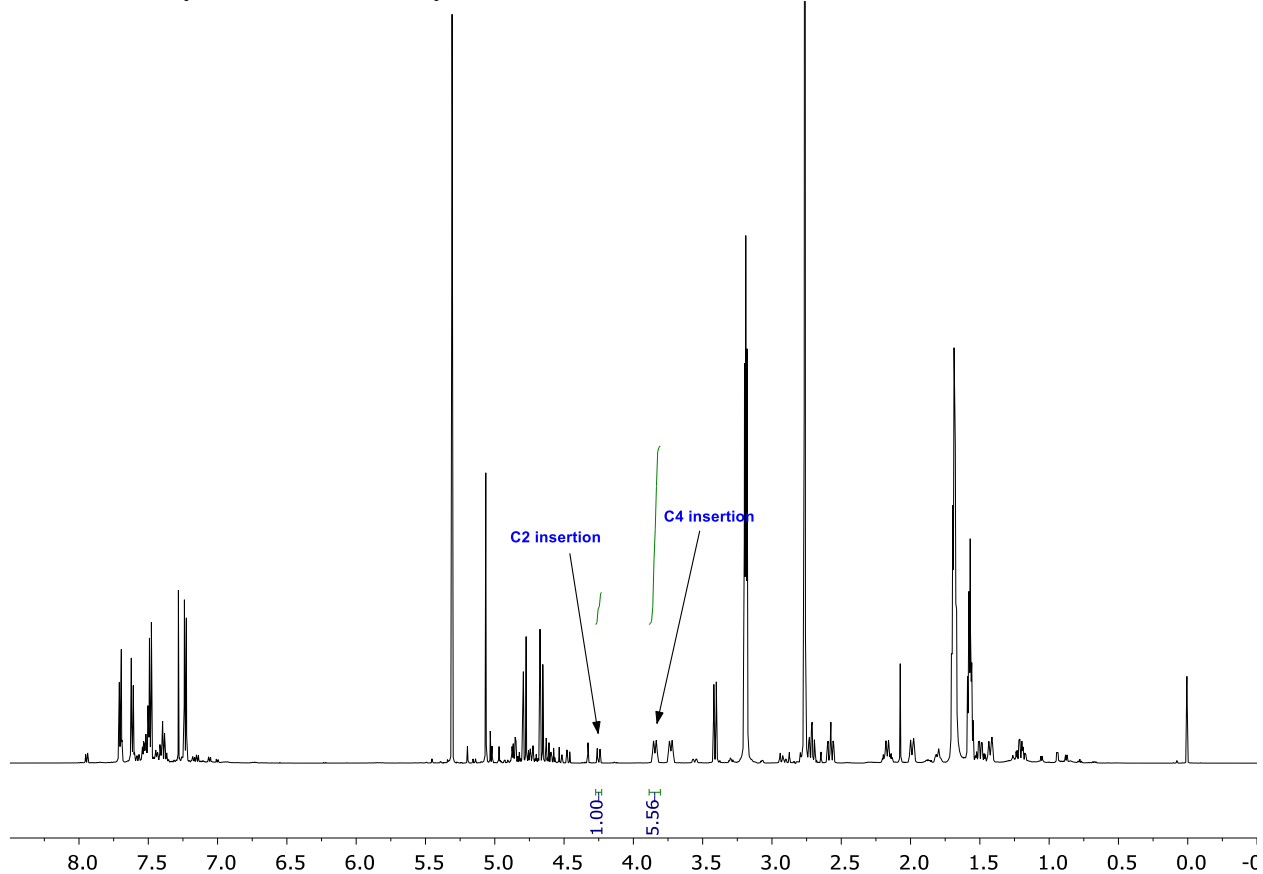


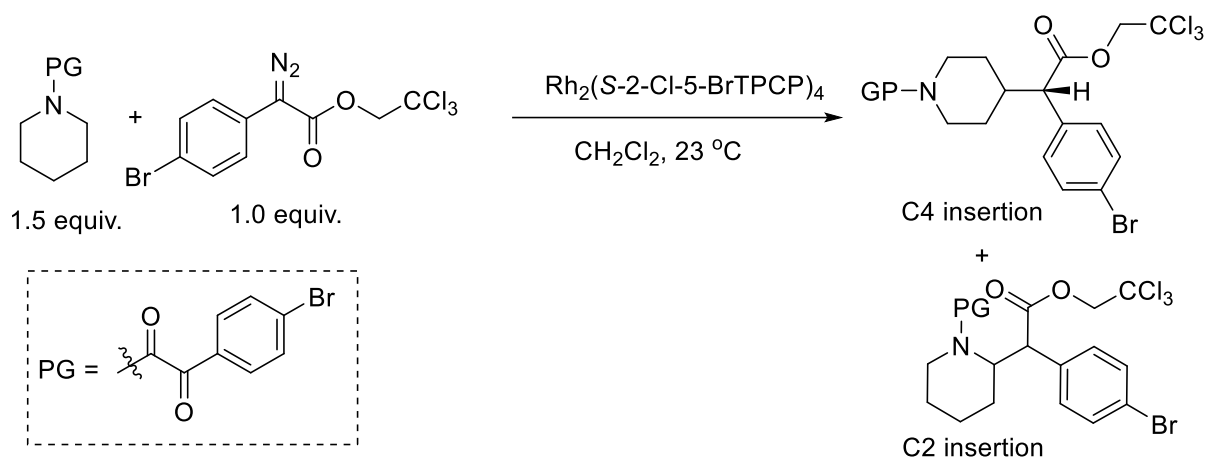
(Table 4, entry 6) (Table S5, entry 8)



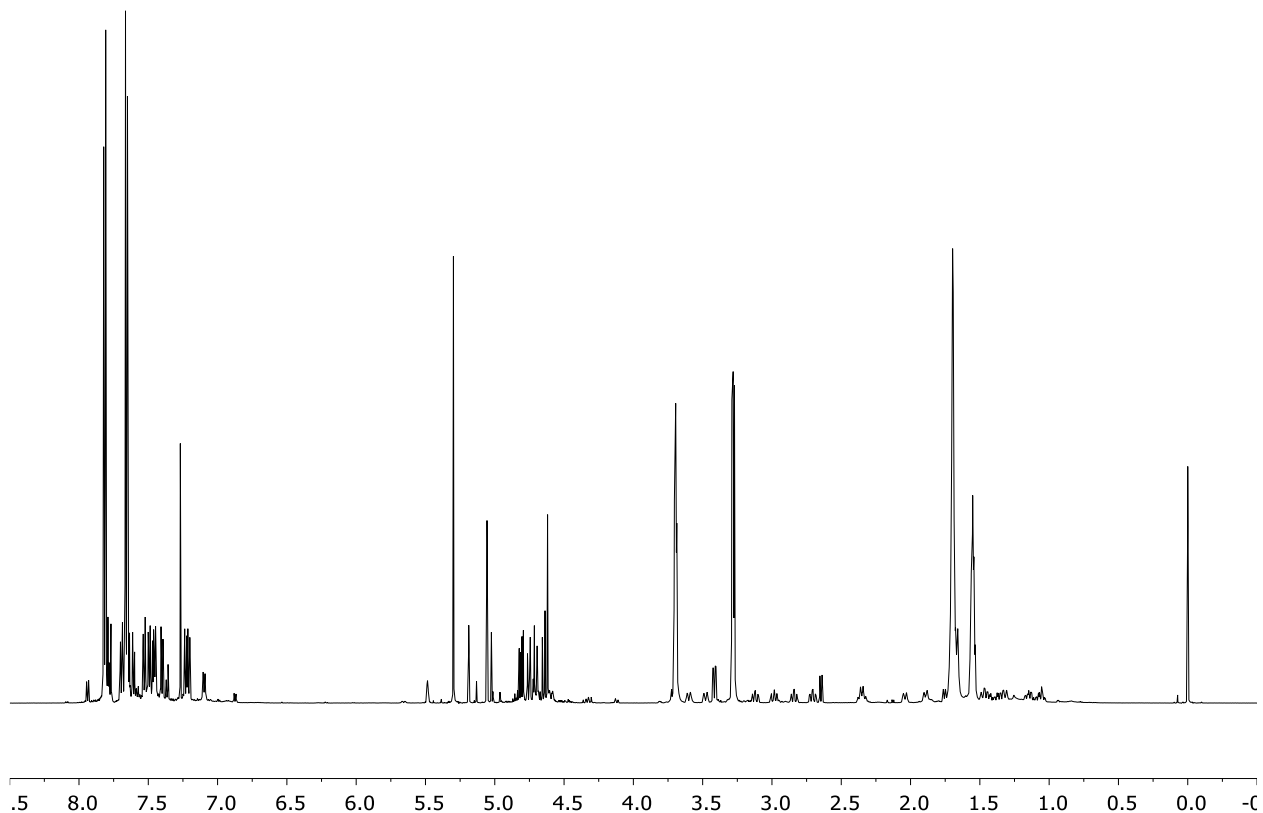


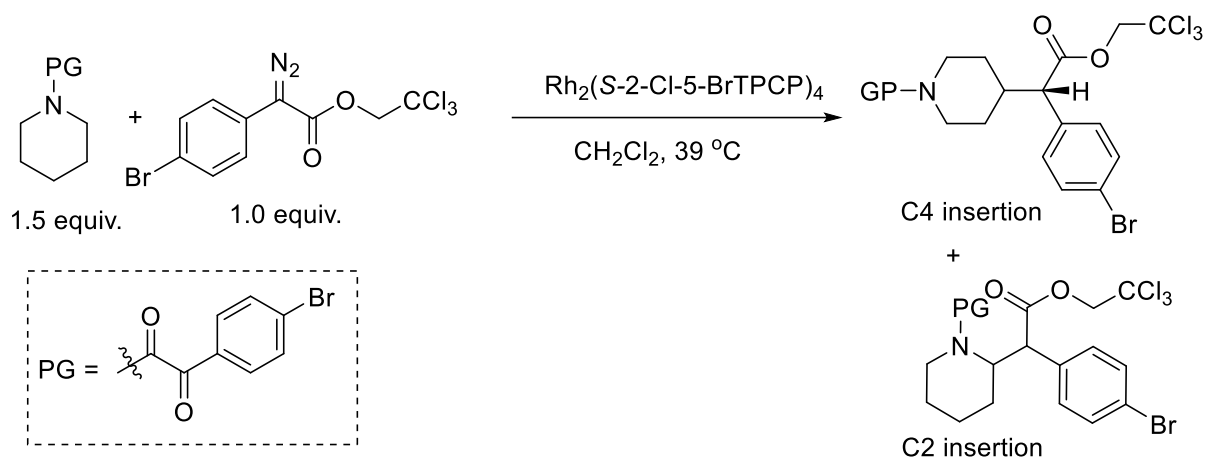
(Table 4, entry 7) (Table S5, entry 10)



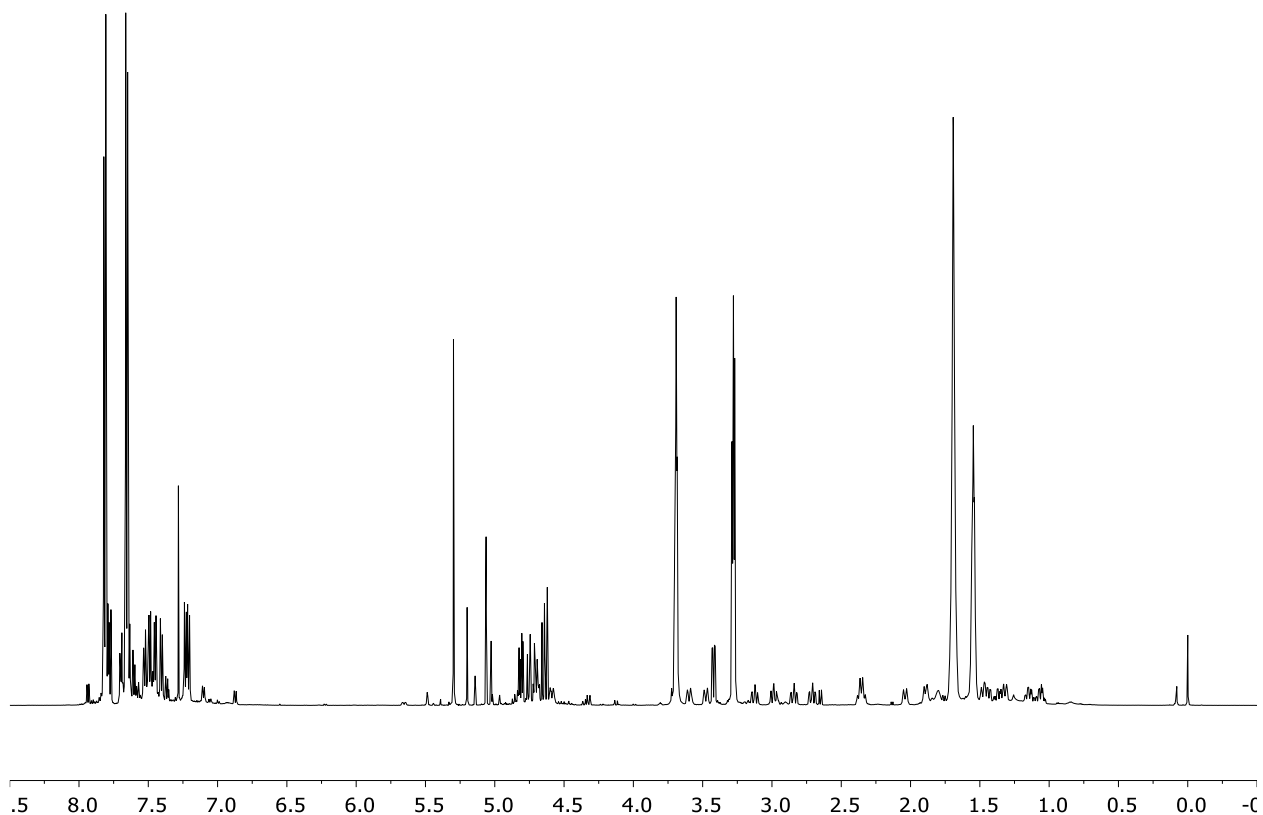


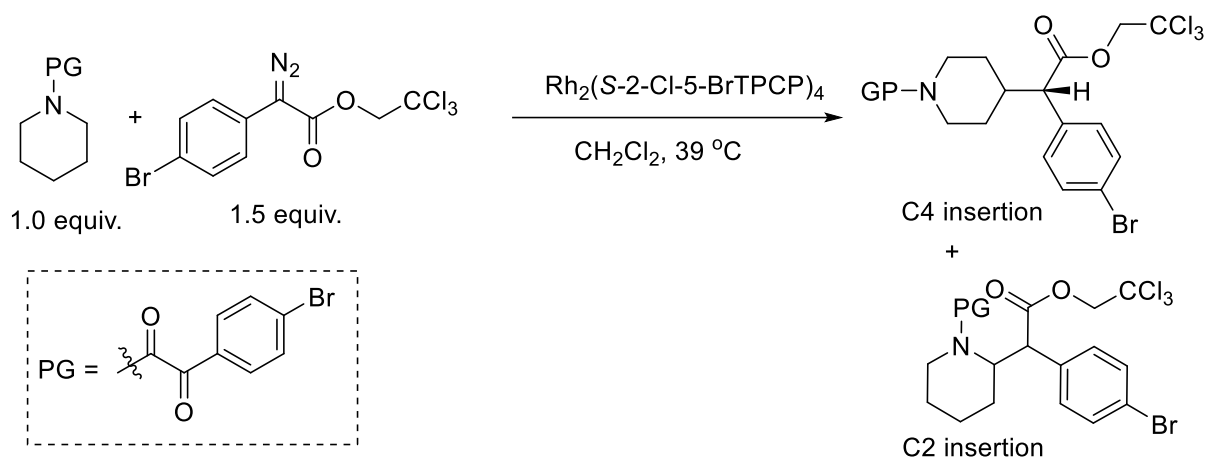
(Table 4, entry 8) (Table S5, entry 11)



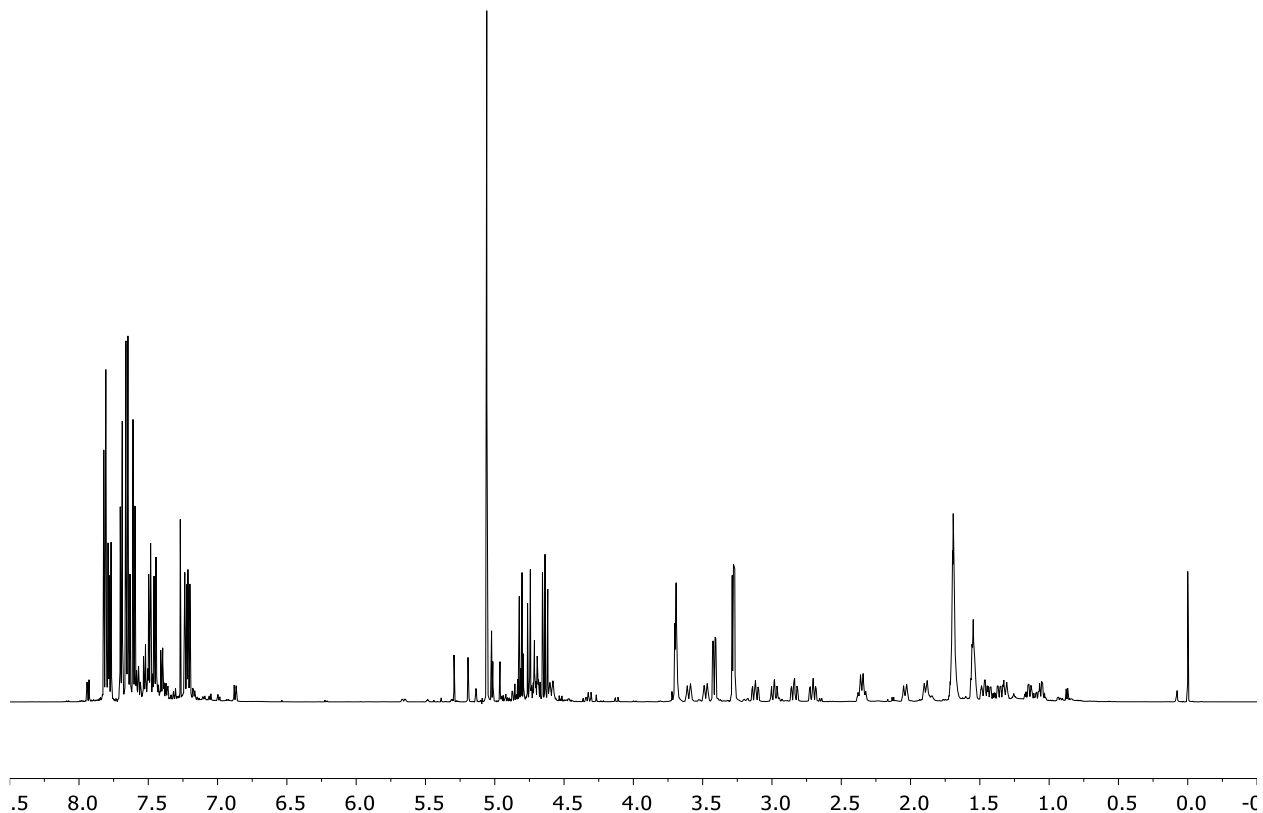


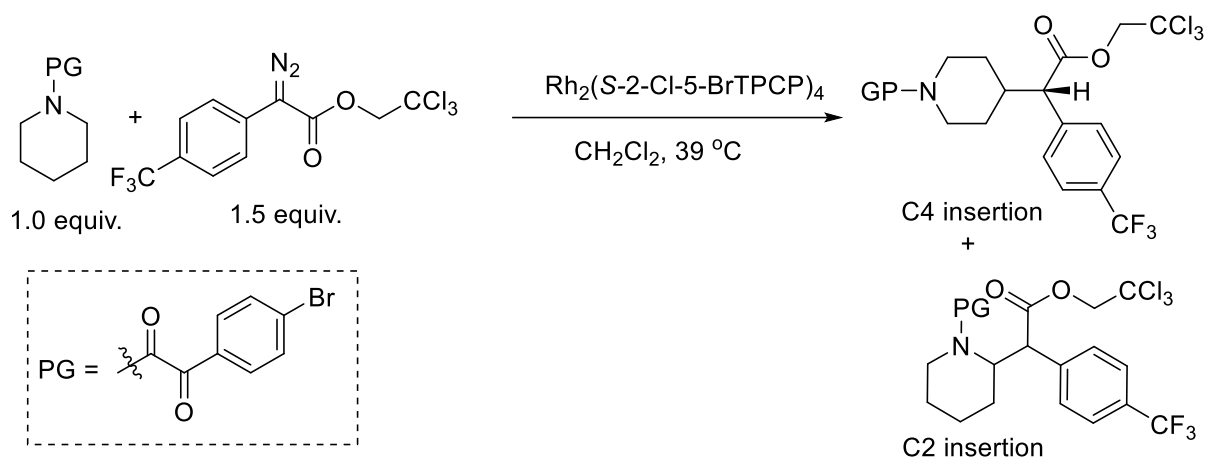
(Table 4, entry 9) (Table S5, entry 12)



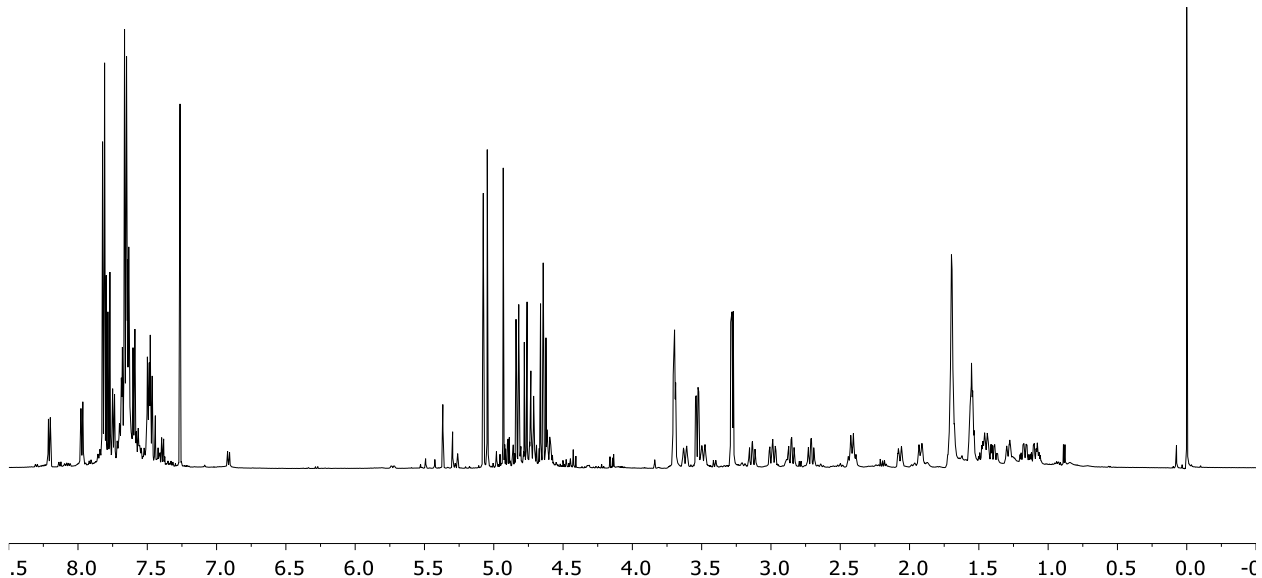


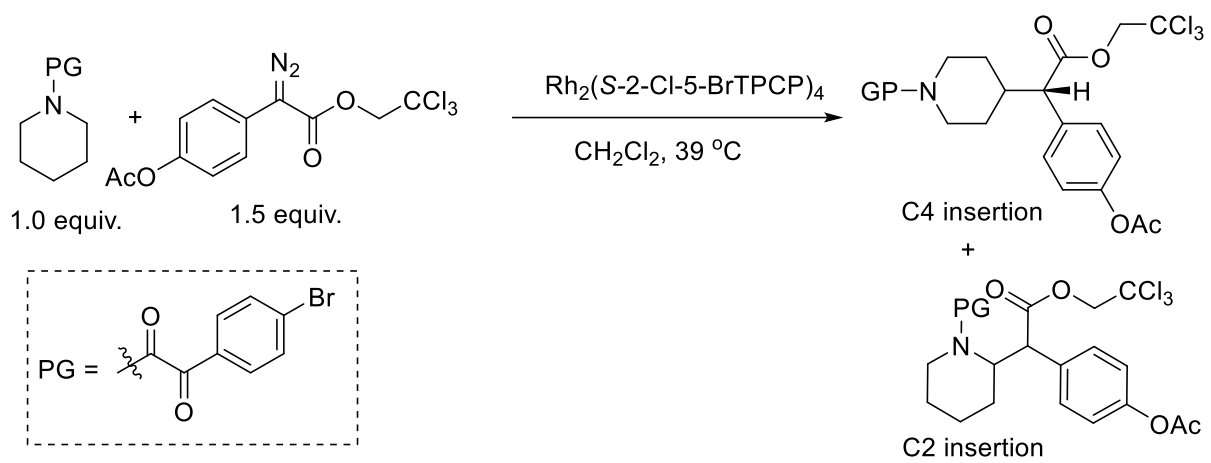
(Table 4, entry 10) (Table S5, entry 13)



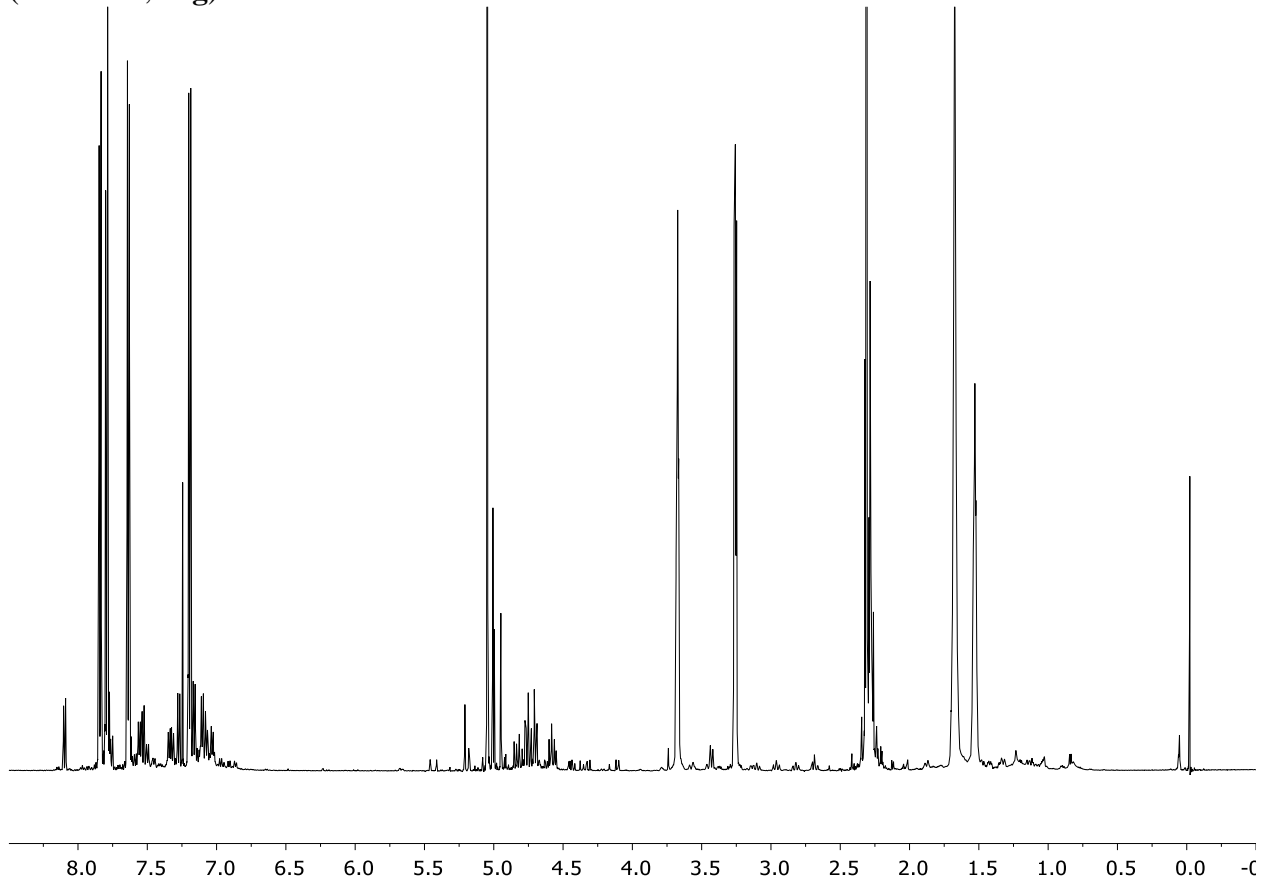


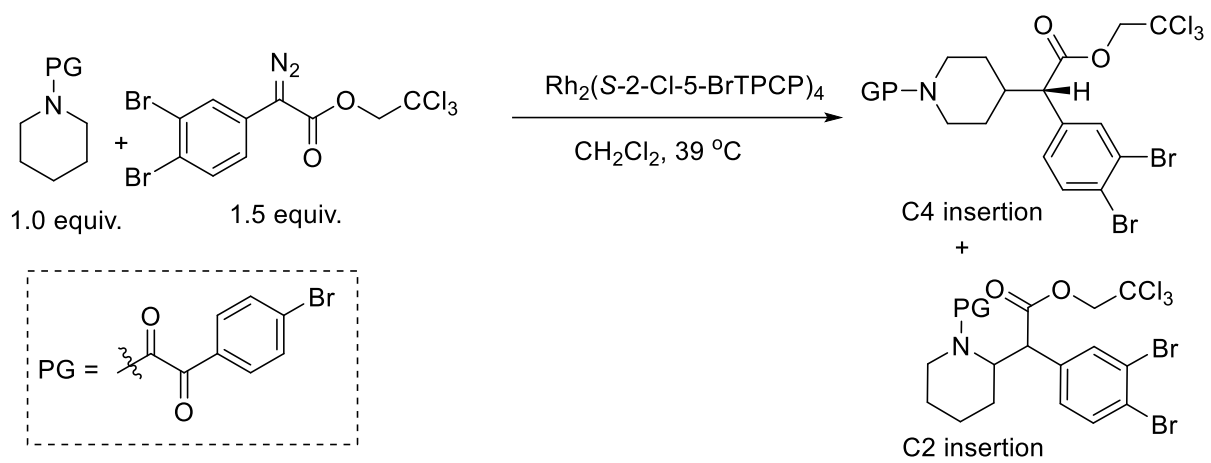
(Scheme 4, **13f**)



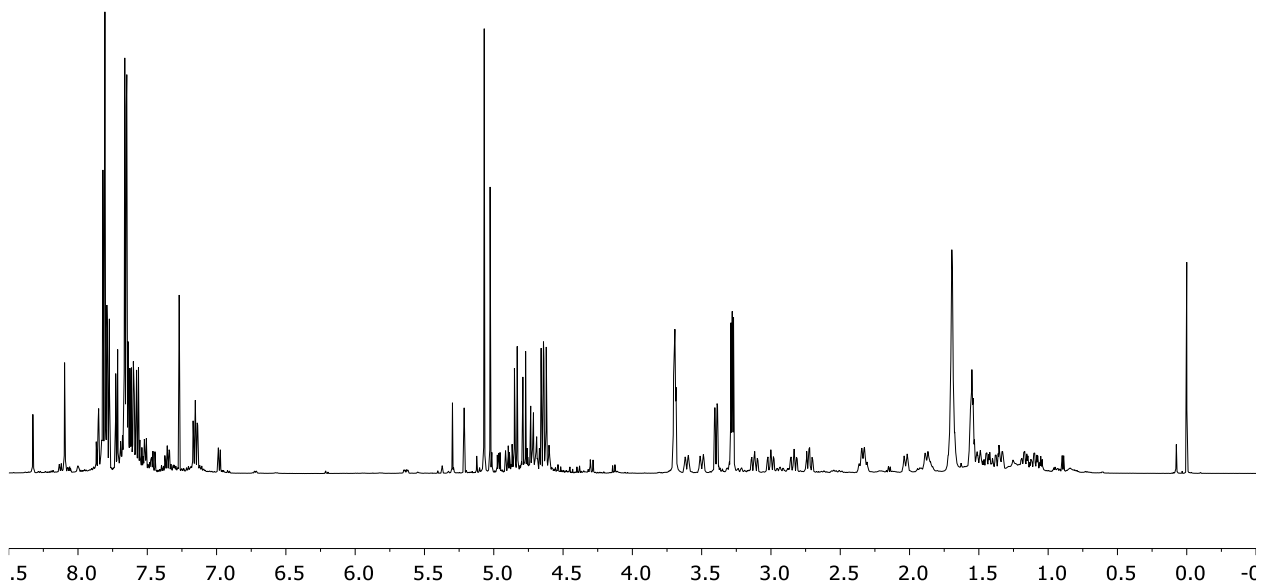


(Scheme 4, **13g**)

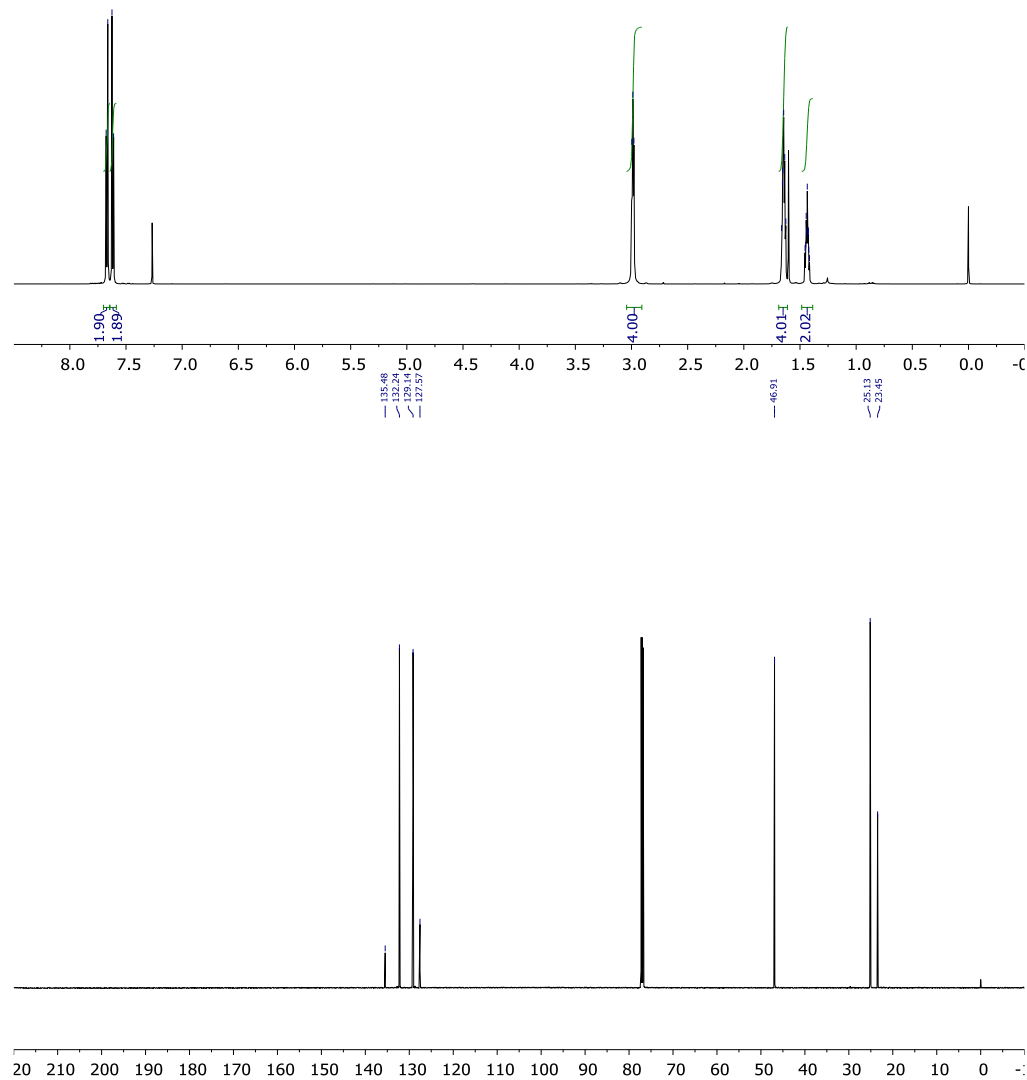


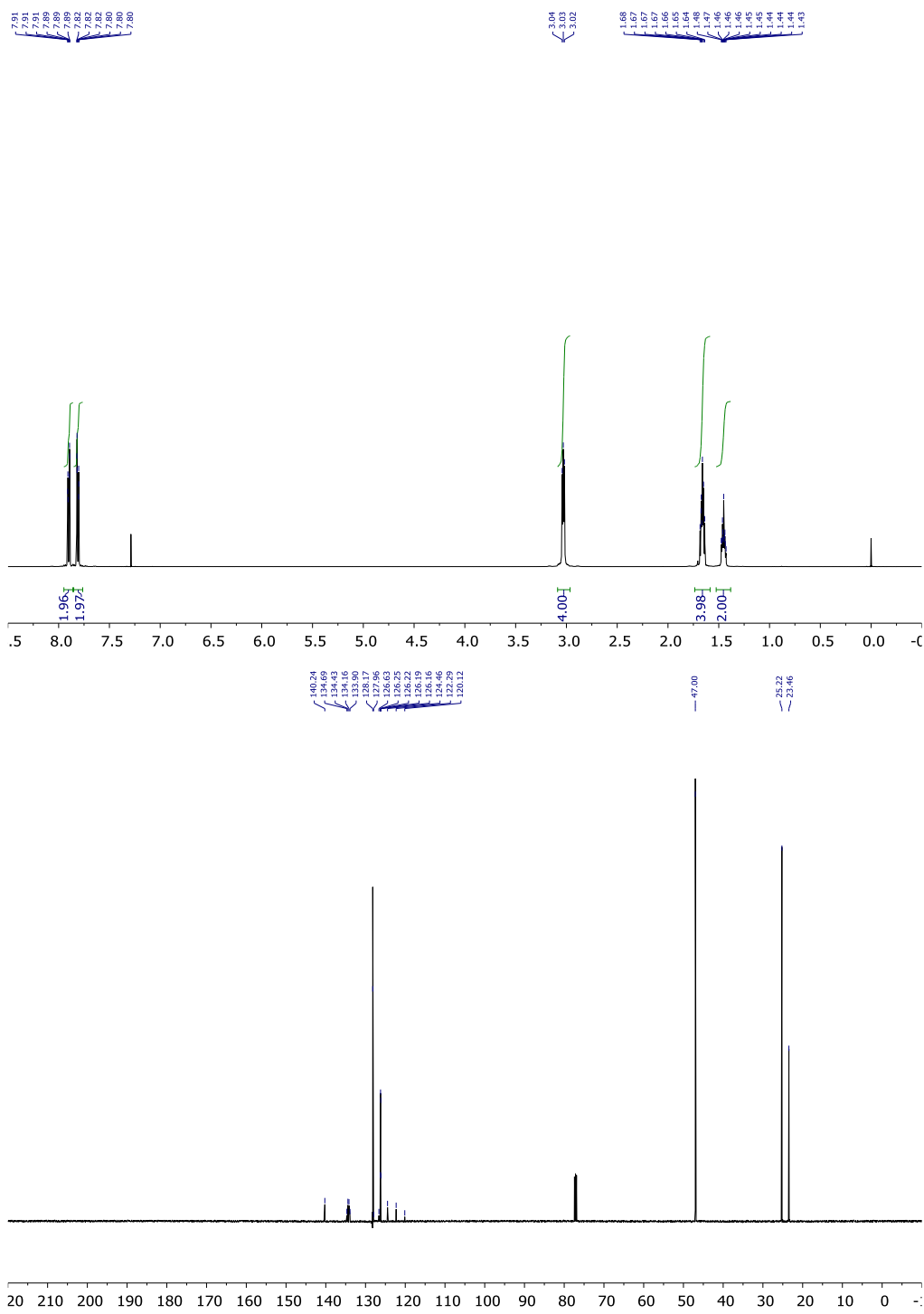
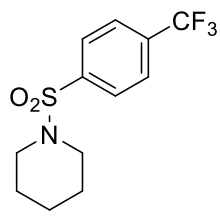


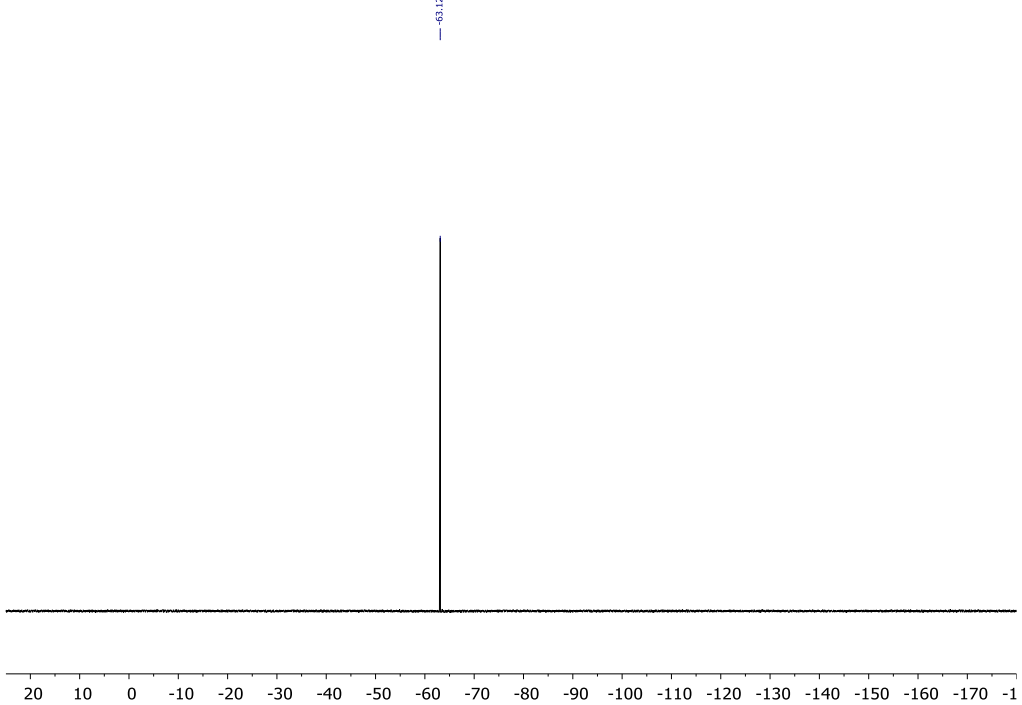
(Scheme 4, **13h**)

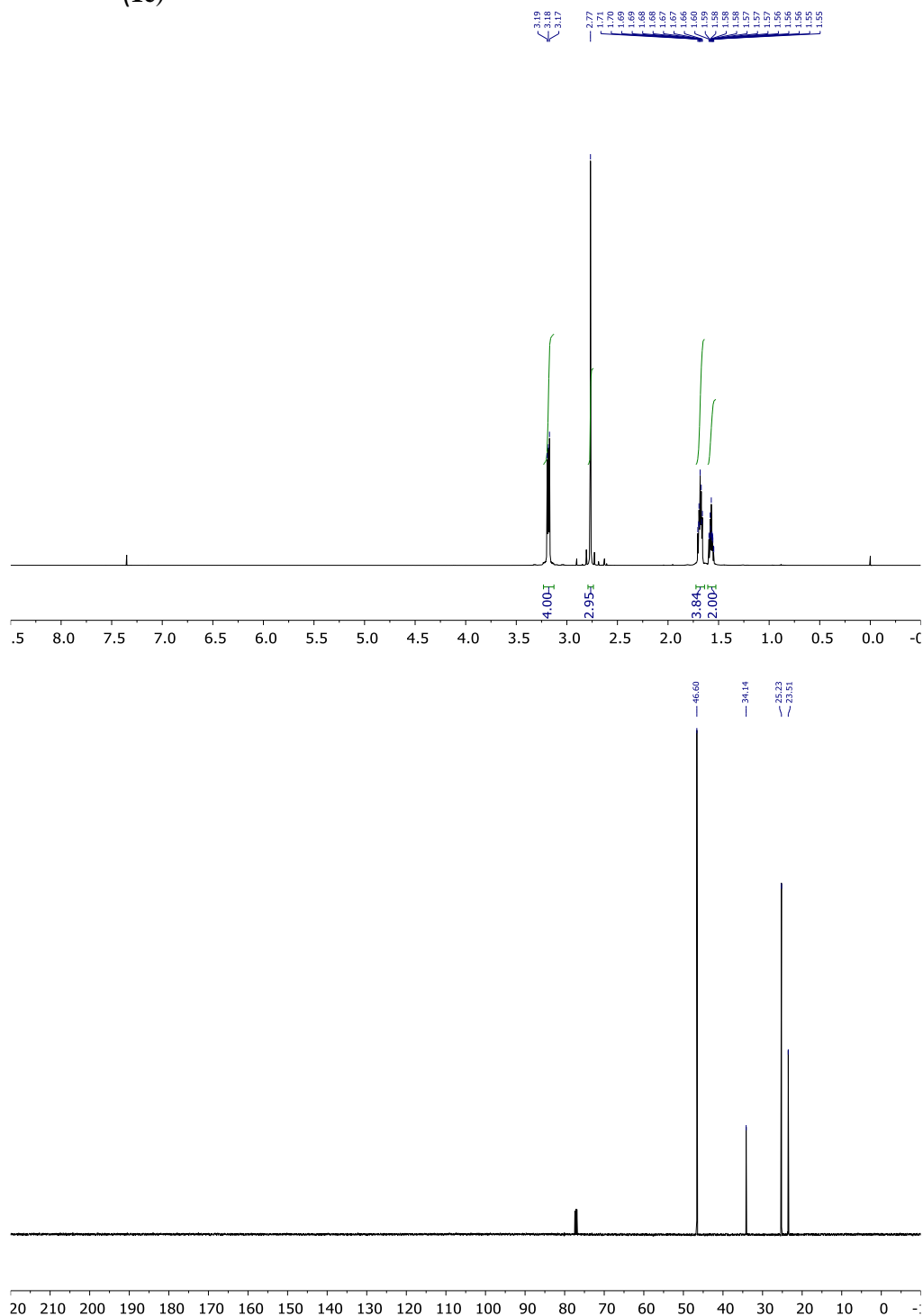
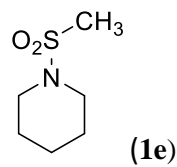


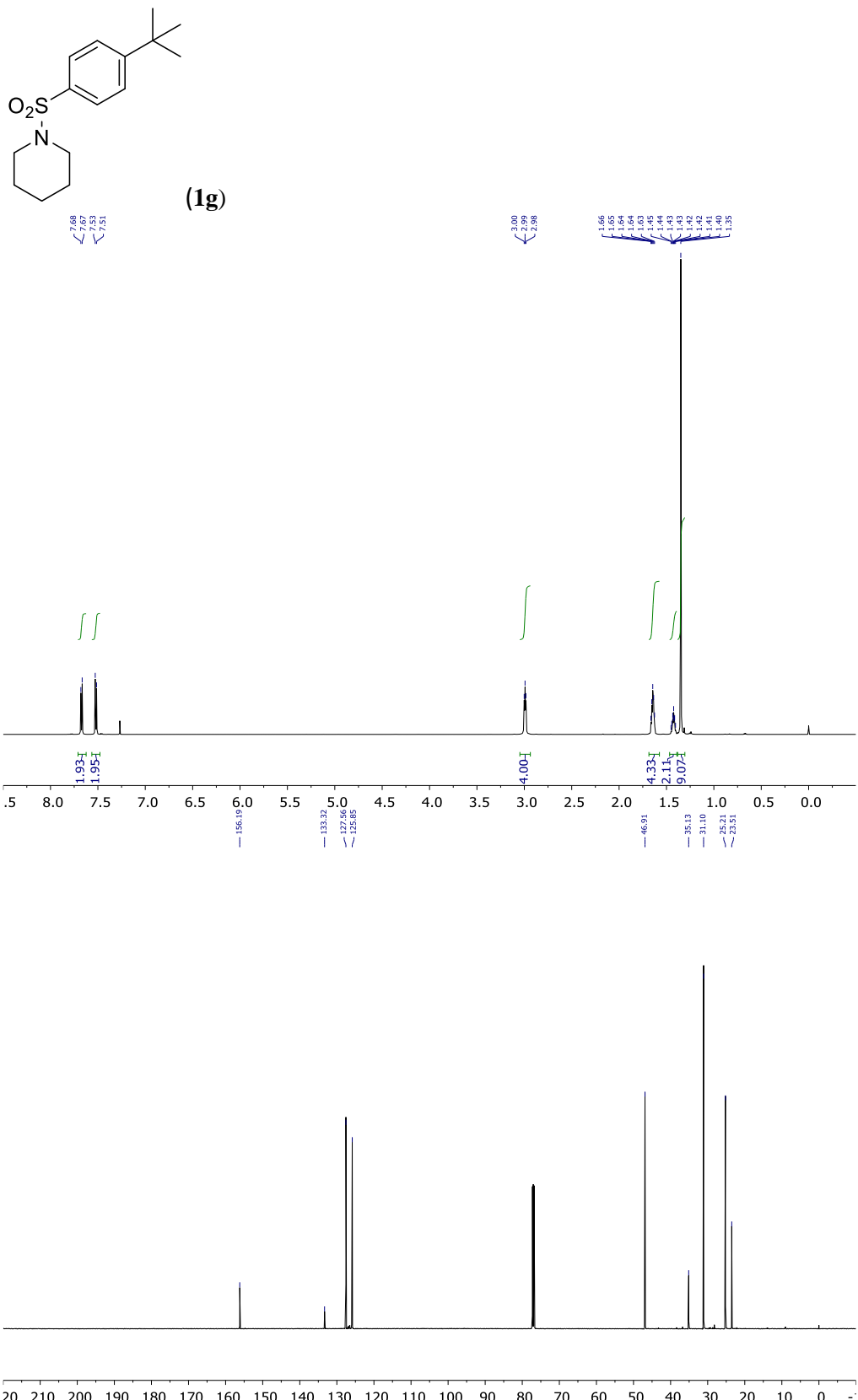
8. Characterization NMR Spectra

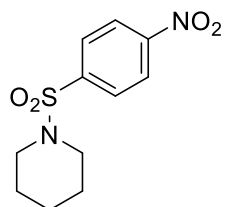




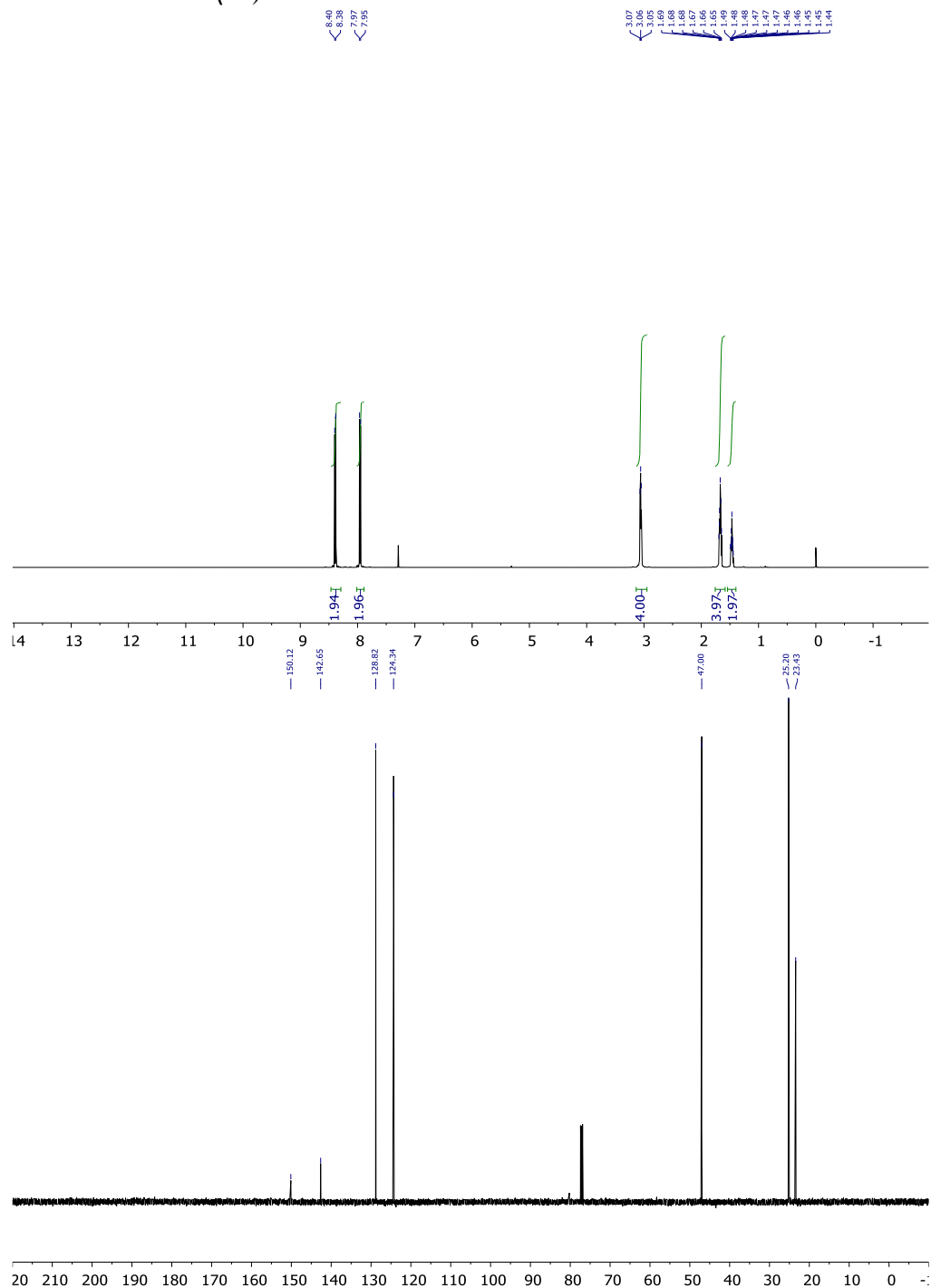


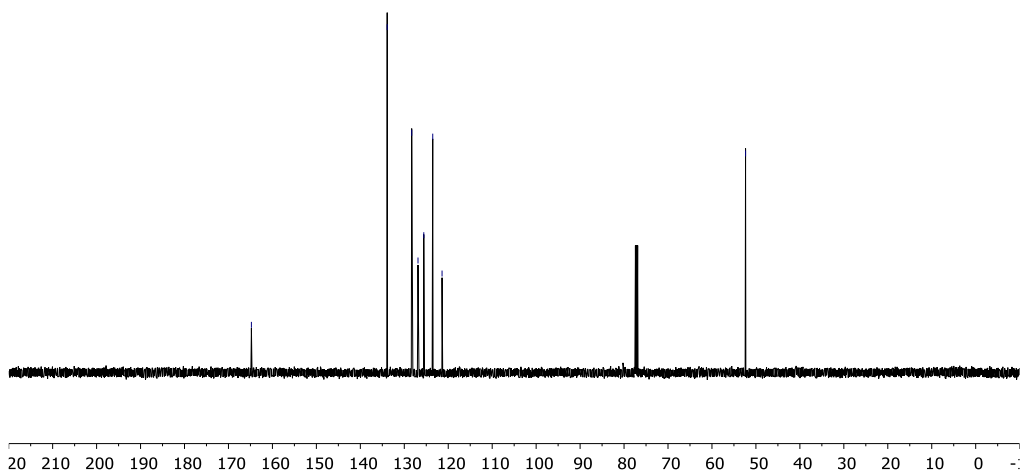
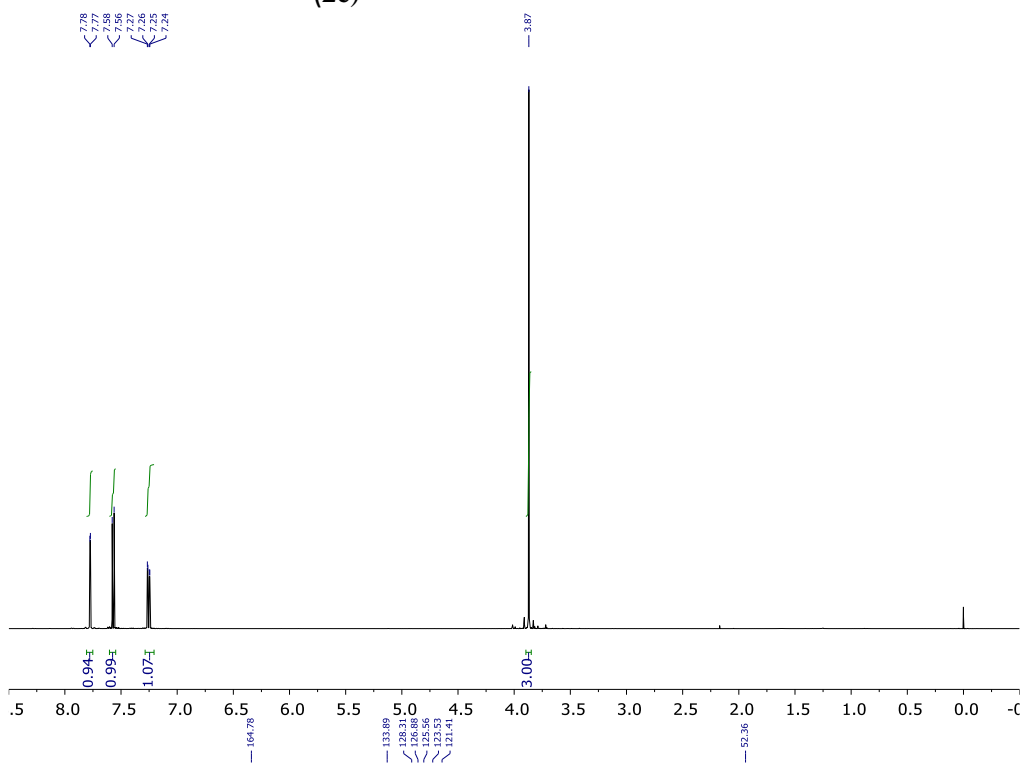
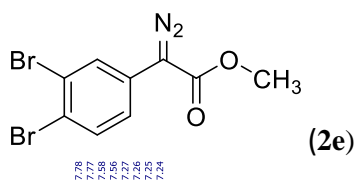


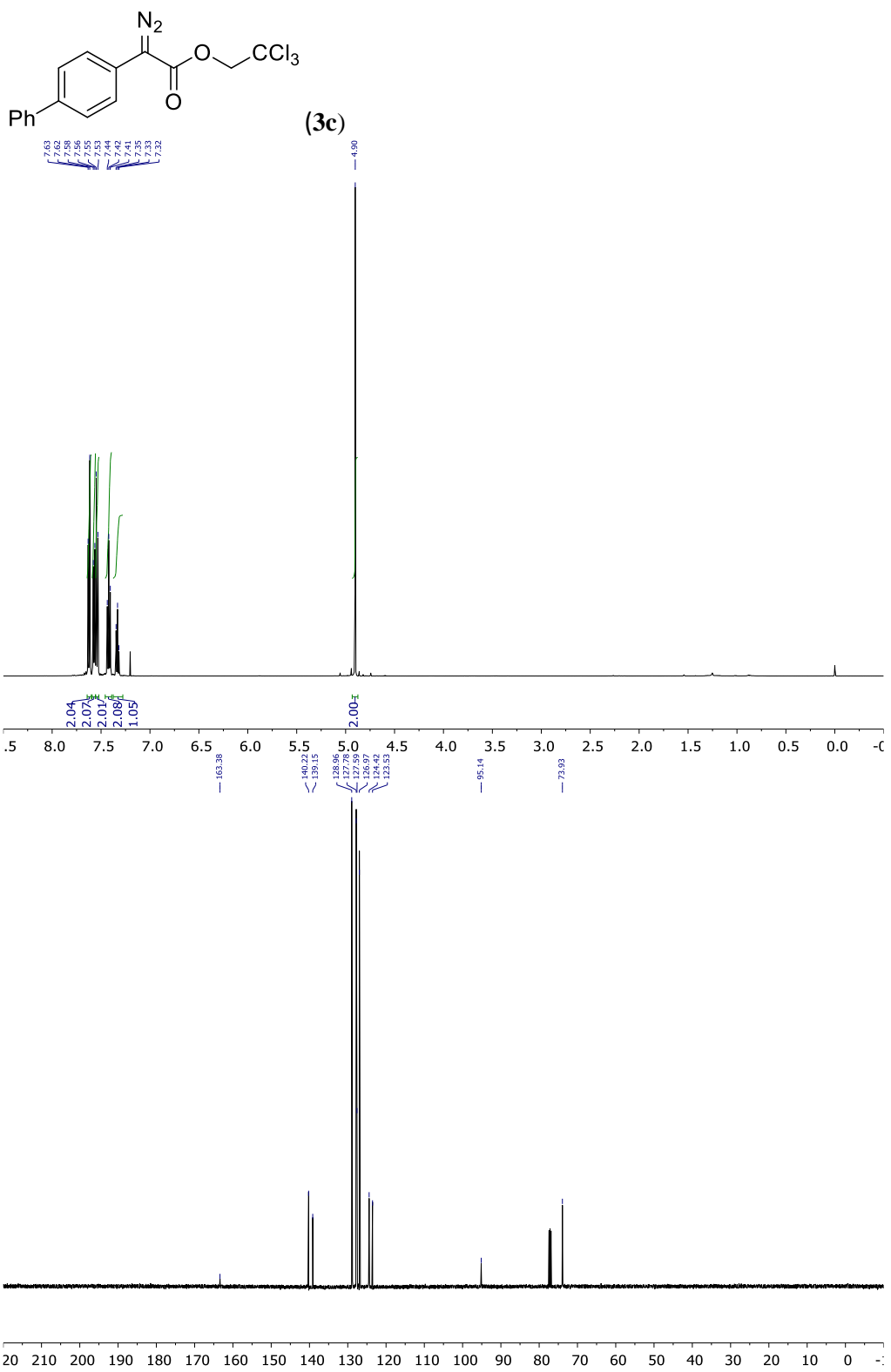


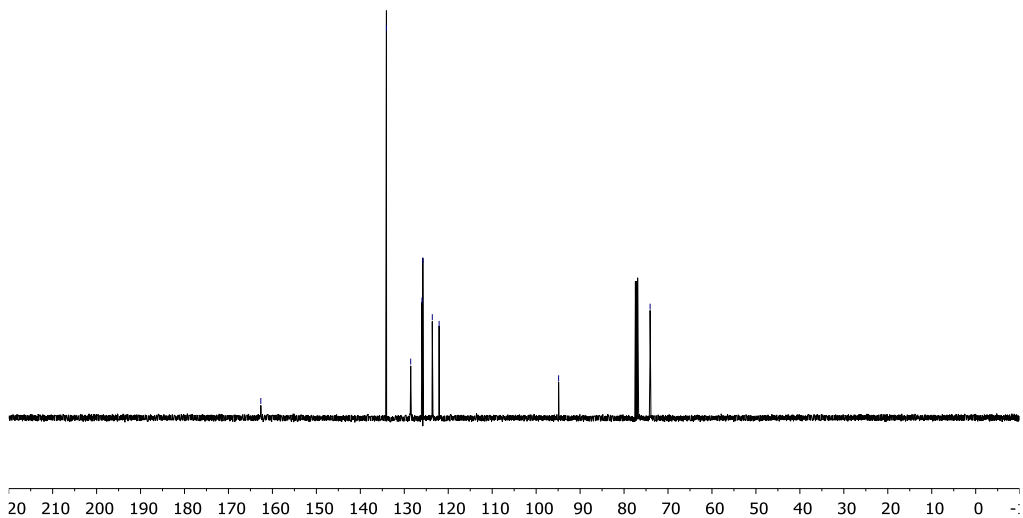
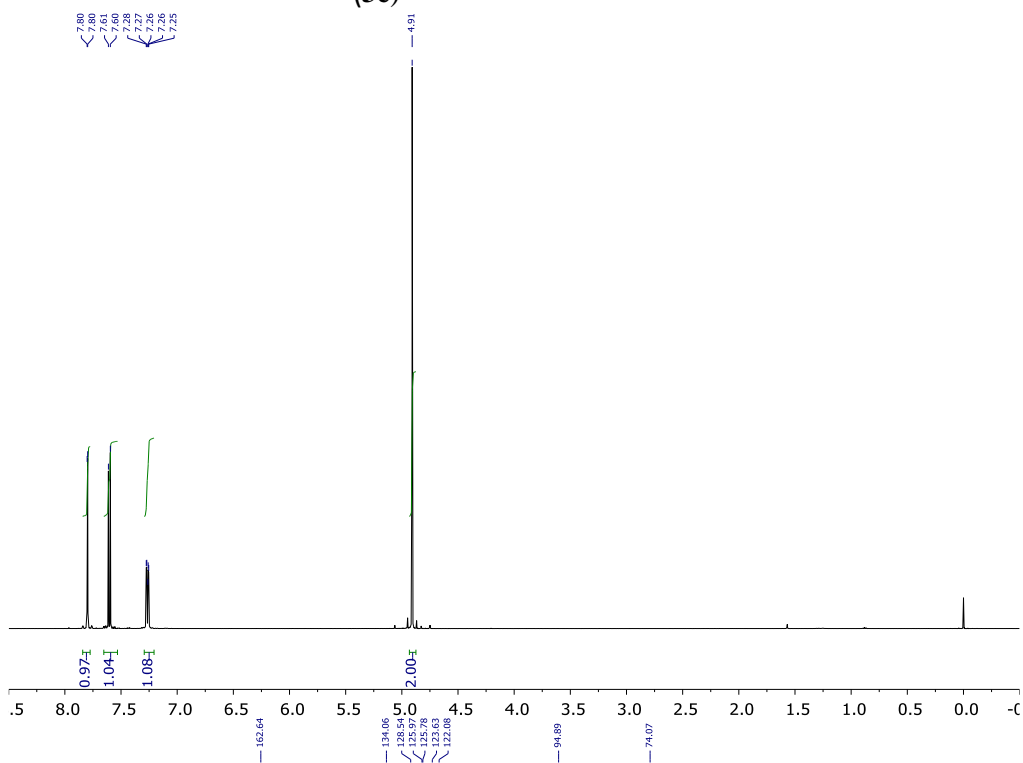
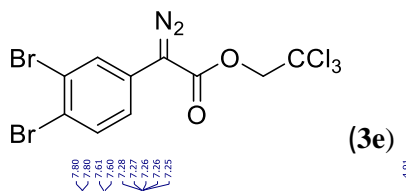


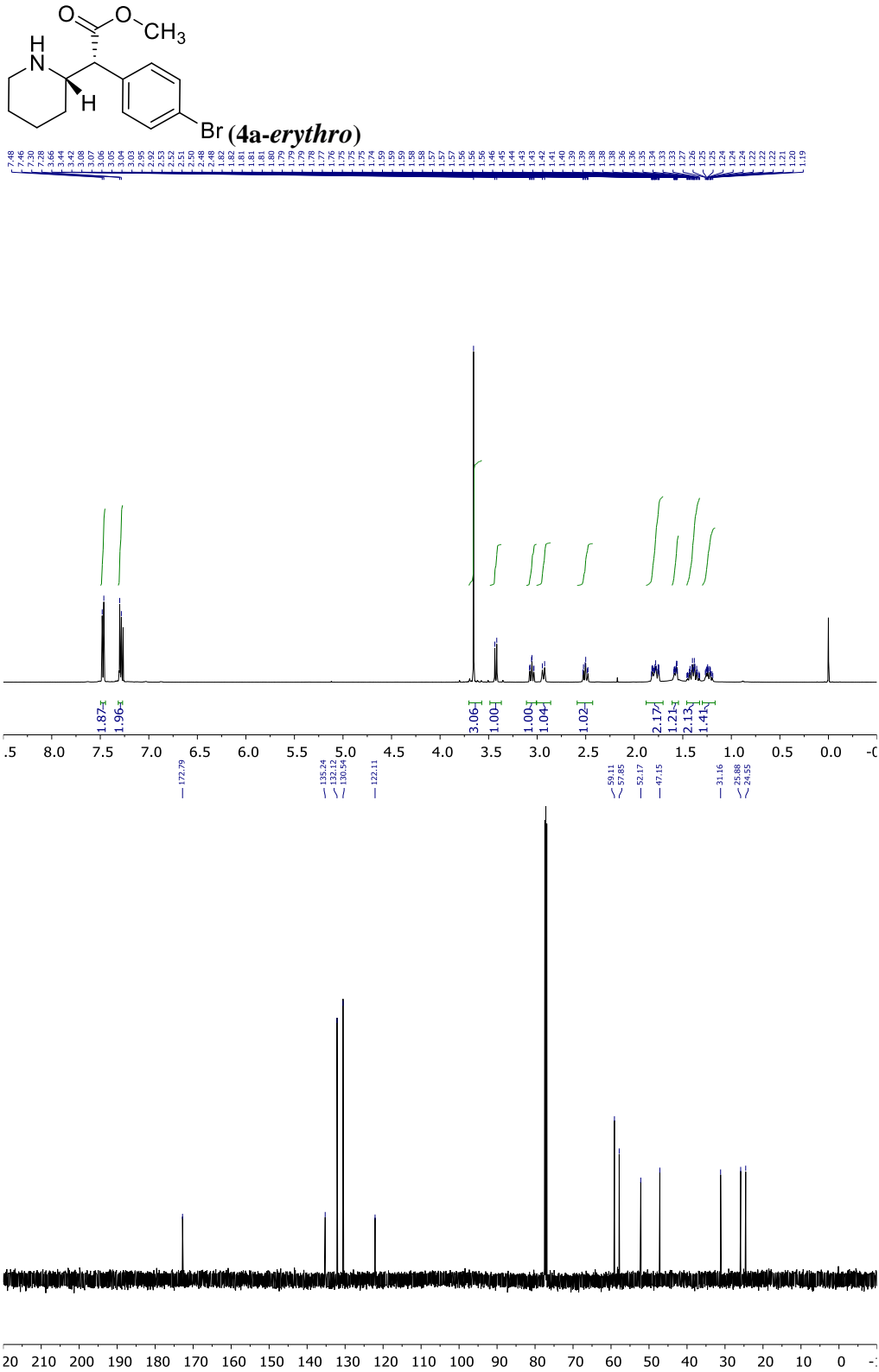
(1h)

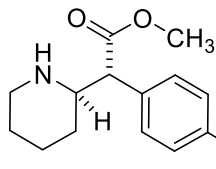




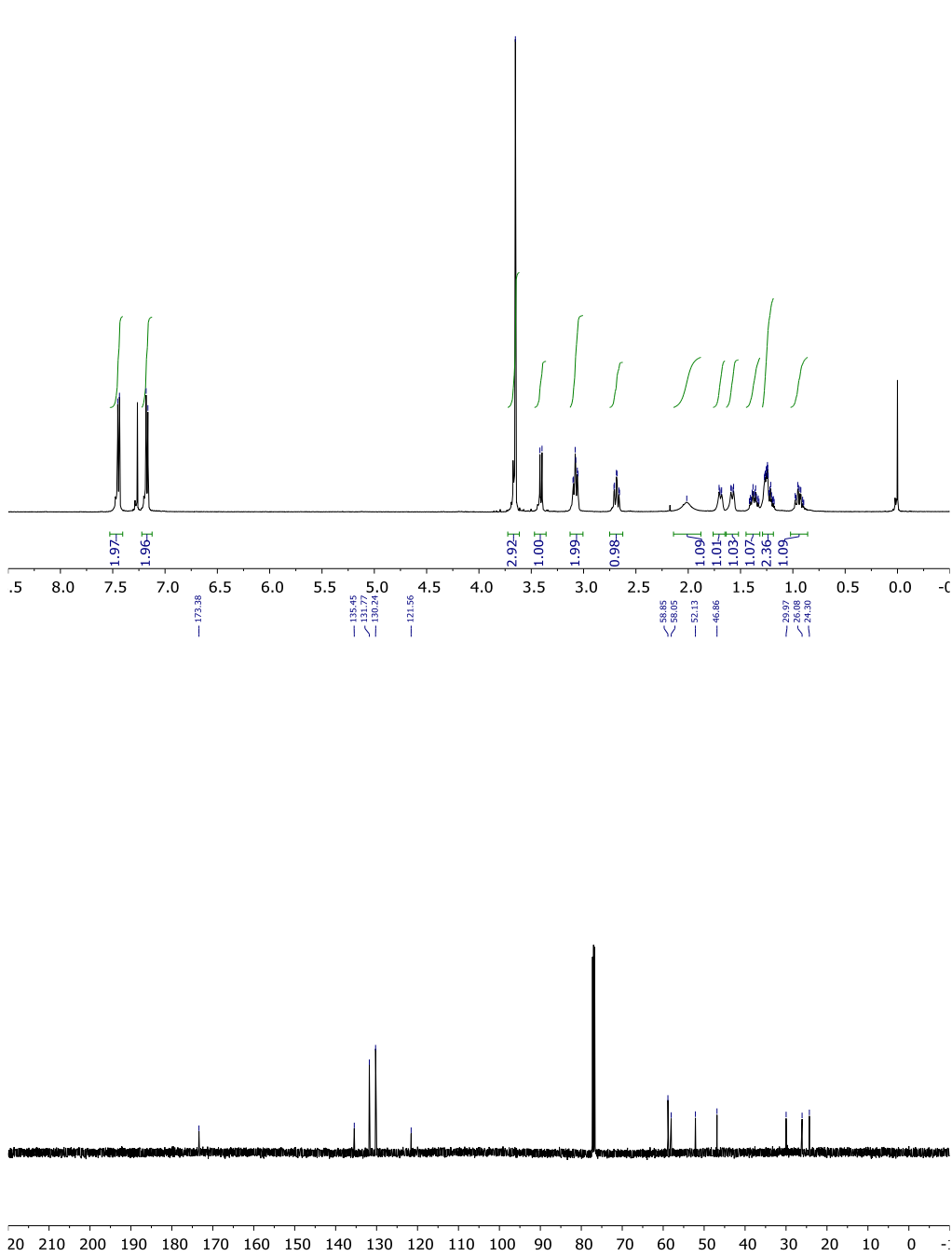


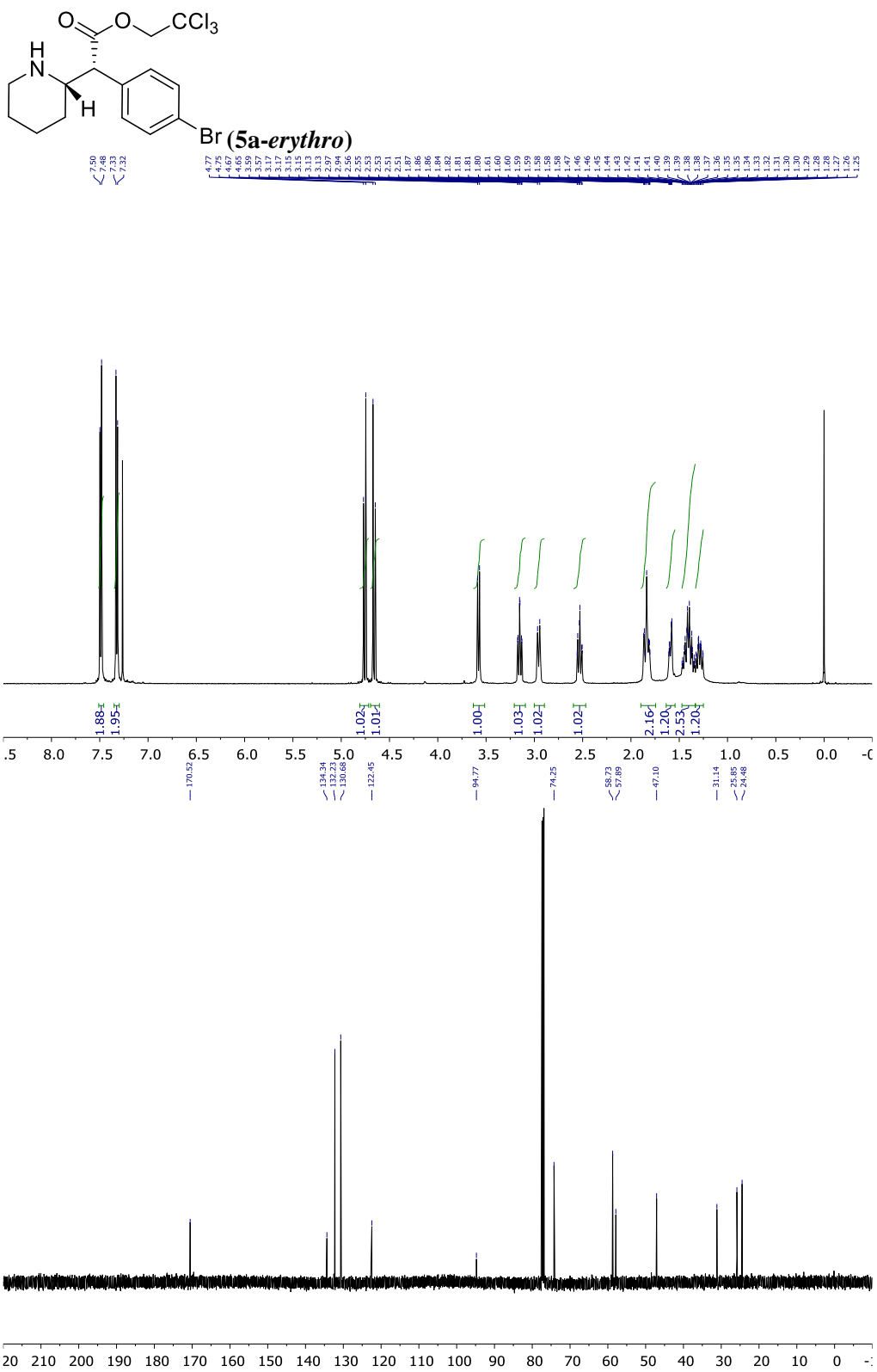


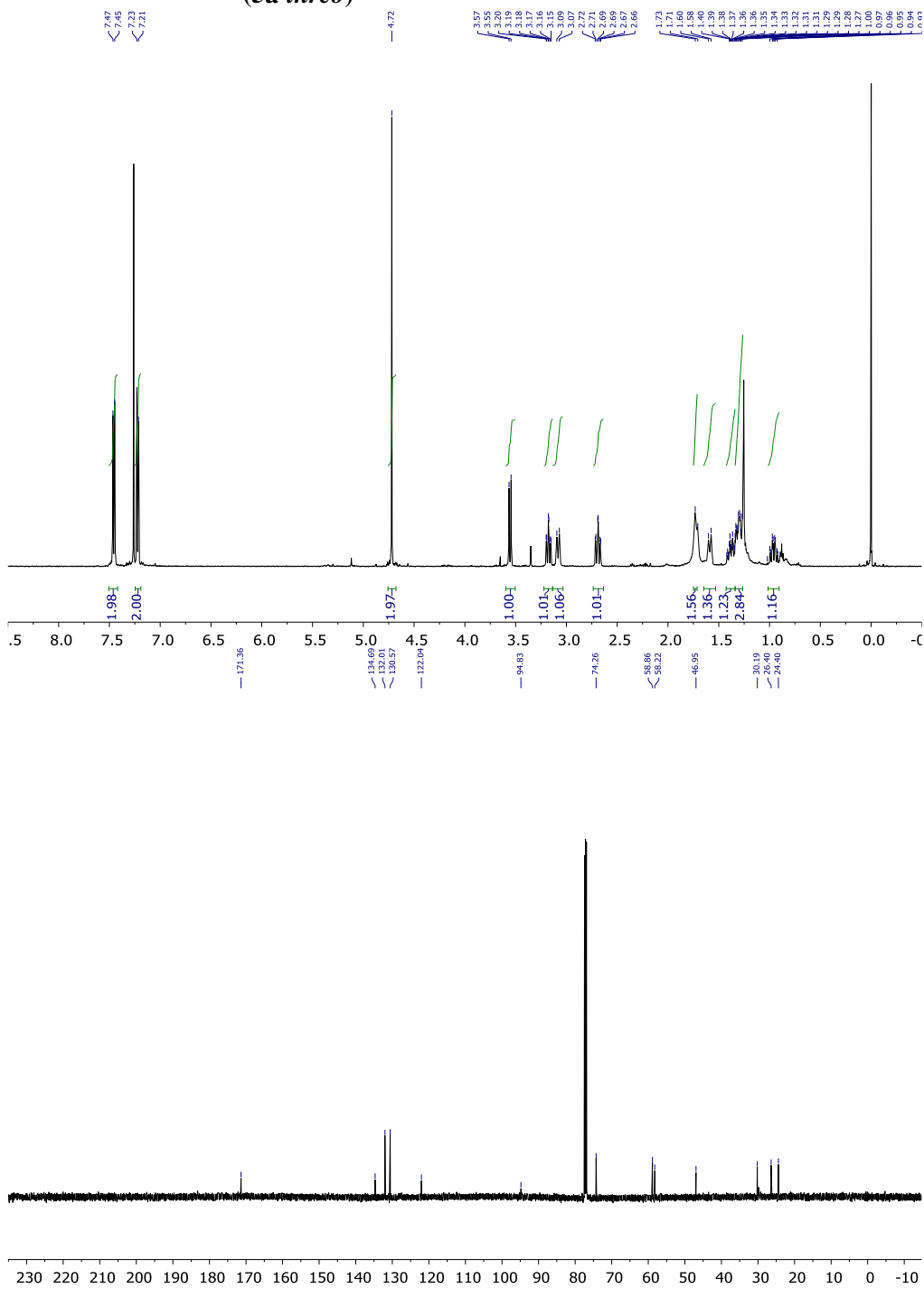
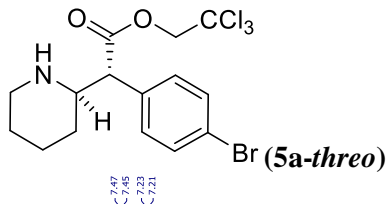


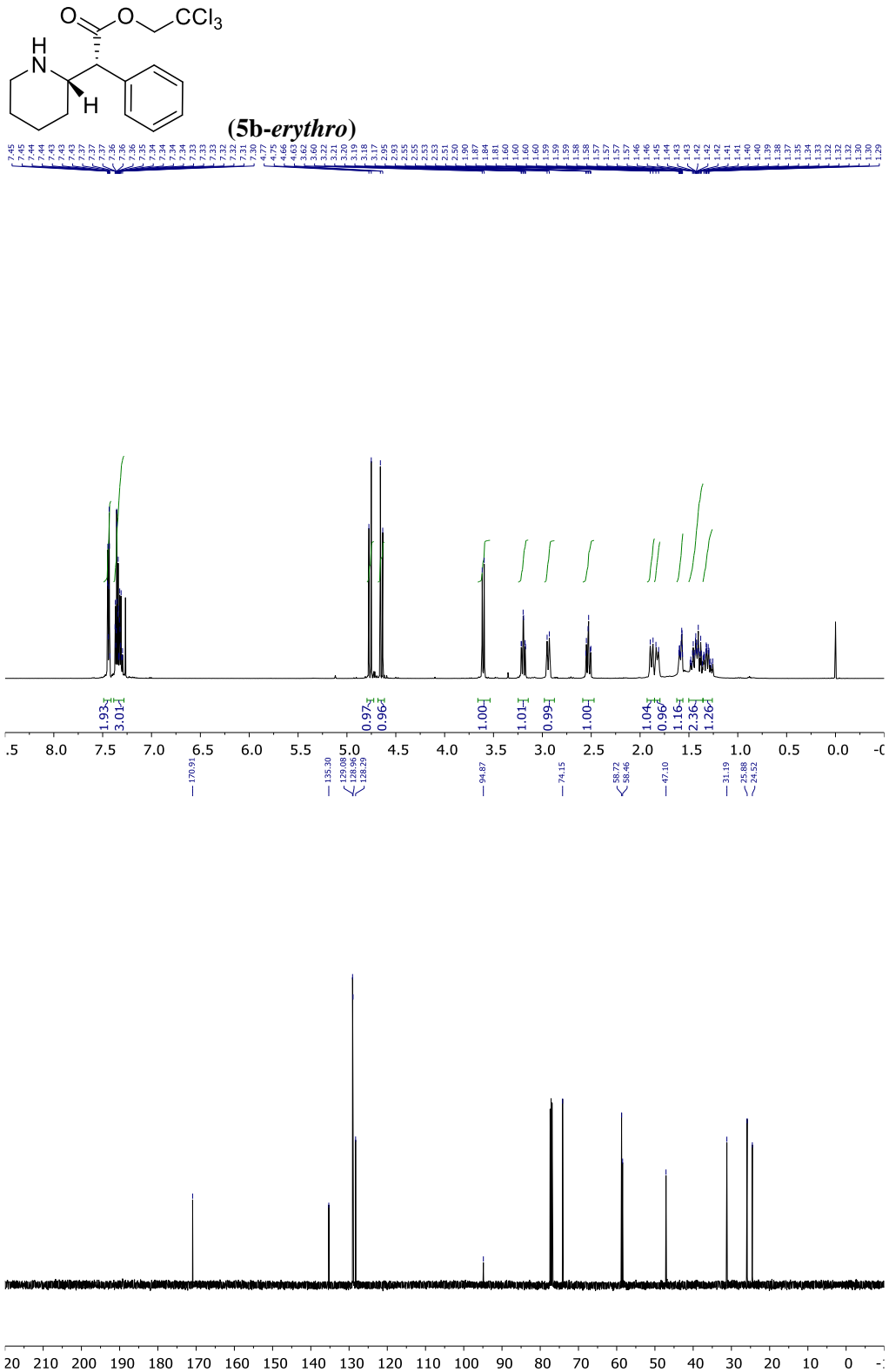


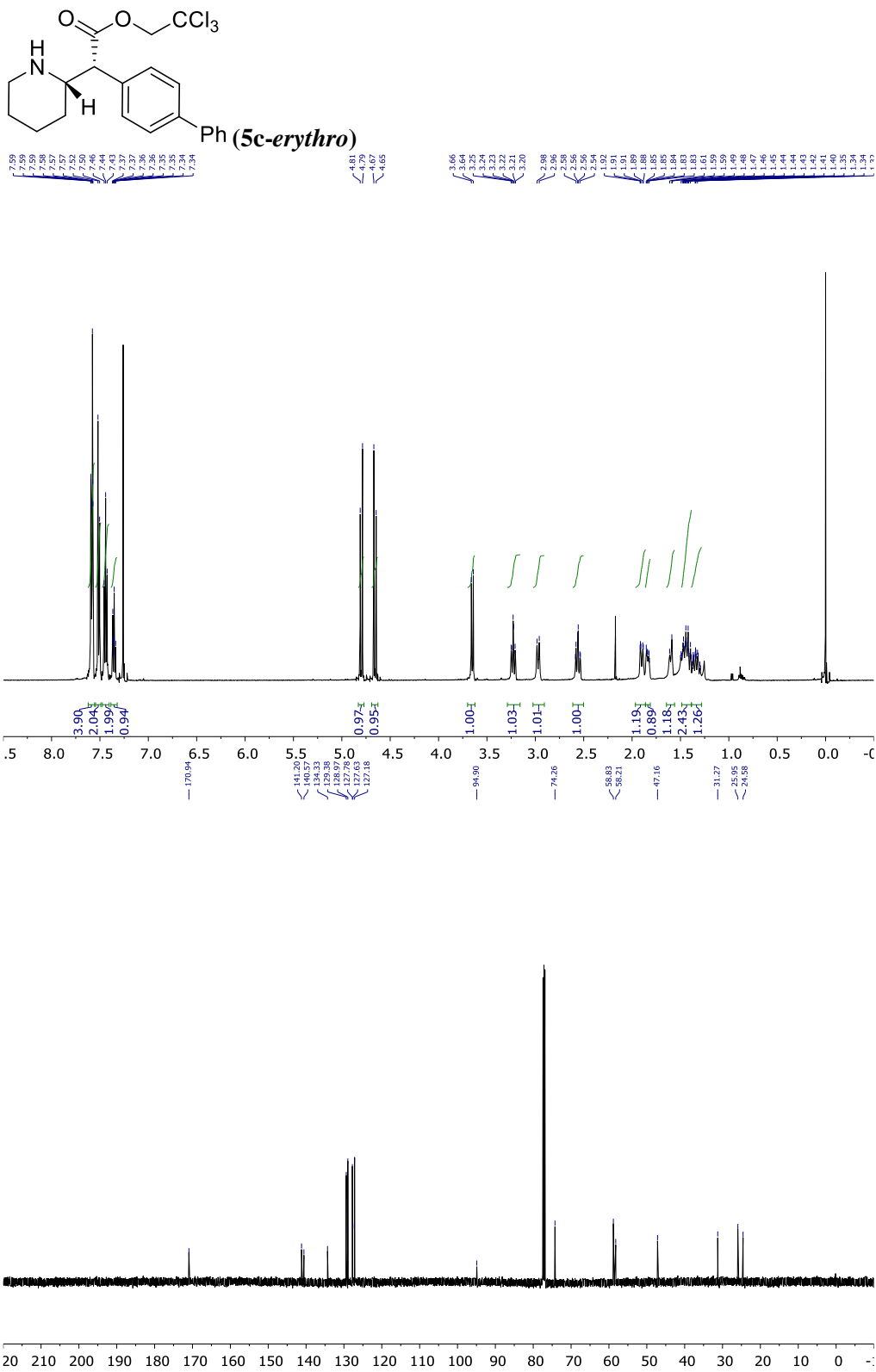
Br (4a-*threo*)

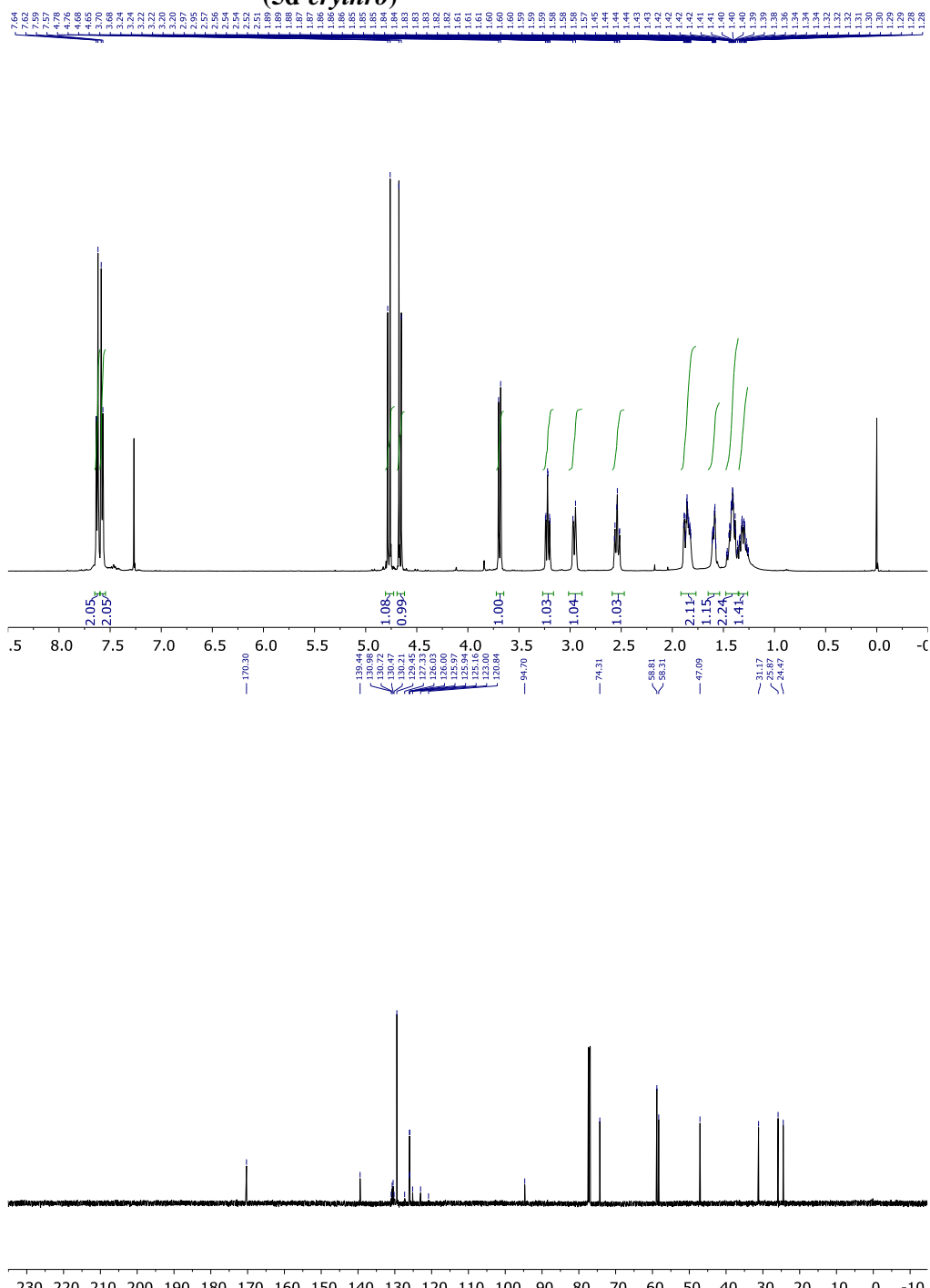
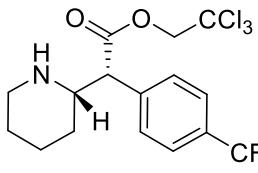


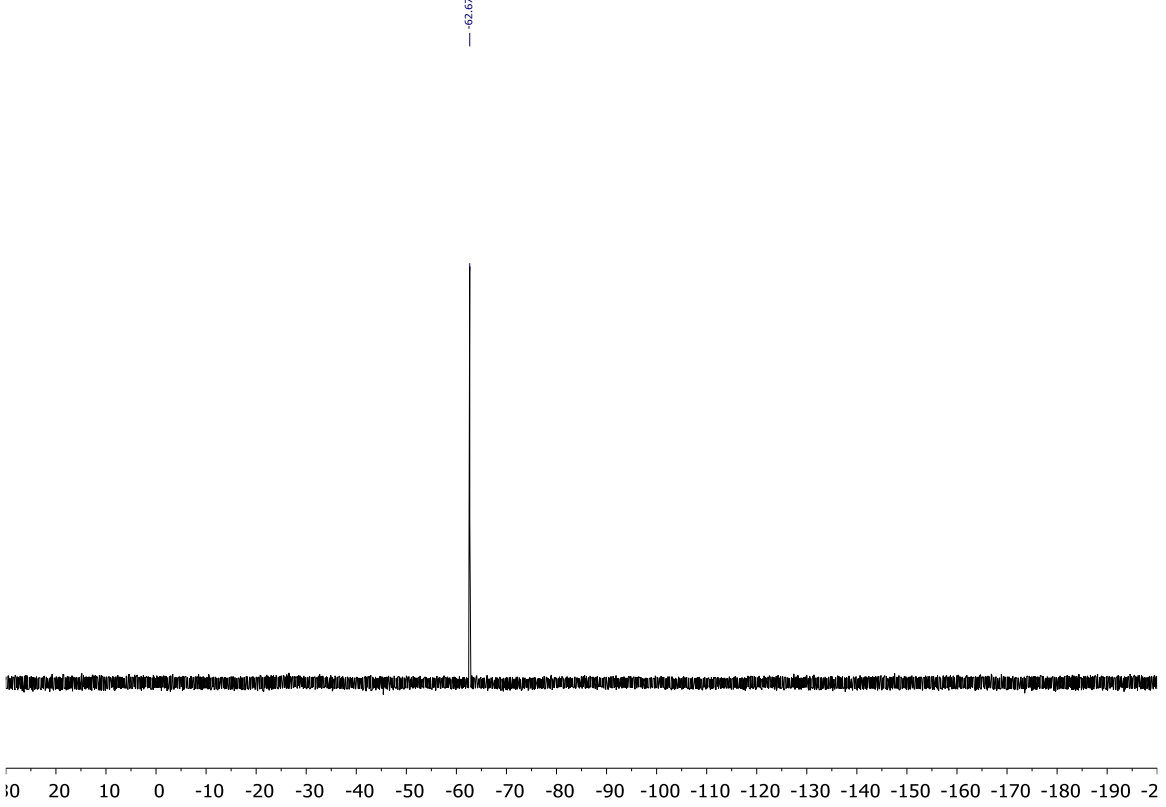


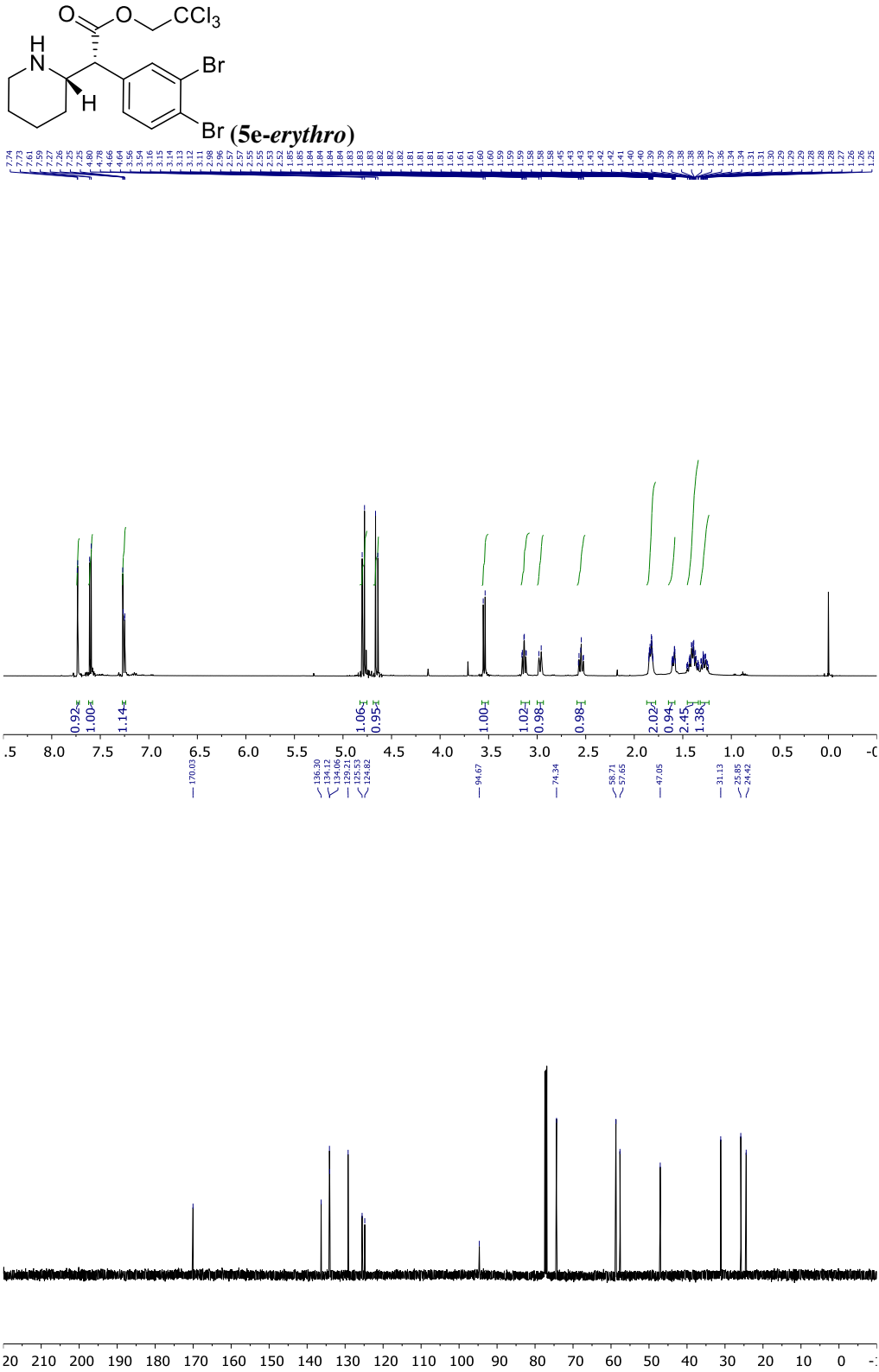


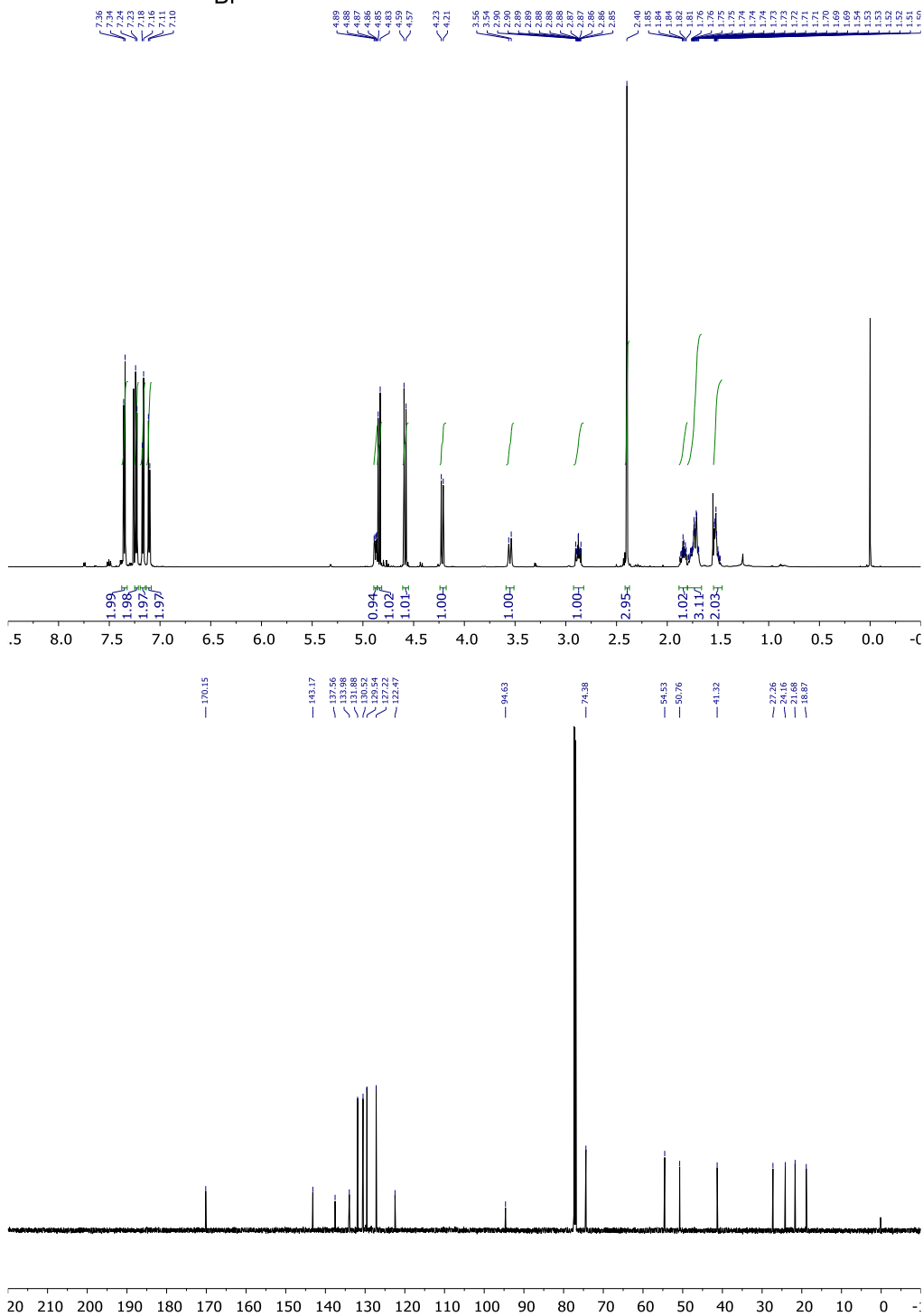
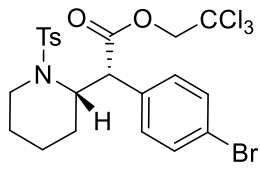


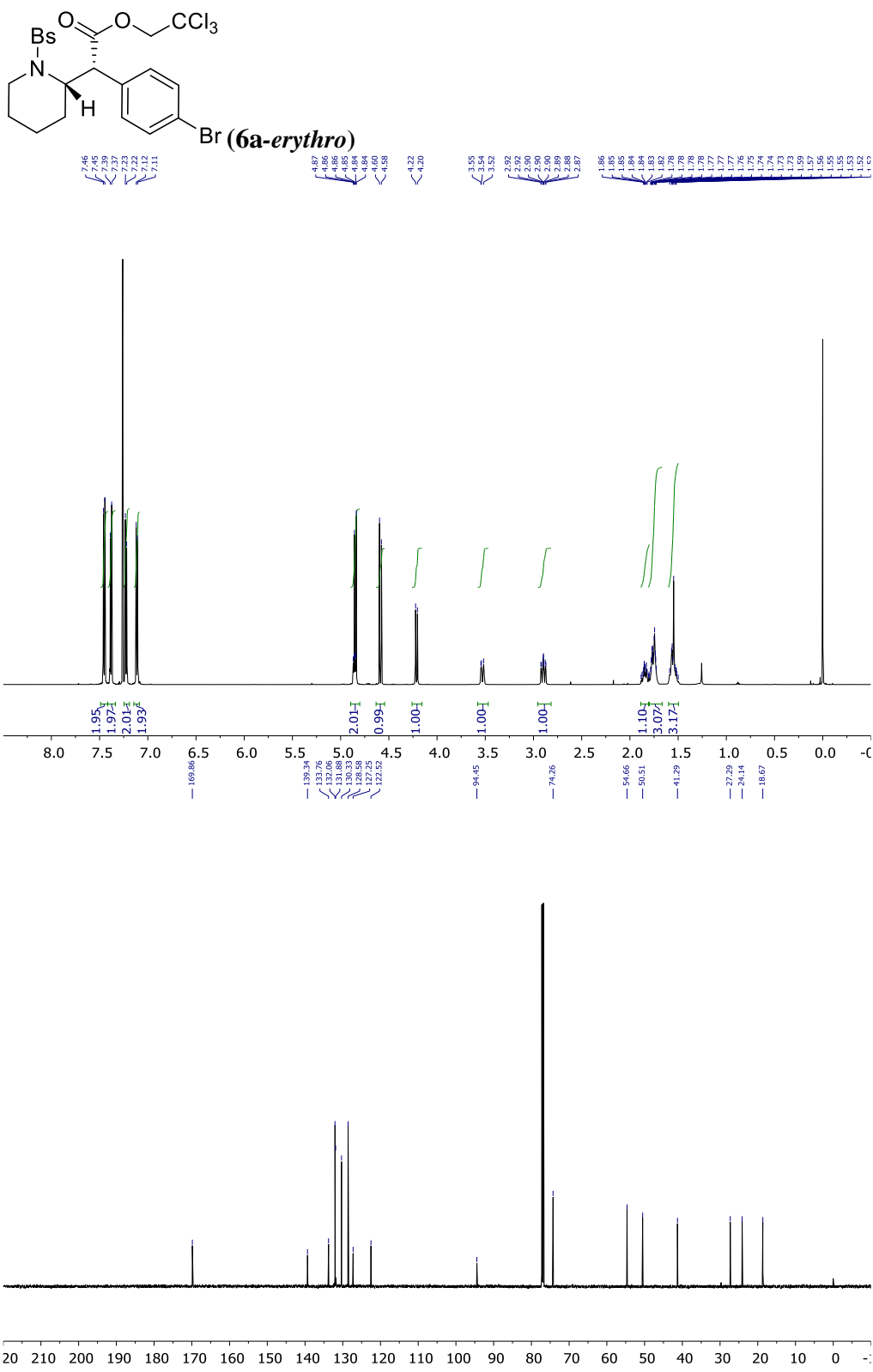


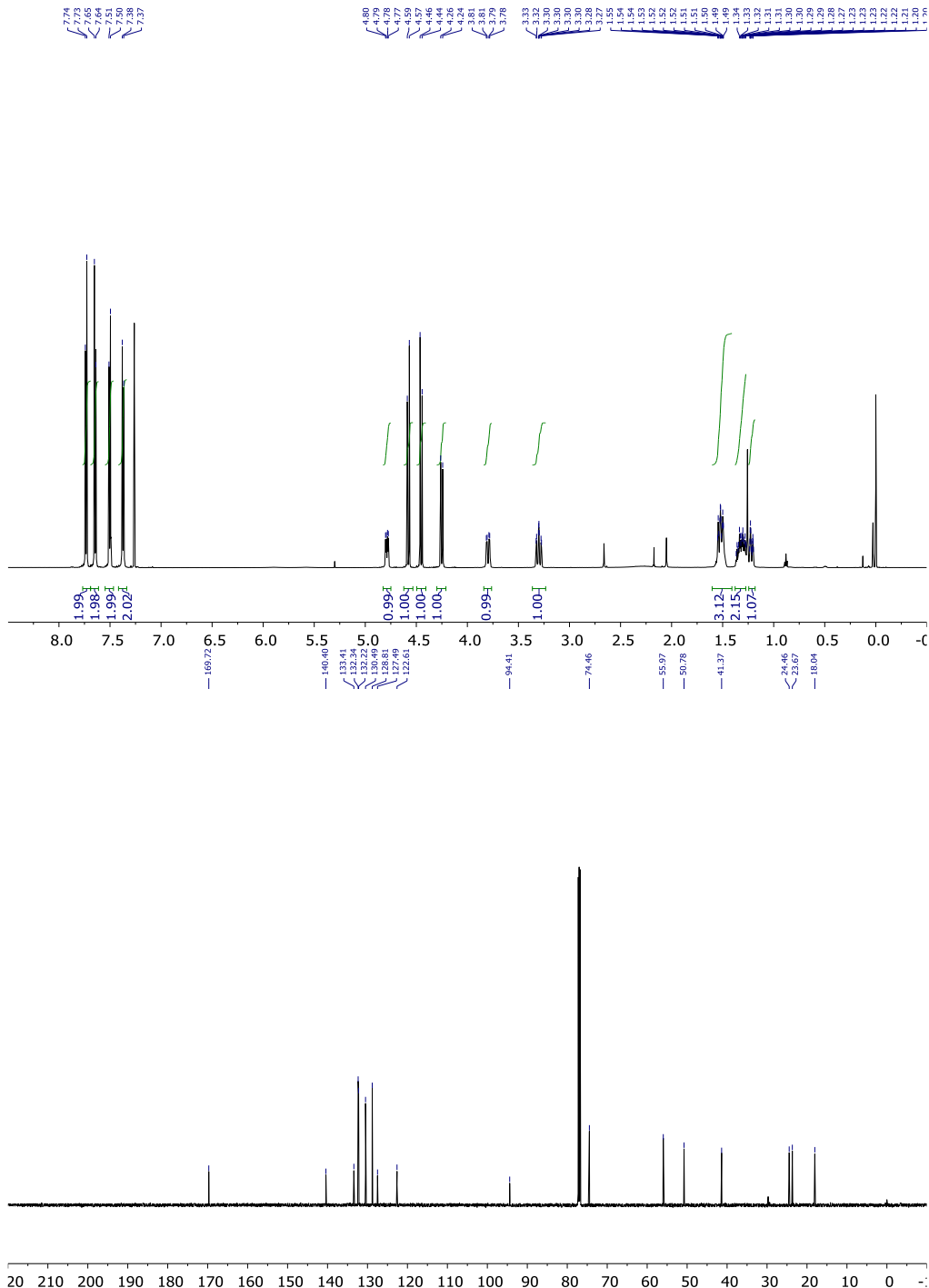
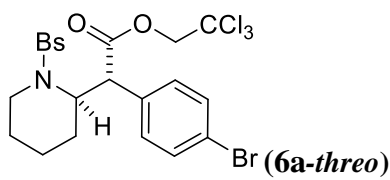


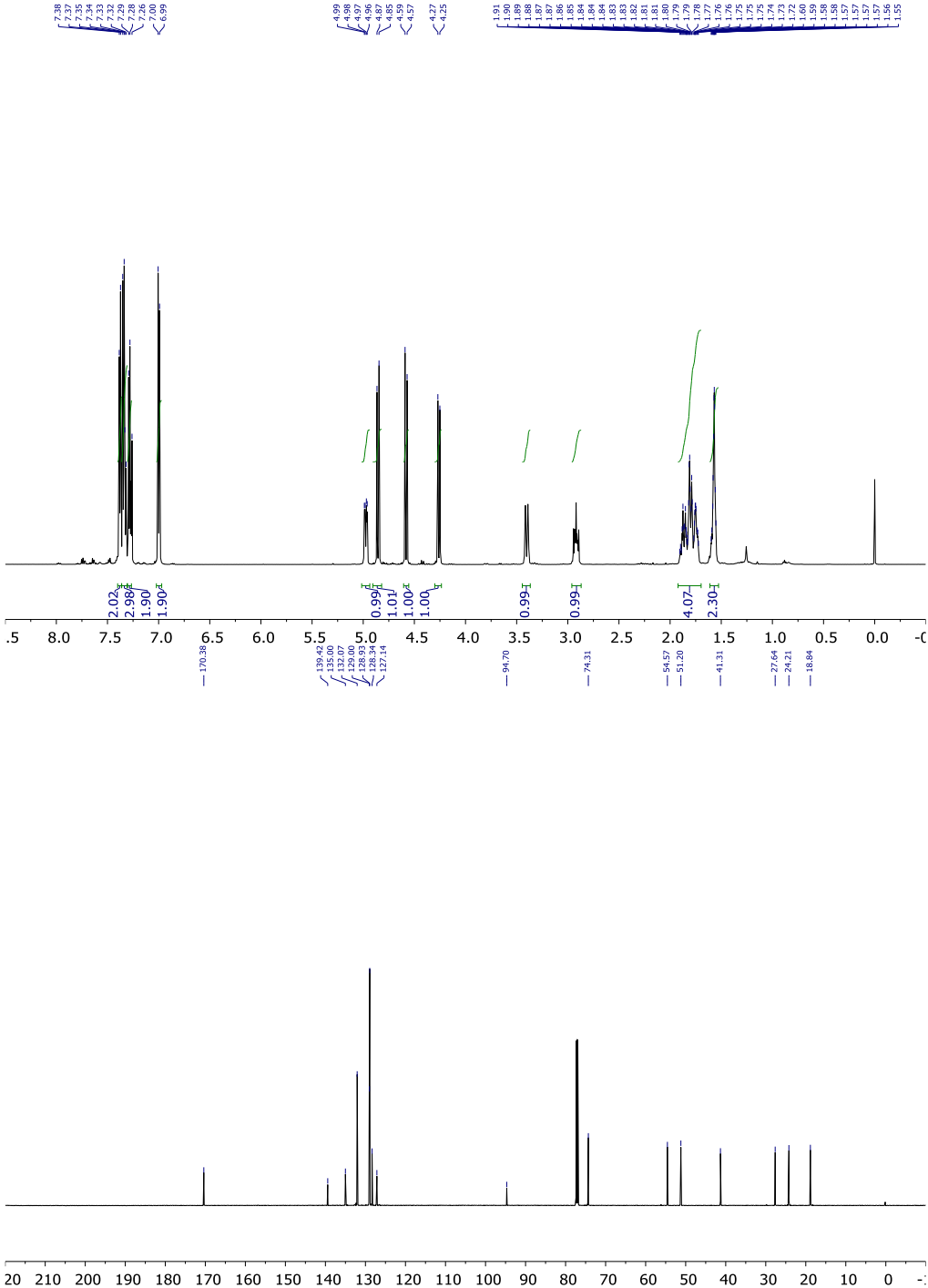
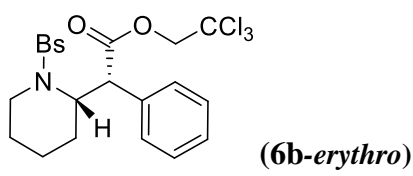


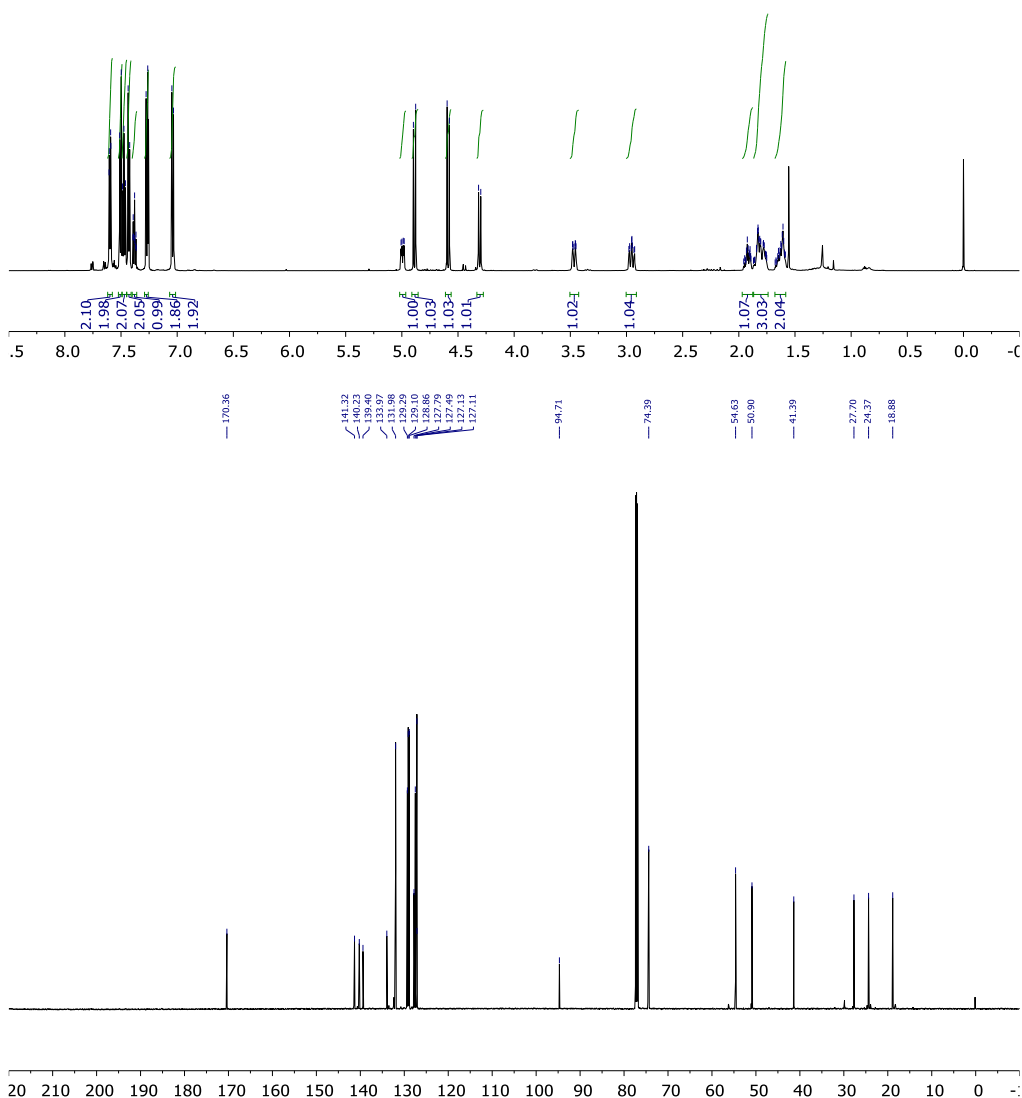
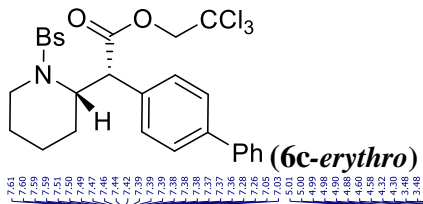


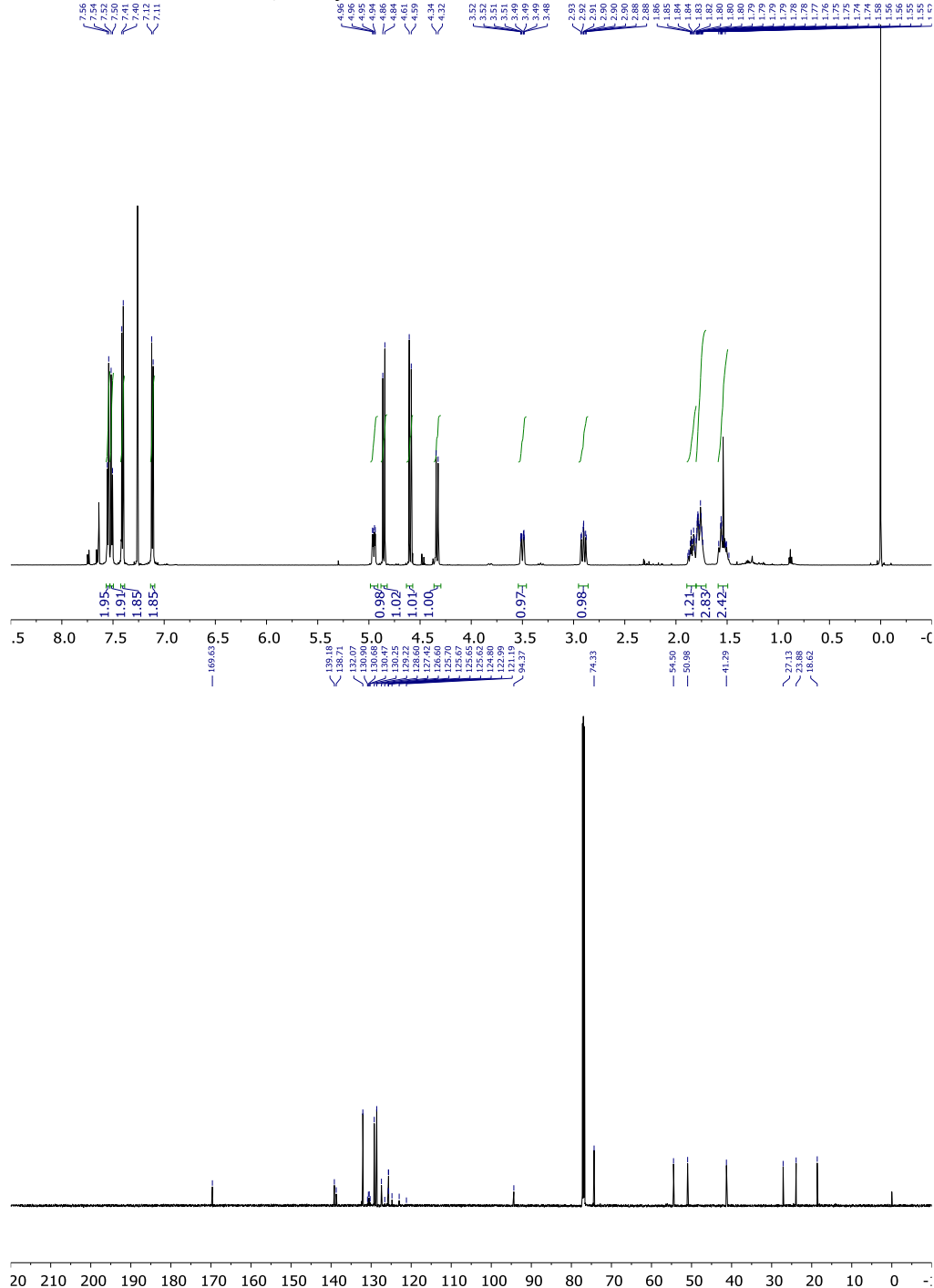
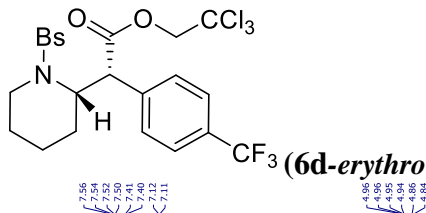


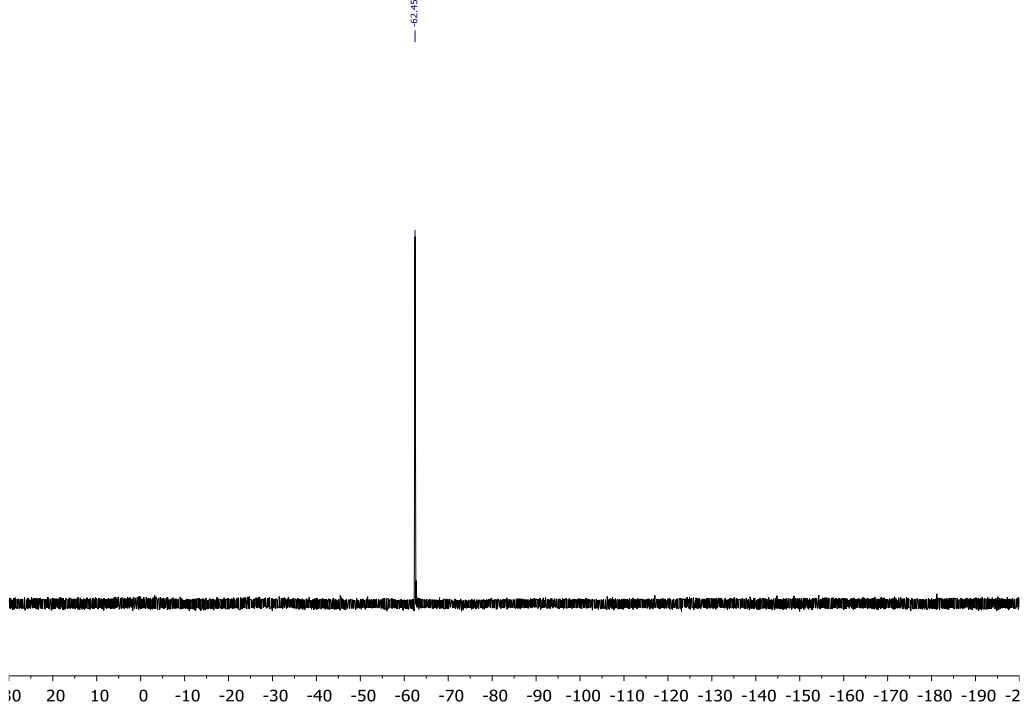


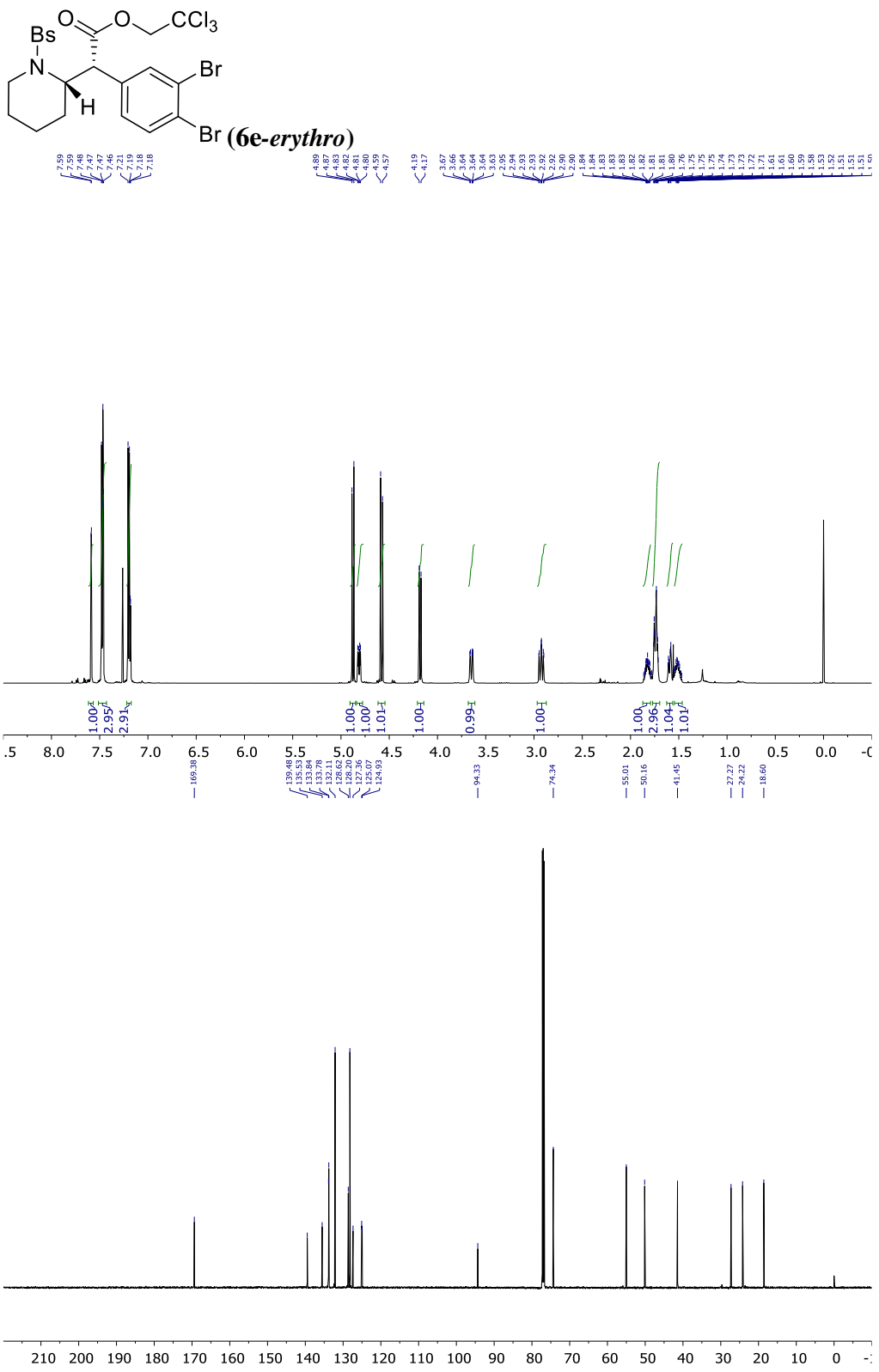


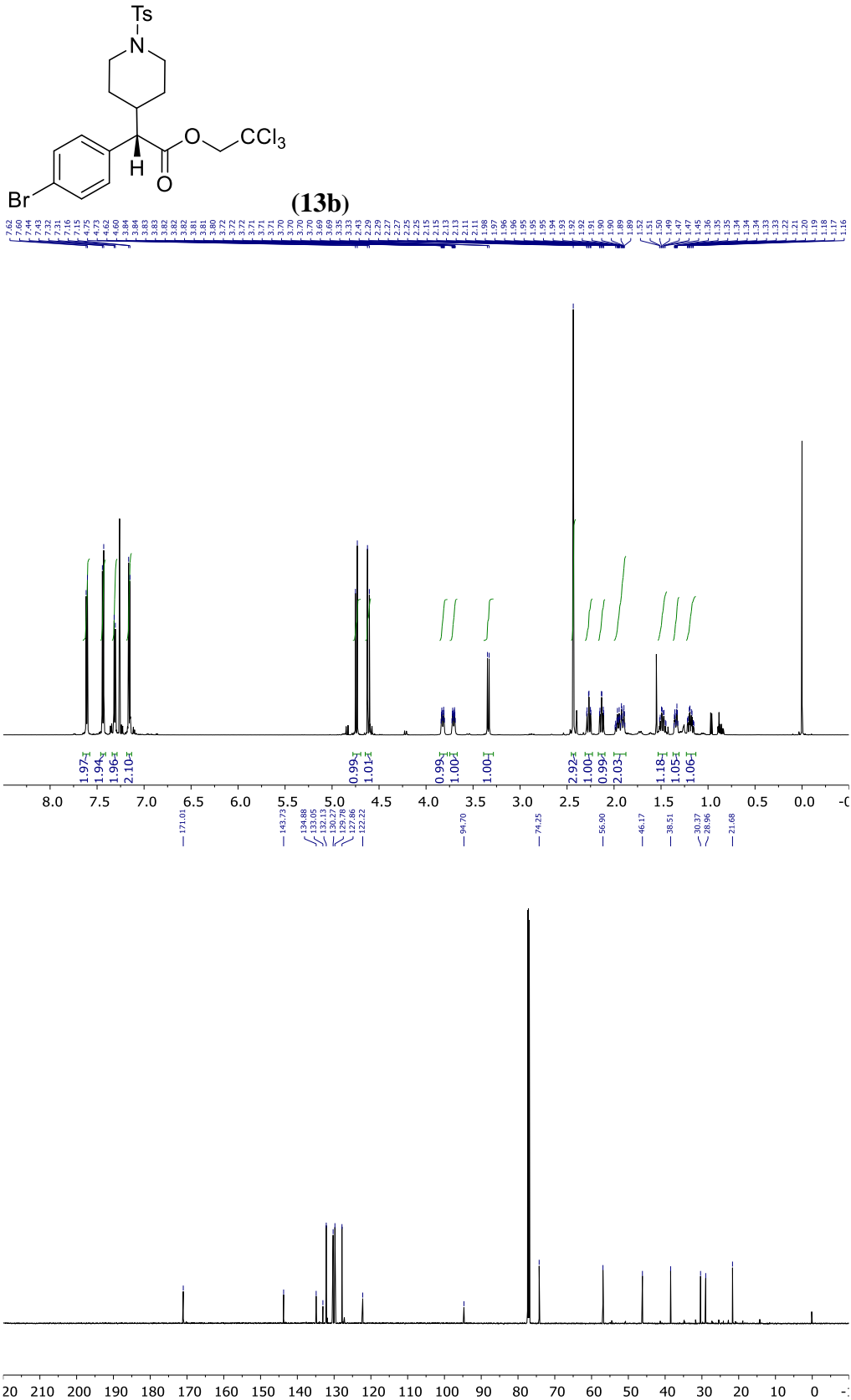


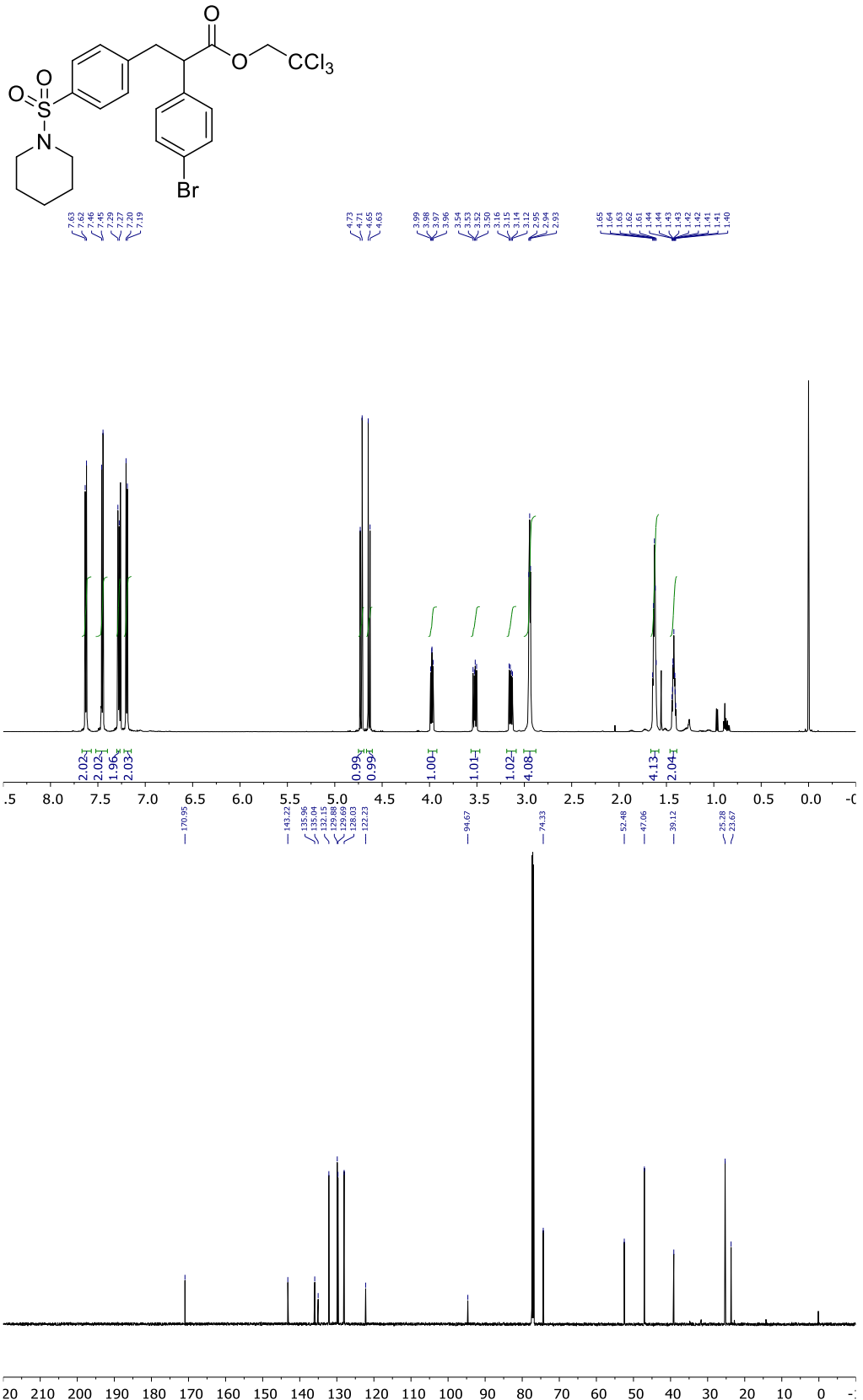


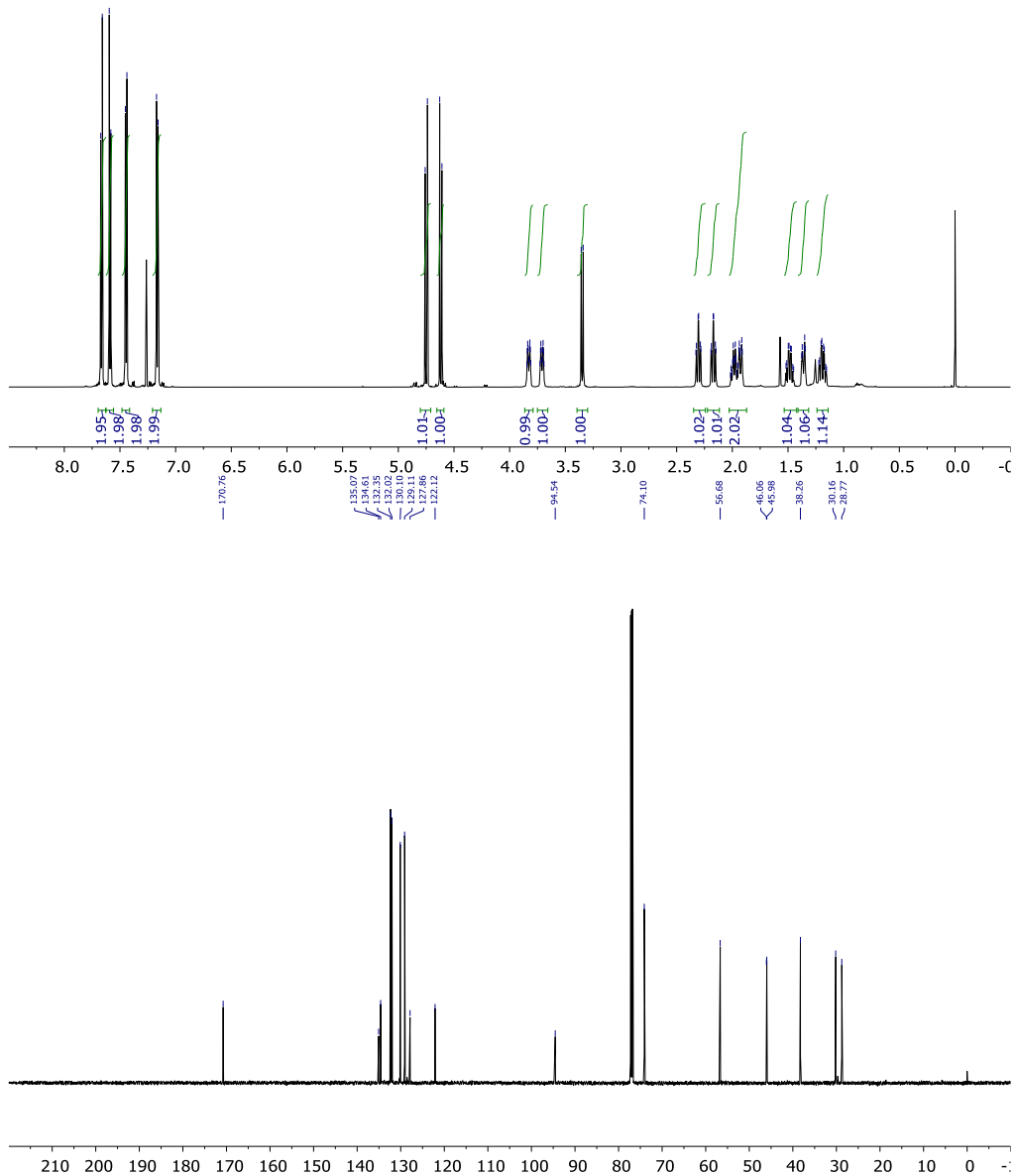
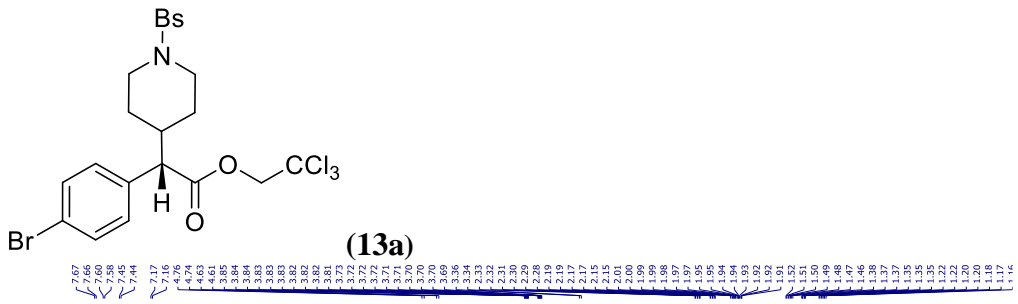


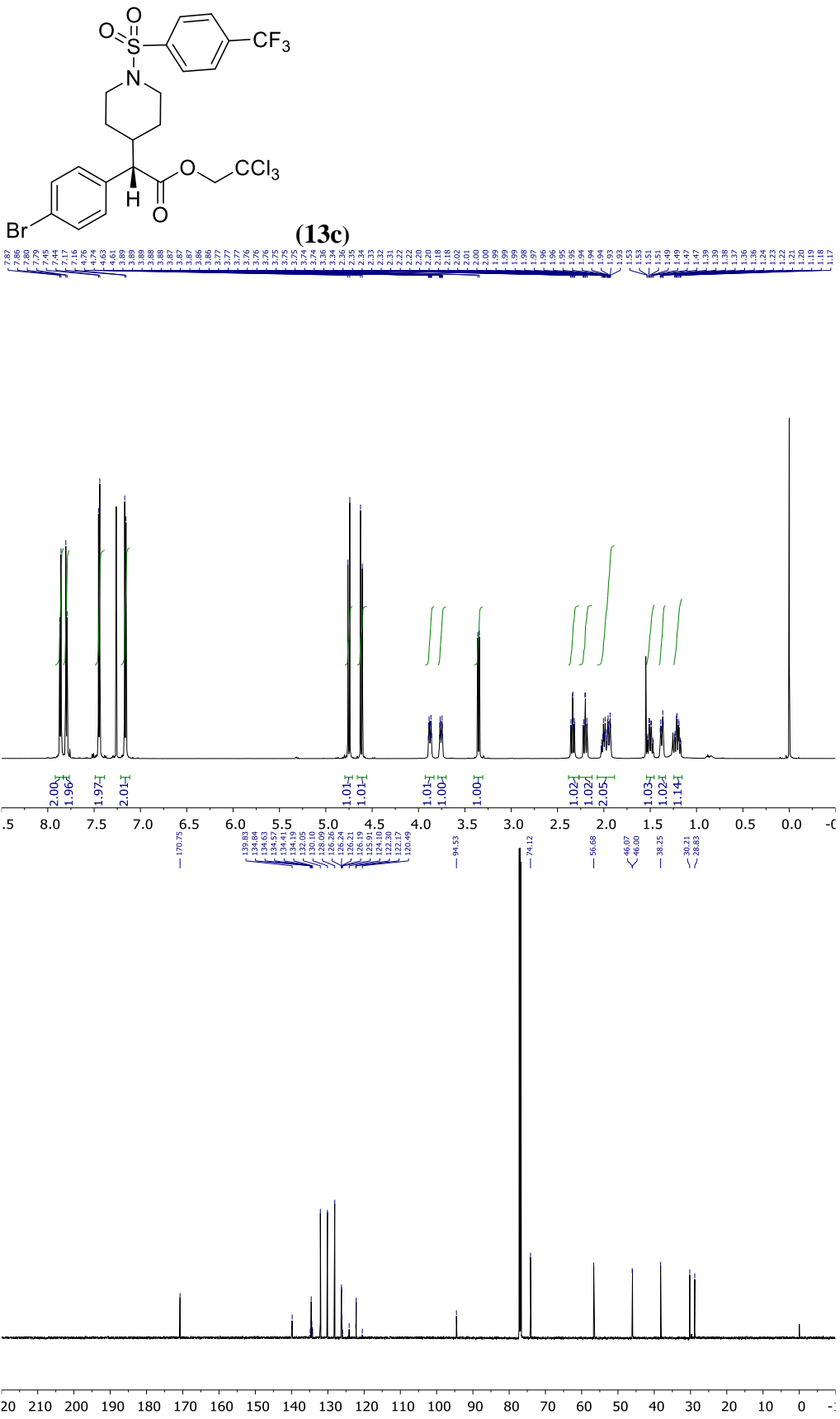


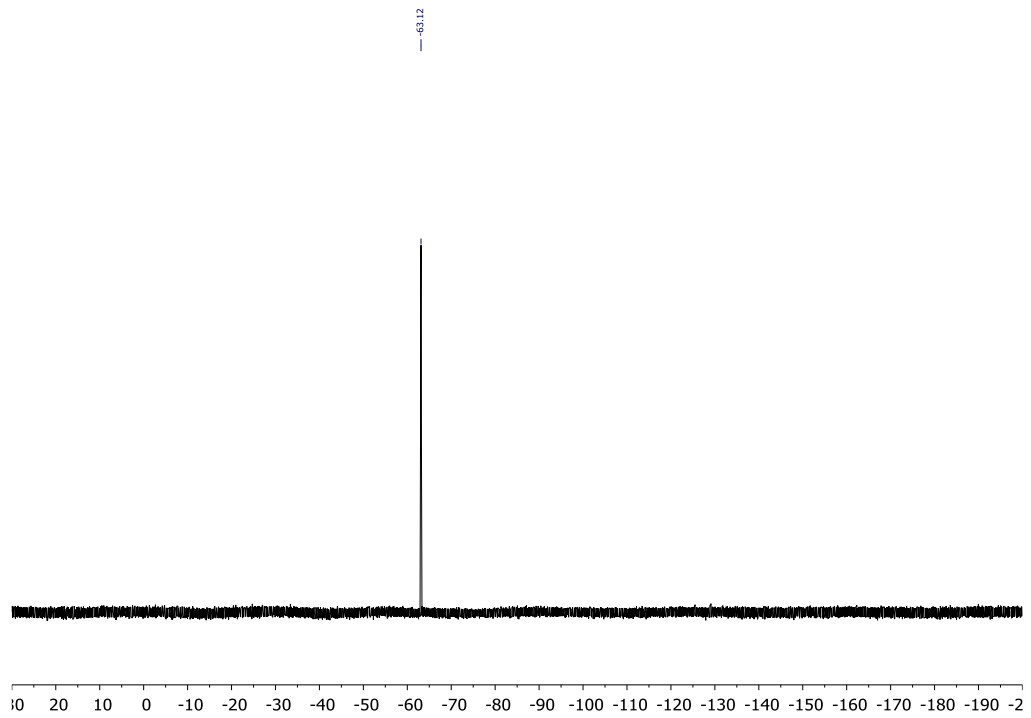


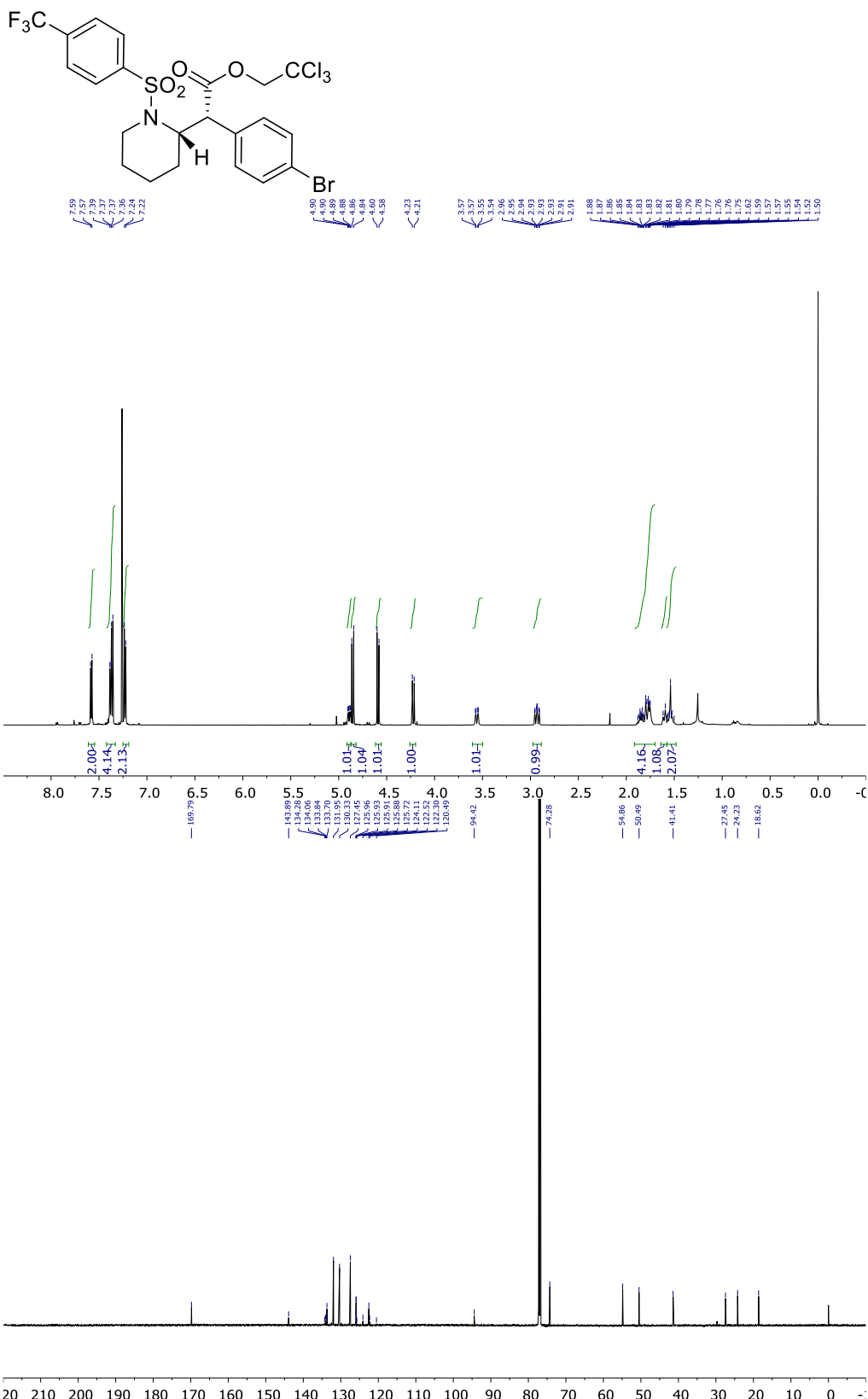


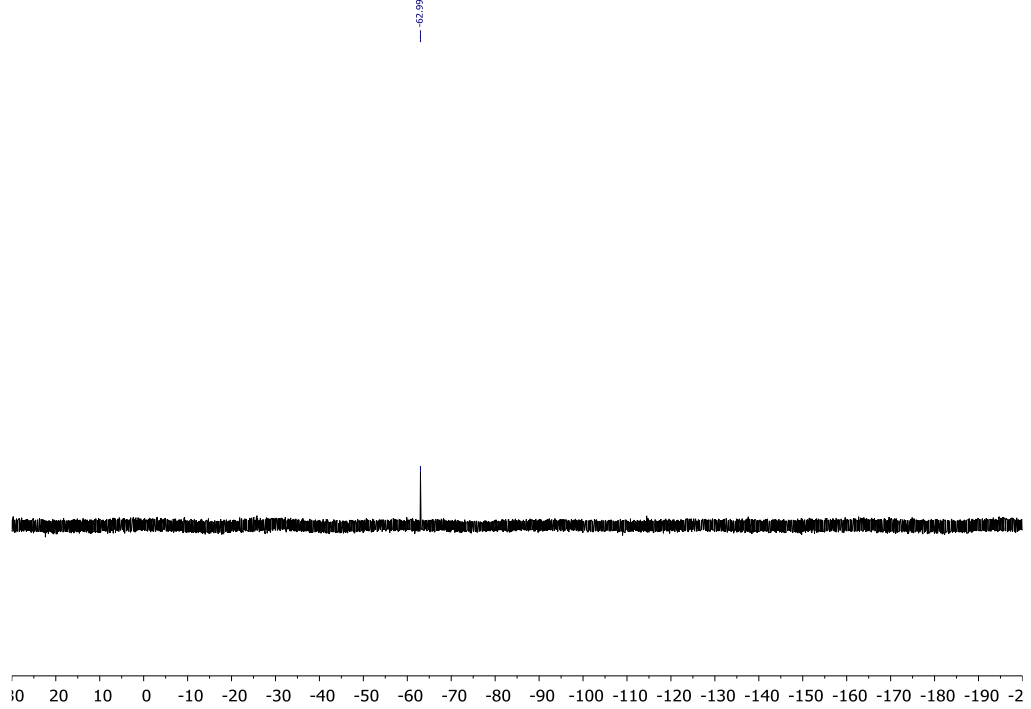


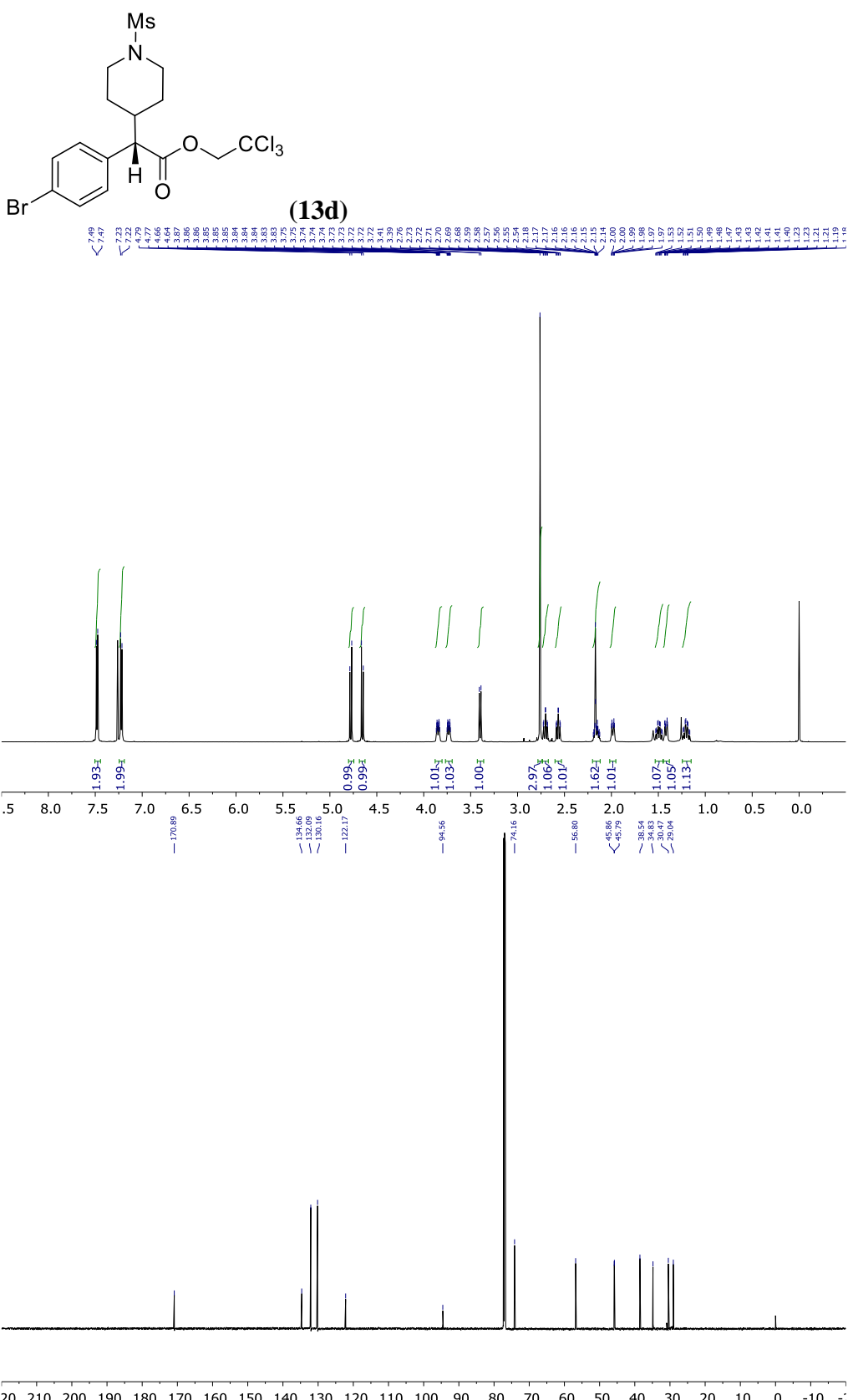


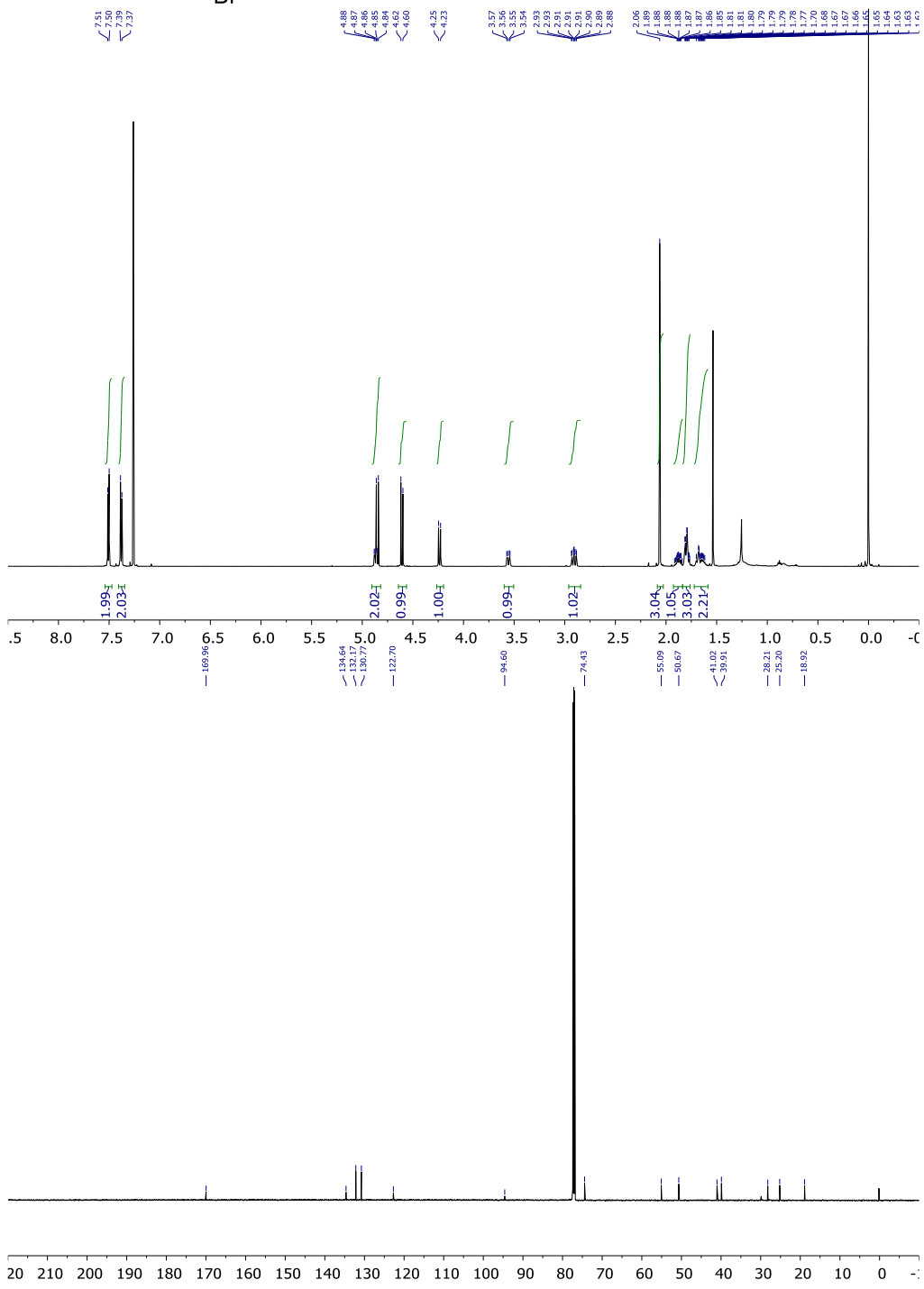
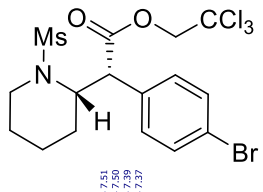


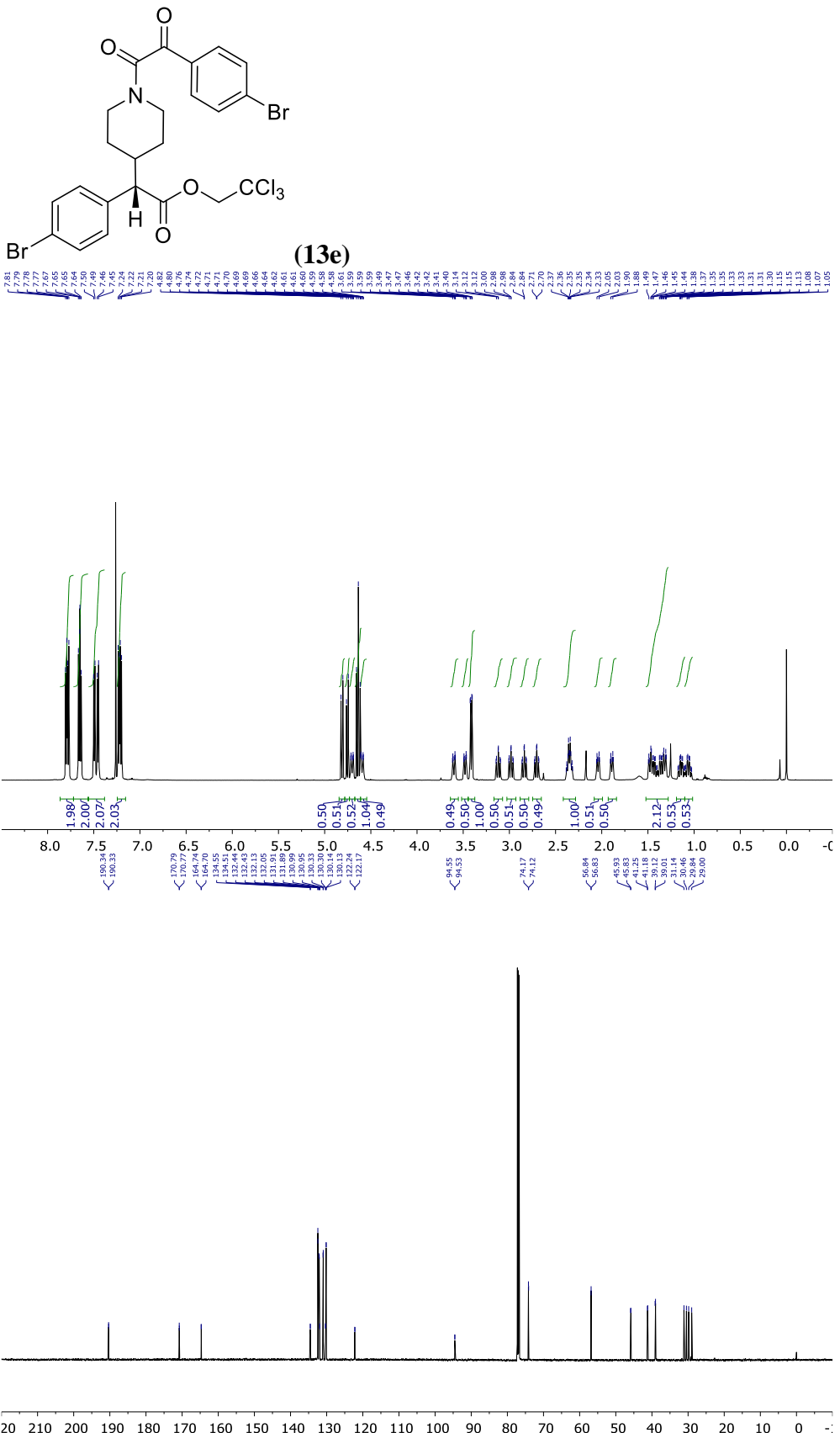


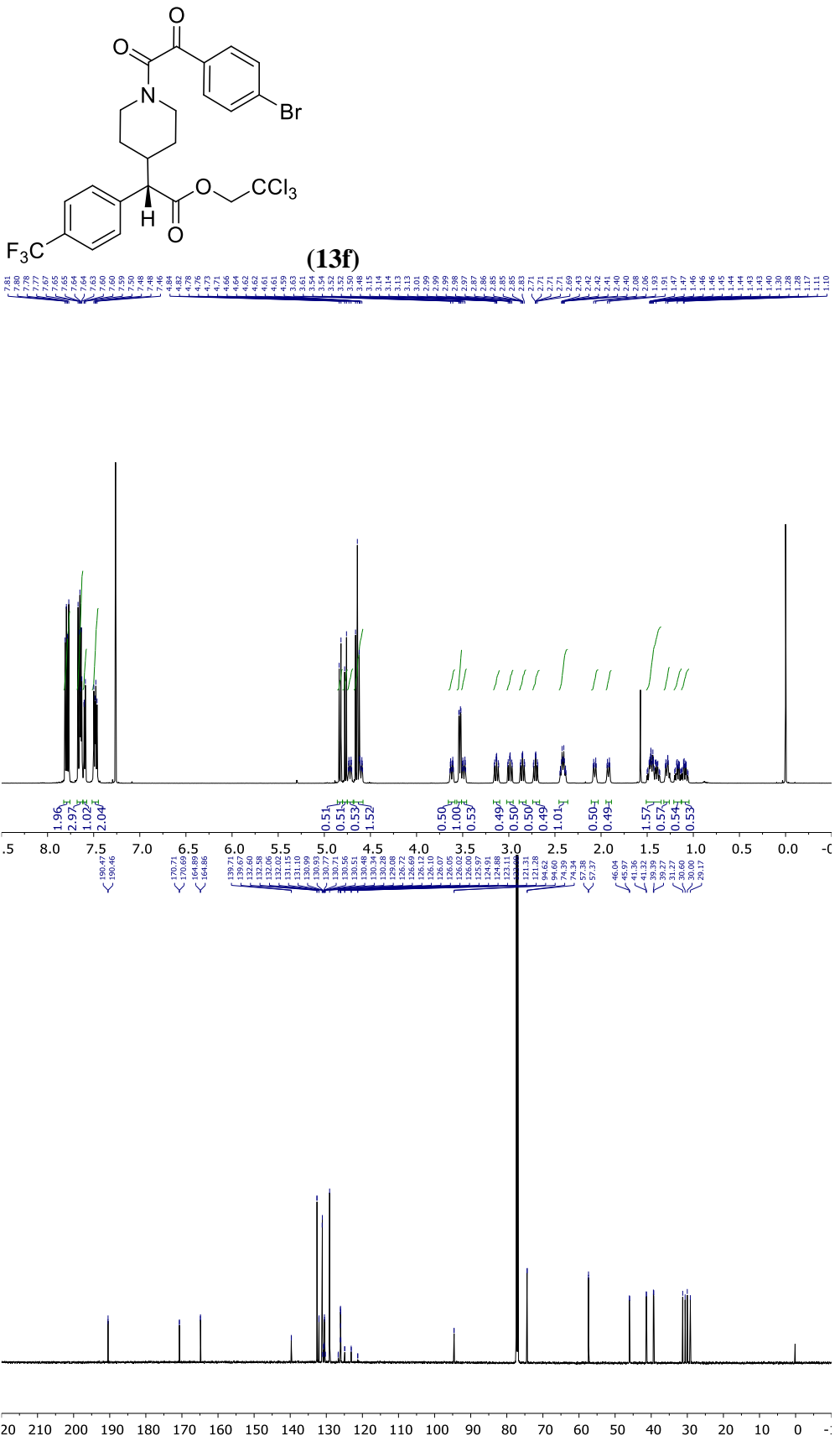


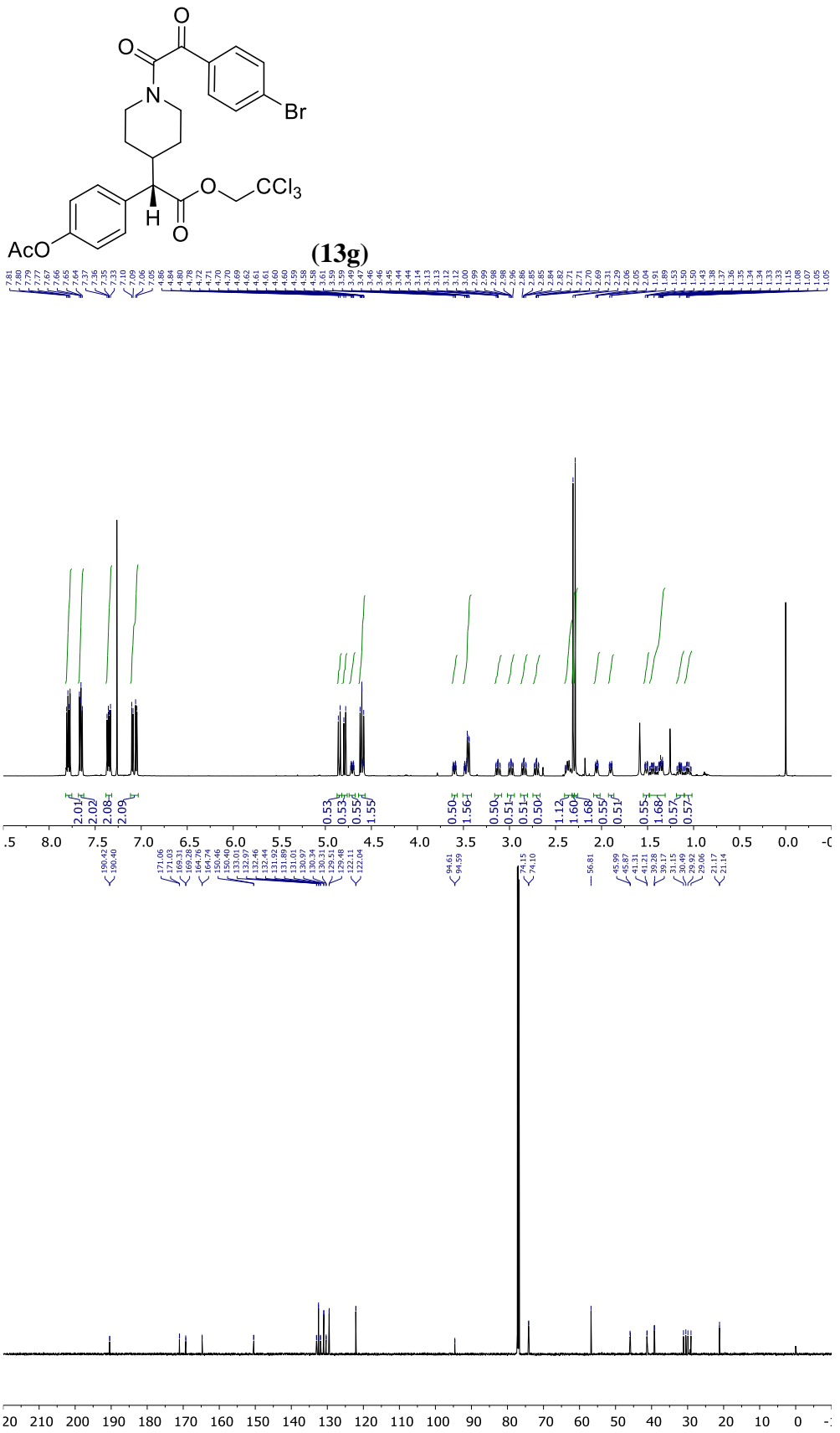


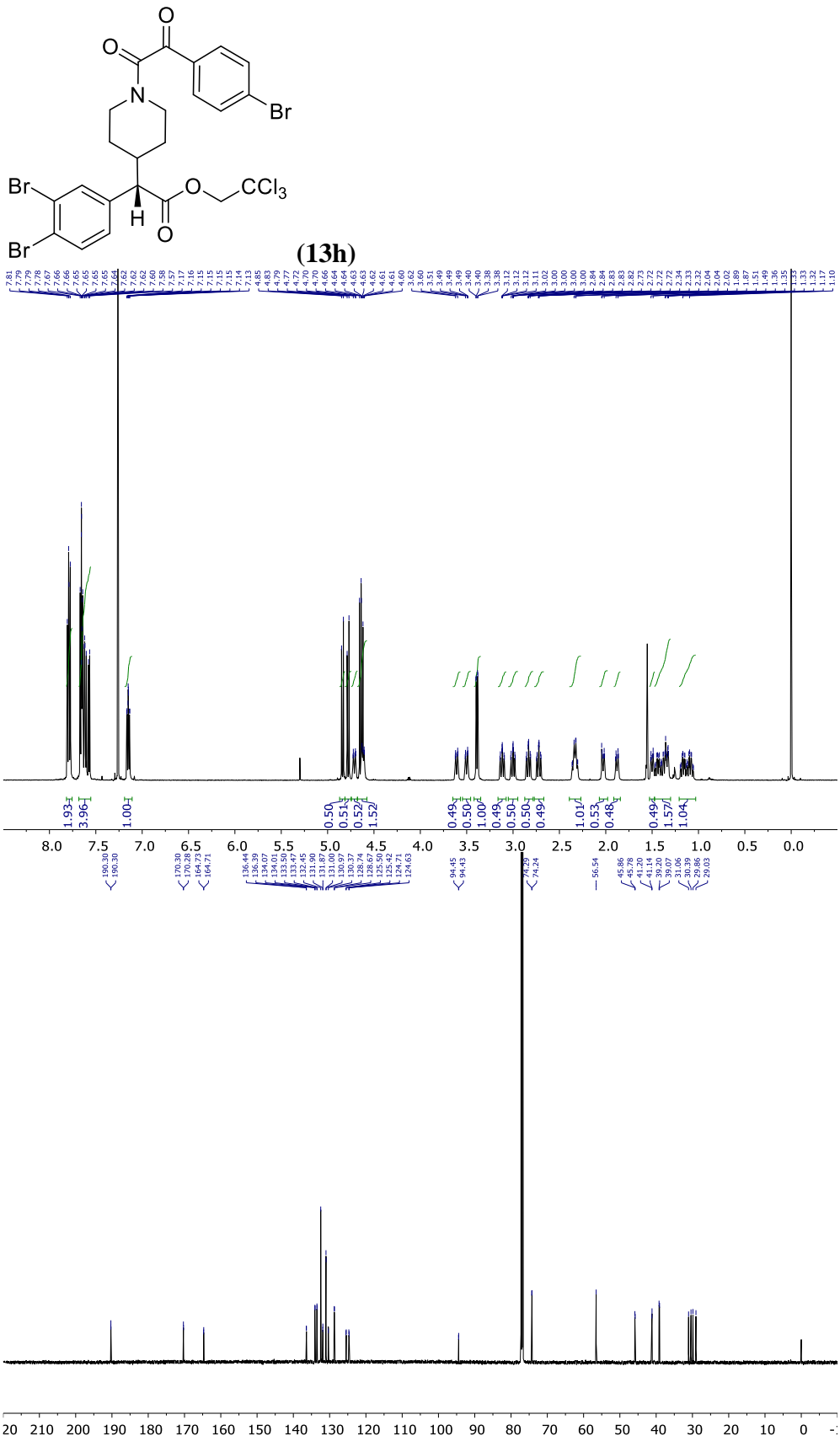


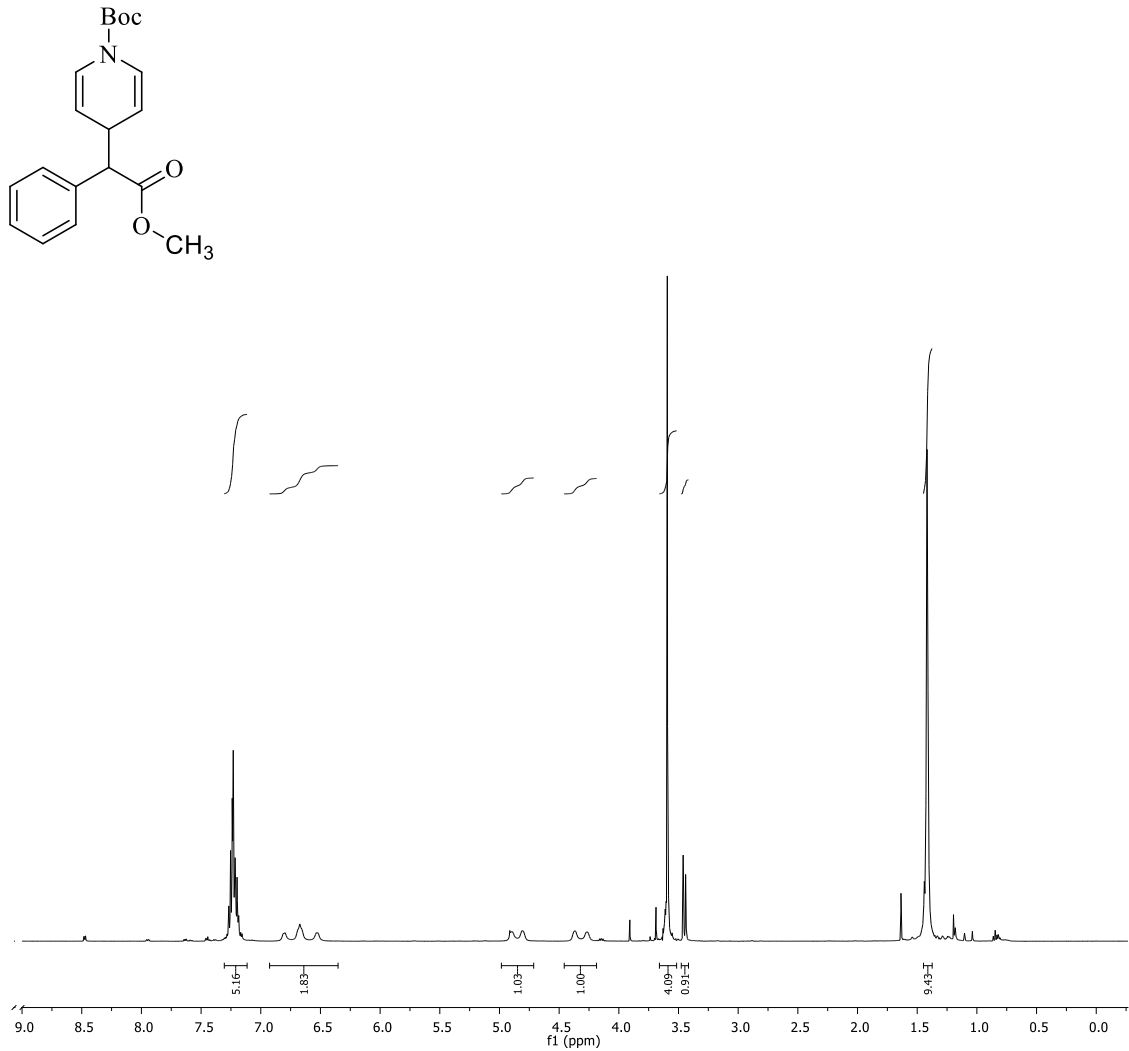


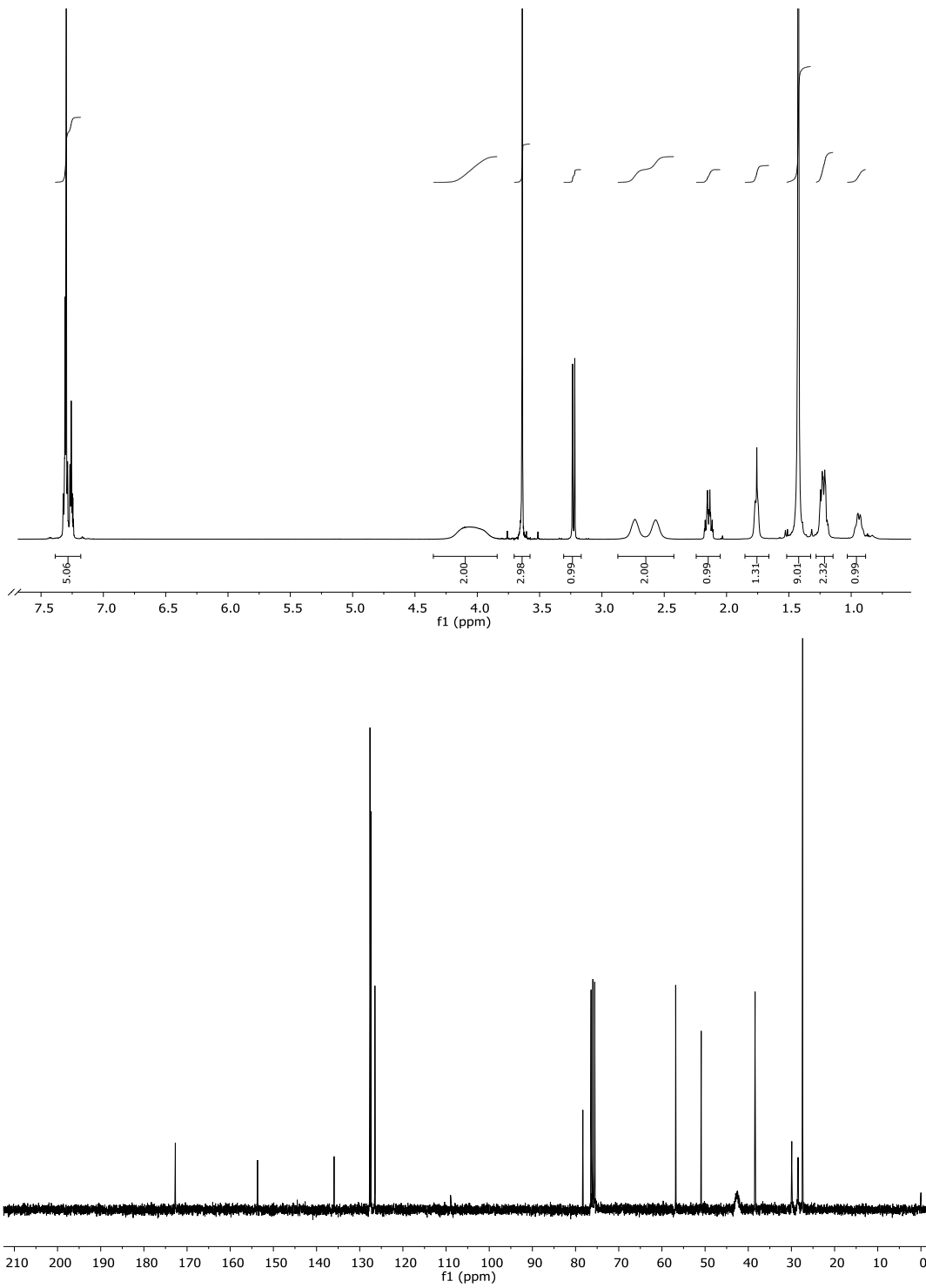
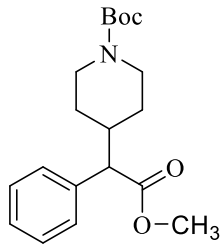


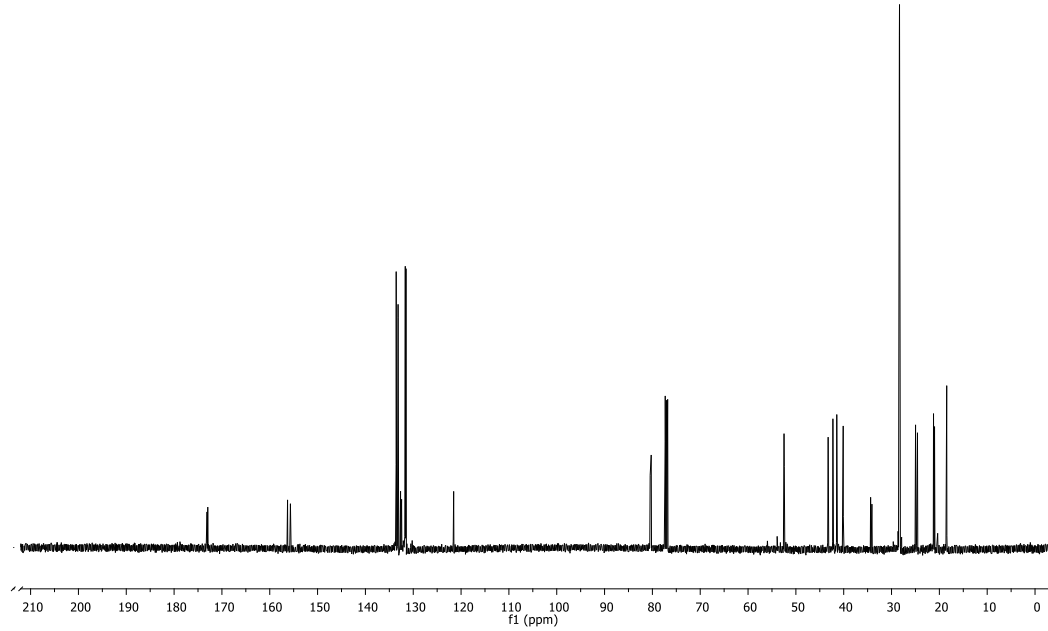
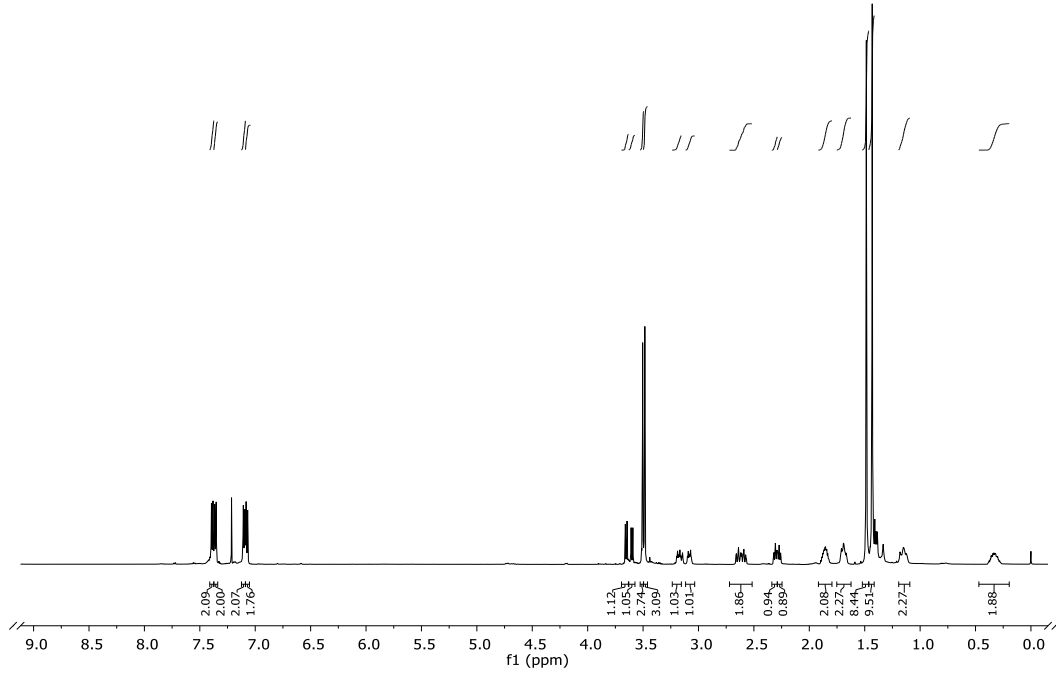
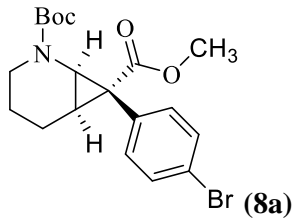


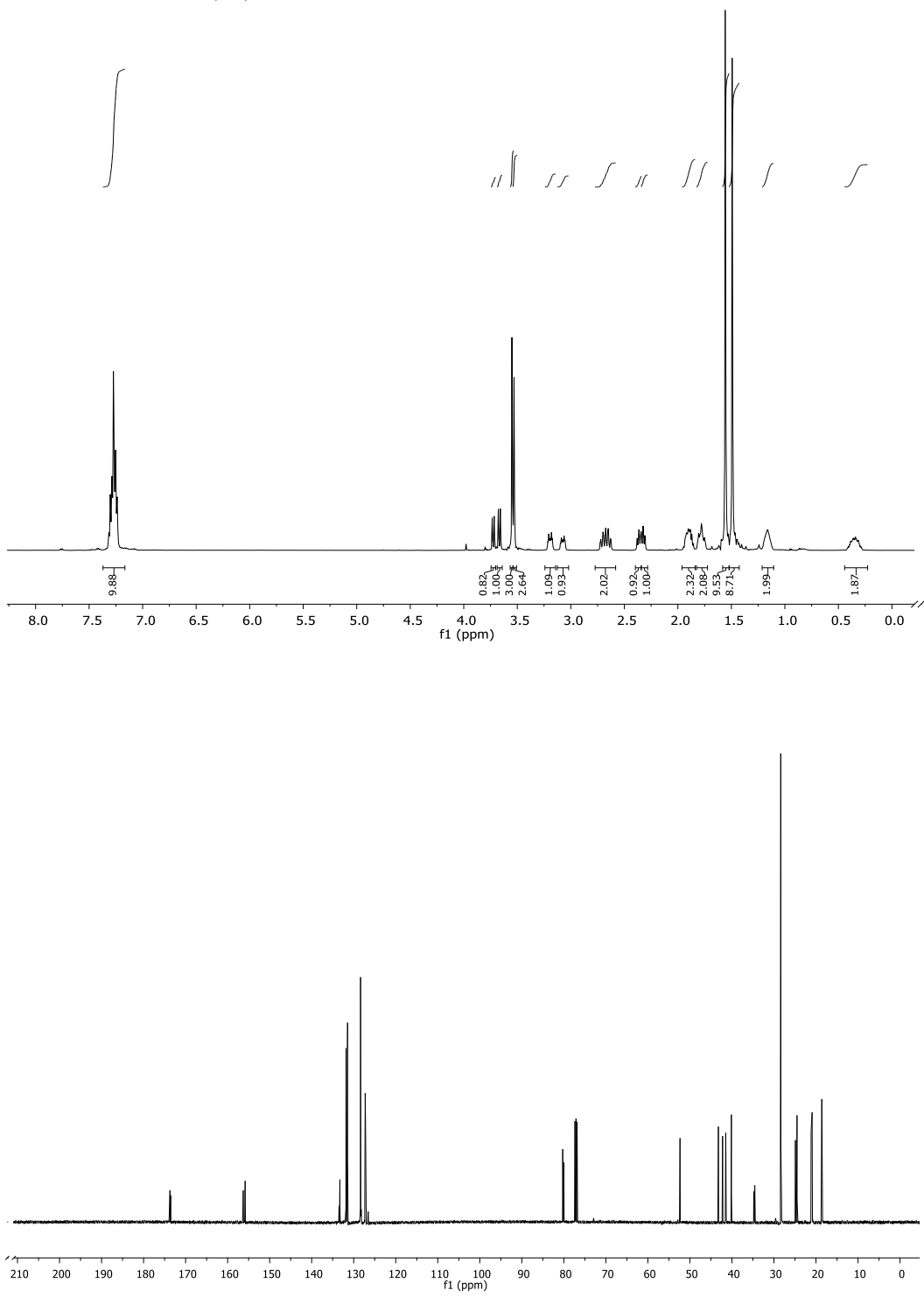
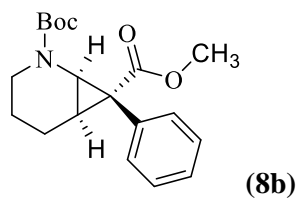


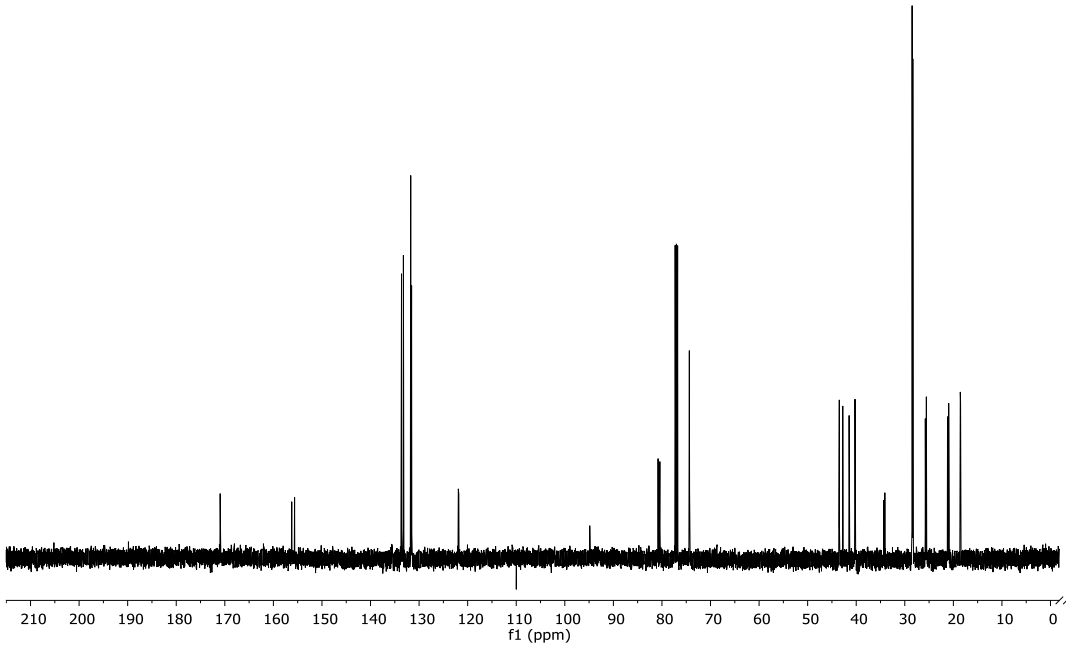
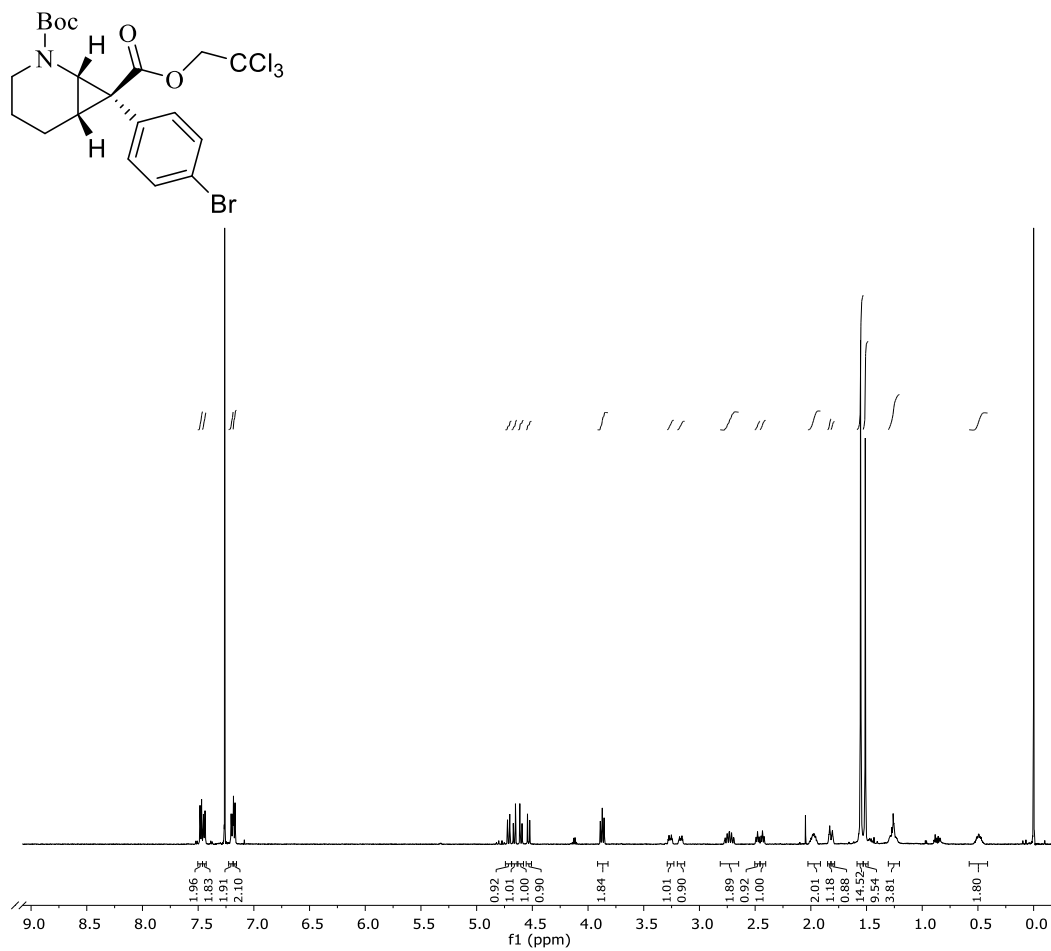


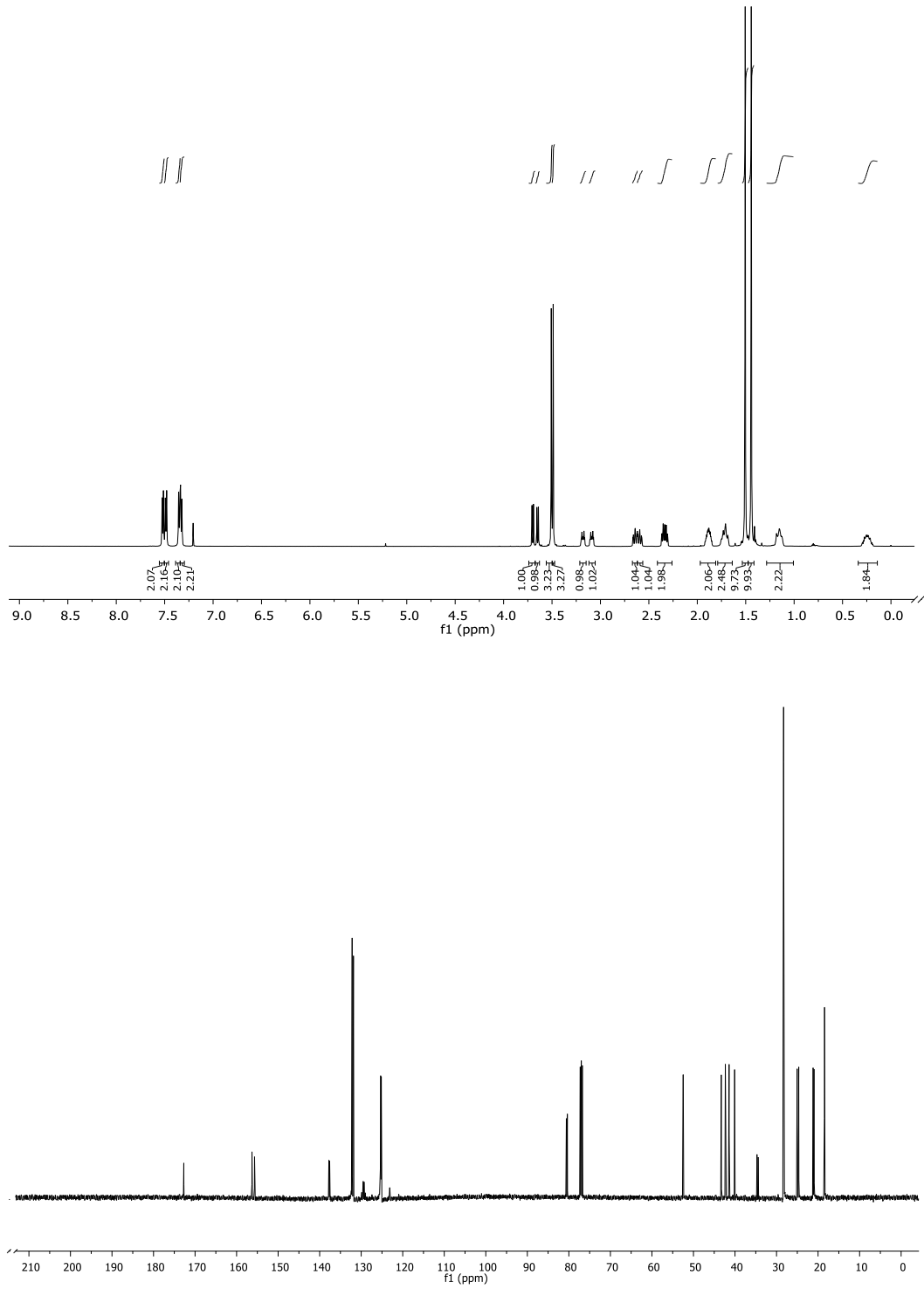
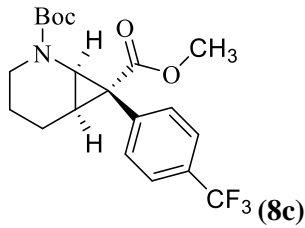


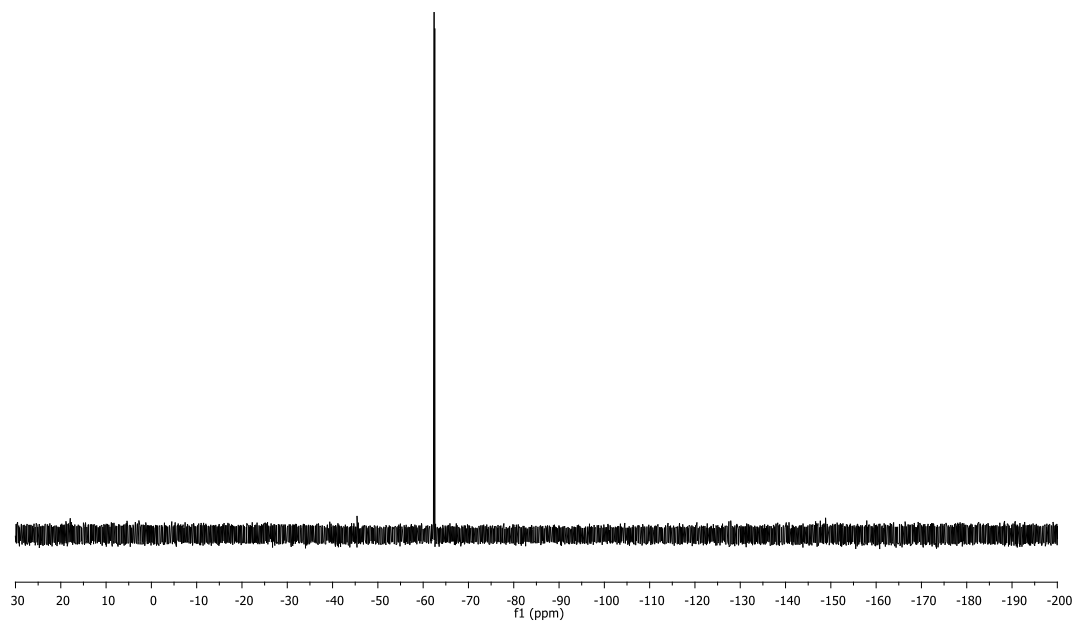


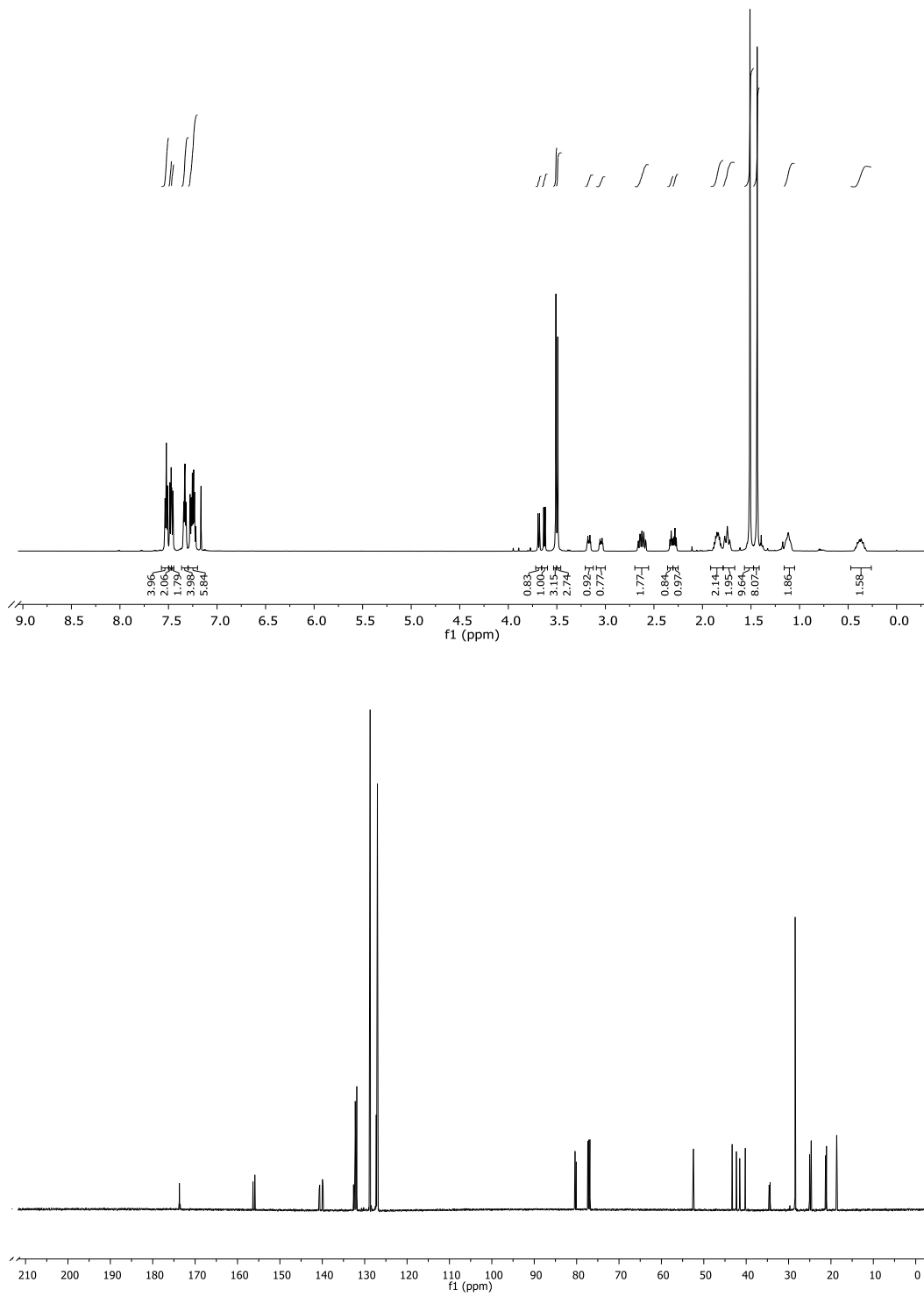
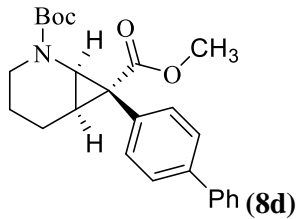


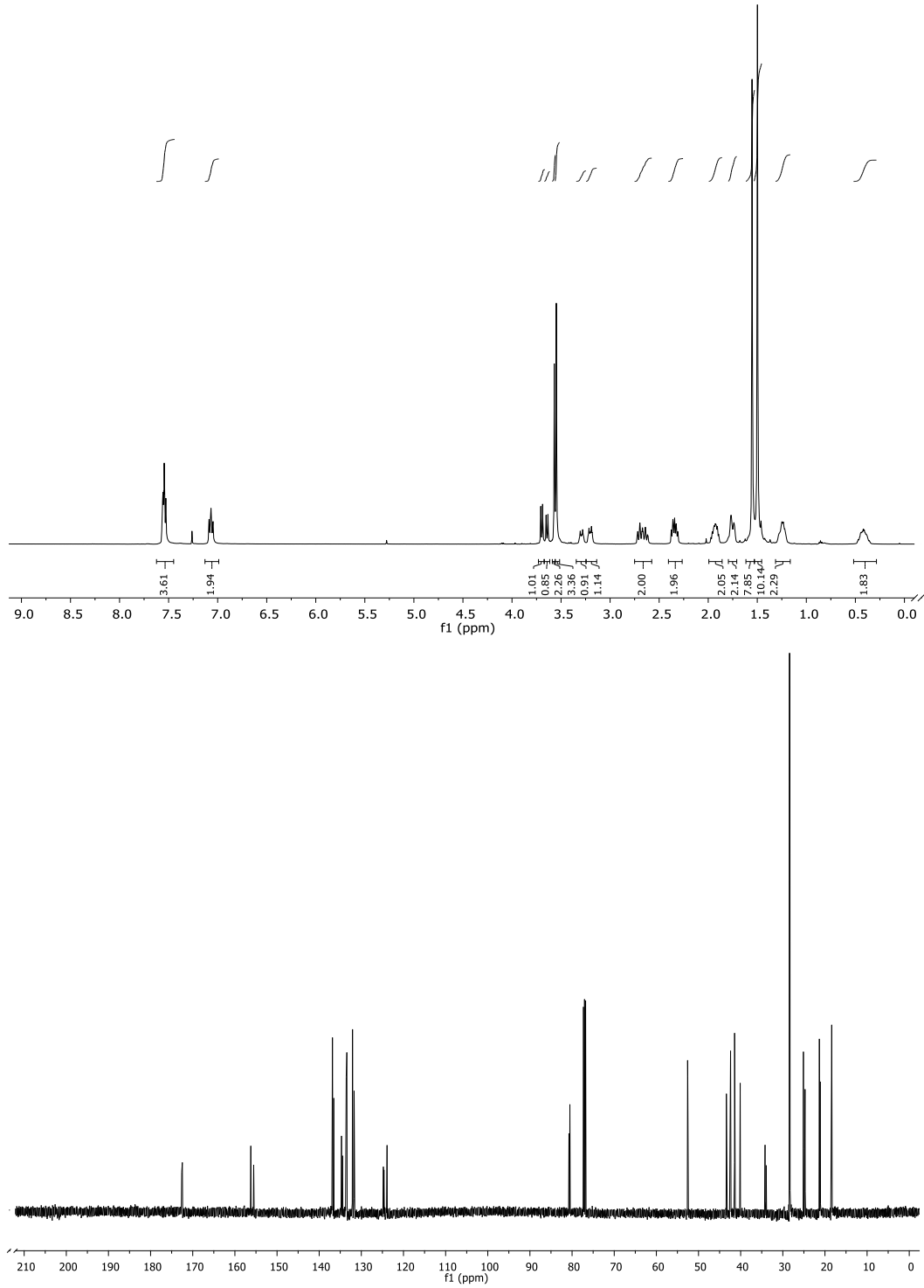
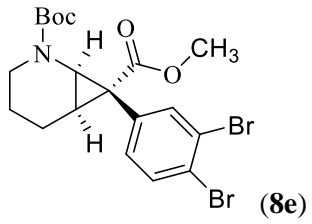


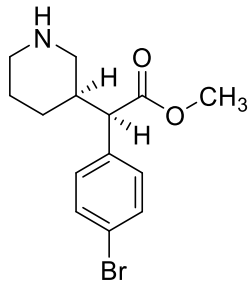




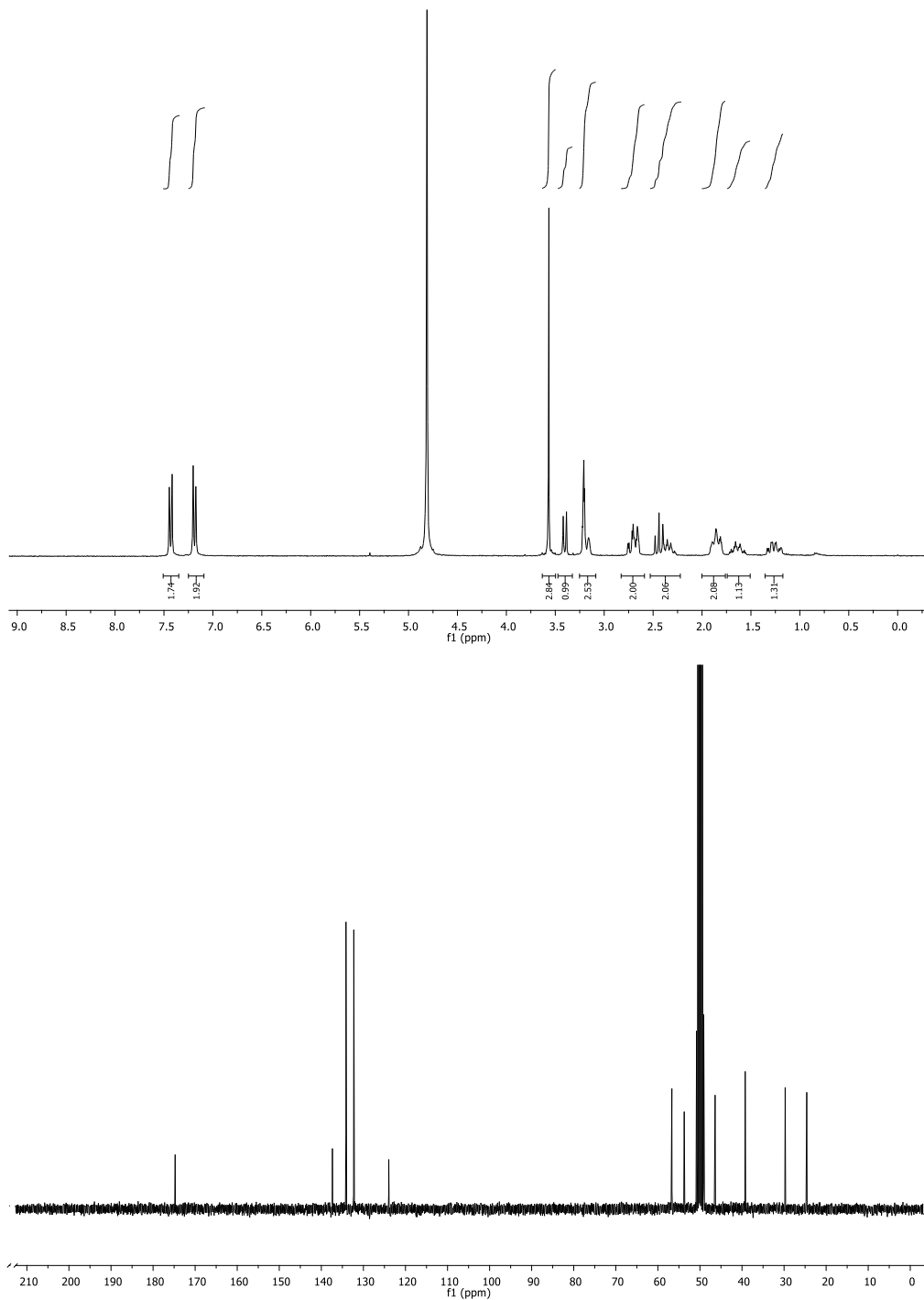


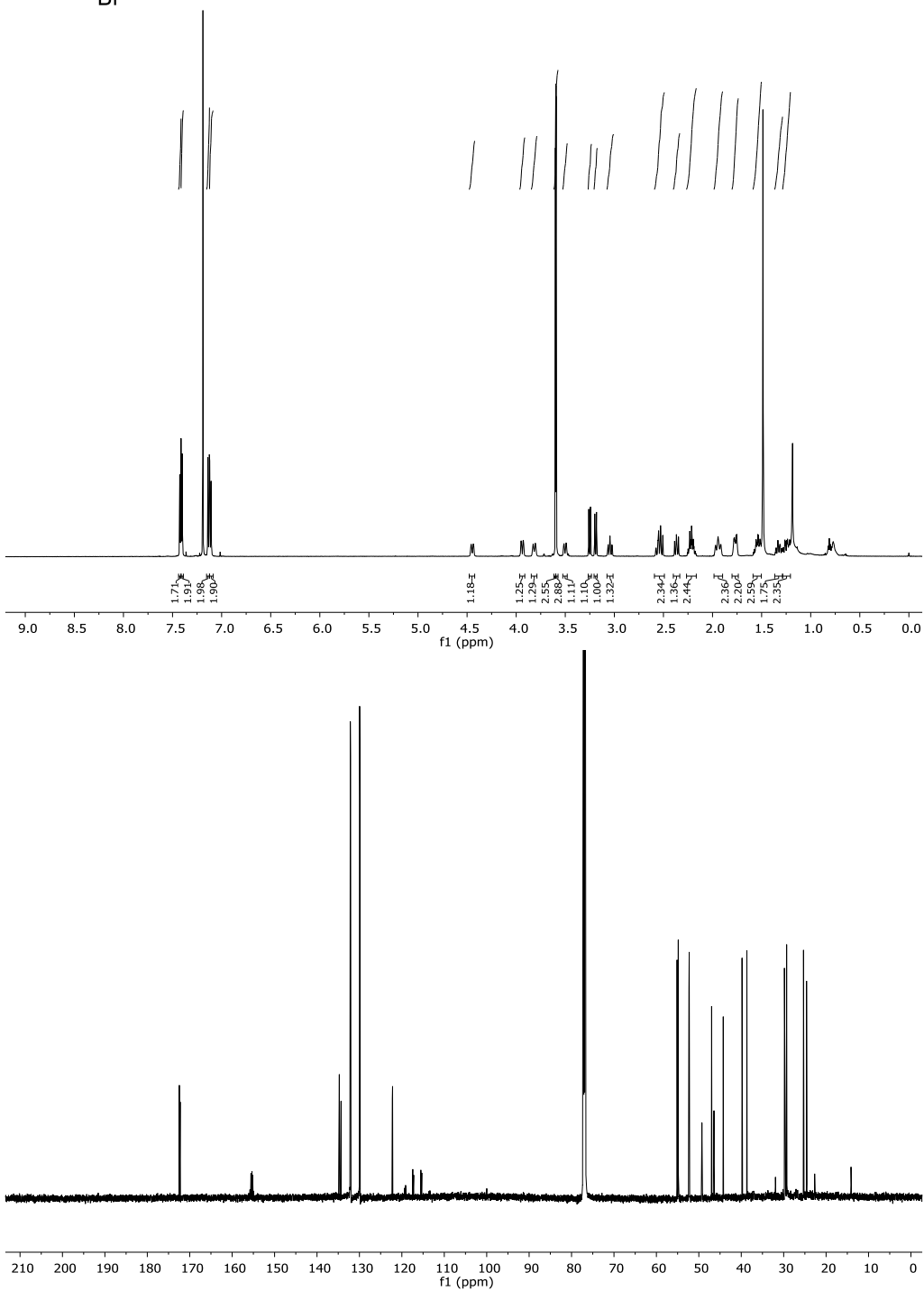
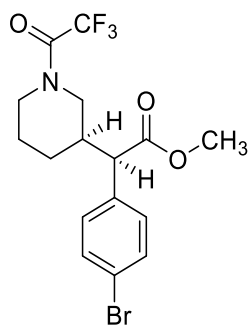


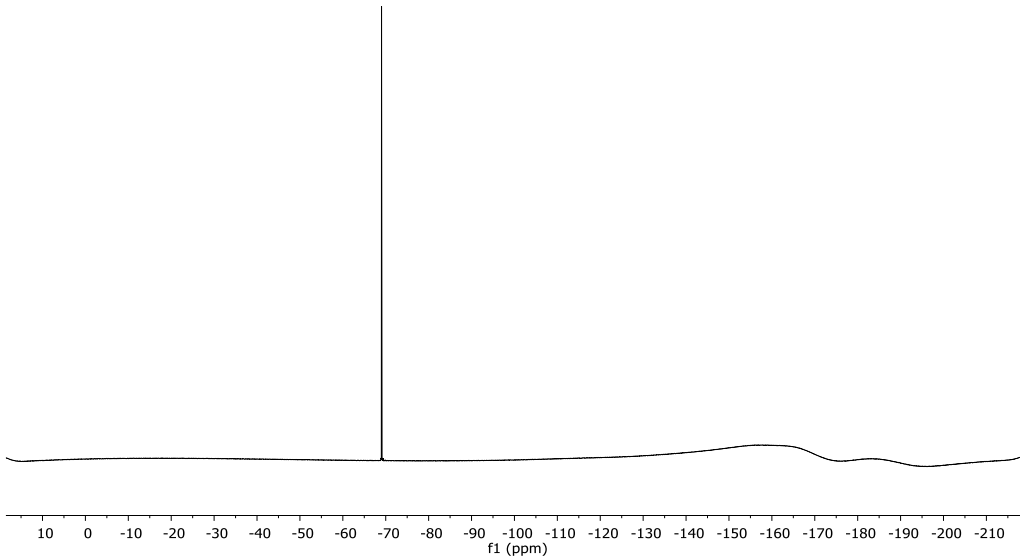


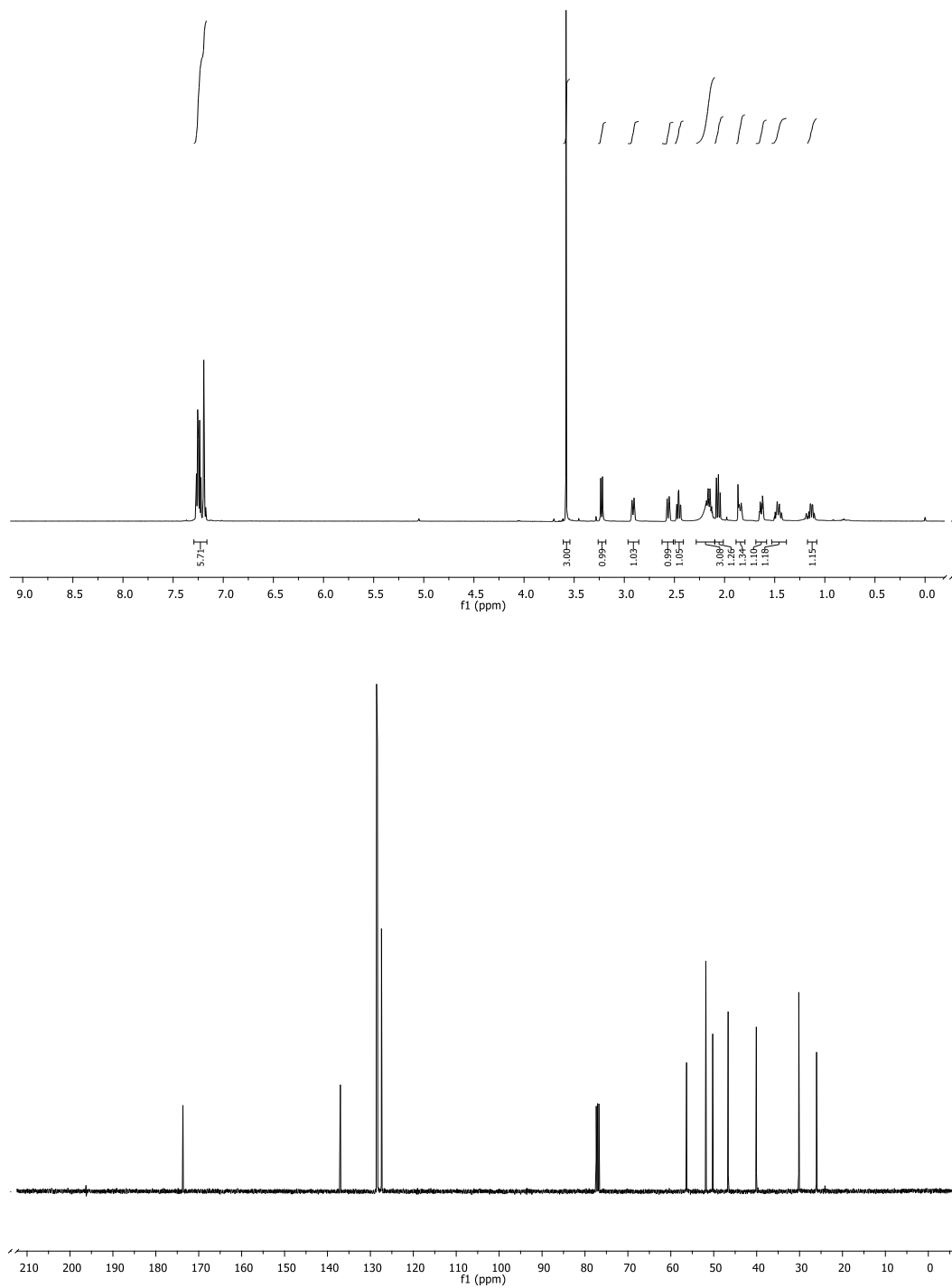
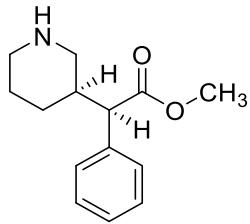


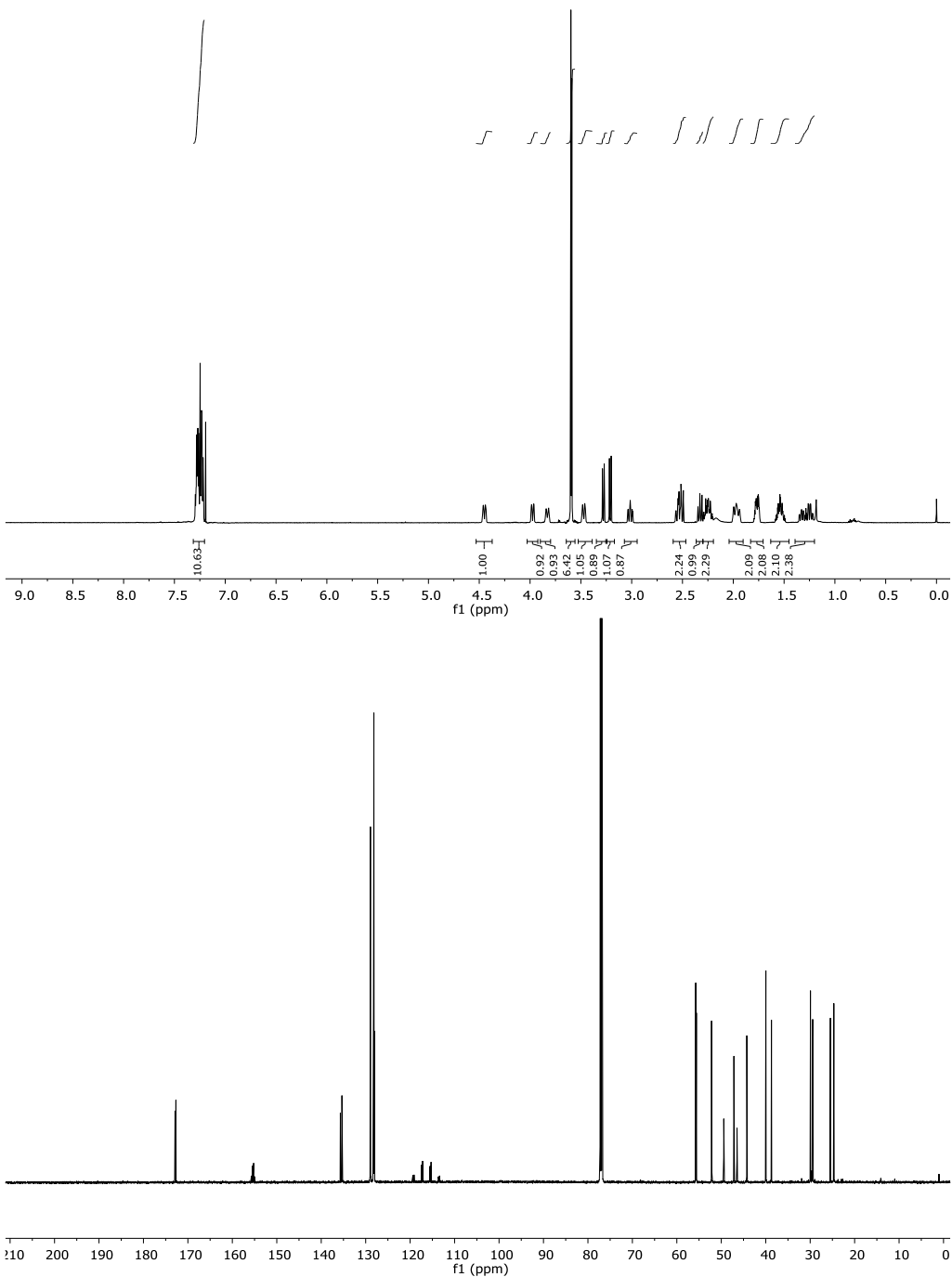
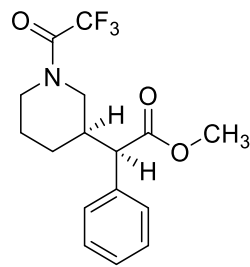
(9a)

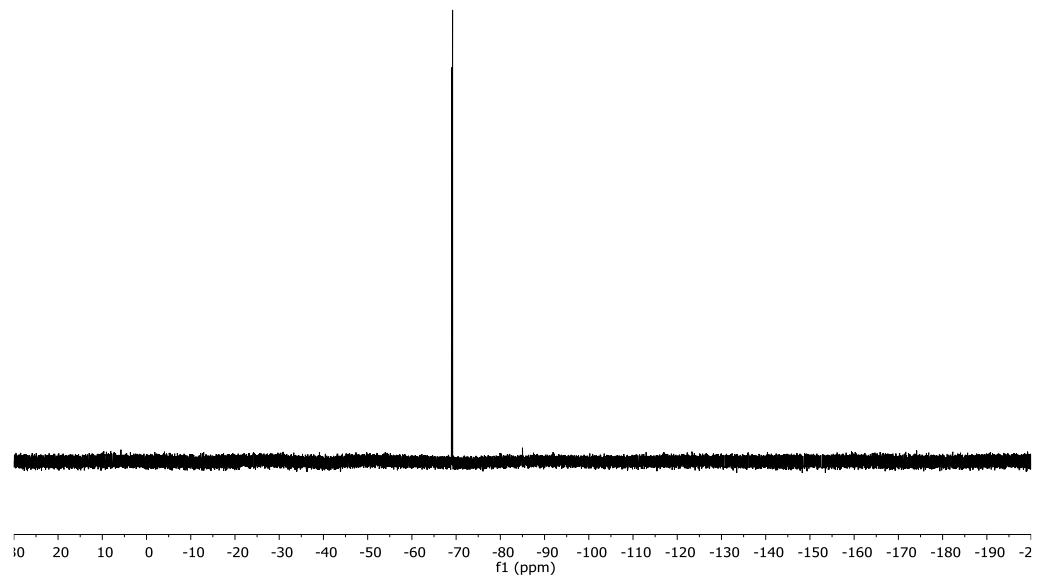


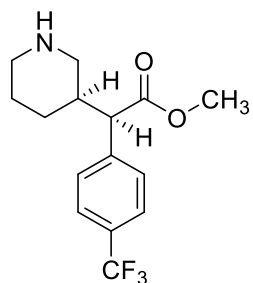




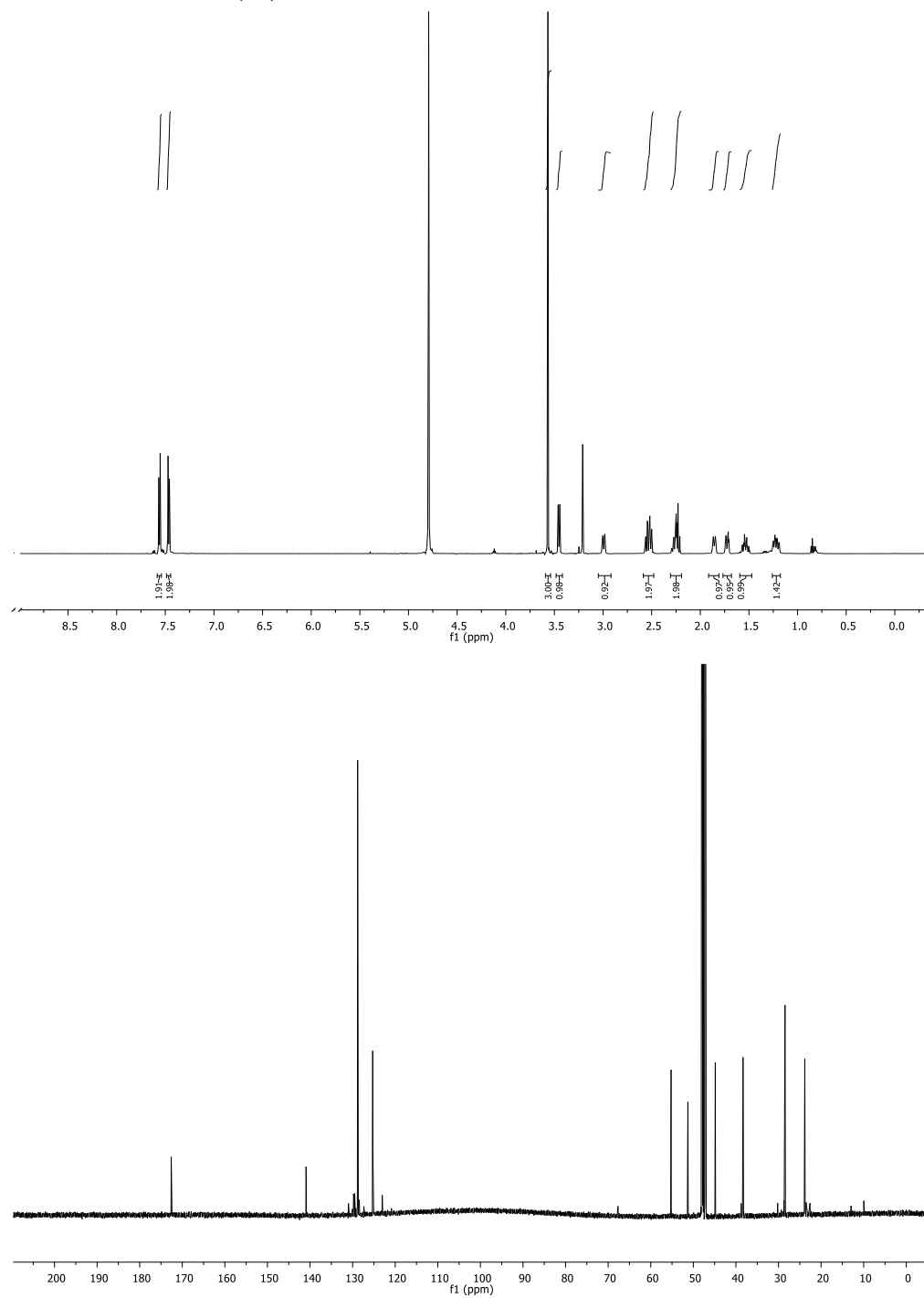


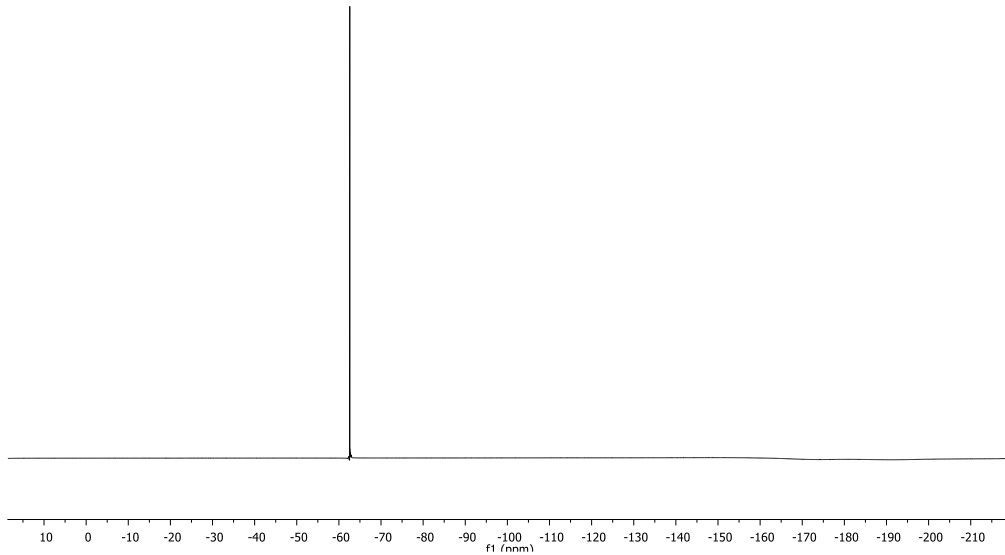


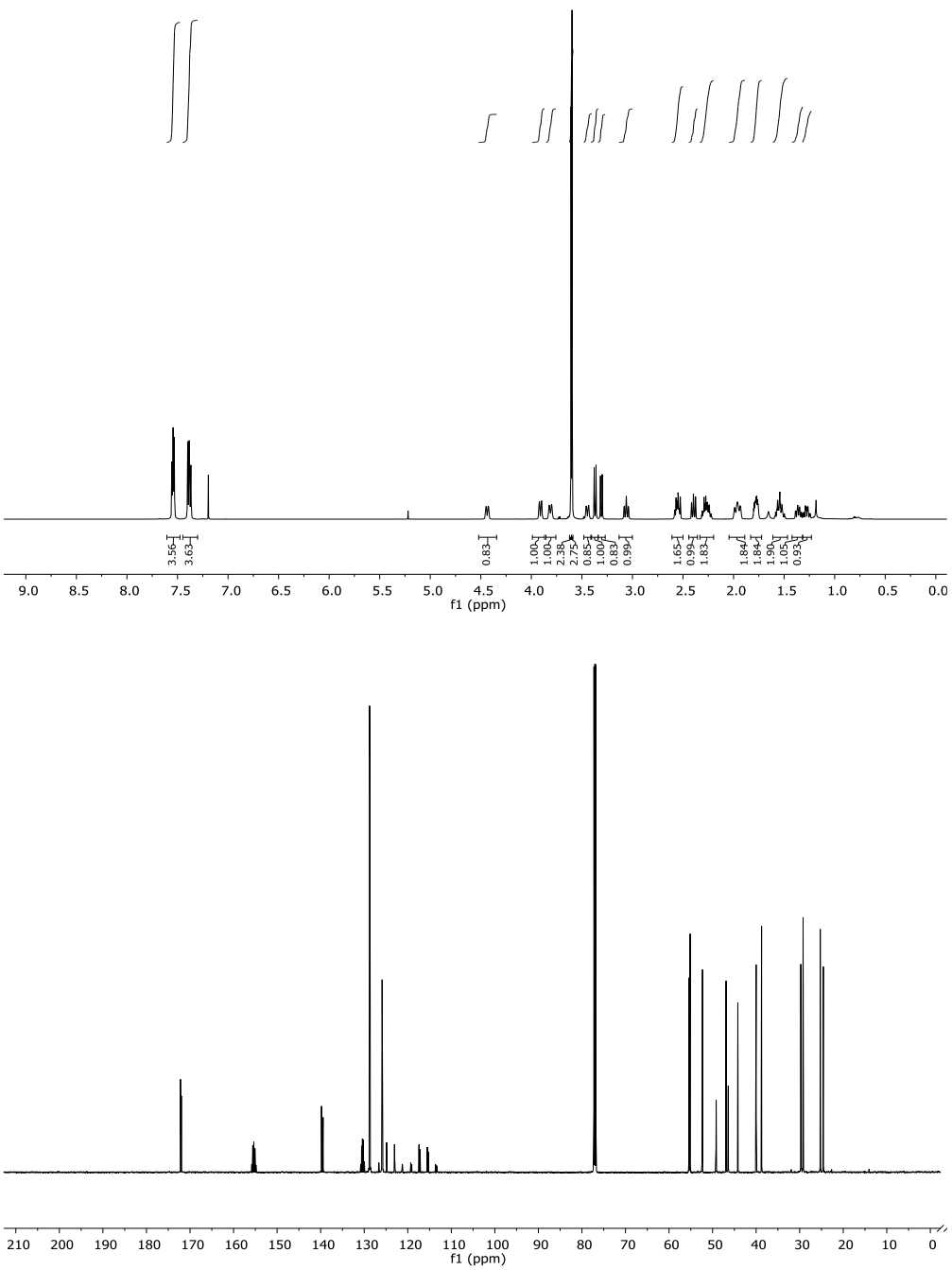
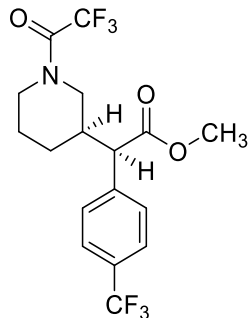


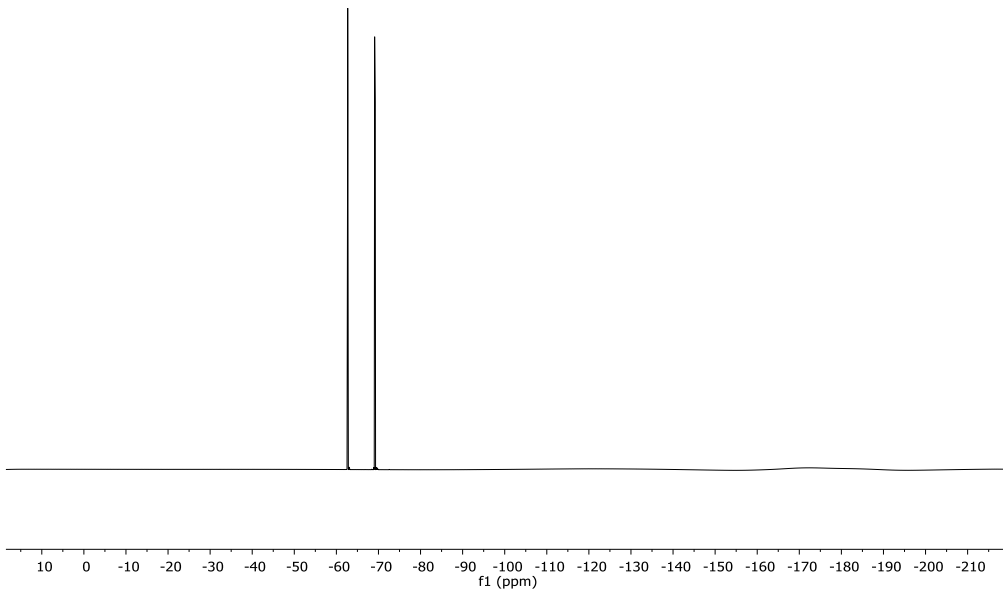


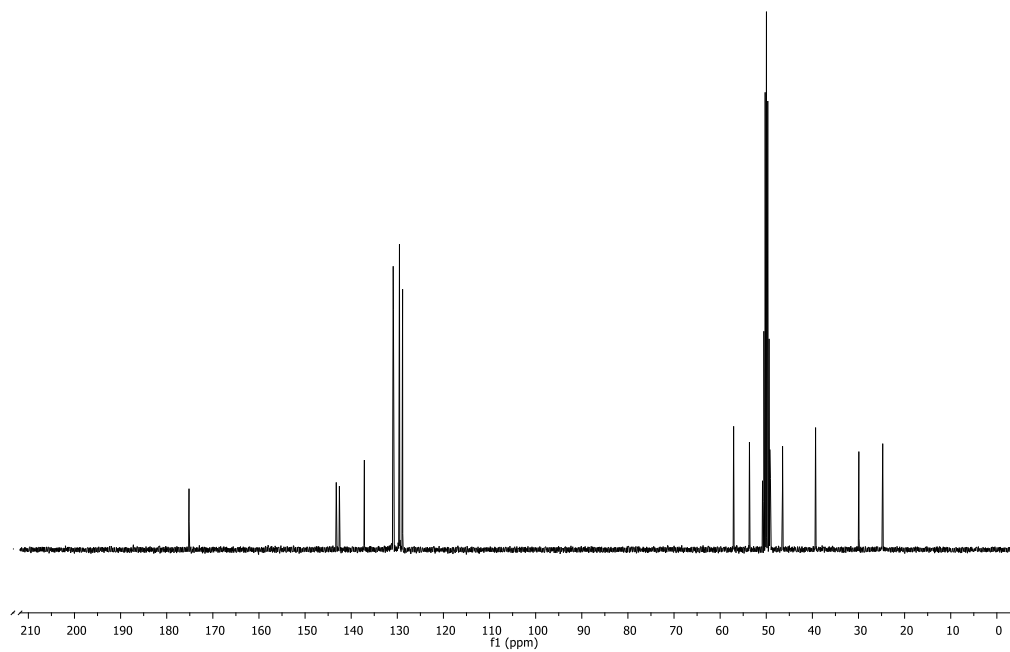
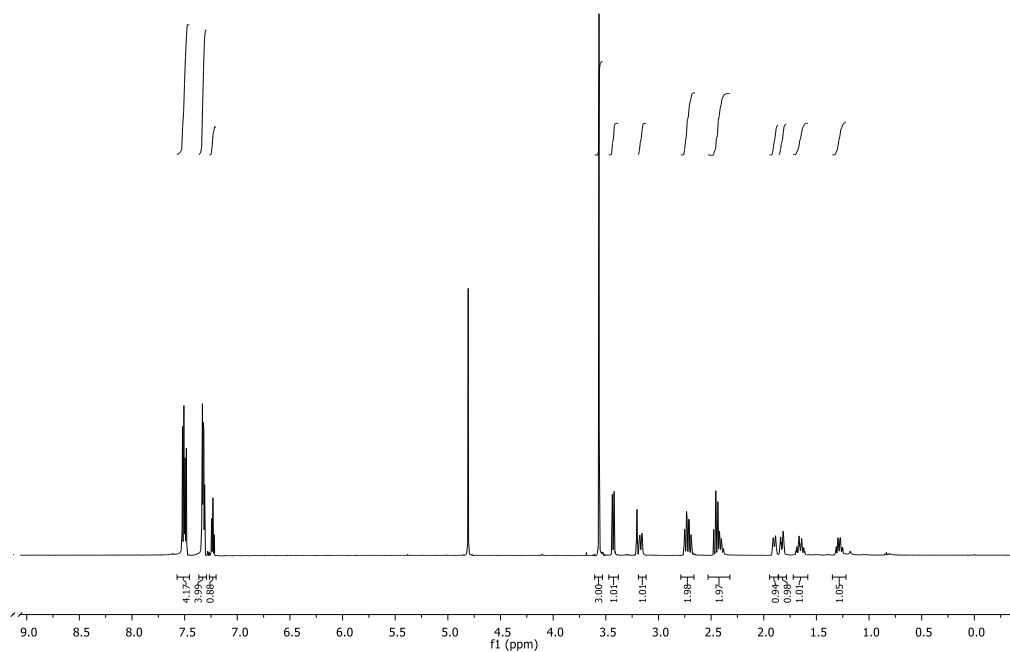
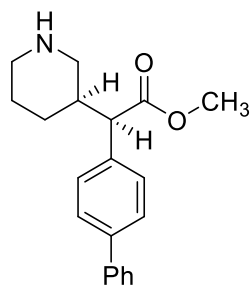
(9c)

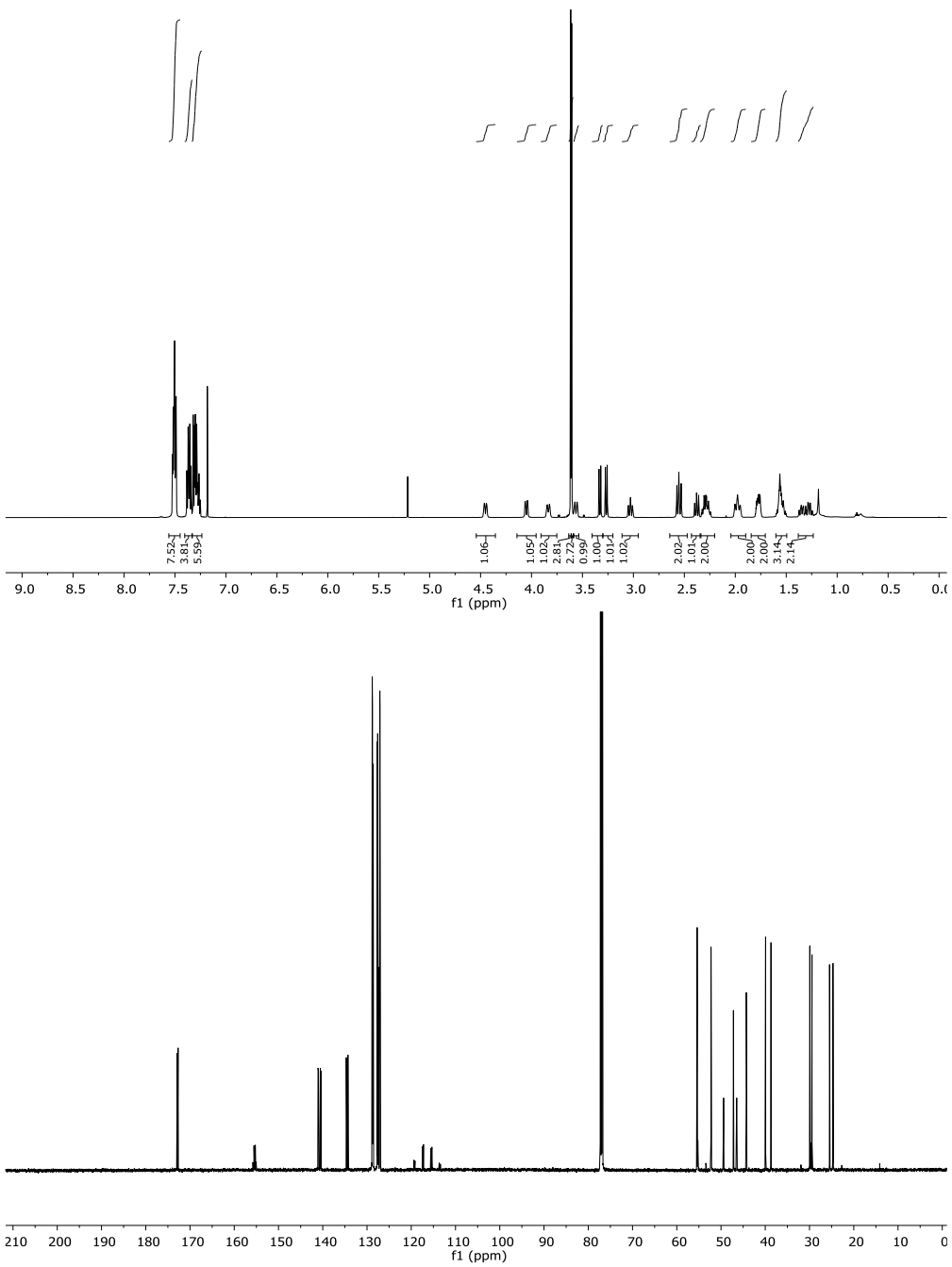
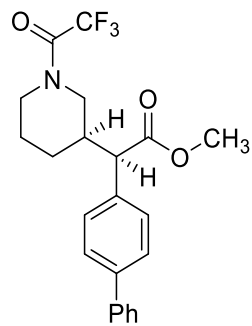


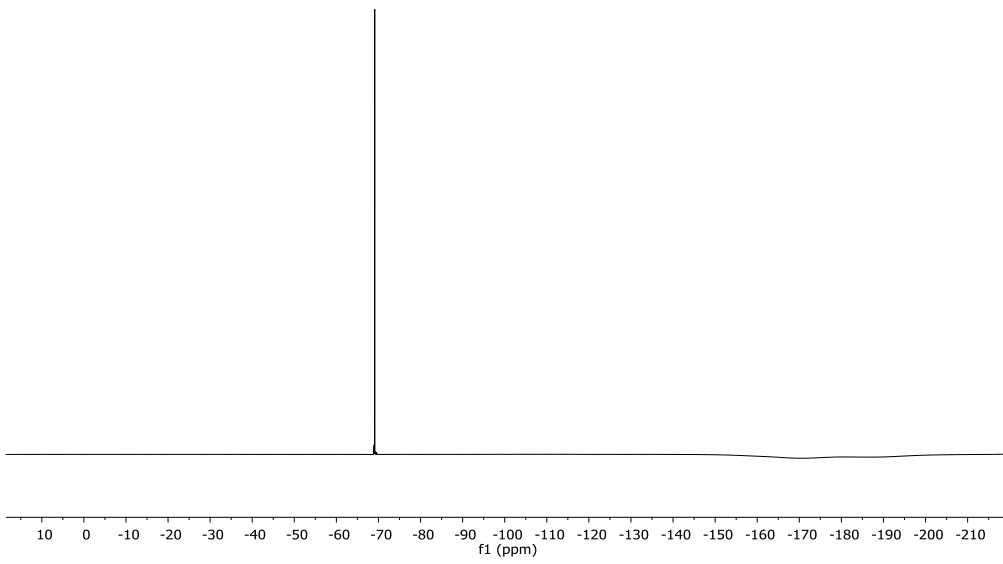


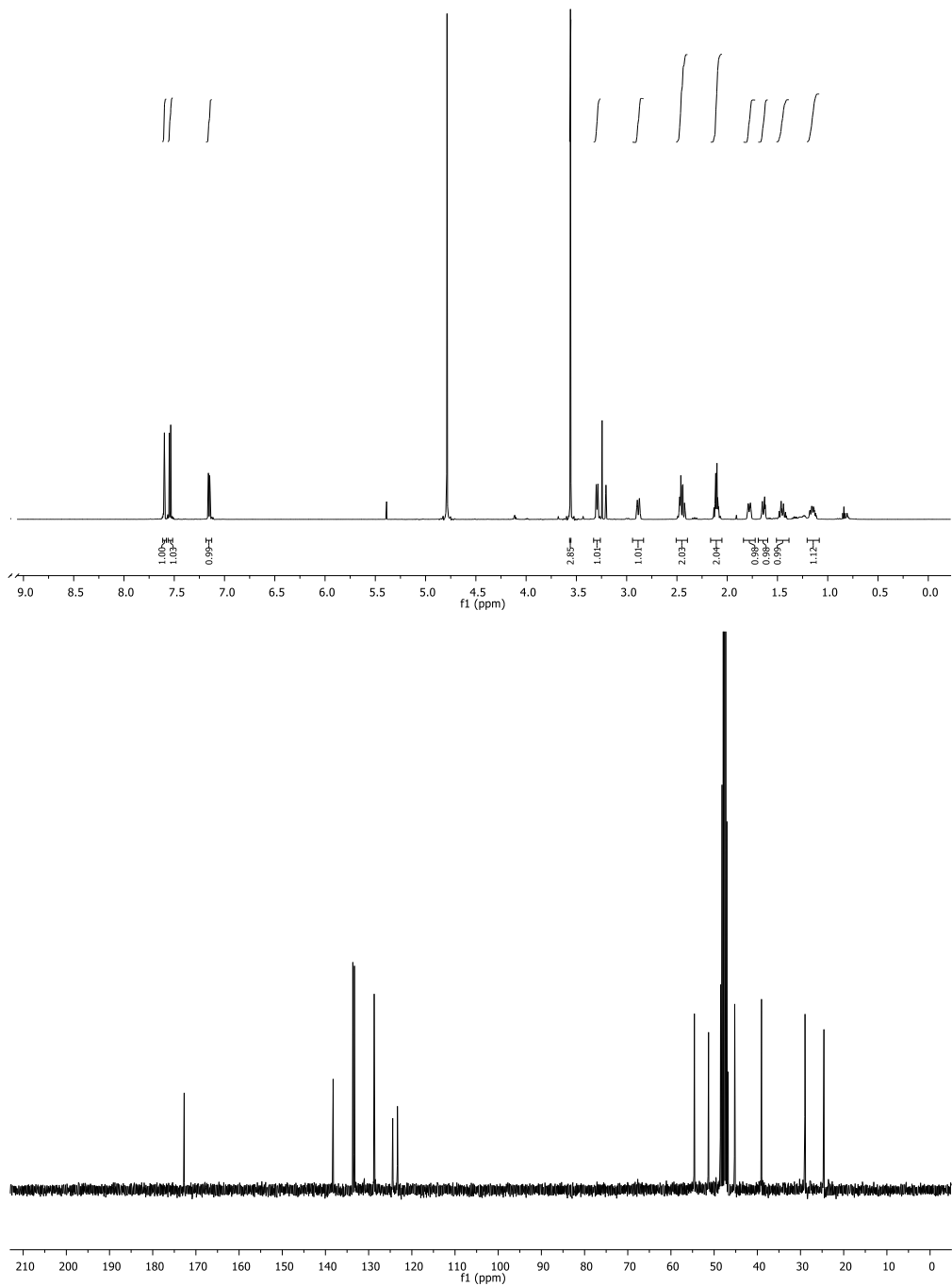
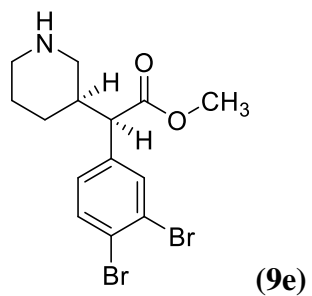


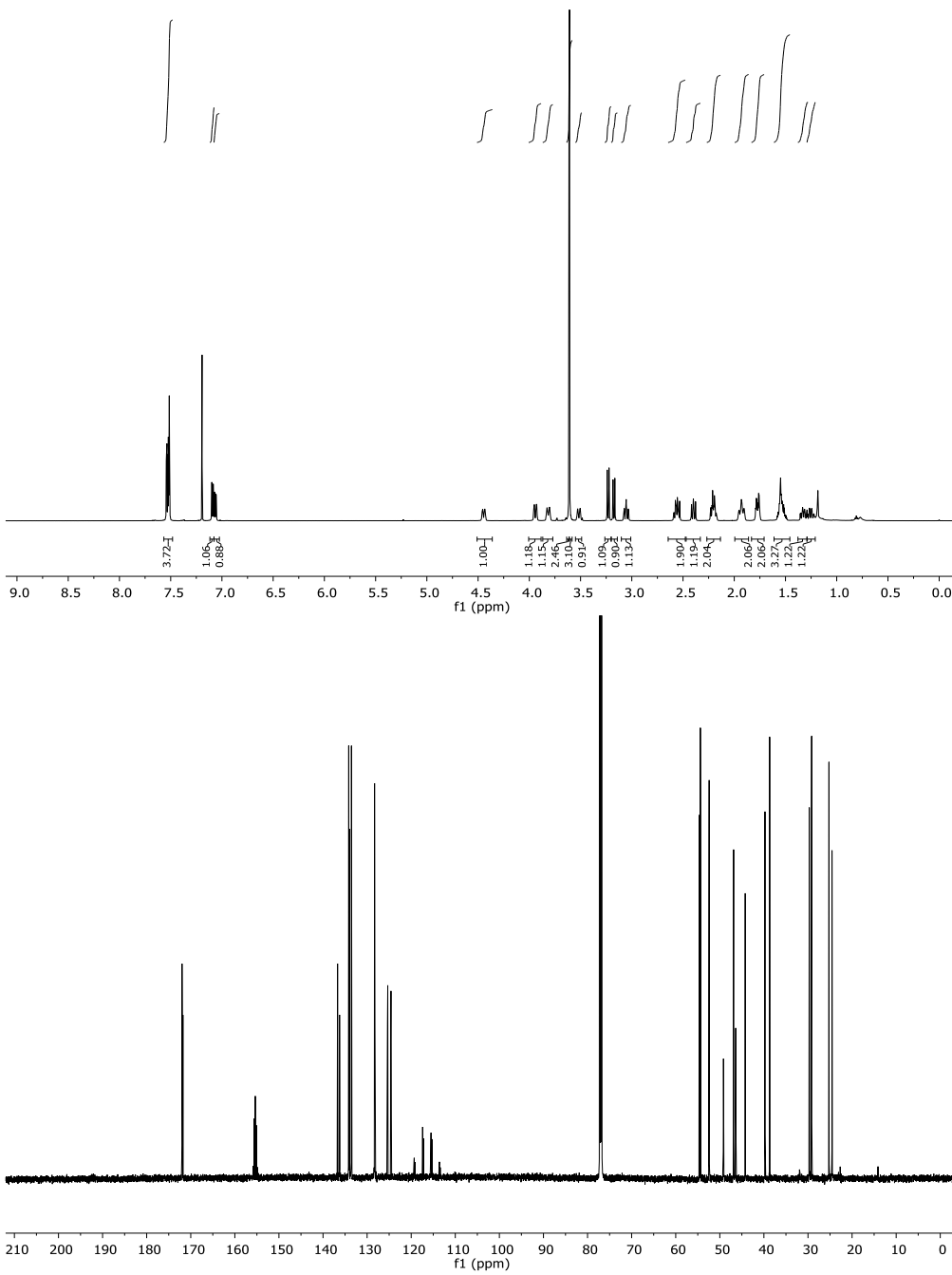
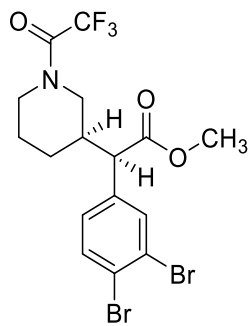


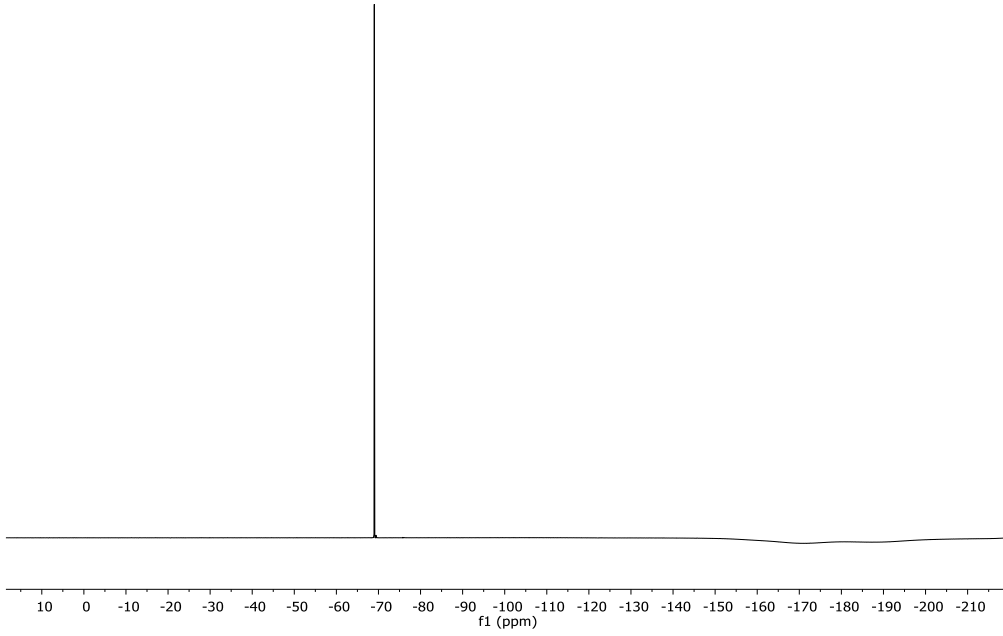






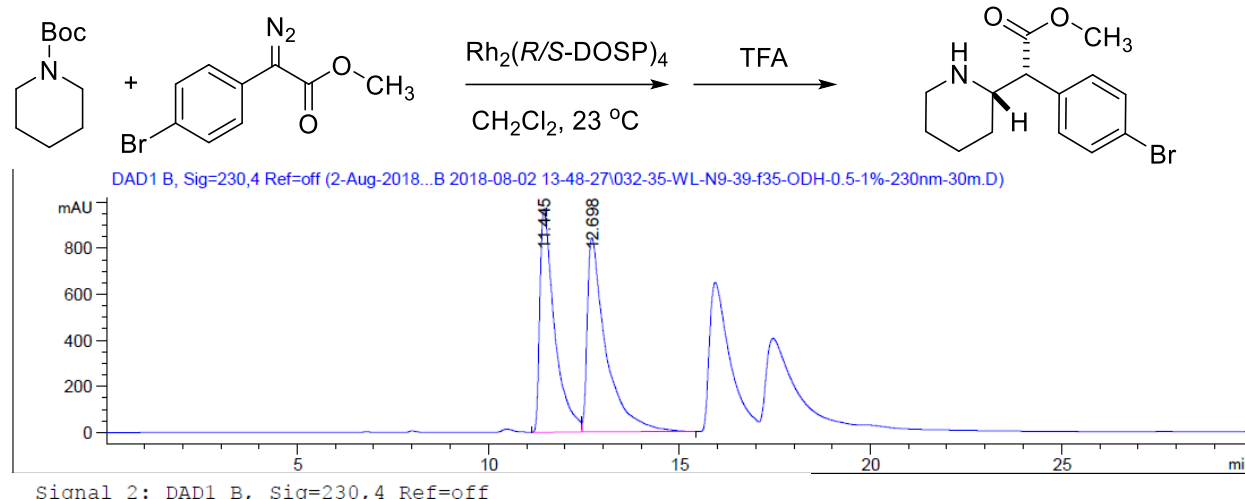




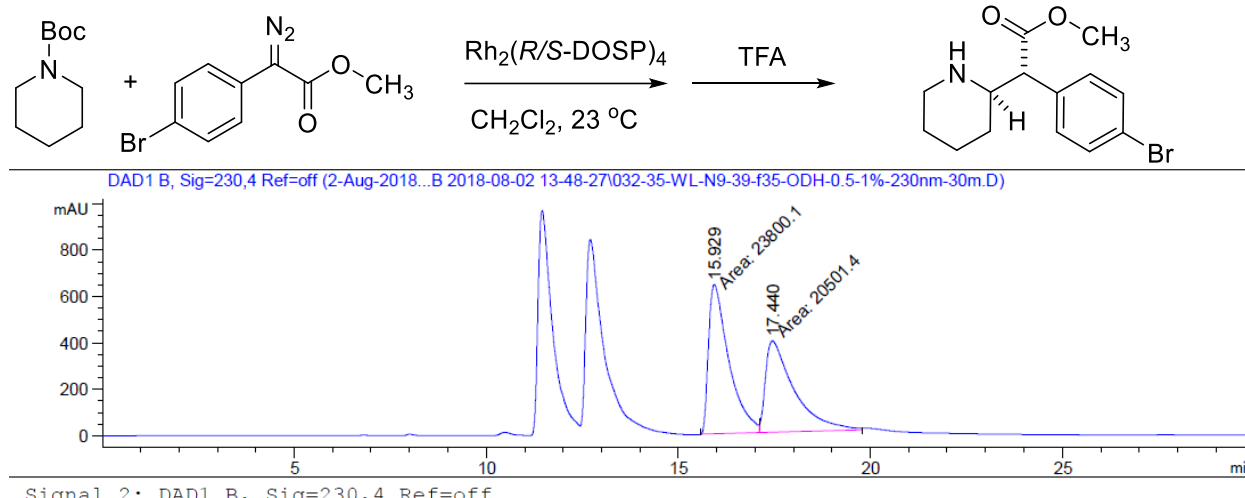


9. HPLC Spectra for Enantioselectivity Determination

10.1. C2 Functionalization Products



Racemic standard



Peak #	RetTime [min]	Type	Width [min]	Area [mAU*s]	Height [mAU]	Area %
1	15.929	MF	0.6162	2.38001e4	643.75751	53.7230
2	17.440	FM	0.8670	2.05014e4	394.11142	46.2770

Totals : 4.43016e4 1037.86893 Racemic standard

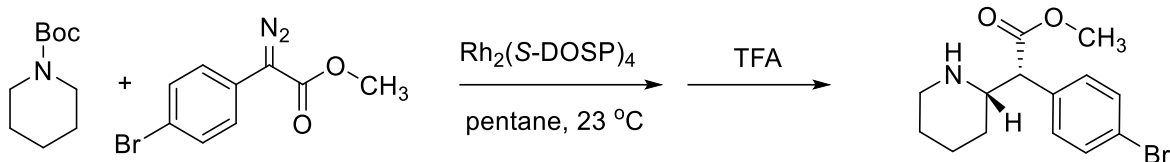
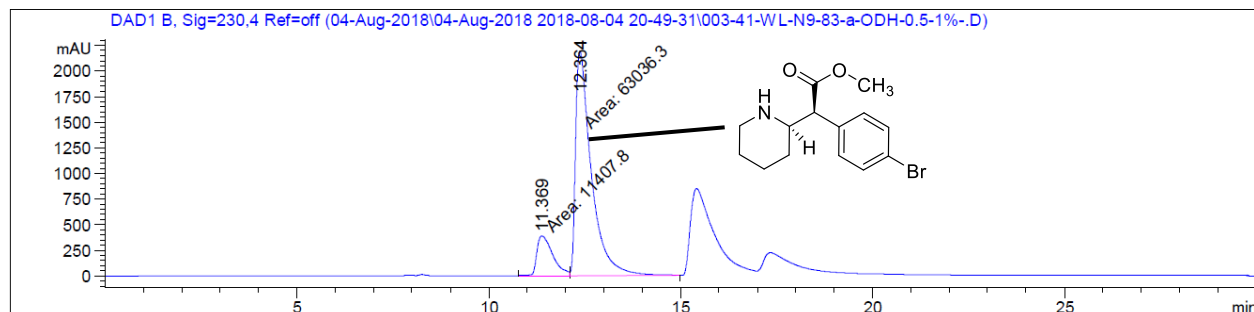


(Table S1, entry 1)



Signal 2: DAD1 B, Sig=230,4 Ref=off

Peak #	RetTime [min]	Type	Width [min]	Area [mAU*s]	Height [mAU]	Area %
----- ----- ----- ----- ----- ----- -----						
1	11.369	MF	0.4861	1.14078e4	391.15503	15.3240
2	12.364	FM	0.4783	6.30363e4	2196.41284	84.6760

Totals : 7.44441e4 2587.56787

→ -69% ee (major diastereomer)

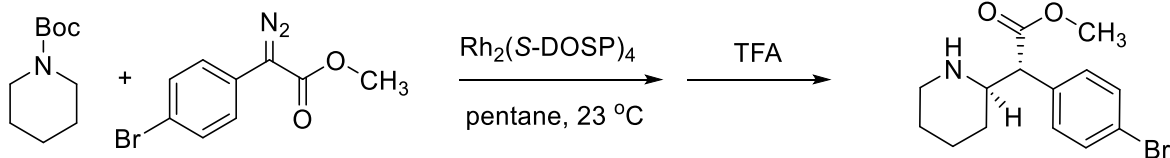
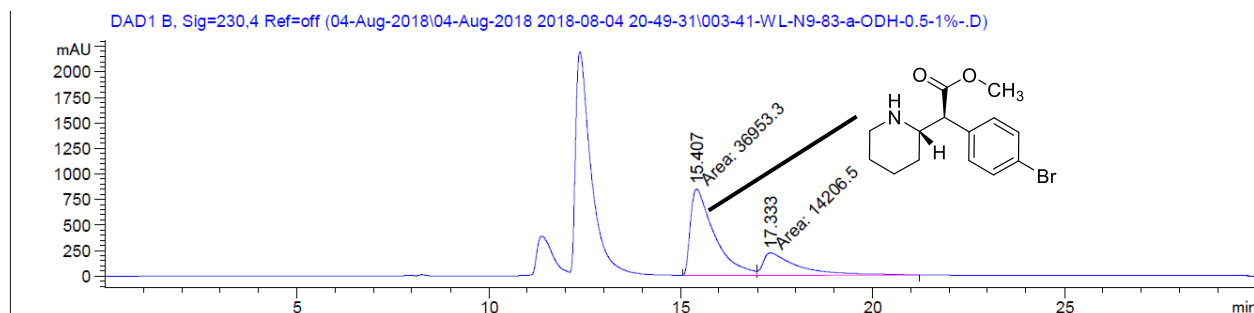


(Table S1, entry 1)



Signal 2: DAD1 B, Sig=230,4 Ref=off

Peak #	RetTime [min]	Type	Width [min]	Area [mAU*s]	Height [mAU]	Area %
----- ----- ----- ----- ----- ----- -----						
1	15.407	MF	0.7243	3.69533e4	850.35370	72.2311
2	17.333	FM	1.0738	1.42065e4	220.51192	27.7689

Totals : 5.11598e4 1070.86562

→ -44% ee (minor diastereomer)

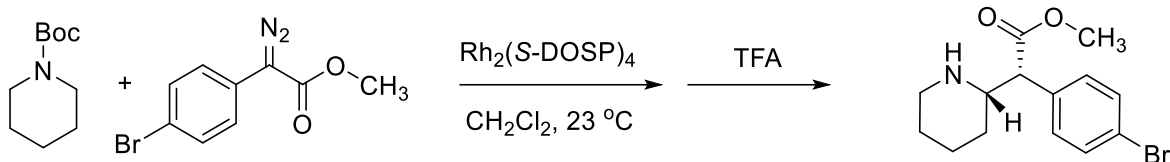
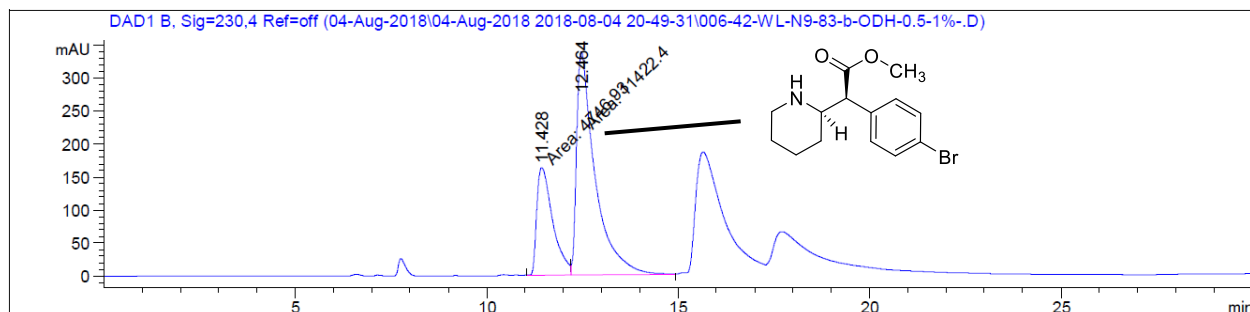


(Table 1, entry 1) (Table S1, entry 2)



Signal 2: DAD1 B, Sig=230,4 Ref=off

Peak #	RetTime [min]	Type	Width [min]	Area [mAU*s]	Height [mAU]	Area %
1	11.428	MF	0.4845	4746.93408	163.28975	29.3577
2	12.464	FM	0.5623	1.14224e4	338.57135	70.6423

Totals : 1.61693e4 501.86110

→ -41% ee (major diastereomer)

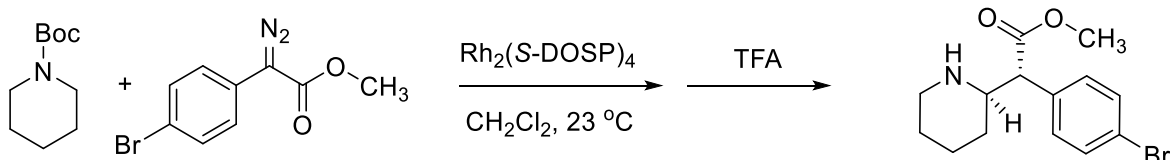
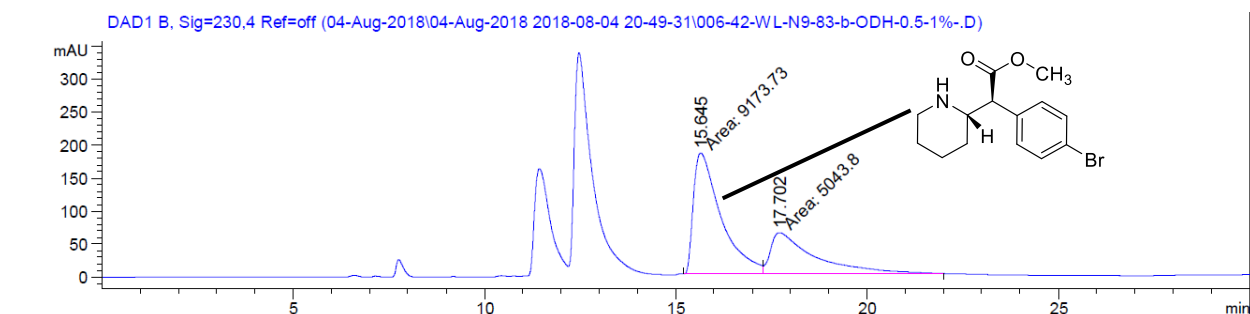


(Table 1, entry 1) (Table S1, entry 2)



Signal 2: DAD1 B, Sig=230,4 Ref=off

Peak #	RetTime [min]	Type	Width [min]	Area [mAU*s]	Height [mAU]	Area %
1	15.645	MF	0.8344	9173.73242	183.24197	64.5241
2	17.702	FM	1.3486	5043.779541	62.33588	35.4759

Totals : 1.42175e4 245.57785

→ -29% ee (minor diastereomer)

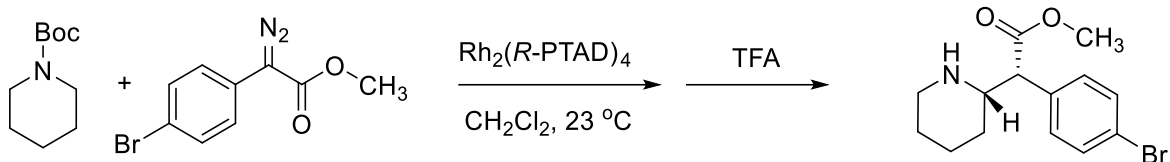
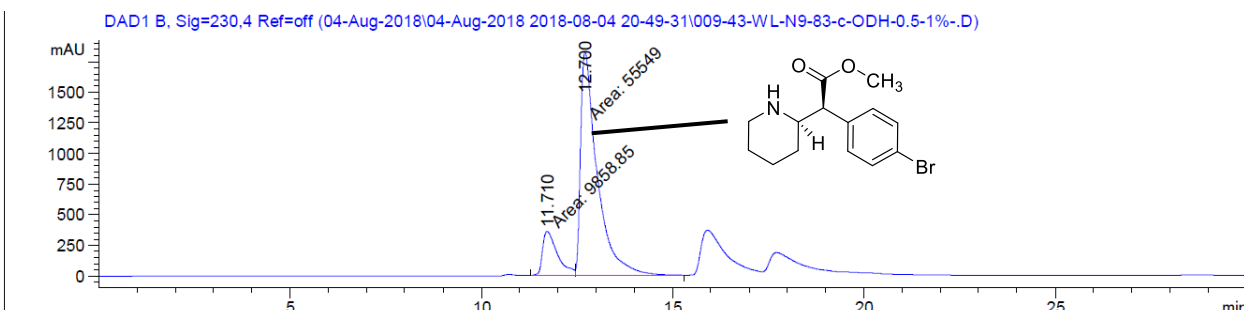


(Table S1, entry 3)



Signal 2: DAD1 B, Sig=230,4 Ref=off

Peak #	RetTime [min]	Type	Width [min]	Area [mAU*s]	Height [mAU]	Area %
1	11.710	MF	0.4549	9858.84961	361.19656	15.0729
2	12.700	FM	0.5069	5.55490e4	1826.51587	84.9271

Totals :

→ -70% ee (major diastereomer)

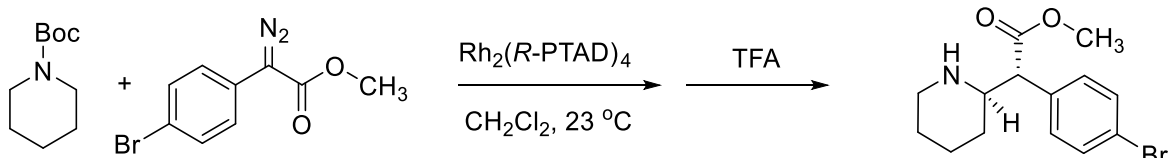
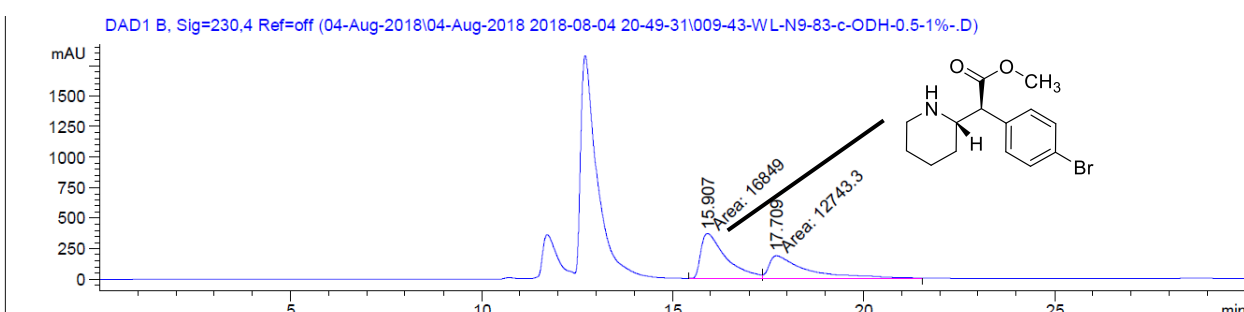


(Table S1, entry 3)



Signal 2: DAD1 B, Sig=230,4 Ref=off

Peak #	RetTime [min]	Type	Width [min]	Area [mAU*s]	Height [mAU]	Area %
1	15.907	MF	0.7638	1.68490e4	367.63730	56.9370
2	17.709	FM	1.1443	1.27433e4	185.60614	43.0630

Totals :

→ -14% ee (minor diastereomer)

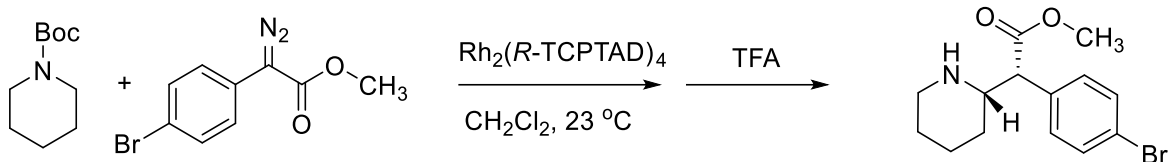
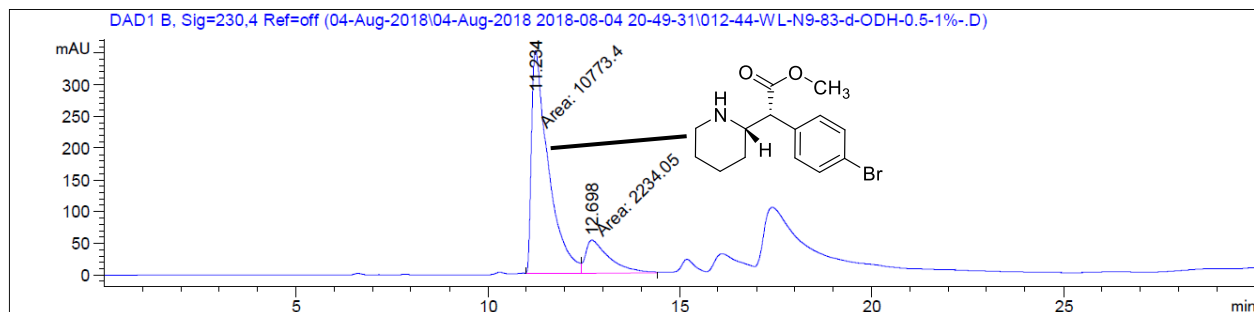


(Table 1, entry 2) (Table S1, entry 4)



Signal 2: DAD1 B, Sig=230,4 Ref=off

Peak #	RetTime [min]	Type	Width [min]	Area [mAU*s]	Height [mAU]	Area %
1	11.234	MF	0.5119	1.07734e4	350.74805	82.8248
2	12.698	FM	0.7135	2234.05225	52.18573	17.1752

Totals : 1.30074e4 402.93378 → 66% ee (major diastereomer)

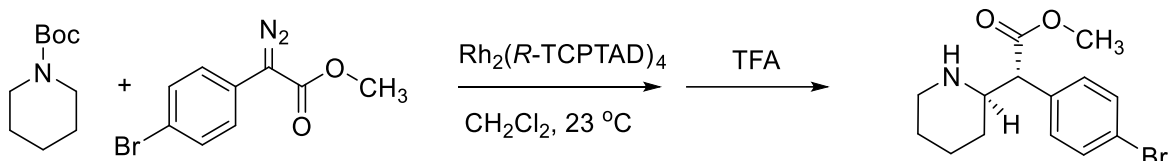
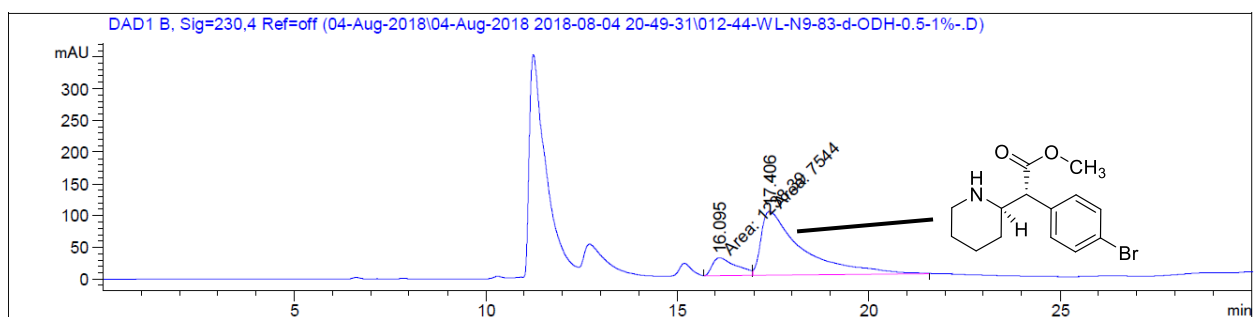


(Table 1, entry 2) (Table S1, entry 4)



Signal 2: DAD1 B, Sig=230,4 Ref=off

Peak #	RetTime [min]	Type	Width [min]	Area [mAU*s]	Height [mAU]	Area %
1	16.095	MF	0.7273	1238.38721	28.37903	14.1008
2	17.406	FM	1.2465	7544.00244	100.86837	85.8992

Totals : 8782.38965 129.24740

→ 72% ee (minor diastereomer)

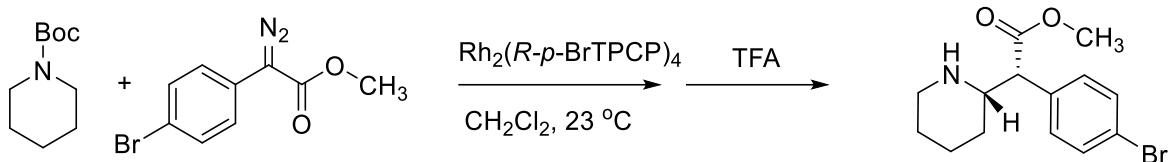
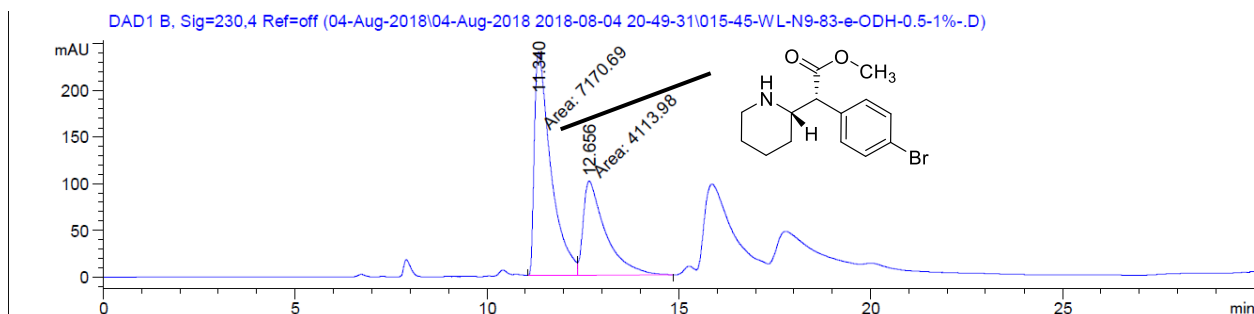


(Table 1, entry 3) (Table S1, entry 5)



Signal 2: DAD1 B, Sig=230,4 Ref=off

Peak #	RetTime [min]	Type	Width [min]	Area [mAU*s]	Height [mAU]	Area %
1	11.340	MF	0.4991	7170.69434	239.46901	63.5436
2	12.656	FM	0.6795	4113.98340	100.90635	36.4564

Totals : 1.12847e4 340.37536 → 27% ee (major diastereomer)

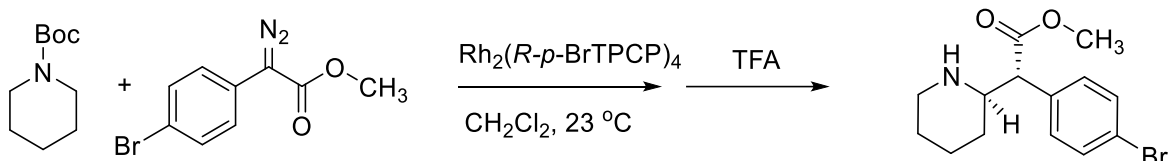
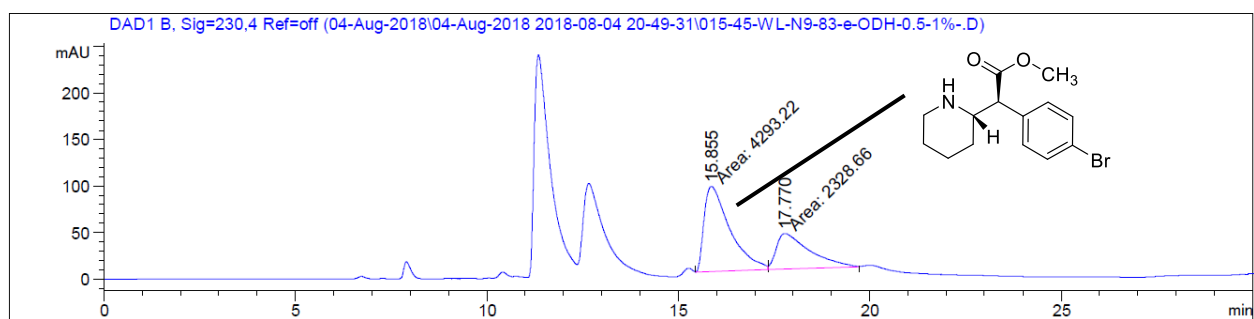


(Table 1, entry 3) (Table S1, entry 5)



Signal 2: DAD1 B, Sig=230,4 Ref=off

Peak #	RetTime [min]	Type	Width [min]	Area [mAU*s]	Height [mAU]	Area %
1	15.855	MF	0.7847	4293.22119	91.18973	64.8338
2	17.770	FM	1.0161	2328.66284	38.19611	35.1662

Totals : 6621.88403 129.38584

→ -30% ee (minor diastereomer)

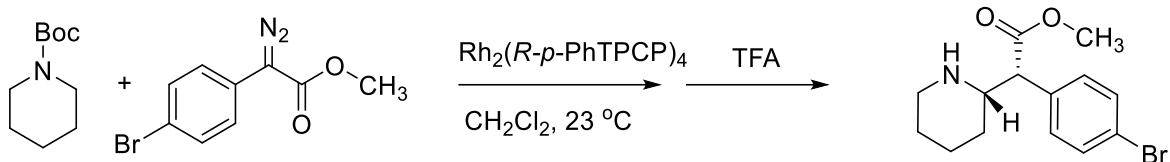
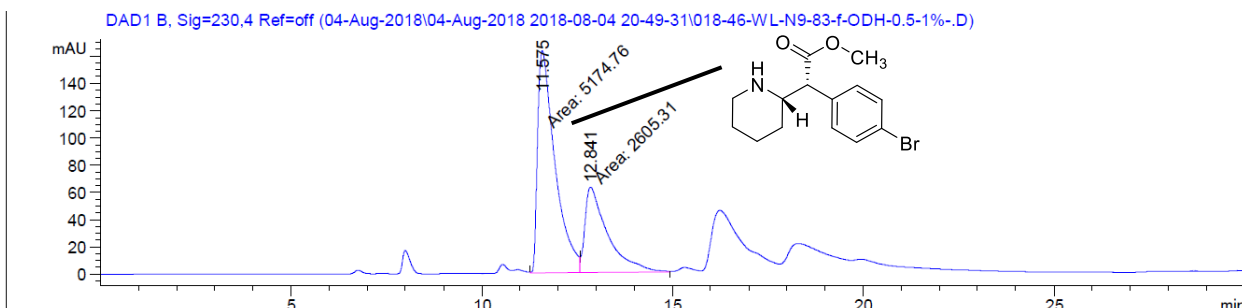


(Table S1, entry 6)



Signal 2: DAD1 B, Sig=230,4 Ref=off

Peak #	RetTime [min]	Type	Width [min]	Area [mAU*s]	Height [mAU]	Area %
1	11.575	MF	0.5285	5174.75732	163.20267	66.5130
2	12.841	FM	0.6917	2605.31250	62.77508	33.4870

Totals : 7780.06982 225.97775

→ 33% ee (major diastereomer)

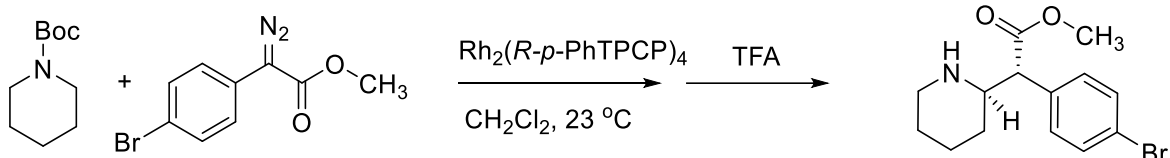
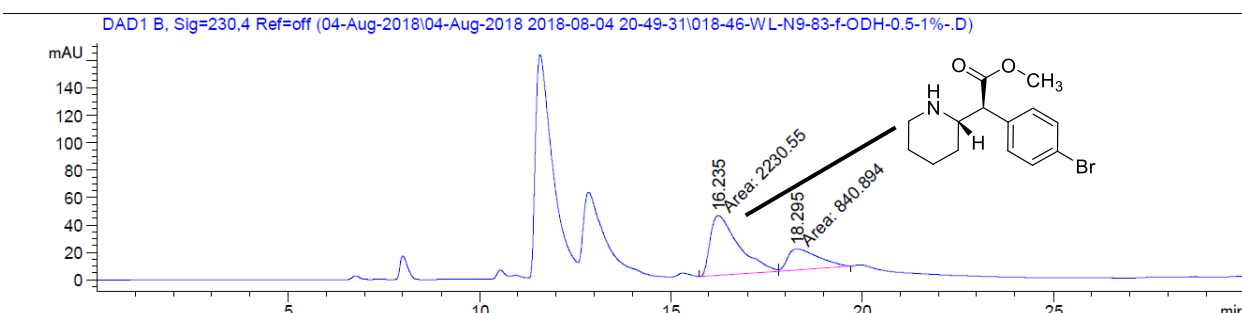


(Table S1, entry 6)



Signal 2: DAD1 B, Sig=230,4 Ref=off

Peak #	RetTime [min]	Type	Width [min]	Area [mAU*s]	Height [mAU]	Area %
1	16.235	MF	0.8545	2230.54614	43.50617	72.6221
2	18.295	FM	0.6483	840.89447	15.20243	27.3779

Totals : 3071.44061 58.70860

→ -45% ee (minor diastereomer)

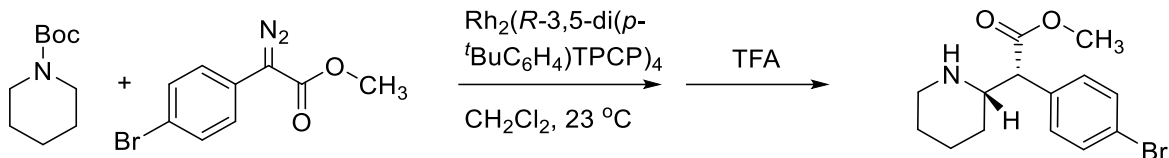
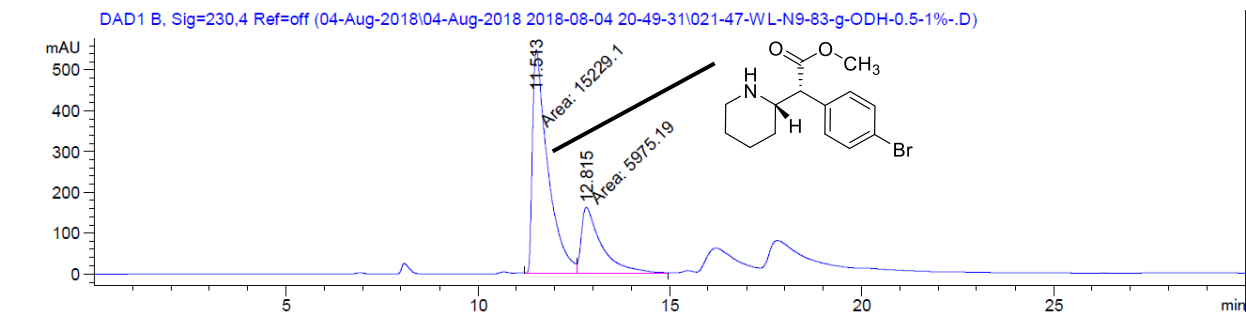


(Table S1, entry 7)



Signal 2: DAD1 B, Sig=230,4 Ref=off

Peak #	RetTime [min]	Type	Width [min]	Area [mAU*s]	Height [mAU]	Area %
1	11.513	MF	0.4633	1.52291e4	547.82129	71.8208
2	12.815	FM	0.6153	5975.18896	161.85378	28.1792

Totals : 2.12043e4 709.67506 → 44% ee (major diastereomer)

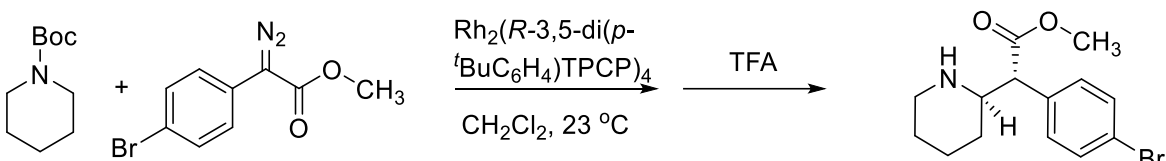
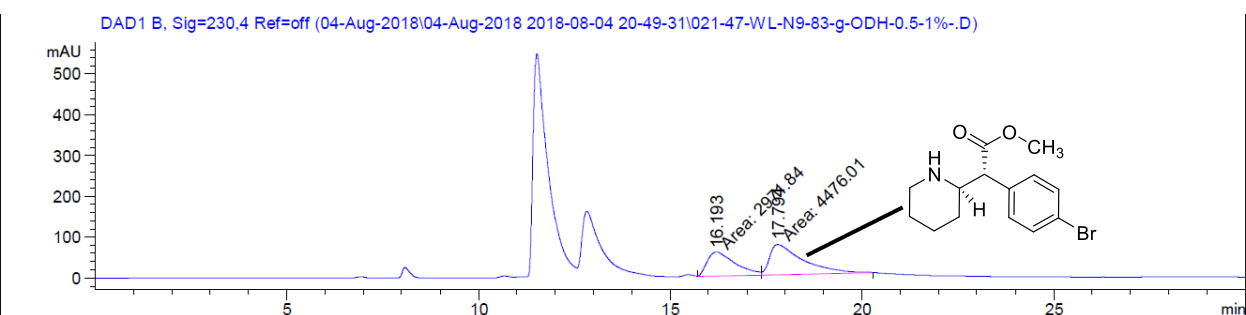


(Table S1, entry 7)



Signal 2: DAD1 B, Sig=230,4 Ref=off

Peak #	RetTime [min]	Type	Width [min]	Area [mAU*s]	Height [mAU]	Area %
1	16.193	MF	0.8420	2971.83643	58.82652	39.9020
2	17.794	FM	1.0082	4476.00732	73.99231	60.0980

Totals : 7447.84375 132.81882 → 20% ee (minor diastereomer)

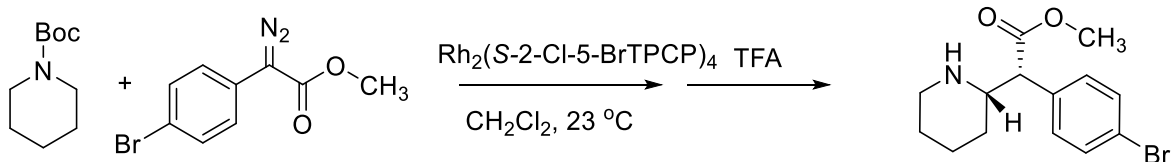
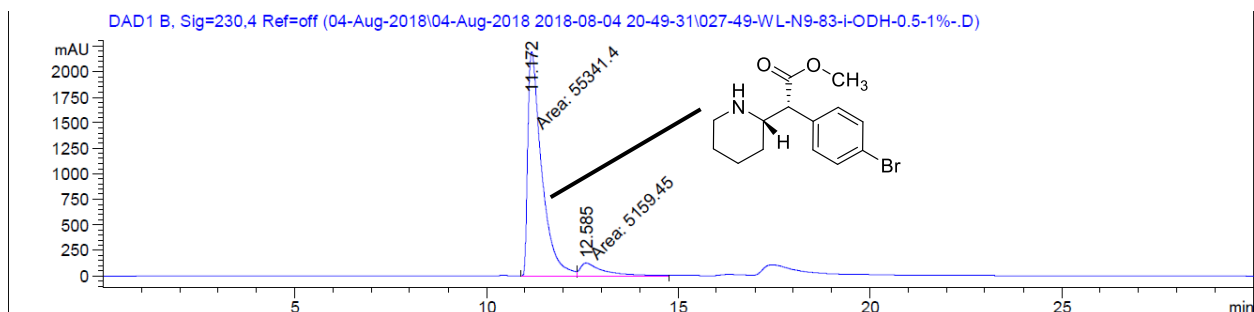


(Table 1, entry 5) (Table S1, entry 8)



Signal 2: DAD1 B, Sig=230,4 Ref=off

Peak #	RetTime [min]	Type	Width [min]	Area [mAU*s]	Height [mAU]	Area %
1	11.172	MF	0.4202	5.53414e4	2195.25513	91.4721
2	12.585	FM	0.6839	5159.44531	125.74113	8.5279

Totals :

→ 83% ee (major diastereomer)

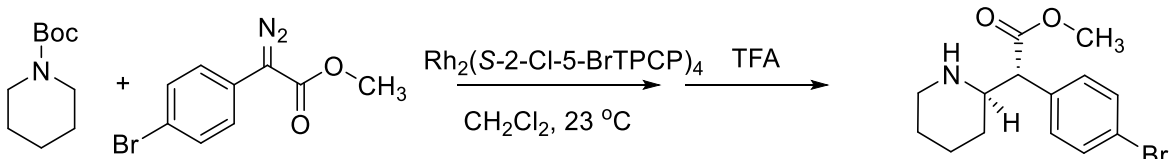
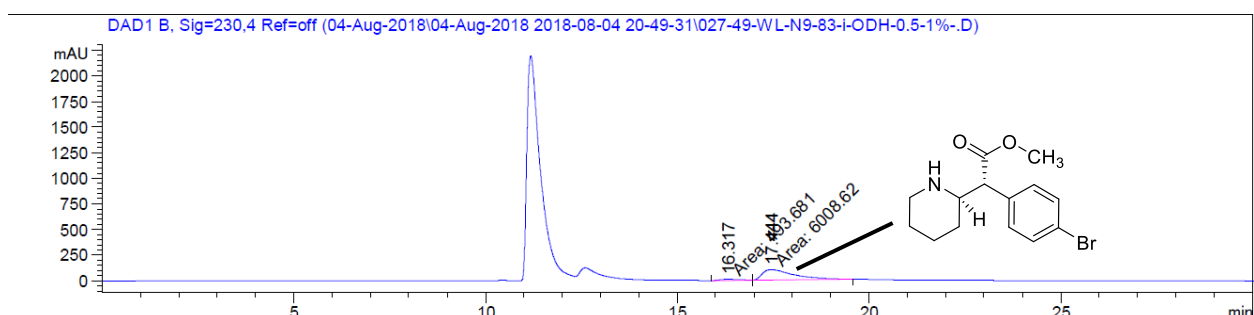


(Table 1, entry 5) (Table S1, entry 8)



Signal 2: DAD1 B, Sig=230,4 Ref=off

Peak #	RetTime [min]	Type	Width [min]	Area [mAU*s]	Height [mAU]	Area %
1	16.317	MF	0.6305	493.68134	13.04979	7.5924
2	17.444	FM	0.6887	6008.62402	102.47517	92.4076

Totals :

→ 85% ee (minor diastereomer)

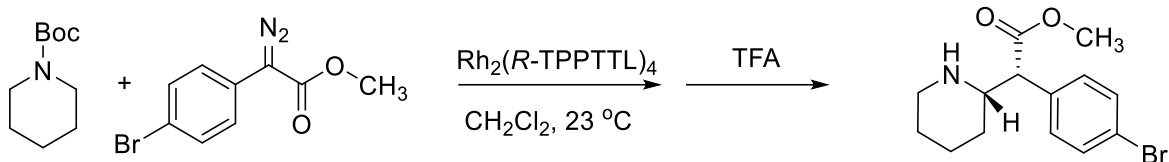
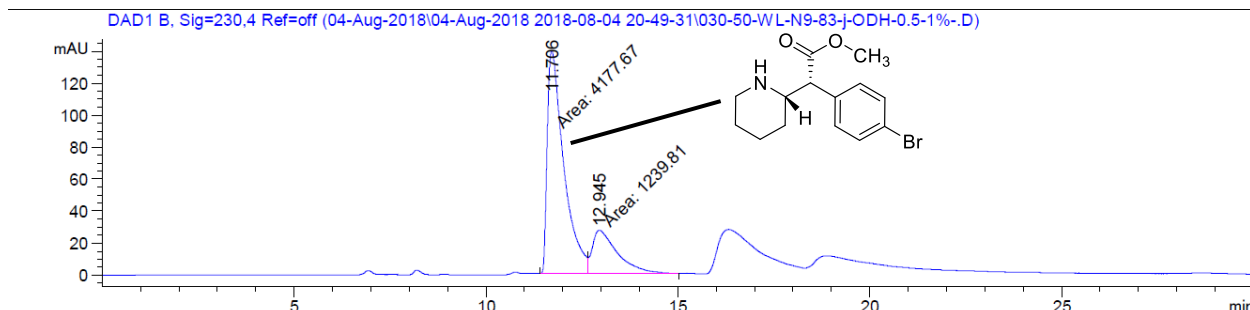


(Table S1, entry 9)



Signal 2: DAD1 B, Sig=230,4 Ref=off

Peak #	RetTime [min]	Type	Width [min]	Area [mAU*s]	Height [mAU]	Area %
1	11.706	MF	0.4993	4177.66504	139.45123	77.1147
2	12.945	FM	0.7599	1239.80676	27.19378	22.8853

Totals :

5417.47180 166.64501

→ 54% ee (major diastereomer)

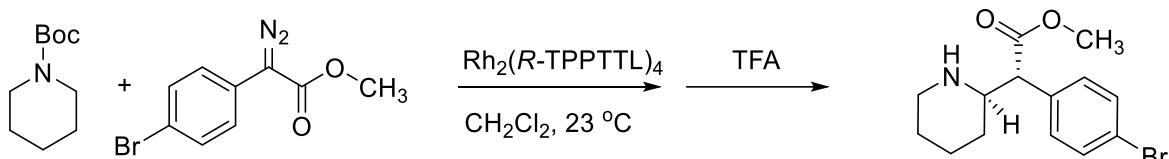
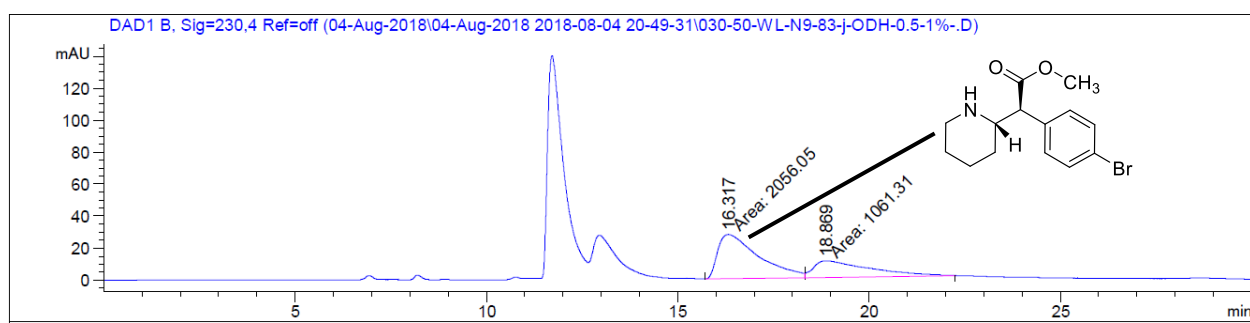


(Table S1, entry 9)



Signal 2: DAD1 B, Sig=230,4 Ref=off

Peak #	RetTime [min]	Type	Width [min]	Area [mAU*s]	Height [mAU]	Area %
1	16.317	MF	1.2393	2056.05444	27.65072	65.9550
2	18.869	FM	1.7064	1061.30603	10.36617	34.0450

Totals :

3117.36047 38.01689

→ -32% ee (minor diastereomer)

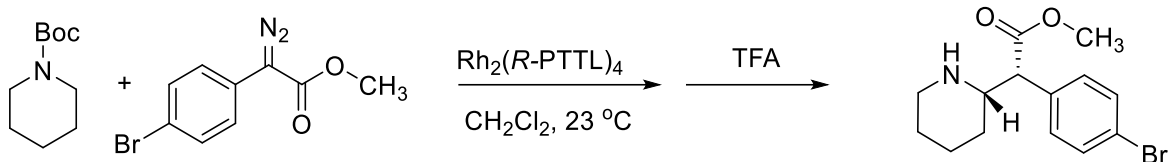
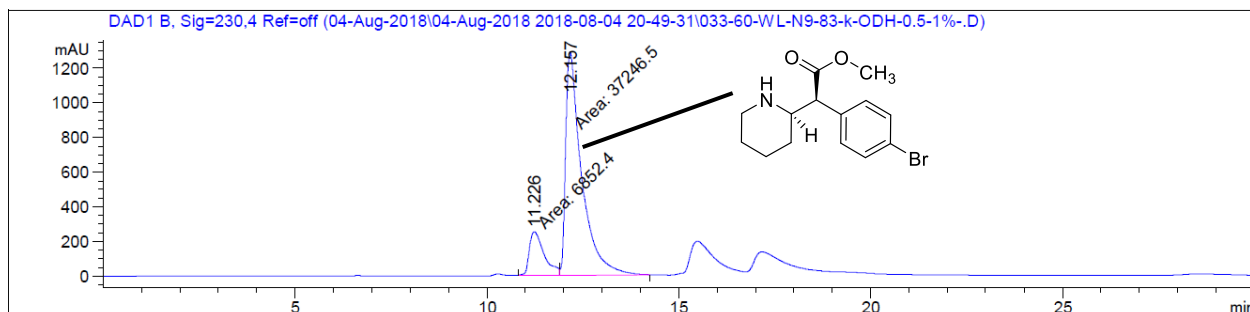


(Table S1, entry 10)



Signal 2: DAD1 B, Sig=230.4 Ref=off

Peak #	RetTime [min]	Type	Width [min]	Area [mAU*s]	Height [mAU]	Area %
1	11.226	MF	0.4520	6852.39844	252.68811	15.5387
2	12.157	FM	0.4810	3.72465e4	1290.56372	84.4613

Totals : 4.40989e4 1543.25183 → -69% ee (major diastereomer)

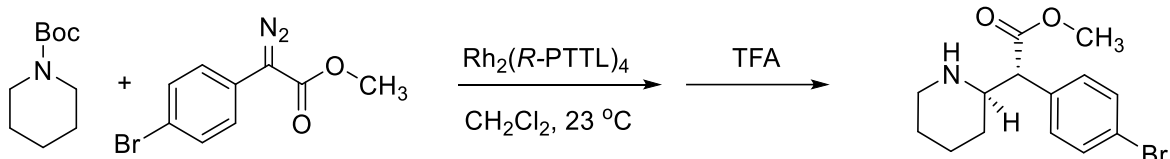
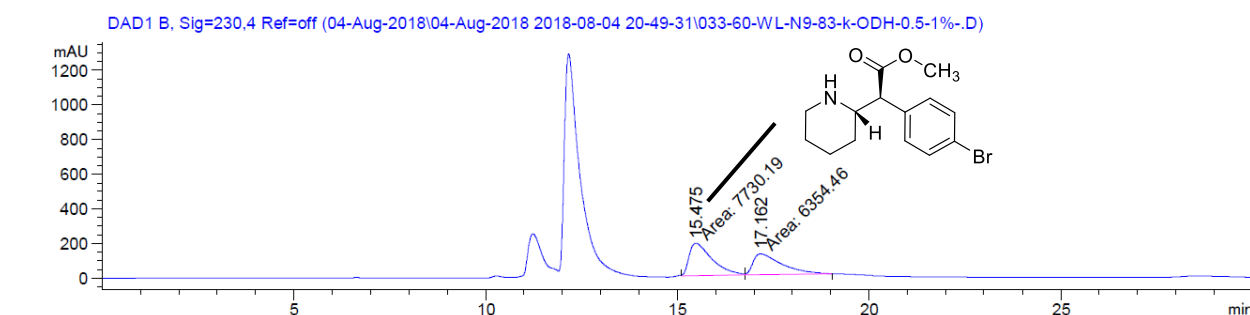


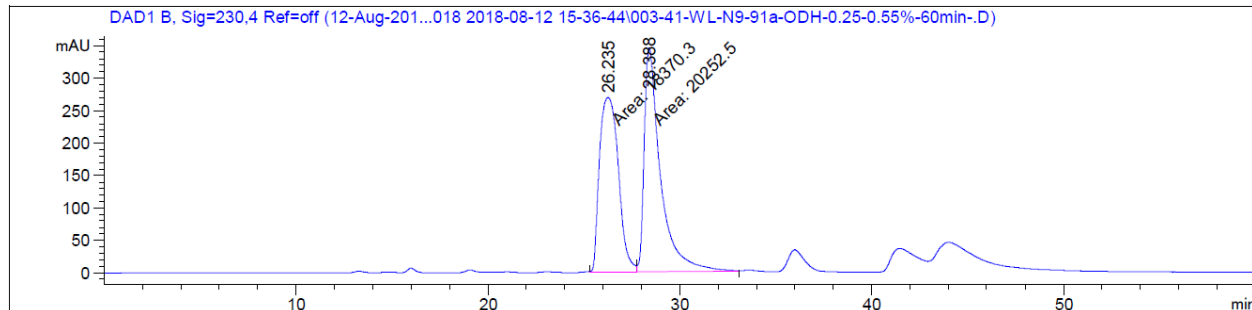
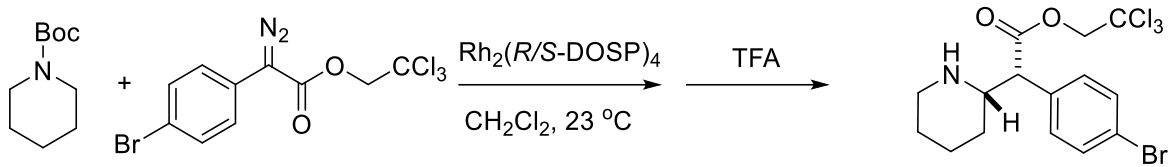
(Table S1, entry 10)



Signal 2: DAD1 B, Sig=230.4 Ref=off

Peak #	RetTime [min]	Type	Width [min]	Area [mAU*s]	Height [mAU]	Area %
1	15.475	MF	0.6927	7730.19336	185.98138	54.8838
2	17.162	FM	0.8777	6354.45508	120.67137	45.1162

Totals : 1.40846e4 306.65276 → -10% ee (minor diastereomer)



Signal 2: DAD1 B, Sig=230,4 Ref=off

Peak #	RetTime [min]	Type	Width [min]	Area [mAU*s]	Height [mAU]	Area %
1	26.235	MF	1.1408	1.83703e4	268.38867	47.5633
2	28.388	FM	0.9793	2.02525e4	344.68665	52.4367

Totals : 3.86228e4 613.07532

Racemic standard

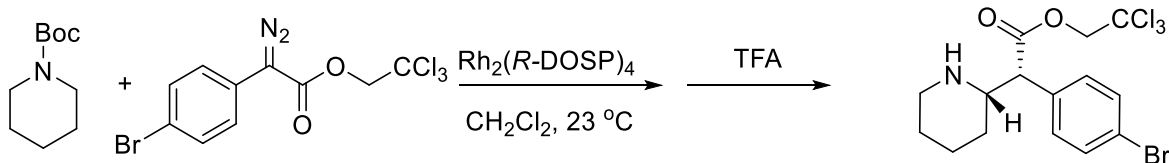
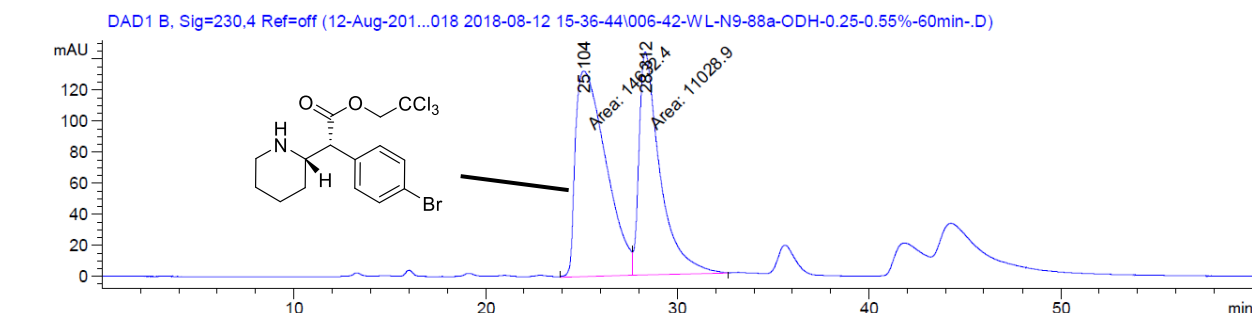


(Table S1, entry 11)



Signal 2: DAD1 B, Sig=230,4 Ref=off

Peak #	RetTime [min]	Type	Width [min]	Area [mAU*s]	Height [mAU]	Area %
1	25.104	MF	1.8405	1.46324e4	132.50249	57.0213
2	28.312	FM	1.2775	1.10289e4	143.88950	42.9787

Totals : 2.56613e4 276.39198

→ 14% ee

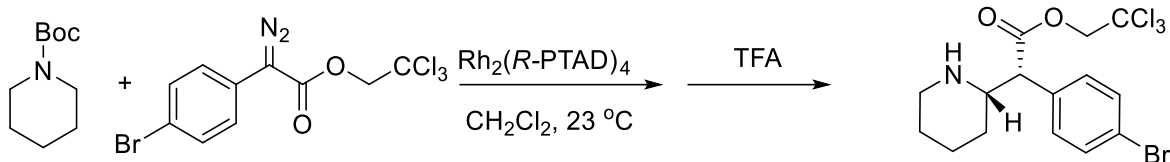
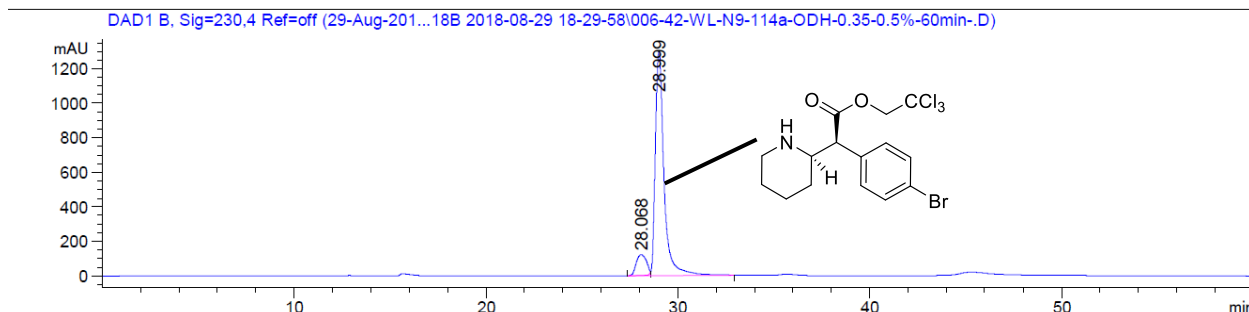


(Table S1, entry 12)



Signal 2: DAD1 B, Sig=230,4 Ref=off

Peak #	RetTime [min]	Type	Width [min]	Area [mAU*s]	Height [mAU]	Area %
1	28.068	BV	E	0.4497	4465.76807	121.68364
2	28.999	VB	R	0.4661	4.08430e4	1301.45325

Totals : 4.53087e4 1423.13689 → -80% ee

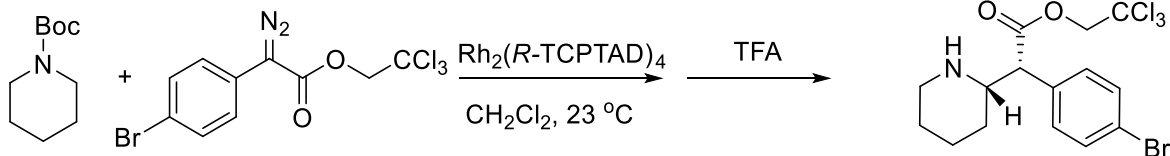
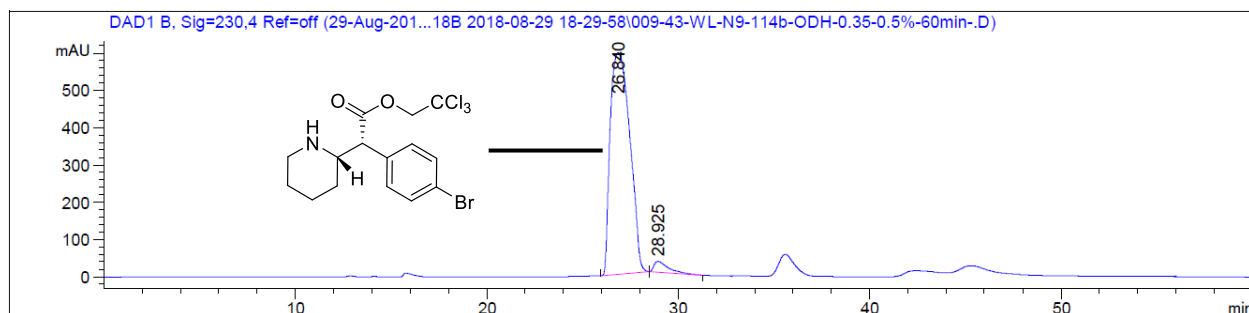


(Table 1, entry 7) (Table S1, entry 13)



Signal 2: DAD1 B, Sig=230,4 Ref=off

Peak #	RetTime [min]	Type	Width [min]	Area [mAU*s]	Height [mAU]	Area %
1	26.840	BB	0.8340	4.23118e4	594.36523	96.4261
2	28.925	BB	0.6203	1568.23633	29.63874	3.5739

Totals : 4.38801e4 624.00398 → 93% ee

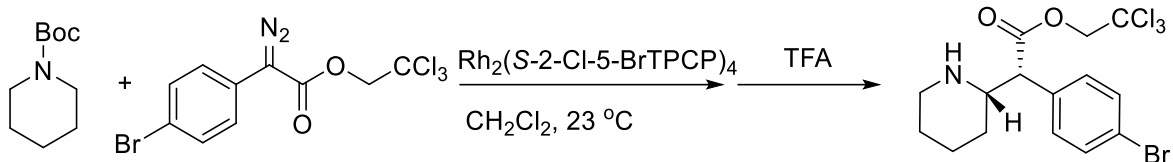
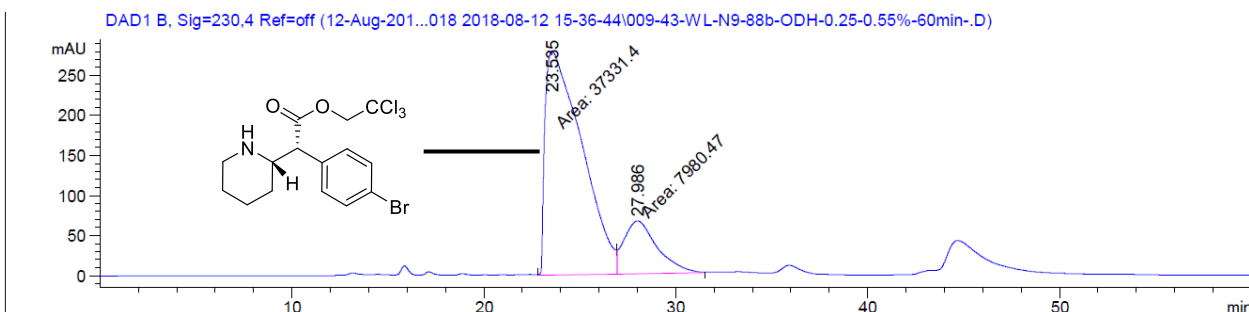


(Table 1, entry 6) (Table S1, entry 14)



Signal 2: DAD1 B, Sig=230,4 Ref=off

Peak #	RetTime [min]	Type	Width [min]	Area [mAU*s]	Height [mAU]	Area %
1	23.535	MF	2.2210	3.73314e4	280.14163	82.3877
2	27.986	FM	2.0146	7980.47217	66.02348	17.6123
Totals :					4.53119e4	346.16512
						→ 65% ee

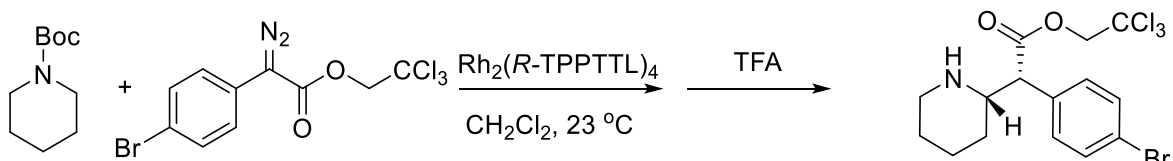
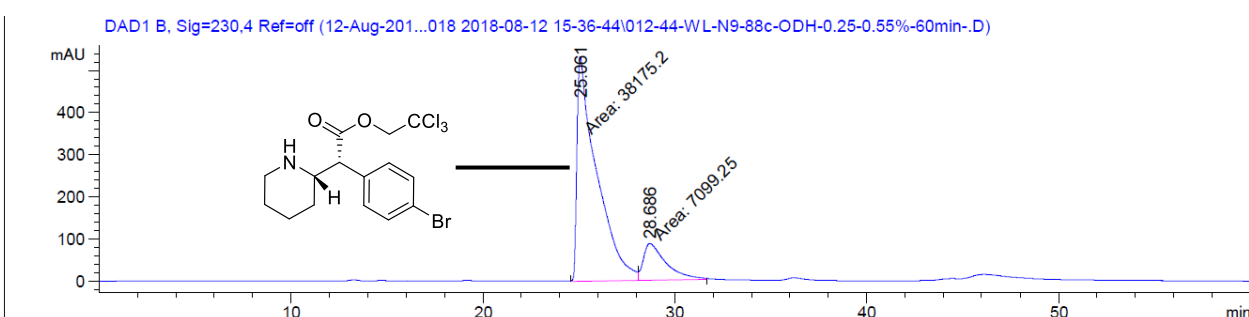


(Table 1, entry 8) (Table S1, entry 15)



Signal 2: DAD1 B, Sig=230,4 Ref=off

Peak #	RetTime [min]	Type	Width [min]	Area [mAU*s]	Height [mAU]	Area %
1	25.061	MF	1.1910	3.81752e4	534.21667	84.3195
2	28.686	FM	1.3590	7099.25146	87.06653	15.6805
Totals :					4.52744e4	621.28320
						→ 69% ee

Totals : 4.52744e4 621.28320 → 69% ee

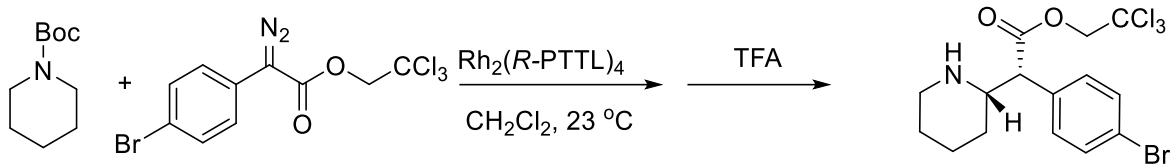
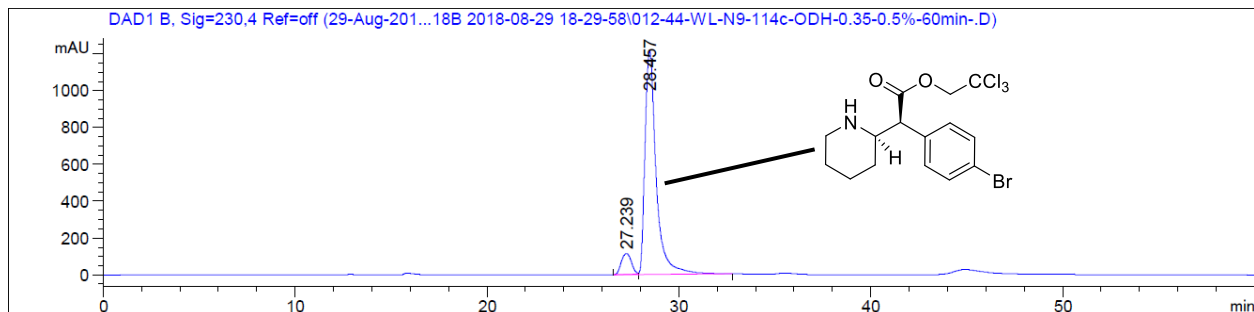


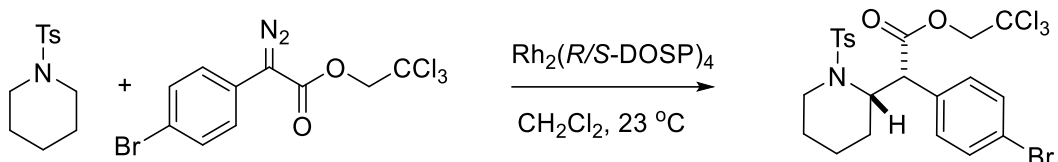
(Table S1, entry 16)



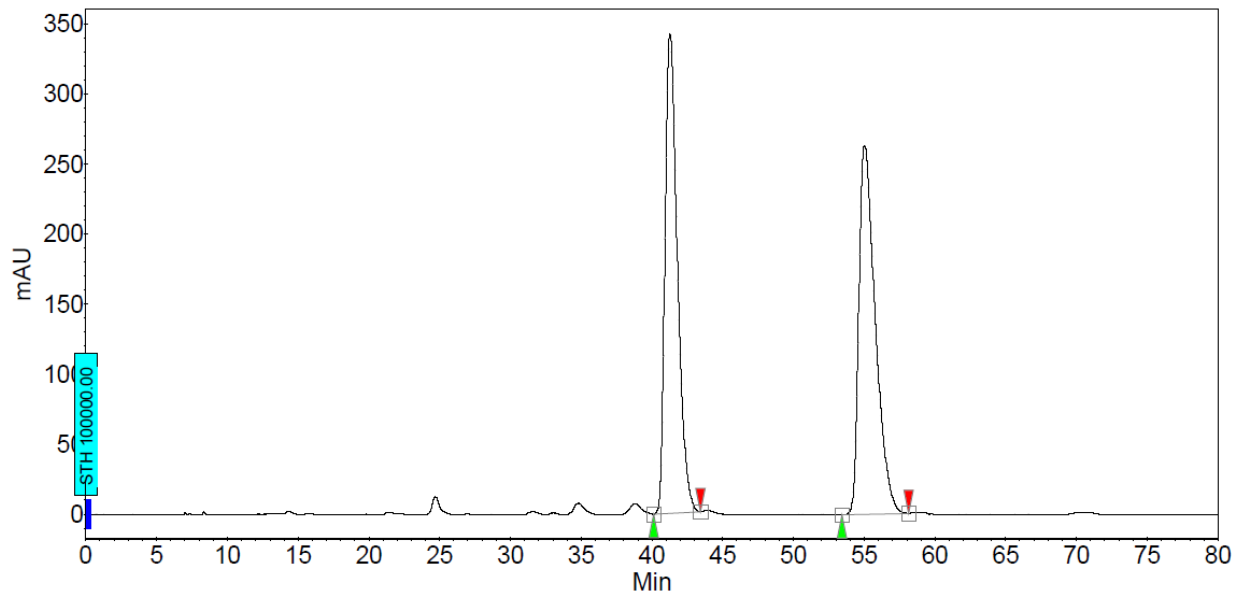
Signal 2: DAD1 B, Sig=230,4 Ref=off

Peak #	RetTime [min]	Type	Width [min]	Area [mAU*s]	Height [mAU]	Area %
1	27.239	BV	E	0.4451	4183.92627	113.63413
2	28.457	VB	R	0.5516	4.92957e4	1219.38342
Totals :					5.34796e4	1333.01756
					→ -84% ee	

Racemic standard



WL-N9-91b-C2-f14-ADH-0.5-5%-230nm-80min-6.DATA - Prostar 325 Absorbance Channel 2 LC1006M831



Peak results :

Index	Name	Time [Min]	Quantity [% Area]	Height [mAU]	Area [mAU.Min]	Area [%]
1	UNKNOWN	41.27	49.39	342.0	346.4	49.391
2	UNKNOWN	55.03	50.61	263.2	355.0	50.609
Total			100.00	605.3	701.4	100.000

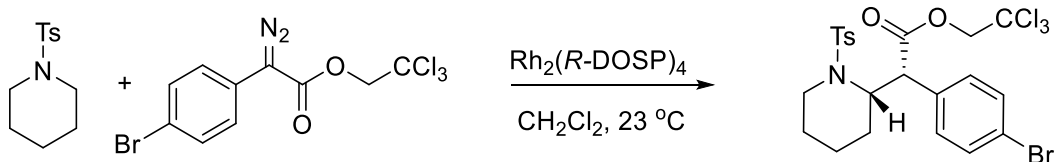
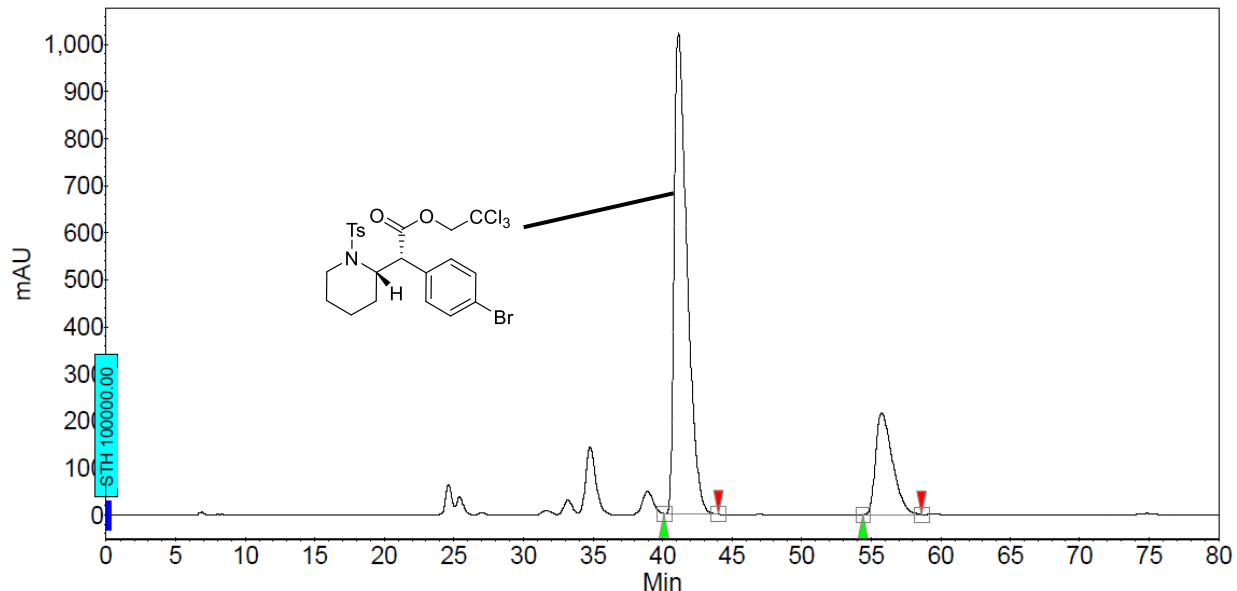


(Table S2, entry 1)

WL-N9-99-f2329-ADH-0.5-5%-230nm-80min-93.DATA - Prostar 325 Absorbance Channel 2 LC1006M831



Peak results :

Index	Name	Time [Min]	Quantity [% Area]	Height [mAU]	Area [mAU.Min]	Area [%]
1	UNKNOWN	41.14	78.46	1022.7	1099.6	78.463
2	UNKNOWN	55.76	21.54	216.3	301.8	21.537
Total			100.00	1238.9	1401.5	100.000

→ 57% ee

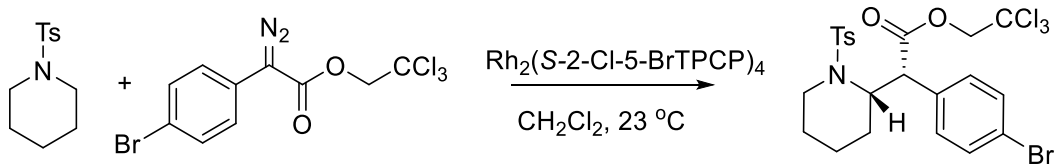
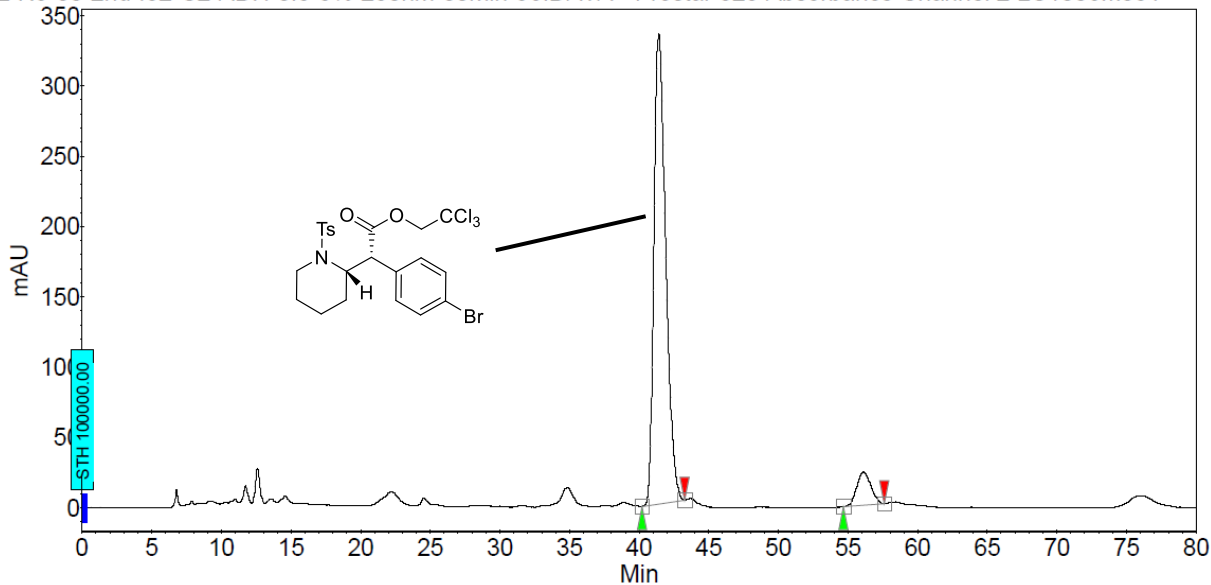


(Table S2, entry 2)

WL-N9-80-2nd-f32-C2-ADH-0.5-5%-230nm-80min-96.DATA - Prostar 325 Absorbance Channel 2 LC1006M831



Peak results :

Index	Name	Time [Min]	Quantity [% Area]	Height [mAU]	Area [mAU.Min]	Area % [%]
1	UNKNOWN	41.40	92.24	334.8	328.1	92.237
2	UNKNOWN	56.11	7.76	23.4	27.6	7.763
Total			100.00	358.3	355.8	100.000

→ 84% ee

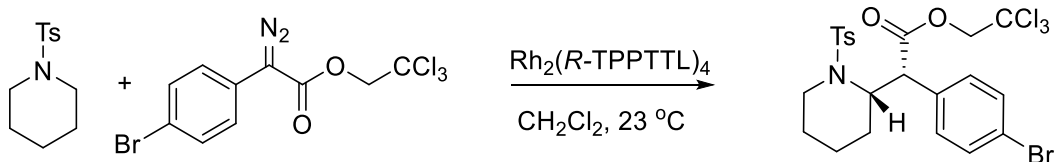
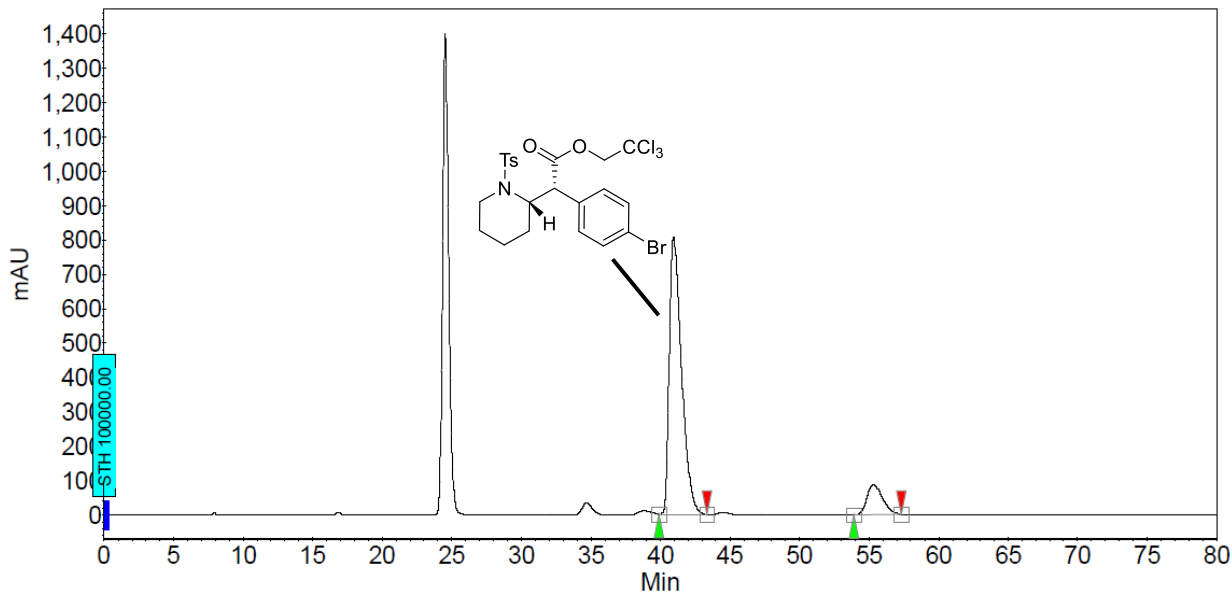


(Table S2, entry 3)

WL-N9-93b-C2-f14-ADH-0.5-5%-230nm-80min-12.DATA - Prostar 325 Absorbance Channel 2 LC1006M831

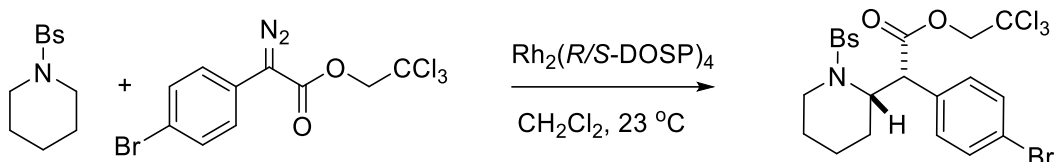


Peak results :

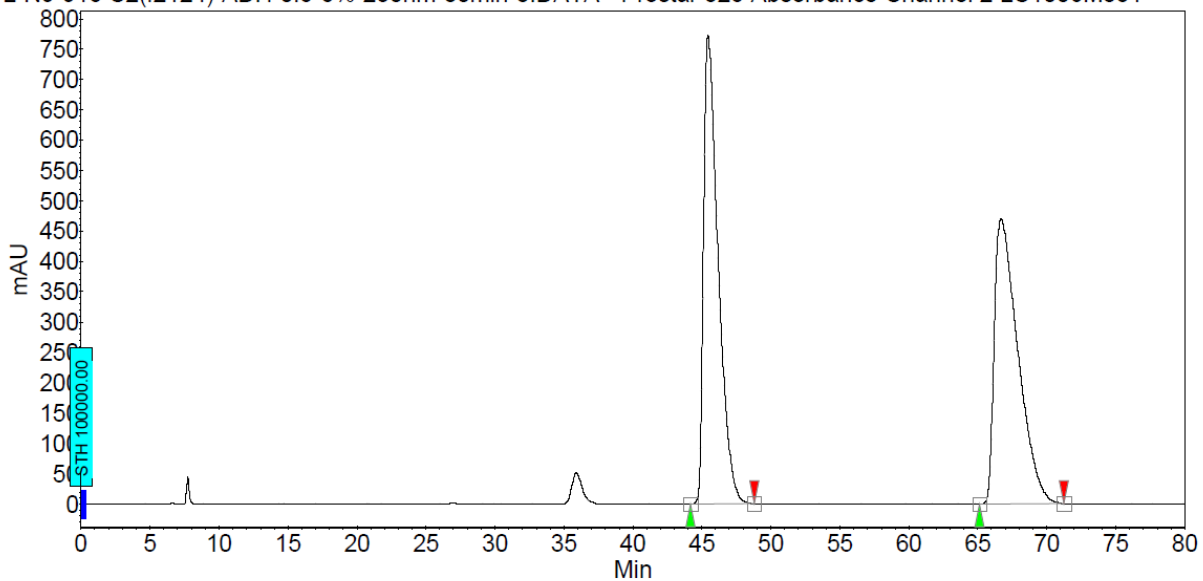
Index	Name	Time [Min]	Quantity [% Area]	Height [mAU]	Area [mAU.Min]	Area [%]
1	UNKNOWN	40.94	88.03	808.2	826.1	88.029
2	UNKNOWN	55.33	11.97	86.2	112.3	11.971
Total			100.00	894.4	938.4	100.000

→ 76% ee

Racemic standard



WL-N9-91c-C2(f2124)-ADH-0.5-5%-230nm-80min-8.DATA - Prostar 325 Absorbance Channel 2 LC1006M831



Peak results :

Index	Name	Time [Min]	Quantity [% Area]	Height [mAU]	Area [mAU.Min]	Area [%]
1	UNKNOWN	45.44	50.39	772.7	947.2	50.386
2	UNKNOWN	66.68	49.61	470.6	932.7	49.614
Total			100.00	1243.3	1879.8	100.000

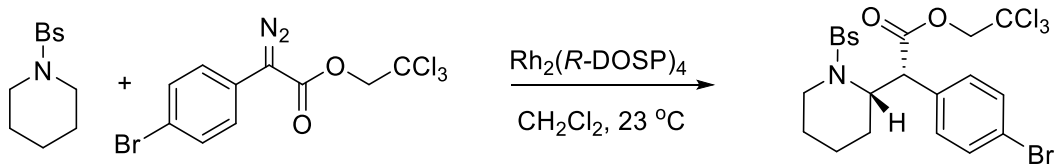
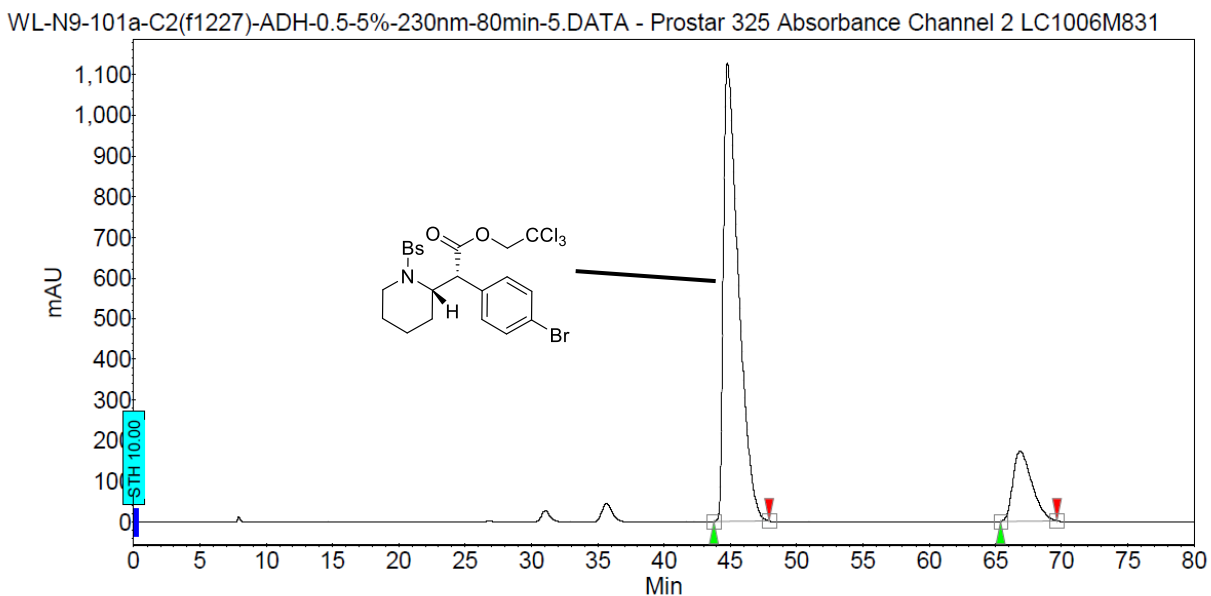


(Table S2, entry 4)



Peak results :

Index	Name	Time [Min]	Quantity [% Area]	Height [mAU]	Area [mAU.Min]	Area % [%]
1	UNKNOWN	44.79	83.71	1128.0	1476.6	83.711
2	UNKNOWN	66.86	16.29	173.2	287.3	16.289
Total			100.00	1301.2	1763.9	100.000

→ 67% ee

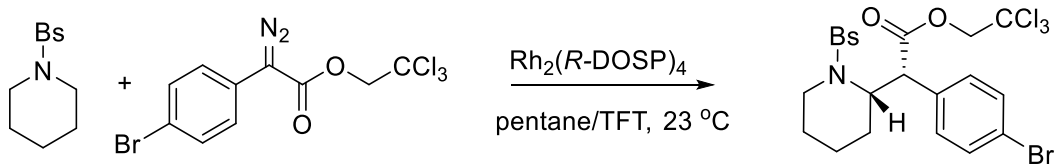
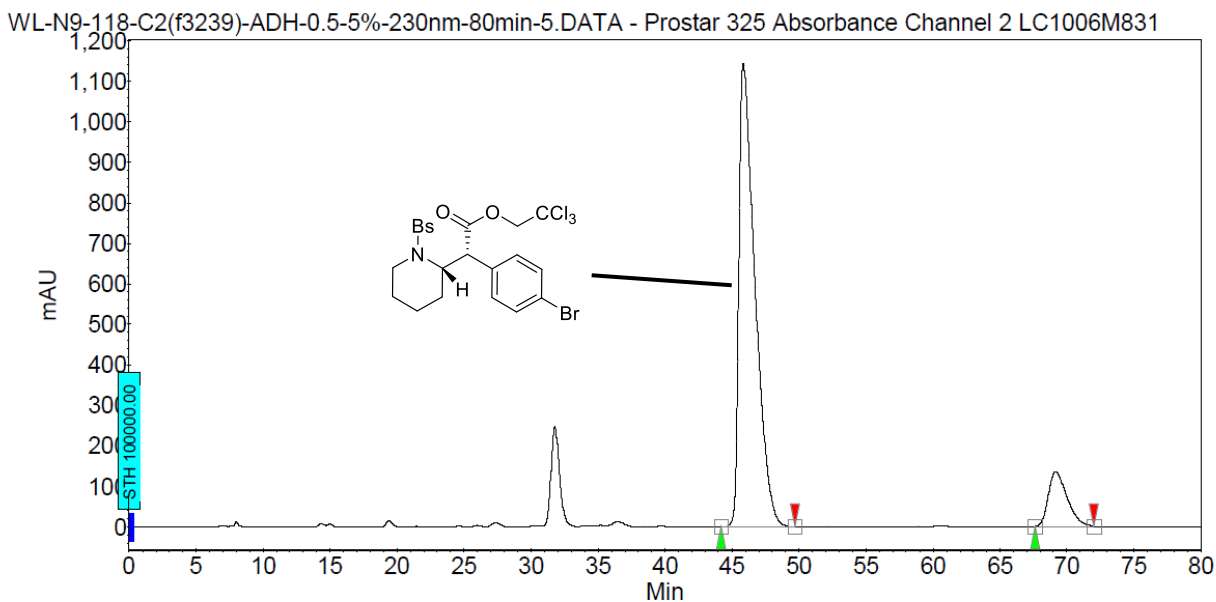


(Table S2, entry 5)



Peak results :

Index	Name	Time [Min]	Quantity [% Area]	Height [mAU]	Area [mAU.Min]	Area [%]
1	UNKNOWN	45.84	87.91	1144.2	1586.9	87.910
2	UNKNOWN	69.15	12.09	133.8	218.2	12.090
Total			100.00	1278.0	1805.1	100.000

→ 76% ee

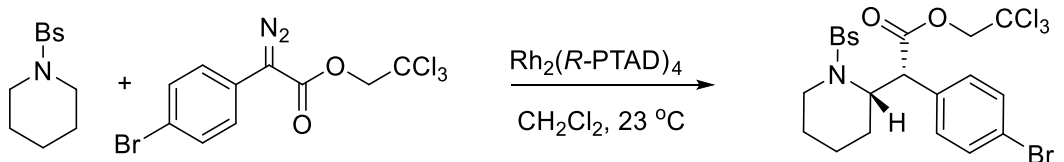
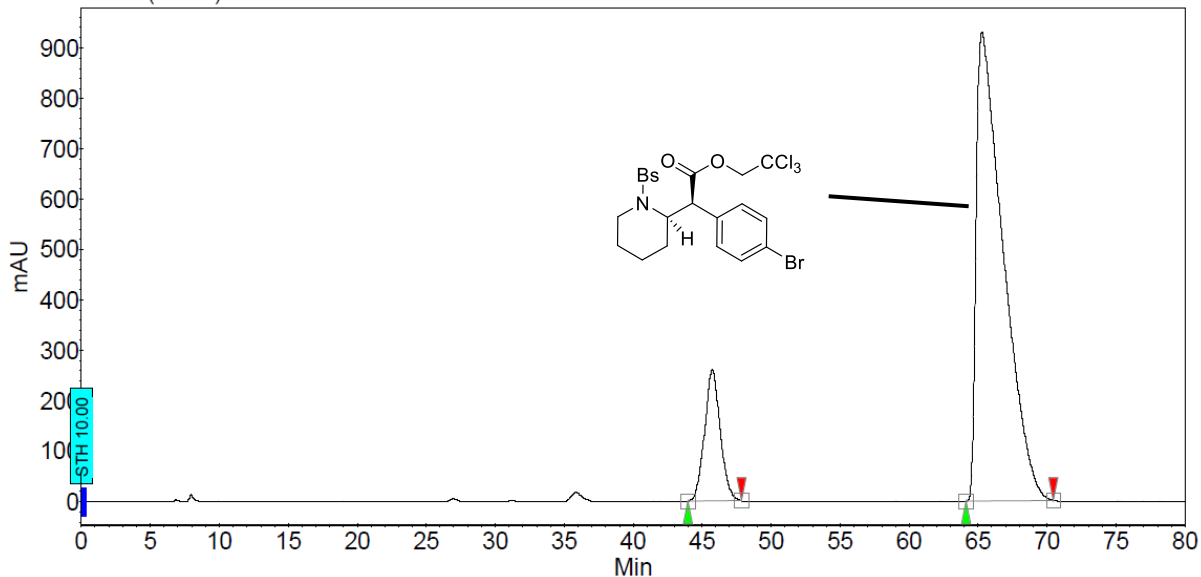


(Table S2, entry 7)

WL-N9-101b-C2(f1326)-ADH-0.5-5%-230nm-80min-2.DATA - Prostar 325 Absorbance Channel 2 LC1006M831



Peak results :

Index	Name	Time [Min]	Quantity [% Area]	Height [mAU]	Area [mAU.Min]	Area % [%]
1	UNKNOWN	45.73	14.01	261.2	343.9	14.011
2	UNKNOWN	65.27	85.99	931.2	2110.4	85.989
Total			100.00	1192.3	2454.3	100.000

→ -72% ee

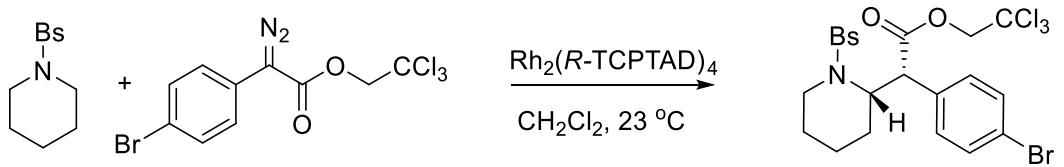
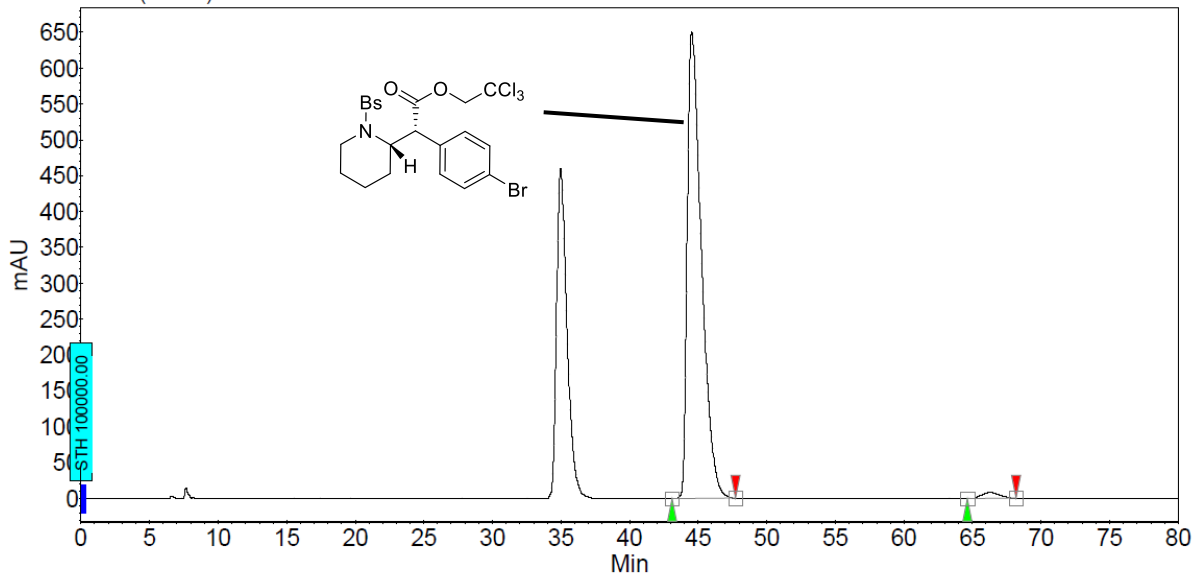


(Table S2, entry 8)

WL-N9-101c-C2(f3032)-ADH-0.5-5%-230nm-80min-32.DATA - Prostar 325 Absorbance Channel 2 LC1006M831



Peak results :

Index	Name	Time [Min]	Quantity [% Area]	Height [mAU]	Area [mAU.Min]	Area % [%]
1	UNKNOWN	44.54	98.50	650.9	776.8	98.498
2	UNKNOWN	66.29	1.50	8.4	11.8	1.502
Total			100.00	659.2	788.6	100.000

→ 97% ee

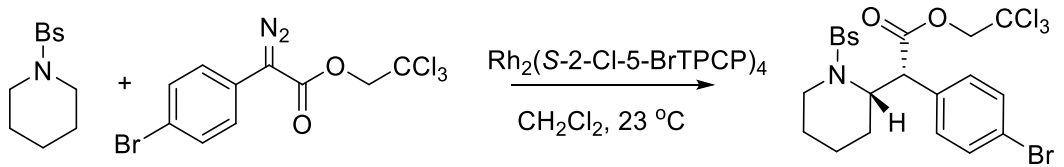
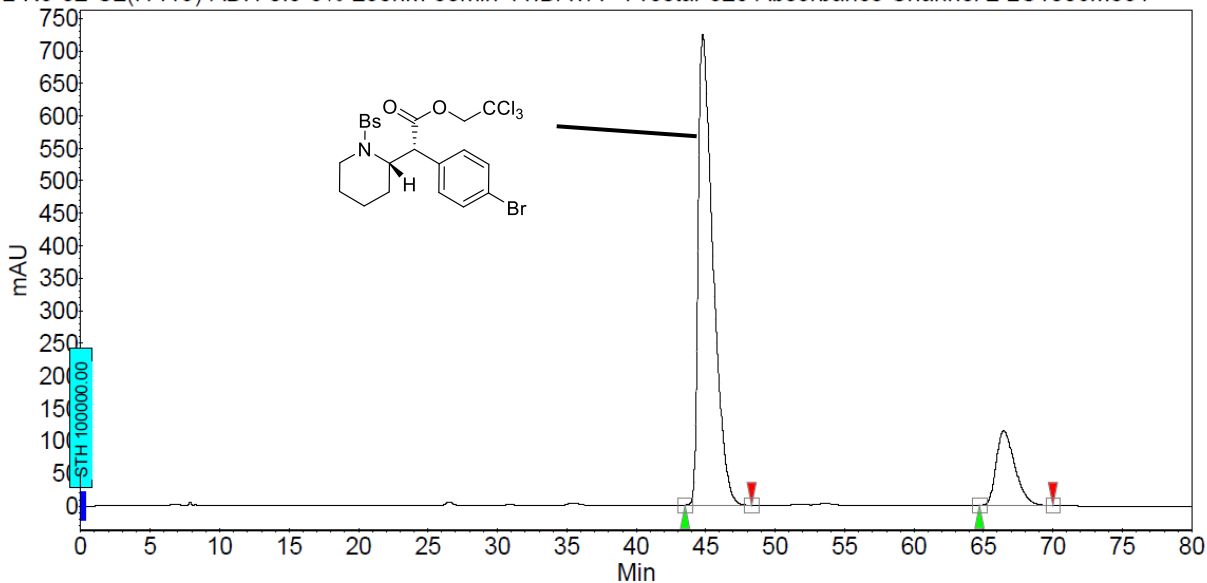


(Table S2, entry 12)

WL-N9-82-C2(f1419)-ADH-0.5-5%-230nm-80min-11.DATA - Prostar 325 Absorbance Channel 2 LC1006M831



Peak results :

Index	Name	Time [Min]	Quantity [% Area]	Height [mAU]	Area [mAU.Min]	Area [%]
1	UNKNOWN	44.79	83.22	724.6	893.8	83.217
2	UNKNOWN	66.46	16.78	115.0	180.3	16.783
Total			100.00	839.6	1074.1	100.000

→ 66% ee

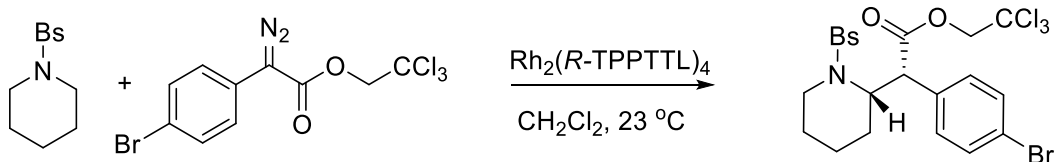
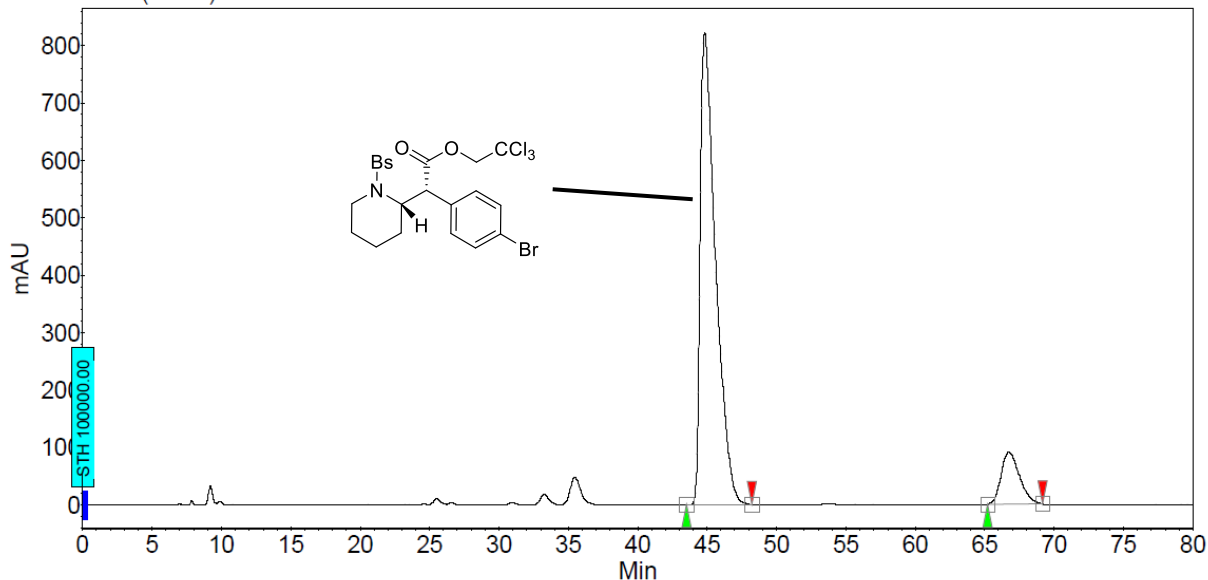


(Table 1, entry 9) (Table S2, entry 13)

WL-N9-93c-C2(f2232)-ADH-0.5-5%-230nm-80min-8.DATA - Prostar 325 Absorbance Channel 2 LC1006M831



Peak results :

Index	Name	Time [Min]	Quantity [% Area]	Height [mAU]	Area [mAU.Min]	Area % [%]
1	UNKNOWN	44.82	88.40	822.6	1054.3	88.399
2	UNKNOWN	66.73	11.60	90.8	138.4	11.601
Total			100.00	913.4	1192.7	100.000

→ 77% ee

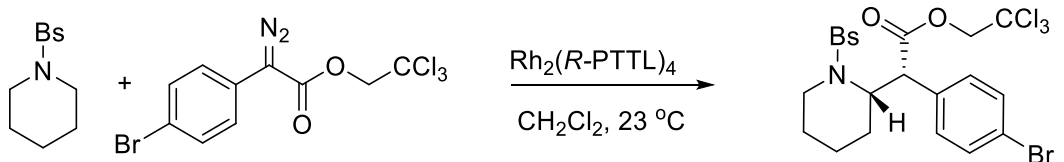
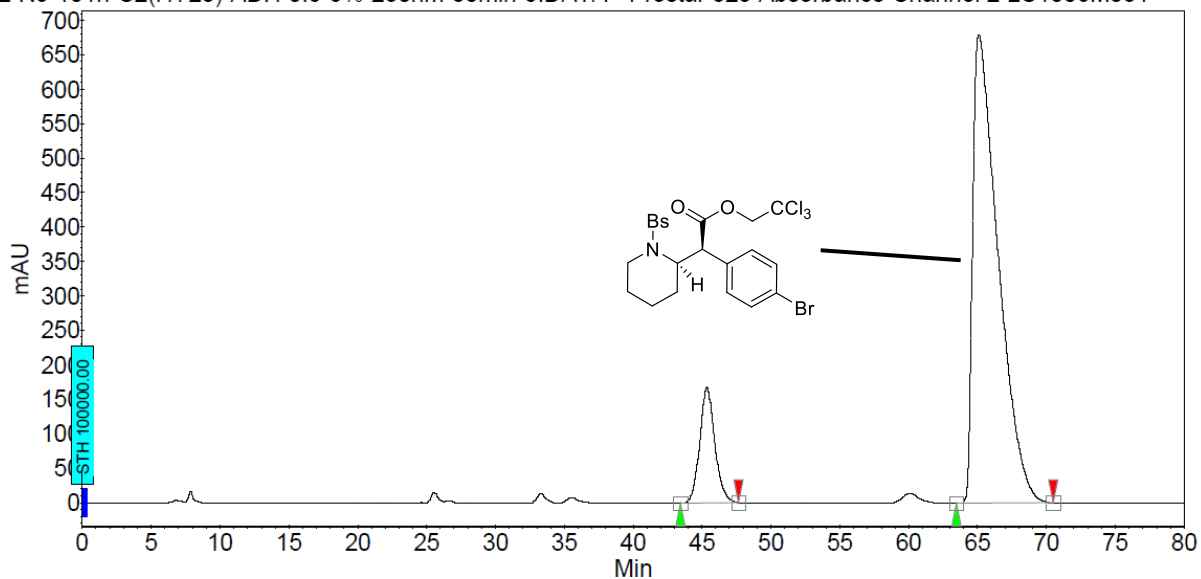


(Table S2, entry 14)

WL-N9-101h-C2(f1728)-ADH-0.5-5%-230nm-80min-5.DATA - Prostar 325 Absorbance Channel 2 LC1006M831



Peak results :

Index	Name	Time [Min]	Quantity (% Area)	Height [mAU]	Area [mAU.Min]	Area % [%]
1	UNKNOWN	45.34	12.78	167.7	212.3	12.780
2	UNKNOWN	65.10	87.22	679.5	1448.6	87.220
Total			100.00	847.3	1660.9	100.000

→ -74% ee

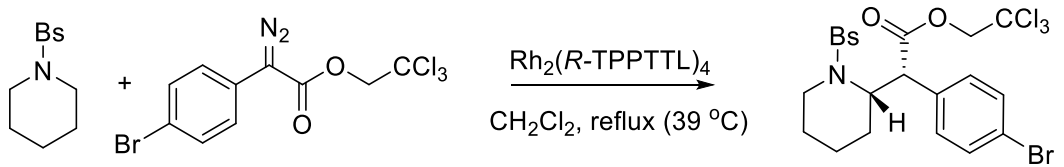
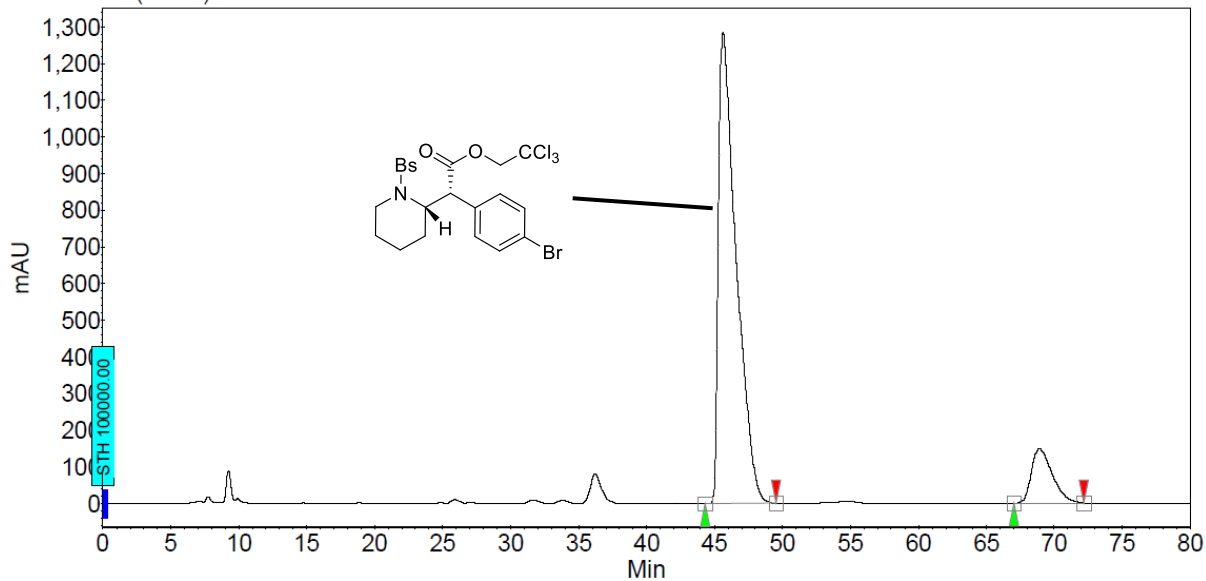


(Table 1, entry 10) (Table S2, entry 15)

WL-N9-149-C2(f1733)-ADH-0.5-5%-230nm-80min-24.DATA - Prostar 325 Absorbance Channel 2 LC1006M831



Peak results :

Index	Name	Time [Min]	Quantity % Area	Height [mAU]	Area [mAU.Min]	Area % [%]
1	UNKNOWN	45.62	88.17	1284.5	1947.8	88.166
2	UNKNOWN	68.90	11.83	148.4	261.4	11.834
Total			100.00	1432.9	2209.2	100.000

→ 76% ee

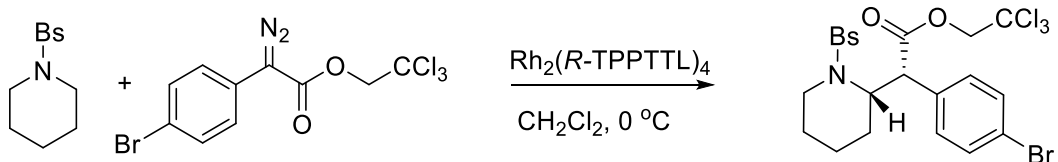
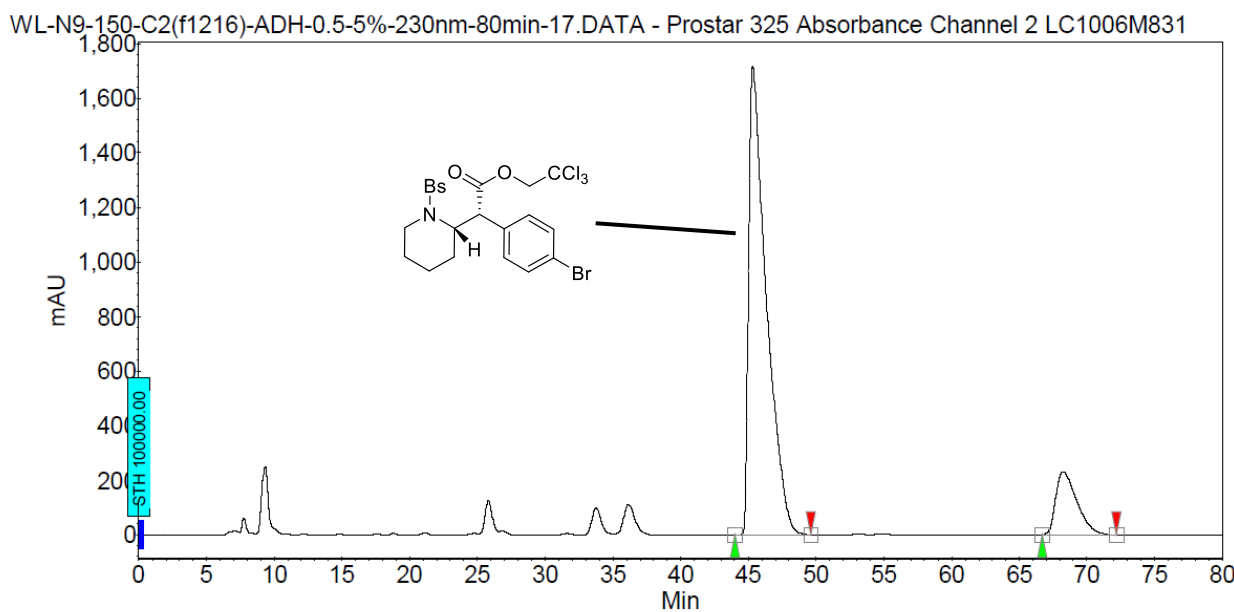


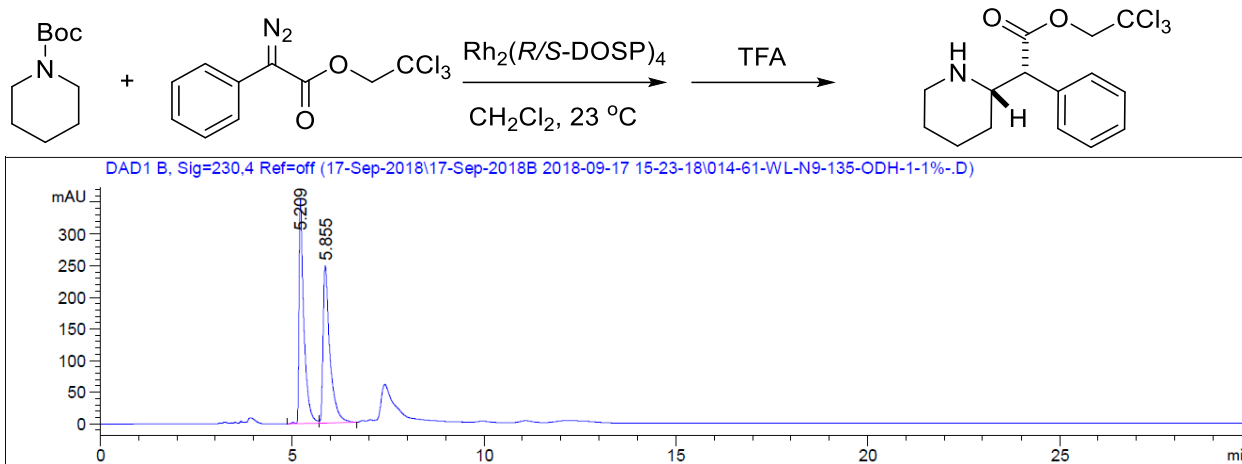
(Table 1, entry 11) (Table S2, entry 16)



Peak results :

Index	Name	Time [Min]	Quantity [% Area]	Height [mAU]	Area [mAU.Min]	Area % [%]
1	UNKNOWN	45.34	86.17	1716.9	2585.7	86.172
2	UNKNOWN	68.25	13.83	230.4	414.9	13.828
Total			100.00	1947.3	3000.6	100.000

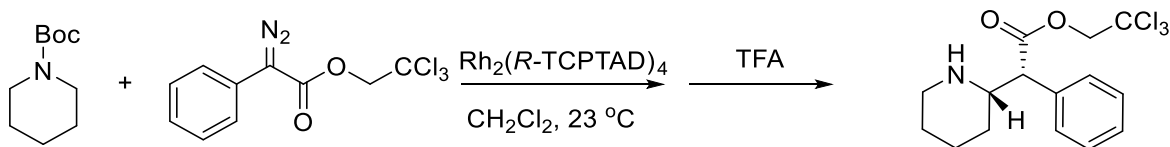
→ 72% ee



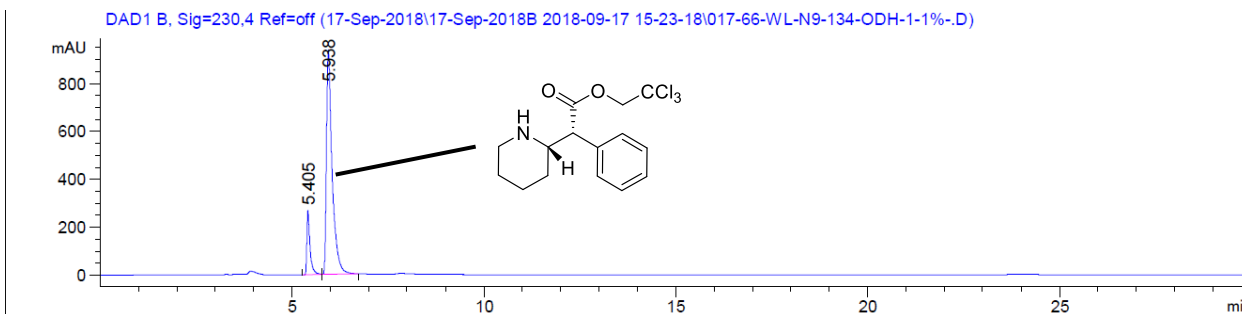
Signal 2: DAD1 B, Sig=230,4 Ref=off

Peak #	RetTime [min]	Type	Width [min]	Area [mAU*s]	Height [mAU]	Area %
1	5.209	VV R	0.1239	3096.28467	355.06827	50.2465
2	5.855	VB	0.1778	3065.90723	248.70621	49.7535

Racemic standard



(Scheme 2, 5b)

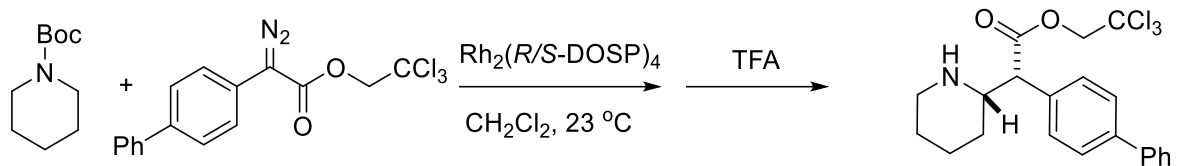


Signal 2: DAD1 B, Sig=230,4 Ref=off

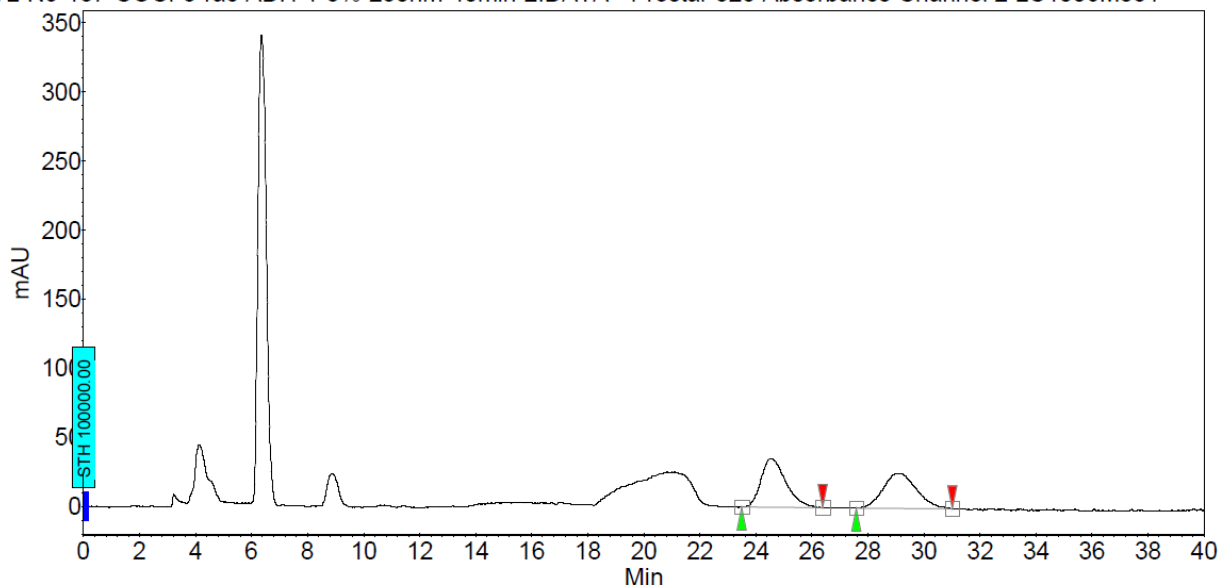
Peak #	RetTime [min]	Type	Width [min]	Area [mAU*s]	Height [mAU]	Area %
1	5.405	BV	0.0828	1545.78625	269.88885	13.6917
2	5.938	VB	0.1506	9744.19141	938.77661	86.3083

Totals : 1.12900e4 1208.66547

→ 73% ee



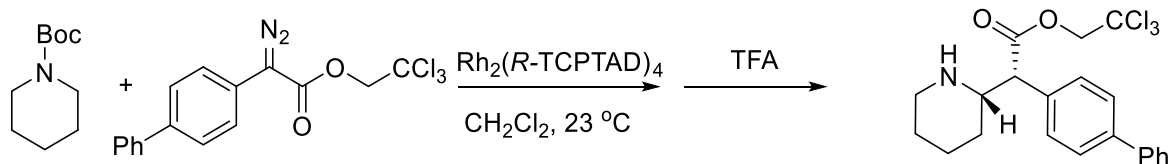
WL-N9-137-COCF3-rac-ADH-1-3%-230nm-40min-2.DATA - Prostar 325 Absorbance Channel 2 LC1006M831



Peak results :

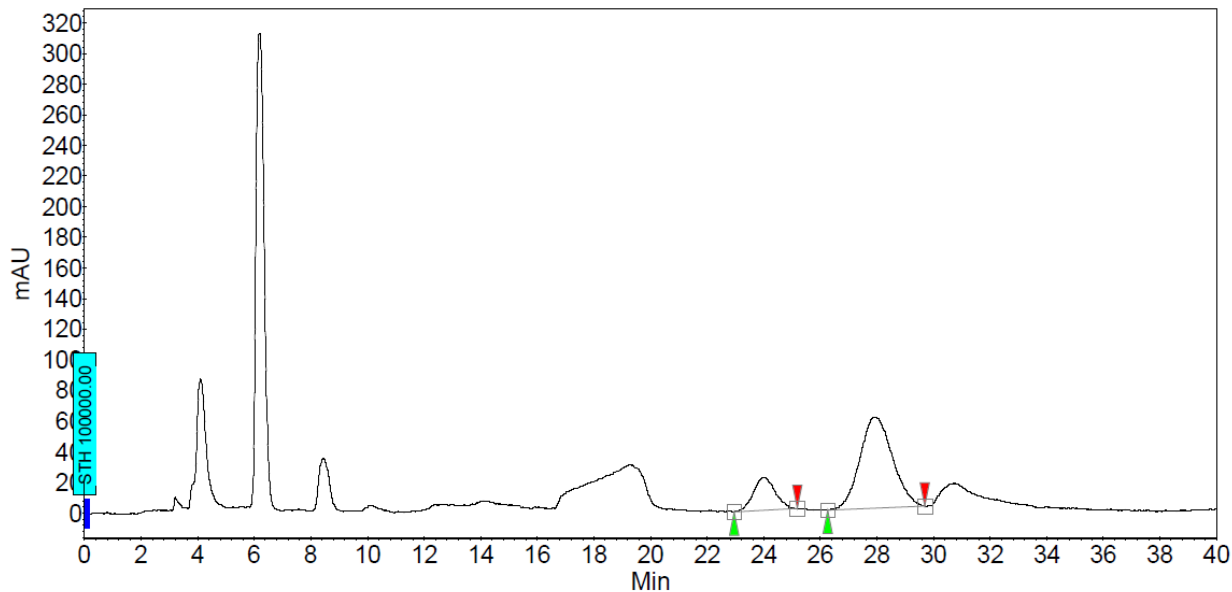
Index	Name	Time [Min]	Quantity [% Area]	Height [mAU]	Area [mAU.Min]	Area % [%]
1	UNKNOWN	24.54	50.97	35.4	36.2	50.967
2	UNKNOWN	29.05	49.03	25.4	34.8	49.033
Total			100.00	60.8	71.0	100.000

Racemic standard



(Scheme 2, **5c**)

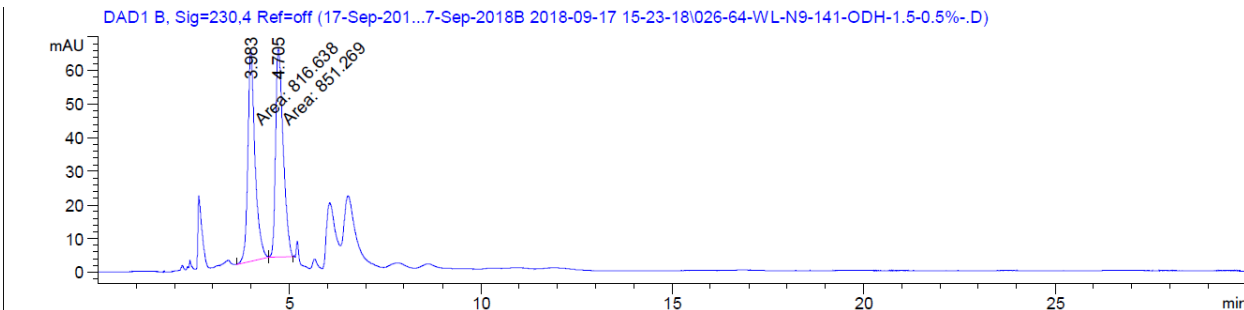
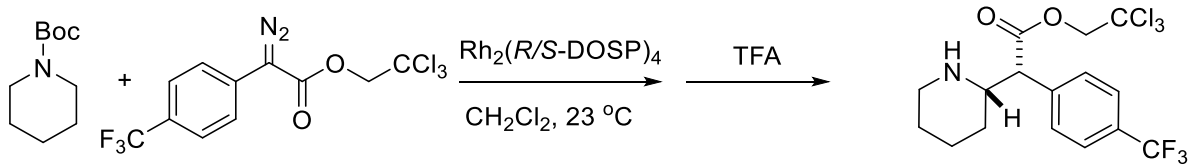
WL-N9-136-COCF3-ADH-1-3%-230nm-40min-5.DATA - Prostar 325 Absorbance Channel 2 LC1006M831



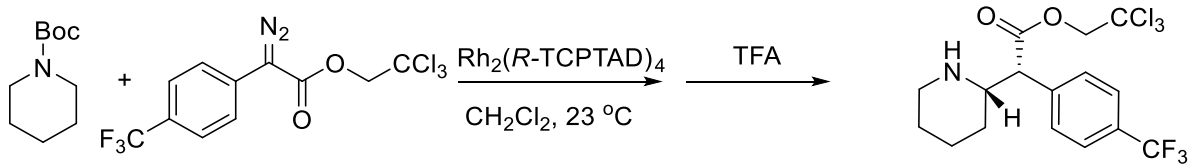
Peak results :

Index	Name	Time [Min]	Quantity [% Area]	Height [mAU]	Area [mAU.Min]	Area [%]
1	UNKNOWN	23.99	19.43	21.2	19.1	19.432
2	UNKNOWN	27.95	80.57	59.4	79.4	80.568
Total			100.00	80.6	98.5	100.000

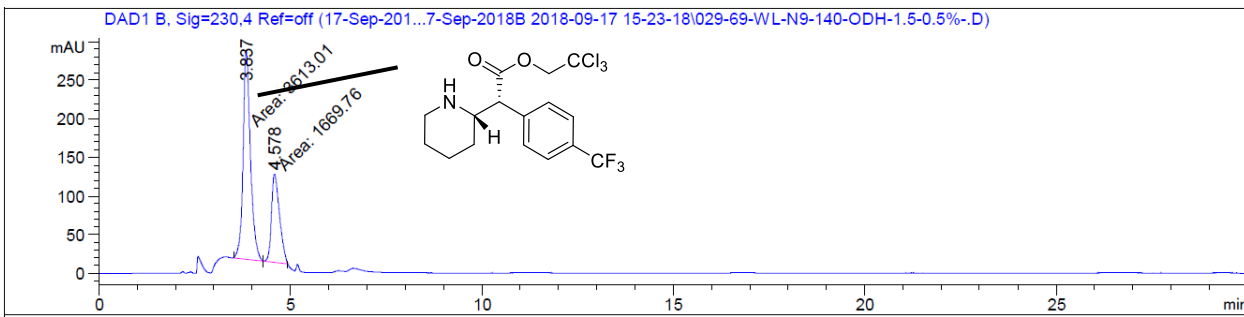
→ 61% ee



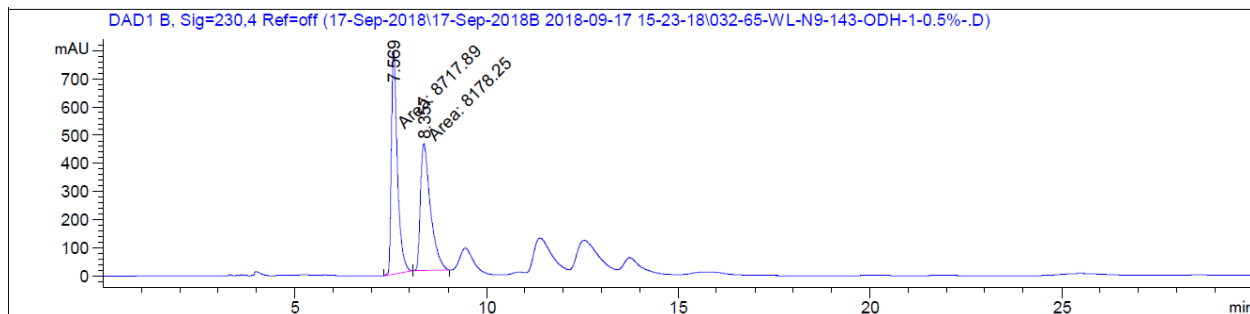
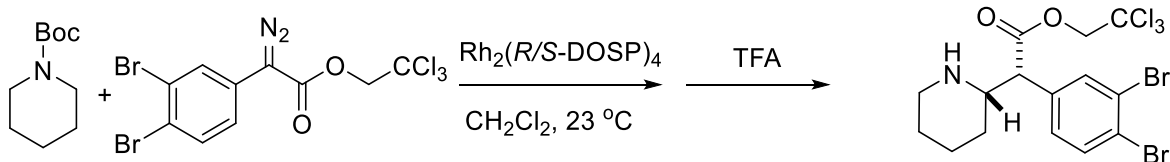
Racemic standard



(Scheme 2, 5d)



→ 37% ee

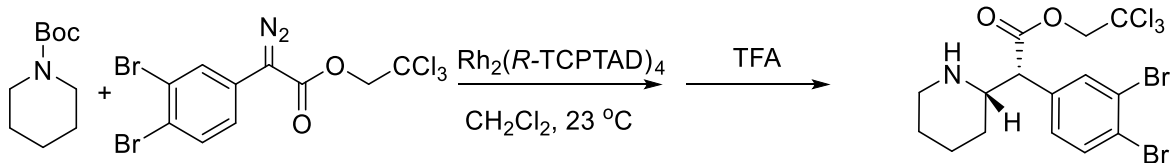


Signal 2: DAD1 B, Sig=230,4 Ref=off

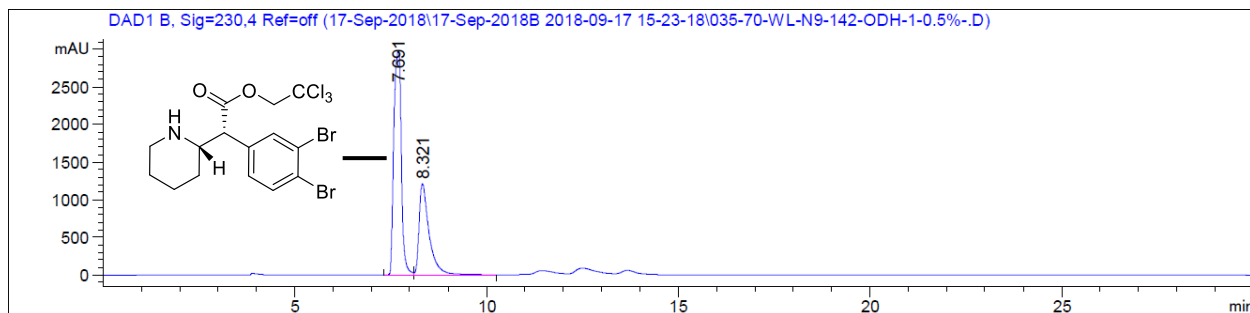
Peak #	RetTime [min]	Type	Width [min]	Area [mAU*s]	Height [mAU]	Area %
1	7.569	MM	0.1831	8717.88770	793.48718	51.5969
2	8.357	MM	0.3031	8178.25439	449.75534	48.4031

Totals : 1.68961e4 1243.24252

Racemic standard



(Scheme 2, 5e)

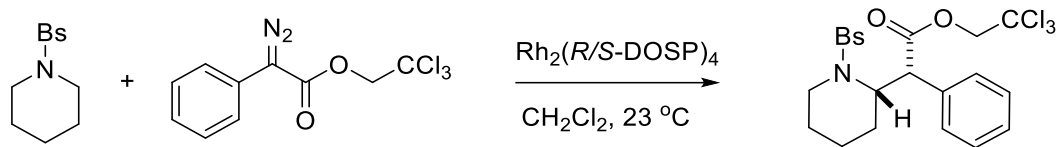


Signal 2: DAD1 B, Sig=230,4 Ref=off

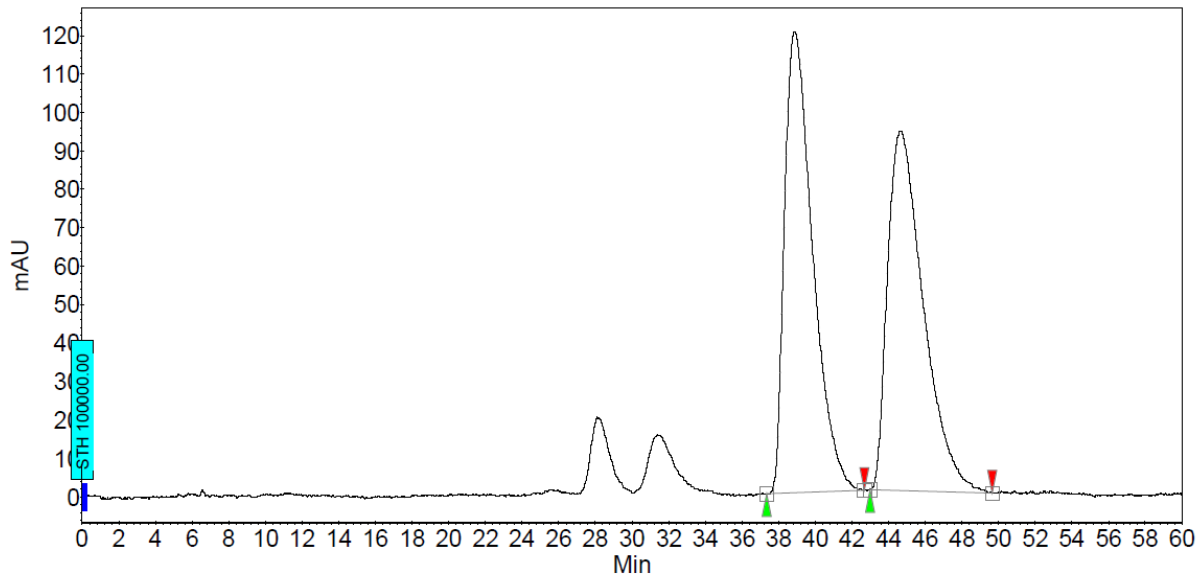
Peak #	RetTime [min]	Type	Width [min]	Area [mAU*s]	Height [mAU]	Area %
1	7.691	BV	0.1630	4.04701e4	2978.64307	64.6349
2	8.321	VB	0.2655	2.21433e4	1212.97864	35.3651

Totals : 6.26134e4 4191.62170

→ 29% ee



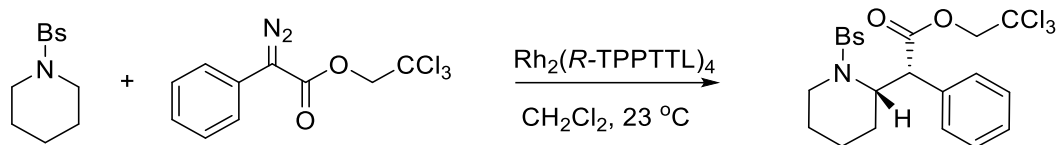
WL-ELN-0009-10H-C2-ODH-0.6-2%-230nm-60min-65.DATA - Prostar 325 Absorbance Channel 2 LC1006M831



Peak results :

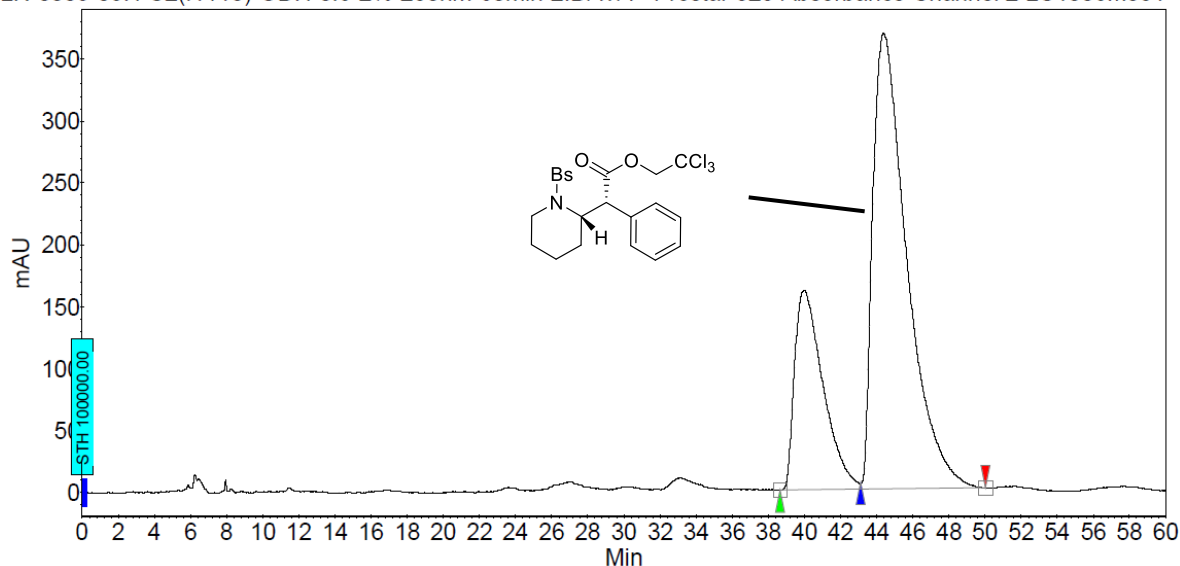
Index	Name	Time [Min]	Quantity [% Area]	Height [mAU]	Area [mAU.Min]	Area [%]
1	UNKNOWN	38.87	50.27	119.9	213.6	50.267
2	UNKNOWN	44.65	49.73	93.5	211.3	49.733
Total			100.00	213.3	424.9	100.000

Racemic standard



(Scheme 2, 6b)

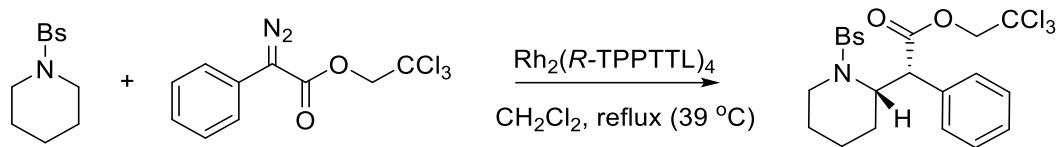
WL-ELN-0009-09H-C2(f1118)-ODH-0.6-2%-230nm-60min-2.DATA - Prostar 325 Absorbance Channel 2 LC1006M831



Peak results :

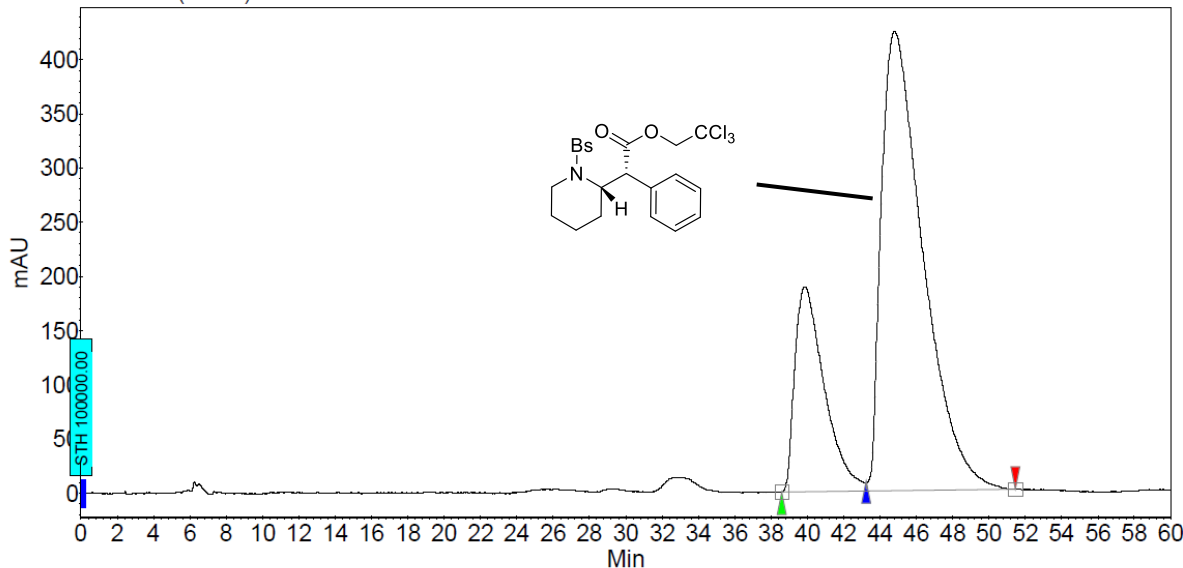
Index	Name	Time [Min]	Quantity [% Area]	Height [mAU]	Area [mAU.Min]	Area % [%]
1	UNKNOWN	39.97	26.79	161.3	294.8	26.792
2	UNKNOWN	44.38	73.21	368.4	805.4	73.208
Total			100.00	529.7	1100.2	100.000

→ 46% ee



(Scheme 2, **6b**)

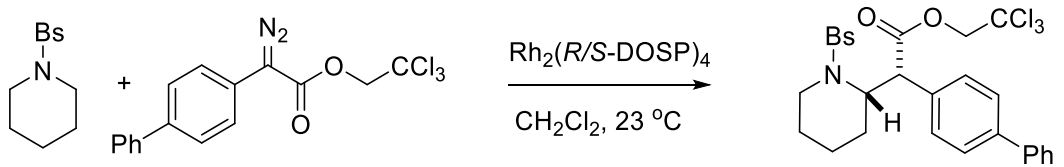
WL-ELN-0009-21H-C2(f3032)-ODH-0.6-2%-230nm-60min-5.DATA - Prostar 325 Absorbance Channel 2 LC1006M831



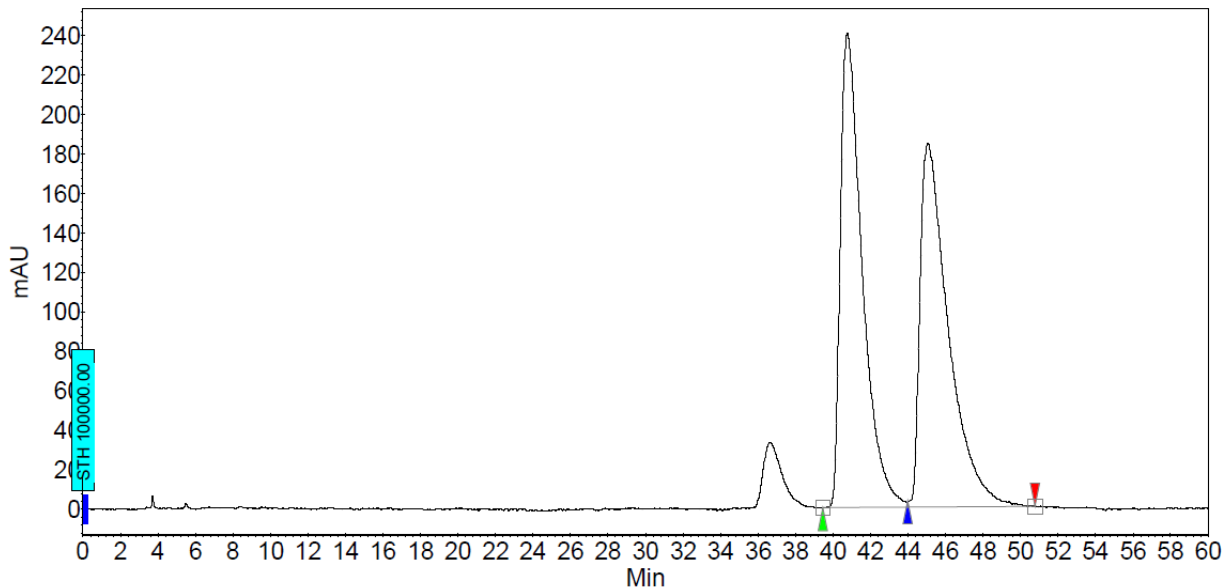
Peak results :

Index	Name	Time [Min]	Quantity [% Area]	Height [mAU]	Area [mAU.Min]	Area [%] [%]
1	UNKNOWN	39.84	24.03	189.2	356.3	24.030
2	UNKNOWN	44.79	75.97	423.9	1126.5	75.970
Total			100.00	613.1	1482.9	100.000

→ 52% ee



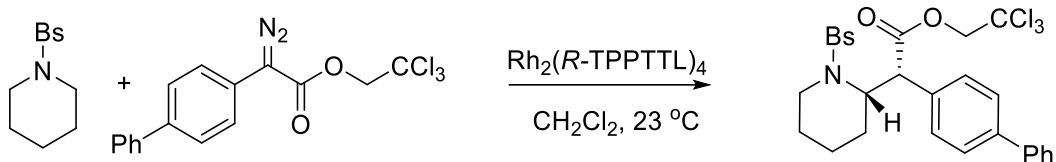
WL-ELN-0009-12Ph-rac-1-10%-230nm-60min-80.DATA - Prostar 325 Absorbance Channel 2 LC1006M831



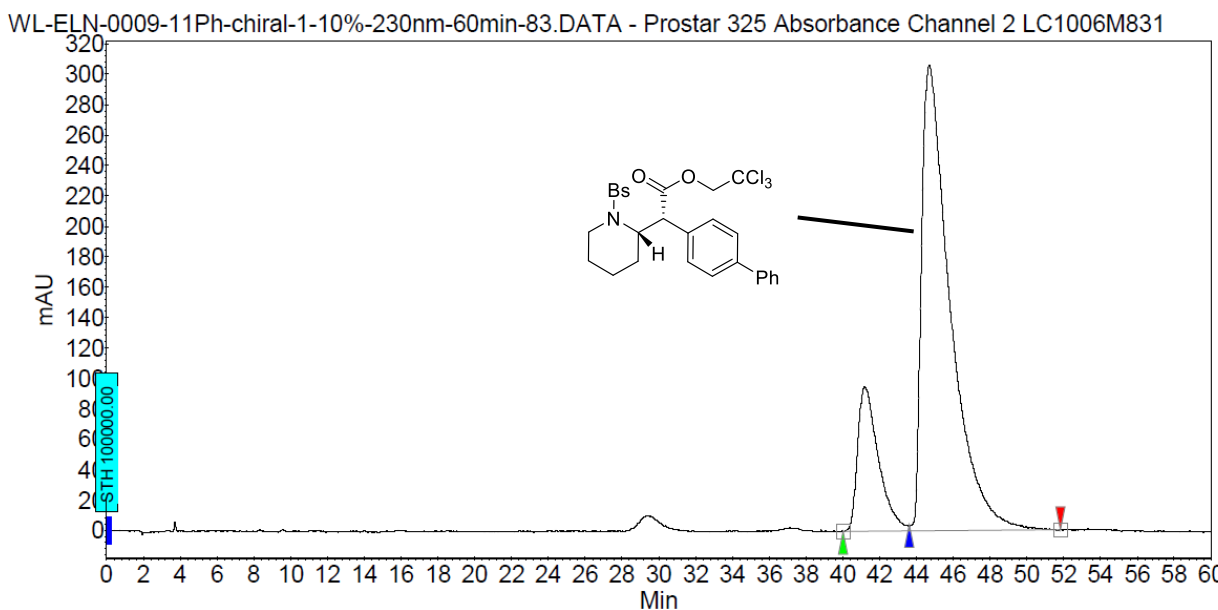
Peak results :

Index	Name	Time [Min]	Quantity [% Area]	Height [mAU]	Area [mAU.Min]	Area % [%]
1	UNKNOWN	40.75	50.12	240.8	325.1	50.124
2	UNKNOWN	45.05	49.88	184.7	323.5	49.876
Total			100.00	425.5	648.5	100.000

Racemic Standard



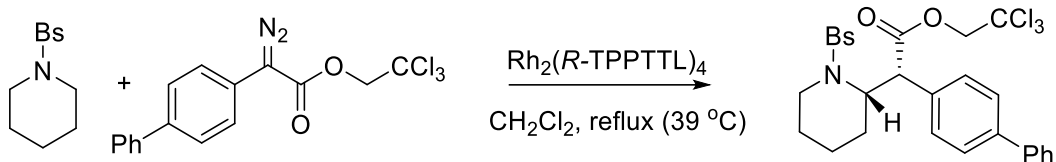
(Scheme 2, **6c**)



Peak results :

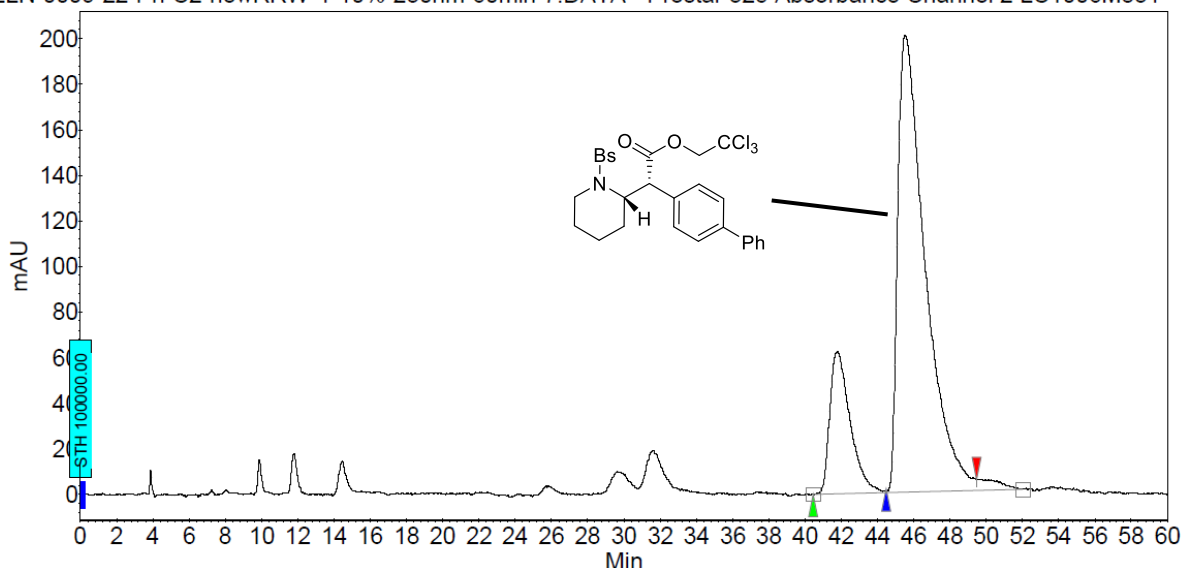
Index	Name	Time [Min]	Quantity [% Area]	Height [mAU]	Area [mAU.Min]	Area % [%]
1	UNKNOWN	41.19	18.37	94.8	124.2	18.365
2	UNKNOWN	44.69	81.63	306.2	552.2	81.635
Total			100.00	401.0	676.4	100.000

→ 63% ee



(Scheme 2, **6c**)

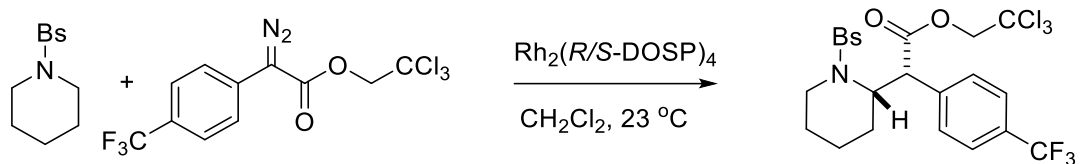
WL-ELN-0009-22-Ph-C2-newRRW-1-10%-230nm-60min-7.DATA - Prostar 325 Absorbance Channel 2 LC1006M831



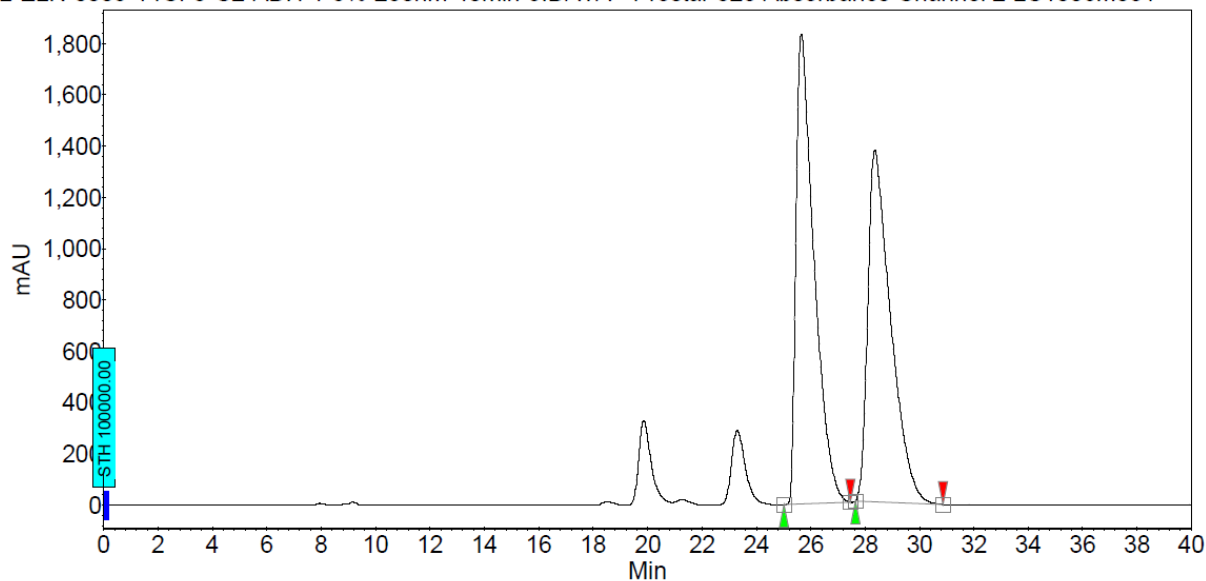
Peak results :

Index	Name	Time [Min]	Quantity [% Area]	Height [mAU]	Area [mAU.Min]	Area [%]
1	UNKNOWN	41.77	18.86	62.5	81.9	18.861
2	UNKNOWN	45.52	81.14	200.5	352.1	81.139
Total			100.00	263.0	434.0	100.000

→ 62% ee



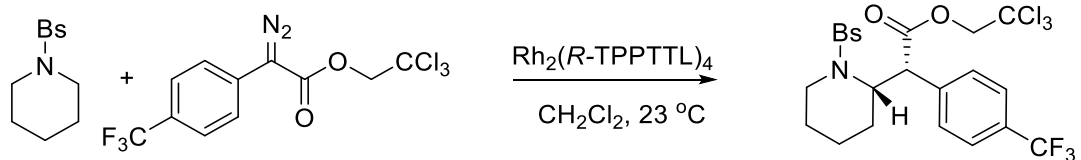
WL-ELN-0009-14CF3-C2-ADH-1-5%-230nm-40min-9.DATA - Prostar 325 Absorbance Channel 2 LC1006M831



Peak results :

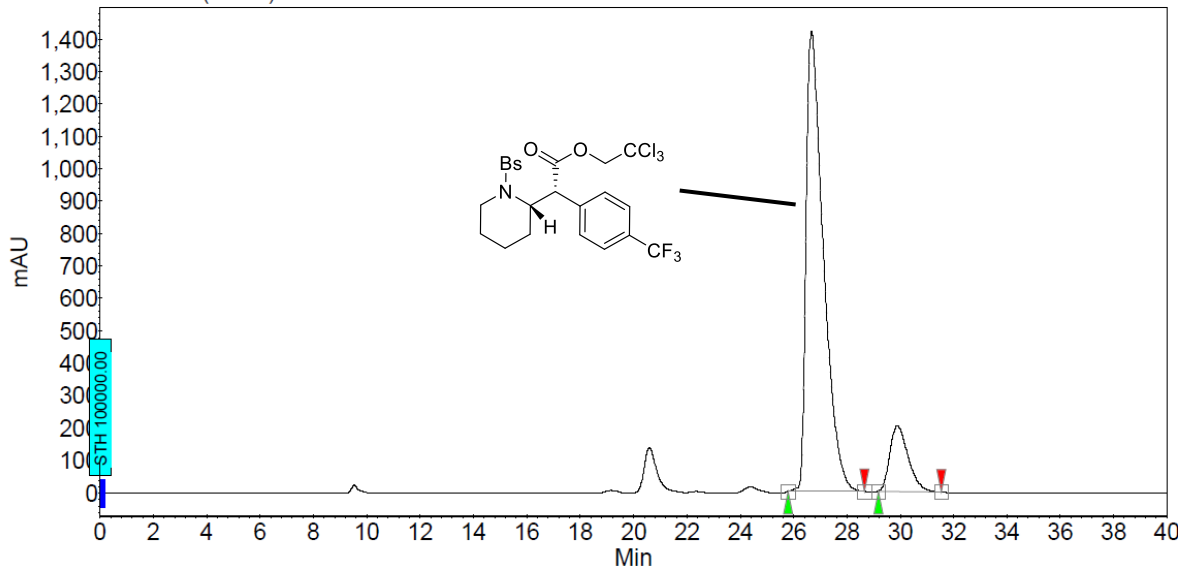
Index	Name	Time [Min]	Quantity [% Area]	Height [mAU]	Area [mAU.Min]	Area [%]
1	UNKNOWN	25.66	51.41	1833.7	1411.2	51.406
2	UNKNOWN	28.36	48.59	1373.8	1334.0	48.594
Total			100.00	3207.4	2745.1	100.000

Racemic standard



(Scheme 2, **6d**)

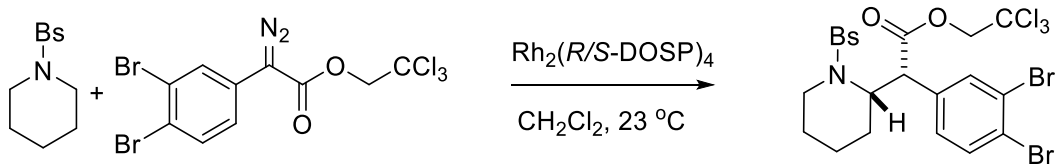
WL-ELN-0009-13CF3-C2(f0713)-ADH-1-5%-230nm-40min-6.DATA - Prostar 325 Absorbance Channel 2 LC1006M831



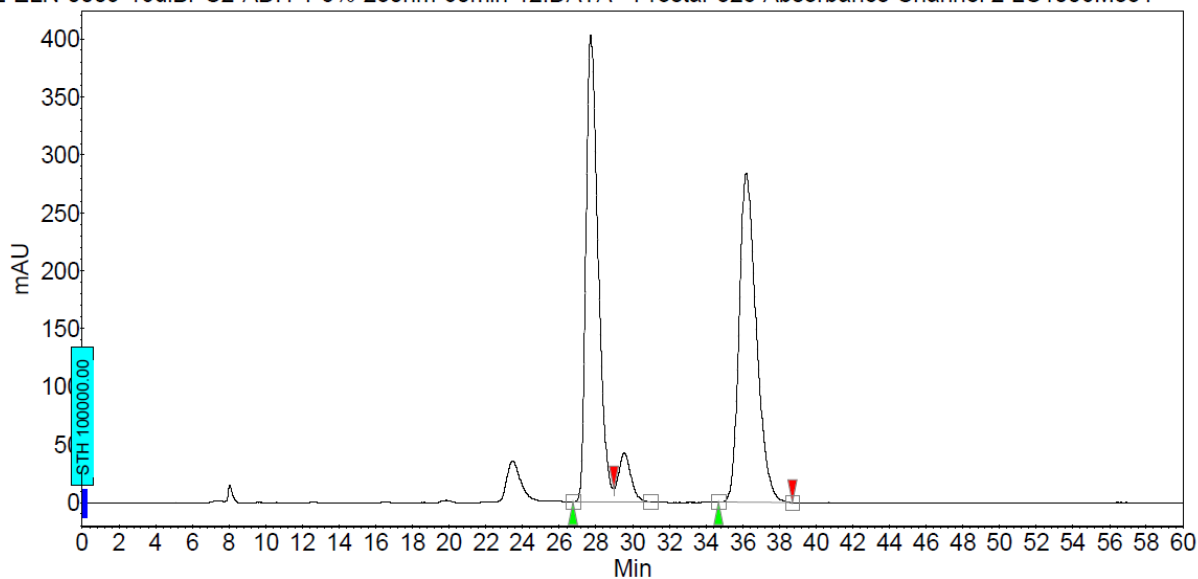
Peak results :

Index	Name	Time [Min]	Quantity [% Area]	Height [mAU]	Area [mAU.Min]	Area % [%]
1	UNKNOWN	26.67	86.83	1421.3	1069.7	86.831
2	UNKNOWN	29.89	13.17	202.9	162.2	13.169
Total			100.00	1624.1	1232.0	100.000

→ 74% ee



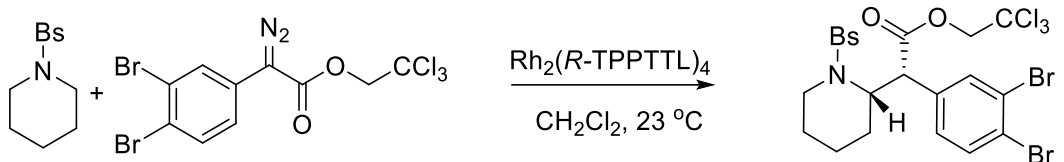
WL-ELN-0009-16diBr-C2-ADH-1-5%-230nm-60min-12.DATA - Prostar 325 Absorbance Channel 2 LC1006M831



Peak results :

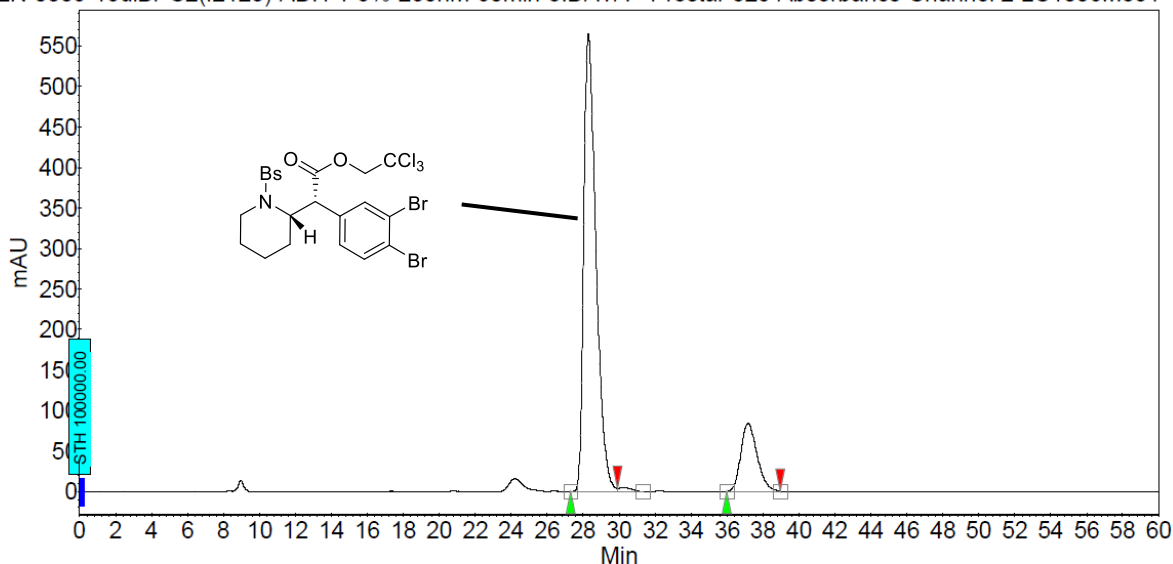
Index	Name	Time [Min]	Quantity [% Area]	Height [mAU]	Area [mAU.Min]	Area % [%]
1	UNKNOWN	27.72	50.09	402.7	309.3	50.086
2	UNKNOWN	36.19	49.91	283.9	308.3	49.914
Total			100.00	686.6	617.6	100.000

Racemic standard



(Scheme 2, **6e**)

WL-ELN-0009-15diBr-C2(f2128)-ADH-1-5%-230nm-60min-3.DATA - Prostar 325 Absorbance Channel 2 LC1006M831

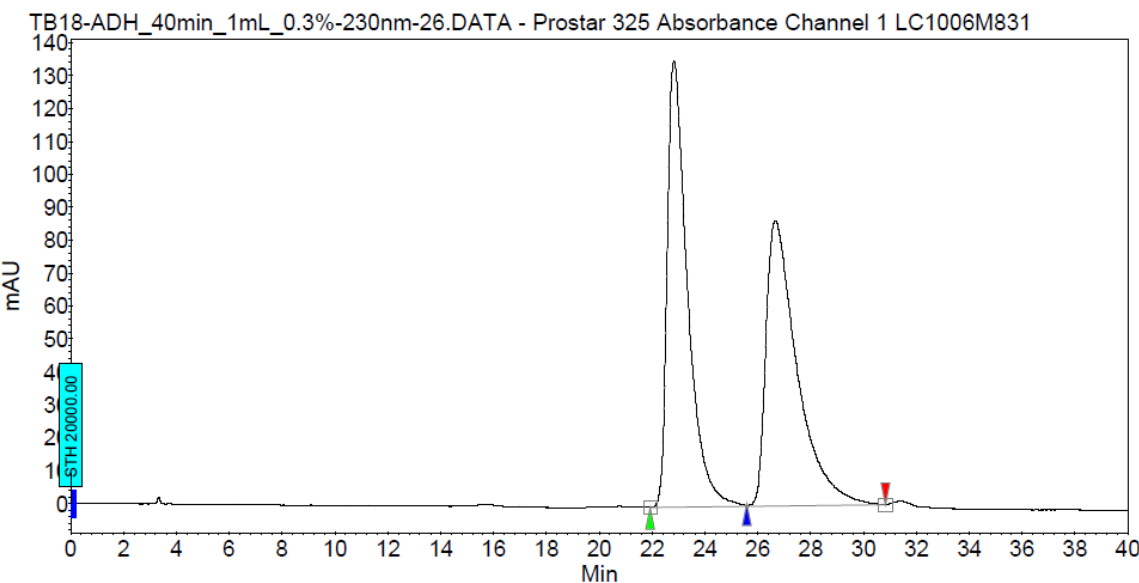
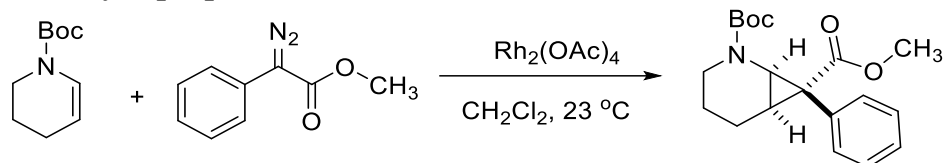


Peak results :

Index	Name	Time [Min]	Quantity [% Area]	Height [mAU]	Area [mAU.Min]	Area [%]
1	UNKNOWN	28.28	83.59	564.9	446.8	83.588
2	UNKNOWN	37.17	16.41	83.9	87.7	16.412
Total			100.00	648.9	534.5	100.000

→ 67% ee

10.2. Cyclopropanation and C3 Functionalization Products



Racemic standard

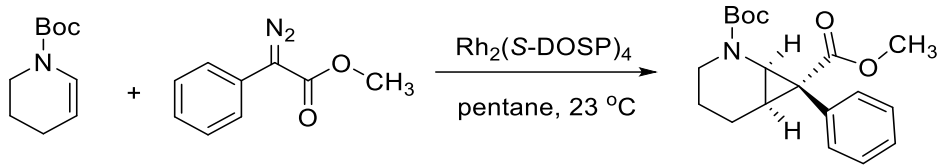
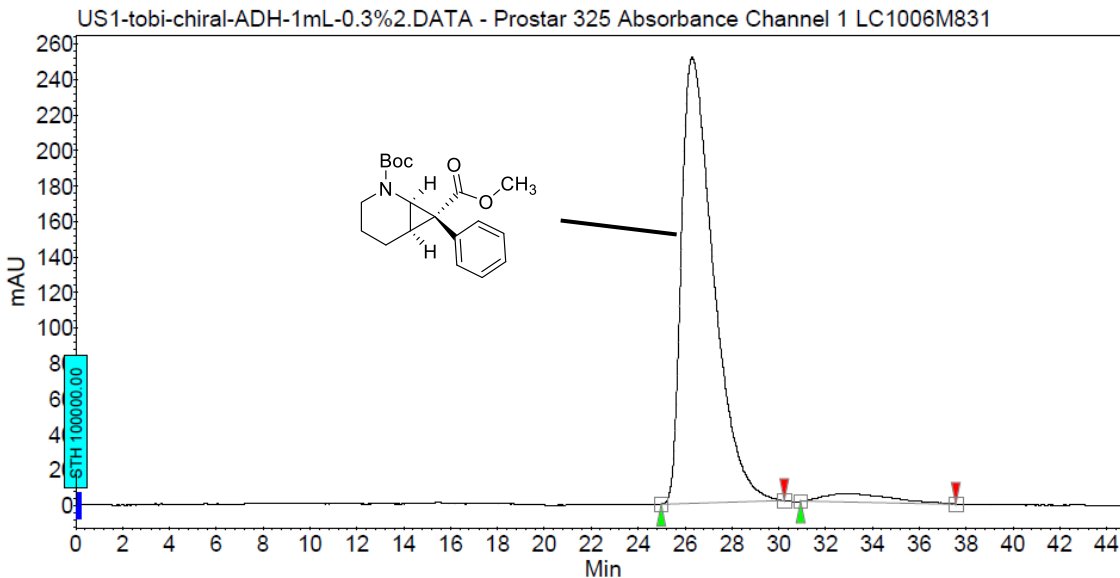


(Table 2, entry 5) (Table S3, entry 1)



→ 92% ee

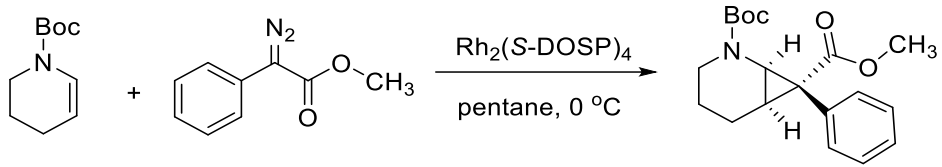
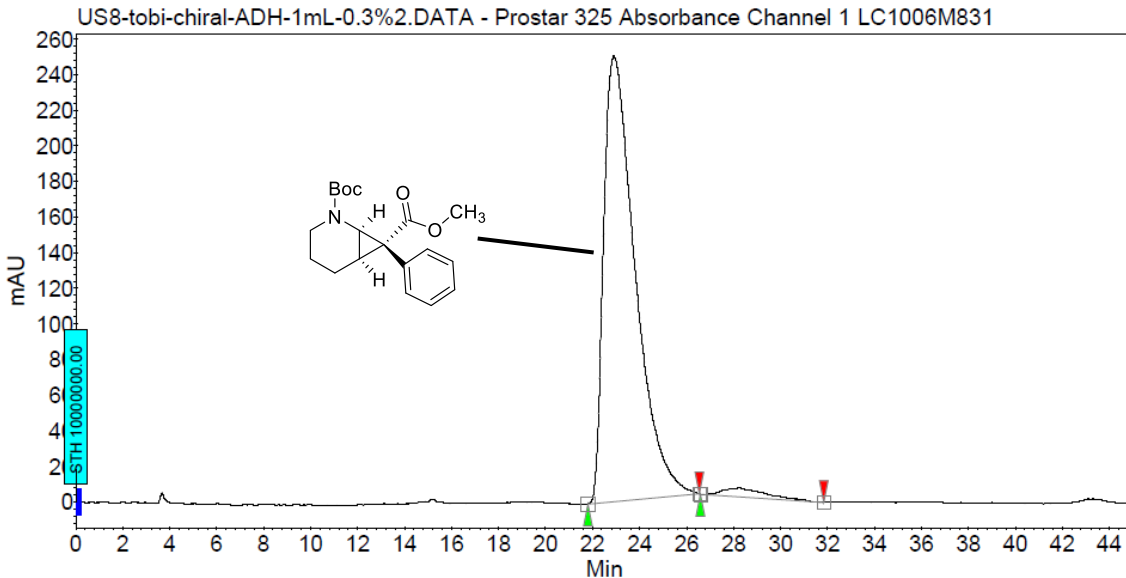


(Table 2, entry 6) (Table S3, entry 2)



Peak results :

Index	Name	Time [Min]	Quantity [% Area]	Height [mAU]	Area [mAU.Min]	Area % [%]
1	UNKNOWN	22.90	97.37	250.2	389.4	97.371
2	UNKNOWN	28.27	2.63	4.9	10.5	2.629
Total			100.00	255.1	399.9	100.000

→ 95% ee

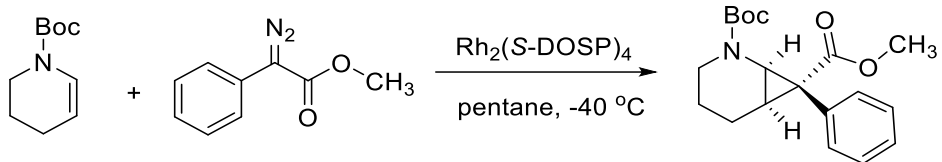
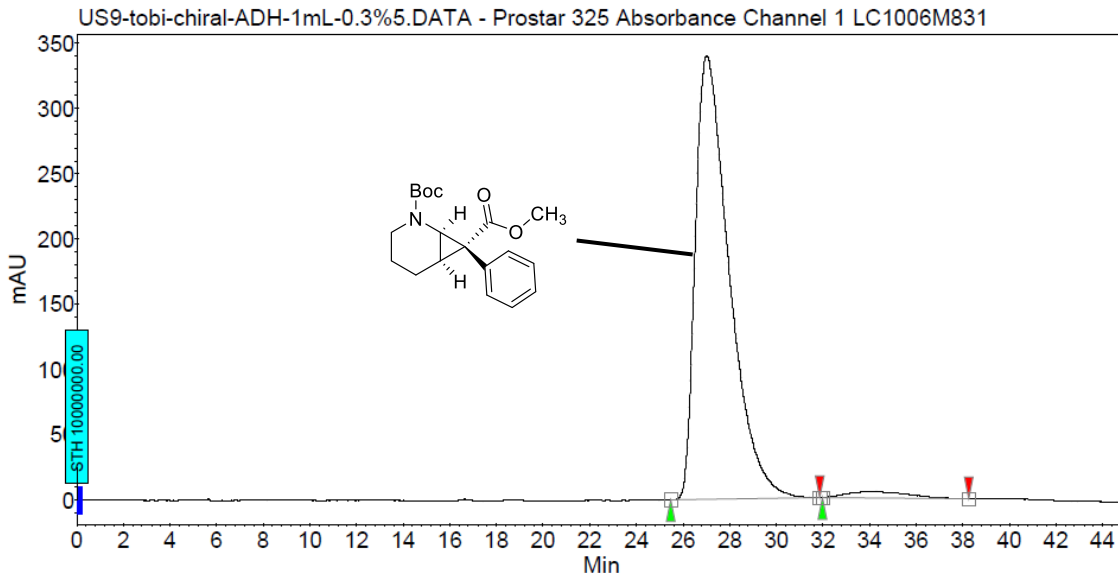


(Table 2, entry 7) (Table S3, entry 3)



Peak results :

Index	Name	Time [Min]	Quantity [% Area]	Height [mAU]	Area [mAU·Min]	Area [%]
1	UNKNOWN	27.02	97.49	339.1	571.7	97.485
2	UNKNOWN	34.38	2.51	5.0	14.7	2.515
Total			100.00	344.1	586.4	100.000

→ 95% ee

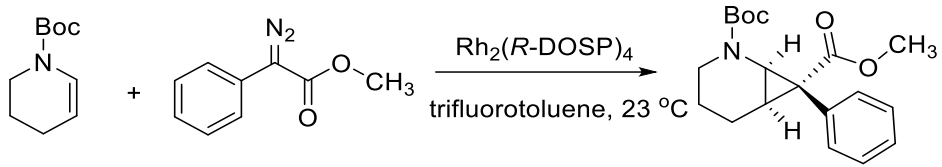
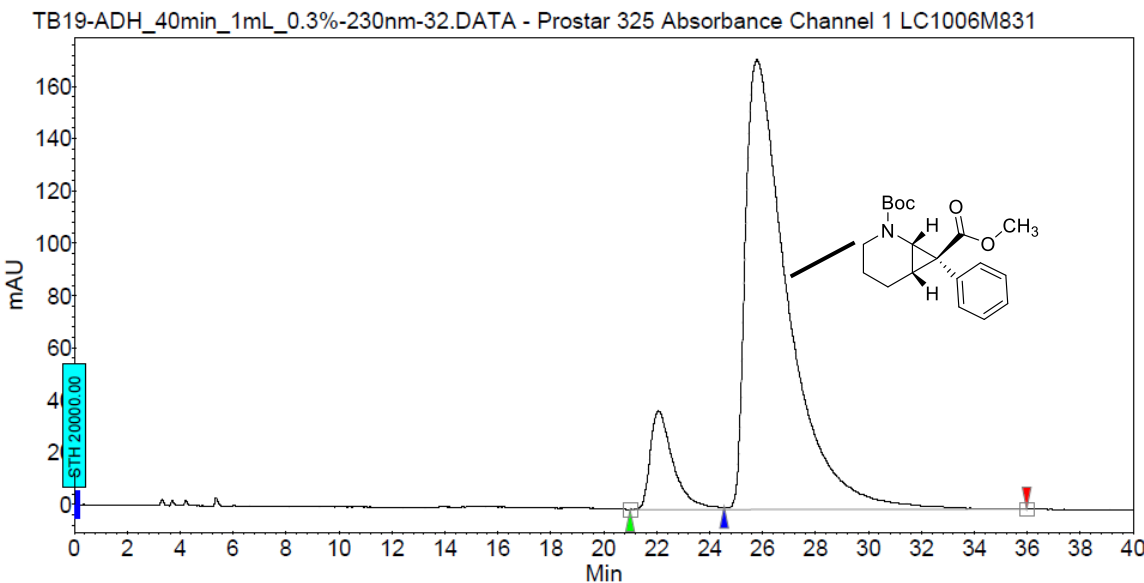


(Table S3, entry 4)



Peak results :

Index	Name	Time [Min]	Quantity [% Area]	Height [mAU]		Area [%]
				Area	[mAU·Min]	
1	UNKNOWN	22.06	10.62	37.8	38.0	10.615
2	UNKNOWN	25.78	89.38	172.1	319.7	89.385
Total			100.00	209.9	357.6	100.000

→ -79% ee

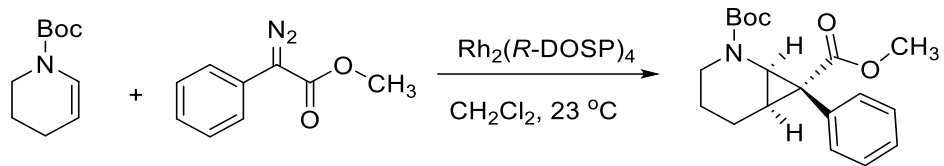
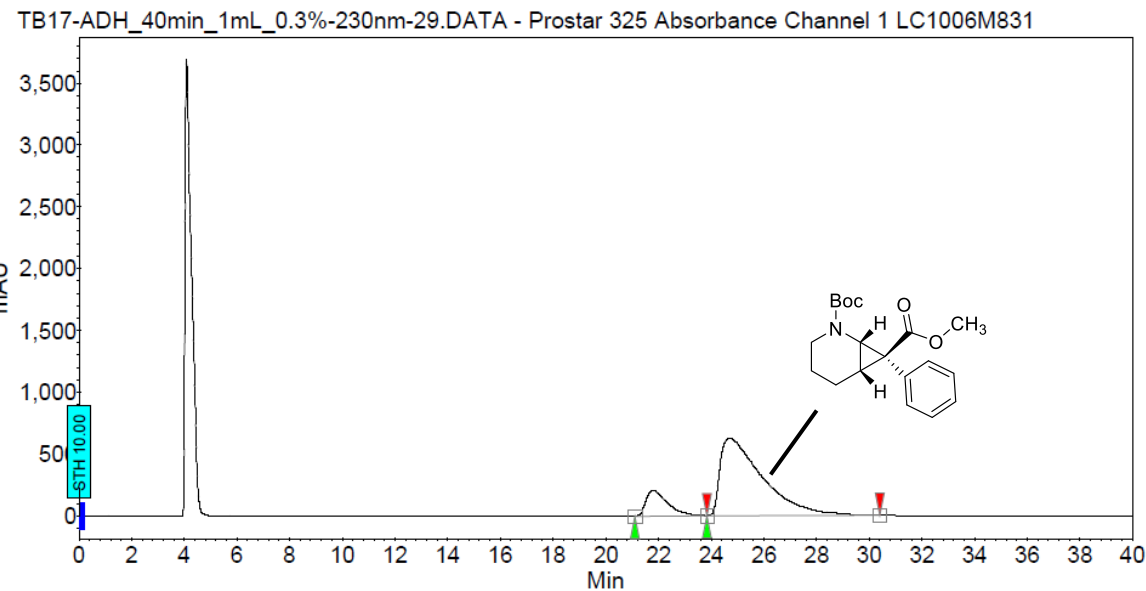


(Table S3, entry 5)



→ -71% ee

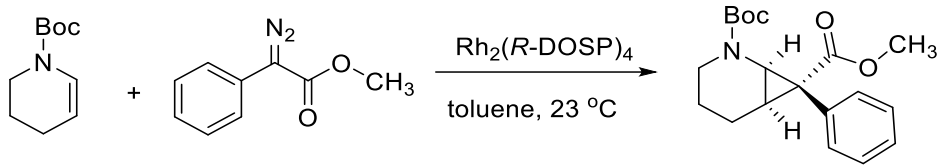
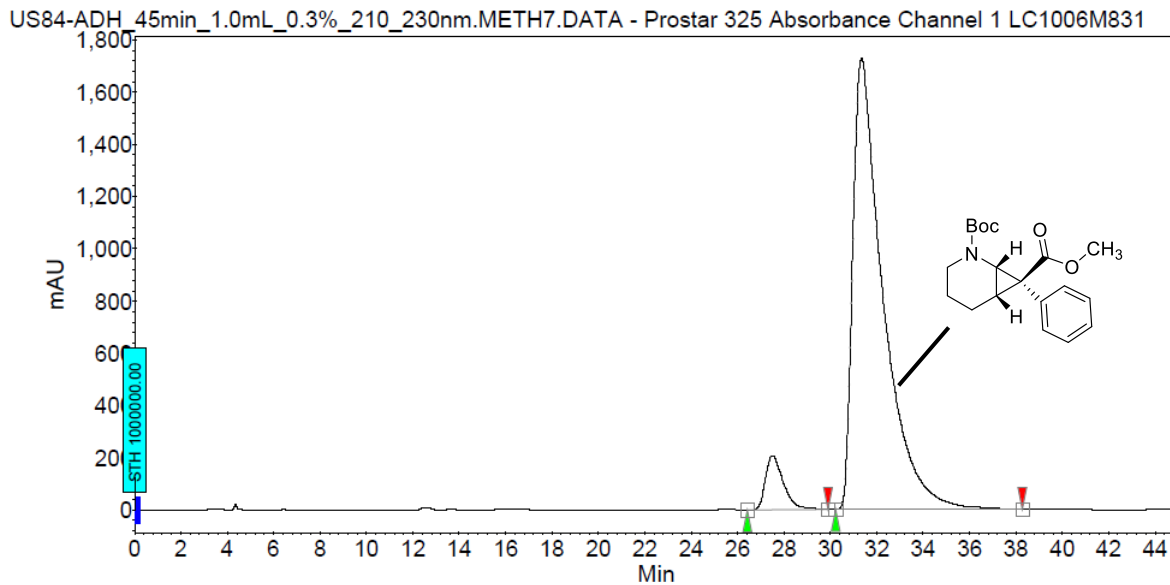


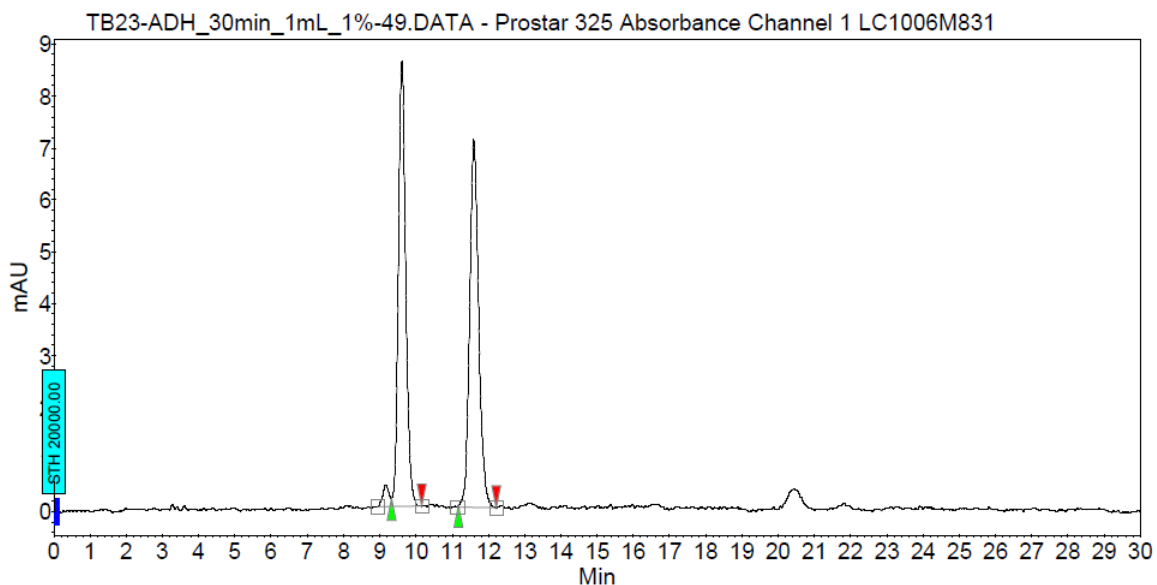
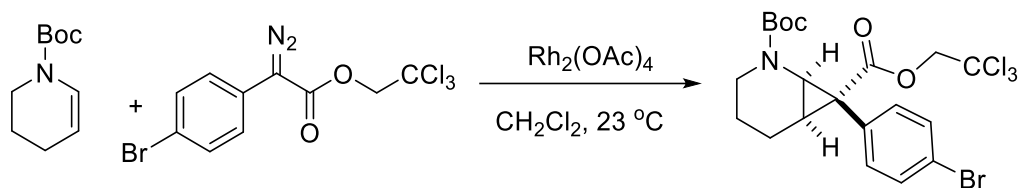
(Table S3, entry 6)



Peak results :

Index	Name	Time [Min]	Quantity [% Area]	Height [mAU]	Area [mAU.Min]	Area % [%]
1	UNKNOWN	27.50	6.62	207.3	185.0	6.619
2	UNKNOWN	31.35	93.38	1726.9	2609.5	93.381
Total			100.00	1934.2	2794.5	100.000

→ -87% ee



Racemic standard

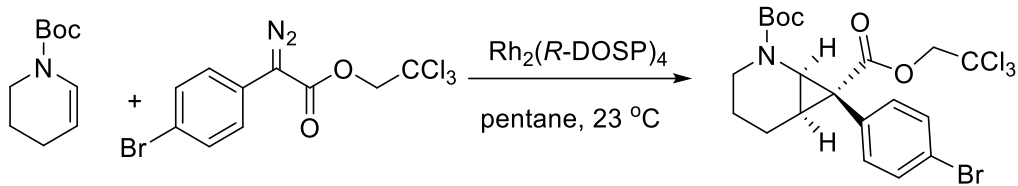
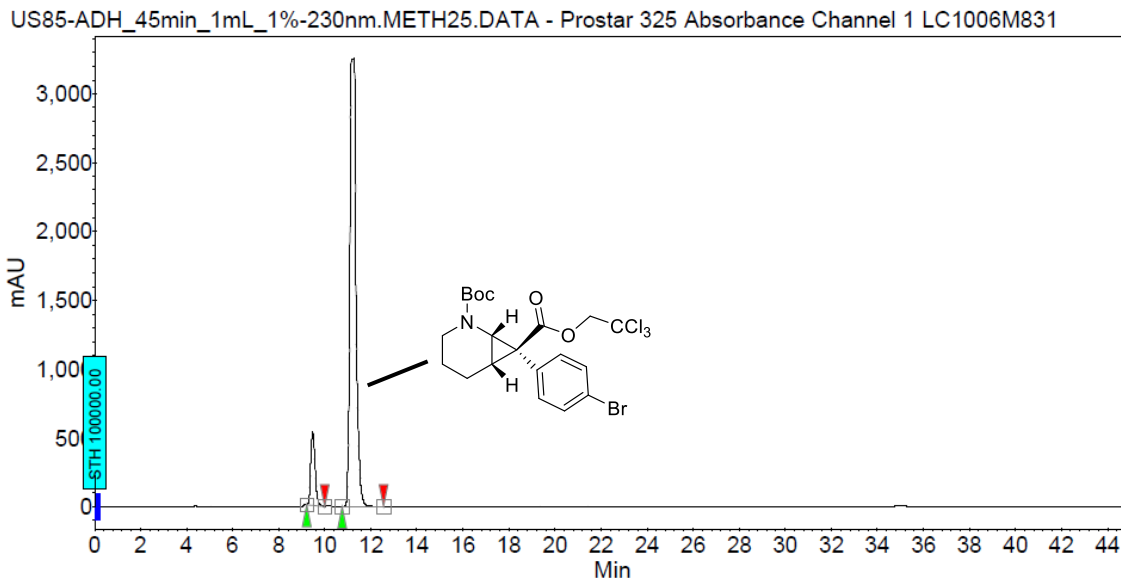
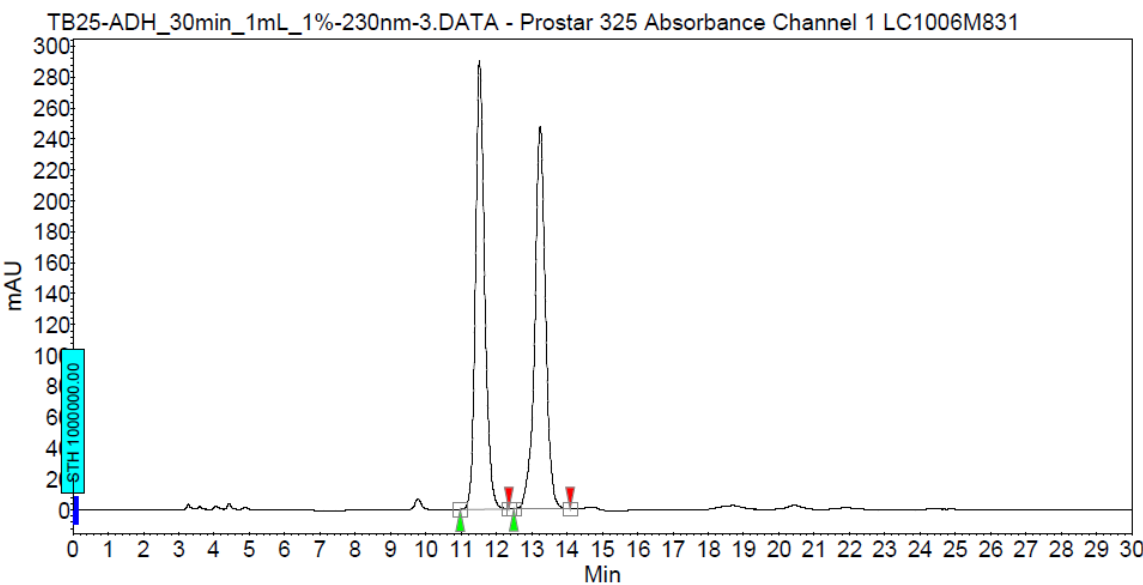
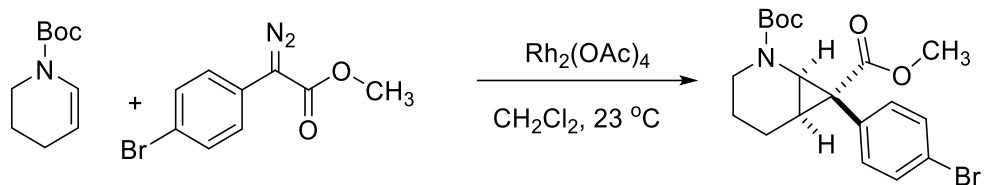


(Table S3, entry 7)



→ -80% ee



Peak results :

Index	Name	Time [Min]	Quantity [% Areal]	Height [mAU]	Area [mAU.Min]	Area % [%]
1	UNKNOWN	11.52	50.00	289.7	87.5	50.001
2	UNKNOWN	13.23	50.00	247.5	87.5	49.999
Total			100.00	537.2	175.0	100.000

Racemic standard

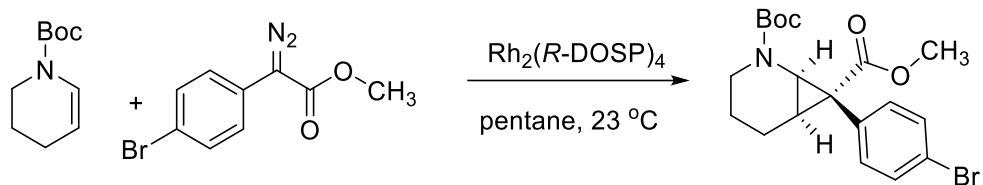
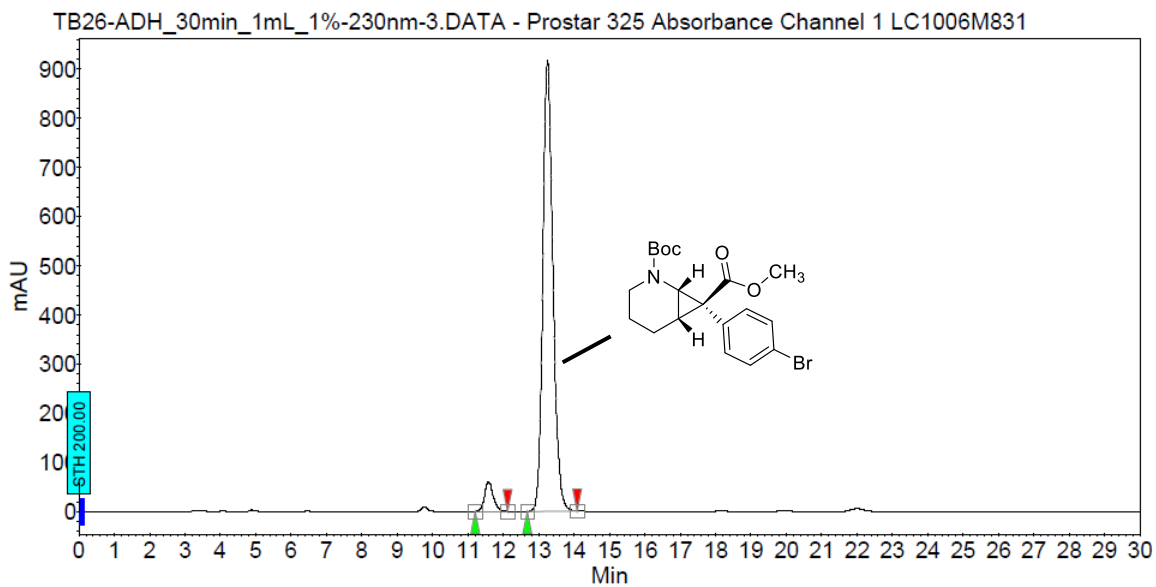


(Table 2, entry 4) (Table S3, entry 8)



Peak results :

Index	Name	Time [Min]	Quantity [% Area]	Height [mAU]	Area [mAU.Min]	Area % [%]
1	UNKNOWN	11.58	5.30	59.9	17.0	5.305
2	UNKNOWN	13.24	94.70	916.1	303.9	94.695
Total			100.00	975.9	320.9	100.000

→ -89% ee

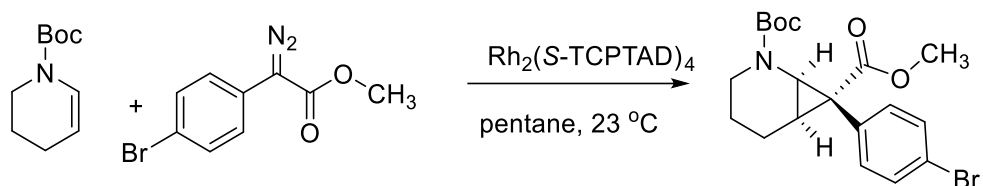
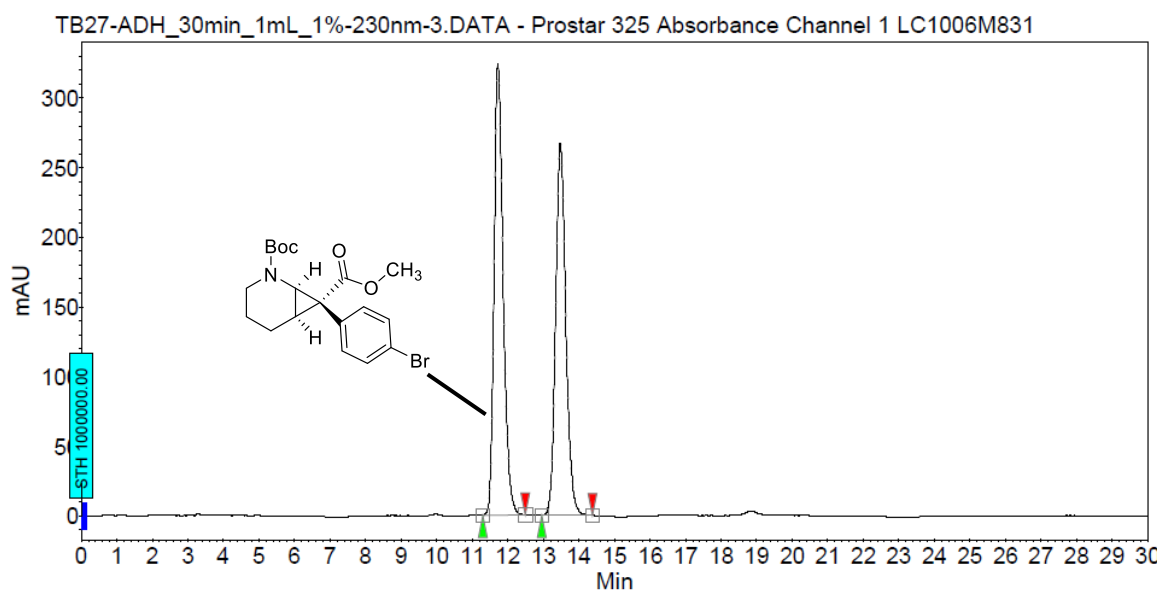


(Table 2, entry 1) (Table S3, entry 9)



Peak results :

Index	Name	Time [Min]	Quantity [% Area]	Height [mAU]	Area [mAU.Min]	Area % [%]
1	UNKNOWN	11.72	51.70	323.6	95.5	51.697
2	UNKNOWN	13.48	48.30	267.0	89.2	48.303
Total			100.00	590.6	184.7	100.000

→ 3% ee

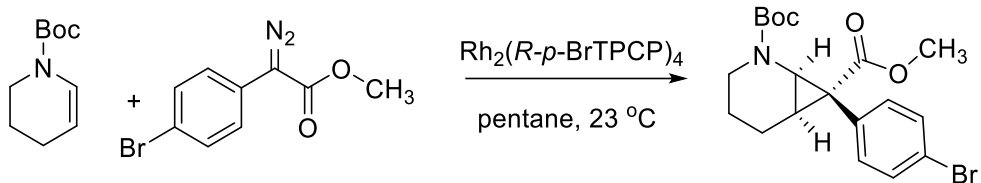
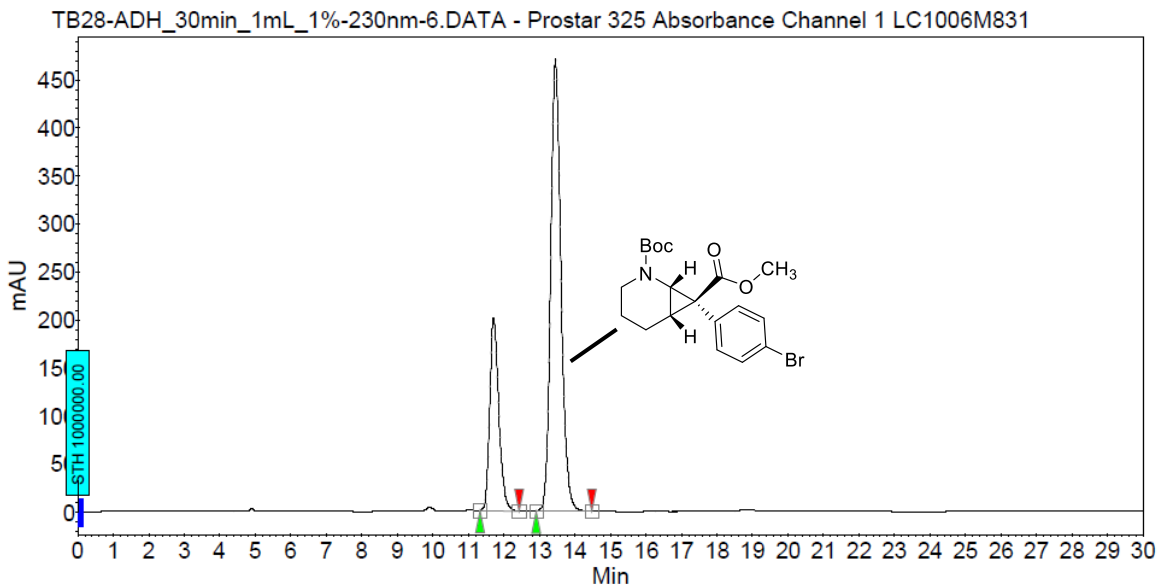


(Table 2, entry 2) (Table S3, entry 10)



Peak results :

Index	Name	Time [Min]	Quantity [% Area]	Height [mAU]	Area [mAU.Min]	Area % [%]
1	UNKNOWN	11.71	27.21	200.5	59.4	27.208
2	UNKNOWN	13.45	72.79	470.4	158.9	72.792
Total			100.00	670.9	218.2	100.000

→ -46% ee

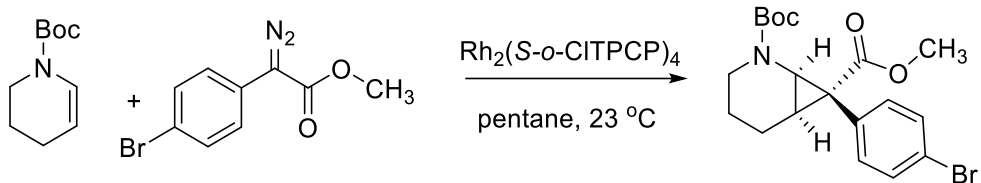
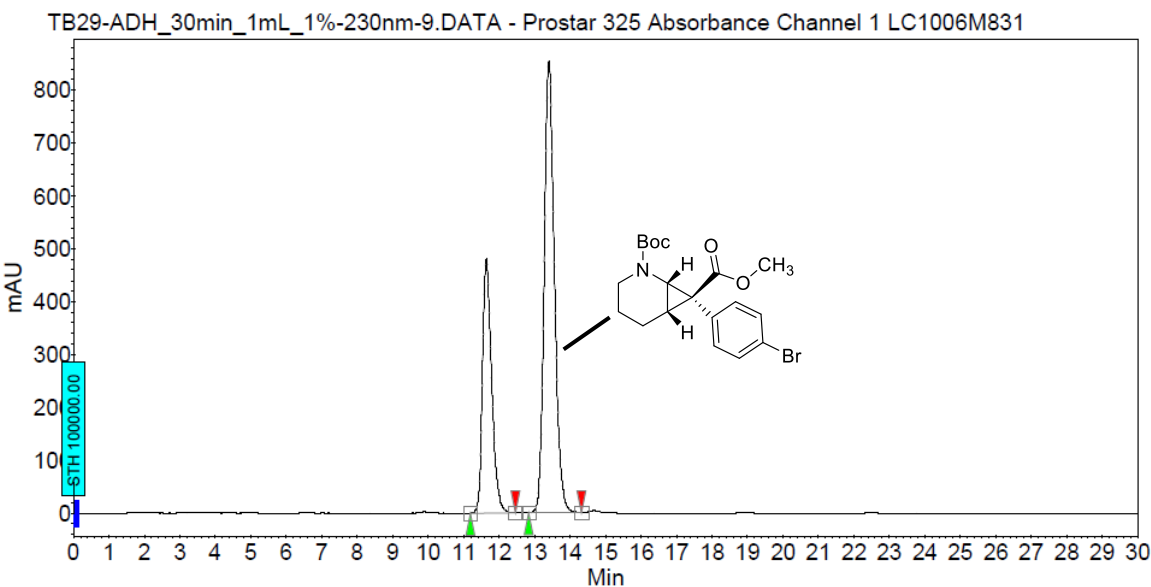


(Table S3, entry 11)



Peak results :

Index	Name	Time [Min]	Quantity [% Area]	Height [mAU]	Area [mAU.Min]	Area % [%]
1	UNKNOWN	11.64	33.41	480.4	143.7	33.413
2	UNKNOWN	13.40	66.59	852.6	286.4	66.587
Total			100.00	1332.9	430.1	100.000

→ -33% ee

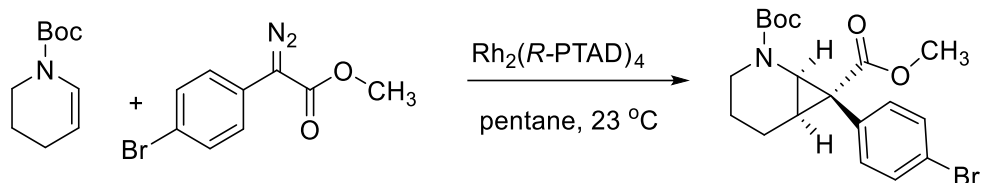
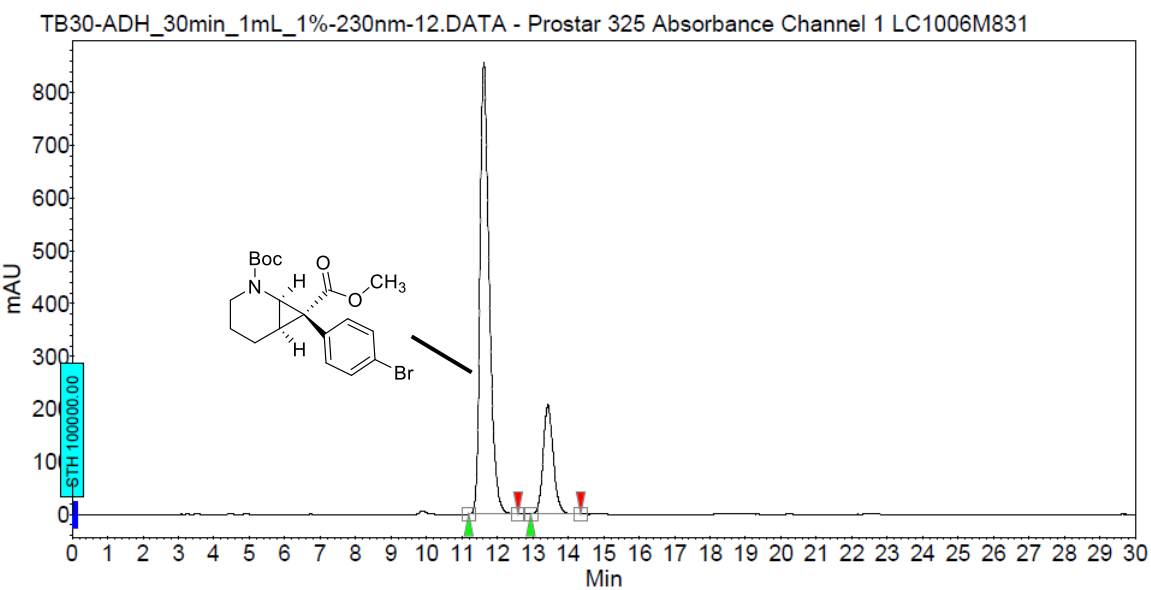


(Table S3, entry 12)



→ 58% ee

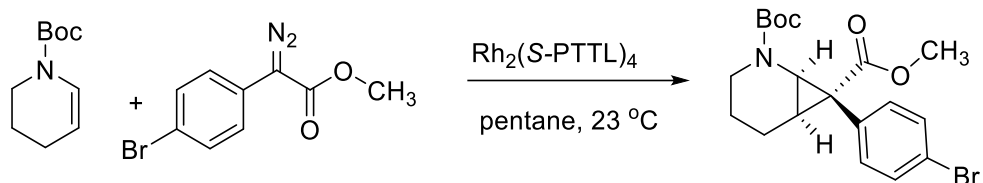
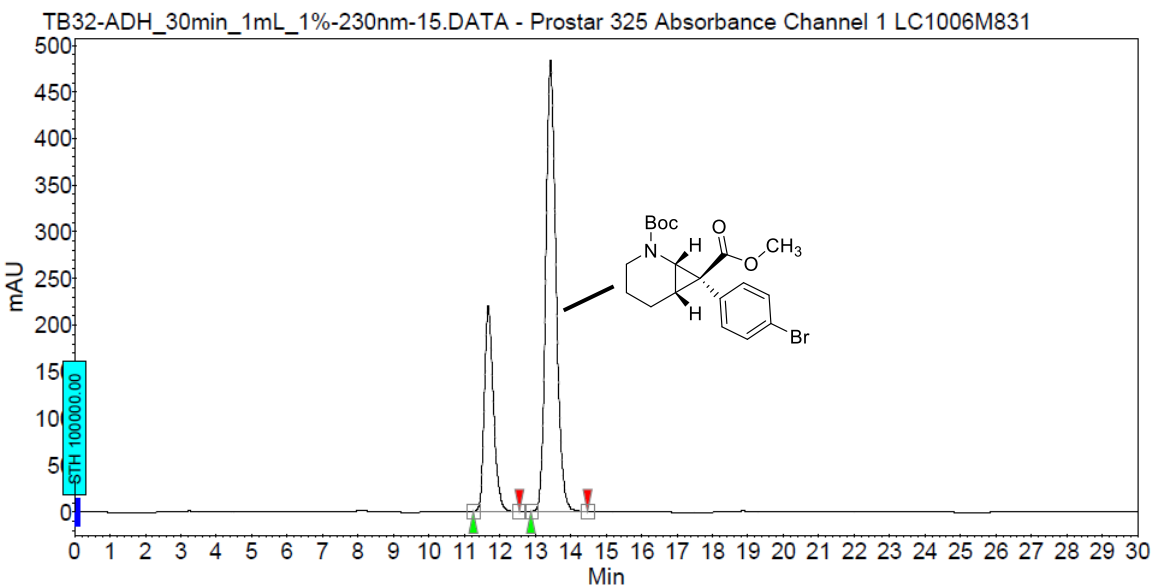


(Table S3, entry 13)



Peak results :

Index	Name	Time [Min]	Quantity [% Area]	Height [mAU]	Area [mAU.Min]	Area % [%]
1	UNKNOWN	11.67	28.69	220.6	65.5	28.691
2	UNKNOWN	13.43	71.31	483.0	162.7	71.309
Total			100.00	703.6	228.1	100.000

→ -43% ee

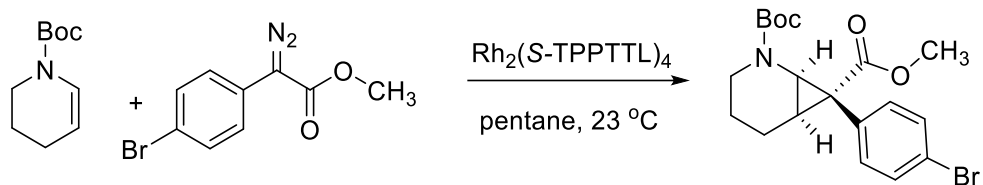
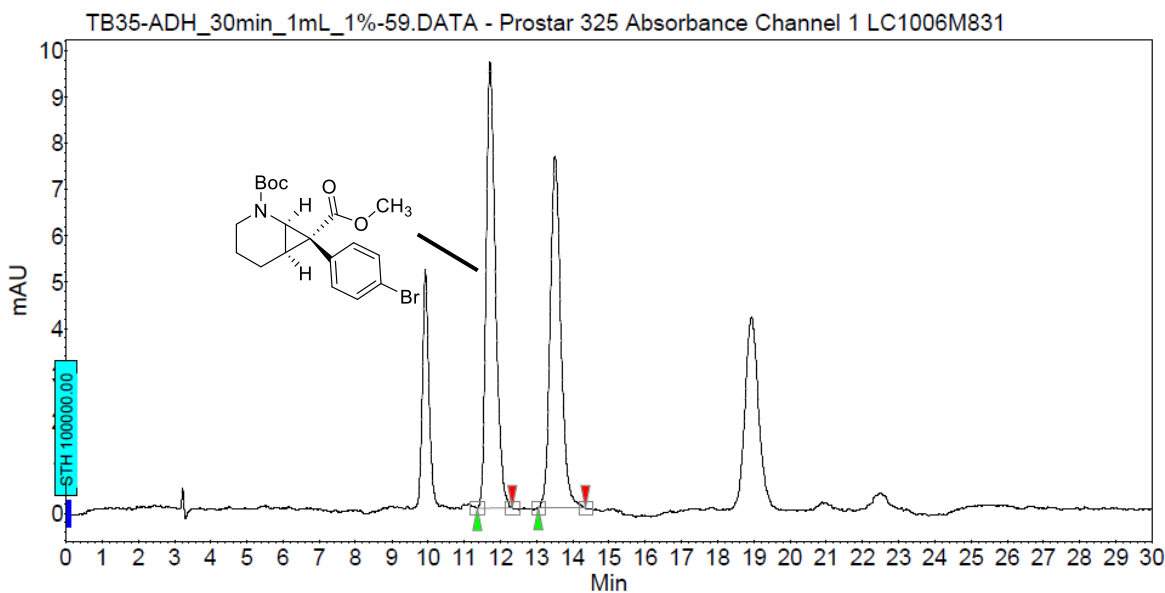


(Table S3, entry 14)



Peak results :

Index	Name	Time [Min]	Quantity [% Area]	Height [mAU]	Area [mAU.Min]	Area % [%]
1	UNKNOWN	11.71	52.40	9.6	2.9	52.401
2	UNKNOWN	13.51	47.60	7.6	2.6	47.599
Total			100.00	17.2	5.5	100.000

→ 5% ee

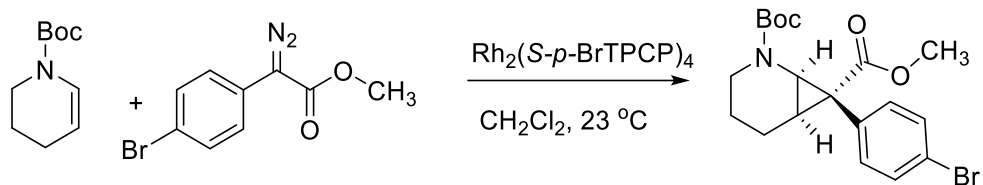
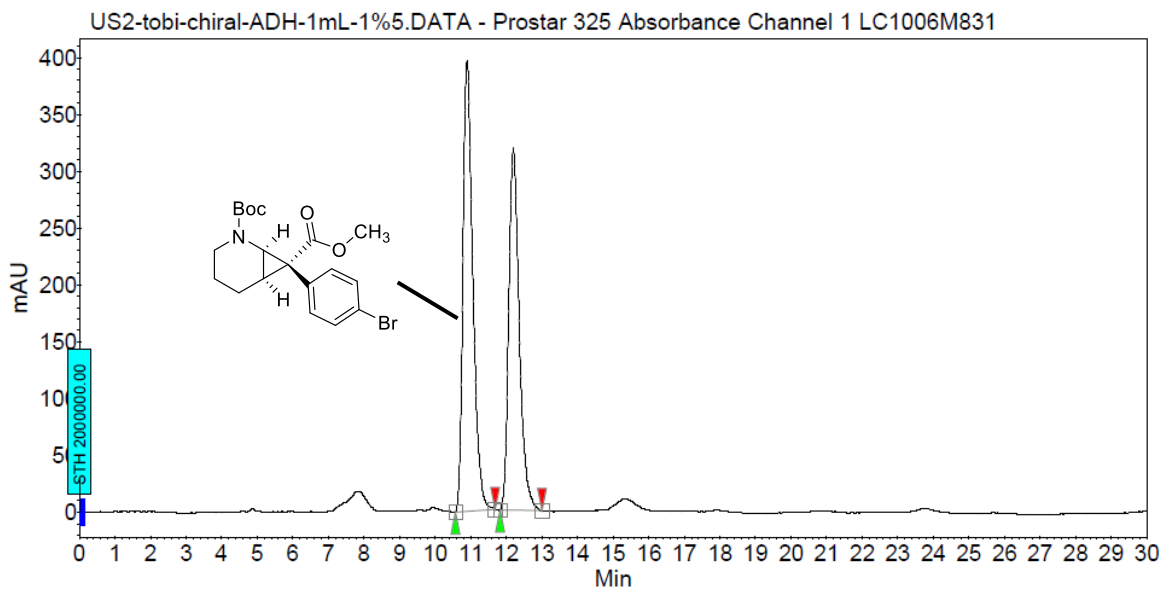


(Table S3, entry 15)



→ 8% ee

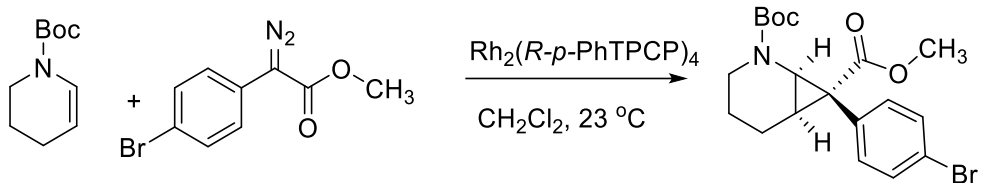
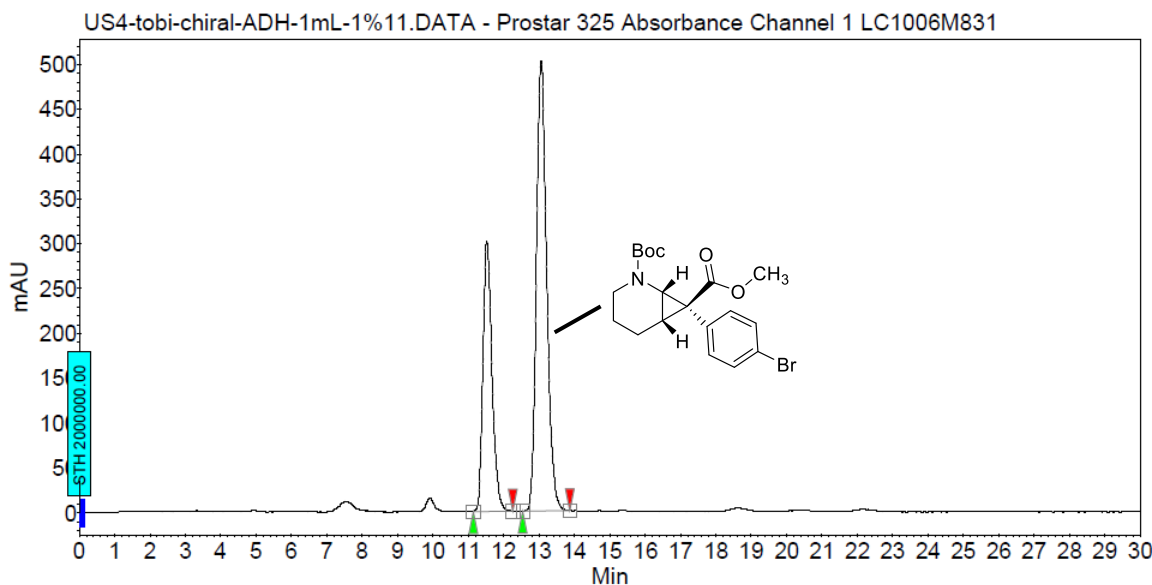


(Table S3, entry 16)



Peak results :

Index	Name	Time [Min]	Quantity [% Area]	Height [mAU]	Area [mAU.Min]	Area % [%]
1	UNKNOWN	11.52	34.78	301.8	89.8	34.782
2	UNKNOWN	13.06	65.22	501.4	168.4	65.218
Total			100.00	803.2	258.2	100.000

→ -30% ee

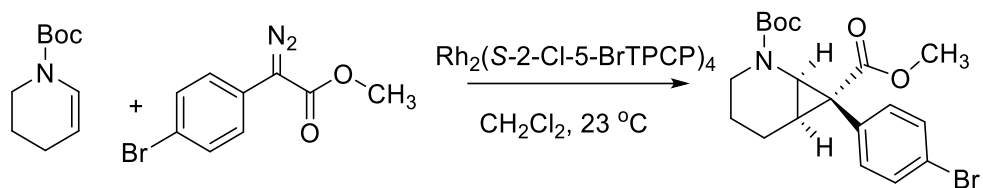
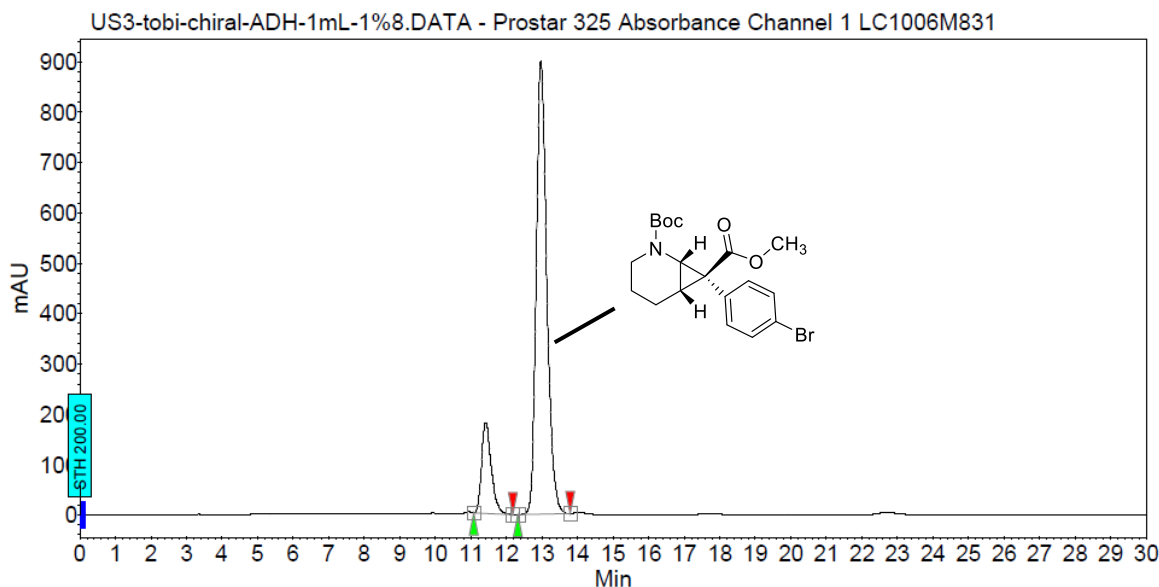


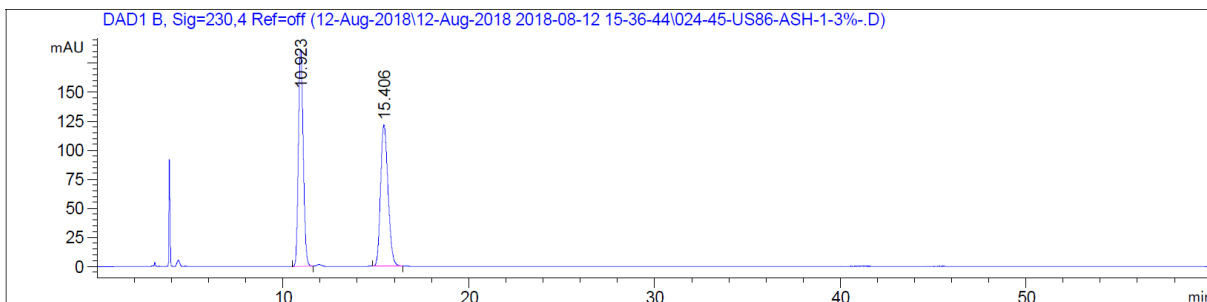
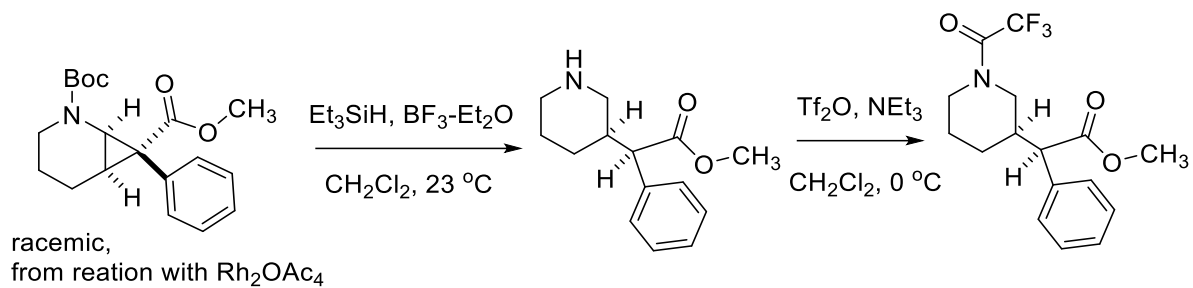
(Table 2, entry 3) (Table S3, entry 17)



Peak results :

Index	Name	Time [Min]	Quantity [% Area]	Height [mAU]	Area [mAU.Min]	Area % [%]
1	UNKNOWN	11.42	15.57	180.9	56.8	15.571
2	UNKNOWN	12.97	84.43	899.6	308.2	84.429
Total			100.00	1080.5	365.0	100.000

→ -69% ee



Signal 2: DAD1 B, Sig=230,4 Ref=off

Peak #	RetTime [min]	Type	Width [min]	Area [mAU*s]	Height [mAU]	Area %
1	10.923	BB	0.2818	3382.68433	186.81001	49.9569
2	15.406	BB	0.4115	3388.52686	121.63947	50.0431
Totals :						6771.21118 308.44948

Racemic standard

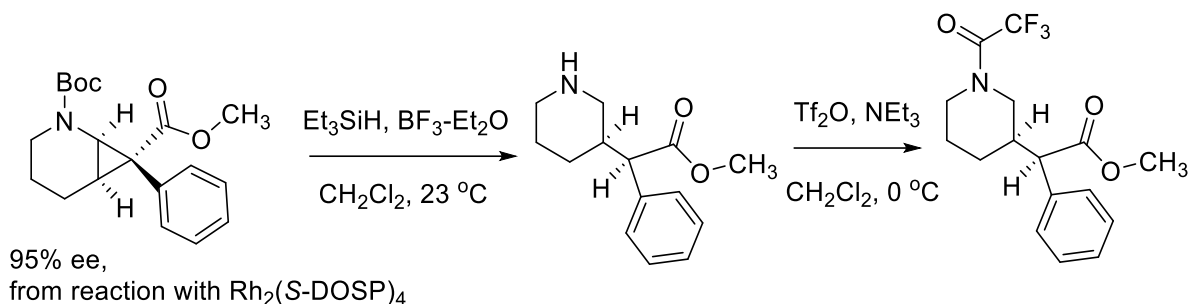
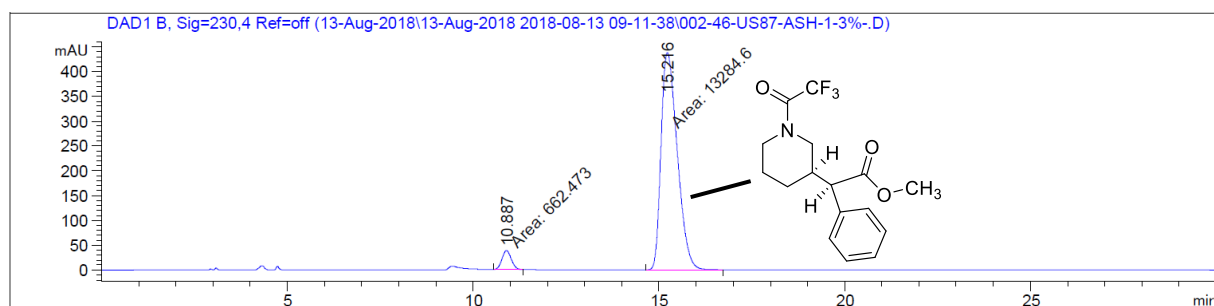


(Table 2, **9b**)



Signal 2: DAD1 B, Sig=230,4 Ref=off

Peak #	RetTime [min]	Type	Width [min]	Area [mAU*s]	Height [mAU]	Area %
1	10.887	MM	0.2891	662.47327	38.18865	4.7499
2	15.216	MM	0.5055	1.32846e4	437.96808	95.2501

Totals : 1.39470e4 476.15673

→ 91% ee

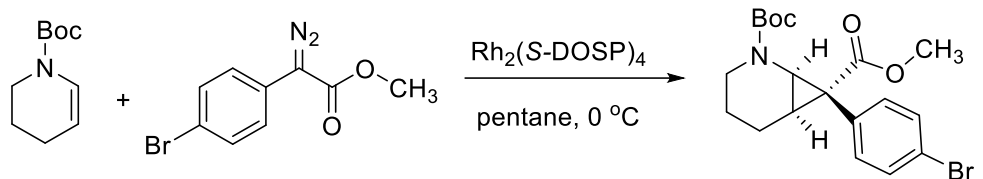
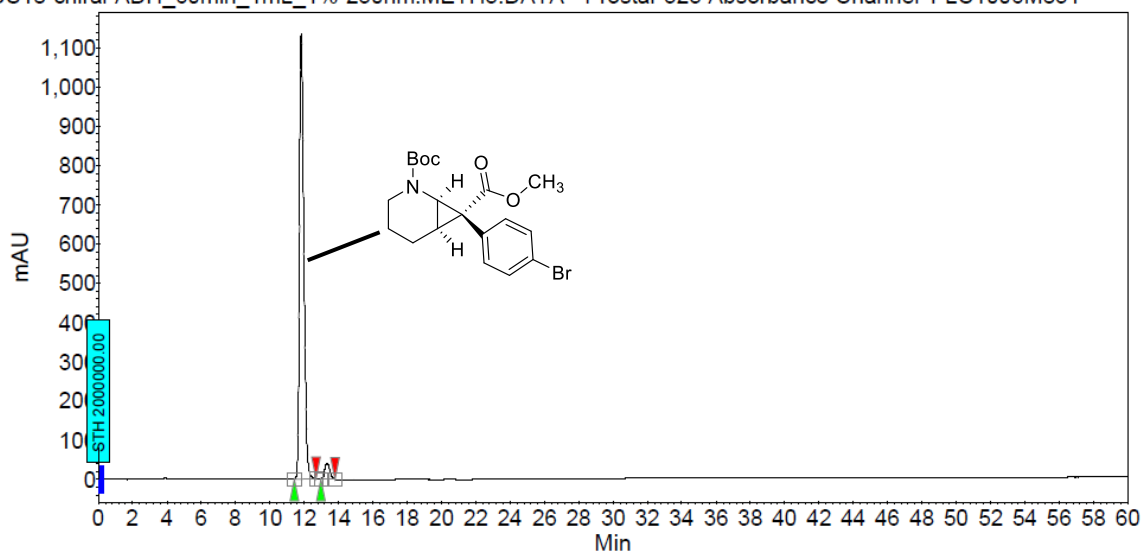


(Table 2, 8a)

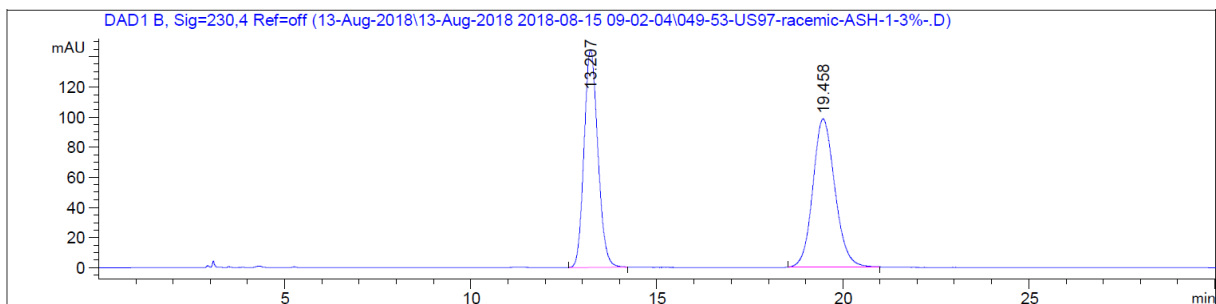
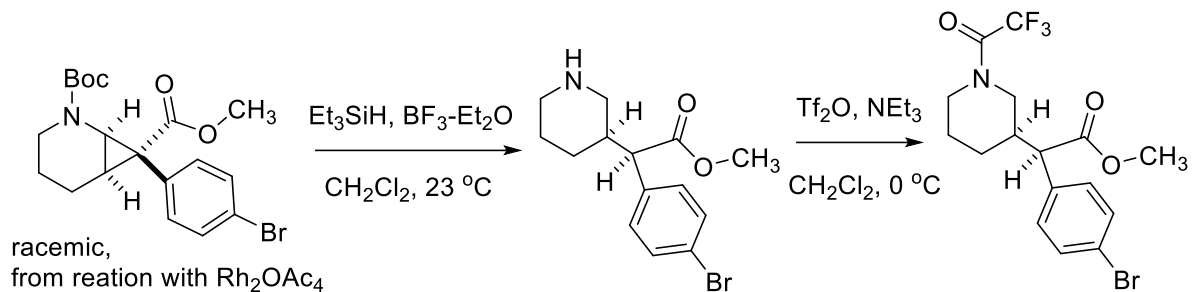
US18-chiral-ADH_60min_1mL_1%-230nm.METH5.DATA - Prostar 325 Absorbance Channel 1 LC1006M831



Peak results :

Index	Name	Time [Min]	Quantity [% Area]	Height [mAU]	Area [mAU·Min]	Area % [%]
1	UNKNOWN	11.83	96.05	1134.2	328.5	96.051
2	UNKNOWN	13.33	3.95	40.9	13.5	3.949
Total			100.00	1175.2	342.0	100.000

→ 92% ee



Signal 2: DAD1 B, Sig=230,4 Ref=off

Peak #	RetTime [min]	Type	Width [min]	Area [mAU*s]	Height [mAU]	Area %
1	13.207	BB	0.3819	3718.29077	144.41826	47.8783
2	19.458	BB	0.5071	4047.83301	98.36426	52.1217
Totals :					7766.12378	242.78252

Racemic Standard

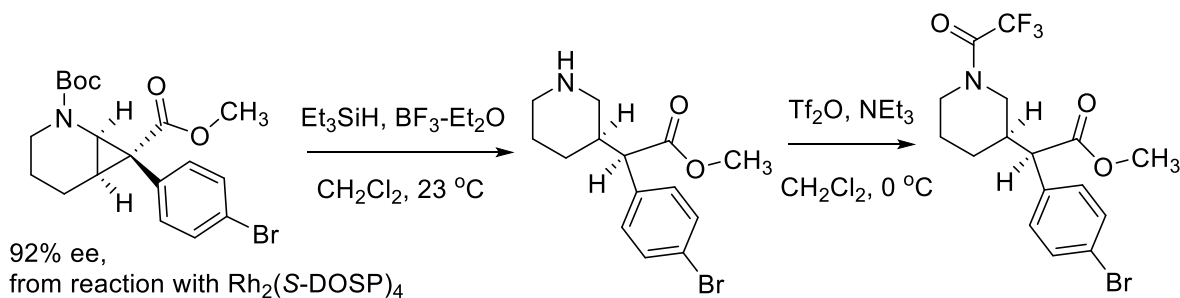
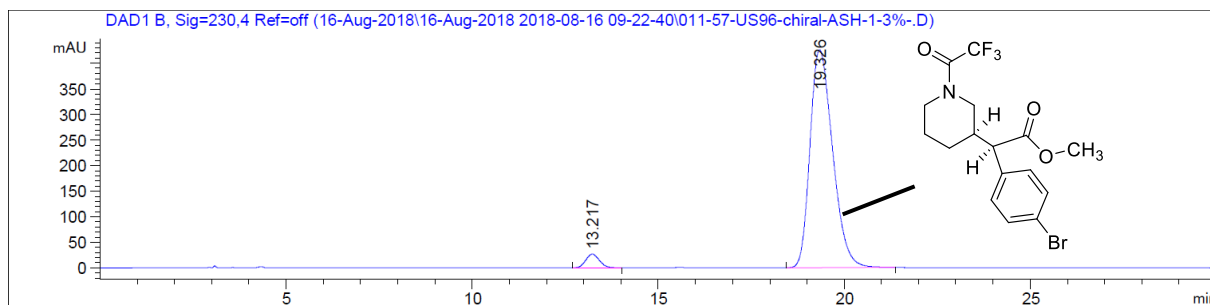


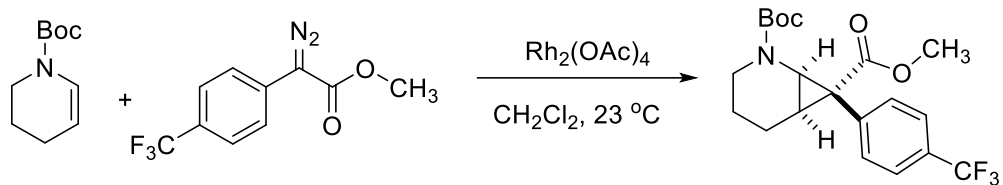
(Table 2, 9a)



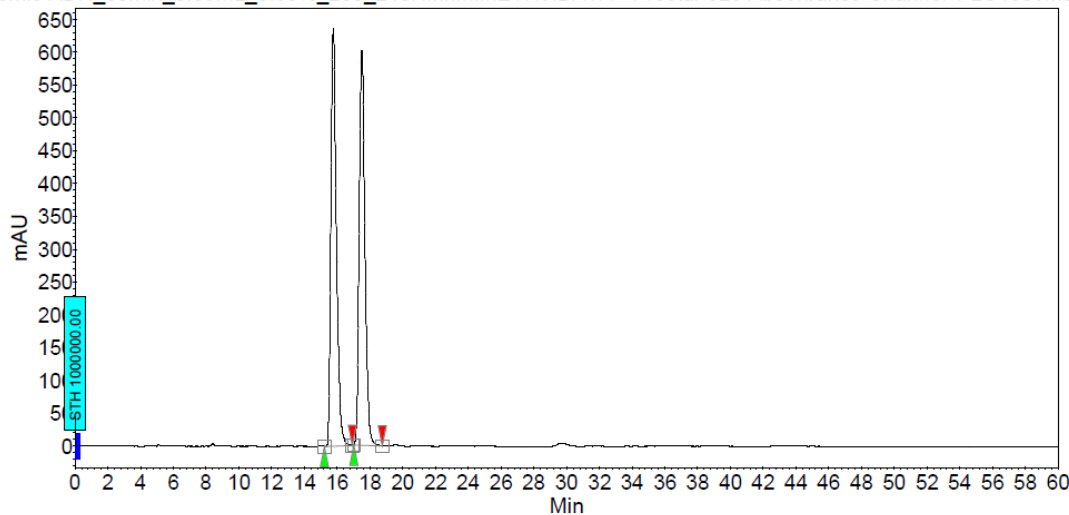
Signal 2: DAD1 B, Sig=230,4 Ref=off

Peak #	RetTime [min]	Type	Width [min]	Area [mAU*s]	Height [mAU]	Area %
1	13.217	BB	0.3150	683.13470	26.83323	3.6499
2	19.326	BB	0.6036	1.80335e4	426.23746	96.3501
Totals :					1.87166e4	453.07069

→ 93% ee



US15-racemic-ADH_60min_0.65mL_0.65%_230_210NMnm.METH5.DATA - Prostar 325 Absorbance Channel 1 LC1006M831



Peak results :

Index	Name	Time [Min]	Quantity [% Area]	Height [mAU]	Area [mAU.Min]	Area [%]
1	UNKNOWN	15.75	50.19	635.7	246.4	50.190
2	UNKNOWN	17.50	49.81	602.1	244.5	49.810
Total			100.00	1237.8	490.9	100.000

Racemic standard

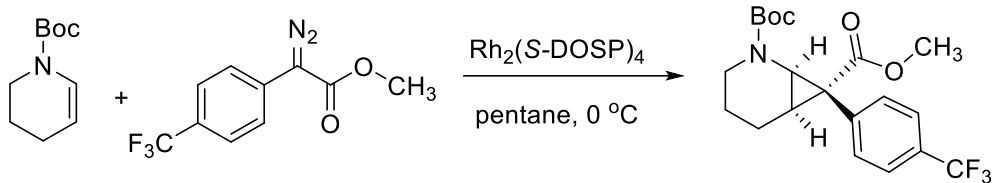
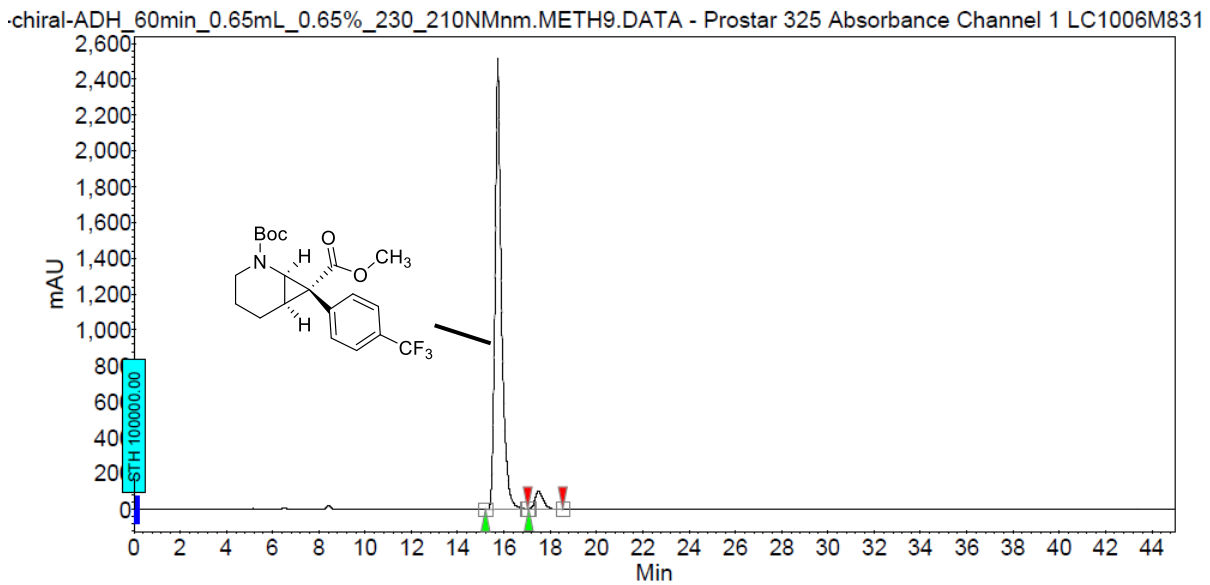


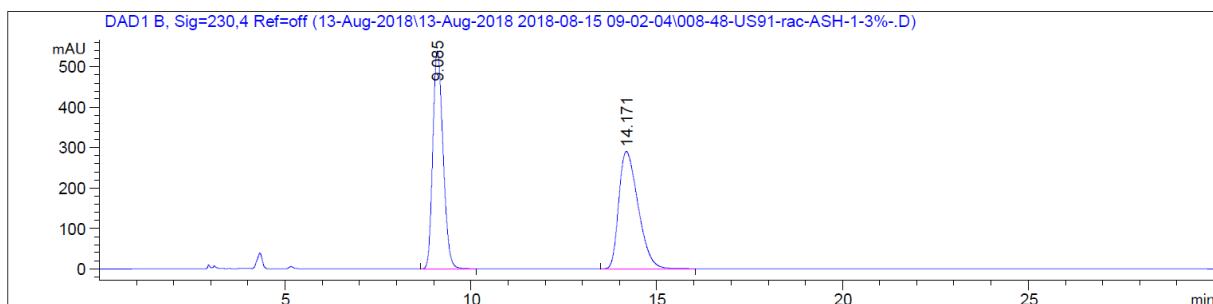
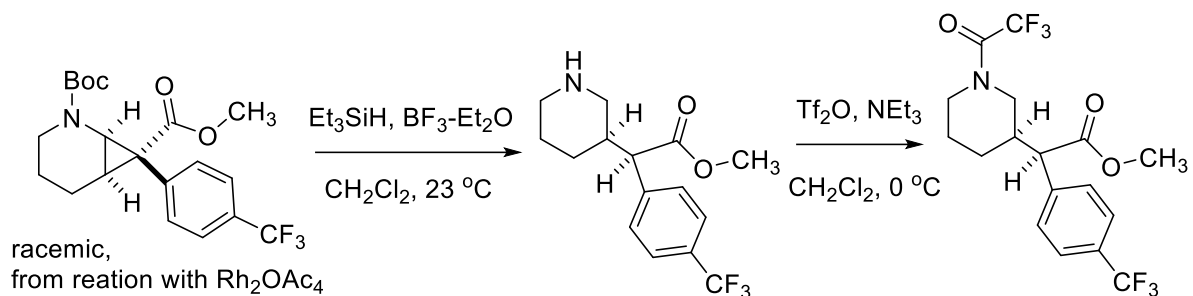
(Table 2, **8c**)



Peak results :

Index	Name	Time [Min]	Quantity [% Area]	Height [mAU]	Area [mAU.Min]	Area % [%]
1	UNKNOWN	15.73	95.12	2512.9	803.2	95.123
2	UNKNOWN	17.49	4.88	100.6	41.2	4.877
Total			100.00	2613.5	844.4	100.000

→ 90% ee



Signal 2: DAD1 B, Sig=230,4 Ref=off

Peak #	RetTime [min]	Type	Width [min]	Area [mAU*s]	Height [mAU]	Area %
<hr/>						
1	9.085	BB	0.2945	1.03478e4	538.94073	49.6662
2	14.171	BB	0.5100	1.04869e4	289.89407	50.3338
Totals :				2.08346e4	828.83481	

Racemic standard

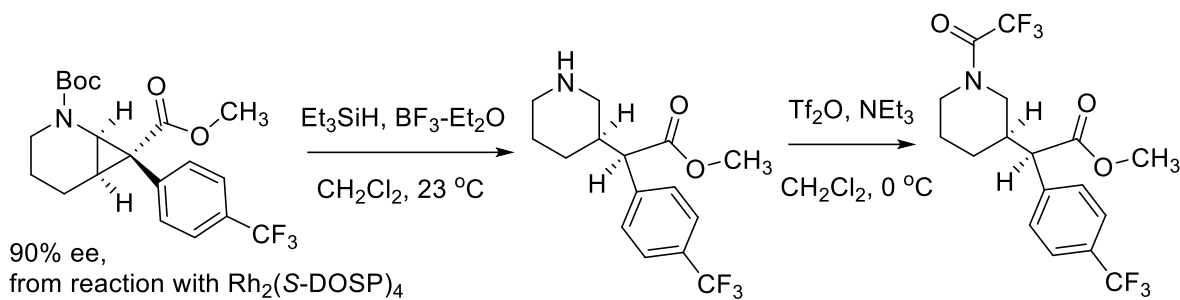
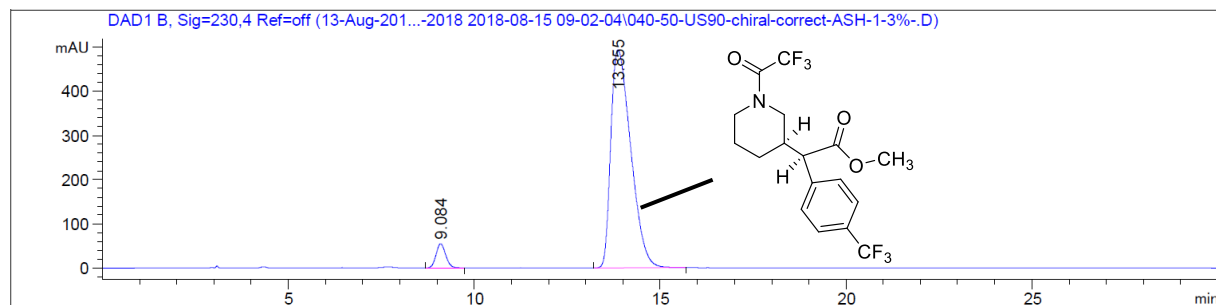
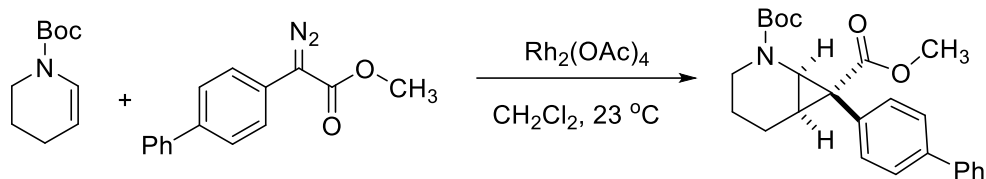


(Table 2, **9c**)

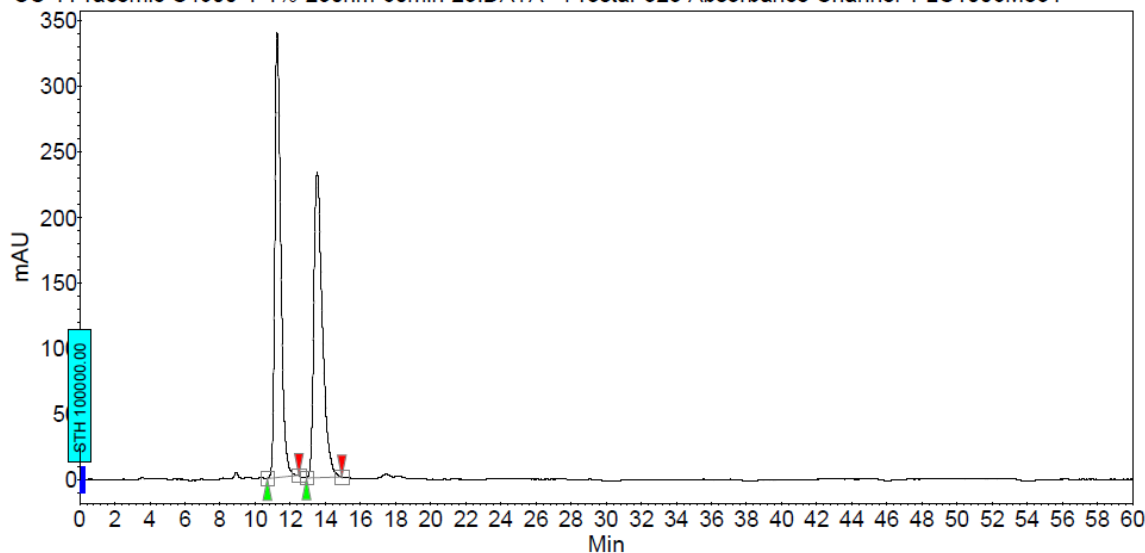


Peak #	RetTime [min]	Type	Width [min]	Area [mAU*s]	Height [mAU]	Area %
1	9.084	BB	0.2710	983.66754	54.66121	5.0685
2	13.855	BB	0.5476	1.84237e4	493.40344	94.9315
Totals :					1.94074e4	548.06465

→ 90% ee



US-11-racemic-S4900-1-1%-230nm-60min-23.DATA - Prostar 325 Absorbance Channel 1 LC1006M831



Peak results :

Index	Name	Time [Min]	Quantity [% Area]	Height [mAU]	Area [mAU.Min]	Area % [%]
1	UNKNOWN	11.26	50.46	339.0	134.2	50.460
2	UNKNOWN	13.53	49.54	232.7	131.8	49.540
Total			100.00	571.8	266.0	100.000

Racemic standard

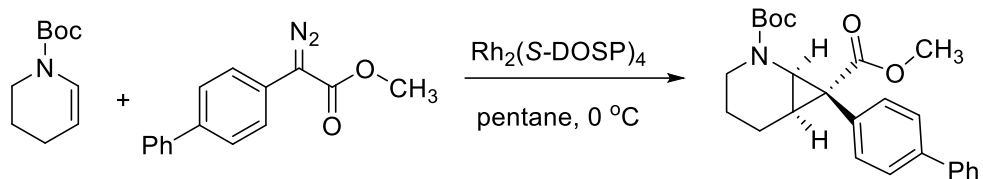
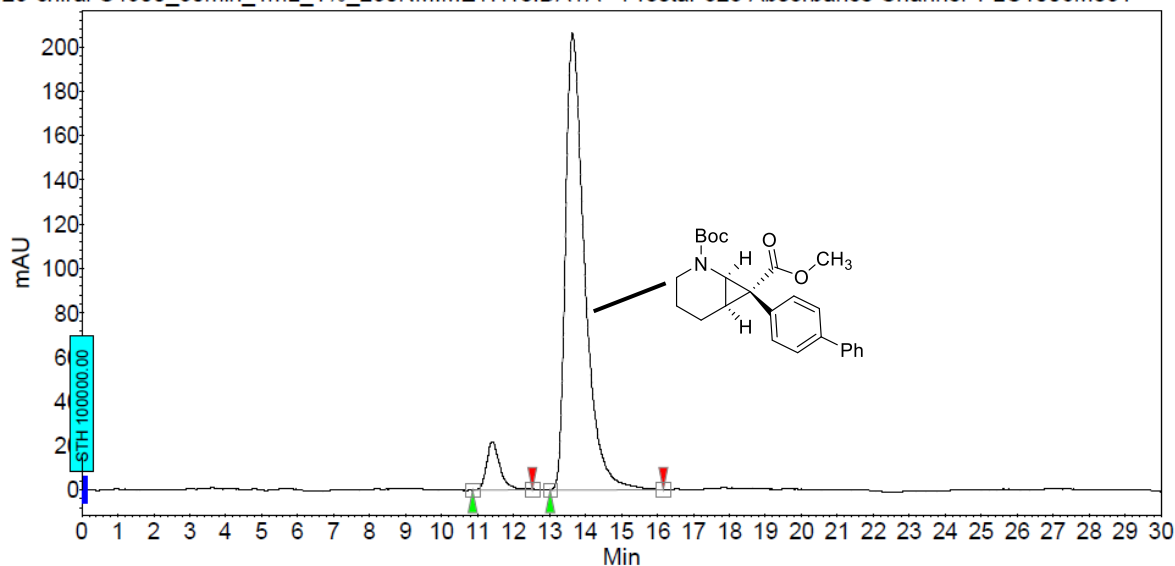


(Table 2, **8d**)

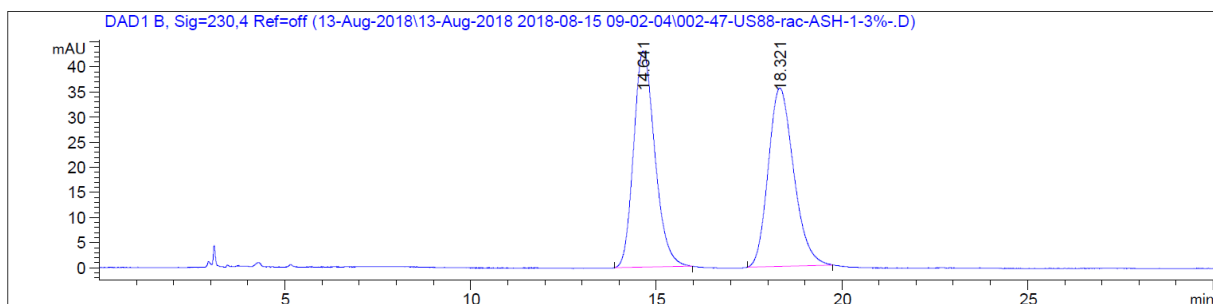
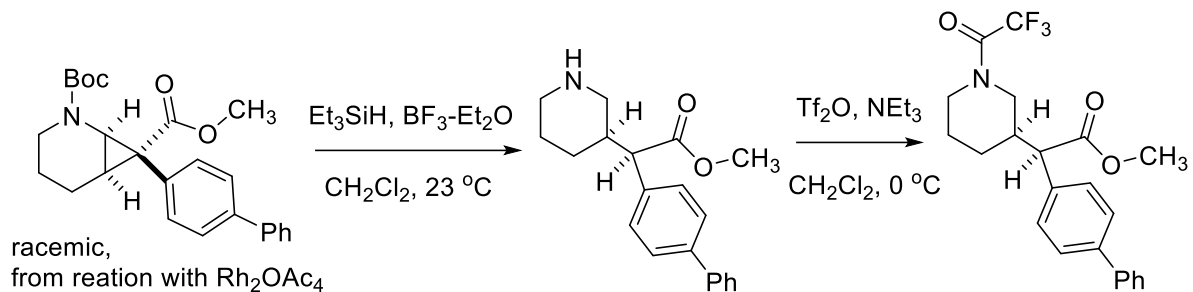
US23-chiral-S4900_30min_1mL_1%_230NM.METH18.DATA - Prostar 325 Absorbance Channel 1 LC1006M831



Peak results :

Index	Name	Time [Min]	Quantity [% Area]	Height [mAU]	Area [mAU.Min]	Area [%]
1	UNKNOWN	11.41	6.92	21.8	9.5	6.925
2	UNKNOWN	13.64	93.08	206.3	127.1	93.075
Total			100.00	228.1	136.6	100.000

→ 86% ee



Peak #	RetTime [min]	Type	Width [min]	Area [mAU*s]	Height [mAU]	Area %
1	14.641	BB	0.4687	1715.65771	43.11946	50.3434
2	18.321	BB	0.5662	1692.25452	35.53103	49.6566
Totals :					3407.91223	78.65049

Racemic standard

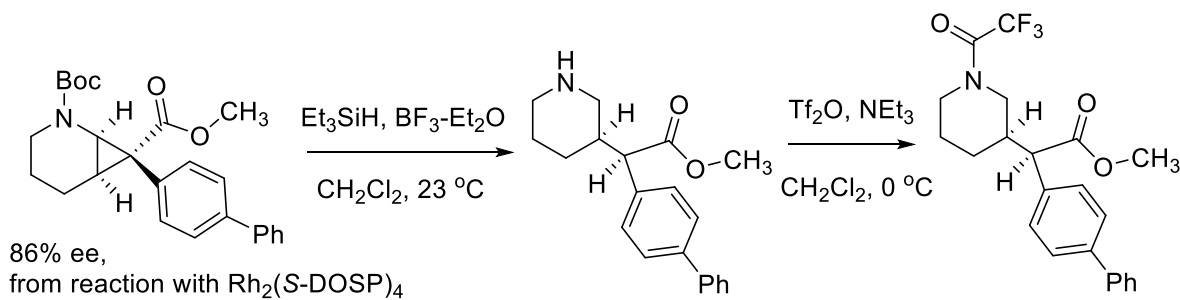
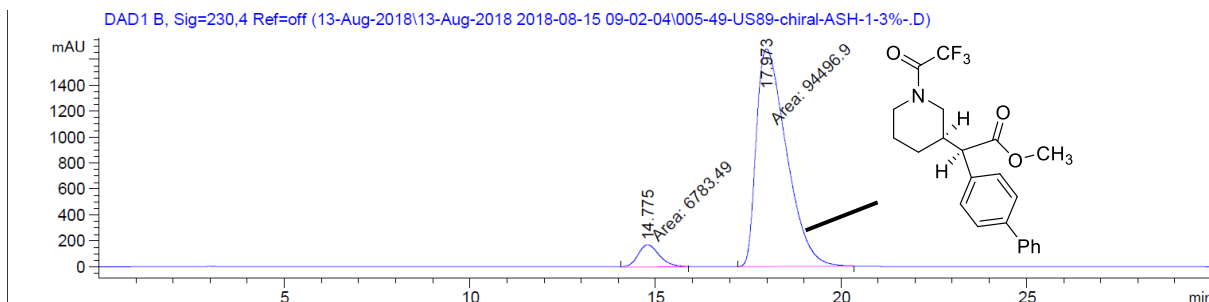


(Table 2, 9d)

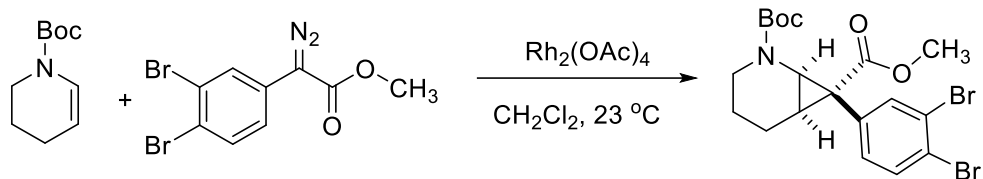


Signal 2: DAD1 B, Sig=230,4 Ref=off

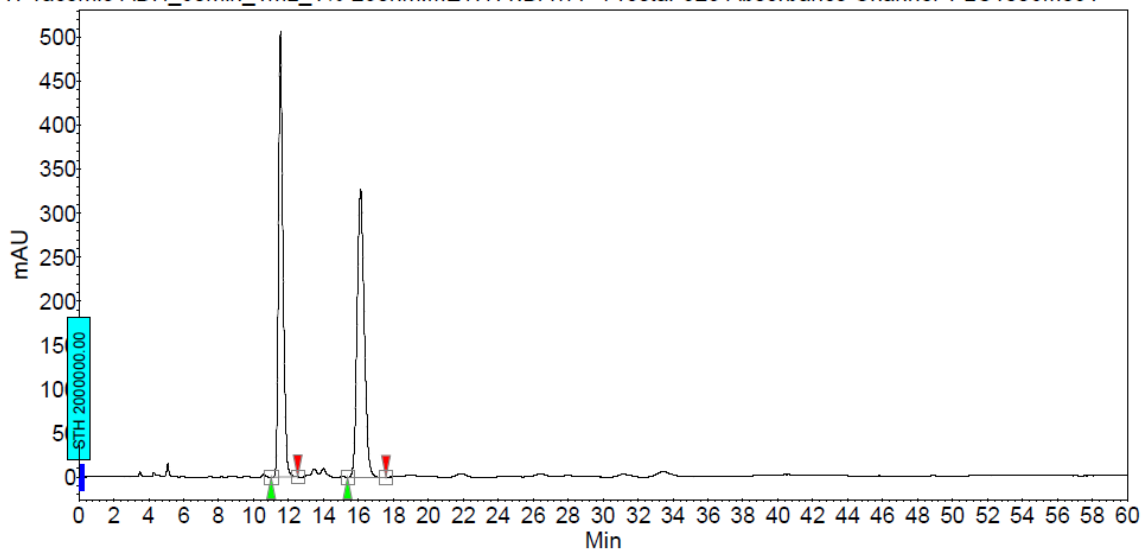
Peak #	RetTime [min]	Type	Width [min]	Area [mAU*s]	Height [mAU]	Area %
1	14.775	MM	0.6639	6783.49316	170.30302	6.6977
2	17.973	MM	0.9392	9.44969e4	1676.85071	93.3023

Totals : 1.01280e5 1847.15373

→ 87% ee



US17-racemic-ADH_60min_1mL_1%-230nm.METH11.DATA - Prostar 325 Absorbance Channel 1 LC1006M831



Peak results :

Index	Name	Time [Min]	Quantity [% Area]	Height [mAU]	Area [mAU Min]	Area % [%]
1	UNKNOWN	11.53	49.47	506.0	151.9	49.469
2	UNKNOWN	16.11	50.53	327.1	155.2	50.531
Total			100.00	833.1	307.1	100.000

Racemic standard

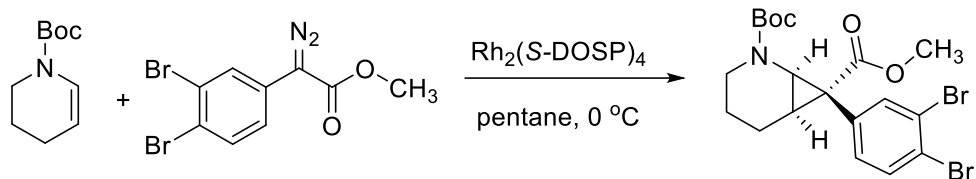
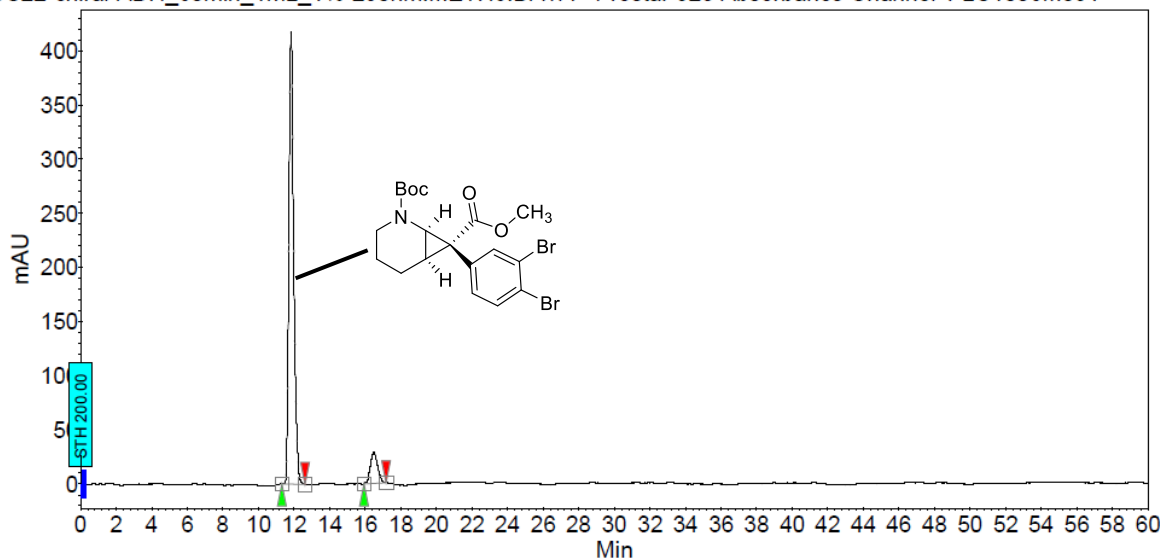


(Table 2, **8e**)

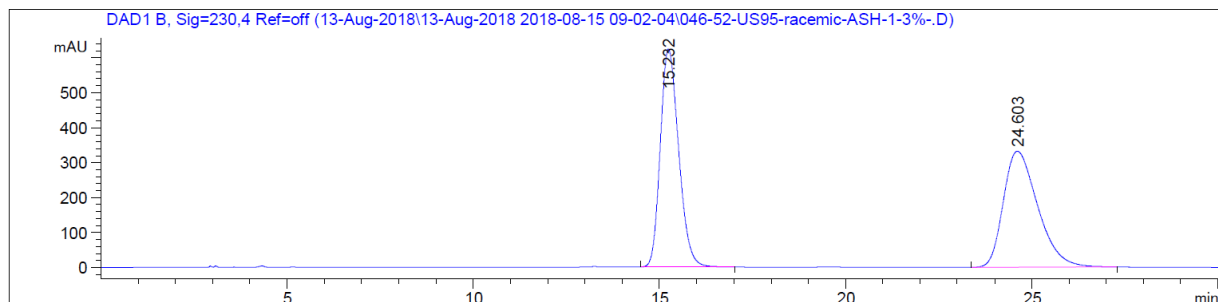
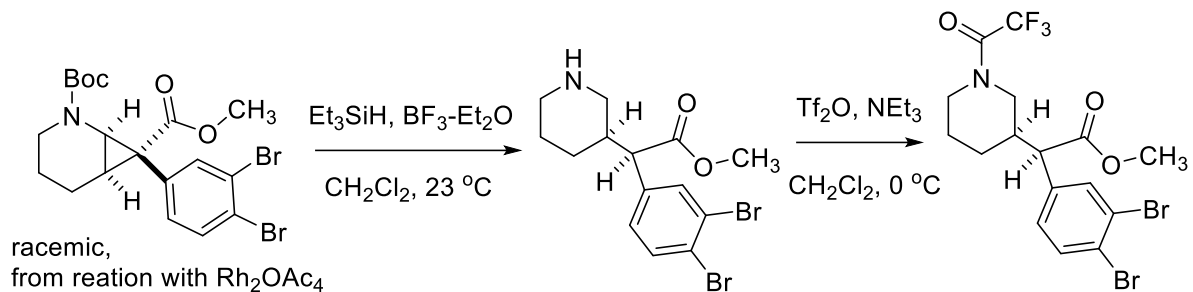
US22-chiral-ADH_60min_1mL_1%-230nm.METH6.DATA - Prostar 325 Absorbance Channel 1 LC1006M831



Peak results :

Index	Name	Time [Min]	Quantity [% Area]	Height [mAU]	Area [mAU.Min]	Area % [%]
1	UNKNOWN	11.82	90.57	417.3	131.9	90.570
2	UNKNOWN	16.48	9.43	29.1	13.7	9.430
Total			100.00	446.4	145.6	100.000

→ 81% ee



Signal 2: DAD1 B, Sig=230,4 Ref=off

Peak #	RetTime [min]	Type	Width [min]	Area [mAU*s]	Height [mAU]	Area %
1	15.232	BB	0.5249	2.13657e4	624.02716	50.0539
2	24.603	BB	0.7578	2.13197e4	332.38715	49.9461
Totals :					4.26853e4	956.41431

Racemic standard

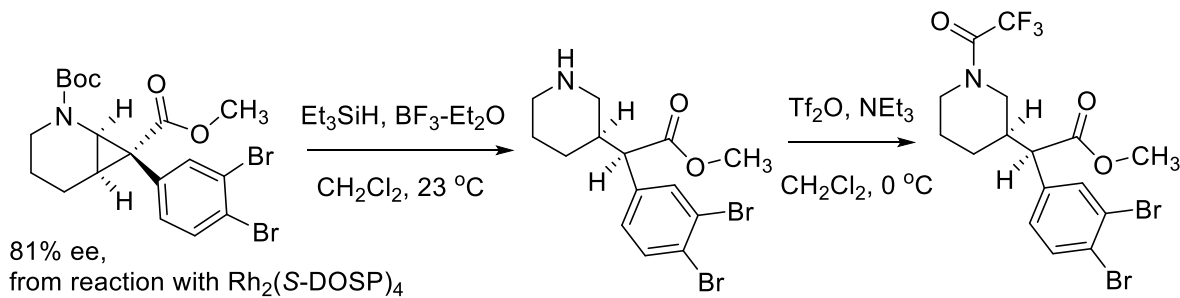
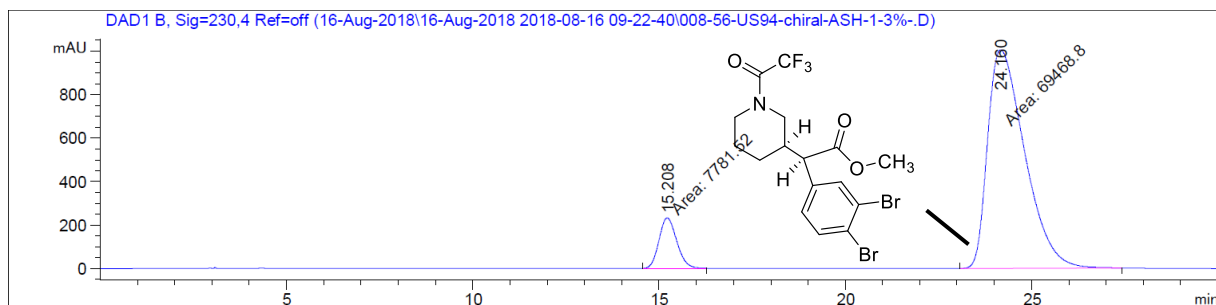


(Table 2, **9e**)



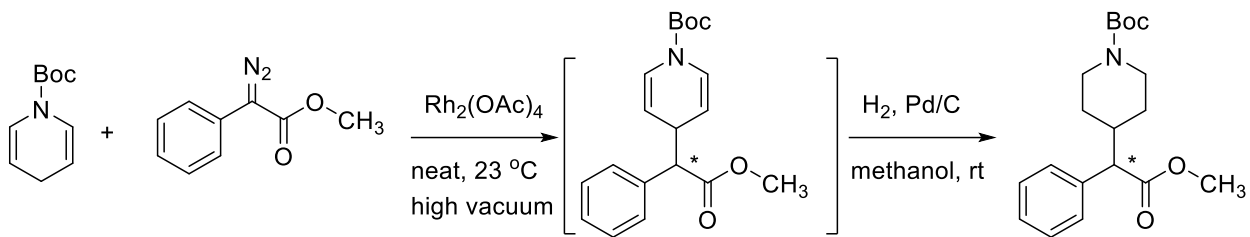
Signal 2: DAD1 B, Sig=230,4 Ref=off

Peak #	RetTime [min]	Type	Width [min]	Area [mAU*s]	Height [mAU]	Area %
1	15.208	MM	0.5562	7781.52002	233.18750	10.0731
2	24.160	MM	1.1523	6.94688e4	1004.77606	89.9269

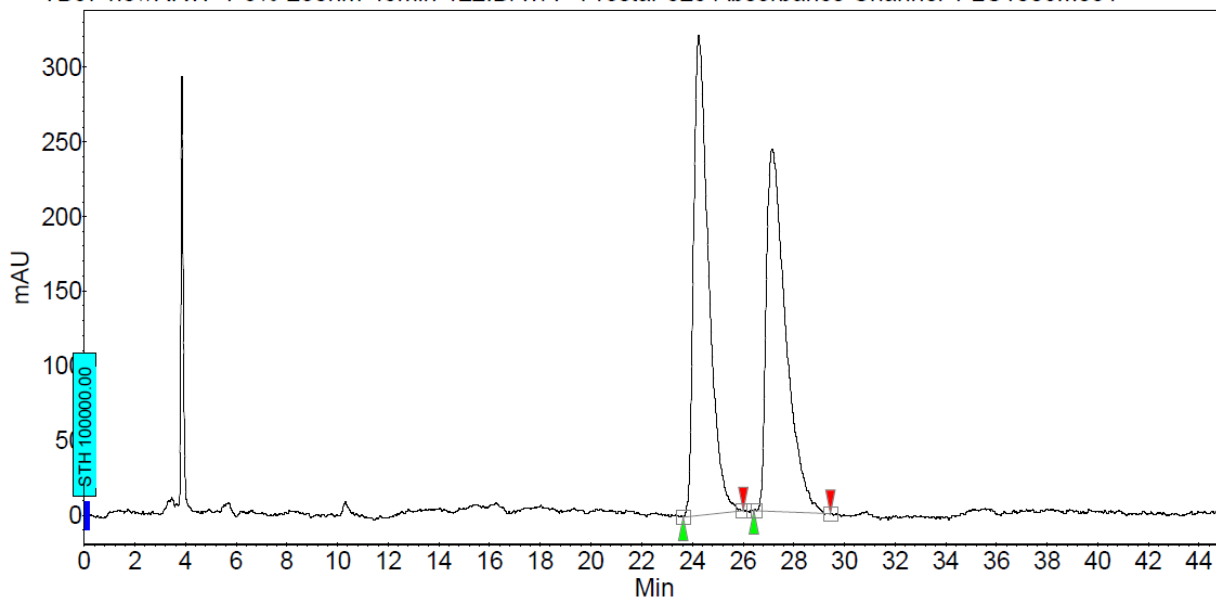
Totals : 7.72503e4 1237.96356

→ 80% ee

10.3. C4 Functionalization Products



TB57-newRRW-1-5%-230nm-45min-122.DATA - Prostar 325 Absorbance Channel 1 LC1006M831



Peak results :

Index	Name	Time [Min]	Quantity [% Area]	Height [mAU]	Area [mAU.Min]	Area % [%]
1	UNKNOWN	24.25	50.52	321.4	221.2	50.515
2	UNKNOWN	27.15	49.48	242.5	216.7	49.485
Total			100.00	563.9	437.9	100.000

Racemic standard

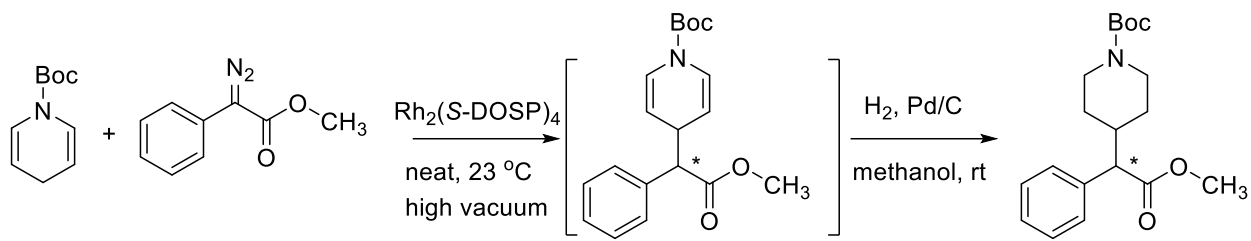
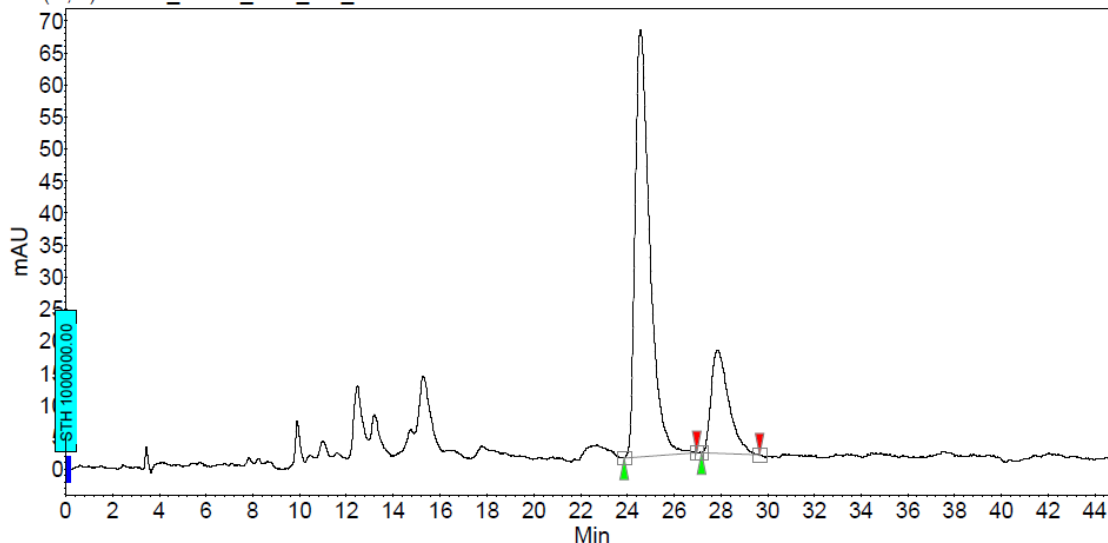


(Table S4, entry 5)

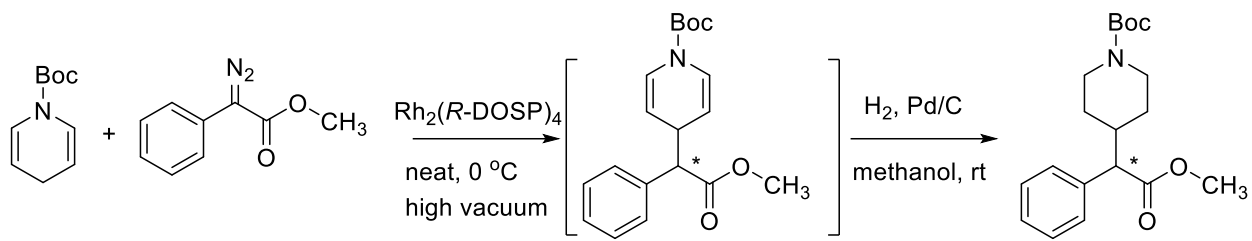
US62-(R,R)-Whelk_45min_1mL_5%_230nm.METH3.DATA - Prostar 325 Absorbance Channel 1 LC1006M831



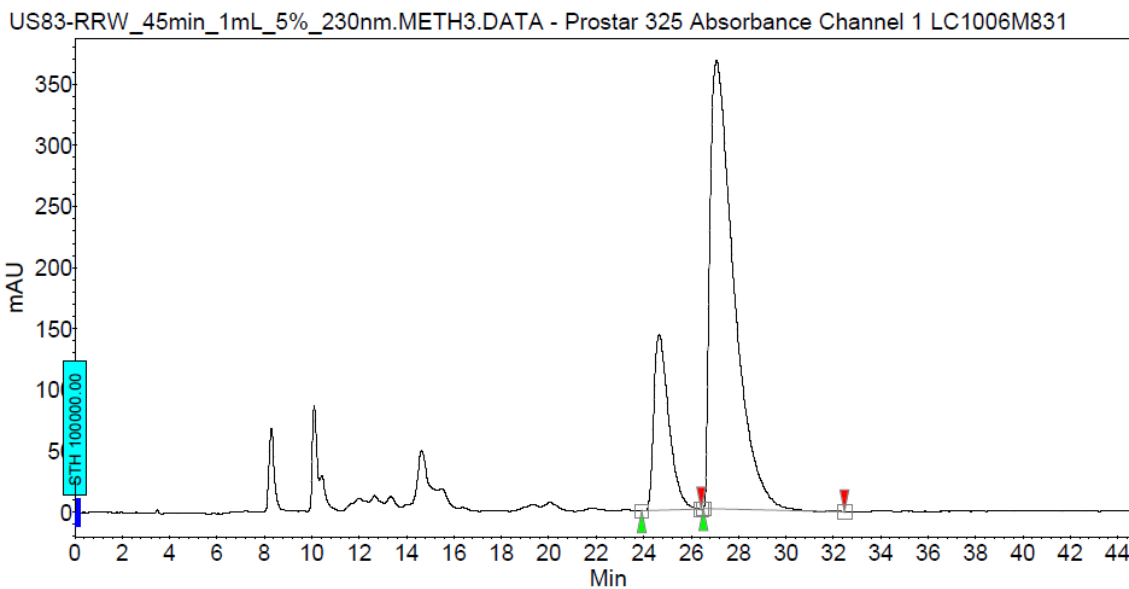
Peak results :

Index	Name	Time [Min]	Quantity [% Area]	Height [mAU]	Area [mAU.Min]	Area % [%]
1	UNKNOWN	24.57	77.70	66.6	48.7	77.704
2	UNKNOWN	27.86	22.30	16.1	14.0	22.296
Total			100.00	82.7	62.7	100.000

→ -55% ee



(Scheme 3) (Table S4, entry 6)



Peak results :

Index	Name	Time [Min]	Quantity [% Area]	Height [mAU]	Area [mAU.Min]	Area [%]
1	UNKNOWN	24.65	19.72	143.3	105.2	19.719
2	UNKNOWN	27.08	80.28	365.6	428.4	80.281
Total			100.00	508.9	533.7	100.000

→ 61% ee

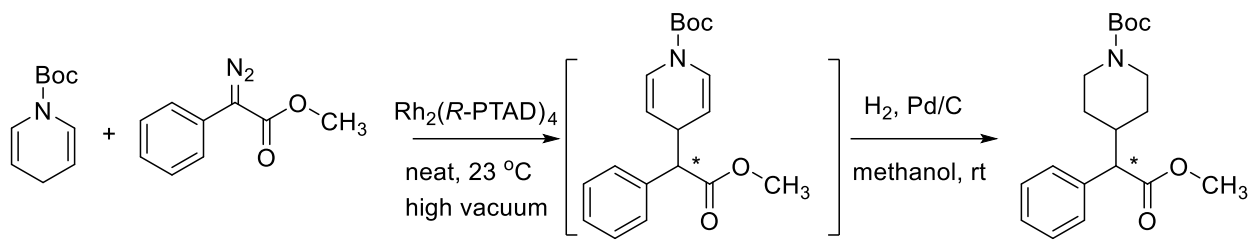
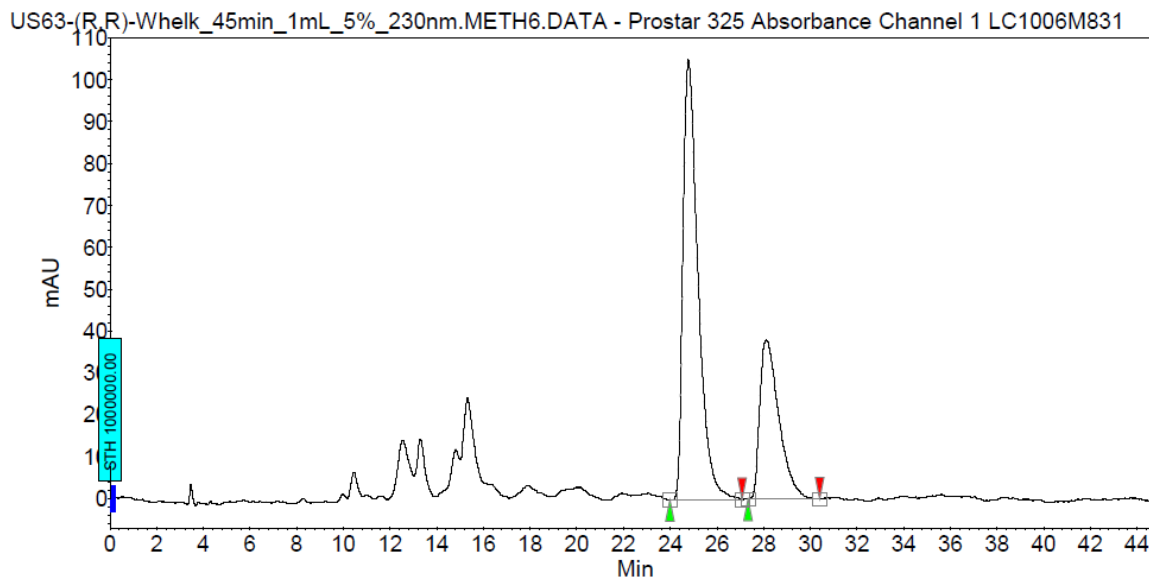


(Table S4, entry 7)



Peak results :

Index	Name	Time [Min]	Quantity [% Area]	Height [mAU]	Area [mAU.Min]	Area % [%]
1	UNKNOWN	24.77	68.58	105.1	78.7	68.577
2	UNKNOWN	28.13	31.42	37.9	36.0	31.423
Total			100.00	143.1	114.7	100.000

→ -37% ee

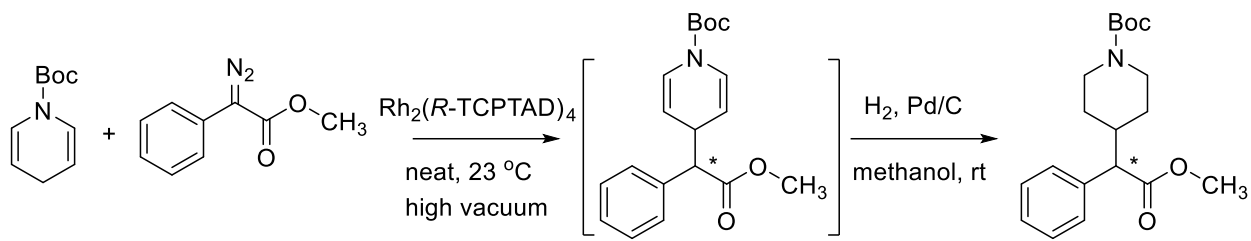
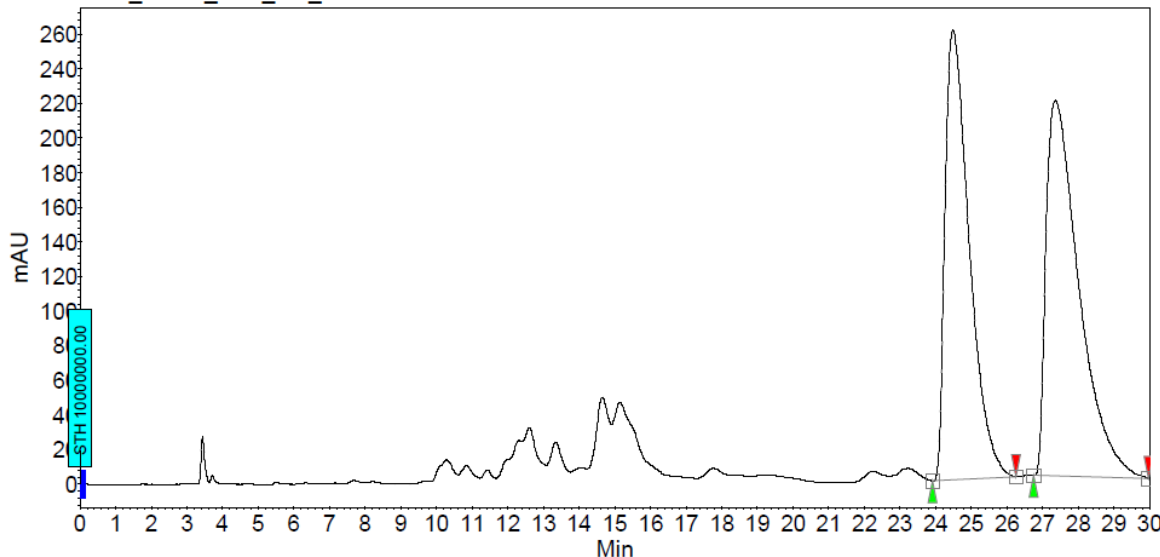


(Table S4, entry 8)

US68-RRW_60min_1mL_5%_230nm.METH18.DATA - Prostar 325 Absorbance Channel 1 LC1006M831



Peak results :

Index	Name	Time [Min]	Quantity [% Area]	Height [mAU]	Area [mAU.Min]	Area % [%]
1	UNKNOWN	24.48	46.92	259.6	204.8	46.918
2	UNKNOWN	27.36	53.08	216.7	231.7	53.082
Total			100.00	476.3	436.5	100.000

→ 6% ee

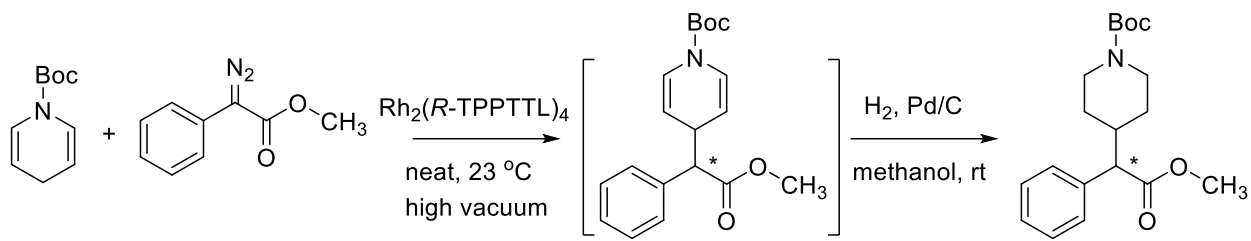
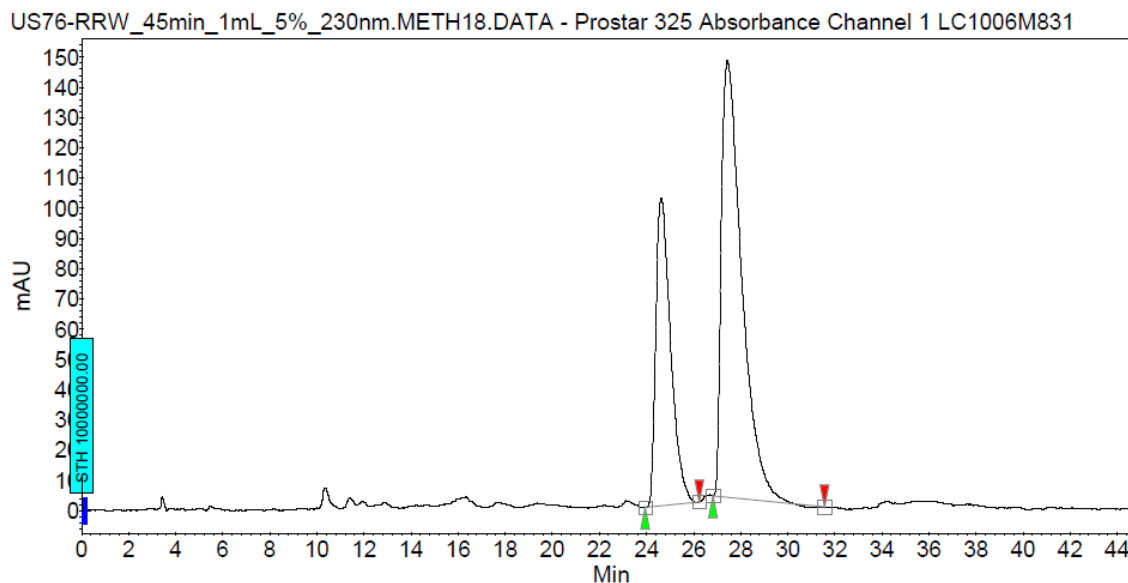


(Table S4, entry 9)



Peak results :

Index	Name	Time [Min]	Quantity [% Area]	Height [mAU]	Area [mAU.Min]	Area % [%]
1	UNKNOWN	24.62	33.79	101.7	74.0	33.794
2	UNKNOWN	27.44	66.21	144.4	145.1	66.206
Total			100.00	246.1	219.1	100.000

→ 32% ee

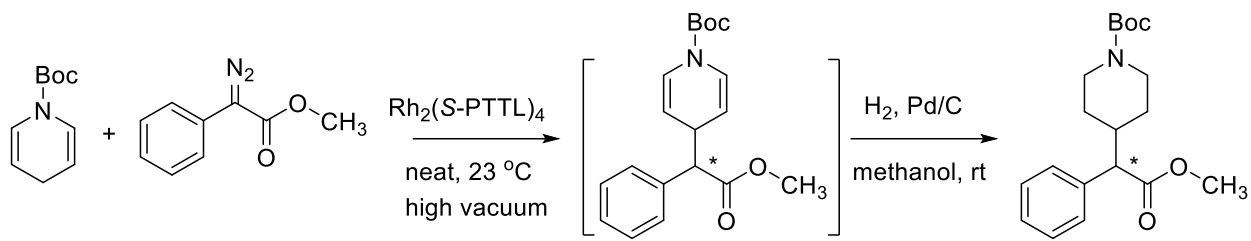
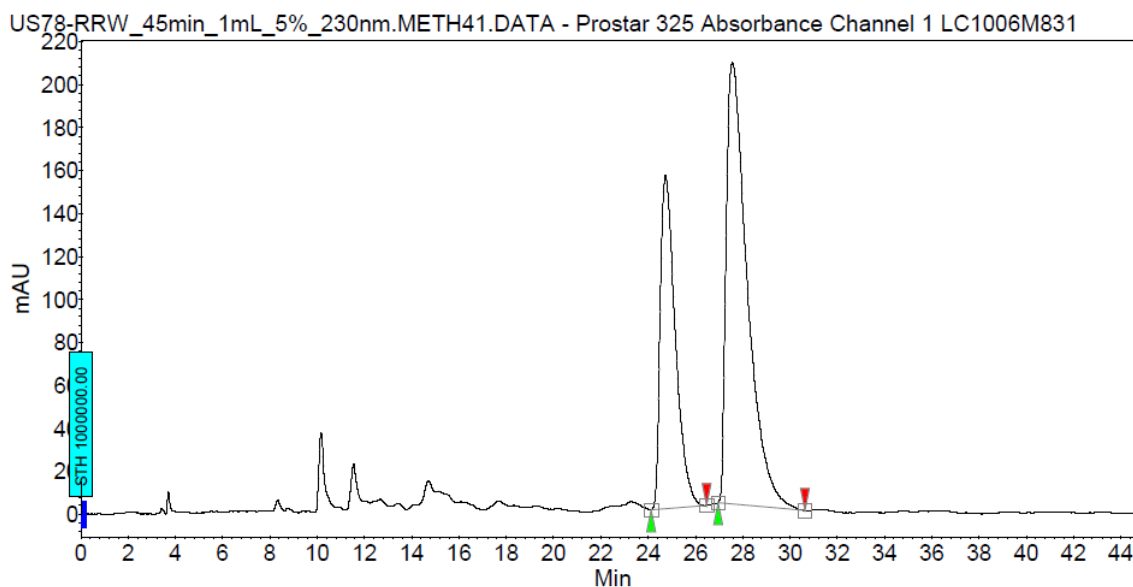


(Table S4, entry 10)



Peak results :

Index	Name	Time [Min]	Quantity [% Area]	Height [mAU]	Area [mAU.Min]	Area % [%]
1	UNKNOWN	24.73	35.09	155.3	114.7	35.085
2	UNKNOWN	27.56	64.91	205.2	212.2	64.915
Total			100.00	360.5	326.9	100.000

→ 30% ee

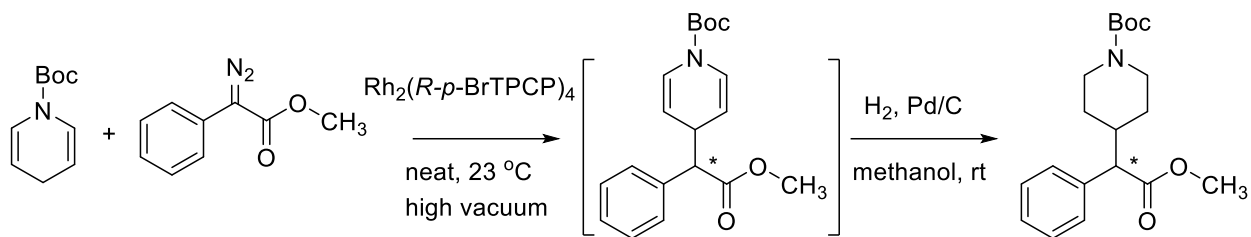
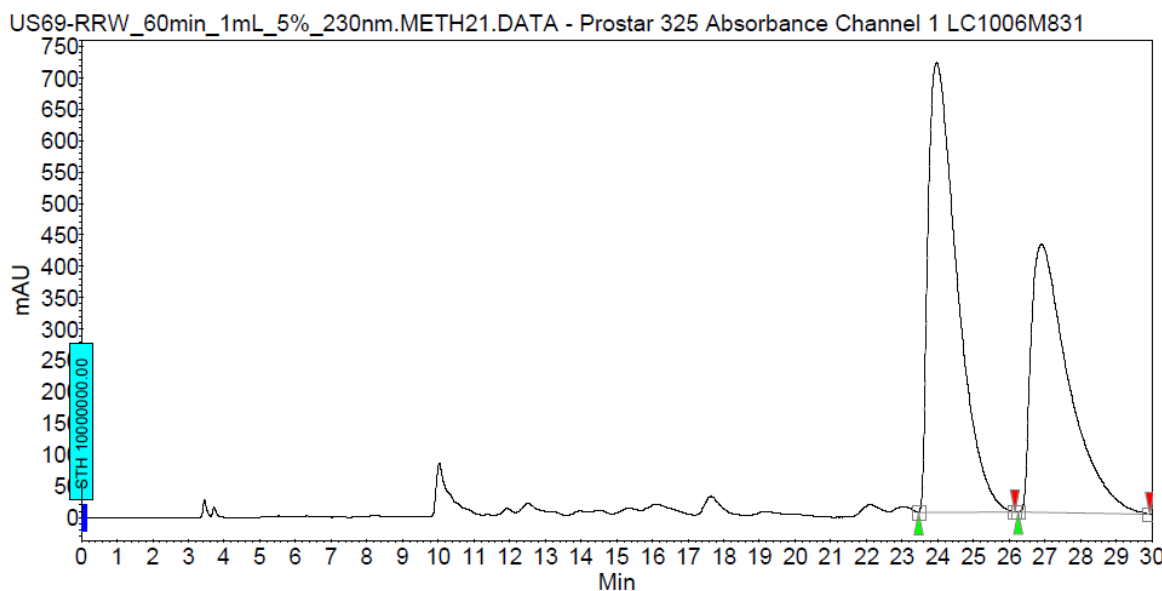


(Table S4, entry 11)



Peak results :

Index	Name	Time [Min]	Quantity [% Area]	Height [mAU]	Area [mAU.Min]	Area [%]
1	UNKNOWN	23.96	56.57	716.0	675.4	56.571
2	UNKNOWN	26.90	43.43	426.6	518.5	43.429
Total			100.00	1142.6	1193.9	100.000

→ -13% ee

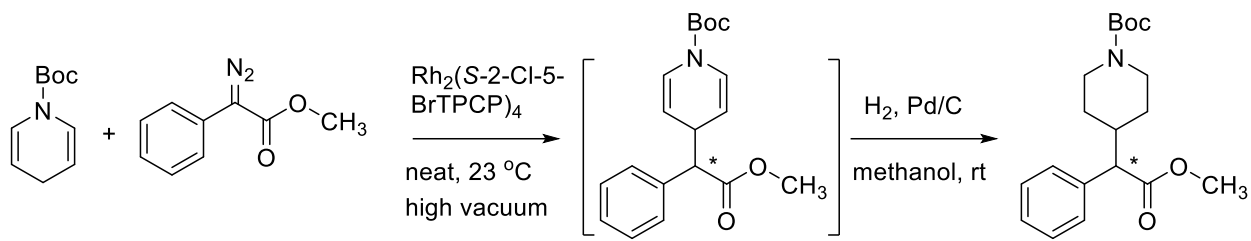
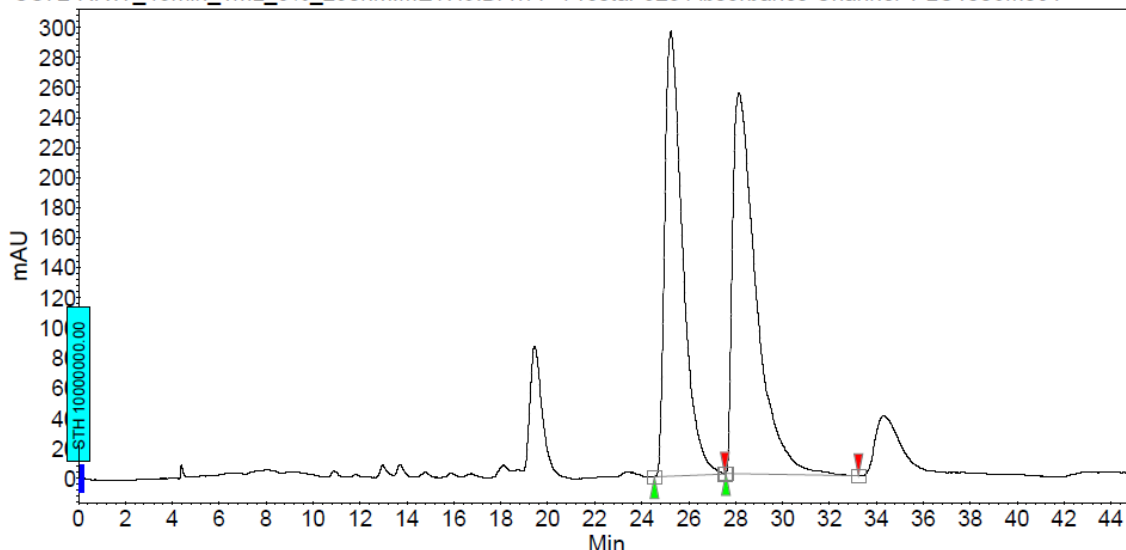


(Table S4, entry 13)

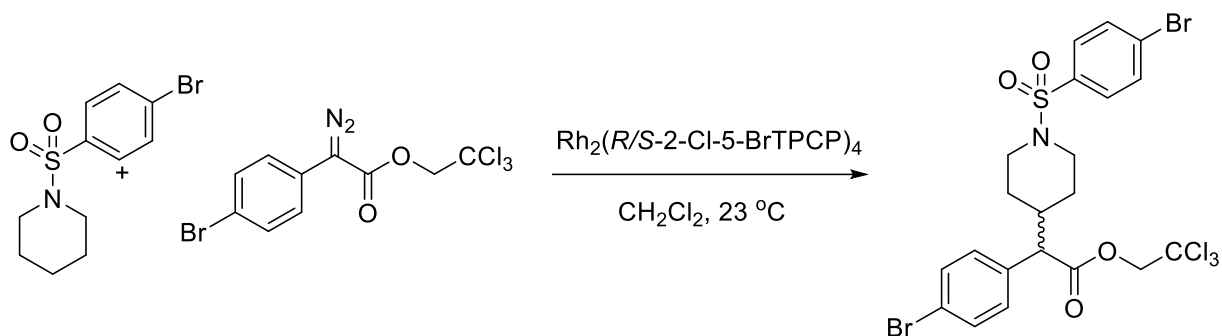
US72-RRW_45min_1mL_5%_230nm.METH9.DATA - Prostar 325 Absorbance Channel 1 LC1006M831



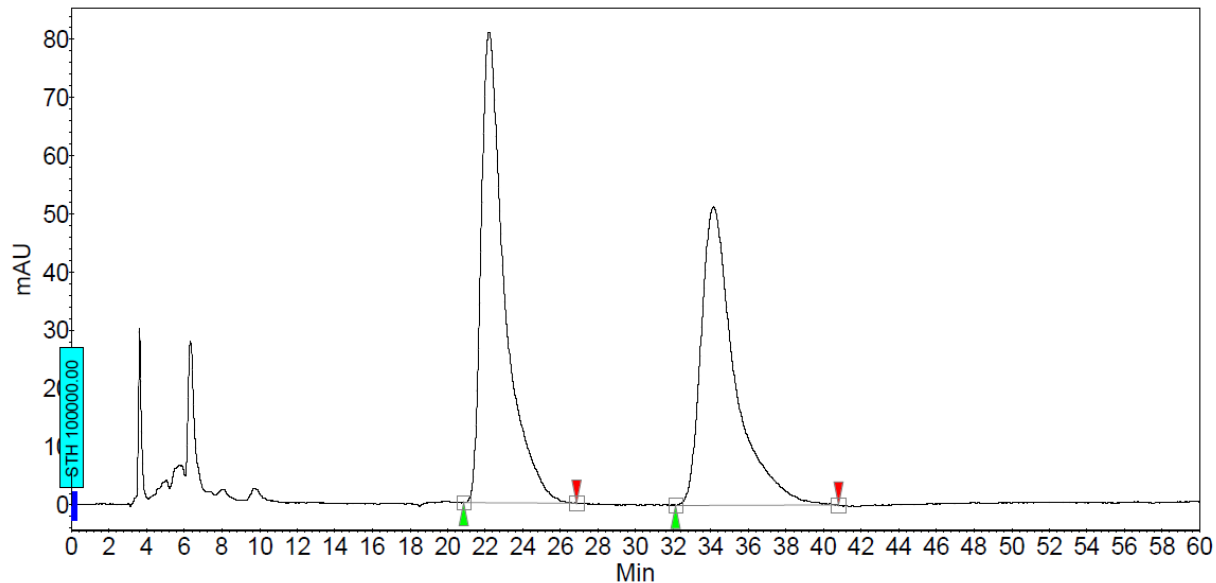
Peak results :

Index	Name	Time [Min]	Quantity [% Area]	Height [mAU]	Area [mAU.Min]	Area [%]
1	UNKNOWN	25.24	46.98	295.8	261.7	46.975
2	UNKNOWN	28.14	53.02	252.8	295.4	53.025
Total			100.00	548.6	557.1	100.000

→ 6% ee



WL-N9-96c-C4-OD-1-15%-230nm-60min-2.DATA - Prostar 325 Absorbance Channel 2 LC1006M831



Peak results :

Index	Name	Time [Min]	Quantity [% Area]	Height [mAU]	Area [mAU.Min]	Area % [%]
1	UNKNOWN	22.21	52.56	80.8	118.0	52.557
2	UNKNOWN	34.15	47.44	51.2	106.5	47.443
Total			100.00	132.0	224.5	100.000

Racemic standard

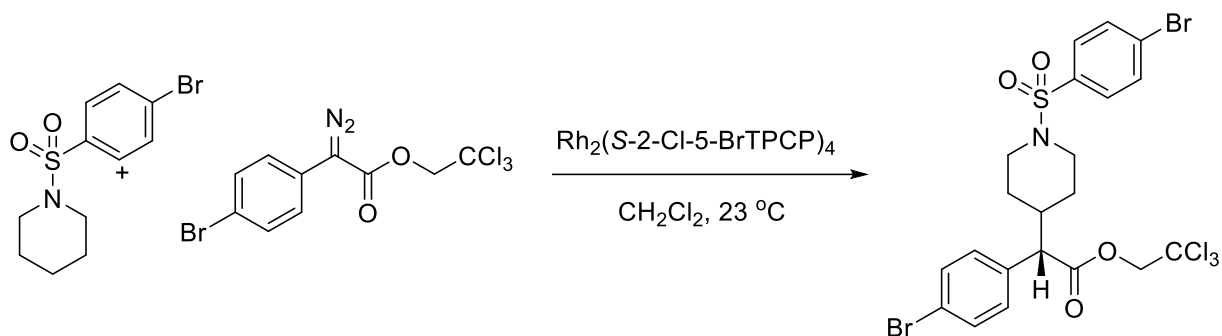
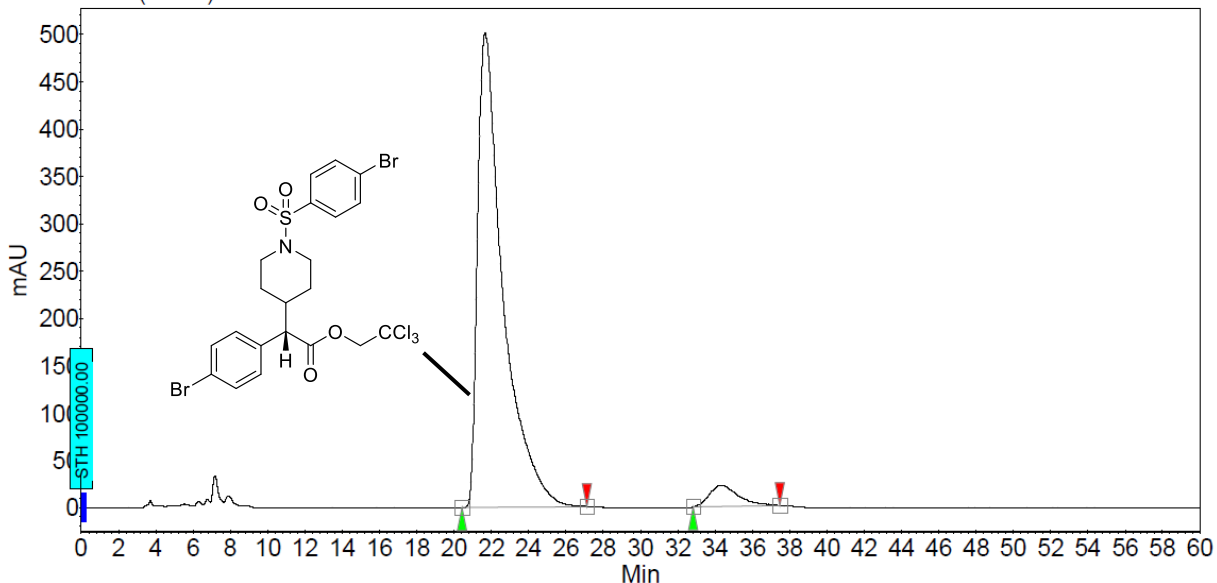


(Table 4, entry 4) (Table S5, entry 5)

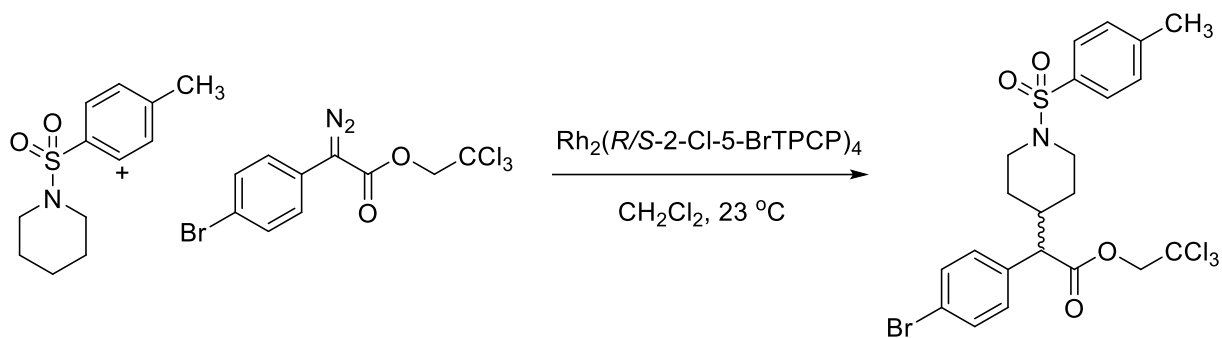
WL-N9-82-C4(f2030)-OD-1-15%-230nm-60min-14.DATA - Prostar 325 Absorbance Channel 2 LC1006M831



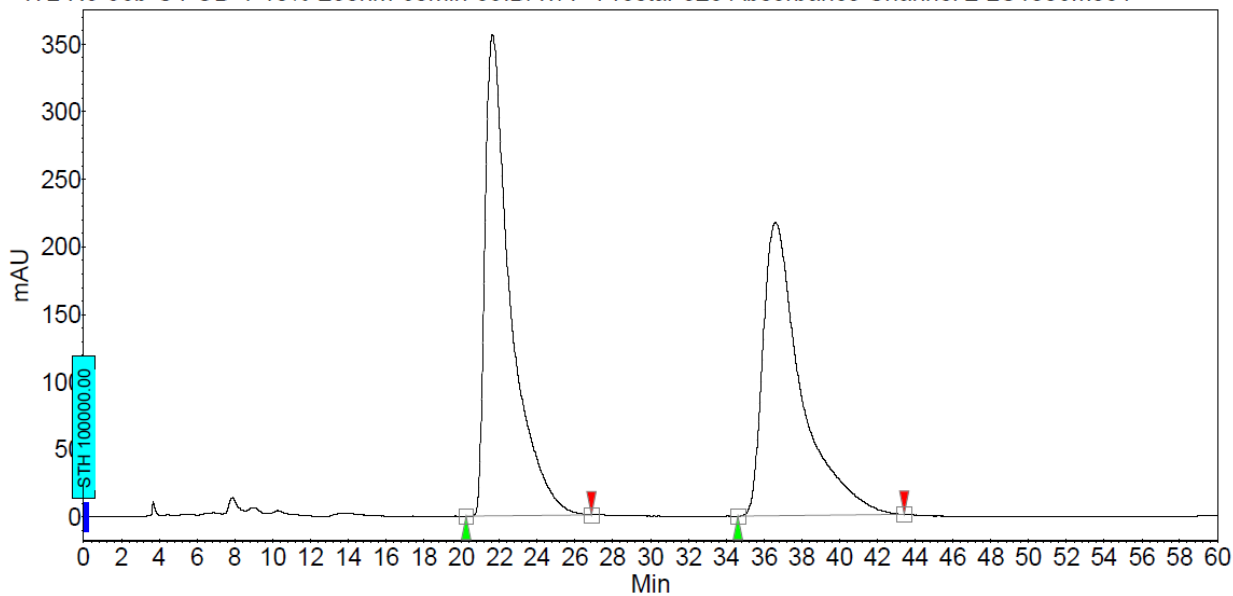
Peak results :

Index	Name	Time [Min]	Quantity [% Area]	Height [mAU]	Area [mAU.Min]	Area [%]
1	UNKNOWN	21.66	95.12	501.8	791.9	95.123
2	UNKNOWN	34.30	4.88	22.4	40.6	4.877
Total			100.00	524.2	832.5	100.000

→ 90% ee



WL-N9-96b-C4-OD-1-10%-230nm-60min-39.DATA - Prostar 325 Absorbance Channel 2 LC1006M831



Peak results :

Index	Name	Time [Min]	Quantity [% Area]	Height [mAU]	Area [mAU.Min]	Area % [%]
1	UNKNOWN	21.64	52.44	357.0	558.3	52.437
2	UNKNOWN	36.61	47.56	217.3	506.4	47.563
Total			100.00	574.2	1064.7	100.000

Racemic standard

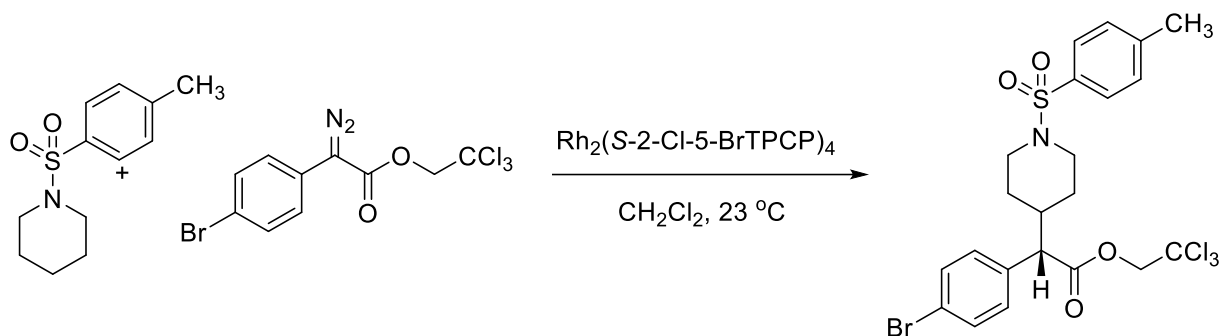
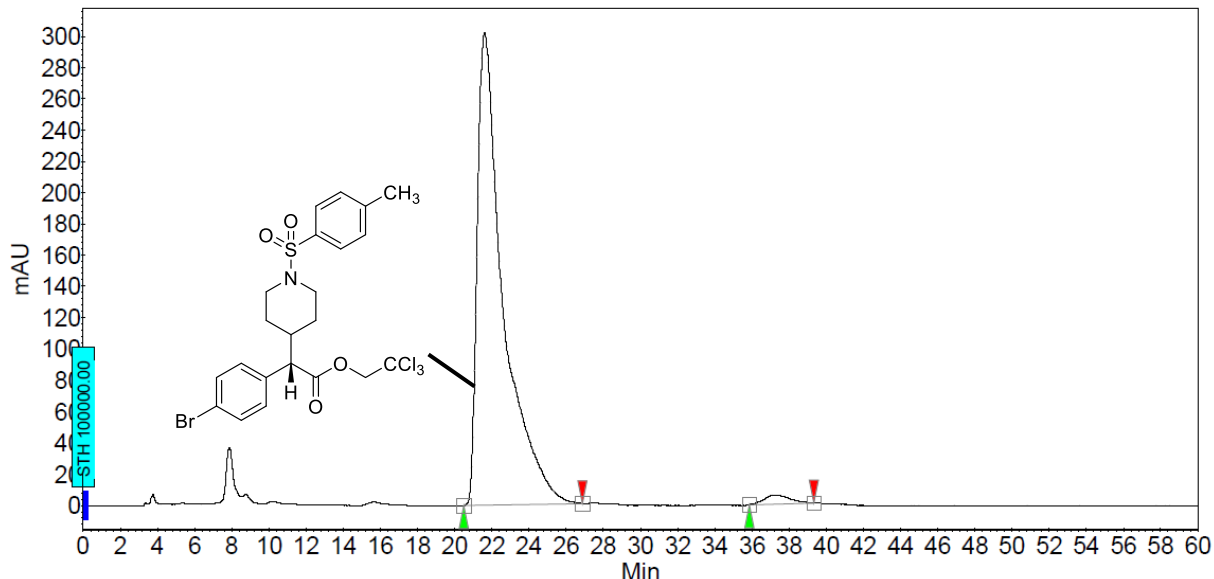


(Table 4, entry 5) (Table S5, entry 6)

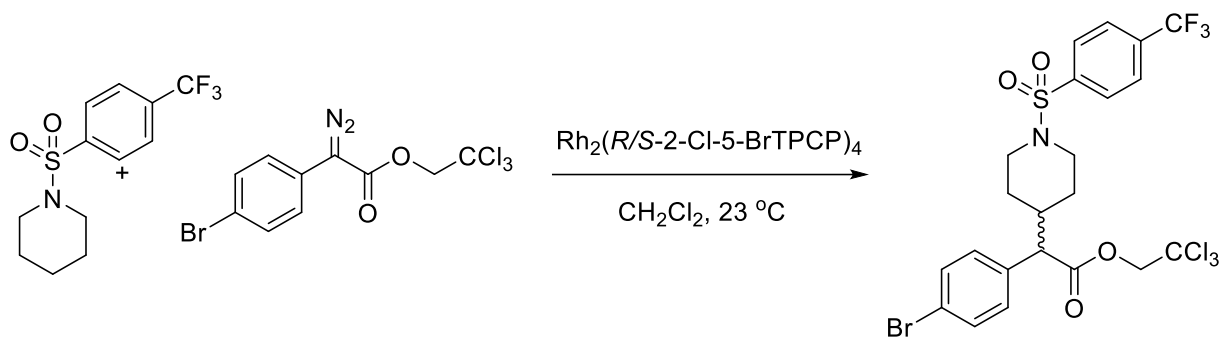
WL-N9-80-2nd-f37-C4-OD-1-10%-230nm-60min-87.DATA - Prostar 325 Absorbance Channel 2 LC1006M831



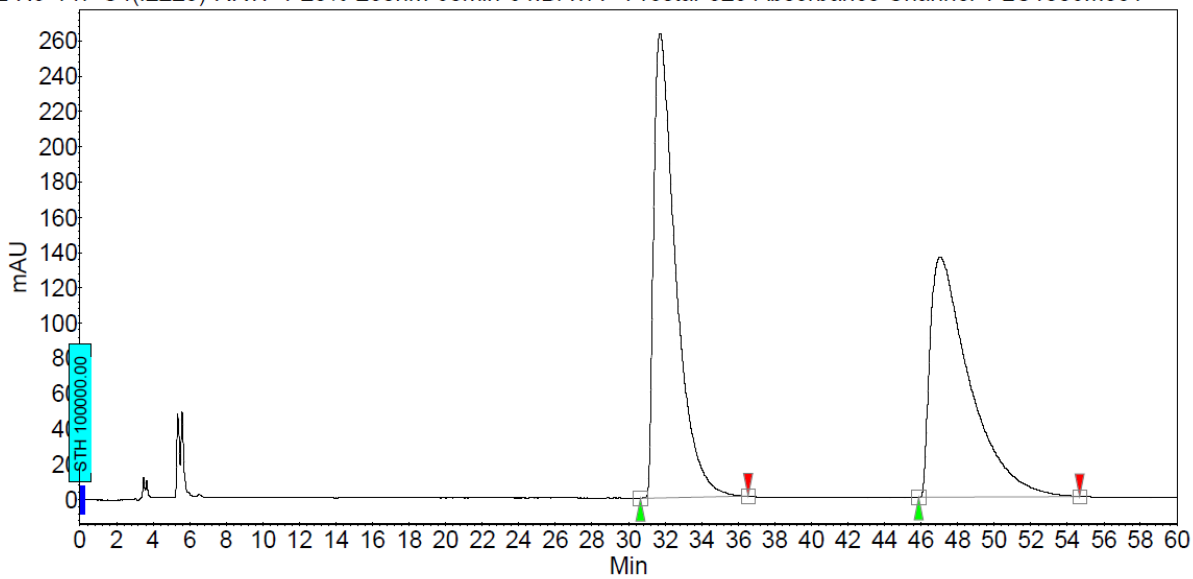
Peak results :

Index	Name	Time [Min]	Quantity [% Area]	Height [mAU]	Area [mAU.Min]	Area % [%]
1	UNKNOWN	21.61	98.15	302.2	486.7	98.149
2	UNKNOWN	37.29	1.85	5.7	9.2	1.851
Total			100.00	308.0	495.9	100.000

→ 96% ee



WL-N9-147-C4(f2223)-RRW-1-20%-230nm-60min-64.DATA - Prostar 325 Absorbance Channel 1 LC1006M831



Peak results :

Index	Name	Time [Min]	Quantity % Area	Height [mAU]	Area [mAU·Min]	Area % [%]
1	UNKNOWN	31.73	51.86	263.1	367.2	51.857
2	UNKNOWN	47.04	48.14	136.1	340.9	48.143
Total			100.00	399.3	708.0	100.000

Racemic standard

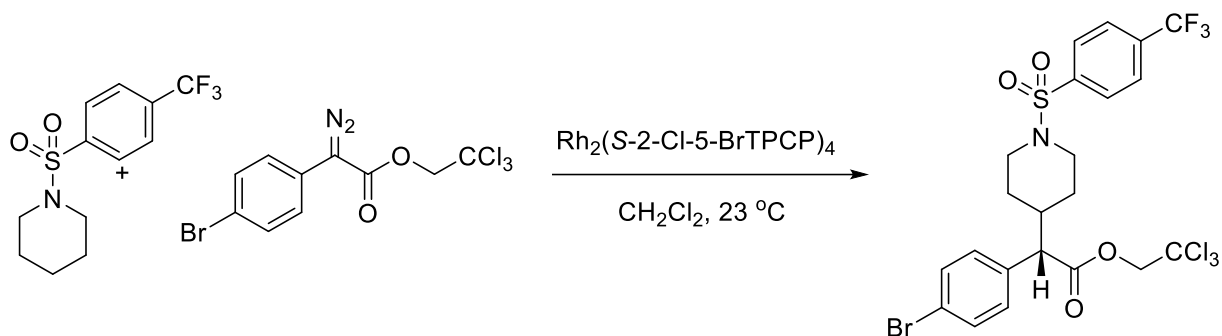
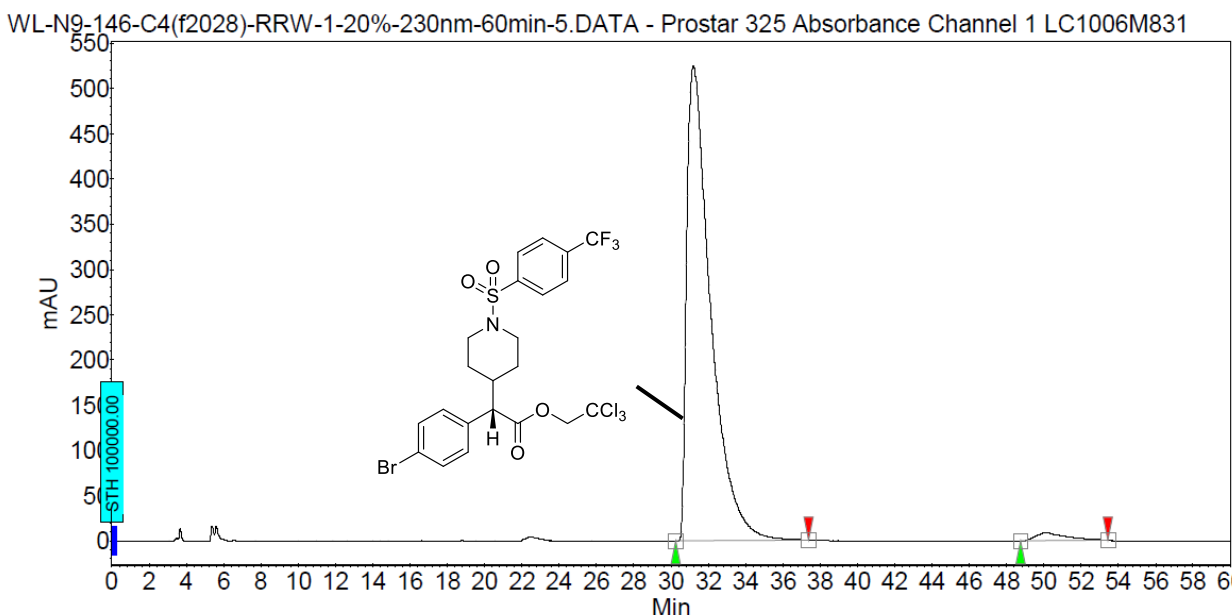
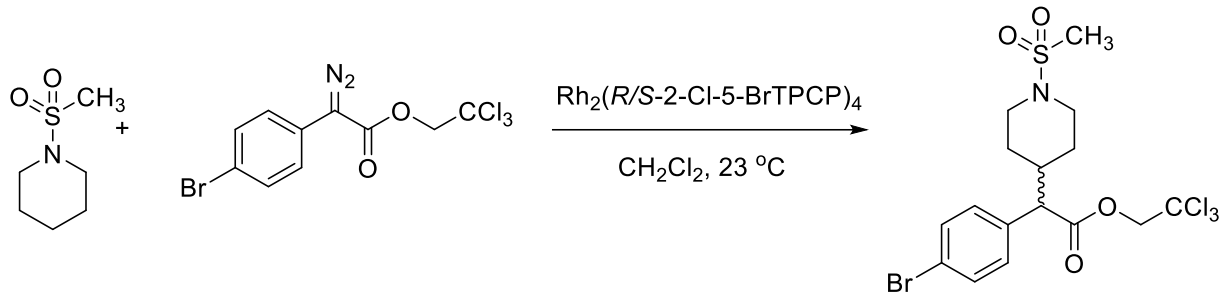


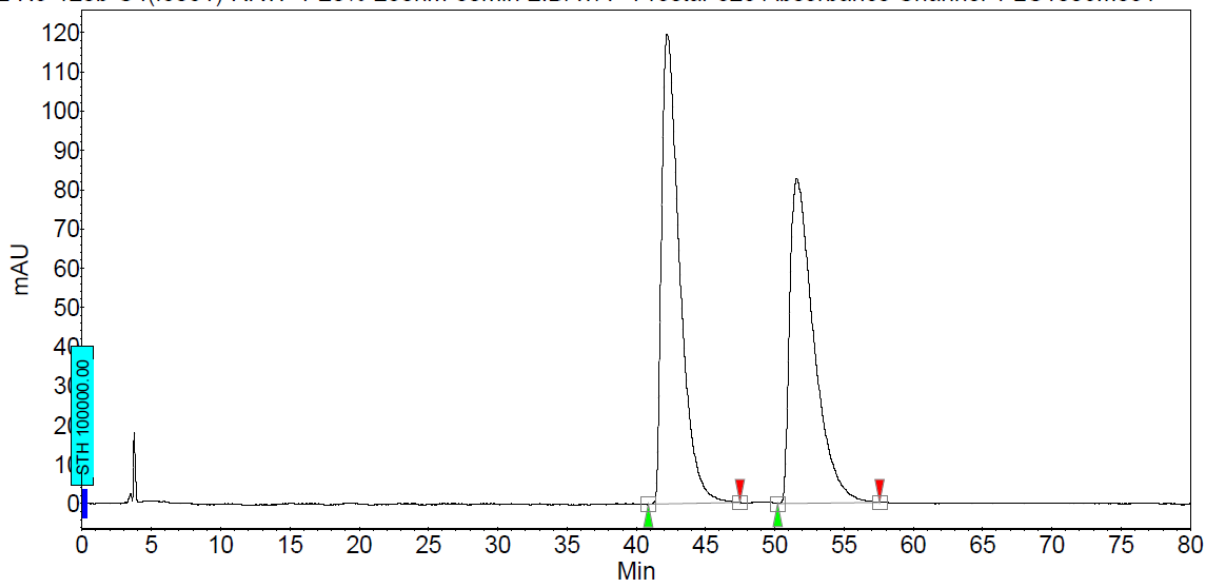
(Table 4, entry 6) (Table S5, entry 8)



→ 96% ee



WL-N9-120b-C4(f5051)-RRW-1-20%-230nm-80min-2.DATA - Prostar 325 Absorbance Channel 1 LC1006M831



Peak results :

Index	Name	Time [Min]	Quantity [% Area]	Height [mAU]	Area [mAU.Min]	Area % [%]
1	UNKNOWN	42.24	52.23	119.7	182.1	52.227
2	UNKNOWN	51.59	47.77	82.7	166.5	47.773
Total			100.00	202.4	348.6	100.000

Racemic standard

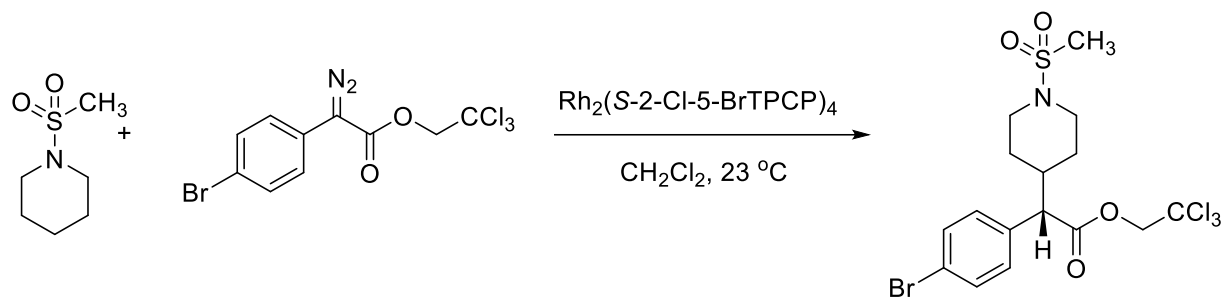
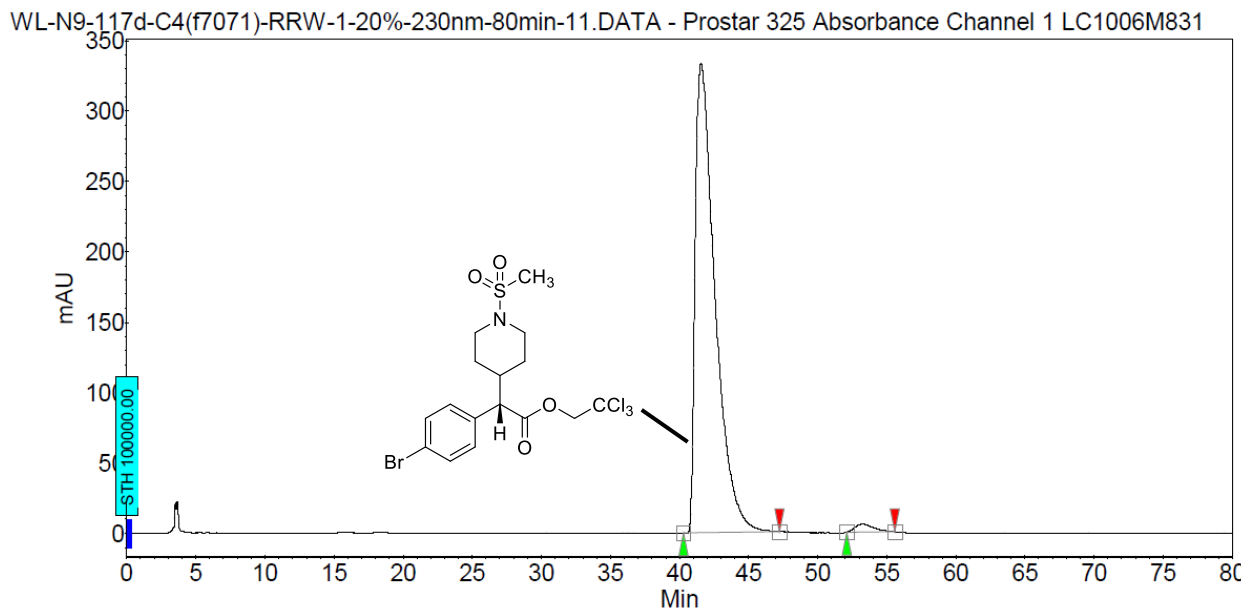


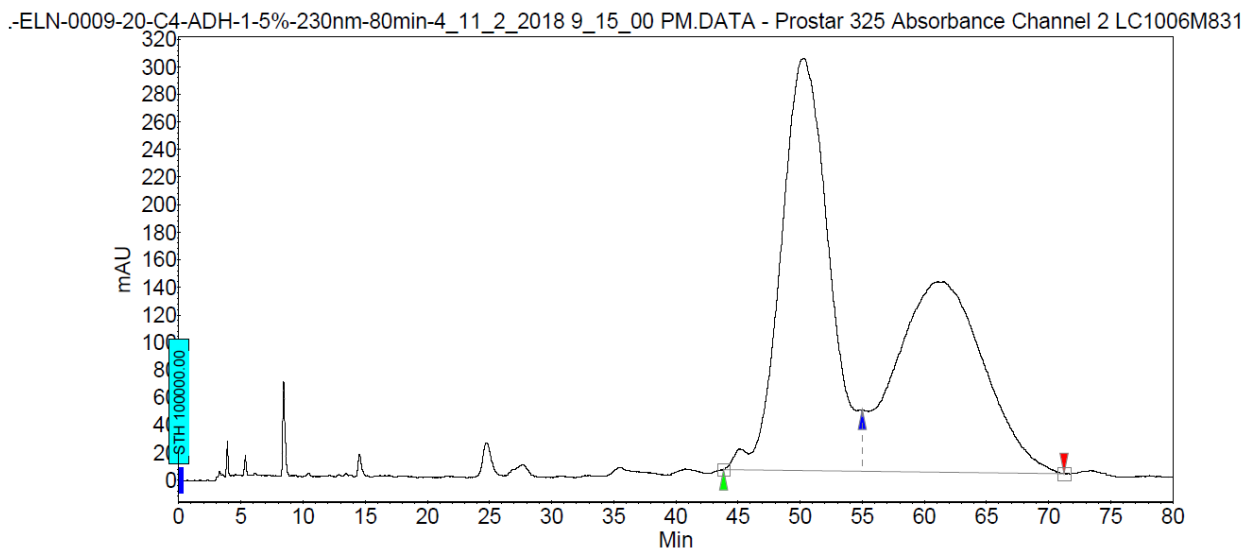
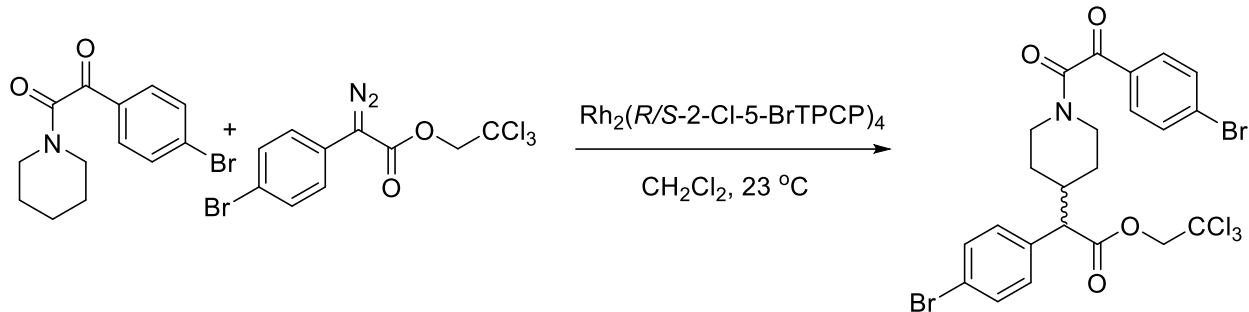
(Table 4, entry 7) (Table S5, entry 10)



Peak results :

Index	Name	Time [Min]	Quantity % Area	Height [mAU]	Area [mAU.Min]	Area % [%]
1	UNKNOWN	41.56	98.41	333.7	556.1	98.413
2	UNKNOWN	53.30	1.59	5.6	9.0	1.587
Total			100.00	339.3	565.1	100.000

→ 97% ee



Peak results :

Index	Name	Time [Min]	Quantity [% Area]	Height [mAU]	Area [mAU.Min]	Area % [%]
1	UNKNOWN	50.31	53.96	299.2	1330.2	53.957
2	UNKNOWN	61.58	46.04	138.3	1135.1	46.043
Total			100.00	437.5	2465.3	100.000

Racemic standard

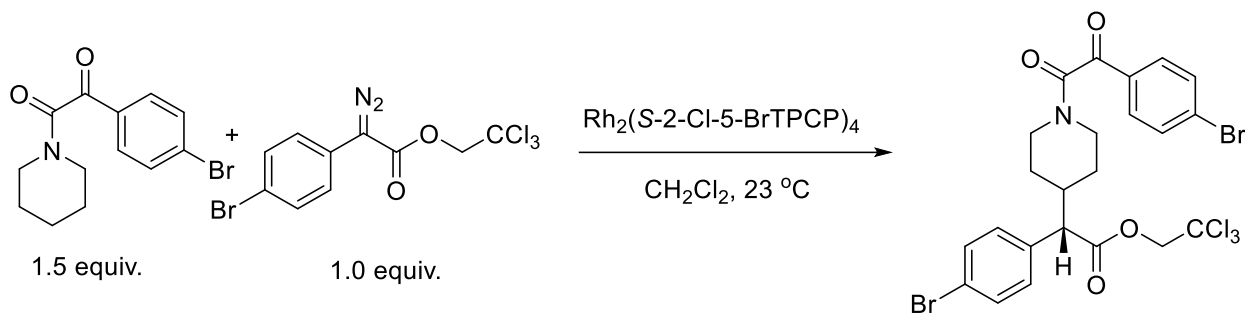
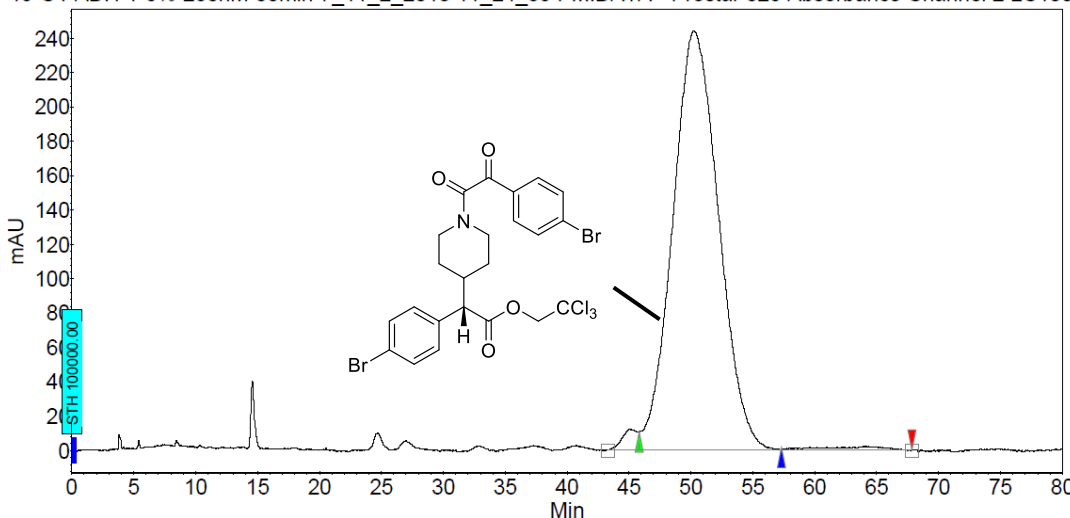


(Table 4, entry 8) (Table S5, entry 11)

-ELN-0009-19-C4-ADH-1-5%-230nm-80min-7_11_2_2018 11_24_35 PM.DATA - Prostar 325 Absorbance Channel 2 LC1006M831



Peak results :

Index	Name	Time [Min]	Quantity [% Area]	Height [mAU]	Area [mAU.Min]	Area % [%]
1	UNKNOWN	50.19	98.74	244.1	1051.0	98.743
2	UNKNOWN	64.18	1.26	2.4	13.4	1.257
Total			100.00	246.5	1064.4	100.000

→ 97% ee

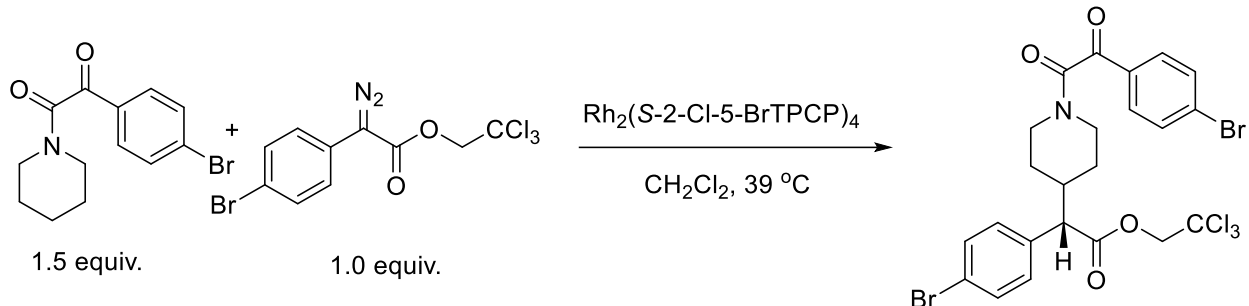
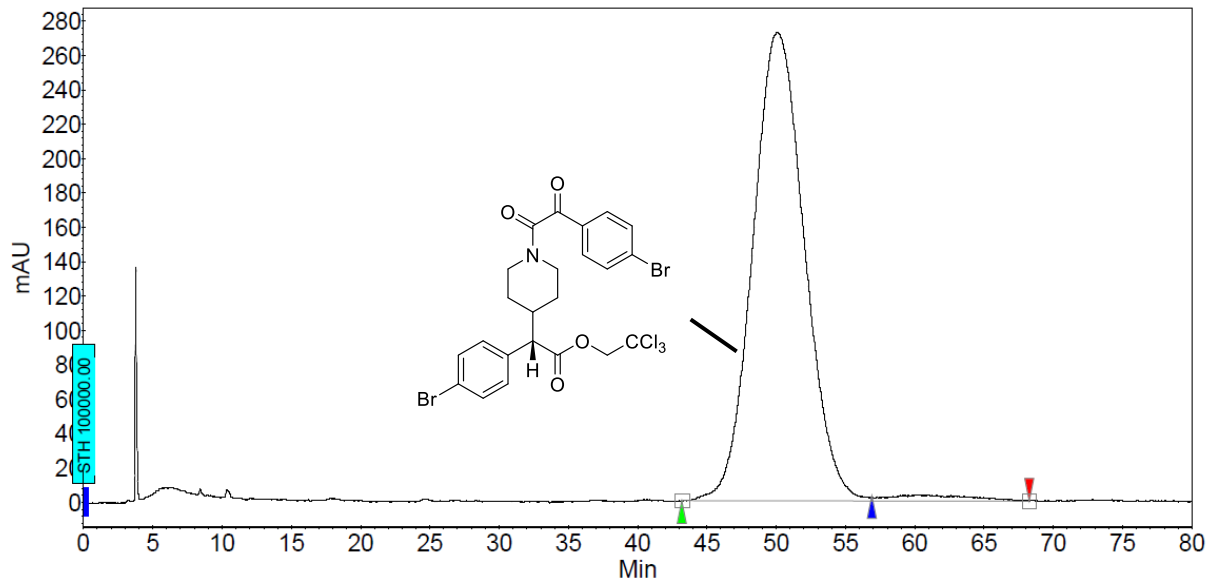


(Table 4, entry 9) (Table S5, entry 12)

WL-ELN-0009-30-C4-ADH-1-5%-230nm-80min-10.DATA - Prostar 325 Absorbance Channel 2 LC1006M831



Peak results :

Index	Name	Time [Min]	Quantity [% Area]	Height [mAU]	Area [mAU.Min]	Area [%]
1	UNKNOWN	50.11	98.02	272.6	1177.5	98.018
2	UNKNOWN	60.24	1.98	3.4	23.8	1.982
Total			100.00	276.0	1201.3	100.000

97% ee

→

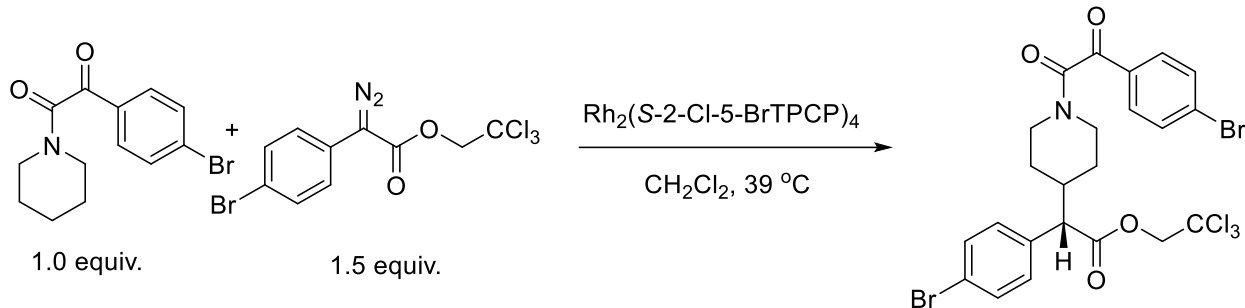
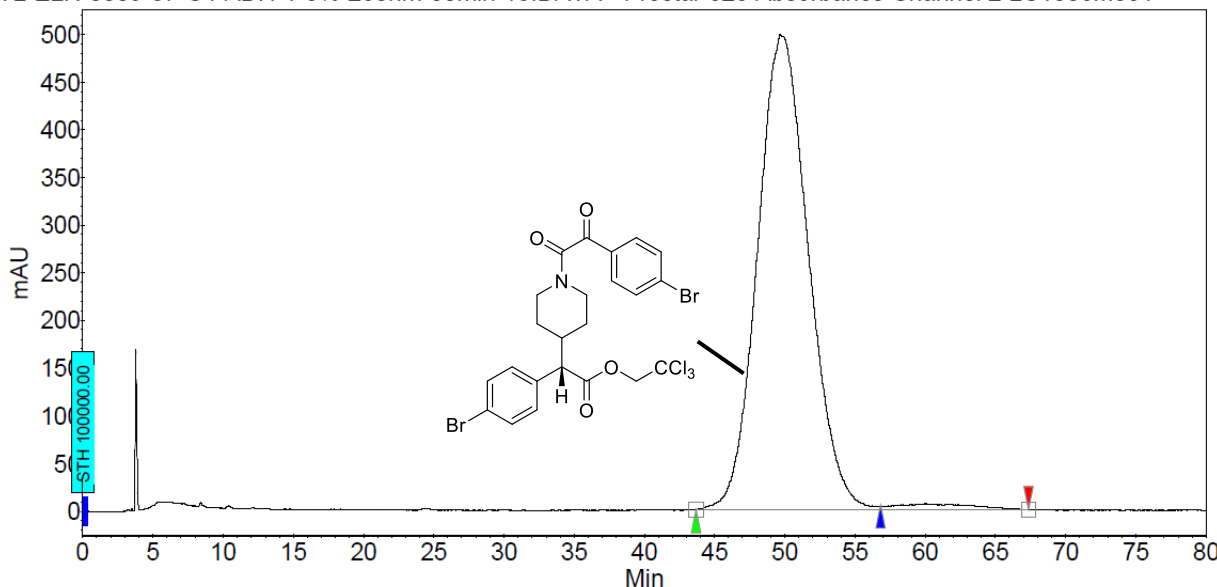


(Table 4, entry 10) (Table S5, entry 13)

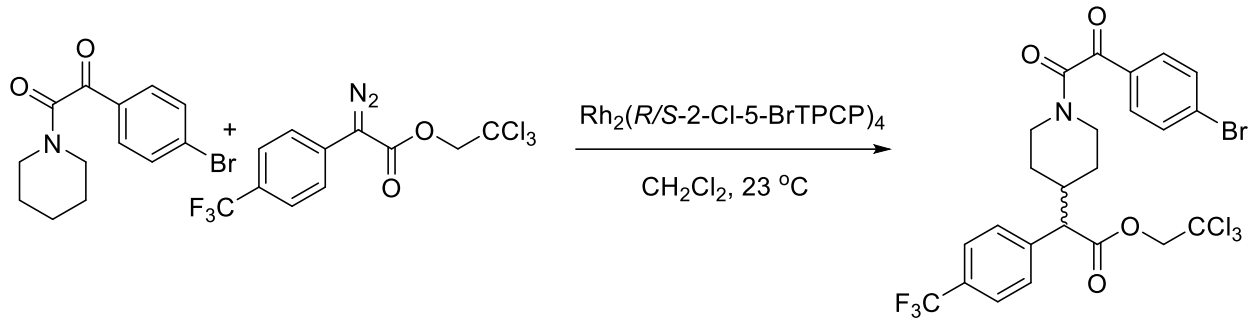
WL-ELN-0009-37-C4-ADH-1-5%-230nm-80min-13.DATA - Prostar 325 Absorbance Channel 2 LC1006M831



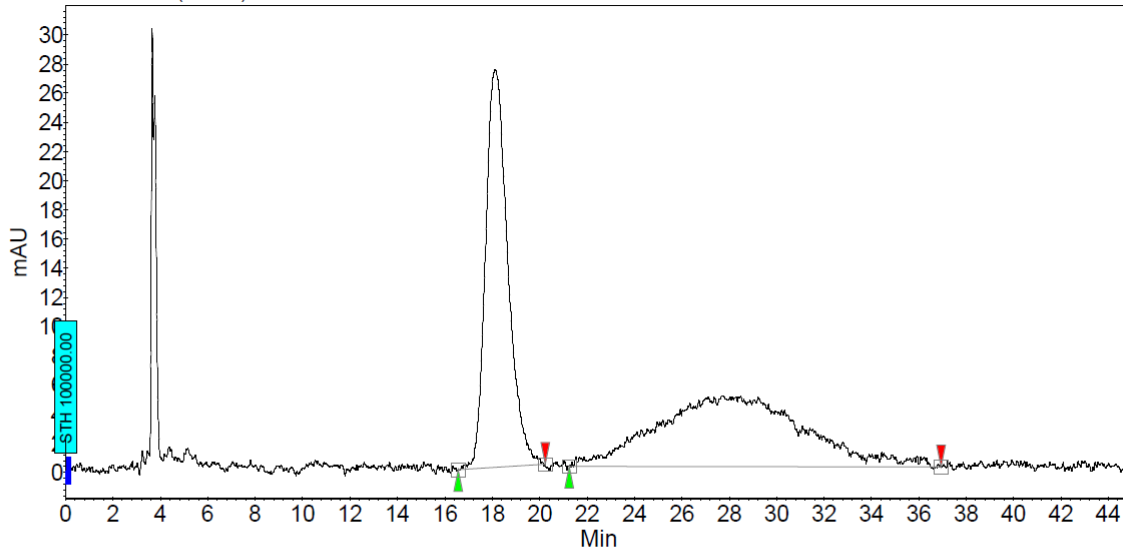
Peak results :

Index	Name	Time [Min]	Quantity [% Area]	Height [mAU]	Area [mAU.Min]	Area % [%]
1	UNKNOWN	49.67	98.13	498.7	2090.5	98.134
2	UNKNOWN	60.07	1.87	5.9	39.8	1.866
Total			100.00	504.6	2130.3	100.000

→ 97% ee



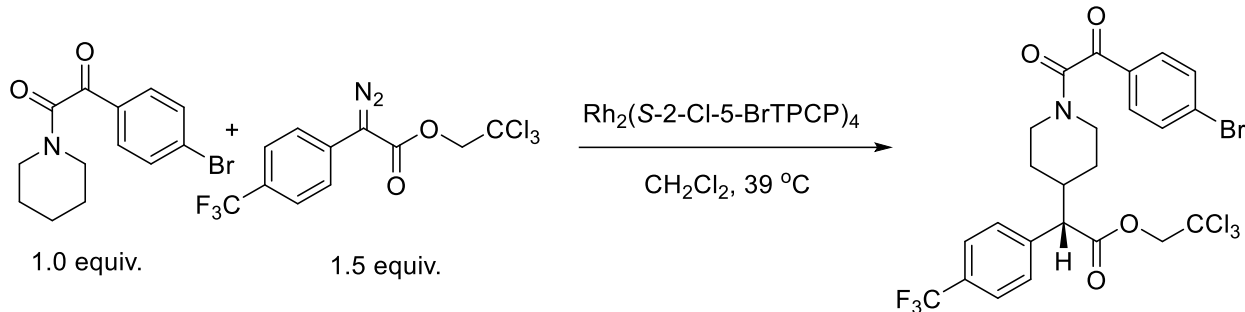
WL-ELN-0009-50rac-C4(f7475)-ODH-1-10%-230nm-45min-17.DATA - Prostar 325 Absorbance Channel 2 LC1006M831



Peak results :

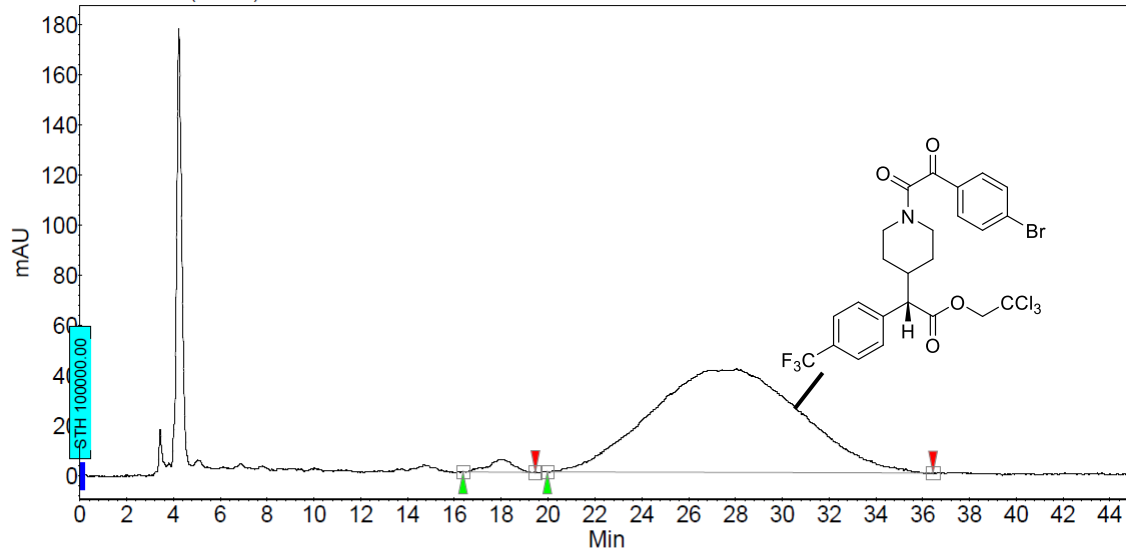
Index	Name	Time [Min]	Quantity [% Area]	Height [mAU]	Area [mAU.Min]	Area % [%]
1	UNKNOWN	18.12	46.14	27.3	29.7	46.135
2	UNKNOWN	27.73	53.86	4.9	34.7	53.865
Total			100.00	32.2	64.4	100.000

Racemic standard



(Scheme 4, 13f)

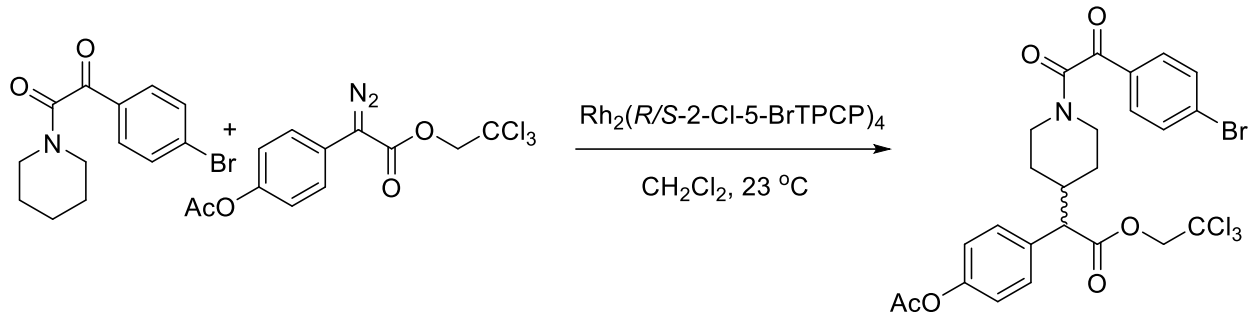
WL-ELN-0009-50chiral-C4(f3846)-ODH-1-10%-230nm-45min-20.DATA - Prostar 325 Absorbance Channel 2 LC1006M831



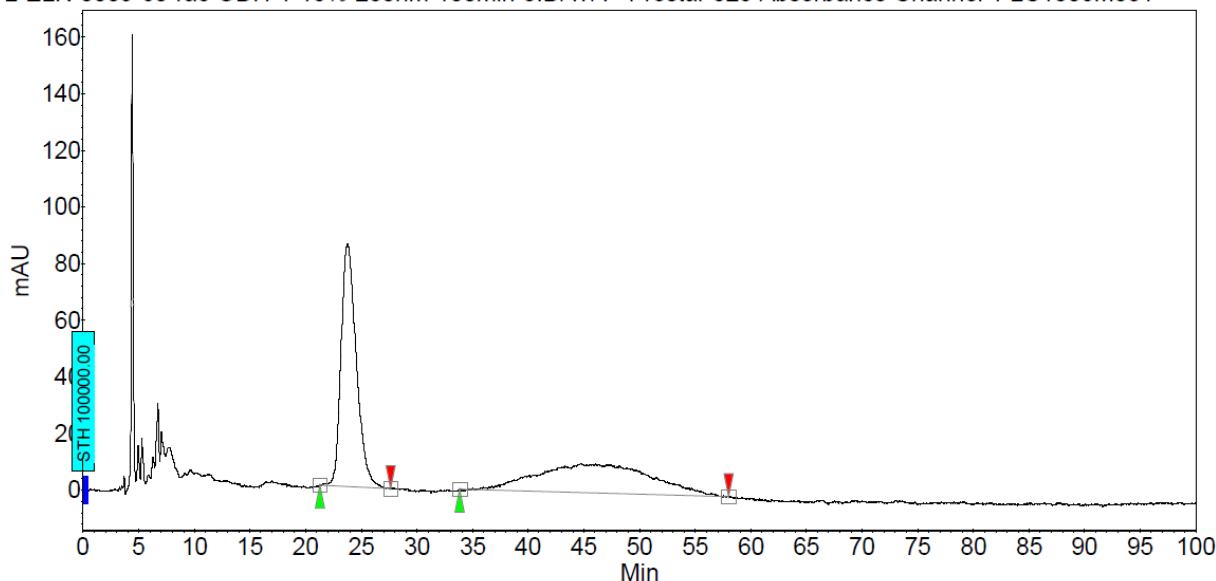
Peak results :

Index	Name	Time [Min]	Quantity [% Area]	Height [mAU]	Area [mAU.Min]	Area % [%]
1	UNKNOWN	18.09	2.04	5.2	6.3	2.039
2	UNKNOWN	28.06	97.96	41.2	304.7	97.961
Total			100.00	46.5	311.1	100.000

→ 96% ee



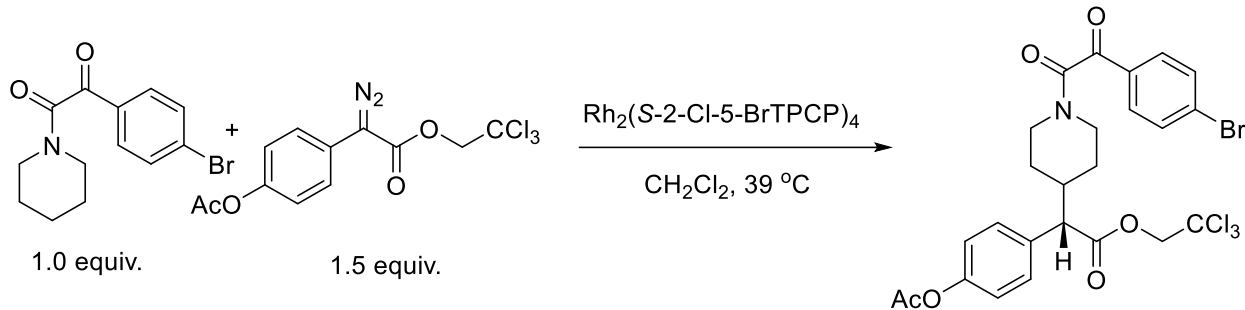
WL-ELN-0009-60-rac-ODH-1-15%-230nm-100min-3.DATA - Prostar 325 Absorbance Channel 1 LC1006M831



Peak results :

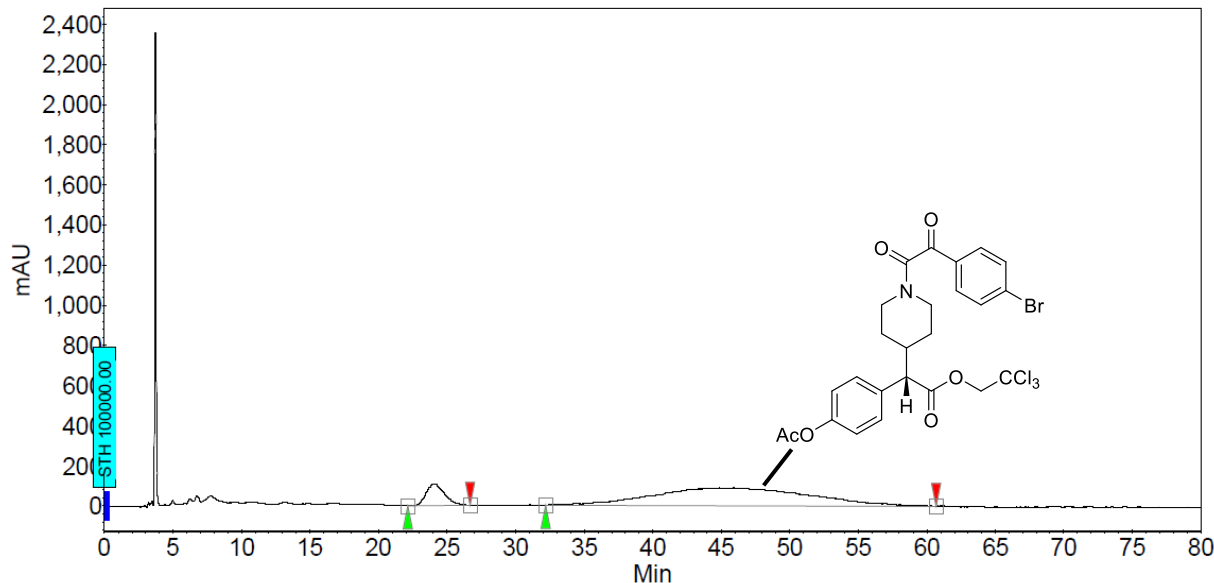
Index	Name	Time [Min]	Quantity [% Area]	Height [mAU]	Area [mAU.Min]	Area % [%]
1	UNKNOWN	23.78	52.58	85.7	136.2	52.576
2	UNKNOWN	46.05	47.42	10.4	122.8	47.424
Total			100.00	96.1	259.0	100.000

Racemic standard



(Scheme 4, 13g)

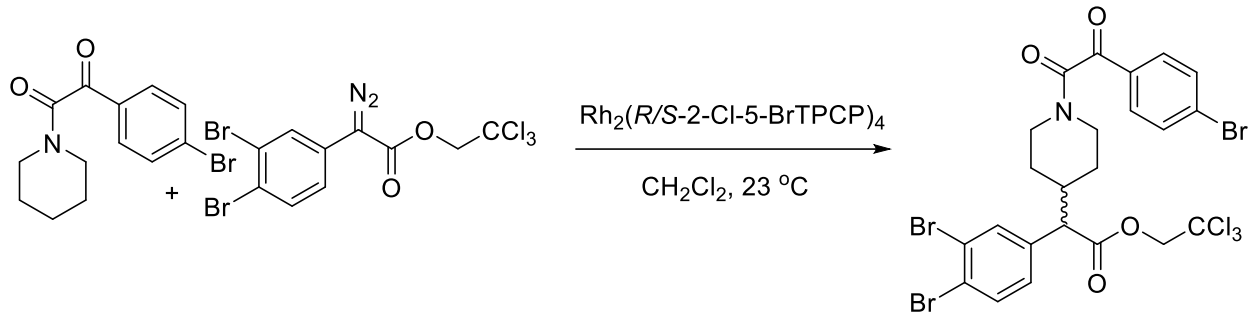
WL-ELN-0009-60-ODH-1-15%-230nm-80min-68.DATA - Prostar 325 Absorbance Channel 1 LC1006M831



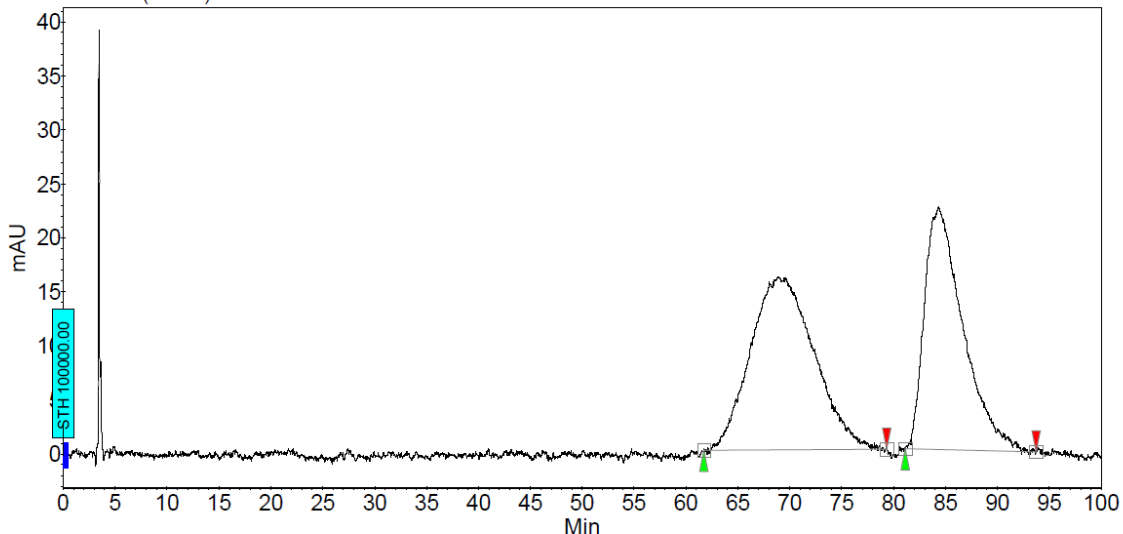
Peak results :

Index	Name	Time [Min]	Quantity [% Area]	Height [mAU]	Area [mAU.Min]	Area % [%]
1	UNKNOWN	23.99	12.50	107.4	167.5	12.499
2	UNKNOWN	45.95	87.50	89.9	1172.7	87.501
Total			100.00	197.3	1340.2	100.000

→ 75% ee



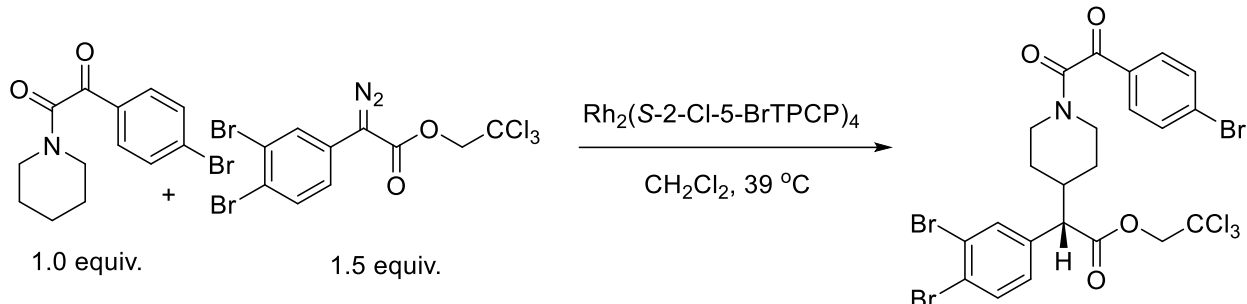
WL-ELN-0009-51rac-C4(f4445)-newRRW-1-20%-230nm-100min-23.DATA - Prostar 325 Absorbance Channel 2 LC1006M831



Peak results :

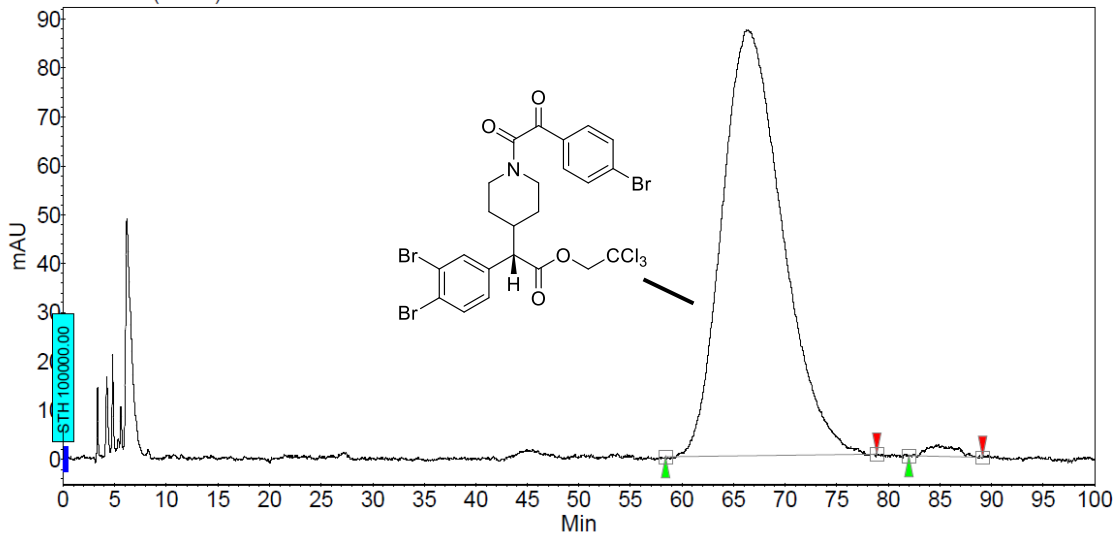
Index	Name	Time [Min]	Quantity [% Area]	Height [mAU]	Area [mAU.Min]	Area % [%]
1	UNKNOWN	68.88	54.19	16.0	114.1	54.189
2	UNKNOWN	84.32	45.81	22.4	96.5	45.811
Total			100.00	38.5	210.6	100.000

Racemic standard



(Scheme 4, **13h**)

VL-ELN-0009-51chiral-C4(f5568)-newRRW-1-20%-230nm-100min-26.DATA - Prostar 325 Absorbance Channel 2 LC1006M831



Peak results :

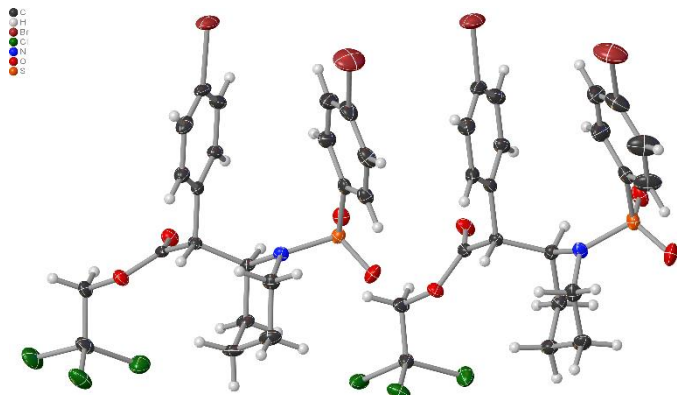
Index	Name	Time [Min]	Quantity [% Area]	Height [mAU]	Area [mAU.Min]	Area % [%]
1	UNKNOWN	66.36	98.76	87.2	589.1	98.760
2	UNKNOWN	84.85	1.24	2.6	7.4	1.240
Total			100.00	89.8	596.5	100.000

→ 98% ee

10. X-Ray Crystallographic Data of the Products for Absolute Stereochemistry

10.1. X-Ray Crystallographic Data for 6a

Crystal Data and Experimental



Experimental. Single colourless needle-shaped crystals of **WL-ELN09-38R-d1** were recrystallised from DCM by slow evaporation. A suitable crystal $0.49 \times 0.10 \times 0.05$ mm³ was selected and mounted on a loop with paratone oil on an XtaLAB Synergy, Dualflex, HyPix diffractometer. The crystal was kept at a steady $T = 111.4(2)$ K during data collection. The structure was solved with the **ShelXT** (Sheldrick, 2015) structure solution program using the Intrinsic Phasing solution method and by using **Olex2** (Dolomanov et al., 2009) as the graphical interface. The model was refined with version 2018/3 of **ShelXL** (Sheldrick, 2015) using Least Squares minimisation.

Crystal Data. $C_{21}H_{20}Br_2Cl_3NO_4S$, $M_r = 648.61$, orthorhombic, $P2_12_12_1$ (No. 19), $a = 6.15074(9)$ Å, $b = 26.3980(4)$ Å, $c = 30.1139(5)$ Å, $a = b = g = 90^\circ$, $V = 4889.51(13)$ Å³, $T = 111.4(2)$ K, $Z = 8$, $Z' = 2$, $m(\text{CuK}_\alpha) = 8.276$ mm⁻¹, 53908 reflections measured, 9424 unique ($R_{int} = 0.0555$) which were used in all calculations. The final wR_2 was 0.0645 (all data) and R_I was 0.0262 ($I > 2\sigma(I)$).

Compound	WL-ELN09-38R-d1
Formula	$C_{21}H_{20}Br_2Cl_3NO_4S$
$D_{\text{calc.}}/\text{g cm}^{-3}$	1.762
m/mm^{-1}	8.276
Formula Weight	648.61
Colour	colourless
Shape	needle
Size/mm ³	$0.49 \times 0.10 \times 0.05$
T/K	111.4(2)
Crystal System	orthorhombic
Flack Parameter	-0.003(6)
Hooft Parameter	-0.007(6)
Space Group	$P2_12_12_1$
$a/\text{\AA}$	6.15074(9)
$b/\text{\AA}$	26.3980(4)
$c/\text{\AA}$	30.1139(5)
a°	90
b°	90
g°	90
$V/\text{\AA}^3$	4889.51(13)
Z	8
Z'	2
Wavelength/Å	1.54184
Radiation type	CuK_α
$Q_{\min}/^\circ$	2.935
$Q_{\max}/^\circ$	72.944
Measured Refl.	53908
Independent Refl.	9424
Reflections with $I > 2\sigma(I)$	9037
R_{int}	0.0555
Parameters	577
Restraints	84
Largest Peak	0.650
Deepest Hole	-0.502
GooF	1.021
wR_2 (all data)	0.0645
wR_2	0.0633
R_I (all data)	0.0281
R_I	0.0262

Structure Quality Indicators

Reflections: $d_{\text{min}}(\text{Cu})$ 0.81 I/σ 29.6 R_{int} 5.55% completeness 100% (IUCr) 100%

Refinement: Shift 0.001 Max Peak 0.7 Min Peak -0.5 Goof 1.021 Flack -0.003(6)

A colourless needle-shaped crystal with dimensions $0.49 \times 0.10 \times 0.05 \text{ mm}^3$ was mounted on a loop with paratone oil. Data were collected using an XtaLAB Synergy, Dualflex, HyPix diffractometer equipped with an Oxford Cryosystems low-temperature device operating at $T = 111.4(2) \text{ K}$.

Data were measured using w scans using CuK_α radiation. The total number of runs and images was based on the strategy calculation from the program **CrysAlisPro** (Rigaku, V1.171.40.37a, 2019). The maximum resolution that was achieved was $Q = 72.944^\circ$ (0.81 \AA).

The diffraction pattern was indexed and the total number of runs and images was based on the strategy calculation from the program **CrysAlisPro** (Rigaku, V1.171.40.37a, 2019) and the unit cell was refined using **CrysAlisPro** (Rigaku, V1.171.40.37a, 2019) on 38372 reflections, 71% of the observed reflections.

Data reduction, scaling and absorption corrections were performed using **CrysAlisPro** (Rigaku, V1.171.40.37a, 2019). The final completeness is 99.90 % out to 72.944° in Q . A numerical absorption correction based on a Gaussian integration over a multifaceted crystal model was performed using **CrysAlisPro** (Rigaku, V1.171.40.37a, 2019). An empirical absorption correction using spherical harmonics as implemented in SCALE3 ABSPACK was also applied. The absorption coefficient m of this material is 8.276 mm^{-1} at this wavelength ($\lambda = 1.542 \text{\AA}$) and the minimum and maximum transmissions are 0.687 and 1.000.

The structure was solved and the space group $P2_12_12_1$ (# 19) determined by the **ShelXT** (Sheldrick, 2015) structure solution program using Intrinsic Phasing and refined by Least Squares using version 2018/3 of **ShelXL** (Sheldrick, 2015). All non-hydrogen atoms were refined anisotropically. Hydrogen atom positions were calculated geometrically and refined using the riding model.

The value of Z' is 2. This means that there are two independent molecules in the asymmetric unit.

The Flack parameter was refined to -0.003(6). Determination of absolute structure using Bayesian statistics on Bijvoet differences using the Olex2 results in -0.007(6). Note: The Flack parameter is used to determine chirality of the crystal studied, the value should be near 0, a value of 1 means that the stereochemistry is wrong and the model should be inverted. A value of 0.5 means that the crystal consists of a racemic mixture of the two enantiomers.

Images of the Crystal on the Diffractometer



C
H
Br
Cl
N
O
S

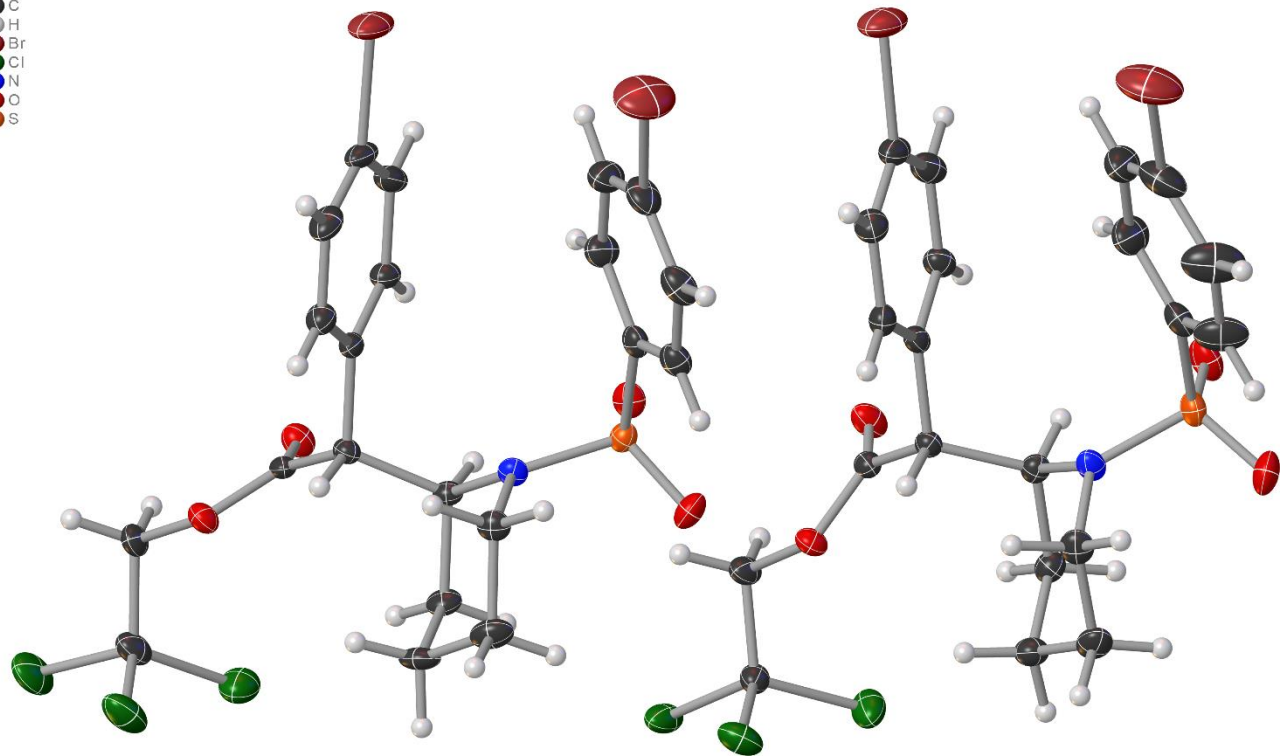


Figure 1: Plot of the asymmetric unit. There are two independent molecules in the asymmetric unit with the same chirality.

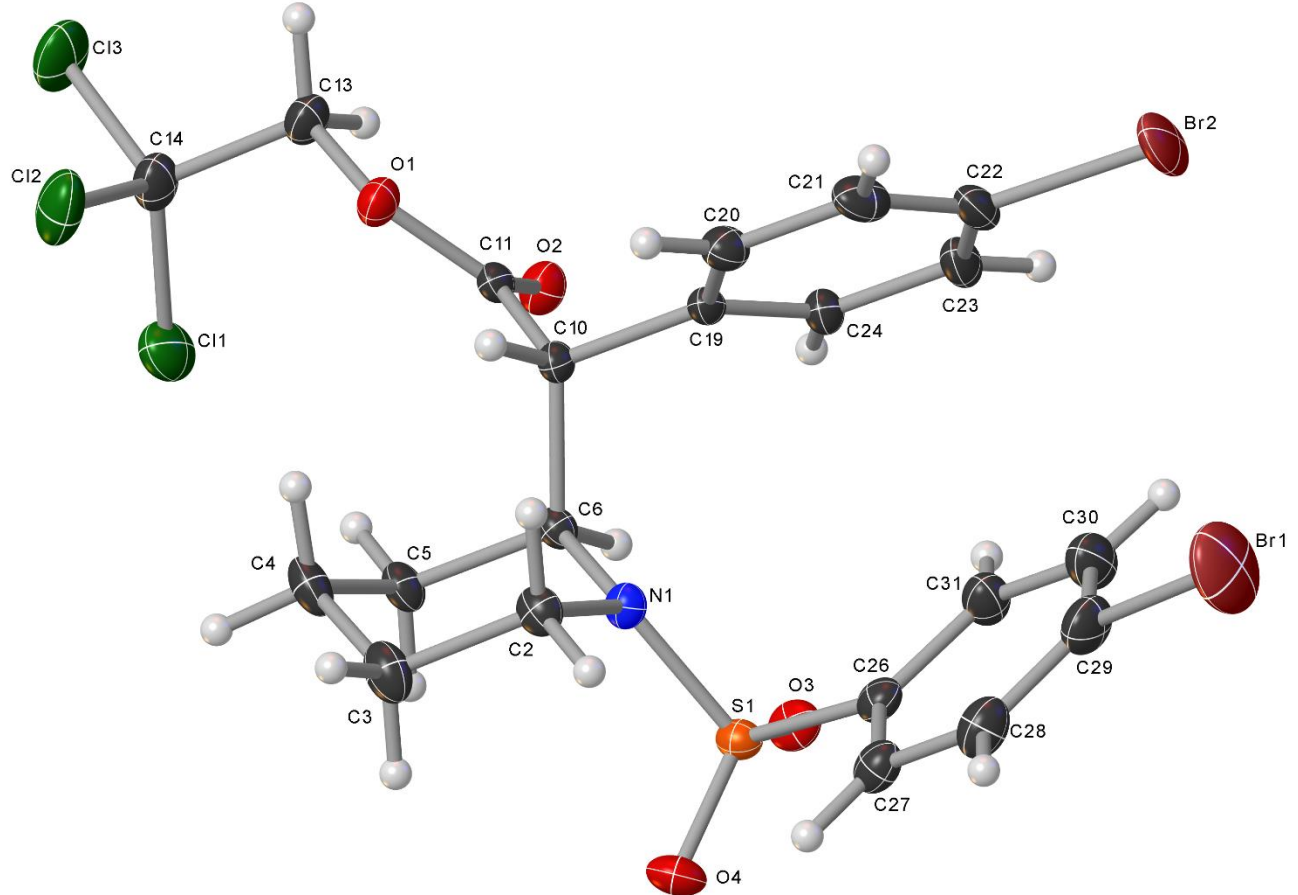
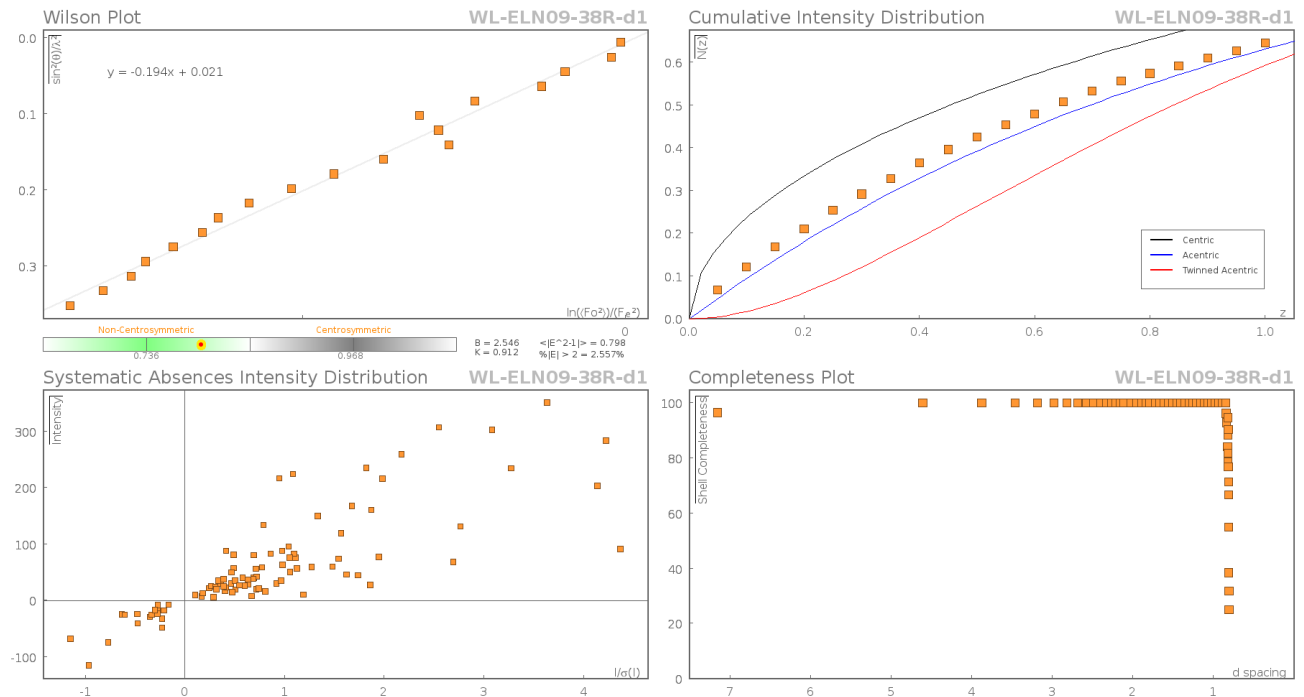
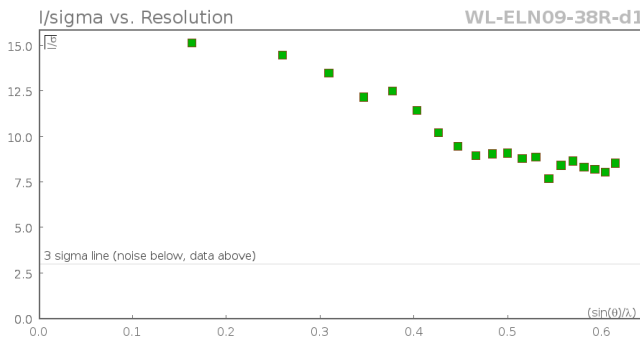


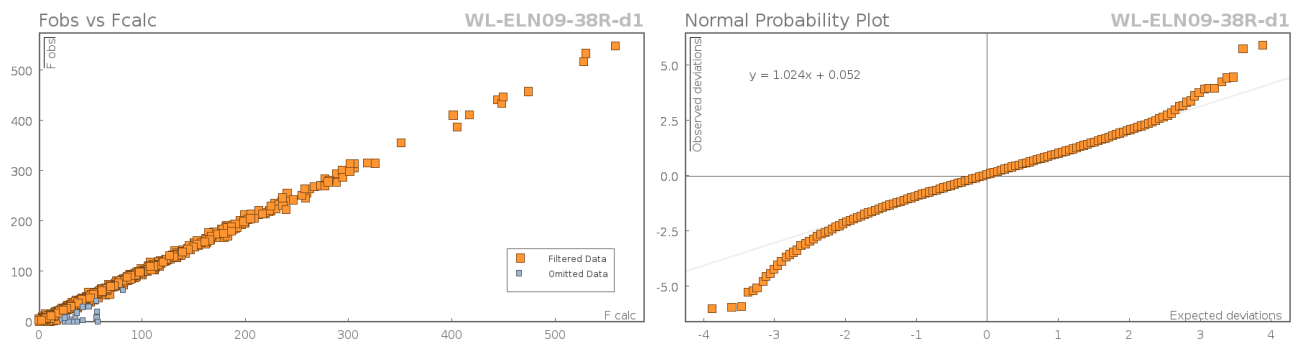
Figure 2: Plot of one of the two independent molecules in the asymmetric unit.

Data Plots: Diffraction Data





Data Plots: Refinement and Data



Reflection Statistics

Total reflections (after filtering)	54043	Unique reflections	9424
Completeness	0.963	Mean I/s	22.96
hkl _{max} collected	(7, 32, 33)	hkl _{min} collected	(-7, -32, -37)
hkl _{max} used	(7, 32, 37)	hkl _{min} used	(-7, 0, 0)
Lim d _{max} collected	100.0	Lim d _{min} collected	0.77
d _{max} used	15.06	d _{min} used	0.81
Friedel pairs	8951	Friedel pairs merged	0
Inconsistent equivalents	25	R _{int}	0.0555
R _{sigma}	0.0338	Intensity transformed	0
Omitted reflections	0	Omitted by user (OMIT hkl)	27
Multiplicity	(12250, 7439, 3904, 1560, 827, 450, 211, 78, 3)	Maximum multiplicity	18
Removed systematic absences	108	Filtered off (Shel/OMIT)	0

Table 1: Fractional Atomic Coordinates ($\times 10^4$) and Equivalent Isotropic Displacement Parameters ($\text{\AA}^2 \times 10^3$) for **WL-ELN09-38R-d1**. U_{eq} is defined as 1/3 of the trace of the orthogonalised U_{ij} .

Atom	x	y	z	U_{eq}
Br1_1	9399.0(11)	6623.9(2)	5923.8(2)	57.82(16)
Br2_1	4129.0(9)	6237.7(2)	7147.5(2)	39.32(12)
Cl1_1	401.7(18)	2394.2(4)	6689.3(3)	34.1(2)
Cl2_1	4311.5(18)	2290.6(4)	7212.2(4)	38.4(2)
Cl3_1	103.5(19)	2097.7(4)	7609.6(4)	40.6(3)
S1_1	4544.3(13)	4550.5(3)	5437.5(2)	17.21(16)
O1_1	2811(4)	3340.6(9)	7132.6(8)	20.7(5)
O2_1	27(4)	3735.4(10)	6789.3(8)	22.9(5)
O3_1	2229(4)	4617.1(10)	5431.8(8)	22.3(5)
O4_1	5601(4)	4342.2(10)	5053.1(7)	24.0(5)
N1_1	5131(4)	4224.0(11)	5879.5(9)	16.4(5)
C2_1	7405(5)	4047.9(14)	5918.7(12)	19.4(7)
C3_1	7617(6)	3498.0(15)	5770.1(14)	26.3(7)
C4_1	6049(6)	3160.0(14)	6025.6(13)	25.0(7)

Atom	x	y	z	<i>U</i>_{eq}
C5_1	3715(6)	3354.4(13)	5966.8(12)	20.0(6)
C6_1	3485(5)	3910.0(12)	6107.5(10)	15.0(5)
C10_1	3747(6)	3977.3(12)	6617.8(10)	16.1(5)
C11_1	1944(6)	3682.4(13)	6846.4(11)	16.6(5)
C13_1	1339(6)	3026.9(14)	7377.8(12)	23.2(7)
C14_1	1552(7)	2477.7(14)	7225.5(13)	26.8(8)
C19_1	3736(6)	4531.7(12)	6754.1(10)	16.1(6)
C20_1	5603(6)	4726.2(14)	6953.7(11)	21.5(7)
C21_1	5702(7)	5234.4(14)	7075.1(11)	26.7(8)
C22_1	3928(7)	5540.5(14)	6994.7(11)	24.4(7)
C23_1	2042(7)	5356.2(14)	6802.3(12)	24.7(7)
C24_1	1961(6)	4845.9(13)	6681.9(11)	19.1(6)
C26_1	5811(6)	5138.4(13)	5545.0(10)	18.8(6)
C27_1	7877(6)	5230.1(14)	5373.7(12)	22.4(7)
C28_1	8925(6)	5681.4(15)	5484.8(13)	27.9(7)
C29_1	7895(7)	6025.1(15)	5758.4(13)	29.9(7)
C30_1	5804(7)	5941.1(15)	5918.8(13)	30.8(8)
C31_1	4773(6)	5492.6(14)	5812.3(12)	25.0(7)
Br1_2	9323.2(10)	7516.7(2)	3726.4(2)	59.28(16)
Br2_2	3339.0(9)	7048.7(2)	4897.6(2)	42.07(13)
Cl1_2	-285.1(18)	3269.3(4)	3886.9(3)	32.9(2)
Cl2_2	3408.3(16)	3118.6(3)	4461.5(3)	31.4(2)
Cl3_2	-895.4(17)	2846.6(3)	4760.9(3)	29.6(2)
S1_2	4047.4(15)	5605.7(3)	2973.3(3)	21.13(18)
O1_2	1707(4)	4153.0(9)	4414.7(8)	19.5(5)
O2_2	-984(4)	4717.8(10)	4300.2(8)	24.8(5)
O3_2	1801(4)	5749.2(11)	2955.3(9)	29.2(6)
O4_2	5151(5)	5457.9(11)	2575.8(8)	29.5(6)
N1_2	4278(5)	5159.9(11)	3342.0(9)	19.2(6)
C2_2	6220(6)	4827.8(14)	3313.8(12)	22.8(7)
C3_2	5676(6)	4327.6(14)	3085.1(12)	25.2(8)
C4_2	3784(6)	4068.9(14)	3319.2(12)	22.7(7)
C5_2	1817(6)	4423.3(14)	3333.5(11)	20.2(7)
C6_2	2330(5)	4936.3(13)	3550.3(11)	17.1(7)
C10_2	2697(5)	4908.7(13)	4061.4(11)	15.2(7)
C11_2	894(6)	4597.2(13)	4270.5(10)	17.4(7)
C13_2	283(6)	3812.3(13)	4640.8(12)	23.0(8)
C14_2	621(6)	3289.5(13)	4443.8(11)	20.6(7)
C19_2	2784(6)	5435.2(13)	4269.0(11)	17.0(7)
C20_2	4696(6)	5591.2(14)	4477.1(11)	20.3(7)
C21_2	4859(7)	6069.0(14)	4668.6(12)	25.6(8)
C22_2	3080(7)	6388.1(14)	4650.0(12)	25.3(8)
C23_2	1162(6)	6244.7(14)	4447.2(12)	25.6(8)
C24_2	1020(6)	5767.0(14)	4256.6(11)	20.8(7)
C26_2	5503(6)	6128.7(14)	3189.2(12)	23.5(7)
C27_2	7523(7)	6241.6(17)	3015.7(17)	37.4(10)
C28_2	8624(7)	6660.9(19)	3173.0(19)	47.9(12)
C29_2	7724(8)	6954.8(16)	3503.2(16)	38.1(10)
C30_2	5690(9)	6848.9(15)	3673.2(14)	37.6(10)
C31_2	4585(8)	6429.7(16)	3514.1(13)	36.2(10)

Table 2: Anisotropic Displacement Parameters ($\times 10^4$) **WL-ELN09-38R-d1**. The anisotropic displacement factor exponent takes the form: $-2p^2[h^2a^{*2} \times U_{11} + \dots + 2hka^* \times b^* \times U_{12}]$

Atom	<i>U</i>₁₁	<i>U</i>₂₂	<i>U</i>₃₃	<i>U</i>₂₃	<i>U</i>₁₃	<i>U</i>₁₂
Br1_1	64.3(4)	29.6(2)	79.5(4)	-9.2(2)	7.9(3)	-22.3(3)
Br2_1	62.3(3)	15.68(19)	40.0(2)	-10.61(16)	11.8(2)	-6.9(2)
Cl1_1	44.0(6)	24.1(5)	34.2(5)	-4.5(4)	1.5(4)	-6.9(4)

Atom	<i>U</i>₁₁	<i>U</i>₂₂	<i>U</i>₃₃	<i>U</i>₂₃	<i>U</i>₁₃	<i>U</i>₁₂
Cl2_1	34.3(5)	28.5(5)	52.3(6)	13.2(4)	7.0(5)	10.7(4)
Cl3_1	48.8(6)	26.2(5)	46.9(6)	14.7(4)	14.2(5)	-4.6(4)
S1_1	16.0(4)	20.5(4)	15.1(3)	-1.1(3)	-1.0(3)	0.8(3)
O1_1	24.0(10)	16.5(10)	21.7(10)	3.9(8)	-0.1(8)	-0.9(8)
O2_1	22.2(8)	20.5(12)	25.9(12)	3.8(10)	0.3(7)	-0.5(7)
O3_1	16.4(12)	27.2(13)	23.3(12)	2.0(10)	-3.6(10)	1.4(11)
O4_1	23.9(12)	32.2(14)	16.0(11)	-5.9(10)	2.0(10)	-0.3(12)
N1_1	13.0(10)	16.9(12)	19.3(12)	0.7(10)	-0.6(8)	1.2(8)
C2_1	13.7(11)	21.1(13)	23.5(16)	-2.0(11)	-2.1(10)	2.7(9)
C3_1	20.7(14)	22.6(13)	35.6(17)	-6.3(11)	-3.8(13)	4.2(10)
C4_1	22.9(12)	18.5(14)	33.4(17)	-9.7(12)	-2.8(11)	3.6(10)
C5_1	21.0(13)	15.7(11)	23.4(16)	-5.6(10)	-1.6(11)	-0.1(9)
C6_1	13.9(11)	14.7(11)	16.4(10)	-2.6(8)	-0.8(8)	-0.1(9)
C10_1	20.0(11)	12.3(10)	15.9(10)	-0.6(7)	-0.8(8)	0.1(9)
C11_1	22.3(8)	12.2(11)	15.4(11)	-1.6(9)	1.0(7)	-0.3(7)
C13_1	27.8(14)	18.5(12)	23.2(14)	5.3(10)	3.2(12)	-0.4(10)
C14_1	30.9(19)	18.4(12)	31.2(18)	4.6(12)	6.3(15)	0.0(12)
C19_1	22.4(13)	12.4(10)	13.6(13)	-0.3(9)	2.1(11)	-1.0(9)
C20_1	25.3(18)	20.7(17)	18.6(16)	-1.6(13)	-0.8(14)	-2.1(15)
C21_1	35(2)	24.8(19)	20.2(17)	-6.2(14)	-0.4(16)	-10.7(17)
C22_1	35.5(16)	16.6(16)	21.0(15)	-4.1(12)	9.1(12)	-1.9(12)
C23_1	35.0(16)	14.2(11)	24.8(16)	-1.6(10)	7.0(12)	-0.7(10)
C24_1	23.7(13)	14.2(11)	19.5(15)	-0.8(9)	1.0(11)	0.5(9)
C26_1	18.4(12)	20.6(14)	17.3(13)	4.3(11)	-2.3(11)	2.3(11)
C27_1	18.7(13)	23.6(14)	24.9(17)	6.1(12)	-0.4(11)	2.4(11)
C28_1	24.2(16)	25.6(14)	33.8(17)	7.9(12)	-1.3(13)	-2.3(11)
C29_1	36.5(16)	21.6(15)	31.5(18)	7.0(13)	1.0(14)	-5.8(12)
C30_1	40.2(16)	21.5(14)	30.6(18)	0.3(12)	7.4(14)	-3.8(13)
C31_1	27.8(16)	20.9(13)	26.5(16)	1.4(12)	6.3(13)	0.1(11)
Br1_2	56.1(3)	25.8(2)	96.0(4)	-10.3(3)	-12.4(3)	-7.1(3)
Br2_2	59.3(3)	20.3(2)	46.6(3)	-13.33(19)	9.1(2)	-5.4(2)
Cl1_2	48.9(6)	26.6(5)	23.1(4)	-2.1(3)	-8.6(4)	-9.1(4)
Cl2_2	27.0(4)	20.0(4)	47.3(5)	3.4(4)	-0.4(4)	3.6(4)
Cl3_2	41.8(5)	15.7(4)	31.4(4)	-1.5(3)	13.3(4)	-5.2(4)
S1_2	22.2(4)	24.1(4)	17.2(4)	5.3(3)	-2.4(3)	0.9(4)
O1_2	21.0(12)	13.6(11)	23.9(12)	2.0(9)	0.3(10)	-1.4(10)
O2_2	19.3(13)	22.5(13)	32.6(13)	6.1(10)	4.4(11)	2.6(11)
O3_2	23.9(13)	32.5(15)	31.2(14)	11.5(12)	-5.3(11)	5.4(12)
O4_2	33.3(15)	41.0(16)	14.2(11)	3.0(11)	1.7(11)	-3.9(13)
N1_2	16.6(14)	20.8(14)	20.1(13)	3.7(11)	1.7(12)	4.8(13)
C2_2	15.4(17)	27.4(19)	25.7(17)	1.6(15)	1.0(14)	5.1(15)
C3_2	22.6(17)	27.6(19)	25.5(17)	-2.8(14)	1.3(15)	10.8(16)
C4_2	25.5(19)	18.3(17)	24.3(17)	-3.1(14)	0.0(14)	1.9(15)
C5_2	19.1(17)	22.8(18)	18.7(16)	-2.3(14)	-0.8(13)	-0.7(15)
C6_2	14.6(15)	18.9(17)	17.7(16)	-0.2(13)	0.6(13)	1.9(14)
C10_2	14.2(15)	15.0(16)	16.4(15)	0.7(13)	-0.3(12)	1.2(13)
C11_2	21.8(17)	15.2(16)	15.3(15)	-0.9(12)	-1.8(13)	0.1(15)
C13_2	30(2)	14.6(16)	24.3(17)	1.6(14)	7.8(15)	-1.8(15)
C14_2	26.0(17)	17.0(16)	18.8(15)	0.6(13)	0.8(14)	-3.2(15)
C19_2	20.3(17)	13.9(16)	16.9(15)	2.4(13)	2.1(13)	0.7(14)
C20_2	23.3(18)	21.5(17)	16.1(15)	1.4(13)	0.2(14)	-0.1(15)
C21_2	31(2)	21.8(18)	24.2(18)	-1.4(14)	-3.3(15)	-3.8(16)
C22_2	38(2)	16.0(17)	21.5(17)	-1.5(14)	7.3(16)	-2.8(16)
C23_2	26.6(19)	19.9(18)	30.4(19)	3.1(15)	8.8(15)	3.0(15)
C24_2	19.9(17)	19.2(17)	23.3(16)	0.9(13)	2.7(14)	2.0(15)
C26_2	26.3(18)	19.9(18)	24.2(17)	8.1(14)	-2.7(15)	0.6(16)
C27_2	21.6(19)	30(2)	60(3)	-10(2)	1.1(19)	5.2(18)
C28_2	22(2)	38(3)	83(4)	-12(2)	6(2)	-2(2)
C29_2	40(2)	21(2)	53(3)	5.6(19)	-9(2)	0.4(18)

Atom	U_{11}	U_{22}	U_{33}	U_{23}	U_{13}	U_{12}
C30_2	61(3)	23.3(19)	28.8(19)	3.2(16)	9(2)	-5(2)
C31_2	50(3)	27(2)	31(2)	3.5(16)	13(2)	-9(2)

Table 3: Bond Lengths in Å for **WL-ELN09-38R-d1**.

Atom	Atom	Length/Å	Atom	Atom	Length/Å
Br1_1	C29_1	1.898(4)	Br1_2	C29_2	1.903(5)
Br2_1	C22_1	1.901(4)	Br2_2	C22_2	1.903(4)
Cl1_1	C14_1	1.777(4)	Cl1_2	C14_2	1.768(3)
Cl2_1	C14_1	1.768(4)	Cl2_2	C14_2	1.774(4)
Cl3_1	C14_1	1.771(4)	Cl3_2	C14_2	1.774(4)
S1_1	O3_1	1.435(3)	S1_2	O3_2	1.434(3)
S1_1	O4_1	1.437(2)	S1_2	O4_2	1.430(3)
S1_1	N1_1	1.626(3)	S1_2	N1_2	1.624(3)
S1_1	C26_1	1.766(4)	S1_2	C26_2	1.769(4)
O1_1	C11_1	1.357(4)	O1_2	C11_2	1.347(4)
O1_1	C13_1	1.432(4)	O1_2	C13_2	1.428(4)
O2_1	C11_1	1.200(4)	O2_2	C11_2	1.202(5)
N1_1	C2_1	1.478(4)	N1_2	C2_2	1.484(4)
N1_1	C6_1	1.478(4)	N1_2	C6_2	1.475(4)
C2_1	C3_1	1.525(5)	C2_2	C3_2	1.526(5)
C3_1	C4_1	1.522(6)	C3_2	C4_2	1.522(5)
C4_1	C5_1	1.535(5)	C4_2	C5_2	1.530(5)
C5_1	C6_1	1.533(5)	C5_2	C6_2	1.536(5)
C6_1	C10_1	1.555(4)	C6_2	C10_2	1.557(5)
C10_1	C11_1	1.520(5)	C10_2	C11_2	1.517(5)
C10_1	C19_1	1.520(4)	C10_2	C19_2	1.525(5)
C13_1	C14_1	1.526(5)	C13_2	C14_2	1.517(5)
C19_1	C20_1	1.394(5)	C19_2	C20_2	1.395(5)
C19_1	C24_1	1.388(5)	C19_2	C24_2	1.395(5)
C20_1	C21_1	1.392(5)	C20_2	C21_2	1.391(5)
C21_1	C22_1	1.379(6)	C21_2	C22_2	1.382(6)
C22_1	C23_1	1.385(6)	C22_2	C23_2	1.381(6)
C23_1	C24_1	1.396(5)	C23_2	C24_2	1.388(5)
C26_1	C27_1	1.393(5)	C26_2	C27_2	1.380(6)
C26_1	C31_1	1.389(5)	C26_2	C31_2	1.381(6)
C27_1	C28_1	1.395(5)	C27_2	C28_2	1.381(7)
C28_1	C29_1	1.379(6)	C28_2	C29_2	1.378(7)
C29_1	C30_1	1.392(6)	C29_2	C30_2	1.380(7)
C30_1	C31_1	1.381(6)	C30_2	C31_2	1.384(6)

Table 4: Bond Angles in ° for **WL-ELN09-38R-d1**.

Atom	Atom	Atom	Angle/°	Atom	Atom	Atom	Angle/°
O3_1	S1_1	O4_1	119.08(15)	C4_1	C3_1	C2_1	110.8(3)
O3_1	S1_1	N1_1	107.16(15)	C3_1	C4_1	C5_1	109.8(3)
O3_1	S1_1	C26_1	109.40(17)	C6_1	C5_1	C4_1	112.0(3)
O4_1	S1_1	N1_1	110.87(15)	N1_1	C6_1	C5_1	110.2(3)
O4_1	S1_1	C26_1	106.53(16)	N1_1	C6_1	C10_1	108.9(3)
N1_1	S1_1	C26_1	102.57(15)	C5_1	C6_1	C10_1	111.9(3)
C11_1	O1_1	C13_1	117.6(3)	C11_1	C10_1	C6_1	108.3(3)
C2_1	N1_1	S1_1	116.2(2)	C11_1	C10_1	C19_1	111.6(3)
C6_1	N1_1	S1_1	121.7(2)	C19_1	C10_1	C6_1	112.1(3)
C6_1	N1_1	C2_1	115.8(3)	O1_1	C11_1	C10_1	110.0(3)
N1_1	C2_1	C3_1	110.9(3)	O2_1	C11_1	O1_1	123.7(3)

Atom	Atom	Atom	Angle°
O2_1	C11_1	C10_1	126.3(3)
O1_1	C13_1	C14_1	109.9(3)
Cl2_1	C14_1	Cl1_1	109.1(2)
Cl2_1	C14_1	Cl3_1	109.8(2)
Cl3_1	C14_1	Cl1_1	108.8(2)
C13_1	C14_1	Cl1_1	110.9(3)
C13_1	C14_1	Cl2_1	110.8(3)
C13_1	C14_1	Cl3_1	107.4(3)
C20_1	C19_1	C10_1	117.9(3)
C24_1	C19_1	C10_1	122.4(3)
C24_1	C19_1	C20_1	119.7(3)
C21_1	C20_1	C19_1	120.3(4)
C22_1	C21_1	C20_1	118.9(4)
C21_1	C22_1	Br2_1	118.2(3)
C21_1	C22_1	C23_1	122.0(3)
C23_1	C22_1	Br2_1	119.7(3)
C22_1	C23_1	C24_1	118.5(4)
C19_1	C24_1	C23_1	120.5(3)
C27_1	C26_1	S1_1	119.2(3)
C31_1	C26_1	S1_1	119.7(3)
C31_1	C26_1	C27_1	121.1(3)
C26_1	C27_1	C28_1	118.8(4)
C29_1	C28_1	C27_1	119.5(4)
C28_1	C29_1	Br1_1	118.7(3)
C28_1	C29_1	C30_1	121.8(4)
C30_1	C29_1	Br1_1	119.5(3)
C31_1	C30_1	C29_1	118.7(4)
C30_1	C31_1	C26_1	120.1(4)
O3_2	S1_2	N1_2	107.54(16)
O3_2	S1_2	C26_2	107.18(18)
O4_2	S1_2	O3_2	119.85(17)
O4_2	S1_2	N1_2	109.44(16)
O4_2	S1_2	C26_2	106.29(18)
N1_2	S1_2	C26_2	105.67(16)
C11_2	O1_2	C13_2	118.3(3)
C2_2	N1_2	S1_2	117.3(2)
C6_2	N1_2	S1_2	120.6(2)
C6_2	N1_2	C2_2	116.2(3)
N1_2	C2_2	C3_2	111.1(3)
C4_2	C3_2	C2_2	110.3(3)
C3_2	C4_2	C5_2	110.1(3)
C4_2	C5_2	C6_2	112.9(3)
N1_2	C6_2	C5_2	109.8(3)
N1_2	C6_2	C10_2	108.7(3)
C5_2	C6_2	C10_2	114.1(3)
C11_2	C10_2	C6_2	109.3(3)
C11_2	C10_2	C19_2	110.5(3)
C19_2	C10_2	C6_2	111.6(3)
O1_2	C11_2	C10_2	109.6(3)
O2_2	C11_2	O1_2	124.3(3)
O2_2	C11_2	C10_2	126.2(3)
O1_2	C13_2	C14_2	107.6(3)
Cl1_2	C14_2	Cl2_2	109.00(19)
Cl1_2	C14_2	Cl3_2	108.98(19)
Cl2_2	C14_2	Cl3_2	108.92(19)
C13_2	C14_2	Cl1_2	110.8(2)
C13_2	C14_2	Cl2_2	110.6(3)
C13_2	C14_2	Cl3_2	108.5(2)
C20_2	C19_2	C10_2	118.9(3)

Atom	Atom	Atom	Angle°
C24_2	C19_2	C10_2	122.3(3)
C24_2	C19_2	C20_2	118.9(3)
C21_2	C20_2	C19_2	121.0(3)
C22_2	C21_2	C20_2	118.6(4)
C21_2	C22_2	Br2_2	118.4(3)
C23_2	C22_2	Br2_2	119.7(3)
C23_2	C22_2	C21_2	121.8(3)
C22_2	C23_2	C24_2	119.0(4)
C23_2	C24_2	C19_2	120.7(3)
C27_2	C26_2	S1_2	119.0(3)
C27_2	C26_2	C31_2	120.8(4)
C31_2	C26_2	S1_2	120.1(3)
C26_2	C27_2	C28_2	119.0(4)
C29_2	C28_2	C27_2	120.1(4)
C28_2	C29_2	Br1_2	119.1(4)
C28_2	C29_2	C30_2	121.2(4)
C30_2	C29_2	Br1_2	119.7(4)
C29_2	C30_2	C31_2	118.6(4)
C26_2	C31_2	C30_2	120.3(4)

Table 5: Hydrogen Fractional Atomic Coordinates ($\times 10^4$) and Equivalent Isotropic Displacement Parameters ($\text{\AA}^2 \times 10^3$) for **WL-ELN09-38R-d1**. U_{eq} is defined as 1/3 of the trace of the orthogonalised U_{ij} .

Atom	x	y	z	U_{eq}
H2A_1	7878.12	4078.71	6224.81	23
H2B_1	8337.85	4259.8	5737.18	23
H3A_1	7311.68	3473.79	5454.82	32
H3B_1	9095.49	3382.98	5819.17	32
H4A_1	6429.89	3160.13	6338.15	30
H4B_1	6154.56	2815	5916.72	30
H5A_1	3294.02	3320.28	5657.86	24
H5B_1	2737.01	3147.89	6143.19	24
H6_1	2037.43	4029.66	6021.31	18
H10_1	5143.27	3829.74	6706.03	19
H13A_1	-140.72	3142.74	7331.61	28
H13B_1	1661.75	3050.47	7692.42	28
H20_1	6786.92	4515.45	7005.93	26
H21_1	6944.63	5365.43	7208.35	32
H23_1	855.32	5567.72	6754.52	30
H24_1	708.01	4715.39	6552.3	23
H27_1	8545.69	4994.98	5188.66	27
H28_1	10307.19	5750	5375.22	33
H30_1	5113.99	6182.34	6094.33	37
H31_1	3383.33	5427.67	5919.62	30
H2A_2	6762.05	4760.48	3610.43	27
H2B_2	7355.69	4999.92	3148.97	27
H3A_2	5296.12	4390.63	2777.42	30
H3B_2	6938.15	4107.47	3090.44	30
H4A_2	4207.67	3978.7	3619.28	27
H4B_2	3403.32	3760.28	3162.62	27
H5A_2	654.73	4260.34	3497.75	24
H5B_2	1305.04	4480.6	3033	24
H6_2	1100.42	5163.79	3494.76	20
H10_2	4085.89	4738.38	4117.17	18
H13A_2	-1215.64	3917.89	4602.47	28
H13B_2	611.2	3808.61	4955.86	28
H20_2	5879.83	5372.31	4487.91	24
H21_2	6138.87	6171.71	4806.34	31
H23_2	-16.97	6465.06	4438.44	31
H24_2	-264.71	5667.18	4119.16	25
H27_2	8132.66	6038.44	2796.3	45
H28_2	9975.73	6744.83	3055.69	57
H30_2	5075.74	7054.71	3890.13	45
H31_2	3217.68	6350.45	3626.39	43

Citations

CrysAlisPro Software System, Rigaku Oxford Diffraction, (2019).

O.V. Dolomanov and L.J. Bourhis and R.J. Gildea and J.A.K. Howard and H. Puschmann, Olex2: A complete structure solution, refinement and analysis program, *J. Appl. Cryst.*, (2009), **42**, 339-341.

Sheldrick, G.M., Crystal structure refinement with ShelXL, *Acta Cryst.*, (2015), **C27**, 3-8.

Sheldrick, G.M., ShelXT-Integrated space-group and crystal-structure determination, *Acta Cryst.*, (2015), **A71**, 3-8.

10.2. X-Ray Crystallographic Data for 8b

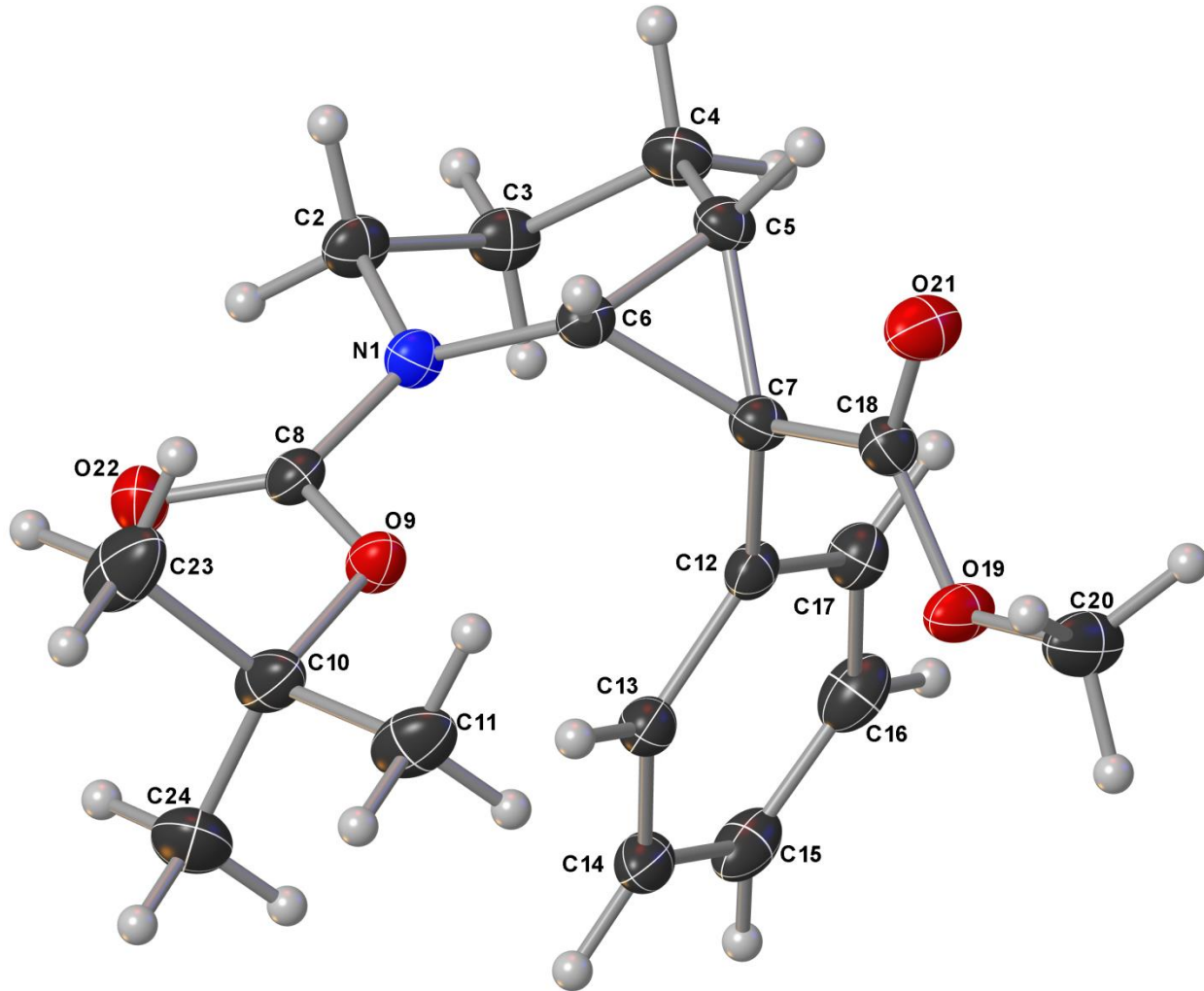


Table 1 Crystal data and structure refinement for US8.

Identification code	US8
Empirical formula	C ₁₉ H ₂₅ NO ₄
Formula weight	331.40
Temperature/K	106(7)
Crystal system	orthorhombic
Space group	P ₂ 12 ₁ 2 ₁
a/Å	8.28903(12)
b/Å	11.79462(19)
c/Å	18.8010(3)
α/°	90
β/°	90
γ/°	90
Volume/Å ³	1838.10(5)
Z	4
ρ _{calc} g/cm ³	1.198
μ/mm ⁻¹	0.678
F(000)	712.0

Crystal size/mm ³	$0.334 \times 0.227 \times 0.128$
Radiation	CuK α ($\lambda = 1.54184$)
2 Θ range for data collection/°	8.85 to 144.684
Index ranges	-9 ≤ h ≤ 9, -14 ≤ k ≤ 14, -21 ≤ l ≤ 23
Reflections collected	17416
Independent reflections	3508 [R _{int} = 0.0424, R _{sigma} = 0.0275]
Data/restraints/parameters	3508/65/307
Goodness-of-fit on F ²	1.064
Final R indexes [I>=2σ (I)]	R ₁ = 0.0264, wR ₂ = 0.0654
Final R indexes [all data]	R ₁ = 0.0272, wR ₂ = 0.0660
Largest diff. peak/hole / e Å ⁻³	0.19/-0.15
Flack parameter	-0.11(6)

Table 2 Fractional Atomic Coordinates ($\times 10^4$) and Equivalent Isotropic Displacement Parameters (Å² $\times 10^3$) for US8. U_{eq} is defined as 1/3 of the trace of the orthogonalised U_{II} tensor.

Atom	x	y	z	U(eq)
O9	6455.8(13)	8047.6(9)	1910.0(6)	22.3(2)
O21	2511.0(13)	8589.1(10)	3446.1(7)	30.2(3)
O22	9112.2(14)	8558.1(10)	1899.5(6)	28.3(3)
O19	3039.0(13)	6722.3(9)	3432.8(7)	27.8(3)
N1	7493.2(15)	8896.1(10)	2857.0(6)	19.9(3)
C12	6212.5(17)	6927.2(12)	3763.2(8)	19.5(3)
C8	7805.6(18)	8504.4(12)	2191.4(8)	20.6(3)
C18	3458.8(18)	7811.0(13)	3491.3(8)	21.8(3)
C6	5881.3(17)	8940.1(12)	3126.8(8)	18.7(3)
C13	6777.9(18)	6219.7(12)	3222.4(8)	21.9(3)
C5	5662.0(18)	9127.7(12)	3905.4(9)	20.9(3)
C7	5230.2(18)	7964.7(12)	3600.3(8)	19.5(3)
C3	8726.1(19)	9061.5(14)	4032.0(9)	24.5(3)
C17	6514(2)	6630.3(13)	4465.8(9)	24.8(3)
C4	7108.6(19)	9357.7(13)	4374.9(8)	24.1(3)
C14	7670.2(19)	5255.8(13)	3384.6(9)	26.5(3)
C2	8776.0(18)	9454.9(13)	3266.2(9)	23.7(3)
C15	8000.4(19)	4984.3(13)	4085.5(10)	29.3(4)
C16	7410(2)	5663.7(14)	4625.7(9)	29.9(4)
C10	6413(2)	7686.0(14)	1162.3(8)	28.6(4)
C11	4692(2)	7259.3(16)	1089.0(10)	34.2(4)
C20	1331(2)	6526.8(15)	3307.9(12)	35.1(4)
C23	6692(3)	8713.8(17)	686.2(10)	43.2(5)
C24	7624(3)	6746.8(16)	1026.9(11)	40.5(4)

Table 3 Anisotropic Displacement Parameters (Å² $\times 10^3$) for US8. The Anisotropic displacement factor exponent takes the form: $-2\pi^2[h^2a^*{}^2U_{11} + 2hka^*b^*U_{12} + \dots]$.

Atom	U ₁₁	U ₂₂	U ₃₃	U ₂₃	U ₁₃	U ₁₂
O9	25.3(5)	22.5(5)	19.1(5)	-0.4(4)	-0.6(4)	-5.0(4)

O21	18.9(5)	23.9(5)	47.8(7)	-1.9(5)	-1.7(5)	2.8(4)
O22	26.1(6)	29.6(6)	29.3(6)	-2.2(5)	7.6(5)	-5.1(5)
O19	18.2(5)	20.3(5)	44.9(7)	-4.1(5)	1.2(5)	-1.0(4)
N1	17.3(6)	20.9(6)	21.6(6)	-1.2(5)	-1.2(5)	-1.4(5)
C12	16.3(7)	18.1(7)	24.2(7)	2.4(5)	0.8(6)	-1.9(5)
C8	22.1(7)	16.4(6)	23.3(7)	2.5(5)	-0.2(6)	-1.9(5)
C18	20.7(7)	22.0(7)	22.7(7)	-1.8(6)	1.9(6)	-0.2(6)
C6	16.6(7)	17.3(6)	22.3(7)	0.1(6)	-1.5(6)	0.6(5)
C13	21.5(7)	20.0(7)	24.2(7)	0.8(6)	2.2(6)	-0.8(6)
C5	19.1(7)	19.7(7)	23.9(7)	-3.0(6)	0.8(6)	2.3(6)
C7	19.1(7)	19.0(7)	20.5(7)	-1.5(5)	0.2(6)	0.9(5)
C3	21.5(8)	24.4(8)	27.7(8)	-2.8(6)	-6.2(6)	-0.3(6)
C17	25.9(7)	24.4(8)	24.3(8)	3.2(6)	0.8(6)	-1.9(6)
C4	27.4(8)	23.0(7)	21.9(7)	-3.7(6)	-3.0(7)	0.3(6)
C14	22.3(7)	20.5(7)	36.6(9)	1.4(6)	7.2(7)	1.1(6)
C2	18.8(7)	23.3(7)	29.1(8)	-2.1(6)	-3.7(6)	-3.1(6)
C15	20.0(7)	22.3(8)	45.5(10)	10.7(7)	-1.5(7)	1.0(6)
C16	29.6(8)	28.3(8)	31.9(8)	11.1(7)	-6.3(7)	-4.0(7)
C10	42.8(10)	24.1(7)	18.8(8)	-1.1(6)	-0.6(7)	-7.5(7)
C11	46.0(11)	29.0(9)	27.5(9)	-0.5(7)	-10.0(8)	-8.8(8)
C20	18.7(8)	28.3(8)	58.3(12)	-10.8(8)	0.5(7)	-2.6(6)
C23	66.8(13)	38.9(10)	24.0(9)	7.7(8)	-3.4(9)	-18.3(10)
C24	51.1(11)	33.1(9)	37.3(10)	-13.1(7)	8.5(9)	-5.8(8)

Table 4 Bond Lengths for US8.

Atom	Atom	Length/Å	Atom	Atom	Length/Å
O9	C8	1.3498(18)	C6	C5	1.492(2)
O9	C10	1.4694(19)	C6	C7	1.551(2)
O21	C18	1.2110(19)	C13	C14	1.390(2)
O22	C8	1.2158(19)	C5	C7	1.529(2)
O19	C18	1.3350(18)	C5	C4	1.513(2)
O19	C20	1.4532(19)	C3	C4	1.528(2)
N1	C8	1.3589(19)	C3	C2	1.513(2)
N1	C6	1.4302(19)	C17	C16	1.394(2)
N1	C2	1.4686(19)	C14	C15	1.383(3)
C12	C13	1.396(2)	C15	C16	1.383(3)
C12	C7	1.501(2)	C10	C11	1.519(3)
C12	C17	1.389(2)	C10	C23	1.524(2)
C18	C7	1.494(2)	C10	C24	1.516(3)

Table 5 Bond Angles for US8.

Atom	Atom	Atom	Angle/°	Atom	Atom	Atom	Angle/°
C8	O9	C10	120.71(12)	C4	C5	C7	124.40(13)
C18	O19	C20	114.82(12)	C12	C7	C6	122.19(12)
C8	N1	C6	121.13(12)	C12	C7	C5	121.85(13)

C8	N1	C2	119.81(12)	C18	C7	C12	117.53(13)
C6	N1	C2	118.31(12)	C18	C7	C6	110.68(13)
C13	C12	C7	121.38(14)	C18	C7	C5	112.98(12)
C17	C12	C13	118.77(14)	C5	C7	C6	57.91(10)
C17	C12	C7	119.79(14)	C2	C3	C4	110.81(13)
O9	C8	N1	109.80(12)	C12	C17	C16	120.48(15)
O22	C8	O9	125.61(13)	C5	C4	C3	114.09(13)
O22	C8	N1	124.59(14)	C15	C14	C13	120.23(15)
O21	C18	O19	123.65(14)	N1	C2	C3	109.94(13)
O21	C18	C7	123.74(14)	C16	C15	C14	119.69(14)
O19	C18	C7	112.60(13)	C15	C16	C17	120.27(16)
N1	C6	C5	117.86(12)	O9	C10	C11	101.86(13)
N1	C6	C7	120.11(12)	O9	C10	C23	109.11(13)
C5	C6	C7	60.30(10)	O9	C10	C24	110.90(14)
C14	C13	C12	120.51(15)	C11	C10	C23	110.63(16)
C6	C5	C7	61.79(10)	C24	C10	C11	111.36(15)
C6	C5	C4	120.16(13)	C24	C10	C23	112.47(16)

Table 6 Hydrogen Atom Coordinates ($\text{\AA} \times 10^4$) and Isotropic Displacement Parameters ($\text{\AA}^2 \times 10^3$) for US8.

Atom	x	y	z	U(eq)
H17	6080(20)	7104(15)	4844(8)	30(5)
H15	8630(20)	4306(12)	4186(10)	33(5)
H14	8030(20)	4770(15)	2996(8)	34(5)
H4A	7130(20)	10172(18)	4474(10)	29(5)
H3A	9600(20)	9426(17)	4278(11)	26(5)
H13	6550(20)	6411(16)	2729(6)	26(5)
H23A	6000(20)	9349(14)	834(12)	45.4(17)
H16	7590(30)	5486(18)	5125(6)	34(5)
H23B	7808(12)	8989(19)	723(12)	45.4(17)
H11A	4520(30)	6980(20)	597(14)	45.4(17)
H5	4680(20)	9538(16)	4021(10)	19(4)
H11B	4520(30)	6620(20)	1423(13)	45.4(17)
H4B	7020(20)	9001(16)	4840(10)	25(5)
H2A	8600(20)	10278(6)	3229(10)	25(5)
H3B	8890(20)	8264(17)	4040(10)	25(5)
H24A	7450(30)	6456(19)	542(6)	45.4(17)
H20A	1250(30)	5702(7)	3240(13)	45.4(17)
H2B	9808(14)	9248(18)	3044(10)	34(5)
H6	5100(20)	9262(16)	2812(10)	20(4)
H24B	7470(30)	6115(13)	1361(9)	45.4(17)
H20B	750(30)	6801(19)	3730(8)	45.4(17)
H11C	3890(30)	7890(20)	1210(12)	45.4(17)
H24C	8735(13)	7020(19)	1090(13)	45.4(17)
H20C	920(30)	6941(17)	2891(8)	45.4(17)

H23C	6500(30)	8473(19)	192(6)	45.4(17)
------	----------	----------	--------	----------

Experimental

Single crystals of C₁₉H₂₅NO₄ [US8] were []. A suitable crystal was selected and [The crystal was mounted on a None] on a XtaLAB Synergy, Dualflex, HyPix diffractometer. The crystal was kept at 106(7) K during data collection. Using Olex2 [1], the structure was solved with the ShelXT [2] structure solution program using Intrinsic Phasing and refined with the ShelXL [3] refinement package using Least Squares minimisation.

1. Dolomanov, O.V., Bourhis, L.J., Gildea, R.J., Howard, J.A.K. & Puschmann, H. (2009), *J. Appl. Cryst.* 42, 339-341.
2. Sheldrick, G.M. (2015). *Acta Cryst. A*71, 3-8.
3. Sheldrick, G.M. (2015). *Acta Cryst. C*71, 3-8.

Crystal structure determination of [US8]

Crystal Data for C₁₉H₂₅NO₄ ($M=331.40$ g/mol): orthorhombic, space group P2₁2₁2₁ (no. 19), $a = 8.28903(12)$ Å, $b = 11.79462(19)$ Å, $c = 18.8010(3)$ Å, $V = 1838.10(5)$ Å³, $Z = 4$, $T = 106(7)$ K, $\mu(\text{CuK}\alpha) = 0.678$ mm⁻¹, $D_{\text{calc}} = 1.198$ g/cm³, 17416 reflections measured ($8.85^\circ \leq 2\Theta \leq 144.684^\circ$), 3508 unique ($R_{\text{int}} = 0.0424$, $R_{\text{sigma}} = 0.0275$) which were used in all calculations. The final R_1 was 0.0264 ($I > 2\sigma(I)$) and wR_2 was 0.0660 (all data).

Refinement model description

Number of restraints - 65, number of constraints - unknown.

Details:

1. Restrained distances

C2-H2A ≈ C2-H2B ≈ C23-H23A ≈ C23-H23B ≈ C23-H23C ≈
 C24-H24B ≈ C24-H24A ≈ C24-H24C ≈ C20-H20A ≈ C20-H20B ≈ C20-H20C
 with sigma of 0.002
 C16-H16 ≈ C17-H17 ≈ C15-H15 ≈ C14-H14 ≈ C13-H13
 with sigma of 0.005

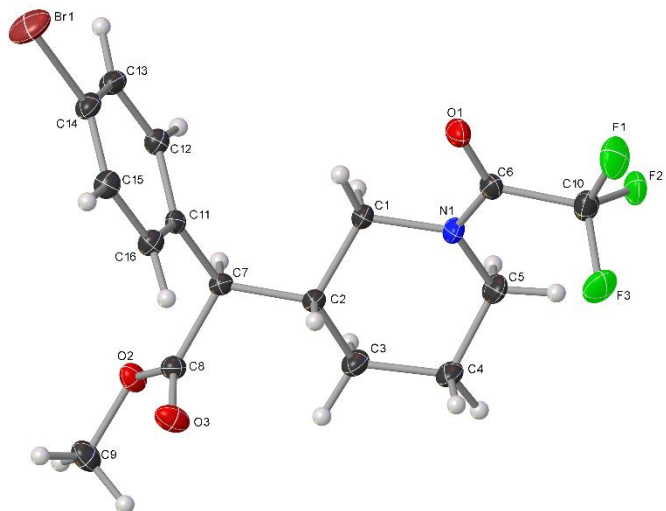
2. Uiso/Uaniso restraints and constraints

Uiso(H24C) = Uiso(H24A) = Uiso(H24B) = Uiso(H11A) = Uiso(H11B) = Uiso(H11C) =
 Uiso(H23C) = Uiso(H23B) = Uiso(H23A) = Uiso(H20C) = Uiso(H20A) = Uiso(H20B)

This report has been created with Olex2, compiled on 2018.07.26 svn.r3523 for OlexSys. Please [let us know](#) if there are any errors or if you would like to have additional features.

10.3. X-Ray Crystallographic Data for N-COCF₃-9a

Crystal Data and Experimental



Experimental. Single colourless needle-shaped crystals of **US96** were chosen from the sample as supplied.. A suitable crystal $0.39 \times 0.12 \times 0.10$ mm³ was selected and mounted on a loop with paratone oil on an XtaLAB Synergy, Dualflex, HyPix diffractometer. The crystal was kept at a steady $T = 100.01(10)$ K during data collection. The structure was solved with the **ShelXT** (Sheldrick, 2015) structure solution program using the Intrinsic Phasing solution method and by using **Olex2** (Dolomanov et al., 2009) as the graphical interface. The model was refined with version 2018/3 of **ShelXL** (Sheldrick, 2015) using Least Squares minimisation.

Crystal Data. $C_{16}H_{17}BrF_3NO_3$, $M_r = 408.21$, monoclinic, $P2_1$ (No. 4), $a = 8.8333(2)$ Å, $b = 8.6844(2)$ Å, $c = 11.4854(3)$ Å, $\beta = 107.078(3)^\circ$, $a = g = 90^\circ$, $V = 842.22(4)$ Å³, $T = 100.01(10)$ K, $Z = 2$, $Z' = 1$, $m(\text{MoK}_\alpha) = 2.485$ mm⁻¹, 20214 reflections measured, 7976 unique ($R_{int} = 0.0321$) which were used in all calculations. The final wR_2 was 0.0993 (all data) and R_I was 0.0406 ($I > 2\sigma(I)$).

Compound	US96
Formula	$C_{16}H_{17}BrF_3NO_3$
$D_{\text{calc.}}/\text{g cm}^{-3}$	1.610
m/mm^{-1}	2.485
Formula Weight	408.21
Colour	colourless
Shape	needle
Size/mm ³	$0.39 \times 0.12 \times 0.10$
T/K	100.01(10)
Crystal System	monoclinic
Flack Parameter	-0.003(3)
Hooft Parameter	0.017(2)
Space Group	$P2_1$
$a/\text{\AA}$	8.8333(2)
$b/\text{\AA}$	8.6844(2)
$c/\text{\AA}$	11.4854(3)
a°	90
b°	107.078(3)
g°	90
$V/\text{\AA}^3$	842.22(4)
Z	2
Z'	1
Wavelength/Å	0.71073
Radiation type	MoK _a
$Q_{\min}/^\circ$	2.412
$Q_{\max}/^\circ$	36.317
Measured Refl.	20214
Independent Refl.	7976
Reflections with $I > 2\sigma(I)$	6370
R_{int}	0.0321
Parameters	217
Restraints	60
Largest Peak	0.969
Deepest Hole	-0.675
GooF	1.019
wR_2 (all data)	0.0993
wR_2	0.0933
R_I (all data)	0.0589
R_I	0.0406

Structure Quality Indicators

Reflections: $d_{\text{min}} (\text{Mo})$ 0.60 I/σ 22.4 R_{int} 3.21% completeness 100% (IUCr) 99%

Refinement: Shift -0.007 Max Peak 1.0 Min Peak -0.7 Goof 1.019 Flack -0.003(3)

A colourless needle-shaped crystal with dimensions $0.39 \times 0.12 \times 0.10 \text{ mm}^3$ was mounted on a loop with paratone oil. Data were collected using an XtaLAB Synergy, Dualflex, HyPix diffractometer equipped with an Oxford Cryosystems low-temperature device operating at $T = 100.01(10) \text{ K}$.

Data were measured using w scans using MoK α radiation. The total number of runs and images was based on the strategy calculation from the program **CrysAlisPro** (Rigaku, V1.171.40.37a, 2019). The maximum resolution that was achieved was $Q = 36.317^\circ$ (0.60 Å).

The diffraction pattern was indexed using the program **CrysAlisPro** (Rigaku, V1.171.40.37a, 2019) and the unit cell was refined using **CrysAlisPro** (Rigaku, V1.171.40.37a, 2019) on 9810 reflections, 49% of the observed reflections. Data reduction, scaling and absorption corrections were performed using **CrysAlisPro** (Rigaku, V1.171.40.37a, 2019). The final completeness is 99.80 % out to 36.317° in Q . A numerical absorption correction based on Gaussian integration over a multifaceted crystal model was performed using **CrysAlisPro** (Rigaku, V1.171.40.37a, 2019). An empirical absorption correction using spherical harmonics as implemented in SCALE3 ABSPACK (Rigaku, V1.171.40.37a, 2019) was also used. The absorption coefficient m of this material is 2.485 mm $^{-1}$ at this wavelength ($\lambda = 0.711 \text{\AA}$) and the minimum and maximum transmissions are 0.448 and 1.000.

The structure was solved and the space group $P2_1$ (# 4) determined by the **ShelXT** (Sheldrick, 2015) structure solution program using Intrinsic Phasing and refined by Least Squares using version 2018/3 of **ShelXL** (Sheldrick, 2015). All non-hydrogen atoms were refined anisotropically. Hydrogen atom positions were located from the difference maps and refined using restraints.

There is a single molecule in the asymmetric unit, which is represented by the reported sum formula. In other words: Z is 2 and Z' is 1.

The Flack parameter was refined to -0.003(3). Determination of absolute structure using Bayesian statistics on Bijvoet differences using the Olex2 results in 0.017(2). Note: The Flack parameter is used to determine chirality of the crystal studied, the value should be near 0, a value of 1 means that the stereochemistry is wrong and the model should be inverted. A value of 0.5 means that the crystal consists of a racemic mixture of the two enantiomers.

Images of the Crystal on the Diffractometer



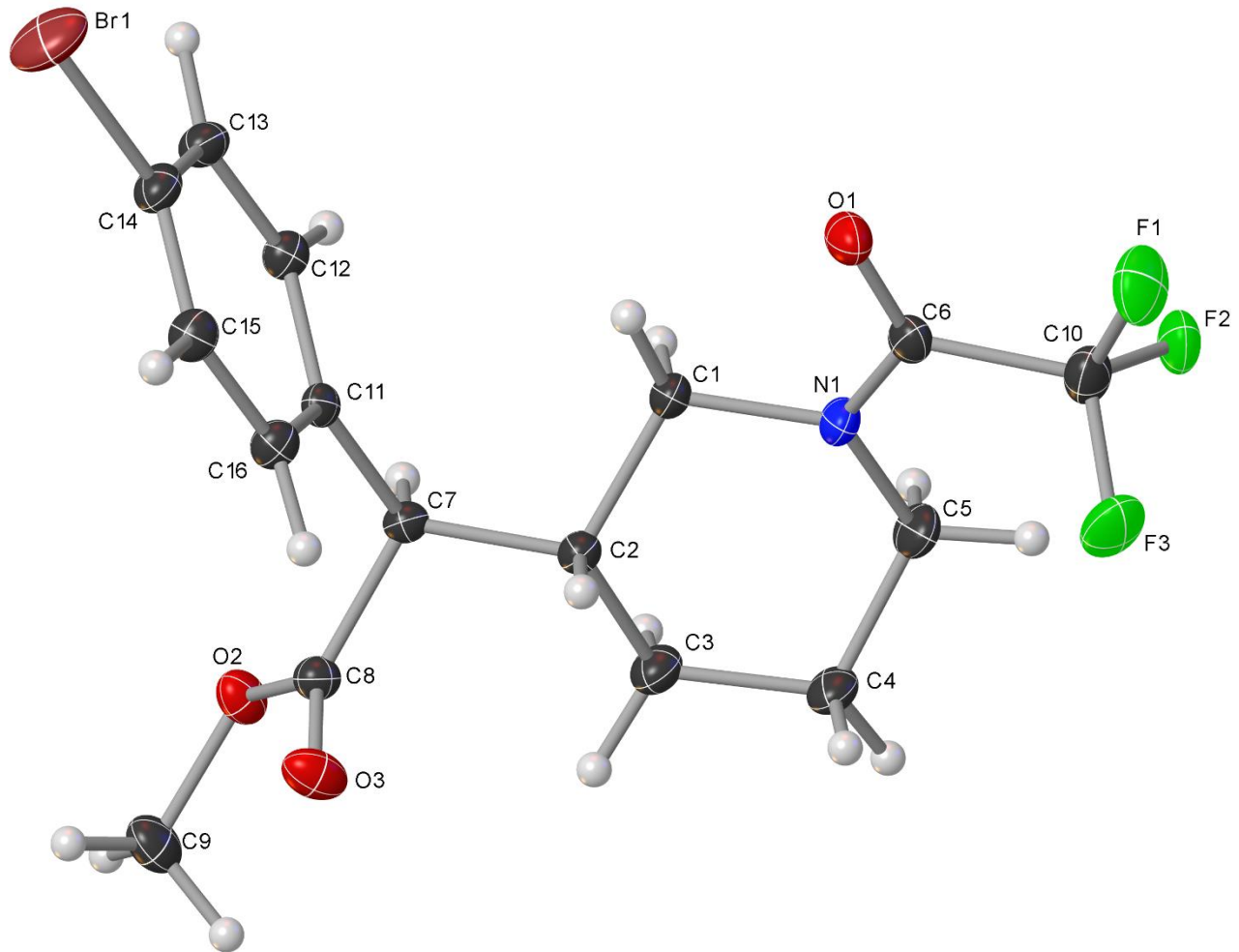
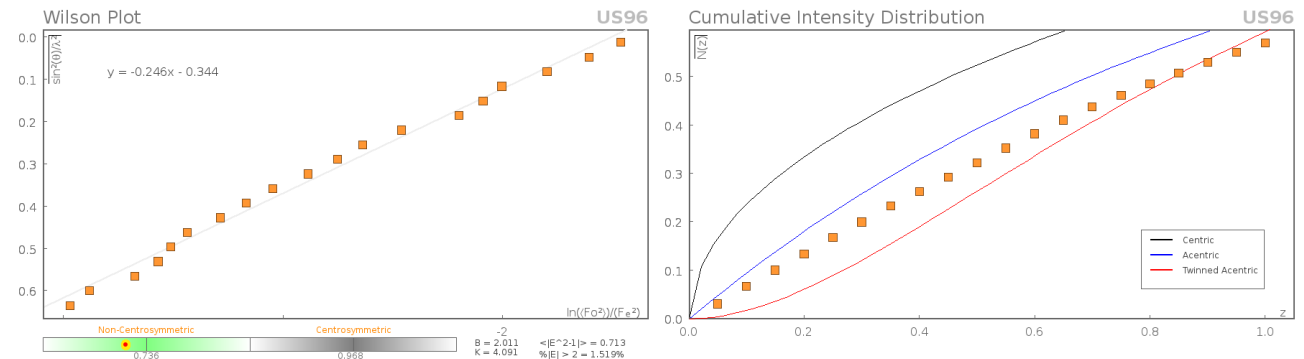
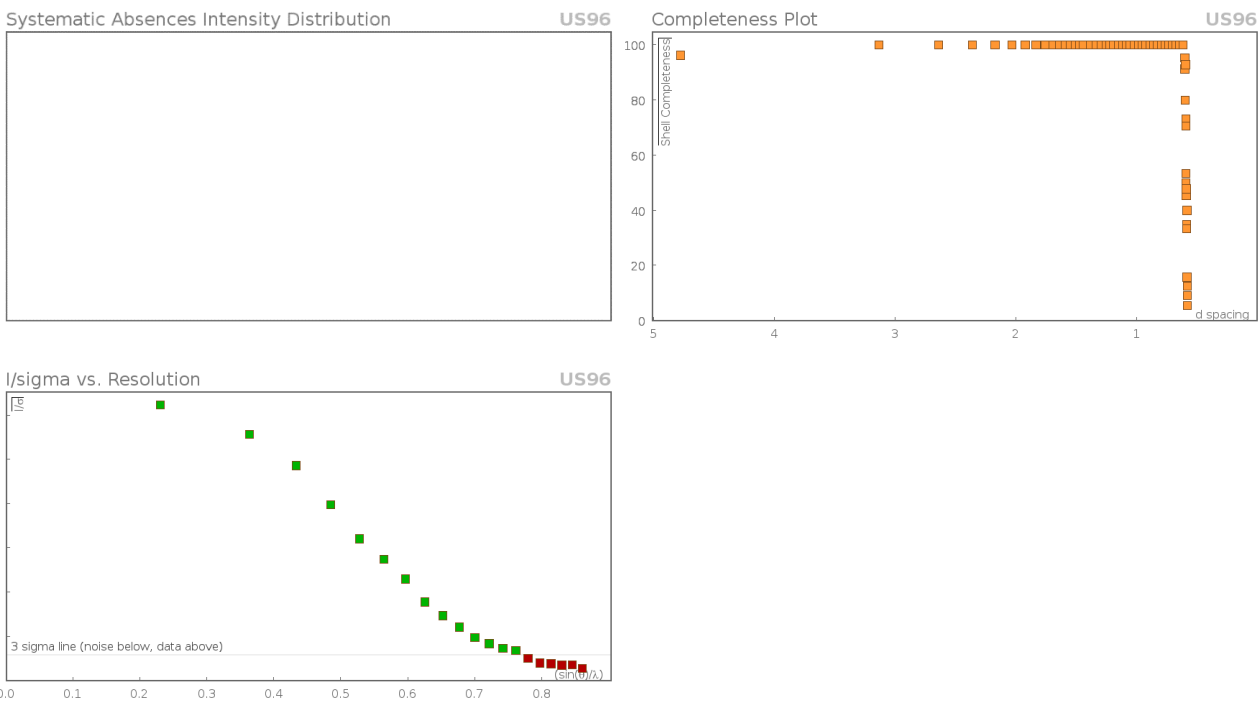


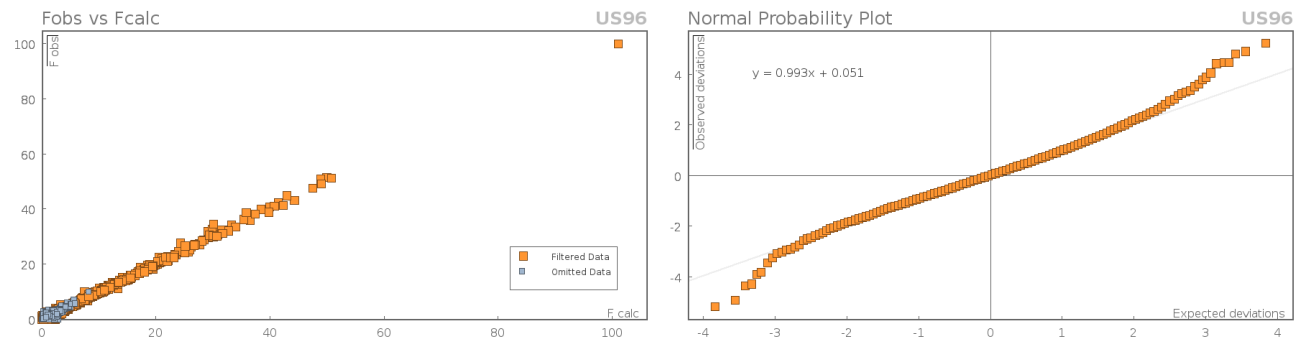
Figure 1:

Data Plots: Diffraction Data





Data Plots: Refinement and Data



Reflection Statistics

Total reflections (after filtering)	20233	Unique reflections	7976
Completeness	0.977	Mean I/s	17.04
hkl _{max} collected	(14, 14, 19)	hkl _{min} collected	(-15, -15, -19)
hkl _{max} used	(14, 14, 19)	hkl _{min} used	(-14, -14, 0)
Lim d _{max} collected	20.0	Lim d _{min} collected	0.6
d _{max} used	8.44	d _{min} used	0.6
Friedel pairs	5055	Friedel pairs merged	0
Inconsistent equivalents	2	R _{int}	0.0321
R _{sigma}	0.0447	Intensity transformed	0
Omitted reflections	0	Omitted by user (OMIT hkl)	19
Multiplicity	(7523, 4412, 1122, 193, 42, 13, 2)	Maximum multiplicity	11
Removed systematic absences	0	Filtered off (Shel/OMIT)	554

Table 1: Fractional Atomic Coordinates ($\times 10^4$) and Equivalent Isotropic Displacement Parameters ($\text{\AA}^2 \times 10^3$) for **US96**. U_{eq} is defined as 1/3 of the trace of the orthogonalised U_{ij} .

Atom	x	y	z	U_{eq}
Br1	10202.9(4)	8500.9(3)	9945.2(3)	36.82(9)
F2	4231.7(17)	8488(2)	815.0(12)	27.3(3)

Atom	x	y	z	U_{eq}
F3	6620(2)	7895(3)	864.7(17)	37.4(4)
F1	6086(3)	10149(2)	1427.8(17)	36.0(4)
O1	6577(2)	9079(2)	3588.8(16)	23.4(4)
O2	7801(2)	1321(2)	6247.6(17)	20.2(3)
O3	9779(2)	2430(2)	5680.9(19)	24.3(4)
N1	5839(3)	6622(2)	2972.0(17)	19.1(4)
C13	7789(3)	6705(3)	8337(2)	19.5(4)
C8	8508(3)	2512(3)	5868(2)	16.6(4)
C6	6098(3)	8109(3)	2796(2)	18.2(4)
C15	10372.1(19)	6546(3)	8005(2)	19.3(4)
C14	9386(3)	7109(3)	8644(2)	19.5(4)
C12	7203(2)	5690(2)	7366.3(19)	16.7(4)
C10	5756(3)	8656(3)	1456(2)	23.7(5)
C4	6180(2)	4074(3)	2157.6(19)	21.9(4)
C2	7271(2)	4617(3)	4413.0(19)	15.5(4)
C11	8173(3)	5083(2)	6719.9(18)	13.8(3)
C16	9765(3)	5526(3)	7041.2(19)	17.7(4)
C7	7480(3)	3946(2)	5697.2(19)	15.2(4)
C3	6548.6(18)	3403(2)	3442.3(19)	21.6(4)
C1	6201(2)	6041(2)	4227.9(17)	18.5(4)
C5	5103(2)	5477(3)	2025.0(16)	22.9(4)
C9	8694(2)	-110(2)	6427.9(13)	24.9(5)

Table 2: Anisotropic Displacement Parameters ($\times 10^4$) **US96**. The anisotropic displacement factor exponent takes the form: $-2p^2/h^2a^{*2} \times U_{11} + \dots + 2hka^* \times b^* \times U_{12}$

Atom	U_{11}	U_{22}	U_{33}	U_{23}	U_{13}	U_{12}
Br1	37.91(15)	42.39(17)	29.57(13)	-21.55(12)	8.97(10)	-11.12(14)
F2	25.9(6)	35.6(8)	16.6(6)	4.6(7)	0.3(5)	5.8(8)
F3	36.7(9)	55.5(12)	26.0(8)	0.5(7)	18.7(7)	9.9(8)
F1	46.8(11)	32.3(9)	28.0(9)	10.3(7)	9.8(8)	-6.4(8)
O1	26.6(9)	20.4(8)	18.7(7)	-1.0(6)	-0.5(7)	3.8(7)
O2	19.8(8)	18.0(8)	24.0(8)	5.6(6)	8.1(6)	0.1(6)
O3	20.6(8)	19.8(8)	36.3(10)	2.5(7)	14.2(8)	1.4(7)
N1	23.5(9)	19.7(9)	11.8(7)	-1.4(6)	1.5(7)	2.3(7)
C13	22.9(11)	20.1(10)	17.2(9)	-2.2(7)	8.3(8)	0.9(9)
C8	17.5(9)	15.7(9)	17.2(9)	-0.3(7)	6.2(7)	0.5(8)
C6	15.5(9)	21.6(11)	16.3(9)	1.2(7)	2.7(7)	3.5(7)
C15	18.1(10)	20.7(10)	18.5(9)	-1.0(7)	4.5(8)	-3.0(8)
C14	23.9(11)	18.7(10)	15.0(9)	-3.1(7)	4.4(8)	-1.8(8)
C12	16.8(10)	16.9(10)	16.6(8)	0.3(6)	5.5(8)	-2.2(7)
C10	23.3(10)	30.5(13)	17.7(9)	3.5(9)	6.7(8)	2.6(10)
C4	29.7(12)	18.7(10)	16.4(9)	-5.1(7)	5.3(8)	0.0(9)
C2	17.1(9)	15.6(9)	13.6(8)	-1.1(6)	4.4(7)	0.6(7)
C11	15.5(9)	13.5(8)	12.9(8)	2.4(6)	4.9(7)	0.2(7)
C16	16.8(10)	19.5(10)	17.4(9)	-0.8(7)	5.9(8)	-1.9(8)
C7	15.7(9)	15.5(9)	15.2(8)	-1.4(6)	5.5(7)	0.3(7)
C3	27.1(10)	20.0(10)	17.4(8)	-3.9(9)	6.2(8)	-0.9(11)
C1	22.6(11)	19.7(9)	12.5(8)	-0.4(7)	3.9(7)	3.7(9)
C5	24.4(11)	25.7(11)	14.2(9)	-4.9(8)	-1.2(8)	0.2(10)
C9	26.2(12)	19.3(11)	29.6(12)	6.8(9)	8.6(10)	3.0(9)

Table 3: Bond Lengths in Å for **US96**.

Atom	Atom	Length/Å	Atom	Atom	Length/Å
Br1	C14	1.892(2)	F3	C10	1.336(3)
F2	C10	1.339(3)	F1	C10	1.332(3)

Atom	Atom	Length/ \AA
O1	C6	1.221(3)
O2	C8	1.346(3)
O2	C9	1.454(3)
O3	C8	1.205(3)
N1	C6	1.337(3)
N1	C1	1.472(3)
N1	C5	1.476(3)
C13	C14	1.394(3)
C13	C12	1.396(3)
C8	C7	1.520(3)
C6	C10	1.554(3)

Atom	Atom	Length/ \AA
C15	C14	1.383(3)
C15	C16	1.396(3)
C12	C11	1.392(3)
C4	C3	1.530(3)
C4	C5	1.526(3)
C2	C7	1.546(3)
C2	C3	1.531(3)
C2	C1	1.533(3)
C11	C16	1.399(3)
C11	C7	1.519(3)

Table 4: Bond Angles in $^{\circ}$ for **US96**.

Atom	Atom	Atom	Angle/ $^{\circ}$
C8	O2	C9	114.76(17)
C6	N1	C1	118.77(18)
C6	N1	C5	126.67(19)
C1	N1	C5	114.41(16)
C14	C13	C12	118.15(15)
O2	C8	C7	110.78(19)
O3	C8	O2	123.9(2)
O3	C8	C7	125.3(2)
O1	C6	N1	126.2(2)
O1	C6	C10	116.9(2)
N1	C6	C10	116.9(2)
C14	C15	C16	119.36(16)
C13	C14	Br1	118.94(17)
C15	C14	Br1	119.41(18)
C15	C14	C13	121.6(2)
C11	C12	C13	121.51(16)
F2	C10	C6	112.5(2)
F3	C10	F2	107.4(2)
F3	C10	C6	112.2(2)
F1	C10	F2	106.5(2)
F1	C10	F3	107.9(2)
F1	C10	C6	110.0(2)
C5	C4	C3	110.50(13)
C3	C2	C7	110.01(17)
C3	C2	C1	110.24(15)
C1	C2	C7	109.42(16)
C12	C11	C16	118.95(19)
C12	C11	C7	119.15(19)
C16	C11	C7	121.90(18)
C15	C16	C11	120.38(16)
C8	C7	C2	109.35(17)
C11	C7	C8	110.08(18)
C11	C7	C2	113.61(17)
C4	C3	C2	111.42(16)
N1	C1	C2	111.10(16)
N1	C5	C4	109.74(15)

Table 5: Hydrogen Fractional Atomic Coordinates ($\times 10^4$) and Equivalent Isotropic Displacement Parameters ($\text{\AA}^2 \times 10^3$) for **US96**. U_{eq} is defined as 1/3 of the trace of the orthogonalised U_{ij} .

Atom	x	y	z	U_{eq}
H13	7054.2	7109	8766.09	0
H15	11513.61	6793	8252.11	0
H16	10442.2	5138.61	6558.3	0
H12	6068.6	5417.5	7083.61	0
H7	6390.6	3577.2	5765.19	0
H1A	5180.3	5776.69	4382.2	0
H3A	5543.4	3001.5	3553.21	0
H5A	4849.4	5968.8	1206.01	0
H4A	7189.01	4295.2	1972.5	0
H4B	5614.2	3339.2	1509.81	0
H2	8319.3	4983.81	4363.79	0
H3B	7265.89	2493.7	3592.3	0
H9A	8091.9	-972.81	6655.61	0
H9B	9698.6	57.9	7095.09	0
H1B	6643.3	6889.21	4811.5	0
H5B	4051.2	5166.29	2103.3	0
H9C	8950.5	-379.1	5663	0

Citations

CrysAlisPro Software System, Rigaku Oxford Diffraction, (2019).

O.V. Dolomanov and L.J. Bourhis and R.J. Gildea and J.A.K. Howard and H. Puschmann, Olex2: A complete structure solution, refinement and analysis program, *J. Appl. Cryst.*, (2009), **42**, 339-341.

Sheldrick, G.M., Crystal structure refinement with ShelXL, *Acta Cryst.*, (2015), **C27**, 3-8.

Sheldrick, G.M., ShelXT-Integrated space-group and crystal-structure determination, *Acta Cryst.*, (2015), **A71**, 3-8.

```

#=====
# PLATON/CHECK-( 70414) versus check.def version of 310314 for Entry: us96
# Data: US96.cif - Type: CIF          Bond Precision C-C = 0.0031 A
# Refl: US96.fcf - Type: LIST4        Temp = 100 K
#           X-Ray      Nref/Npar = 19.8
# Cell 8.8333(2) 8.6844(2) 11.4854(3)    90 107.078(3)    90
# Wavelength 0.71073   Volume Reported 842.22(4) Calculated 842.22(4)
# SpaceGroup from Symmetry P 21   Hall: P 2yb      monoclinic
#           Reported P 1 21 1   P 2yb      monoclinic
# MoietyFormula C16 H17 Br F3 N O3
#   Reported C16 H17 Br F3 N O3
# SumFormula C16 H17 Br F3 N O3
#   Reported C16 H17 Br F3 N O3
# Mr     = 408.21[Calc], 408.21[Rep]
# Dx,gcm-3 = 1.610[Calc], 1.610[Rep]
# Z     = 2[Calc], 2[Rep]
# Mu (mm-1)= 2.485[Calc], 2.485[Rep]
# F000   = 412.0[Calc], 412.0[Rep] or F000' = 411.68[Calc]
# Reported T Limits: Tmin=0.448      Tmax=1.000 AbsCorr=GAUSSIAN
# Calculated T Limits: Tmin=0.715 Tmin'=0.378 Tmax=0.784
# Reported Hmax= 14, Kmax= 14, Lmax= 19, Nref= 7976 , Th(max)= 36.317
# Obs in FCF Hmax= 14, Kmax= 14, Lmax= 19, Nref= 7976[ 4290], Th(max)= 36.317
# Calculated Hmax= 14, Kmax= 14, Lmax= 19, Nref= 8160[ 4292], Ratio=1.86/0.98
# Reported Rho(min) = -0.68, Rho(max) = 0.97 e/Ang**3 (From CIF)
# Calculated Rho(min) = -0.57, Rho(max) = 0.88 e/Ang**3 (From CIF+FCF data)
# w=1/(\sigma**2(Fo**2)+(0.0578P)**2), P=(Fo**2+2*Fc**2)/3
# R= 0.0406( 6369), wR2= 0.0993( 7976), S = 1.019 (From CIF+FCF data)
# R= 0.0406( 6369), wR2= 0.0993( 7976), S = 1.019 (From FCF data only)
# R= 0.0406( 6370), wR2= 0.0993( 7976), S = 1.019, Npar= 217, Flack -0.003(3)
# Number Bijvoet Pairs = 3686 ( 95%) ( 2523 Selected for: Parsons -0.001(2)
# P2(tr) 1.000, P3(tr) 1.000, P3(tw) 0.000, Student-T Nu 18.85, Hooft -0.001(4)
#=====

For Documentation: http://http://www.platonssoft.nl/CIF-VALIDATION.pdf
#=====
```

```

#=====
>>> The Following Improvement and Query ALERTS were generated - (Acta-Mode) <<<
#=====

Format: alert-number_ALERT_alert-type_alert-level text
```

```

751_ALERT_4_C Bond Calc 0.99000, Rep 0.9877(15) ..... Senseless su
C13 -H13 1.555 1.555 # 14
751_ALERT_4_C Bond Calc 0.99000, Rep 0.9875(15) ..... Senseless su
C15 -H15 1.555 1.555 # 19
751_ALERT_4_C Bond Calc 0.99000, Rep 0.9867(18) ..... Senseless su
C12 -H12 1.555 1.555 # 21
751_ALERT_4_C Bond Calc 0.99000, Rep 0.9940(17) ..... Senseless su
C4 -H4A 1.555 1.555 # 24
751_ALERT_4_C Bond Calc 1.00000, Rep 0.9960(16) ..... Senseless su
C4 -H4B 1.555 1.555 # 25
751_ALERT_4_C Bond Calc 1.00000, Rep 0.9959(16) ..... Senseless su
C2 -H2 1.555 1.555 # 29
751_ALERT_4_C Bond Calc 0.99000, Rep 0.9865(17) ..... Senseless su
C16 -H16 1.555 1.555 # 32
751_ALERT_4_C Bond Calc 1.04000, Rep 1.039(2) ..... Senseless su
C7 -H7 1.555 1.555 # 33
751_ALERT_4_C Bond Calc 1.00000, Rep 0.9964(16) ..... Senseless su
C3 -H3A 1.555 1.555 # 34
751_ALERT_4_C Bond Calc 1.00000, Rep 0.9955(17) ..... Senseless su
C3 -H3B 1.555 1.555 # 35
751_ALERT_4_C Bond Calc 1.00000, Rep 0.9952(16) ..... Senseless su
C1 -H1A 1.555 1.555 # 36
751_ALERT_4_C Bond Calc 1.00000, Rep 0.9955(16) ..... Senseless su
C1 -H1B 1.555 1.555 # 37
751_ALERT_4_C Bond Calc 1.00000, Rep 0.9968(16) ..... Senseless su
C5 -H5A 1.555 1.555 # 38
751_ALERT_4_C Bond Calc 1.00000, Rep 0.9966(16) ..... Senseless su
C5 -H5B 1.555 1.555 # 39
751_ALERT_4_C Bond Calc 1.00000, Rep 0.9973(14) ..... Senseless su
C9 -H9A 1.555 1.555 # 40
751_ALERT_4_C Bond Calc 1.00000, Rep 0.9980(17) ..... Senseless su
C9 -H9B 1.555 1.555 # 41
```

751_ALERT_4_C Bond Calc 1.00000, Rep 0.9971(17) Senseless su
 C9 -H9C 1.555 1.555 # 42
 752_ALERT_4_C Angle Calc 123.00, Rep 123.2(2) Senseless su
 C14 -C13 -H13 1.555 1.555 1.555 # 6
 752_ALERT_4_C Angle Calc 119.00, Rep 118.6(2) Senseless su
 C12 -C13 -H13 1.555 1.555 1.555 # 7
 752_ALERT_4_C Angle Calc 121.00, Rep 121.4(2) Senseless su
 C14 -C15 -H15 1.555 1.555 1.555 # 15
 752_ALERT_4_C Angle Calc 119.00, Rep 119.1(2) Senseless su
 C16 -C15 -H15 1.555 1.555 1.555 # 16
 752_ALERT_4_C Angle Calc 121.00, Rep 121.12(19) Senseless su
 C13 -C12 -H12 1.555 1.555 1.555 # 20
 752_ALERT_4_C Angle Calc 117.00, Rep 117.3(2) Senseless su
 C11 -C12 -H12 1.555 1.555 1.555 # 22
 752_ALERT_4_C Angle Calc 109.00, Rep 109.25(18) Senseless su
 C3 -C4 -H4A 1.555 1.555 1.555 # 29
 752_ALERT_4_C Angle Calc 113.00, Rep 113.2(2) Senseless su
 C3 -C4 -H4B 1.555 1.555 1.555 # 30
 752_ALERT_4_C Angle Calc 113.00, Rep 113.35(19) Senseless su
 C5 -C4 -H4A 1.555 1.555 1.555 # 32
 752_ALERT_4_C Angle Calc 106.00, Rep 106.01(19) Senseless su
 C5 -C4 -H4B 1.555 1.555 1.555 # 33
 752_ALERT_4_C Angle Calc 104.00, Rep 104.41(17) Senseless su
 H4A -C4 -H4B 1.555 1.555 1.555 # 34
 752_ALERT_4_C Angle Calc 109.00, Rep 108.81(18) Senseless su
 C7 -C2 -H2 1.555 1.555 1.555 # 35
 752_ALERT_4_C Angle Calc 112.00, Rep 112.00(17) Senseless su
 C3 -C2 -H2 1.555 1.555 1.555 # 38
 752_ALERT_4_C Angle Calc 106.00, Rep 106.28(18) Senseless su
 C1 -C2 -H2 1.555 1.555 1.555 # 40
 752_ALERT_4_C Angle Calc 120.00, Rep 120.5(2) Senseless su
 C15 -C16 -H16 1.555 1.555 1.555 # 45
 752_ALERT_4_C Angle Calc 119.00, Rep 119.1(2) Senseless su
 C11 -C16 -H16 1.555 1.555 1.555 # 46
 752_ALERT_4_C Angle Calc 106.00, Rep 105.65(19) Senseless su
 C8 -C7 -H7 1.555 1.555 1.555 # 48
 752_ALERT_4_C Angle Calc 110.00, Rep 109.54(18) Senseless su
 C2 -C7 -H7 1.555 1.555 1.555 # 49
 752_ALERT_4_C Angle Calc 108.00, Rep 108.30(17) Senseless su
 C11 -C7 -H7 1.555 1.555 1.555 # 52
 752_ALERT_4_C Angle Calc 108.00, Rep 108.14(16) Senseless su
 C4 -C3 -H3A 1.555 1.555 1.555 # 54
 752_ALERT_4_C Angle Calc 114.00, Rep 114.42(17) Senseless su
 C4 -C3 -H3B 1.555 1.555 1.555 # 55
 752_ALERT_4_C Angle Calc 110.00, Rep 110.17(16) Senseless su
 C2 -C3 -H3A 1.555 1.555 1.555 # 56
 752_ALERT_4_C Angle Calc 108.00, Rep 108.19(17) Senseless su
 C2 -C3 -H3B 1.555 1.555 1.555 # 57
 752_ALERT_4_C Angle Calc 104.00, Rep 104.23(19) Senseless su
 H3A -C3 -H3B 1.555 1.555 1.555 # 58
 752_ALERT_4_C Angle Calc 108.00, Rep 107.82(18) Senseless su
 N1 -C1 -H1A 1.555 1.555 1.555 # 60
 752_ALERT_4_C Angle Calc 110.00, Rep 109.61(18) Senseless su
 N1 -C1 -H1B 1.555 1.555 1.555 # 61
 752_ALERT_4_C Angle Calc 110.00, Rep 110.10(17) Senseless su
 C2 -C1 -H1A 1.555 1.555 1.555 # 62
 752_ALERT_4_C Angle Calc 114.00, Rep 113.52(18) Senseless su
 C2 -C1 -H1B 1.555 1.555 1.555 # 63
 752_ALERT_4_C Angle Calc 104.00, Rep 104.35(16) Senseless su
 H1A -C1 -H1B 1.555 1.555 1.555 # 64
 752_ALERT_4_C Angle Calc 110.00, Rep 109.58(19) Senseless su
 N1 -C5 -H5A 1.555 1.555 1.555 # 66
 752_ALERT_4_C Angle Calc 110.00, Rep 109.65(19) Senseless su
 N1 -C5 -H5B 1.555 1.555 1.555 # 67
 752_ALERT_4_C Angle Calc 113.00, Rep 113.39(19) Senseless su
 C4 -C5 -H5A 1.555 1.555 1.555 # 68
 752_ALERT_4_C Angle Calc 110.00, Rep 110.19(18) Senseless su
 C4 -C5 -H5B 1.555 1.555 1.555 # 69
 752_ALERT_4_C Angle Calc 104.00, Rep 104.13(17) Senseless su
 H5A -C5 -H5B 1.555 1.555 1.555 # 70
 752_ALERT_4_C Angle Calc 112.00, Rep 111.72(18) Senseless su
 O2 -C9 -H9A 1.555 1.555 1.555 # 71

752_ALERT_4_C Angle Calc 108.00, Rep 107.89(17) Senseless su
O2 -C9 -H9B 1.555 1.555 1.555 # 72
752_ALERT_4_C Angle Calc 109.00, Rep 109.19(17) Senseless su
O2 -C9 -H9C 1.555 1.555 1.555 # 73
752_ALERT_4_C Angle Calc 109.00, Rep 109.33(17) Senseless su
H9A -C9 -H9B 1.555 1.555 1.555 # 74
752_ALERT_4_C Angle Calc 109.00, Rep 109.37(17) Senseless su
H9A -C9 -H9C 1.555 1.555 1.555 # 75
752_ALERT_4_C Angle Calc 109.00, Rep 109.29(18) Senseless su
H9B -C9 -H9C 1.555 1.555 1.555 # 76
911_ALERT_3_C Missing # FCF Refl Between THmin & STh/L= 0.600 2 Why ?

#=====

002_ALERT_2_G Number of Distance or Angle Restraints on AtSite 26 Note
760_ALERT_1_G CIF Contains no Torsion Angles ? Info
791_ALERT_4_G The Model has Chirality at C2 R Verify
791_ALERT_4_G The Model has Chirality at C7 R Verify
795_ALERT_4_G C-Atom in CIF Coordinate List out of Sequence .. C8 Note
860_ALERT_3_G Number of Least-Squares Restraints 60 Note
910_ALERT_3_G Missing # of FCF Reflections Below Th(Min) 1 Why ?

#=====

ALERT_Level and ALERT_Type Summary

=====

58 ALERT_Level_C = Check. Ensure it is Not caused by an Omission or Oversight
7 ALERT_Level_G = General Info/Check that it is not Something Unexpected

1 ALERT_Type_1 CIF Construction/Syntax Error, Inconsistent or Missing Data.
1 ALERT_Type_2 Indicator that the Structure Model may be Wrong or Deficient.
3 ALERT_Type_3 Indicator that the Structure Quality may be Low.
60 ALERT_Type_4 Improvement, Methodology, Query or Suggestion.

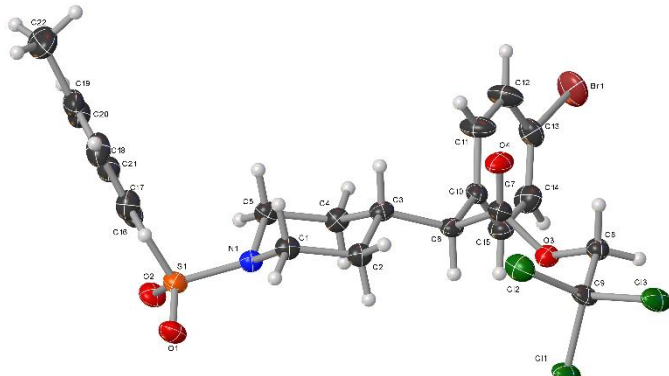
#=====

0 Missing Experimental Info Issue(s) (Out of 54 Tests) - 100 % Satisfied
0 Experimental Data Related Issue(s) (Out of 28 Tests) - 100 % Satisfied
2 Structural Model Related Issue(s) (Out of 117 Tests) - 98 % Satisfied
63 Unresolved or to be Checked Issue(s) (Out of 223 Tests) - 72 % Satisfied

#=====

10.4. X-Ray Crystallographic Data for 13b

Crystal Data and Experimental



Experimental. Single colourless prism-shaped crystals of **WL-N9-80-f34** were chosen from the sample as supplied. A suitable crystal $0.35 \times 0.21 \times 0.11 \text{ mm}^3$ was selected and mounted on a loop with paratone oil on an XtaLAB Synergy-S diffractometer. The crystal was kept at a steady $T = 100.01(10)$ K during data collection. The structure was solved with the **ShelXT** (Sheldrick, 2015) structure solution program using the Intrinsic Phasing solution method and by using **Olex2** (Dolomanov et al., 2009) as the graphical interface. The model was refined with version 2018/3 of **ShelXL** (Sheldrick, 2015) using Least Squares minimisation.

Crystal Data. $C_{22}H_{23}BrCl_3NO_4S$, $M_r = 583.73$, orthorhombic, $P2_12_12_1$ (No. 19), $a = 5.60602(6) \text{ \AA}$, $b = 20.3318(2) \text{ \AA}$, $c = 21.4309(2) \text{ \AA}$, $a = b = g = 90^\circ$, $V = 2442.71(4) \text{ \AA}^3$, $T = 100.01(10)$ K, $Z = 4$, $Z' = 1$, $m(\text{CuK}_\alpha) = 6.365 \text{ mm}^{-1}$, 24631 reflections measured, 4842 unique ($R_{int} = 0.0422$) which were used in all calculations. The final wR_2 was 0.0855 (all data) and R_I was 0.0326 ($I > 2\sigma(I)$).

Compound	WL-N9-80-f34
Formula	$C_{22}H_{23}BrCl_3NO_4S$
$D_{\text{calc.}}/\text{g cm}^{-3}$	1.587
m/mm^{-1}	6.365
Formula Weight	583.73
Colour	colourless
Shape	prism
Size/mm ³	$0.35 \times 0.21 \times 0.11$
T/K	100.01(10)
Crystal System	orthorhombic
Flack Parameter	-0.001(8)
Hooft Parameter	-0.007(6)
Space Group	$P2_12_12_1$
$a/\text{\AA}$	5.60602(6)
$b/\text{\AA}$	20.3318(2)
$c/\text{\AA}$	21.4309(2)
a°	90
b°	90
g°	90
$V/\text{\AA}^3$	2442.71(4)
Z	4
Z'	1
Wavelength/ \AA	1.54184
Radiation type	CuK_α
$Q_{\min}/^\circ$	2.996
$Q_{\max}/^\circ$	77.056
Measured Refl.	24631
Independent Refl.	4842
Reflections with $I > 2\sigma(I)$	4758
R_{int}	0.0422
Parameters	290
Restraints	12
Largest Peak	0.675
Deepest Hole	-0.722
GooF	1.057
wR_2 (all data)	0.0855
wR_2	0.0851
R_I (all data)	0.0335
R_I	0.0326

Structure Quality Indicators

Reflections:	d min (Cu)	0.79	I/σ	39.7	R _{int}	4.22%	complete 100% (IUCr)	100%	
Refinement:	Shift	-0.004	Max Peak	0.7	Min Peak	-0.7	GooF	1.057	Flack 0.001(8)

A colourless prism-shaped crystal with dimensions $0.35 \times 0.21 \times 0.11$ mm³ was mounted on a loop with paratone oil. Data were collected using an XtaLAB Synergy, Dualflex, HyPix diffractometer equipped with an Oxford Cryosystems low-temperature device operating at $T = 100.01(10)$ K.

Data were measured using w scans using CuK_a radiation. The total number of runs and images was based on the strategy calculation from the program **CrysAlisPro** (Rigaku, V1.171.40.37a, 2019). The maximum resolution that was achieved was $Q = 77.056^\circ$ (0.79 Å).

The diffraction pattern was indexed and then the total number of runs and images was calculated from the program **CrysAlisPro** (Rigaku, V1.171.40.37a, 2019). The unit cell was refined using **CrysAlisPro** (Rigaku, V1.171.40.37a, 2019) on 20665 reflections, 84% of the observed reflections.

Data reduction, scaling and absorption corrections were performed using **CrysAlisPro** (Rigaku, V1.171.40.37a, 2019). The final completeness is 100.00 % out to 77.056° in Q . A numerical absorption correction based on Gaussian integration over a multifaceted crystal model was performed using (Rigaku Oxford Diffraction, 2019). An empirical absorption correction using spherical harmonics as implemented in SCALE3 ABSPACK was also performed. The absorption coefficient m of this material is 6.365 mm⁻¹ at this wavelength ($\lambda = 1.542\text{\AA}$) and the minimum and maximum transmissions are 0.158 and 0.975.

The structure was solved and the space group $P2_12_12_1$ (# 19) determined by the **ShelXT** (Sheldrick, 2015) structure solution program using Intrinsic Phasing and refined by Least Squares using version 2018/3 of **ShelXL** (Sheldrick, 2015). All non-hydrogen atoms were refined anisotropically. Hydrogen atom positions were calculated geometrically and refined using the riding model. Hydrogen atom positions were calculated geometrically and refined using the riding model.

There is a single molecule in the asymmetric unit, which is represented by the reported sum formula. In other words: Z is 4 and Z' is 1.

The Flack parameter was refined to -0.001(8). Determination of absolute structure using Bayesian statistics on Bijvoet differences using the Olex2 results in -0.007(6). Note: The Flack parameter is used to determine chirality of the crystal studied, the value should be near 0, a value of 1 means that the stereochemistry is wrong and the model should be inverted. A value of 0.5 means that the crystal consists of a racemic mixture of the two enantiomers.

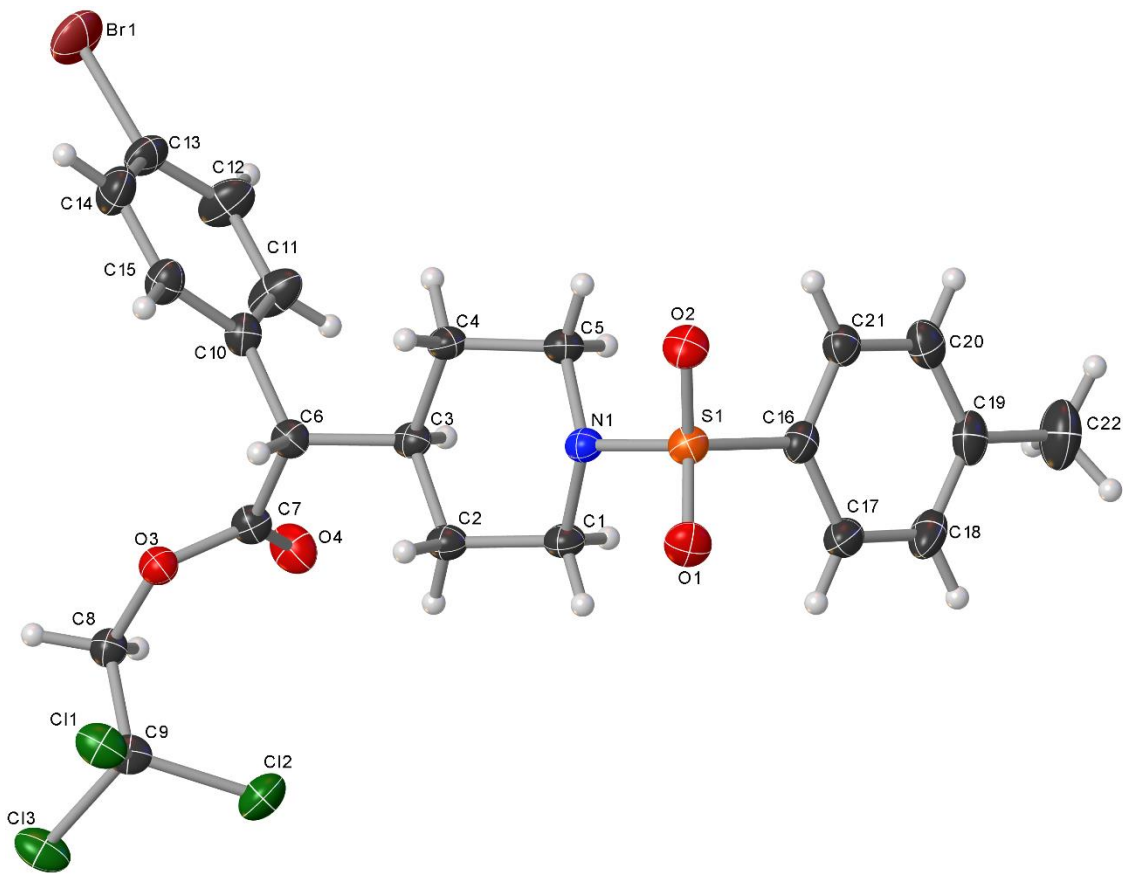


Figure 1:

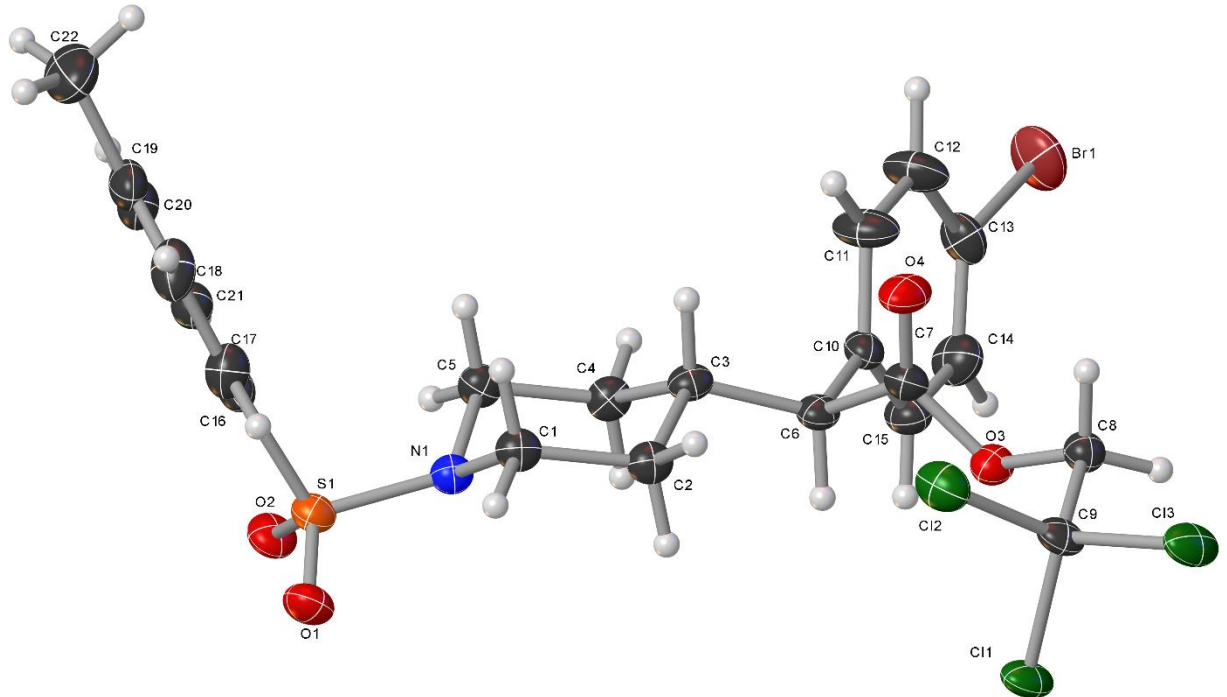
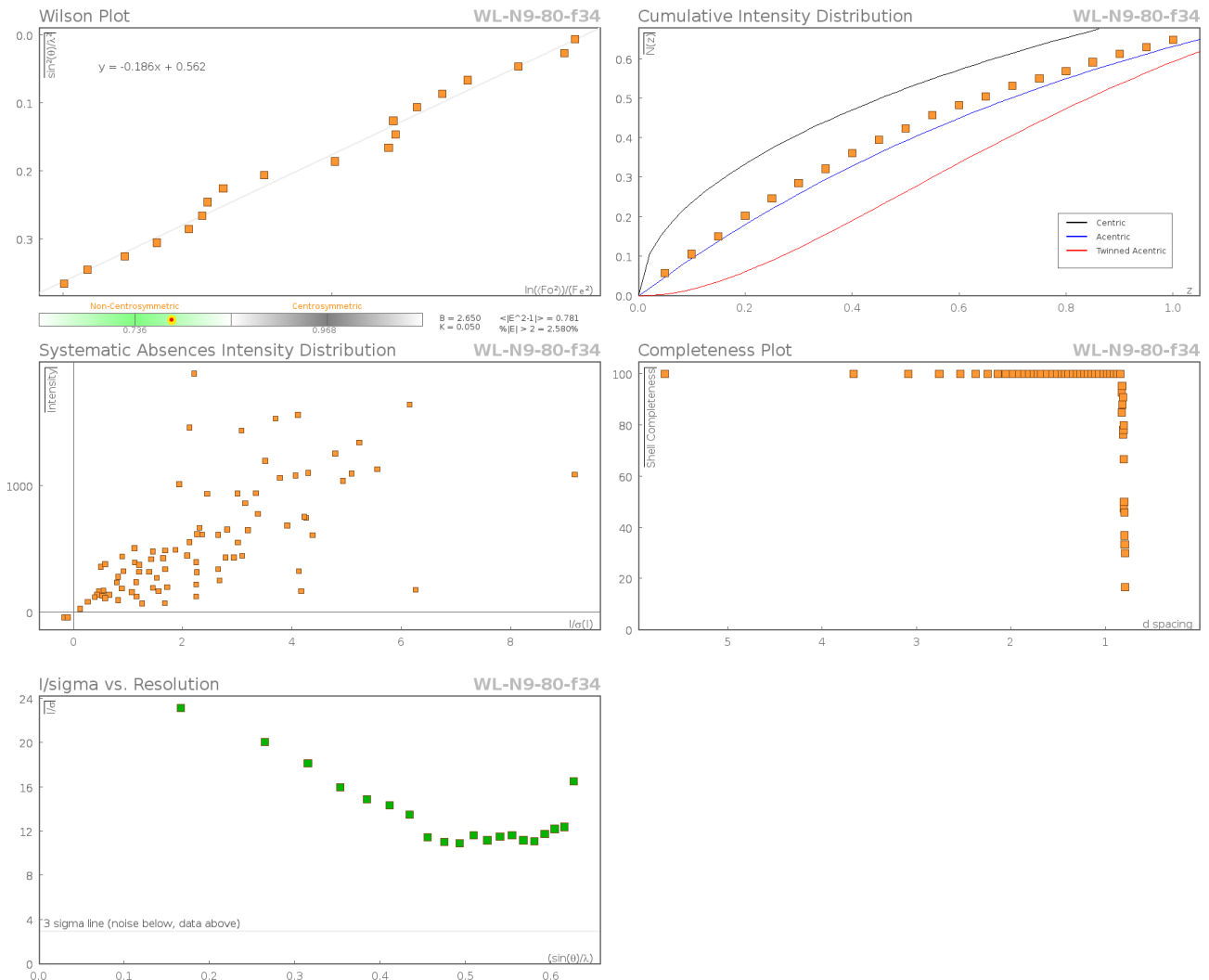
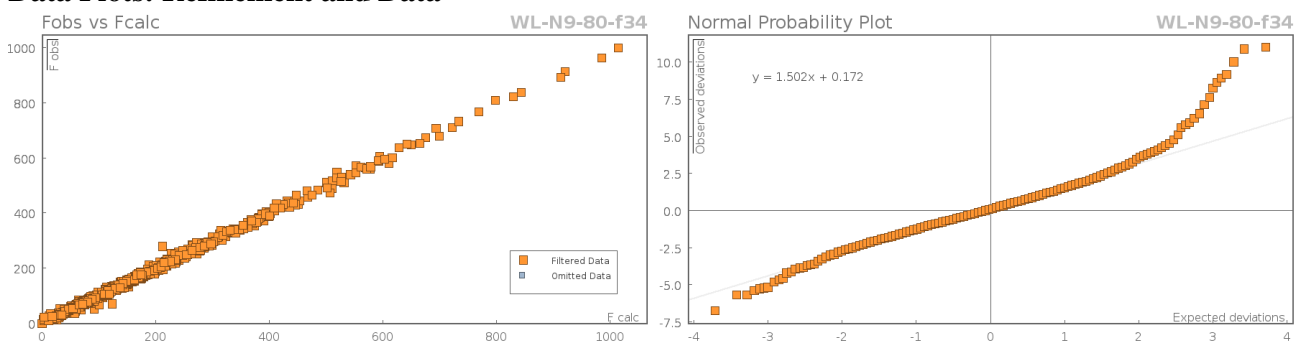


Figure 2:

Data Plots: Diffraction Data



Data Plots: Refinement and Data



Reflection Statistics

Total reflections (after filtering)	24719
Completeness	0.94
hkl _{max} collected	(6, 22, 26)
hkl _{max} used	(6, 25, 26)
Lim d _{max} collected	100.0
d _{max} used	14.75
Friedel pairs	2903

Unique reflections	4842
Mean I/s	28.61
hkl _{min} collected	(-6, -25, -25)
hkl _{min} used	(-6, 0, 0)
Lim d _{min} collected	0.77
d _{min} used	0.79
Friedel pairs merged	0

Inconsistent equivalents	16	R_{int}	0.0422
R_{sigma}	0.0252	Intensity transformed	0
Omitted reflections	0	Omitted by user (OMIT hkl)	0
Multiplicity	(4573, 3499, 1890, 963, 416, 172, 56, 13, 2)	Maximum multiplicity	16
Removed systematic absences	88	Filtered off (Shel/OMIT)	0

Images of the Crystal on the Diffractometer

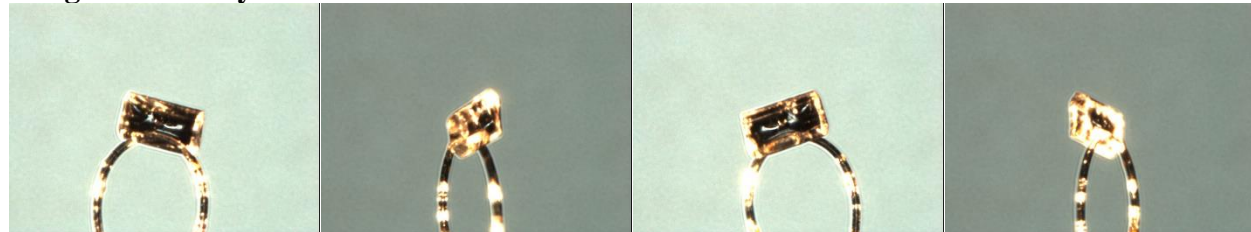


Table 1: Fractional Atomic Coordinates ($\times 10^4$) and Equivalent Isotropic Displacement Parameters ($\text{\AA}^2 \times 10^3$) for **WL-N9-80-f34**. U_{eq} is defined as 1/3 of the trace of the orthogonalised U_{ij} .

Atom	x	y	z	U_{eq}
Br1	2801.8(11)	1784.5(2)	4307.8(3)	49.52(16)
C1	6633(7)	6324.1(18)	4797.0(17)	24.8(7)
C2	6167(7)	5869.2(18)	4242.4(18)	25.2(7)
C3	5315(7)	5184.6(18)	4444.8(16)	22.5(7)
C4	7009(7)	4906.9(17)	4939.5(16)	24.8(8)
C5	7411(7)	5382.3(17)	5473.4(16)	25.3(7)
C6	5239(7)	4718.2(18)	3879.1(17)	22.6(7)
C7	3332(7)	4912.0(18)	3407.4(18)	24.8(8)
C8	2607(7)	4960.3(17)	2306.5(16)	23.9(7)
C9	3411(7)	5610.5(19)	2020.5(18)	25.9(8)
C10	4745(7)	3992.7(19)	4029.2(17)	24.2(7)
C11	2689(8)	3809(2)	4339(2)	38.7(10)
C12	2144(8)	3148(2)	4433(2)	40.3(10)
C13	3686(8)	2680.8(18)	4212(2)	31.1(9)
C14	5814(9)	2844(2)	3932(2)	36.6(10)
C15	6298(7)	3507(2)	3837.6(19)	29.3(8)
C16	7868(7)	6777.2(18)	6246.6(17)	25.3(7)
C17	6642(8)	7360(2)	6117.9(19)	31.8(9)
C18	4942(9)	7578(2)	6537(2)	37.0(10)
C19	4397(8)	7229(2)	7076(2)	34.5(9)
C20	5640(8)	6651(2)	7192.3(19)	34.2(10)
C21	7353(8)	6420.8(19)	6782.5(17)	27.7(8)
C22	2503(10)	7463(3)	7523(2)	54.5(14)
Cl1	6532.4(16)	5608.4(5)	1900.9(4)	31.8(2)
Cl3	1966.4(16)	5695.7(6)	1286.8(4)	35.6(2)
Cl2	2634.7(19)	6285.6(4)	2500.5(5)	35.7(2)
N1	8391(6)	6000.3(14)	5214.8(14)	22.0(6)
O1	10817(5)	7001.9(14)	5336.0(14)	32.3(6)
O2	11531(5)	6036.9(14)	6019.9(13)	29.8(6)
O3	4142(5)	4807.2(13)	2820.3(12)	24.3(5)
O4	1346(5)	5097.9(16)	3531.3(14)	33.8(7)
S1	9909.2(16)	6464.1(4)	5693.8(4)	24.63(19)

Table 2: Anisotropic Displacement Parameters ($\times 10^4$) **WL-N9-80-f34**. The anisotropic displacement factor exponent takes the form: $-2p^2[h^2a^{*2} \times U_{11} + \dots + 2hka^* \times b^* \times U_{12}]$

Atom	U_{11}	U_{22}	U_{33}	U_{23}	U_{13}	U_{12}
Br1	59.0(3)	26.0(2)	63.6(3)	-7.0(2)	-3.3(3)	-13.6(2)

Atom	U_{11}	U_{22}	U_{33}	U_{23}	U_{13}	U_{12}
C1	24.1(18)	23.4(14)	27.0(14)	4.0(12)	-1.1(13)	3.9(14)
C2	24.0(17)	24.9(12)	26.6(14)	3.6(11)	-0.4(12)	3.3(11)
C3	18.6(16)	23.9(13)	24.9(17)	1.9(12)	2.9(13)	5.4(11)
C4	28(2)	20.6(16)	25.9(17)	3.0(14)	-0.2(15)	3.5(16)
C5	27.2(18)	23.2(12)	25.3(16)	3.3(11)	-0.4(14)	0.4(12)
C6	15.3(16)	27.0(18)	25.6(17)	0.0(14)	1.6(14)	2.7(14)
C7	20.7(18)	26.0(18)	27.8(18)	0.8(15)	1.5(15)	-2.2(15)
C8	21.0(18)	25.0(17)	25.7(17)	-1.1(13)	-0.6(14)	1.2(15)
C9	14.2(16)	31.6(19)	31.8(18)	4.0(16)	-2.6(14)	0.3(15)
C10	17.1(14)	28.3(18)	27.2(16)	-4.6(14)	-0.3(12)	-0.4(13)
C11	25.7(15)	29.0(18)	62(2)	2.2(18)	17.1(17)	3.5(14)
C12	29(2)	30(2)	62(3)	5.3(19)	12(2)	-5.0(18)
C13	34(2)	19.7(17)	39(2)	-0.8(16)	-5.3(18)	-4.4(16)
C14	41(2)	29(2)	40(2)	-7.6(19)	6.0(19)	3.4(19)
C15	25(2)	29.2(19)	34(2)	-4.2(17)	5.6(16)	-0.1(16)
C16	21.4(18)	25.5(17)	28.9(17)	-6.1(14)	-5.1(15)	2.1(16)
C17	39(2)	26.1(19)	30.3(19)	-1.4(15)	-5.1(17)	4.5(17)
C18	38(2)	33(2)	41(2)	-12.6(18)	-11(2)	15(2)
C19	31(2)	40(2)	33(2)	-15.2(18)	-2.3(17)	-1.1(19)
C20	37(2)	39(2)	26.9(19)	-5.7(17)	-1.3(17)	-4.7(19)
C21	27(2)	28.8(18)	27.2(17)	-3.2(15)	-2.4(15)	2.0(17)
C22	47(3)	63(3)	54(3)	-26(3)	8(3)	4(3)
Cl1	14.4(4)	46.4(5)	34.6(5)	6.4(4)	-1.4(3)	-0.9(4)
Cl3	18.9(4)	54.6(6)	33.2(4)	12.0(4)	-6.5(4)	0.4(4)
Cl2	31.5(5)	24.6(4)	50.9(6)	-3.6(4)	1.8(5)	1.9(4)
N1	20.3(15)	21.5(12)	24.2(14)	1.9(10)	0.4(11)	3.2(11)
O1	26.8(15)	33.1(15)	37.1(15)	2.7(12)	2.7(12)	-7.6(12)
O2	17.6(13)	35.1(14)	36.8(14)	0.4(12)	-4.6(11)	6.2(11)
O3	20.0(12)	26.7(13)	26.3(13)	0.2(10)	-0.1(10)	4.5(11)
O4	18.2(14)	50.2(18)	32.8(15)	0.1(13)	3.8(11)	5.9(13)
S1	18.5(4)	26.3(4)	29.1(4)	0.6(4)	-0.2(4)	0.8(3)

Table 3: Bond Lengths in Å for **WL-N9-80-f34**.

Atom	Atom	Length/Å	Atom	Atom	Length/Å
Br1	C13	1.900(4)	C10	C11	1.381(6)
C1	C2	1.528(5)	C10	C15	1.379(5)
C1	N1	1.486(5)	C11	C12	1.394(6)
C2	C3	1.534(5)	C12	C13	1.369(6)
C3	C4	1.531(5)	C13	C14	1.376(6)
C3	C6	1.540(5)	C14	C15	1.390(6)
C4	C5	1.515(5)	C16	C17	1.398(5)
C5	N1	1.479(5)	C16	C21	1.388(5)
C6	C7	1.523(5)	C16	S1	1.766(4)
C6	C10	1.535(5)	C17	C18	1.382(6)
C7	O3	1.355(5)	C18	C19	1.391(7)
C7	O4	1.205(5)	C19	C20	1.389(7)
C8	C9	1.525(5)	C19	C22	1.507(6)
C8	O3	1.432(4)	C20	C21	1.383(6)
C9	Cl1	1.769(4)	N1	S1	1.633(3)
C9	Cl3	1.777(4)	O1	S1	1.429(3)
C9	Cl2	1.770(4)	O2	S1	1.438(3)

Table 4: Bond Angles in ° for **WL-N9-80-f34**.

Atom	Atom	Atom	Angle°	Atom	Atom	Atom	Angle°
N1	C1	C2	108.3(3)	C12	C13	Br1	117.6(3)
C1	C2	C3	112.5(3)	C12	C13	C14	122.0(4)
C2	C3	C6	110.2(3)	C14	C13	Br1	120.3(3)
C4	C3	C2	109.7(3)	C13	C14	C15	117.8(4)
C4	C3	C6	109.6(3)	C10	C15	C14	121.8(4)
C5	C4	C3	112.3(3)	C17	C16	S1	119.5(3)
N1	C5	C4	108.3(3)	C21	C16	C17	120.2(4)
C7	C6	C3	112.5(3)	C21	C16	S1	120.1(3)
C7	C6	C10	105.1(3)	C18	C17	C16	118.8(4)
C10	C6	C3	115.6(3)	C17	C18	C19	121.9(4)
O3	C7	C6	109.9(3)	C18	C19	C22	121.5(4)
O4	C7	C6	125.7(4)	C20	C19	C18	118.0(4)
O4	C7	O3	124.3(4)	C20	C19	C22	120.4(5)
O3	C8	C9	108.7(3)	C21	C20	C19	121.4(4)
C8	C9	Cl1	110.4(3)	C20	C21	C16	119.5(4)
C8	C9	Cl3	107.8(3)	C1	N1	S1	118.0(2)
C8	C9	Cl2	111.5(3)	C5	N1	C1	110.8(3)
Cl1	C9	Cl3	108.8(2)	C5	N1	S1	116.7(2)
Cl1	C9	Cl2	109.2(2)	C7	O3	C8	118.6(3)
Cl2	C9	Cl3	109.1(2)	N1	S1	C16	107.00(17)
C11	C10	C6	120.7(3)	O1	S1	C16	108.36(18)
C15	C10	C6	120.8(3)	O1	S1	N1	106.86(17)
C15	C10	C11	118.5(4)	O1	S1	O2	119.84(18)
C10	C11	C12	120.9(4)	O2	S1	C16	107.54(18)
C13	C12	C11	118.8(4)	O2	S1	N1	106.62(17)

Table 5: Torsion Angles in ° for **WL-N9-80-f34**.

Atom	Atom	Atom	Atom	Angle°
Br1	C13	C14	C15	175.8(3)
C1	C2	C3	C4	-50.8(4)
C1	C2	C3	C6	-171.5(3)
C1	N1	S1	C16	67.6(3)
C1	N1	S1	O1	-48.3(3)
C1	N1	S1	O2	-177.6(3)
C2	C1	N1	C5	-63.4(4)
C2	C1	N1	S1	158.5(3)
C2	C3	C4	C5	51.7(4)
C2	C3	C6	C7	-67.2(4)
C2	C3	C6	C10	172.0(3)
C3	C4	C5	N1	-58.3(4)
C3	C6	C7	O3	142.4(3)
C3	C6	C7	O4	-41.3(5)
C3	C6	C10	C11	58.2(5)
C3	C6	C10	C15	-124.3(4)
C4	C3	C6	C7	172.0(3)
C4	C3	C6	C10	51.2(4)
C4	C5	N1	C1	64.4(4)
C4	C5	N1	S1	-156.8(3)
C5	N1	S1	C16	-68.2(3)
C5	N1	S1	O1	175.9(3)
C5	N1	S1	O2	46.6(3)
C6	C3	C4	C5	172.8(3)
C6	C7	O3	C8	-179.9(3)
C6	C10	C11	C12	175.0(4)
C6	C10	C15	C14	-175.8(4)

Atom	Atom	Atom	Atom	Angle°
C7	C6	C10	C11	-66.5(5)
C7	C6	C10	C15	111.0(4)
C9	C8	O3	C7	102.7(4)
C10	C6	C7	O3	-91.0(3)
C10	C6	C7	O4	85.3(5)
C10	C11	C12	C13	-0.1(8)
C11	C10	C15	C14	1.8(6)
C11	C12	C13	Br1	-176.5(4)
C11	C12	C13	C14	3.7(7)
C12	C13	C14	C15	-4.4(7)
C13	C14	C15	C10	1.6(7)
C15	C10	C11	C12	-2.6(7)
C16	C17	C18	C19	-0.9(7)
C17	C16	C21	C20	-0.8(6)
C17	C16	S1	N1	-87.6(3)
C17	C16	S1	O1	27.3(4)
C17	C16	S1	O2	158.1(3)
C17	C18	C19	C20	0.8(7)
C17	C18	C19	C22	-178.6(4)
C18	C19	C20	C21	-0.7(6)
C19	C20	C21	C16	0.7(6)
C21	C16	C17	C18	0.9(6)
C21	C16	S1	N1	87.5(3)
C21	C16	S1	O1	-157.6(3)
C21	C16	S1	O2	-26.7(4)
C22	C19	C20	C21	178.7(4)
N1	C1	C2	C3	56.4(4)
O3	C8	C9	Cl1	47.9(3)
O3	C8	C9	Cl3	166.7(2)
O3	C8	C9	Cl2	-73.7(3)
O4	C7	O3	C8	3.7(6)
S1	C16	C17	C18	176.0(3)
S1	C16	C21	C20	-175.9(3)

Table 6: Hydrogen Fractional Atomic Coordinates ($\times 10^4$) and Equivalent Isotropic Displacement Parameters ($\text{\AA}^2 \times 10^3$) for **WL-N9-80-f34**. U_{eq} is defined as 1/3 of the trace of the orthogonalised U_{ij} .

Atom	x	y	z	U_{eq}
H1A	7255.43	6742.14	4651.97	30
H1B	5158.82	6405.53	5021.04	30
H2A	7622	5824.44	4001.22	30
H2B	4968.63	6066.72	3974.96	30
H3	3710.53	5220.95	4622.86	27
H4A	6350.34	4500.53	5102.61	30
H4B	8529.19	4805.18	4746.22	30
H5A	5915.99	5469.06	5686.06	30
H5B	8519.72	5194.75	5771.77	30
H6	6789.61	4742.76	3669.28	27
H8A	970.9	4996.29	2449.79	29
H8B	2685.81	4613.49	1996.42	29
H11	1653.94	4131.43	4485.7	46
H12	759.22	3026.49	4642.13	48
H14	6892.78	2521.31	3810.52	44
H15	7708.63	3626.63	3639.39	35
H17	6965.32	7597.88	5756.69	38
H18	4139.21	7968.83	6455.13	44
H20	5312.28	6413.43	7553.11	41
H21	8155.34	6030.09	6865.49	33
H22A	2752.47	7263.5	7924.14	82
H22B	959.11	7340.46	7367.64	82
H22C	2589.51	7932.25	7562.54	82

Citations

CrysAlisPro Software System, Rigaku Oxford Diffraction, (2019).

O.V. Dolomanov and L.J. Bourhis and R.J. Gildea and J.A.K. Howard and H. Puschmann, Olex2: A complete structure solution, refinement and analysis program, *J. Appl. Cryst.*, (2009), **42**, 339-341.

Sheldrick, G.M., Crystal structure refinement with ShelXL, *Acta Cryst.*, (2015), **C27**, 3-8.

Sheldrick, G.M., ShelXT-Integrated space-group and crystal-structure determination, *Acta Cryst.*, (2015), **A71**, 3-8.

```

#=====
# PLATON/CHECK-( 70414) versus check.def version of 310314 for Entry: wl-n9-80
# Data: WL-N9-80-f34.cif - Type: CIF      Bond Precision C-C = 0.0057 A
# Refl: WL-N9-80-f34.fcf - Type: LIST4          Temp = 100 K
#           X-Ray      Nref/Npar = 9.9
# Cell 5.60602(6) 20.3318(2) 21.4309(2)    90     90     90
# Wavelength 1.54184  Volume Reported 2442.71(4) Calculated 2442.70(4)
# SpaceGroup from Symmetry P 21 21 21 Hall: P 2ac 2ab orthorhombic
#           Reported P 21 21 21   P 2ac 2ab orthorhombic
# MoietyFormula C22 H23 Br Cl3 N O4 S
#   Reported C22 H23 Br Cl3 N O4 S
#   SumFormula C22 H23 Br Cl3 N O4 S
#   Reported C22 H23 Br Cl3 N O4 S
# Mr      = 583.73[Calc], 583.73[Rep]
# Dx,gcm-3 = 1.587[Calc], 1.587[Rep]
# Z       = 4[Calc], 4[Rep]
# Mu (mm-1) = 6.365[Calc], 6.365[Rep]
# F000   = 1184.0[Calc], 1184.0[Rep] or F000' = 1189.49[Calc]
# Reported T Limits: Tmin=0.158      Tmax=0.975 AbsCorr=GAUSSIAN
# Calculated T Limits: Tmin=0.257 Tmin'=0.086 Tmax=0.497
# Reported Hmax= 6, Kmax= 25, Lmax= 26, Nref= 4842 , Th(max)= 77.056
# Obs in FCF Hmax= 6, Kmax= 25, Lmax= 26, Nref= 4842[ 2864], Th(max)= 77.055
# Calculated Hmax= 7, Kmax= 25, Lmax= 27, Nref= 5151[ 2982], Ratio=1.62/0.94
# Reported Rho(min) = -0.72, Rho(max) = 0.68 e/Ang**3 (From CIF)
# Calculated Rho(min) = -0.67, Rho(max) = 0.85 e/Ang**3 (From CIF+FCF data)
# w=1/[sigma**2(Fo**2)+(0.0436P)**2+ 2.2178P], P=(Fo**2+2*Fc**2)/3
# R= 0.0326( 4758), wR2= 0.0856( 4842), S = 1.057 (From CIF+FCF data)
# R= 0.0326( 4758), wR2= 0.0856( 4842), S = 1.057 (From FCF data only)
# R= 0.0326( 4758), wR2= 0.0855( 4842), S = 1.057, Npar= 290, Flack -0.001(8)
# Number Bijvoet Pairs = 1978 ( 91%) ( 1899 Selected for: Parsons 0.003(5)
# P2(tr) 1.000, P3(tr) 1.000, P3(tw) 0.000, Student-T Nu 19.05, Hooft -0.012(6)
#=====
```

For Documentation: <http://www.platonsoft.nl/CIF-VALIDATION.pdf>

```
#=====
```

```

#=====
>>> The Following Improvement and Query ALERTS were generated - (Acta-Mode) <<<
#=====
```

Format: alert-number_ALERT_alert-type_alert-level text

```

090_ALERT_3_C Poor Data / Parameter Ratio (Zmax > 18) ..... 9.88 Note
761_ALERT_1_C CIF Contains no X-H Bonds ..... Please Check
762_ALERT_1_C CIF Contains no X-Y-H or H-Y-H Angles ..... Please Check
#=====
003_ALERT_2_G Number of Uiso or Uij Restrained non-H Atoms ... 7 Why ?
142_ALERT_4_G su on b - Axis Small or Missing ..... 0.00020 Ang.
143_ALERT_4_G su on c - Axis Small or Missing ..... 0.00020 Ang.
434_ALERT_2_G Short Inter HL..HL Contact Cl1 .. Cl3 . 3.32 Ang.
791_ALERT_4_G The Model has Chirality at C6 ..... S Verify
860_ALERT_3_G Number of Least-Squares Restraints ..... 12 Note
912_ALERT_4_G Missing # of FCF Reflections Above STh/L= 0.600 99 Note
#=====
```

ALERT_Level and ALERT_Type Summary

3 ALERT_Level_C = Check. Ensure it is Not caused by an Omission or Oversight
 7 ALERT_Level_G = General Info/Check that it is not Something Unexpected

2 ALERT_Type_1 CIF Construction/Syntax Error, Inconsistent or Missing Data.

2 ALERT_Type_2 Indicator that the Structure Model may be Wrong or Deficient.

2 ALERT_Type_3 Indicator that the Structure Quality may be Low.

4 ALERT_Type_4 Improvement, Methodology, Query or Suggestion.

#=====

2 Missing Experimental Info Issue(s) (Out of 54 Tests) - 96 % Satisfied

0 Experimental Data Related Issue(s) (Out of 28 Tests) - 100 % Satisfied

4 Structural Model Related Issue(s) (Out of 117 Tests) - 97 % Satisfied

4 Unresolved or to be Checked Issue(s) (Out of 223 Tests) - 98 % Satisfied

#=====